



***Proceedings of the Third Meeting  
of  
the International Group on Research Reactors  
(IGORR-III)***

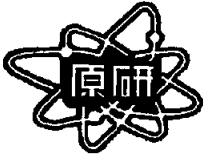


September 30 ~ October 1, 1993  
Naka Research Establishment, JAERI, Naka, Ibaraki, Japan

Organized and Sponsored by  
***Japan Atomic Energy Research Institute***

in Cooperation with  
***Committee for International Group on Research Reactors***

***Japan Atomic Energy Research Institute***



***Proceedings of the Third Meeting  
of  
the International Group on Research Reactors  
(IGORR-III)***

September 30 ~ October 1, 1993  
Naka Research Establishment, JAERI, Naka, Ibaraki, Japan

Organized and Sponsored by  
***Japan Atomic Energy Research Institute***

in Cooperation with  
***Committee for International Group on Research Reactors***

***Japan Atomic Energy Research Institute***

# **International Group on Research Reactors IGORR**

## **Charter**

The International group on Research Reactors was formed to facilitate the sharing of knowledge and experience among those institutions and individuals who are actively working to design, build, and promote new research reactors or to make significant upgrades to existing facilities.

### **IGORR Organizing Committee**

- J. Ahlf, *Joint Research Center - Petten***
- P. Armbruster, *Institut Laue-Langevin***
- J. D. Axe, *Brookhaven National Laboratory***
- A. Axmann, *Hahn Meitner Institute***
- K. Böning, *Technischen Universität München***
- C. Desandre, *Technicatome***
- A. F. DiMeglio, *AIEA***
- B. Farnoux, *Laboratory Leon Brillouin***
- J. Ganley, *General Atomics***
- O. K. Harling, *Massachusetts Institute of Technology***
- R. F. Lidstone, *Whitshell Nuclear Research Establishment***
- S. Matsuura, *Japan Atomic Energy Research Institute***
- J. C. McKibben, *University of Missouri***
- H. Nishihara, *Research Reactor Institute, Kyoto University***
- Y. V. Petrov, *St Petersburg Nuclear Physics Institute***
- H. J. Roegler, *Interatom***
- J. M. Rowe, *National Institute for Standard and Technology***
- C. D. West, *Oak Ridge National Laboratory***



IGORR-III

THE 3 RD MEETING OF THE INTERNATIONAL GROUP ON RESEARCH REACTORS

September 30 - October 1, 1993, Naka -machi, Ibaraki-ken, Japan

## IGORR-III

### 3rd Meeting of the International Group on Research Reactors September 30-October 1, 1993 Naka-machi, Ibaraki-ken, Japan

#### AGENDA

##### Wednesday, September 29

Registration

Evening  
(at Hotel Crystal Plaza)

##### Thursday, September 30

	<b>Speakers (min.)</b>	<b>Session times</b>	
Registration (final)		9:00 a.m.	(15)
Welcome and Opening	S. Matsuura	9:15 a.m.	(15)
Organization	E. Shirai	9:30 a.m.	(10)
Agenda	C. D. West	9:40 a.m.	(5)

##### I. Operating Research Reactors and Facility Upgrades (H. Nishihara)

RSG-GAS	B. Arbie	9:45 a.m.	(20)
R2-Studsvik	M. Grounes	10:05 a.m.	(20)
BREAK		10:25 a.m.	(25)
BR2	E. Koonen	10:50 a.m.	(20)
NIST	H. Prask	11:10 a.m.	(20)
JRR-3M	E. Shirai	11:30 a.m.	(20)
FRJ-2 Status	J. Wolters	11:50 a.m.	(20)
ORPHEE Upgrades	B. Farnoux	0:10 p.m.	(20)
LUNCH		0:30 p.m.	(75)

##### II. Research Reactors in Design and Construction (C. Desandre)

FRM-II	K. Böning	1:45 p.m.	(20)
MAPLE-MTR	A. Lee	2:05 p.m.	(20)
ANS	C. D. West	2:25 p.m.	(30)
BREAK		2:55 p.m.	(35)
KMRR (Current status)	J. T. Lee	3:30 p.m.	(20)
KMRR (Residual heat removal)	I. C. Lim	3:50 p.m.	(20)
REX 2000	F. Merchie	4:10 p.m.	(20)
HTTR Program	T. Tanaka	4:30 p.m.	(20)
TRIGA (TRIGA reactors of higher power density)	W. L. Whitemore	4:50 p.m.	(20)

\* This paper was not presented at IGORR-III meeting.

ADJOURN

5:10 p.m.

DEPART FOR CONFERENCE RECEPTION AT TOKAI-KAIKAN 5:30 p.m.

CONFERENCE RECEPTION <b>Friday, October 1</b>		6:00 p.m. (90)
<b><u>III. Research, Development and Analysis Results</u></b>		<b>(K. Böning)</b>
Instrumentation of Fuel Element and Fuel Plate at CERCA	J. P. Durand	9:00 a.m. (15)
The Use of Reprocessed Uranium in CERCA	G. Harbonnier	9:15 a.m. (15)
Two Safety-related Design Features of Reactor PIK that is Under Construction	K. Konoplev	9:30 a.m. (15)
Present Status of PIK Gadolinium Control	Y. V. Petrov	9:45 a.m. (15)
Core Thermal Hydraulic Tests for ANS	M. Kaminaga	10:00 a.m. (15)
Results from the ANS Research Work	C. D. West	10:15 a.m. (15)
BREAK		10:30 a.m. (20)
OSIRIS: The First MTR with a New Instrumentation and Control System Based on Logics of Vote	C. Joly	10:50 a.m. (20)
Probabilistic Safety Analysis for FRJ-2	J. Wolters	11:10 a.m. (20)
Neutron Sources for the Research of Condensed Matter	W. Knop	11:30 a.m. (20)
Development of Supermirror and Neutron Bender	K. Soyama	11:50 a.m. (20)
PHOTOGRAPH		0:10 p.m. (20)
LUNCH		0:30 p.m. (70)
<b><u>IV. Workshop on R&amp;D Needs</u></b>		<b>(C. D. West)</b> 1:40 p.m. (80)
<b><u>V. Business Session</u></b>		<b>(C. D. West)</b> 3:00 p.m. (20)
Closing	C. D. West	3:20 p.m. (10)
Technical Tour to JRR-3M		3:30 p.m. (120)

## CONTENTS

### Welcome and Opening Address

#### I. Operating Research Reactors and Facility Upgrades

<b>I-1</b> Status Report on The Indonesian Multipurpose Reactor, RSG-GAS .....	3
<i>Bakri ARBIE and Sutaryo SUPADI (BATAN)</i>	
<b>I-2</b> Studsvik's R2 Reactor - Review of Activities .....	11
<i>Mikael Grounes, Hans Tomani, Christian Gröslund, Hans Rundquist and Kurt Sköld (Studsvik Nuclear AB)</i>	
<b>I-3</b> Ongoing Refurbishment Activities and Strategy for The Future Operation of The BR2 Reactor .....	47
<i>E. Koonen and P. Gubel (C.E.N./S.C.K.)</i>	
<b>I-4</b> The Reactor and Cold Neutron Research Facility at NIST .....	59
<i>H. J. Prask and J. M. Rowe (NIST)</i>	
<b>I-5</b> Present Status of JRR-3M .....	76
<i>Eiji SHIRAI (JAERI)</i>	
<b>I-6</b> Status of FRJ-2 Refurbishment of Tank Pipes and Essential Results of Aging Analysis .....	87
<i>G. Hansen, G. Thamm and M. Thomé (Forschungszentrum Jülich GmbH)</i>	
<b>I-7</b> Upgrade of The Experimental Facilities of The ORPHEE Reactor .....	115
<i>B. Farnoux and P. Breant (CEN Saclay)</i>	

#### II. Research Reactors in Design and Construction

<b>II-1</b> Status of The FRM-II Project .....	137
<i>Klaus Böning (Technische Universität München)</i>	
<b>II-2</b> Progress Towards A New Canadian Irradiation-Research Facility .....	144
<i>A. G. Lee and R. F. Lidstone (AECL Research)</i>	
<b>II-3</b> A Status Report on The Advanced Neutron Source Project .....	155
<i>Colin D. West (ORNL)</i>	
<b>II-4</b> The Design Characteristics and Current Status of KMRR .....	163
<i>J. T. Lee, J. B. Lee and B. K. Kim (KAERI)</i>	
<b>II-5</b> The Residual Heat Removal System of KMRR and Flap Valve Design .....	172
<i>I. C. Lim, Y. S. Yang, H. T. Chae and C. Park (KAERI), C.H. Han (Samshin Limited)</i>	
<b>II-6</b> Preliminary Conceptual Studies of REX 2000 .....	186
<i>F. Merchie, C. Baas, A. Ballagny, M. Chagrot, G. Farry, M. Branier and A. Pattou (CEA, France)</i>	
<b>II-7</b> Present Status of High-Temperature engineering Test Reactor (HTTR) Program .....	191
<i>Toshiyuki TANAKA, Osamu BABA, Shusaku SHIOZAWA, Minoru OKUBO and Toshiaki TOBIOKA (JAERI)</i>	
<b>II-8</b> TRIGA Research Reactors with Higher Power Density .....	205
<i>W. L. Whittemore (General Atomics)</i>	
* This paper was not presented at IGORR-III meeting.	

### III. Research, Development and Analysis Results

III-1 Instrumentation of Fuel Elements and Fuel Plates .....	211
<i>J. P. Durand and Y. Fanjas (CERCA)</i>	
III-2 Mechanism of $^{232}\text{U}$ Production in MTR Fuel Evolution of Activity in Reprocessed Uranium .....	219
<i>G. Harbonnier, B. Lelièvre, Y. Fanjas and SJP. Naccache (CERCA)</i>	
III-3 Two Design Aspects Connected with The Safety of The PIK Reactor Presently under Construction .....	230
<i>V. V. Gostev, A. S. Zakharov, K. A. Konoplev, N. V. Levandovskii, L. M. Ploshchanskii and S. L. Smolsky (Petersburg Nuclear Physics Institute)</i>	
III-4 Present Status of PIK Gadolinium Control .....	252
<i>Y. V. Petrov, E. A. Garusov and V. A. Shustov (Petersburg Nuclear Physics Institute)</i>	
III-5 Core Thermal Hydraulic Tests for ANS .....	264
<i>Masanori KAMINAGA (JAERI), M. Siman-Tov, D. K. Felde, G. L. Yoder and Colin D. West (ORNL)</i>	
III-6 Some Results from The ANS Research Work.....	273
<i>Colin D. West (ORNL)</i>	
III-7 OSIRIS : The First MTR with A New Instrumentation and Control System Based on Digital Logic of Vote .....	285
<i>C. Joly, C. Thiercelin, J. Corre, J. F. Dubois and G. De Contenson (C.E.A. Saclay)</i>	
III-8 Probabilistic Safety Analysis for FRJ-2 Motivation, Methodology and Results.....	301
<i>J. Wolters (Forschungszentrum Jülich GmbH)</i>	
III-9 Neutron Sources for The Research of Condensed Matter .....	313
<i>W. Knop (GKSS)</i>	
III-10 Development of Supermirror and Neutron Bender.....	325
<i>Kazuhiko SOYAMA, Masatoshi SUZUKI (JAERI) and Yuji KAWABATA (Research Reactor Institute, Kyoto University)</i>	

### IV. Workshop on R&D Needs

Report on The Workshop on R&D Needs .....	333
<i>Colin D. West (ORNL) and Klaus Böning (Technische Universität München)</i>	

### V. Business Session

IGORR Business Meeting .....	337
<i>Colin D. West (ORNL)</i>	

### IGORR-III Participants List



**WELCOME AND OPENING ADDRESS**

**by**

**Shojiro MATSUURA**

**Executive Director**

**Japan Atomic Energy Research Institute**

## Welcome and Opening Address

### Shojiro MATSUURA

Good morning gentlemen, I am Shojiro MATSUURA, an executive director of JAERI and the director general of Tokai Research Establishment. On behalf of the organizing committee of IGORR and JAERI, it is my great pleasure to open the IGORR-III here, in the Naka Fusion Research Establishment of JAERI, and to express our cordial welcome to all of participants. First of all, I would like to express my deep gratitude to all participants for their cooperation and especially to Dr. West for his continuous significant contribution keeping the IGORR activities. I cannot believe, we can continue the IGORR activities without his leadership and contribution. At the same time, I greatly thank our staff for their large effort to arrange this IGORR meeting.

In preparation for any meetings, the most important issues will be to decide a good time, a convenient place and a suitable program for the meeting. Our staff, the working party for this meeting, had struggled for arranging these issues, because autumn is usually very busy season for many kinds of conferences. For example, there was a very big nuclear conference, "Global '93", in the United States, before last week. Last week, we had a little bit exotic meeting, the 7th International Conference on Emerging Nuclear Energy System (ICENES '93), at Makuhari in Chiba city. Next week, we will have an another reactor relating meeting on "Reduced Enrichment for Research and Test Reactors (RERTR)". And then, after next week, we will have an Autumn Meeting of the Atomic Energy Society of Japan. Therefore, it was very difficult for them to fix this IGORR meeting in sometime in this autumn. Finally, our working party had decided to take this week for this IGORR-III, taking into consideration of convenience for persons who are attending to ICENES '93 and RERTR.

The next point is to decide a place for the meeting. Some persons wonder why this meeting is held in this Naka Establishment, not in Tokai Establishment or Oarai Establishment. Our JAERI has several research and test reactors. In Tokai we have several reactors and in Oarai we have the Japan Material Test Reactor and also we are constructing a new High Temperature Test Reactor. Although we don't have any research or test reactors in this Naka Establishment, we use this place. Because we don't have a quite nice size and nicely facilitated meeting room in Tokai Establishment and in Oarai Establishment. We have a very big auditorium in Tokai, but it's too big for this meeting. Therefore our working party decided to use this quite nice size and facilitated meeting room. I believe this is a very good chance for the participants to see another side of JAERI's activity in this Naka Establishment which is dedicated for fusion research and in the next door there is a nice exhibition place. Many fusion small facilities are exhibited in the next room. I hope, some of you enjoy such kind of one face of fusion research.

Most important point of meeting is of course the program of meeting. This meeting has participants from 13 (thirteen) countries, and total number of participants is about more than hundred and 35 (thirty-five) participants from abroad. I believe it's a quite good number and also we have 25 (twenty-five) papers. I'm expecting we can hear the very recent information in research reactor activities all over the world. Especially, we have a very new presentation in this third meeting. In addition to the first and the second meeting of IGORR, we have 5 (five) new presentation, one is from Indonesia, RSG-GAS reactor's by Dr. Bakri, a Swedish reactor R2 Studsvik by Dr. Grounes, first presentation from Korea KMRR by Dr. Lee and Lim, a new French program for the research reactor REX 2000 by Dr. Merchie and HTTR of Japan, High Temperature Test Reactor presently under construction by Dr. Tanaka. I believe, we can touch the new information for such a new program of research reactors.

Thinking of the circumstances surrounding research reactors all over the world, I feel, we are in very delicate stage, because the number of people to use research reactors or the peoples wanting to use research reactors are increasing right now. For example, since we started revised JRR-3, JRR-3M, number of Japanese researcher is very much increased and still the trend is continuing. Because recently the utilization field of neutrons is so much widened, so the number of researchers is increasing. I observe this situation is similar in all over the world. But first generation research reactor is aging year after year and right now the world economic condition is not so good. Every country is in some tight financial conditions. Japan is also in very tight financial condition after the broken of economical babble. But as I said, first generation research reactor is aged and number of researchers is increasing, so we have to continue our effort to upgrade the present research reactors or to construct new research reactors for future utilization of many kinds of research. I think this IGORR is big chance to exchange information for the upgrading and new program and also a very nice chance to exchange our experience for such upgrading and establishing new program. I hope this IGORR-III will be a very fruitful meeting. Thank you.

## **SESSION I**

# **Operating Research Reactors and Facility Upgrades**

## STATUS REPORT ON THE INDONESIAN MULTIPURPOSE REACTOR, RSG-GAS

Bakri ARBIE and Sutaryo SUPADI

BATAN INDONESIA

## ABSTRACT

RSG-GAS, a 30 MW multipurpose reactor, and located at Serpong Atomic Energy Research Center, went to its first criticality on July 29, 1987. Its nominal power was just achieved in March, 1992 by operating the full core configuration (core-VI) after successive five transition core commissioning operation. By then, the reactor performed as expected to produce thermal neutron flux in the order of  $10^{14}$  n/(cm<sup>2</sup>.sec) safely to support research, radioisotope production as well as material testing including man power development.

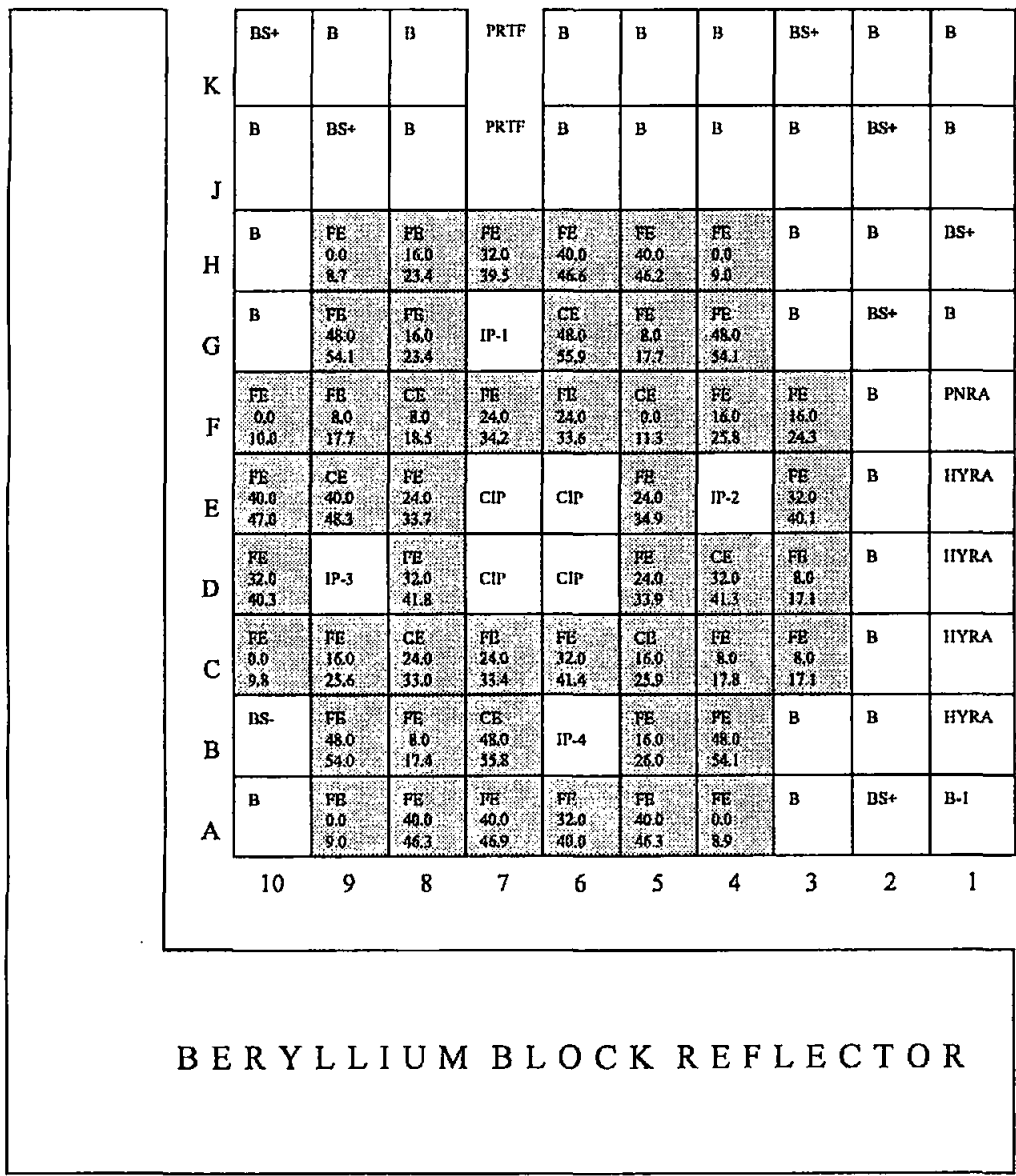
The long commissioning activities and experiences are outlined in the paper. Main characteristics of the reactor is also presented. Nowadays, the reactor is operating at core no. 9, in weekly modes, mainly for radioisotope production. Some facilities for neutronic experiment, material and fuel testing are being commissioned.

Study of silicide fuels to replace the oxide ones is in progress. Several silicide fuel elements with similar specification to the existing oxide fuels have been inserted in the core since 1989. In five years, the RSG-GAS is expected to operate with the silicide fuel.

Introduction

The Indonesian Multipurpose Reactor RSG-GAS has recently completed 6 years of operation. The reactor plays an important role in the Centre for Nuclear Industry Development, at Puspptek, Serpong to serve other supporting laboratories, namely, radioisotope production, nuclear material science, reactor fuel element development, reactor safety, waste treatment, radiometallurgy and nuclear-mechano laboratories.

The nominal power of 30 MWt was achieved on March 23, 1992 after completion of 5 transition cores commissioning operation so called power ascent test, since its first criticality in July, 1987. The commissioning took rather long time due to strategy complexities of in-core fuel management starting with all fuel elements were of fresh (zero burn-up) to reach 7 different burn-up levels of typical working core (TWC) as illustrated in Figure 1. By keeping



BERYLLIUM BLOCK REFLECTOR

Note:  
 B = Beryllium, BS- = Beryllium Stopper without stopper, BS+ = Beryllium Stopper with stopper, HYRA = Hydraulic Rabbit System, PNRA = Pneumatic Rabbit System  
 FE/CE = Fuel Element/ Control Element  
 xx.x = burn-up BOC  
 yy.y = burn-up EOC

FIGURE 1: DESIGN TWC OF RSG-GAS

the constant power density of fuel element, the reactor was started operating with the first core consisting of 18 fuel elements and possessing nominal power of 10 MW thermal. The following cores were built by adding some fuel elements in ascending the power until full core at core No.VI, with 30 MW power achieved.

During commissioning operation, experiences were gained in the matter of O & M, utilization even solving the problems arosed.

As of today, the reactor is operating routinely in weekly mode to serve the radioisotope production as well as other experiments. Some experiment facilities such as power ramp test and beam tubes experiment have been commissioned. The facility called in-pile loop will be totally commissioned next year.

Upon completion of all experiment facilities, the reactor should be operated optimum in a safe manner to support the national nuclear industry development including man-power in facing the nuclear power program. The RSG-GAS itself has been planned to operate with silicide fuels in the form of  $U_3Si_2Al$  in 5 years. Test of 4 home made silicide fuels was started in the core No.3, in 1989. So far, until core No.9, those fuel elements indicate no problem.

### Nuclear Commissioning

The first criticality of the RSG-GAS as mentioned before achieved on July 29, 1987. This successful stage was then followed to be able to operate the reactor with the power of 10 MW at the first core. The President of the Republic of Indonesia innaugurated the reactor on August 20, 1987 and the RSG was then ready for its operation and utilization.

The nominal power of 30 MW thermal was achieved on 23 rd March 1992 at the sixth core containing 40 standard fuel elements and 8 control fuel elements. Nuclear commissioning seemed to be quite long about 5 1/2 years. The reason is that :

- during commissioning, the RSG-GAS was applied not only for fuel elements testing, but also for experiments using neutron beams, isotope production and silicon doping.
- commissioning was interrupted quite long because of inpile loop and neutron guide tube installations.
- occurence of disturbance operation and reactor systems failures.

However, the above conditions have given enhancement in operations, staff management analysis, maintenance and repair stages. In addition, thermohydraulic and neutronic calculations were also verified by experiments.

As explained before, to achieve the nominal power of 30 MW thermal, it was formulated and configured transition cores. Transition cores were started with the power of 10 MW thermal. At that time, the core possessed 12 standard fuel elements and 6 control fuel elements. Transition cores ended at the sixth core which was called the optimum core

configuration possessing the power of 30 MW thermal. It was noted that during nuclear and non nuclear commissioning period, the research reactor responsible for the RSG-GAS operation had about a hundred staff and technicians. At that time, some problems arose, staff most likely should know not only his field but also others. Fortunately, because of staff's hardworking, dilligence, and one-to-another cooperation as well as cooperating with the reactor supplier and its experts, all problems arose were finally solved.

Prior to detailed information of the RSG-GAS core, the RSG-GAS uses fuel elements with 19.75 % uranium enrichment. The fuel elements form in  $U_3O_8$ -Al. Each fuel element contains about 250 grams of U-235, while control fuel element only contains roughly 154 grams. The fuel element is a fuel plate type consisting of 21 fuel plates, while a control fuel elements containing 15 fuel plates. The fuel type absorber is made of AgInCd. For complete information, table 1 shows nuclear design parameters of the RSG-GAS.

**Table 1. Nuclear Design Parameters of the RSG-GAS**

No.	Parameter	Value
1.	Nominal Power, MW	30
2.	Amount of standard fuel elements	40
3.	Amount of control fuel elements	8
4.	Amount of absorbers	8
5.	Cycle length, full power days	25
6.	Fraction of Burn-up at BOC, %	23.3
7.	Fraction of Burn-up at EOC, %	31.3
8.	Average fraction of spent fuel element Burn-up, %	53.7
9.	Excess Reactivity at BOC, %	9.2
10.	Control Rod Reactivity, %	- 14.5
11.	Shut down Reactivity, %	- 5.3
12.	Shut down Reactivity at Stuck Rod, %	- 3.2



## Utilization of RSG-GAS

Since the RSG-GAS achieved first criticality in July 1987, the RSG-GAS was then applied for energy, non-energy programs and radioisotope production services. Figure 2 shows the RSG-GAS and its facilities.

For energy services, R & D activities are supported by availability of power ramp test facility (PRTF) and wet neutron radiography. They are both located at the edge of the reactor core. The PRTF is applied for testing the fuel element of power reactor, particularly the endurance of fuel element during power ramp. By this facility, it is able to indentify the characteristic interaction between the pellets and cladding of the fuel element. The wet neutron radiography facility is utilized for performing "radiography" using thermal neutron from the reactor. The object is mainly either fuel pellet or fuel pin. Last but not least, the equipment called inpile loop which will however be commissioning. The loop located at CIP is applied for testing fuel element of power reactor and this will be available at the beginning of 1995.

For non-energy services, the RSG-GAS is supported by low and high speed rabbit systems which are located at the edge of the core. Both systems, especially for a high speed rabbit system, are utilized for Neutron Activation Analysis (NAA). The NAA is able to carry out a high sensitivity analysis that can not be detected by chemical analysis. It can be used also for both measuring air contamination and minerals and analyzing a material composition etc.

Neutron Transmutation Doping Facility is utilized to perform neutron irradiation on a silicon sample. By this irradiation, a part of silicon atom will be transmuted into phosphor atom (dopant). The irradiated sample is then becoming a semi-conductor material.

In addition to the above mention, the RSG-GAS has two tangential and four radial beam tubes. Beam tube S2 which is tangential is applied for dry neutron radiography. This system is able to carry out the performance of "radiography" whose the irradiated sample is a little bit bigger than the sample irradiated in the wet neutron radiography. Beam tubes S4, S5 and S6 are subsequently applied for Triple Axis Spectrometer, High Resolution Small Angle Neutron Scattering (HRSANS), and neutron diffractometer. Those systems are utilized for R & D in material science.

For radioisotope production services, central irradiation position (CIP) is so far utilized to irradiate U-235 for Molybdenum-99 production. In the near future, production of Ir-192, TeO<sub>2</sub>, S as well as P which will be irradiated in irradiation position will be achieved at commercial scales.

Summary of all facilities possessed by the RSG-GAS is shown in table 2.

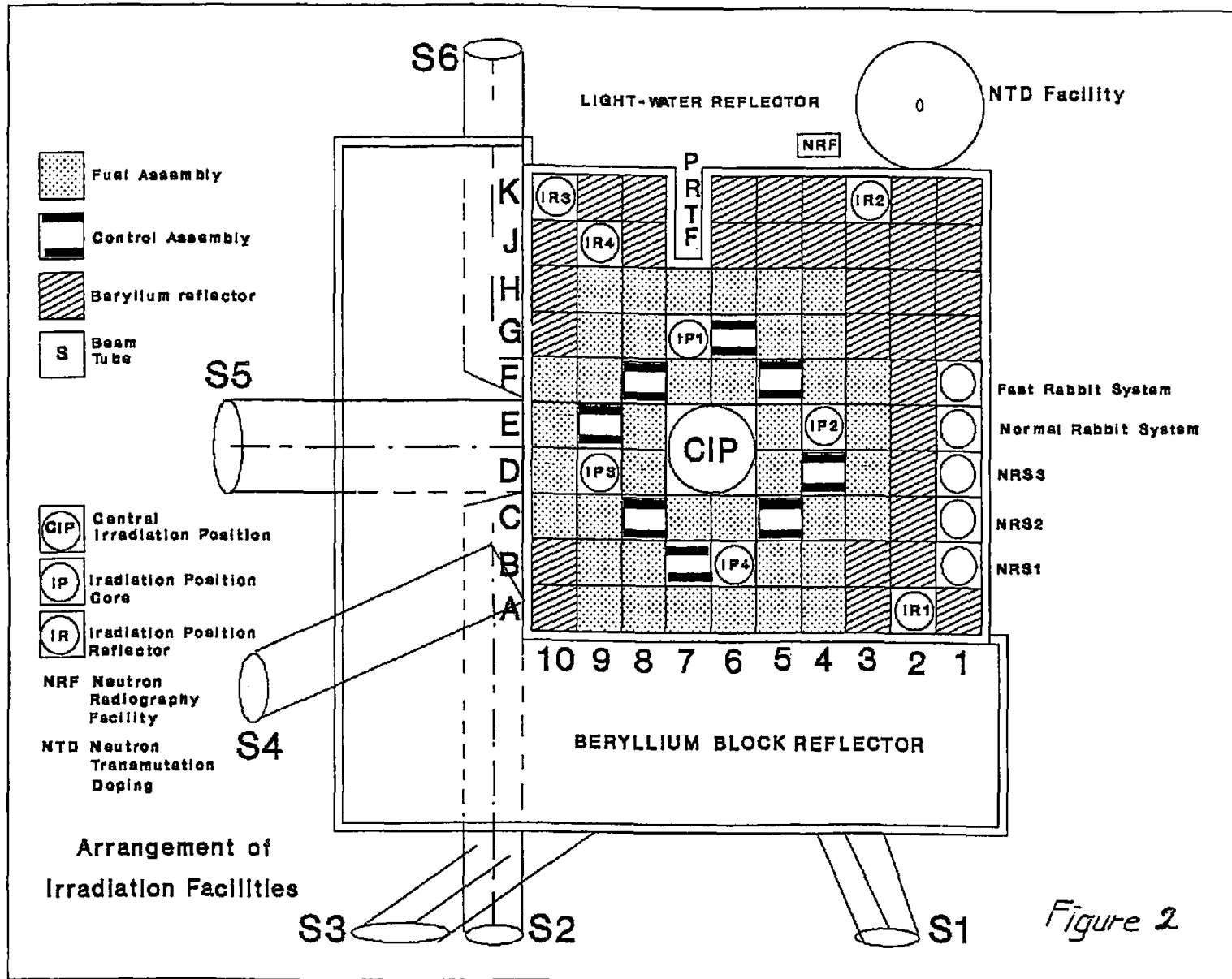


Figure 2

**Table 2. Irradiation Facilities at RSG-GAS**

FACILITY	NO.	THERMAL NEUTRON FLUX n/cm <sup>2</sup> .sec. (Calculated)	APPLICATION	NOTE
Horizontal Tube	6	$0.5 \times 10^9$	Neutron scattering research and Dry Neutron Radiography and Radioisotope Production	Instrumented loop
Central Incore Hole	1	$2 \times 10^{14}$	PWR-fuel Bundle Test 4 x 4 matrix PHWR-fuel Bundle, 16 rods	Instrumented loop
Incore Hole	4	$7.5 \times 10^{13}$	Research and Development for Fuel-pin and Material, Radioisotope Production and MTR Fuel Test	Instrumented capsule
On-power Loading	1	$0.3 \times 10^{10}$	NTD of silicon, max.7" diameter	Instrumented capsule
Pneumatic Tube	1	$0.2 \times 10^{10}$	NAA, short live Nuclide Study	Uninstrumented capsule
Hydraulic Tube	4	$0.2 \times 10^{10}$	NAA	Uninstrumented capsule
Adjacent Core	2	$0.4 \times 10^{10}$	Power Ramp Test of PWR fuel-pin and Wet Neutron Radiography	Instrumented loop

## Conclusion

During nuclear and non-nuclear commissioning, we faced a lot of difficulties in terms of equipments installation, repair as well as operation. However, those were very beneficial for us to face the next step of operation, maintenance as well as carrying out R & D activities. This is surely very useful for us to face nuclear power plants which will be built in the near future.

The RSG-GAS and its facilities which were established as a central of excellence in Asia Pacific regions in 1989 are open to those interested in doing R & D activities with mutual benefit agreements.

## Future Program

Starting the year 1994, a five year program for operation, utilization and R & D in RSG-GAS is outlined :

- a. **Availability and Reliability**  
The availability and reliability of the RSG-GAS will be increased to support optimum utilization safely, by ways :
  - optimizing the O & M schedule
  - establishing and develop the operability of irradiation and experiment facilities
  - promoting the man-power ability
- b. **Fuel Conversion**  
Study, analysis test and development of silicide fuels as substitute of oxide fuel is expected to complete in 1999.
- c. **Computer Code**  
Computer code systems for design, analysis and operation of the reactor and its system are expected to be established by 1997 for supporting the safe and optimum reactor operation and utilization.

## References

1. Safety Analysis Report of the RSG-GAS volume 8, Batan, Jakarta, 1986.
2. Nuclear Commissioning Report of the RSG-GAS, PRSG - BATAN, Serpong, February 1993.
3. Non-Nuclear Commissioning Report of the RSG-GAS, PRSG - BATAN, Serpong, February 1993.
4. Planned Irradiation Facilities of the MPR-GA. Siwabessy for R & D Program, B. Arbie et.al, Published paper, 1987.

## STUDSVIK'S R2 REACTOR - REVIEW OF ACTIVITIES

Mikael Grounes, Hans Tomani, Christian Gräslund, Hans Rundquist and Kurt Sköld

STUDSVIK NUCLEAR AB, S-611 82, NYKÖPING, SWEDEN

### Abstract

A general description of the R2 reactor, its associated facilities and its history is given. The facilities and range of work are described for the following types of activities: fuel testing, materials testing, neutron transmutation doping of silicon, activation analysis, radioisotope production and basic research including thermal neutron scattering, nuclear chemistry and neutron capture radiography.

### 1 Introduction

STUDSVIK AB is a subsidiary of Vattenfall AB, performing R&D work and associated activities, primarily in the nuclear energy field. STUDSVIK AB is a commercial company, active in the areas of services, supply of special equipment and systems and also consulting. STUDSVIK NUCLEAR AB, which is the largest subsidiary within the STUDSVIK group, is one of the direct offsprings of AB Atomenergi, the origin of the STUDSVIK group, which was formed in 1947. The STUDSVIK group has about 520 employees and a turnover of about 400 MSEK/year.

During the 1950's and 60's, an ambitious nuclear program was launched in Sweden. The experience and competence gained from a large number of advanced projects constitutes the basis upon which the present activities of STUDSVIK NUCLEAR are based. Among the fuel- and materials-related experiences are the design, construction and operation of a fuel manufacturing plant for uranium dioxide fuel in Stockholm, a pilot line for mixed-oxide fuel in Studsvik, the design and manufacture and initial operation of the Ågesta pressurized heavy water reactor, and the design, manufacture and irradiation proof testing for the Marviken boiling heavy water reactor. Ambitious R&D programs for heavy water reactor super-heater fuel and fast heavy water reactor fuel and materials have also been carried out. Since the 1970's, the efforts have been concentrated on light water reactor fuel and materials, and the originally domestic R&D programs have been expanded so that a large fraction is now financed by non-Swedish sponsors.

Neutron activation analysis and radioisotope production as well as beam tube experiments for basic research applications were started in the 1960's. In 1977 neutron transmutation doping of silicon began.

The facilities of interest in this connection are the R2 Test Reactor, the Hot Cell Laboratory, the Lead Cell Laboratory and various other laboratories, all located at Studsvik, 100 kilometers south of Stockholm.

## 2 The R2 reactor

### 2.1 General Description of the R2 Reactor

The R2 reactor is a tank-in-pool reactor, see Figure 1 and Table 1, in operation since 1960 and originally similar to the Oak Ridge Research Reactor, ORR (1). The reactor core is contained within an aluminum vessel at one end of a large open pool, which also serves as a storage for spent fuel. Light water is used as core coolant and moderator. The reactor power was increased to 50 MW(th) in 1969. In 1984-85 a new reactor vessel was installed.

The R2 reactor has a high neutron flux, see Table 1, and special equipment for performing sophisticated in-pile experiments. An important feature of the R2 test reactor is that it is possible to run fuel experiments up to and beyond failure of the cladding; that is not possible in a commercial power reactor.

**Table 1** Technical Data for the R2 Test Reactor.

Power	50 MW(th)
Moderator/coolant	H <sub>2</sub> O
Reflector	D <sub>2</sub> O, Be
Fuel length	600 mm
Fuel assembly length	924 mm
Fuel assembly cross section	79x82 mm <sup>2</sup>
Number of fuel plates per assembly	18
Neutron flux in experimental positions	
Thermal	(0.3-2.5) x 10 <sup>14</sup> n/(cm <sup>2</sup> -sec)
Fast (>1 MeV)	(0.5-2.0) x 10 <sup>14</sup> n/(cm <sup>2</sup> -sec)
Primary flow	1 350 kg /sec
Coolant temperature: Inlet	≤ 35 °C
Outlet	≤ 45 °C

The coolant water is circulated through the reactor vessel and flows through pipes and a large decay tank below the reactor hall to an adjoining building containing pumps and heat exchangers cooled with sea water.

The present core configuration is shown in Figure 2. The components of the core are arranged in an 8x10 lattice, typically comprising 46 fuel elements, 6 control rods, about 12 beryllium reflector assemblies and a number of in-pile loops, irradiation rigs and aluminum fillers. Rows No 1 and 10 consist of beryllium reflector assemblies. The composition of the core can be altered to suit the experimental program.

The R2 driver fuel assemblies are, since the beginning of 1993, of the LEU type. They have 18 curved fuel plates containing an aluminum-clad aluminum silicide matrix. The initial fuel content is 450g  $^{235}\text{U}$  per fuel assembly, enriched to less than 20 %. The burnup of the spent fuel of this type reaches about 65 %.

The control rods consist of an upper neutron absorbing section of cadmium and a lower fuel section. They are moved vertically by drive mechanisms placed below the reactor vessel.

The reactor vessel is 4.5 m high and 1.6 m in diameter. The design pressure is 3.3 bars.

Some of the irradiation facilities in the R2 reactor have been described in the literature (2–4), and details are given below. Most base irradiations of test fuel (that is irradiations at constant power, where fuel burnup is accumulated under well-defined conditions) are performed in boiling capsules (BOCA rigs). Some base irradiations and all ramp tests (that is irradiations under power changes) are performed in one of the two in-pile loops, which can be operated under either BWR or PWR pressure and temperature conditions. The ramp tests, simulating power transients in power reactor fuel, are achieved by the use of  $^3\text{He}$  as a variable neutron absorber. Structural materials, such as samples of Zircaloy cladding, steels for pressure vessels and vessel internals and candidate materials for advanced reactors can also be irradiated in special rigs either in the loops or in special NaK-filled irradiation rigs in fuel element positions with a well-controlled irradiation temperature. Special equipment for in-pile corrosion experiments in the loops are under development.

The R2 core has an active fuel length of 600 mm. Most fuel rods irradiated are segments of power reactor fuel rods, so-called rodlets, with lengths in the range 300 to 600 mm. Non-destructive examinations of fuel rods can be performed in the R2 pool during short pauses in the irradiation program or between various phases of an experiment, see Section 3. All the handling and all the examinations are performed with the fuel rods in a vertical position; this is advantageous with respect to possible movements of fuel fragments etc.

Associated with the R2 reactor is the 1 MW(th) swimming pool R2-0 reactor, which is located in the same pool, see Figure 3. The basic research performed by use of R2-0 is briefly described in Section 10.

## 2.2 Boiling Capsules (BOCA rigs)

The Boiling Capsule (BOCA) facility for irradiation of BWR and PWR fuel rods was introduced in 1973.

The in-pile part of a BOCA rig consists of a bare stainless steel pressure thimble containing a shroud with flow entrance ports at the bottom and exit ports at the top. The lower part of this shroud is located in the reactor core region. A fuel test rod bundle consisting of 4 (or 5) rodlets is located inside the shroud. The BOCA is filled with highly purified pressurized water from a special pressurization system. Figure 4 shows a simplified BOCA flow diagram. BOCA system technical and operational data are given in Table 2.





### 2.3 In-Pile Loops

Data for the two loops used in the current LWR fuel R&D programs are shown in Table 3 (2-3). Data for other loops, e.g. for the testing of HTR fuel, are described elsewhere (5) and will not be discussed here. Each LWR fuel loop utilizes two diagonally adjacent fuel element positions in the R2 test reactor, see Figure 2.

The two loops are pressurized in order that test fuel rods can be investigated at realistic operating conditions for either PWR (loop No 1) or BWR (both loops) type power reactors.

**Table 3** Characteristics of the R2 in-pile loops.

Loop No	1	2
Type	PWR	BWR
Pressure, bars	30-150	30-90
Coolant temperature, °C	220-325	220-285
Coolant flow rate, kg/sec	2.5-4.0	2.5-5.0
Max cooling capacity, kW	150	400
Neutron flux, $10^{14}n/(cm^2\cdot s)$		
Thermal	0.6-1.2	0.5-1.0
Fast (>1 MeV)	0.8-1.50	0.7-1.3
Gamma heating in stainless steel, W/g	5-10	5-8

The loops can be used for irradiation at constant power of up to 4-5 test fuel rods simultaneously, and for power ramp tests of single rods. The test rods to be ramp tested are installed in the loop in special capsules, which in turn are inserted in a special test rig. The loops can also be used for irradiation testing of structural materials, e.g. Zircaloy test specimens and steel specimens of various types. A technique for in-pile corrosion tests in the loops with on-line corrosion potential measurements is being developed.

The in-pile part of the loops are of a U-tube design, taking up two core positions and thus providing two test positions in the R2 core, one of which can be used for ramp tests (Figure 5). The U-tube is isolated from the reactor primary coolant by a gas gap containing CO<sub>2</sub>. Heat losses from the tube to the reactor coolant are therefore quite small, which facilitates accurate test rod power measurement.

The working in-core inside diameter of these in-pile pressure tubes is 45.5 mm. The useful length in the core is 670 mm. The main features of the loops are presented in Figure 6.

## 2.4 Ramp Test Facility

Ramp testing in the R2 reactor began in 1969. Originally, the tests were performed by rapid power increases of the whole reactor. This mode of operation had two disadvantages: safety restrictions limited the maximum allowable power increase and financial restrictions limited the number of tests that could be performed since other experiments, which would have been disturbed by the ramp tests, had to be unloaded from the reactor at considerable expense.

In the present Ramp Test Facility, introduced in 1973, the fuel rod power during a ramp test in a loop is controlled by variation of the  $^3\text{He}$  gas pressure in a stainless steel double minitube coil screen which surrounds the fuel rod test section. The principle of operation of this system is based on the fact that  $^3\text{He}$  absorbs neutrons in proportion to its density, which can be varied as required by proper application of pressure.

The axial location of the minitube coil screen in the loop U-tubes is shown in Figure 6. The efficiency of the  $^3\text{He}$  neutron absorber system makes it possible to increase test rod power by a factor of 1.8 to 2.2 (depending on the fissile content of the fuel). The  $^3\text{He}$  absorber system is designed to achieve a 100 % power increase within 90 seconds, when operating with the normal pressure variation (bellows system).

In order to achieve a higher power increase than a factor of about 2, the reactor power must be increased before or simultaneously with the " $^3\text{He}$  ramping". This technique with combined ramp systems is called "double step up-ramping", Figure 7. The technique makes it possible to increase the test fuel rod power by a factor of about three.

An important advantage of the R2 Ramp Test Facility is that test rods, one at a time, can be loaded and unloaded during reactor operation. This is done by means of a lock vessel built onto an axial drive mechanism with about 3.5 m stroke. This lock vessel is bolted on top of a lock valve (ball type valve) fixed on top of the ramp rig. For BWR pressure conditions and normal rod lengths there is a 4-rod revolver lock vessel with a mechanical chain drive. For tests of PWR fuel rods and longer than normal rods, there exists a selection of rod lock vessels and dedicated hydraulic drives. Figure 6 shows a ramp rig with a hydraulic drive.

In the Ramp Test Facility ramp rates can be achieved in the range of 0.01 W/(cm·min) to about 3 000 W/(cm·min).

The power (linear heat generation rate in the fuel rod) is measured calorimetrically by the use of two inlet thermocouples, two outlet thermocouples, a venturi flowmeter and a pressure gage. The special calibration techniques employed have been described (3). The estimated uncertainty ( $\pm 1\sigma$ ) is 2.3 % when the most common rod lengths (0.3–1.4 m) are used. The reproducibility obtained, when a fuel rod is irradiated several times in the same ramp rig, is  $\pm 1\%$ . For fast ramps the discrepancy between the terminal power aimed at and the one obtained is less than  $\pm 1$  kW/m.

The axial thermal neutron flux distribution is measured by activation of cobalt wires in dummy rods and by gamma scanning of the ramp tested fuel rods.

Each test rod is mounted in a separate stainless steel "capsule" (a shroud open at both ends), primarily as a safety measure and to facilitate the removal and handling of test rods that fail in the course of a power ramp. The "capsule" with the fuel rod is connected to the actuating rod which is used to move the fuel rod axially between the rod changing device and the in-pile

section of the rig. There is a small floating push-rod built in at the bottom guide plug of the capsule. This push-rod transmits the elongation movements of the test rod to the LVDT type elongation detector built into the bottom of the ramp test rig.

## 2.5 Fuel Rod Failure Detection System

Fuel rod failures in the loops are detected by a Čerenkov-type radiation sensor which monitors the activity of the loop coolant water. The Čerenkov detector is installed in a by-pass circuit in order to increase the detection system sensitivity by decreasing the background  $^{16}\text{N}$  activity produced in the loop coolant water. The  $^{16}\text{N}$  background activity is decreased by the introduction of a delay time due to the fact that the Čerenkov detector is positioned in the by-pass circuit.

The system detects fuel rod failure after  $155 \pm 10$  seconds. This degree of failure detection capability has been verified experimentally. An example of system operation during a ramp test where the rod failed is shown in Figure 8.

However, the moment of failure is also registered instantaneously by the rod elongation measurement system as a sudden rod contraction and also often by the power measurement system as a small thermal "spike" (3,6,7).

## 2.6 Defect Fuel Degradation Studies

The Ramp Test Facility is utilized with a new test technique to investigate the potential degradation of defected test fuel rodlets. A test of this type, to be used at the R2 test reactor, has to fulfil certain experimental constraints, i.e.

- 1 the length of the test fuel rodlets should not exceed the active core height (600 mm) of the R2 test reactor
- 2 the release of fission products and fuel material from the defect fuel must be minimized in order that the contamination of the in-pile loop circuit water be tolerable.

Both these requirements can be met with the unique but simple test technique adopted. Instead of an artificial primary defect (drilled hole etc) the primary defect is now simulated by a special device at the top end of the fuel rodlet (8). This device contains an enclosed small reservoir of liquid water in the "extension plenum", Figure 9. This extra plenum is connected with the normal plenum volume of the rodlet through a tiny tube (the "steam snorkel") in such a manner that only water in the form of steam will communicate with the plenum volume and the interconnected void space of the interior of the rodlet. Heat is transferred to the enclosed water reservoir from the surrounding pressurized loop water at the start of the operation until the pressure and temperature of the whole system are in balance, simulating either BWR or PWR operating conditions.

An important experimental feature of this arrangement is the possibility of post-irradiation puncture and subsequent collection of released fission gases and hydrogen from the closed system of the individual rodlets being irradiation tested.

### **3 Pool-side examination**

The general appearance of the irradiated fuel rods can be studied by visual inspection in the R2 pool (3). The following phenomena can also be investigated in detail:

Dimensional changes, ridge formation, rod bow and creep-down can be investigated with equipment for profilometry and length measurements. The existence and location of fuel rod defects can be established by means of eddy current testing.

The axial distribution of certain nuclides is determined by axial gamma scanning of fuel rods or of cladding samples. Data obtained before ramp tests are used as a check on the burnup profile during the base irradiation. Data obtained after ramp testing are used to check the power profile during the R2 irradiation and for studies of the fission product redistribution.

Neutron radiography can be used to study the general appearance and dimensions of the fuel, the extent of filling out of pellet dishing, of center porosities and of center melting (9, 10). This type of examination also reveals the presence of special fuel cracks, interpellet gaps etc. Indications of cladding failure and of structural changes in the fuel can also be observed. In cases where there is no leakage of fission products from failed fuel rods neutron radiography is an important tool since cladding leaks are indicated by the existence of hydrides in the cladding or by the presence of water.

### **4 Post irradiation examination**

Post-irradiation examination of irradiated fuel is performed in STUDSVIK's well-equipped Hot Cell Laboratory, which has been described in a separate publication (11).

Post-irradiation examinations of structural and cladding materials are performed in STUDSVIK's versatile Lead Cell Laboratory, which contains equipment for mechanical testing, corrosion testing and metallography. Among the different types of post-irradiation tests performed are tensile tests, fatigue tests, low-cycle fatigue tests, creep tests, impact test, stress corrosion tests and microscopy (optical microscopy, SEM/EPMA, both with image analysis, and TEM).

### **5 Fuel R&D**

Much of STUDSVIK NUCLEAR's R&D work in the fuel area has been concentrated on fuel testing, which can be made in the R2 test reactor with high precision under realistic water reactor conditions. This type of work was started in the early 1960's. In a very general sense the purpose of fuel testing can be described as follows:

- Increasing of reactor availability by decreasing fuel-related operational power restrictions, defining the operational power limits.
- Acquisition of experimental data for fuel-related safety considerations.
- Decrease of fuel costs by making increases in fuel burnup possible.

The fuel testing activities can be divided into a number of well-defined steps as follows:

- Base irradiation, performed
  - in a power reactor, or
  - in STUDSVIK's R2 test reactor.
- Power ramping and/or other in-pile measurements, performed
  - in STUDSVIK's R2 test reactor.
- Non-destructive testing between different phases of an experiment, performed
  - in STUDSVIK's R2 test reactor pool, or
  - in the Hot Cell Laboratory.
- Destructive post-irradiation examinations, performed
  - in STUDSVIK's Hot Cell Laboratory, or
  - in the sponsor's hot cell laboratory.

Fuel examination can be performed on standard (full-size) fuel rods from power reactors, which can be investigated in the Hot Cell Laboratory. If required, some types of tests could also be performed on such fuel rods in the R2 test reactor. However, due to the rather large initiation costs, such tests have not yet been performed. It should be noted, however, that short fuel rodlets, suitable for ramp testing and other on-line measurements in the R2 test reactor, can now be fabricated from irradiated full-size power reactor fuel rods by the STUDEFAB refabrication process.

Fuel testing in the R2 test reactor is usually performed on fuel segments (rodlets) of 300–1000 mm length. However, tests have also been performed on full-size demonstration reactor fuel rods with up to 2.5 m length. In those cases only the lower 0.6 meters were irradiated. Irradiation at constant power is performed in boiling capsules (BOCA rigs) in fuel element positions, or in pressurized water in-pile loops operating under BWR or PWR pressure/temperature conditions, as described in Sections 2.2 and 2.3 above.

Ramp tests incorporating a very fast-responding test rod power measuring system and associated on-line measurements, such as rod elongation and noise measurements for studies of the rod thermal performance, are performed in the pressurized water loops.

The ramp tests are a form of integral performance tests where the complex interplay between the pellets and the cladding of a power reactor fuel rod is reproduced. The primary test objectives are:

- Determination of the failure boundary and the failure threshold, see Figures 10 (17) and 11.
- Establishing of the highest "conditioning" ramp rate that safely avoids failure occurrence.
- Study of the failure initiation and progression under short time over-power transient operation beyond the failure threshold.

- Proof testing of potential pellet-clad interaction (PCI) remedies.

Other, more specific test objectives have also been pursued in some projects.

The fuel testing projects executed at Studsvik have been organized under three different types of sponsorship:

#### **International (multilateral) fuel projects**

- Jointly sponsored internationally on a world-wide basis.
- Project information remains restricted to the project participants throughout the project's duration and some predetermined time after project completion.

#### **Bilateral fuel projects**

- Sponsored by one single organization, or a few co-operating organizations.
- Project information remains restricted to the sponsor, sometimes published later.

#### **In-house R&D work**

- Sponsored by STUDSVIK NUCLEAR.

Several new hot-lab techniques have also been introduced in recent years (11). The STUDEFAB process for fabrication of rodlets from full-size fuel was mentioned above. Fuel ceramography can include scanning electron microscopy (SEM) and electron probe microanalysis (EPMA).

Descriptions of the fuel testing facilities and the techniques used were given in Section 2 above. The noise measurements introduced for studies of the rod thermal performance have been described elsewhere (12-14). Several other novel testing techniques have also been introduced (15). A very fast ramp rate, up to 3 000 W/(cm·min) can be used to obtain fast power transients and to determine the pellet-clad interaction/stress-corrosion cracking (PCI/SCC) failure boundary. The double step up-ramping technique was described in Section 2.4. On-line elongation measurements can be performed during ramp tests, Figure 8. Test fuel rods can be fitted with on-line pressure transducers through a refabrication process.

Since 1975, a series of international fuel R&D projects addressing the PCI/SCC failure phenomenon have been conducted under the management of STUDSVIK NUCLEAR (15-18). These projects are pursued under the sponsorship of different groups of fuel vendors, nuclear power utilities, national R&D organizations and, in some cases, licensing authorities in Europe, Japan and the U.S. In most of the projects the clad failure occurrence was studied under power ramp conditions utilizing the special ramp test facilities of the R2 reactor. The current projects are not limited to PCI/SCC studies but also include other aspects of fuel performance, such as end-of-life rod overpressure (19-21) and defect fuel degradation (22-24). An overview of the projects that have been completed and that are currently in progress or planned has been published (18), see also Appendix 1. In most cases, the test fuel was base irradiated in commercially operating light water power reactors. In some instances the base irradiation took place in BOCA rigs in the R2 reactor.

In general, the international fuel R&D projects can be divided into two main categories:

- Projects aimed at decreasing the fuel costs by increasing fuel utilization and reactor availability.
- Projects providing data for fuel-related safety considerations.

A typical example of the former category is the SUPER-RAMP project (25), where several groups of fuel from different fuel vendors and with different "PCI remedies" were tested. A summary of some of the data from this category of projects is shown in Figure 10. Reviews of the projects in the latter category have also been published (26-27).

A third category of fuel R&D projects, dealing with defect fuel degradation, has been introduced in recent years, first by bilateral projects with Swedish participants (22, 23) and later in an ongoing international project, the Defect Fuel Degradation Experiment (DEFEX) (24). These projects consist of experimental studies in the R2 test reactor of secondary damage formation in fuel rodlets with simulated fretting defects.

The test data are often used as "benchmarking" data in the project participants' own fuel modeling work. In recent years many ramp test data have also been analyzed with the INTERPIN code, developed by STUDSVIK (28-30). INTERPIN is a fuel performance code which satisfies real-time simulation requirements when implemented on a minicomputer. In its analyzing mode it can also be used on a desktop computer. The model incorporates a comprehensive set of physical submodels, each of which is optimized for bench-marking efficiency. The code utilizes a novel, non-linear numerical technique which enables the handling of large time-steps without use of iterations.

European, Japanese and U.S. fuel manufacturers and research organizations have also for many years been utilizing the R2 test reactor and the associated hot-cell laboratories for bilaterally sponsored research\*). General Electric Co. has executed several series of ramp tests at R2, as part of the efforts to develop the zirconium barrier fuel concept. Some of the ramp techniques requested were innovative, for example the "double ramping" of the test rods. Exxon Nuclear Co. (later Advanced Nuclear Fuels Corporation, later Siemens Nuclear Power Corporation, now Siemens Power Corporation) is another major customer as well as Hitachi Ltd. and Toshiba Corporation. Mitsubishi Heavy Industries, Ltd. has performed combined power cycling and ramp tests. Tests have also been performed on behalf of other organizations but the results have not always been published.

During the 1970's extensive series of HTR fuel irradiations were performed in a special HTR gas loop system operating with on-line measurements and analyses of the released fission gas and of the fuel temperature (5).\*)

STUDSVIK NUCLEAR's in-house R&D work is mainly associated with improvements of test irradiation techniques, instrumentation and post-irradiation examination, all in support of ongoing or upcoming irradiation projects. Progress in these areas has made it possible to achieve important progress in fuel research. For example, the characterization of the PCI failure progression in some recent projects was only made feasible through a combination of several new techniques. These included a very fast ramp execution using a ramp rate of up to 3 000 W/(cm·min), compared to the previous maximum of 200 W/(cm·min), a prompt detection of the

---

\*) A list of available publications can be obtained upon request from the authors.

through-failure event using the on-line elongation detector and a subsequent special clad bore inspection technique. Another result of the in-house R&D work is the noise measurement technique mentioned above.

STUDSVIK NUCLEAR has also been carrying out an in-house R&D program aimed at improving the performance of LWR fuel by the utilization of a design concept with cladding tubes which have been "rifled" on a micro-scale (31). Results of R2 irradiations of such fuel and the associated modeling work have been published (32-39).

## 6 Materials R&D

The R&D work in this area consists of studies of irradiation effects in structural materials. These types of studies have been concentrated on pressure vessel steels, stainless steels and nickel-base alloys (for super-heater and fast reactor cladding) during the 1960's and on zirconium alloys since the 1970's. The early pressure vessel steel work comprised investigations of different potential pressure vessel materials, of different materials variables, and of the influence of different irradiation conditions (neutron fluence, irradiation temperature etc). Recent work has been concentrated on accelerated irradiation of materials actually used in pressure vessels under as realistic conditions as possible. Recent work on stainless steels has to a large extent been concentrated on fusion reactor materials within the Next European Torus (NET) program, where tensile tests, fatigue tests, and stress corrosion tests have been performed after irradiation to displacement doses of up to 10 dpa. Some work, including post-irradiation creep and fatigue tests and crack propagation studies (including CT tests) has also recently been performed on potential FBR vessel materials. Among the in-pile tests performed stress-relaxation tests can be mentioned. In-pile corrosion tests in the R2 test reactor with on-line corrosion potential measurements are under development. The work on zirconium alloys is continuing and is being expanded in order to include in-pile corrosion studies.

Originally structural materials (pressure vessel steels, stainless steels, nickel-base alloys and aluminum alloys) were to a large extent irradiated in rigs in fuel element positions either in contact with the reactor coolant water (temperature about 60 °C) or in rigs where the heat-transfer conditions were closely defined and the specimen temperatures were measured but not regulated. Later rigs containing in-pile furnaces for constant temperature irradiations were introduced. Besides numerous detailed publications review papers were published on the early pressure steel work (40) and on the corresponding work on the other structural materials (41). During this period extensive work was also pursued on cladding materials for superheated reactors and for steam-cooled fast reactors. Some work was also performed on early Swedish candidates for FBR pressure vessel materials (42, 43).

During the 1970's the in-pile loops in the R2 test reactor became available for irradiations of specimens of structural materials. Such specimens are now irradiated either in rigs that only allow irradiations during whole 400 hour reactor cycles or in rigs where shorter irradiations, down to less than an hour, are possible. The specimens are either in direct contact with the loop water (temperature selected in the range 230-350 °C or in some cases specimens of pressure vessel steels have been nickel plated in order to avoid corrosion problems during longer irradiations. Later new types of in-pile rigs for fuel element positions have also been developed where the specimens are heated by gamma heating. In these rigs close temperature control (about  $\pm 10$  °C in the range 250-350 °C) has been maintained by placing the specimens in specimen holders filled with a NaK alloy. The temperature is monitored by thermocouples placed in some specimens or in the NaK adjacent to the specimens.



Temperature control is achieved by changes of the He/Ne gas mixture in the gap between the capsule containing specimens and NaK and the rig secondary containment. Varieties of these rigs are also used up to a temperature of 550 °C.

## 7 Neutron transmutation doping

Neutron transmutation doping of silicon for industrial use in electric power components is done in a facility which is shown in Figure 12. Three shelves with silicon ingots can be irradiated simultaneously, but only the bottom shelf is shown in the figure. The silicon ingots are loaded manually onto the irradiation facility, which is situated in the R2 reactor pool, in front of the reactor vessel. The ingots perform a horizontal helical movement on the shelves in front of the core. The neutron flux is monitored through self-powered neutron detectors and the velocity of the ingots and hence the neutron fluence is controlled by a computer. After completion of the irradiation the ingots are removed from the shelves to a conveyor which slowly transports them to the pool surface. A permanent radiation instrument monitors the dose rate and in order to avoid hand doses to the operators the ingots are lifted with a crane. They are then stored for a few days in order to let the  $^{31}\text{Si}$  and  $^{32}\text{P}$  activities decay. The decontamination is done by rinsing in demineralized water.

Silicon ingots with lengths up to 600 mm and diameters from 60 to 152 mm are treated routinely. The target resistivity of the resulting conducting material usually lies in the 30–300 ohmcm range. The high uniformity and precision of the irradiation guarantees less than 5 % axial variation and a radial gradient which is better than 2 and 4 % for the minimum and maximum diameters, respectively. The day-to-day constancy of the operation of the facility is monitored by means of cobalt monitors attached to some of the silicon ingots.

The irradiated material is shipped in compliance with IAEA regulations. The bulk material must have a specific activity of less than 7.4 Bq/g before it is shipped as non-radioactive material. For the nonfixed surface contamination a limit of 0.4 Bq/cm<sup>2</sup> is maintained taking the ALARA principle into consideration. Application of these values to the process normally gives a turnover time of three weeks at Studsvik.

## 8 Neutron activation analysis

The present set-up for neutron activation analysis (NAA) permits multi-element determination by instrumental and radiochemical NAA of around 50 elements in trace concentrations. The samples which are investigated are of biological, environmental, industrial, or geological origin.

The samples usually require little or no pre-treatment, and after weighing they are pneumatically transported in plastic capsules to a position close to the reactor core. Having been irradiated the samples are left to decay in a storage unit for a suitable period of time, before the gamma radiation is registered with a Ge(Li) or a high purity Ge detector. The thermal and epithermal fluxes are measured with a Zr monitor. Thus the automatic data evaluation system gives an absolute determination of the composition of the sample from the intensity of the gamma spectrum, which is characteristic of each element.

Neutron activation analysis in theory permits determination of around 70 elements. In practice the number is limited to some 30 elements when using instrumental NAA. Application of radiochemical NAA increases this number.

Many elements can be determined at sub-ppb( $10^{-9}$ ) levels, but high concentrations of disturbing elements may be troublesome because of spectrum interferences. Sometimes corrections have to be made for other reasons, for instance due to interfering nuclear reactions. Neither the lightest elements nor lead and sulphur can be detected. Some examples of STUDSVIK NUCLEAR projects for which instrumental NAA has proved to be an efficient method are:

- Multi-element studies of geological samples, with special interest in rare earth elements and iridium.
- Uranium, thorium and other elements in sediment.
- Trace elements in metallurgical products.
- Trace elements in food-stuff.

## 9 Radioisotope production

Radioisotopes can be produced over a wide range of conditions in several irradiation positions in and around the R2 vessel. The operational cycle of the reactor, however, to some degree limits the number of isotopes that are produced routinely.

There are six permanent rigs in the reactor core which are used for radioisotope irradiation. One of them can be loaded and unloaded during reactor operation. The maximum flux which can be obtained for irradiation is as high as  $3 \times 10^{14}$  n/(cm<sup>2</sup>-s). The permanent rigs can be supplemented with temporary installations.

<sup>192</sup>Ir is produced by irradiation in the core positions. The specific activity of the resulting product is higher than 350 Ci/g. The encapsulated isotope is used industrially for gamma radiography. <sup>169</sup>Yb, which is also produced, has the same application.

Eu is irradiated with the aim to extract <sup>153</sup>Gd, which is used for sources in bone scanners. <sup>32</sup>P and <sup>35</sup>S are examples of isotopes produced in R2, which are used for biological research. There is also a wide variety of radioisotopes being produced for medical research and therapy, such as <sup>85</sup>Sr, <sup>89</sup>Sr, <sup>86</sup>Rb, <sup>155</sup>Cd, <sup>110</sup>Ag, <sup>51</sup>Cr, <sup>59</sup>Fe, <sup>45</sup>Cs, <sup>47</sup>Cs, <sup>90</sup>Y, <sup>186</sup>Re and <sup>63</sup>Ni.

A few other isotopes are produced routinely. <sup>24</sup>Na for example is delivered to the Swedish defence forces for training purposes.

## 10 Beam tube experiments

The R2 and R2-0 reactors serve as sources of thermal neutrons for a wide variety of basic research applications. The beam tubes at the R2 reactor are used for thermal neutron scattering experiments, see Figure 13 and Table 4. The R2-0 reactor, which is mobile in the pool, is in one position used as source for a neutron capture radiography facility and in the other position as source for a facility for nuclear physics and nuclear chemistry experiments based on an on-line isotope separator. Researchers from the universities have easy access to the facilities through the Studsvik Neutron Research Laboratory (44). The laboratory is organized as a department at the

University of Uppsala but serves users from all Swedish universities. The instruments are also available for outside users.

In connection with the replacement of the reactor vessel, a large D<sub>2</sub>O box was installed on the outside of the core box. The reentrant beam tubes end at positions close to the thermal flux peak in the D<sub>2</sub>O. Two tangential beam tubes were installed through a region in the biological shield which was previously inaccessible. The new beam tubes are rectangular with height 18 cm and width 8 cm. The larger vertical divergence of the beams increases the flux at the experimental positions. With these modifications substantial improvements in the thermal flux and in the ratio of thermal to fast flux at the experimental positions are achieved. The research performed involves, for example, structure determinations in crystals and amorphous systems, studies of magnetic phenomena in condensed matter and of excitations in disordered systems.

**Table 4** Neutron scattering instrumentation at the R2 reactor.

Neutron beam tube	Instrumentation
H1	Service instrument
H3	Time-of-flight spectrometer for thermal neutrons
H5	Single-crystal diffractometer
H6	Diffractometer for protein studies
H7	Diffractometer for disordered structures
H8	Powder diffractometer
H10, H10A	Diffractometers for polarized neutrons

A thermal neutron facility for neutron capture radiography (NCR) is located at the R2-0 reactor, see Figure 14. A very pure thermal neutron field is produced by moderation of the fast neutrons from the reactor in a large D<sub>2</sub>O volume positioned immediately outside the pool liner and adjacent to the reactor core, which is located immediately inside the pool liner. At the outer edge of the D<sub>2</sub>O volume irradiations can be made in a thermal flux over a large area (30x30 cm<sup>2</sup>). The thermal flux used in recent experiments has varied between 6x10<sup>8</sup> and 5x10<sup>9</sup> n/(cm<sup>2</sup>-s), corresponding to a reactor power of 25 to 200 kW. The facility is used extensively for biomedical research and has proved to be an efficient tool for studying the distribution of boron loaded compounds with a specific affinity for certain tumors.

A variety of nuclear physics and nuclear chemistry research programs are based on the on-line isotope separator OSIRIS at the R2-0 reactor. The main activity is aimed at studies of the properties of short-lived neutron-rich nuclides. The programs include determination of fission yields including branching ratios for gamma decay from fission products and determination of the antineutrino spectrum at a nuclear reactor. The system utilizes a novel method for plasma creation and allows higher temperatures, up to 2500 °C, and thereby shorter delay times for the released fission products. This has increased the number of nuclides available considerably and has increased the production yields of many short-lived isotopes by factors of 10<sup>2</sup>-10<sup>3</sup>.

## References

- 1 COLE, T E, COX, J A  
Design and Operation of the ORR.  
Peaceful Uses of Atomic Energy. Proc. Int. Conf.,  
Geneva, 1–13 September 1958.  
Vol. 10. UN IAEA, New York & Vienna 1959, p 86–106.  
(A/CONF. 15/P/420).
- 2 SANDKLEF, S, TOMANI, H  
Irradiation Facilities for LWR Fuel Testing in the Studsvik R2 Reactor.  
AB Atomenergi, Sweden (1973). (AE-478).
- 3 RÖNNBERG, G, BERGENLID, U, TOMANI, H  
Power Ramp Test Technique at Studsvik.  
Proc. KTG/ENS/JRC Meeting on Ramping and Load Following  
Behaviour of Reactor Fuel, Petten,  
The Netherlands, 1978. (EUR 6623 EN, p 37–51).
- 4 SANDKLEF, S, BODH, R  
Neutron Absorber Techniques Developed in the Studsvik R2 Reactor.  
Irradiation Facilities for Research Reactors. IAEA, Vienna, 1973  
(STI/PUB/316), p 213–231. (IAEA/SM-165/37).  
Also AB Atomenergi, Sweden 1973. (AE-468).
- 5 SANDKLEF, S  
Irradiation Facilities for Coated Particle Fuel Testing in the Studsvik R2 Reactor.  
AB Atomenergi, Sweden (1973). (AE-467).
- 6 BERGENLID, U, MOGARD, H, RÖNNBERG, G  
Experimental Observations of the PCI Failure Occurrence on  
Power Ramping.  
IAEA Specialists' Meeting on Pellet-Cladding  
Interaction in Water Reactors. Risö, Denmark,  
22–26 September 1980. (IAEA IWGFPT/8, p 121–127).  
Also Res Mechanica Letters 1(1981), p 229–234.
- 7 BERGENLID, U, RÖNNBERG, G  
Observations of Cladding Failure During Ramp Tests.  
IAEA Specialists' Meeting on Power Ramping and Cycling  
Behaviour of Water Reactor Fuel. Petten, the Netherlands,  
8–9 September 1982. (IAEA IWGFPT/14, p 55–71).  
Also Res Mechanica 12(1984): 4, p 297–301.
- 8 TOMANI, H  
Studsvik AB, Sweden. Patent Pending.

- 9 BERGENLID, U, GUSTAFSSON, I  
Examination of Fuel Rods by Means of Neutron Radiography.  
Post-Irradiation Examination. Grange-over-Sands, UK,  
13-16 May 1980. Proc. of the Conf. BNES,  
London 1981, p 49-53.
- 10 BERGENLID, U, GUSTAFSSON, I  
Examination of Fuel Rods by Means of Neutron Radiography.  
Neutron Radiography. J P Barton & P von der Hardt (Eds).  
Brussels 1983, p 349-353.
- 11 FORSYTH, R S, (Ed.)  
The Hot Cell Laboratory - a Short Description of Programs,  
Facilities and Techniques.  
Studsvik Energiteknik AB, Sweden (1986). (STUDSVIK/NF(P)-86/29).
- 12 OGUMA, R, SCHRIRE, D, BERGDAHL, B-G  
Fuel Rod Thermal Performance Studies Based on Noise Analysis.  
Studsvik Energiteknik AB, Sweden (1986). (STUDSVIK-NF(P)-86/08).
- 13 OGUMA, R, BERGDAHL, B-G, SCHRIRE, D  
Application of a Recursive Identification Technique to Noise Analysis  
for Fuel Performance Study.  
Specialists' Meeting on Reactor Noise (SMORN-V), Munich, FRG, 12-16 October 1987.
- 14 SCHRIRE, D, OGUMA, R  
The Thermal Response of a Fuel Rod with a Small Xenon-Filled Gap.  
Studsvik Energiteknik AB, Sweden 1988.  
(STUDSVIK/NF(P)-88/13).
- 15 MOGARD, H, GROUNES, M  
STUDSVIK's International Fuel R&D Projects - a Review.  
Studsvik Energiteknik AB, Sweden (1986). (STUDSVIK-86/2).
- 16 MOGARD, H, RÖNNBERG, G  
LWR fuel research at Studsvik - a review.  
ENC'86, Geneva, 1986, Transactions, Vol. 4 (1986), p 59-66.
- 17 MOGARD, H, KJAER-PEDERSEN, N  
A Review of STUDSVIK's International Power Ramp Test Projects.  
Studsvik Energiteknik AB, Sweden (1985).  
(STUDSVIK-85/6).  
Also Performance of Fuel and Cladding Material under Reactor  
Operating Conditions, G. Mülding & W. Dietz, (Eds),  
Kernforschungszentrum Karlsruhe, FRG, (1986), p 63-71.

- 18 GROUNES, M, DJURLE, S, LYSELL, G, MOGARD, H  
Review of STUDSVIK's International Fuel R&D Projects.  
IAEA Technical Committee Meeting on Fission-Gas Release and  
Fuel-Rod Chemistry Related to Extended Burnup.  
Pembroke, Ont., Canada, 28 April - 1 May 1992.  
(IAEA-TECDOC-697, p 124-130).
- 19 SCHRIRE, D  
Rod Overpressure Experiment (ROPE) - Pre-Project.  
Studsvik Energiteknik AB, Sweden 1987.  
(STUDSVIK/NF(P)-87/43).
- 20 SCHRIRE, D  
Sweden's International Fuel Rod Overpressure Experiments.  
Nuclear Europe Worldscan (1991): 1-2, p 60-61.
- 21 GROUNES, M, TOMANI, H  
Tying up Fuel Rod Overpressure Problems with ROPE I and II.  
Nuclear Engineering International 37 (1992): 451, p 30, 32.
- 22 MOGARD, H, GROUNES, M, TOMANI, H  
Test Reactor Investigation of the Process of Degradation  
of Defect LWR Fuel.  
Jahrestagung Kerntechnik '91. INFORUM, Bonn 1991, p 339-342.
- 23 MOGARD, H, GROUNES, M, TOMANI, H  
Experimental Studies in the R2 Test Reactor of Secondary Damage  
Formation in LWR Fuel Rods with Simulated Fretting Defects.  
Jahrestagung Kerntechnik '92. INFORUM, Bonn 1992, p. 353-356.
- 24 MOGARD, H, GROUNES, M, TOMANI, H, LYSELL, G  
Studies in the R2 Test Reactor of Secondary Damage Formation in  
LWR Fuel Rods with Simulated Defects.  
IAEA Technical Committee Meeting on Fuel Failure in Normal Operation  
of Water Reactors: Experience, Mechanisms and Management.  
Dimitrovgrad, Russian Federation, 26-29 May 1992. (IAEA-TECDOC-709, p 184-192).
- 25 MOGARD, H, HECKERMAN, H  
The International SUPER-RAMP Project at Studsvik.  
Proc. ANS Topical Meeting on Light Water Reactor Fuel Performance,  
Orlando, Fla, USA, 21-24 April 1985. ANS, LaGrange Park, Ill 1985.  
(DOE/NE/34130-1, Vol. 2, p 6-17 to 6-33).
- 26 MOGARD, H, DJURLE, S, GROUNES, M, LYSELL, G, KJAER-PEDERSEN, N  
Effects of High Power Transients on the Operational Status of LWR  
Fuel - Experimental and Analytical Investigations at Studsvik.  
Proc International ENS/ANS Conference on Thermal Reactor Safety,  
"NUCSAFE 88". Avignon, France, 2-7 October 1988, p 181-190.

- 27 MOGARD, H, DJURLE, S, GROUNES, M, LYSELL, G  
Effects of High Power Transients on the Operational Status of LWR Fuel –  
Experimental Investigations at Studsvik.  
IAEA Technical Committee Meeting on Behaviour of Core Materials and Fission  
Product Release in Accident Conditions in LWRs. Aix-en-Provence,  
France, 16–20 March 1992.  
(IAEA-TECDOC-706, p 28–34).
- 28 KJAER-PEDERSEN, N  
A Novel Fuel Rod Performance Simulation Methodology for Predictive,  
Interpretive and Educational Purposes.  
Structural Mechanics in Reactor Technology (SMiRT9), Vol C, p 53–61.  
Balkema, Rotterdam 1987.
- 29 KJAER-PEDERSEN, N  
A Novel Fuel Performance Simulation Methodology for Predictive,  
Interpretive and Educational Purposes.  
Res Mechanica 25 (1988), p 321–338.
- 30 KJAER-PEDERSEN, N  
Correlation Between the Potential for Thermal Feedback and Some  
Principal Fuel Rod State Variables.  
IAEA Specialists' Meeting on Water Reactor Fuel Element Performance  
Modelling in Steady State, Transient and Accident Conditions.  
Preston, UK, September 19–22, 1988.(IAEA IWGFPT/32, p 302–306).
- 31 MOGARD, H  
Suppression of PCI Induced Defects by Lightly Undulating the Bore  
Surface of the Fuel Cladding.  
Studsvik Energiteknik AB, Sweden 1977. (STUDSVIK-77/2).
- 32 MOGARD, H, BERGENLID, U, DJURLE, S, LYSELL, G, RÖNNBERG, G  
Irradiation Testing of an Advanced Fuel Cladding Designed for Load-Follow and  
Extended Burnup Operation.  
IAEA International Symposium on Improvements in Water Reactor Fuel  
Technology and Utilization. Stockholm, Sweden, 15–19 September 1986.  
IAEA, Vienna 1987, p 335–351.(IAEA-SM-288/15).
- 33 MOGARD, H, BERGENLID, U, DJURLE, S, LYSELL, G, RÖNNBERG, G  
Irradiation Testing of an Advanced Fuel Cladding Designed for Load-Follow and  
Extended Burnup Operation.  
Studsvik Energiteknik AB, Sweden 1986. (STUDSVIK-86/1).
- 34 KJAER-PEDERSEN, N, KINOSHITA, M Y, MOGARD, H  
Comparative Studies of Axial Gas Mixing in Fuel Rods with Standard  
and Rifled Cladding.  
IAEA Technical Committee Meeting on Power Ramping, Cycling and Load Following  
Behaviour of Water Reactor Fuel. Lyon, France, 18–21 May 1987. (IAEA IWGFPT/28,  
p 25–32 and IAEA-TC-624/13).

- 35 KJAER-PEDERSEN, N, MOGARD, H  
In-Reactor Performance of Fuel with Rifled Cladding.  
ANS Topical Meeting on LWR Fuel Performance,  
Williamsburg, Va, USA, 17-20 April 1988, p 284.
- 36 MOGARD, H, DJURLE, S, LYSELL, G, OGUMA, R  
Continued Irradiation Testing of Fuel with Rifled Cladding:  
Thermal Behaviour and PCI Failure Resistance.  
Enlarged Halden Group Meeting,  
Loen, Norway, May 9-13, 1988.
- 37 KJAER-PEDERSEN, N, MOGARD, H  
Controlling Overall Fission Gas Release by Controlling Axial  
Gas Mixing.  
IAEA Specialists' Meeting on Water Reactor Fuel  
Element Performance Modelling in Steady State, Transient and  
Accident Conditions. Preston, UK, September 19-22, 1988.  
(IAEA IWGFPT/32, p 269-278).
- 38 MOGARD, H, KJAER-PEDERSEN, N  
Improved PCI and FGR Performance of LWR Fuel using  
Rifled Cladding.  
Technical Committee Meeting on Fuel  
Performance of High Burnup for Water Reactors.  
Studsvik, Sweden 5-8 June 1990. (IAEA IWGFPT/36, p 147-159).
- 39 MONTGOMERY, R O, RASHID, Y R, KJAER-PEDERSEN, N  
Theoretical Evaluation of Rifled Cladding for LWR Fuel.  
Nucl. Eng & Des 132 (1992), p 309-316.
- 40 GROUND, M  
Review of Swedish work on Irradiation effects in Pressure Vessel  
Steels and on the Significance of the Data Obtained.  
Effects of Radiation on Structural Metals, ASTM STP 426.  
Am Soc Testing Mats, 1967, p 224-259.
- 41 GROUND, M  
Review of Swedish work on Irradiation effects in Canning and  
Core Support Materials. Effects of Radiation on Structural Metals,  
ASTM STP 426. Am Soc Testing Mats, 1967, p 200-223.
- 42 GROUND, M  
Irradiation Effects in Pressure Vessel Materials for Steam-Cooled  
Fast Reactors.  
Irradiation Effects in Structural Alloys for Thermal and Fast Reactors,  
ASTM STP 457. Am Soc Testing Mats, 1969, p 156-179.
- 43 GROUND, M, RAO, S  
New Alloy Steels for Nuclear reactor Pressure Vessels and  
Vessel Internals.  
Trans ASM 62 (1969), p 902-914.



- 44 **The STUDSVIK NEUTRON RESEARCH LABORATORY**  
**User Guide for the Neutron Research Facilities of the Studsvik Neutron**  
**Research Laboratory, August 1991.**

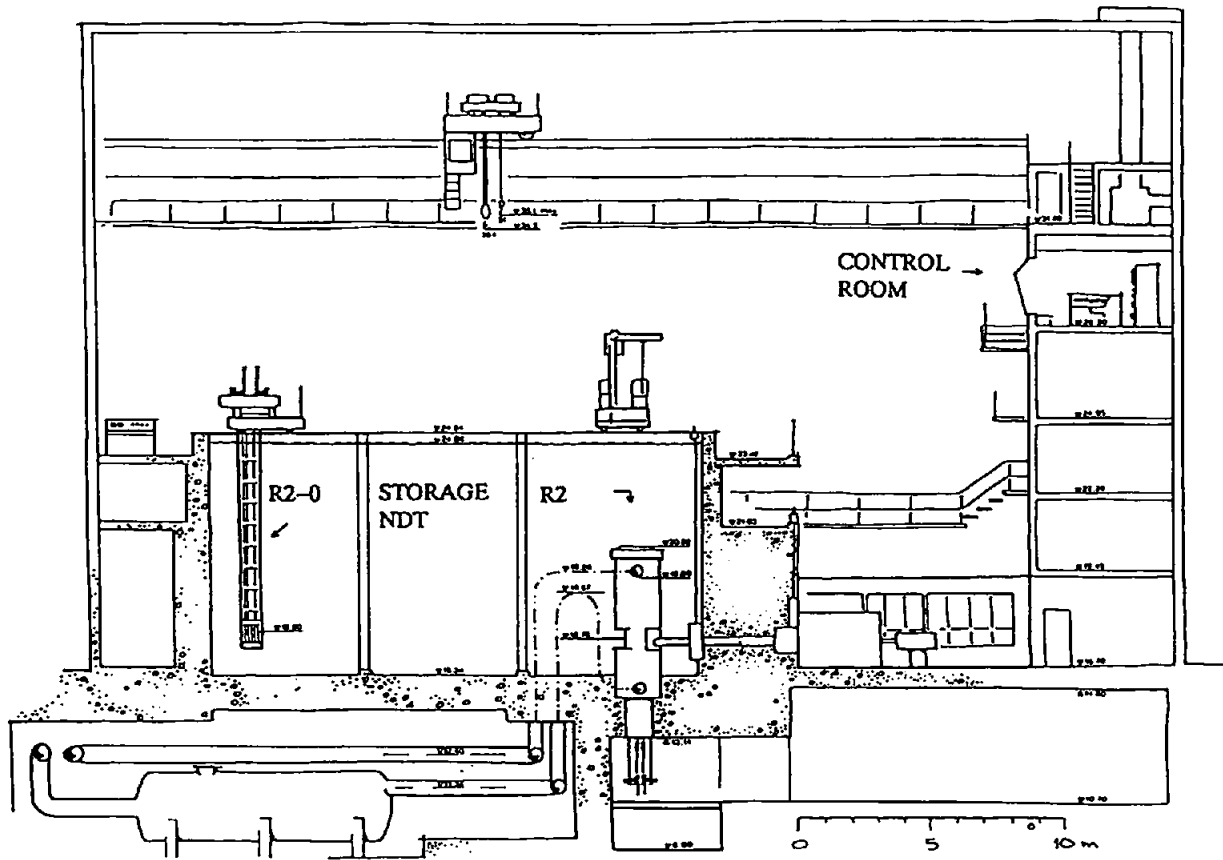


**Figure 1**  
The R2 Test Reactor – General Arrangement.

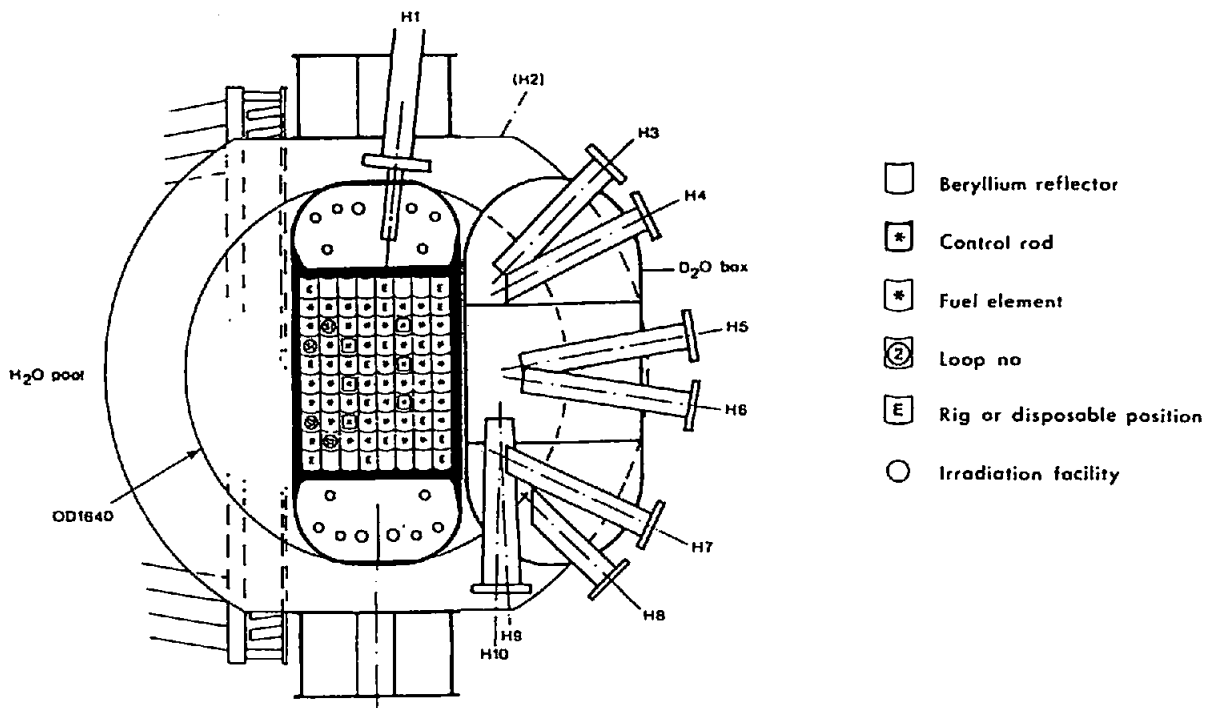


**Figure 2**  
The R2 Test Reactor – Core Configuration.

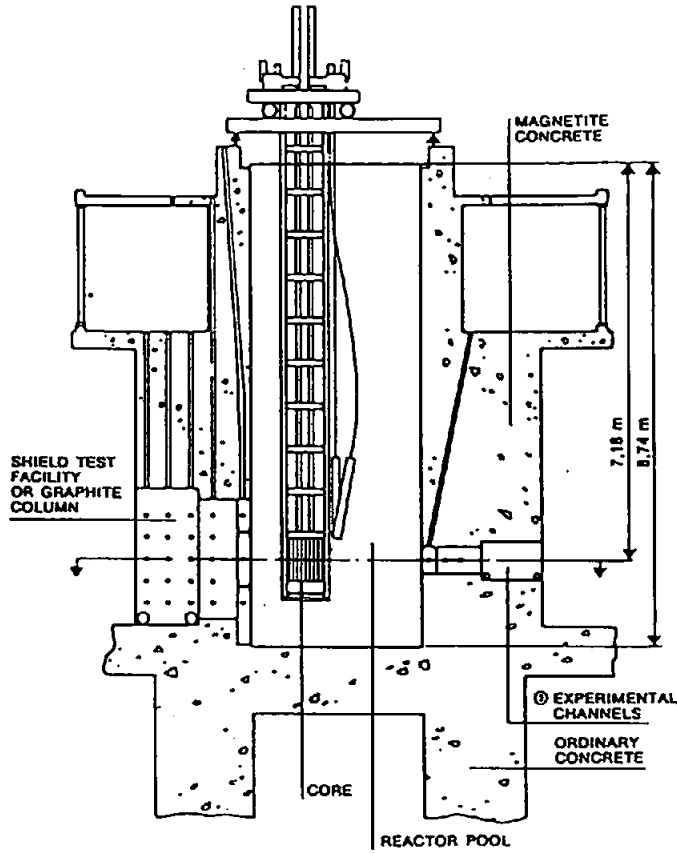


Figure 3  
The R2-0 Reactor.

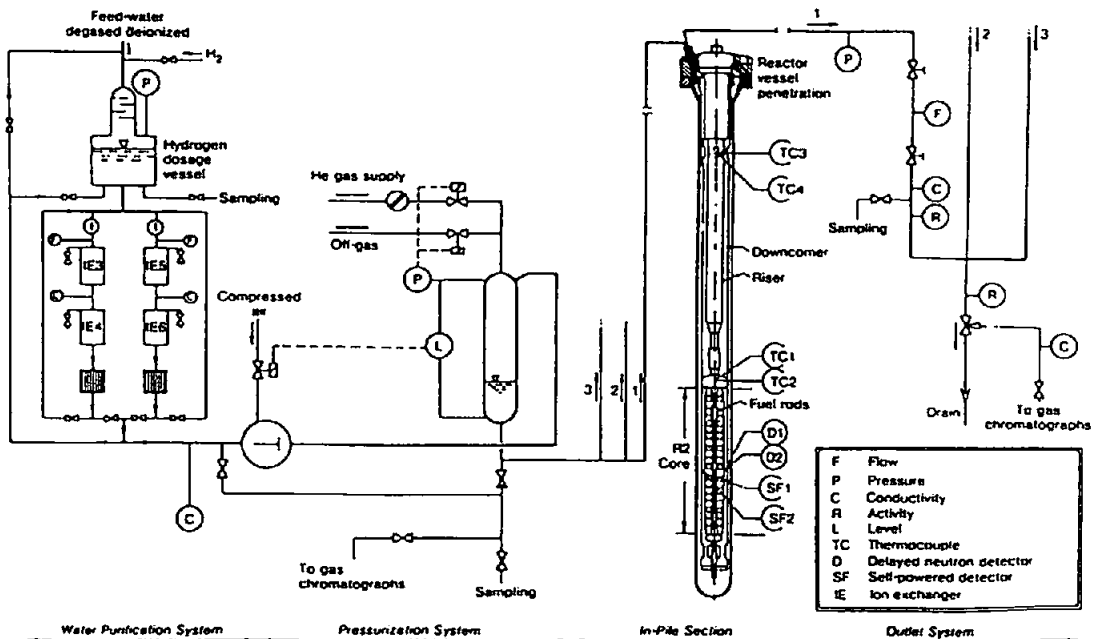
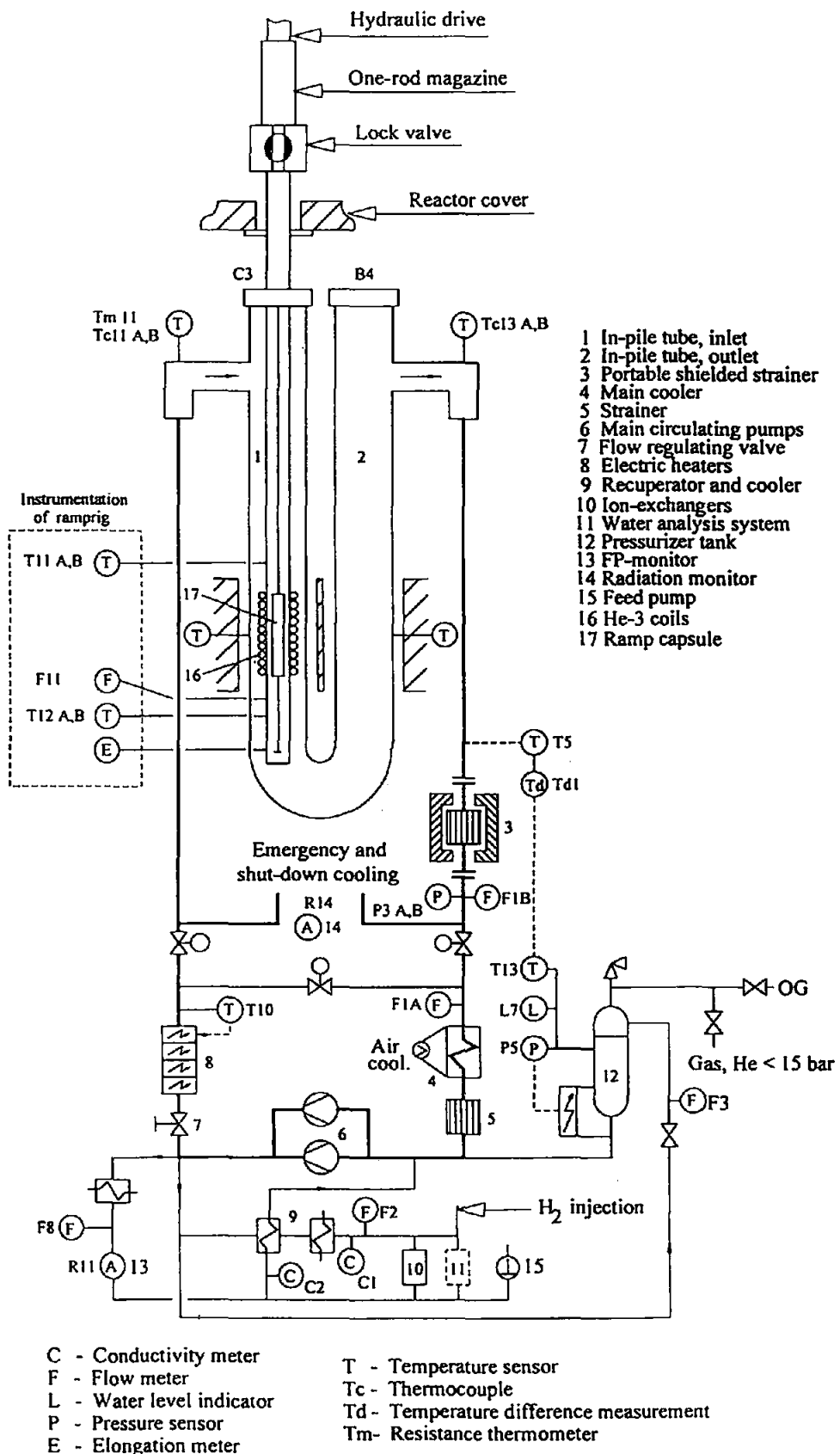
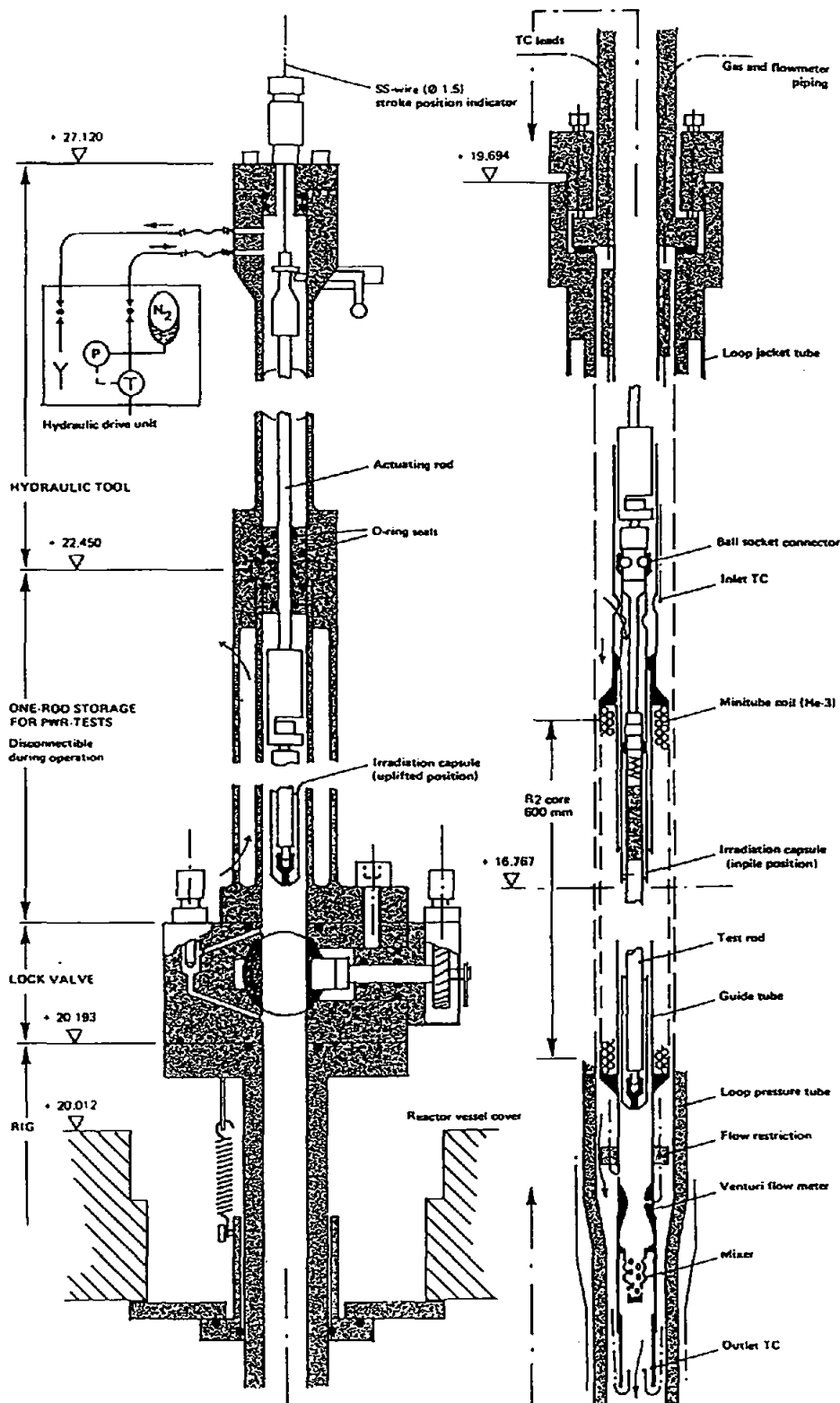


Figure 4  
BOCA Rig in R2 - Simplified Flow Sheet and In-Pile  
Part of a Boiling Capsule.



**Figure 5**  
Loop No 1 in R2 with Ramp Test Rig – Simplified Flow Diagram.



**Figure 6**  
 Loop No. 1 in R2 - PWR Ramp Testing Facility.

Recent versions include a transducer in the lower part of the rig. This transducer is used to monitor the length changes in the fuel rod. These changes are monitored continuously, see Figure 8.

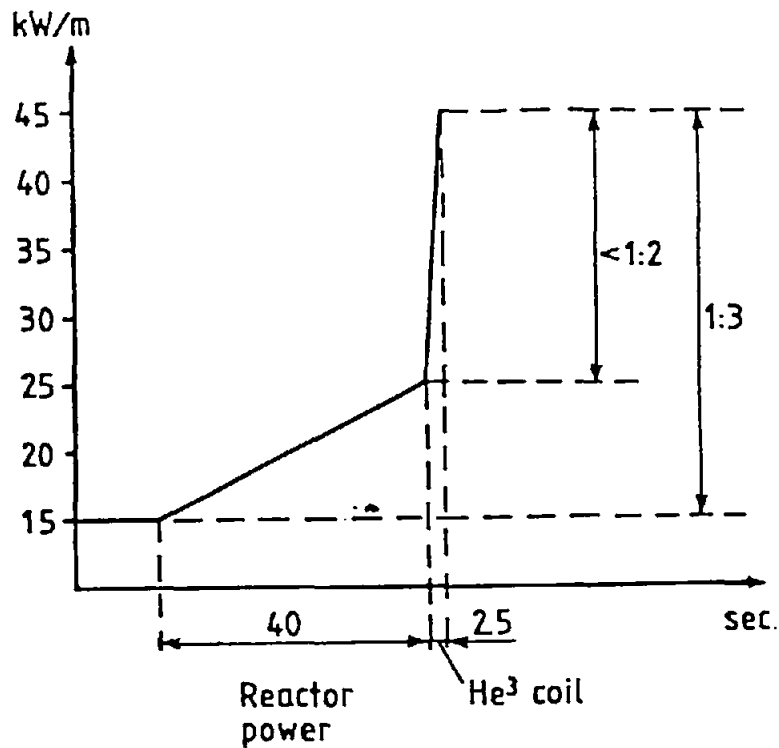


**Figure 7**  
Schematic Rod Power vs. Time Diagram for Double Step Up-Ramping.

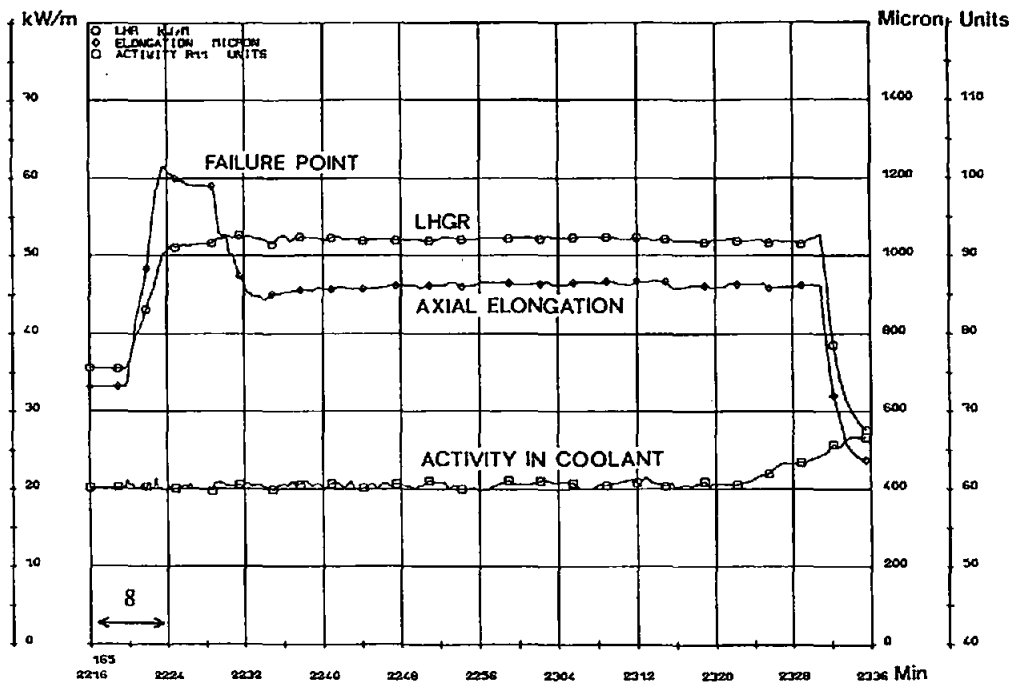


**Figure 8**  
On-line Measurements During a Ramp Test Showing a PCI Failure Event.

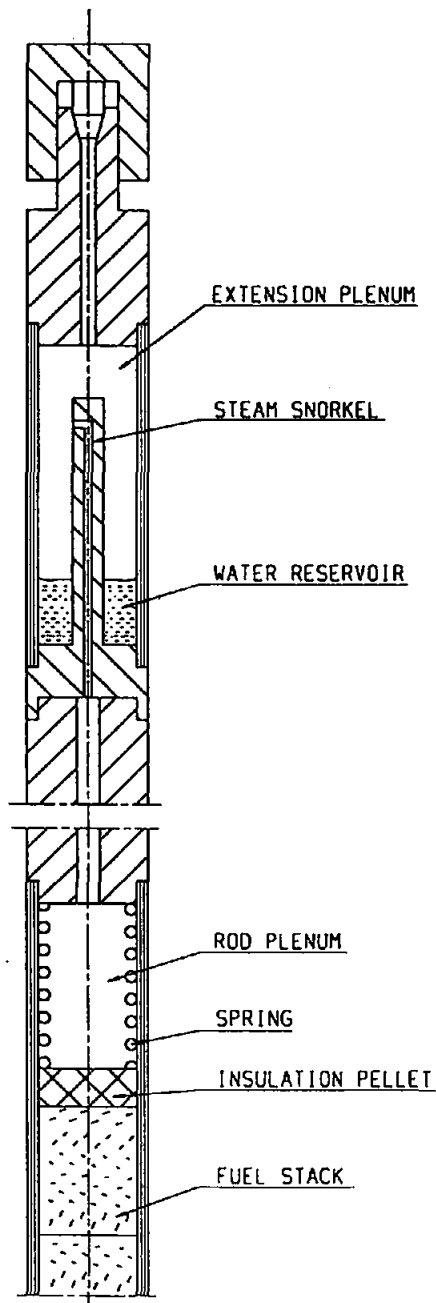


**Figure 9**  
Array Simulating Primary Defects in Fuel Rods (Patent Pending).

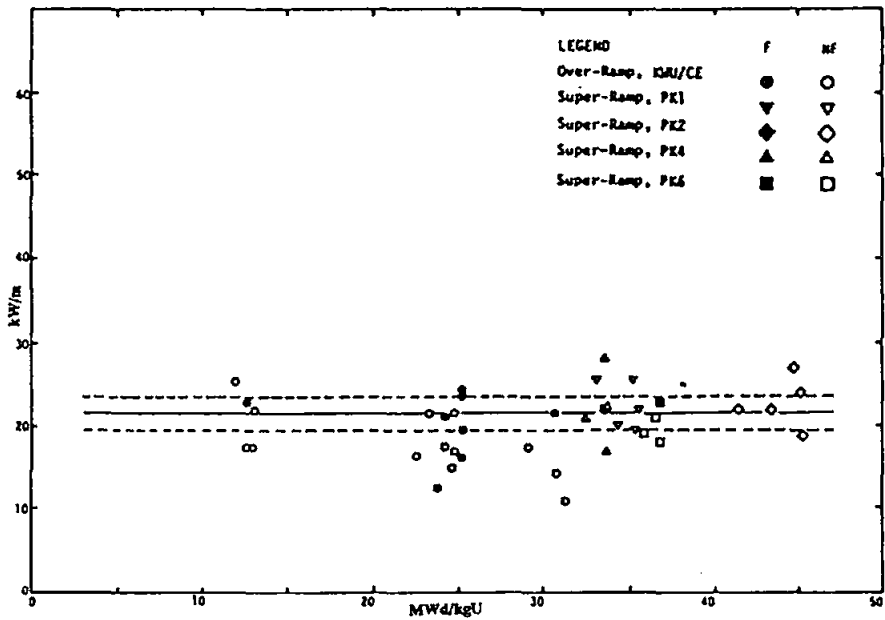
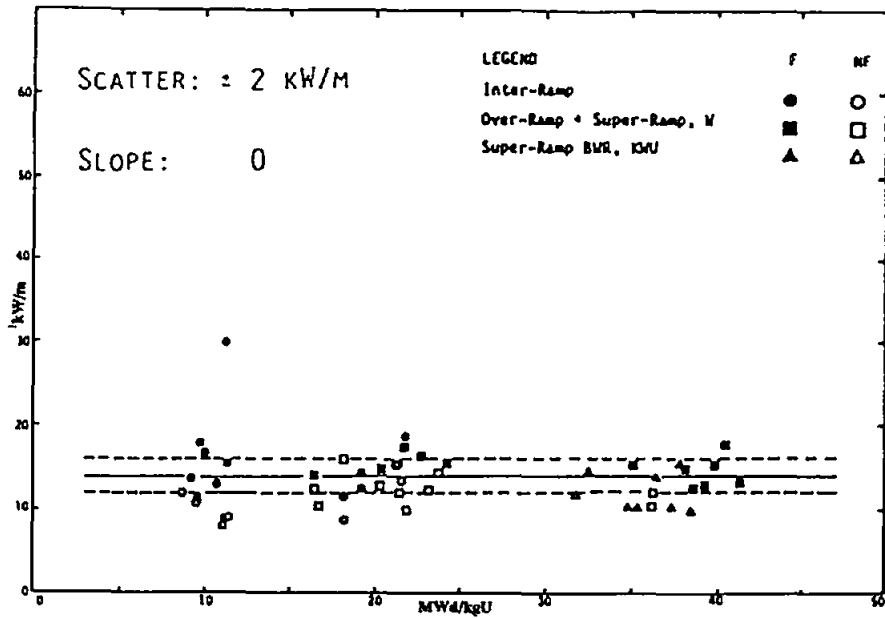


**Figure 10**  
 Summary of Some Data From the INTER-RAMP, OVER-RAMP and SUPER-RAMP Projects. The Incremental Failure Threshold as a Function of Burn-Up for Different Groups of Fuel Rods.



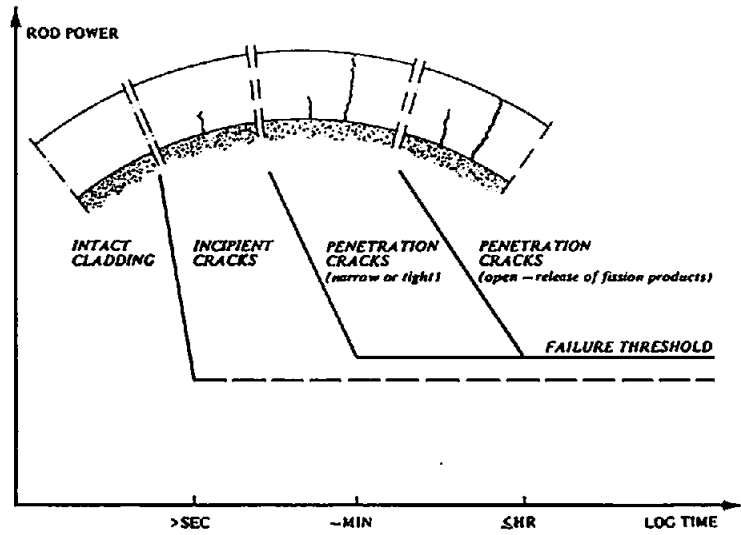


**Figure 11**  
Schematic PCI Failure Progression Diagram.

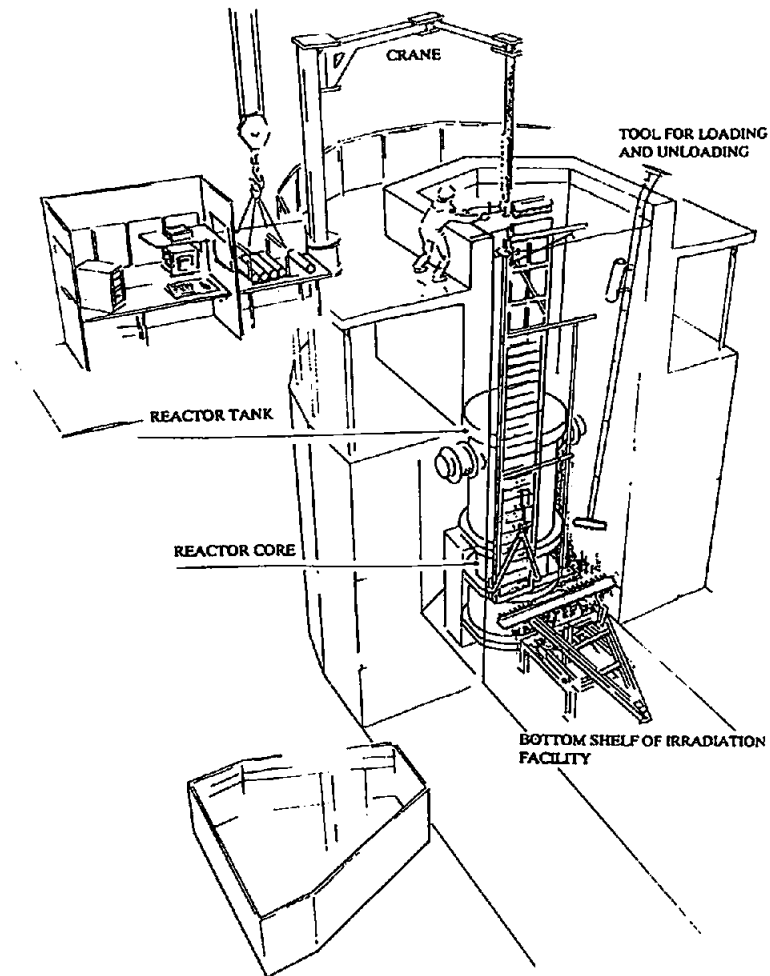


**Figure 12**  
Silicon Irradiation Facility.

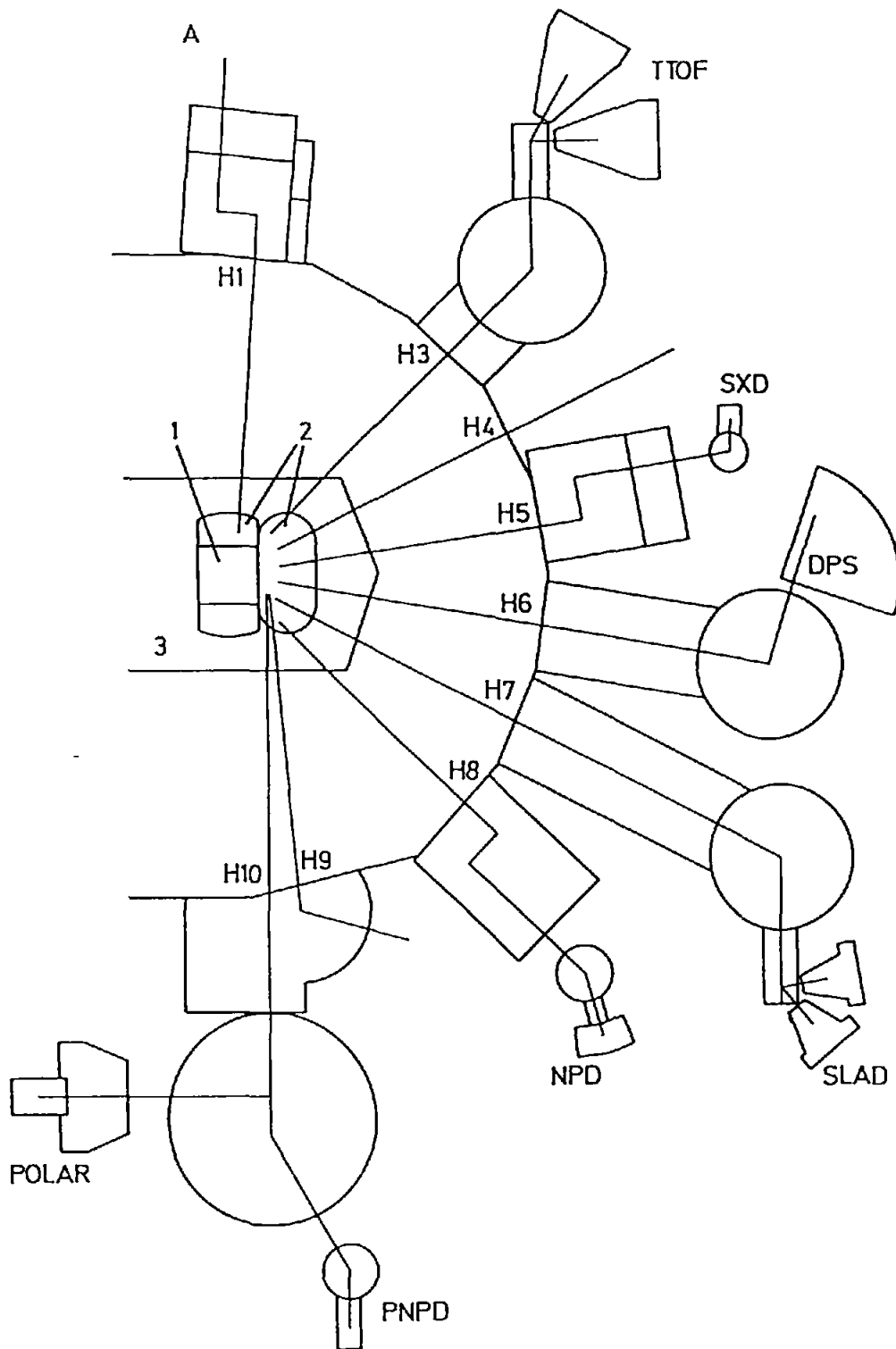


**Figure 13**  
Neutron Scattering Instruments at the R2 Reactor.

1. Reactor core    2. D<sub>2</sub>O moderator    3. Reactor pool  
TTOF: Time-of-flight spectrometer for thermal neutrons  
SXD: Single-crystal spectrometer  
DPS: Diffractometer for protein studies  
SLAD: Diffractometer for disordered system  
NPD: Powder diffractometer  
POLAR, PNPD: Diffractometers for polarized neutrons.

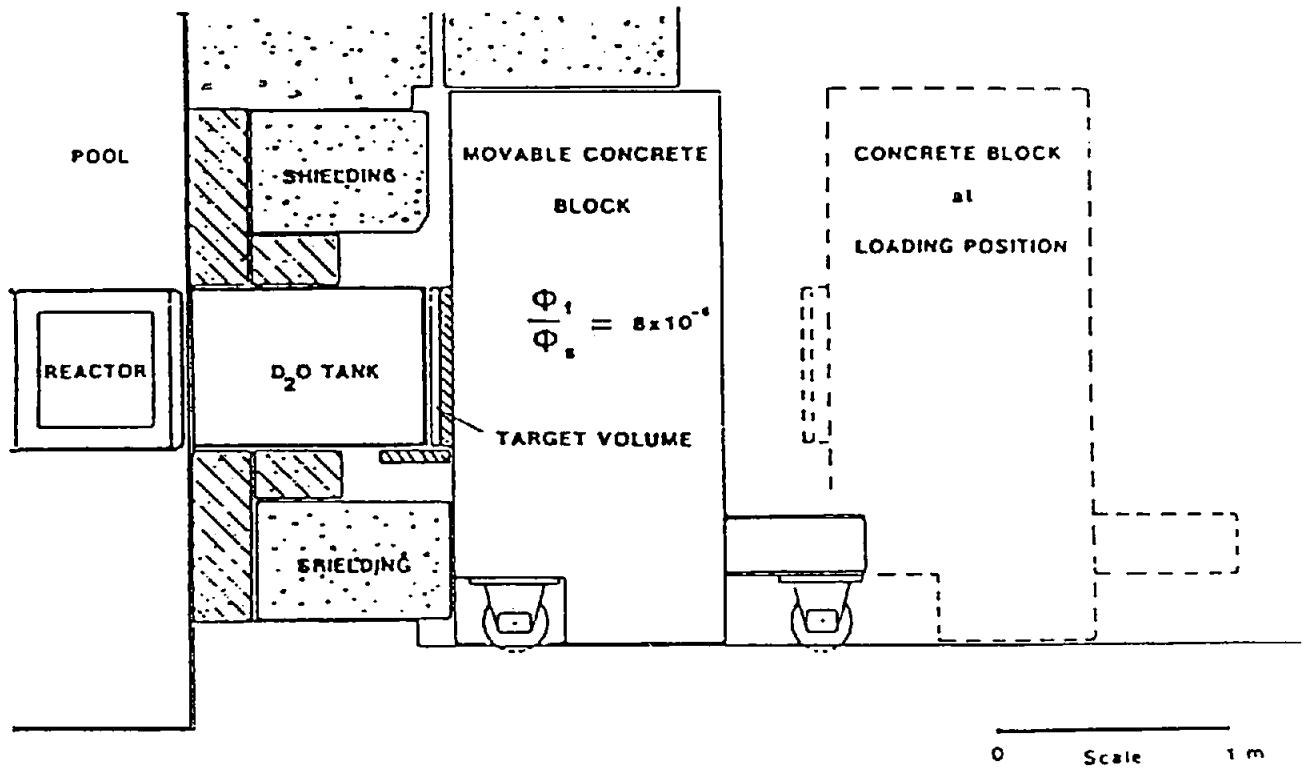


**Figure 14**  
The R2-0 Thermal Neutron Facility for Neutron Capture Radiography.

## Appendix 1

### Overview of STUDSVIK NUCLEAR's International Fuel R&D Projects 1975–1991

Project (duration)	Fuel Type (No of rods)	Base Irradiation (MWd/kgU)	Research Objectives	Data published
INTER-RAMP (1975–79)	BWR (20)	R2 (10–20)	Failure threshold Failure mechanism Clad heat treatment Modeling data	Yes (Ref 1,2) *)
OVER-RAMP (1977–80)	PWR (39)	Obrigheim (10–30) BR-3 (15–25)	Failure threshold Design parameters Modeling data	Yes (Ref 3,4)
DEMO-RAMP I (1979–82)	BWR (5)	Ringhals I (15)	PCI remedies (Annular, niobia doped pellets)	Yes (Ref 5)
DEMO-RAMP II (1980–82)	BWR (8)	Würgassen (25–29)	Failure threshold PCI damage by overpower transients	Yes (Ref 6,7)
SUPER-RAMP (1980–83)	BWR (16)	Würgassen (30–35) Monticello (30)	Failure threshold High burn-up effects PCI remedies Safe ramp rate Gd fuel	Yes (Ref 8)
	PWR (28)	Obrigheim (33–45) BR-3 (28–33)	Design parameters Modeling data	Yes (Ref 8)
SUPER-RAMP EXTENSION (1984–86)	BWR (9)	Oskarshamn 2 (27–31)	Safe ramp rate	No
	PWR (4)	Obrigheim (30–35)	Resolve unexplained failure resistance	No
TRANS-RAMP I (1982–84)	BWR (5)	Würgassen (18)	Failure boundary Crack init. and prop. Structural changes Fission gas release Modeling data	Yes (Ref 6,9)

\*) References, see p. 25

## Appendix 1, cont.

Project (duration)	Fuel Type (No of rods)	Base Irradiation (MWd/kgU)	Research Objectives	Data published
TRANS-RAMP II (1982-86)	PWR (7)	Zorita (30)	Failure boundary Crack init. and prop. Structural changes Fission gas release Modeling data	Yes (Ref 10)
ROPE I (1986-89)	BWR (4)	Ringhals (36)	Investigate clad creep- out as a function of rod overpressure	No
SUPER-RAMP II/9x9 (1987-91)	BWR (4)	Dresden (30)	PCI performance	Yes (Ref 11)

## Appendix 1 – References

- 1 THOMAS, G  
The Studsvik INTER–RAMP Project: An International Power Ramp  
Experimental Program.  
J Nucl Materials 87 (1979), p. 215–226 also Proc KTG/ENS/JRC Meeting on Ramping  
and Load Following Behaviour of Reactor Fuel. Petten, The Netherlands, Nov 30 – Dec 1,  
1978. H. Röttger, Ed. (EUR 6623 EN, p 95–106).
- 2 MOGARD, H et al.  
The Studsvik INTER–RAMP Project – An International Power Ramp  
Experimental Program.  
ANS Topical Meeting on LWR Fuel Performance. Portland,  
Oregon, USA, April 29 – May 3, 1979, p 284–294. (DOE/ET/34007–1).
- 3 DJURLE, S  
The Studsvik OVER–RAMP Project.  
Studsvik Energiteknik AB; Sweden. 1981. (STUDSVIK–STOR–37).
- 4 HOLLOWELL, T E, KNUDSEN, P, MOGARD, H  
The International OVER–RAMP Project at Studsvik.  
Proc. ANS Topical Meeting on LWR Extended Burnup – Fuel Performance  
and Utilization. Williamsburg, VA, USA, 4–8 April 1982, Vol. 1, p 4–5 to 4–18.
- 5 FRANKLIN, D G, DJURLE, S, HOWL, D  
Performance of Niobia–Doped Fuel in Power–Ramp Tests.  
Nuclear Fuel Performance. Stratford–upon–Avon, UK, 25–29 March 1985.  
Proc. BNES, London 1985. Vol. 1, p 141–147.
- 6 BERGENLID, U et al.  
The Studsvik Power Transient Programs DEMO–RAMP II and TRANS–RAMP I.  
IAEA Specialists' Meeting on Pellet–Cladding Interaction in Water Reactor Fuel.  
Seattle, WA, USA, 3–5 October 1983. (IAEA IWGFPT/18, p 50–55).
- 7 MOGARD, H et al.  
The International DEMO–RAMP II Project at Studsvik.  
Nuclear Technology 69(1985):2, p 236–242.
- 8 MOGARD, H, HECKERMANN, H  
The International SUPER–RAMP Project at Studsvik.  
Proc. ANS Topical Meeting on Light Water Reactor Fuel Performance.  
Orlando, FL, USA, 21–24 April 1985. ANS, La Grange Park, IL, 1985.  
(DOE/NE/34130–1, Vol. 2, p 6–17 to 6–33).
- 9 MOGARD, H et al.  
The International TRANS–RAMP I Fuel Project.  
Fuel Rod Internal Chemistry and Fission Product Behaviour.  
Technical Committee Meeting, Karlsruhe, FRG, 11–15 November 1985.  
Proc. (IAEA IWGFPT/25, p 157–167).

- 10 MOGARD, H, HOWL, D A, GROUNES, M  
The International TRANS-RAMP II Fuel Project – A Study of the  
Effects of Rapid Power Ramping on the PCI Resistance of PWR Fuel.  
ANS Topical Meeting on LWR Fuel Performance.  
Williamsburg, Va, USA, 17–20 April, 1988, p 232–244.
- 11 HOWE, T, DJURLE, S, LYSELL, G  
Ramp Testing of 9x9 BWR Fuel.  
Fuel for the 90's. International Topical Meeting on LWR Fuel Performance,  
Avignon, France, 21–24 April, 1991, Vol 1, p 828–837.

## Appendix 2

### Overview of STUDEVIK NUCLEAR's Ongoing and Planned International Fuel R&D Projects

Project (duration)	Fuel Type (No of rods)	Base Irrad (MWd/kgU)	Research Objectives
TRANS-RAMP IV (1988-91)	PWR (7)	Gravelines (20-25)	Influence of non-penetrating cracks on PCI failure resistance
ROPE II (1990-93)	PWR (6)	Ringhals Obrigheim (> 40)	Investigate clad creep-out as a function of rod overpressure
DEFEX*) (1993-95)	BWR (6)	Initially unirradiated rodlets	Study secondary damage formation in fuel rods with simulated fretting defects
SUPER-RAMP III (NS**), 1994-97)	PWR (ND)**)	ND (> 40/ > 55)	PCI performance
TRANS-RAMP III (NS, 1994-96)	BWR	ND	.Same as TR IV
DEFEX II (NS, 1995-97)	BWR +PWR	ND (10-20)	Same as DEFEX

\*) DEFEX = Defect Fuel Degradation Experiment

\*\*\*) NS = Not yet started

ND = Not decided



Ongoing Refurbishment Activities and Strategy  
For the Future Operation of the BR2 Reactor

E. Koonen and P. Gubel

*BR2 Department  
Belgian Nuclear Research Center  
C.E.N./S.C.K.  
Boeretang 200  
B-2400 MOL, Belgium*

Tel.: 00 32 14 332407

Fax.: 00 32 14 320513

**Abstract:**

The operation of the BR2 reactor with its second Be-matrix is foreseen up to mid-1995 or mid-1996.

A life extension for another 15 years is envisaged considering programmatic, financial and technical aspects.

At present, the second phase of the refurbishment programme is being executed. The major activities of this programme can be grouped under two headings: safety reassessment and ageing issues. The expected outcome end '93 is an assessment report defining extent, chosen options, prioritized activities, budget and a tentative planning for the preparation and execution of the refurbishment. These aspects together with the prospects of possible cooperation with other parties for the refurbishment programme and the future operation of BR2 will be evaluated by the CEN/SCK Board who has to take a decision early in 1994.

Various scenarios are now being considered and evaluated for the refurbishment and the future BR2 operation regime.

**Table of Contents**

1. INTRODUCTION.
2. PRESENT STATUS, PROBLEMS AND PERSPECTIVES.
3. NEEDS FOR REFURBISHMENT.
4. STRATEGY.
5. 2nd PHASE REFURBISHMENT PROGRAMME.
6. FUTURE OPERATION.
7. CONCLUSION.

## 1. INTRODUCTION

The BR2 reactor (Mol, Belgium) went critical for the first time on the 29th June 1961. It was put into service with an experimental loading in January 1963. On the 31st December 1978, the reactor was shut down to replace its beryllium matrix. All of 1979 and the first half of 1980 were devoted to this task. Routine operation of the reactor was resumed in July 1980. During the last two years (1991-1992), the operation regime of the reactor was perturbed by the installation of the CALLISTO loop: the duration of the shut downs was limited by the maximum allowed antireactivity due to the He-3 poisoning.

The BR2 is a high flux engineering test reactor which differs from comparable materials testing reactors by its specific core array.

The core is composed of hexagonal beryllium blocks with central channels. These channels form a twisted hyperboloidal bundle and hence are close together at the midplane but more apart at the lower and upper ends where the channels penetrate through the covers of the reactor pressure vessel. With this array, a high fuel density is achieved in the middle part of the vessel (reactor core) while leaving enough space at the extremities for easy access to the channel openings (cf. figure 1.).

The standard BR2 fuel elements consist of several concentric tubular shells (up to 6) of uranium-aluminium alloy clad by aluminium which provide a central channel for locating irradiation experiments. Besides these fuel element channels which offer a particularly high fast neutron flux (up to  $7 \times 10^{14}$  n/cm<sup>2</sup>.s), a large number of channels exist in the beryllium matrix where no fuel elements are loaded.

These reflector channels can be occupied by experiments which demand only a thermal neutron flux or they are obturated by beryllium filling plugs.

## 2. PRESENT STATUS, PROBLEMS AND PERSPECTIVES

The BR2 reactor is at present operating routinely on the basis of 168 days per year - 8 cycles of 21 operation days. -

During shutdowns, short irradiation campaigns may be organized for ramping tests of fuel rods in dedicated irradiation devices.

This routine operation regime was reestablished by the end of 1992 after the successful installation and commissioning of the CALLISTO loop. This loop is composed of three in-pile sections connected to a common out-pile equipment and allows for the irradiation of 27 (3x9) fuel rods in representative PWR conditions.

Besides irradiations executed in the frame of various programmes for material and fuel research, the BR2 reactor is also used for the production of valuable radioisotopes for medical and industrial applications and silicon doping.

In 1992, a new irradiation device, called SIDONIE- Silicon Doping by Neutron Irradiation -, was successfully commissioned and put into service. This unique irradiation device allows for the production of 25 T/year of high quality silicon.

At the present operation regime, a continuation of the operation until ~ mid-1995 is authorized. This time constraint is derived from the maximum fast fluence -  $6.4 \times 10^{22}$  nvt,  $E > 1$  Mev - imposed for the beryllium matrix; this physical limit is dictated by the operation license which also provides for guidance and rules on surveillance and evaluation of the matrix degradation.

A life extension of the present matrix is under consideration: it would allow continuation and completion of on-going irradiation programmes, and also provide more flexibility for the preparation of the refurbishment programme.

The envisaged life extension is of ~ one year corresponding to a ~ 6% increase of the maximum fast fluence: indeed the operation license demands a safety re-evaluation of the reactor by mid-1996.

A safety study has been carried out to evaluate the conditions under which a limited life extension of the beryllium matrix can be justified. On this basis, a request for modification of the actual operation license has been recently submitted to the Authorities.

As for most European research reactors, the operation of BR2 is facing several increasing constraints with regard to safety, radioprotection and protection of the environment.

Meeting these growing requirements constitutes a challenge for an installation designed more than 35 years ago.

Various social, economical and technical factors, internal as well as external, concur to constitute a threat for future operation: on one hand a diminishing demand for irradiations and on the other increasing costs for the fuel cycle, the treatment and disposal of waste and the necessary provisions for decommissioning.

In particular, all evolutions and problems related to the HEU fuel-cycle, procurement of fresh HEU and disposal of the spent fuel, are closely followed and studied.

Up to now fresh HEU material has been procured from the U.S.A. without major difficulties: indeed BR2 has been recognized by the U.S. as one of the facilities still requiring highly enriched (93%) uranium in order to keep its unique characteristics. The availability of U.S. origin material after 1995 is however questionable. Alternative sources of material have to be looked for, in particular the reutilization of reprocessed HEU material in combination with a slightly higher density.

The back-end of the fuel-cycle has become a preoccupying problem since the non-renewal of the U.S. off-site policy for U.S. origin fuel irradiated in foreign countries. Different alternate solutions have been examined, compared and are still being evaluated: storage pool expansion with a complete reshuffling, using high density storage racks, dry storage or reprocessing. A reconduction of the U.S. off-site policy has been announced. Nevertheless many

uncertainties - delay for implementation, costs... - still subsist and do not yet allow for a balance of advantages and disadvantages of this solution against the above mentioned alternatives.

A license is expected for a limited storage pool expansion with two conditions: first the storage pool should be inspected and refurbished and secondly an alternate solution to wet storage should be available for an operation after 1996. To satisfy the refurbishment requirement for the storage pool, a limited number of fuel elements have to be evacuated to A.E.A./Dounreay for storage and a possible reprocessing is being negotiated.

### 3. NEEDS FOR REFURBISHMENT

The unavoidable replacement of the beryllium matrix constitutes a first reason for a refurbishment programme (fig. 1). According to the operation license, other inspections and tests like the inspection of the reactor vessel have to be carried out. The duration of the necessary shutdown for replacement of the matrix and the required inspections/tests should be approximately ~1 year provided the new matrix is available in due time.

The first matrix has been replaced previously in the period 1979-80. This time however, the intention is to use for replacement at least part of the BR02 matrix after minor adaptations (see § 5.2a).

The operation license for BR2 states that the safety should be reassessed by June 30 1996. This corresponds to a decennial safety review of the entire plant. A life extension programme for another 15-20 years requires therefore that the entire installation must be critically reviewed with respect to the status of the installations, the operating experience and the evolution of the safety standards. Aspects such as availability and reliability should certainly not be forgotten in a perspective of a continued operation.

The requirement to build a new safety case in compliance with modern safety standards constitutes the second need for a comprehensive refurbishment programme, the extent of which will be defined by the results of the on-going studies (see § 5).

### 4. STRATEGY

The BR2 reactor is one of the most performing research reactors in the world. An operation after the year 2000 however is only justified if there is a growing need for European and international nuclear research in the field of new, (r)evolutionary materials, fuels and reactor types.

Therefore a quantitative outlook on the future irradiation needs is now being made. The results of this analysis together with the conclusions of the technical and financial evaluation for the refurbishment programme should be available by end of 1993. These aspects together with the prospects of possible cooperation with other parties for the refurbishment programme and the future

operation of BR2 will be assessed by the CEN/SCK Board. A decision on the future of BR2 is expected early 1994.

In function of the prospects for future irradiation programmes and the time needed for the phases 3 and 4 of the refurbishment (respectively preparation and execution), an optimum date for the refurbishment shutdown will be defined. The remaining operation period will be devoted to continue and possibly terminate all on-going irradiations programmes and to proceed with all pre-shutdown activities (design, procurement of materials and components,...).

## 5. 2nd PHASE REFURBISHMENT PROGRAMME

Phase 1 established the feasibility and defined a work programme for phase 2 [1].

The second phase, now underway, has to be executed in 18 months, mainly with in-house staff.

A temporary project management structure has been set up for this purpose.

A budget of ~ 3 M \$ US has been allocated and a tight planning established.

The expected outcome end '93 is an assessment report defining extent, chosen options, prioritized activities, budget and a tentative planning for phases 3 and 4 of the refurbishment programme [2].

The major activities of phase 2 can be grouped under two headings : safety reassessment and ageing issues.

### 5.1. Safety reassessment

The aim is to prepare a new safety case in compliance with modern standards. All risk-significant systems and functions are being reviewed in order to assure that the safety goals are met, or to define technically possible complementary provisions if required.

#### a. Probabilistic Safety Assessment :

The existing deterministic safety case is being complemented by a level 1 + probabilistic safety assessment (PSA), in order to assess the risk profile of facility.

The information produced is used as follows [3]:

- the PSA indicates the reliability expected of the safety-related systems. The refurbishment issues are then adressed in a way to ensure that the reliability expectations are achieved during future operation.
- for those plant items which are in the risk significant sequences, increasing the reliability will lead to a reduction of risk. The refurbishment options considered should then lead to improvements in reliability and hence reductions in the overall risk of core degradation and radioactive releases.

- for those plant items which are not in the risk significant sequences, any refurbishment can be considered, as even a reduction in reliability will not lead to an increase in the overall risk.

Some important issues, that have been identified, and some contemplated refurbishment issues are listed here below [4]:

- adequacy of nuclear control with respect to diversity and segregation ;
- reliability of process trip instruments ;
- duplication of isolation valves of the primary circuit in the reactor pool;
- modifications to reduce the likelihood of pool drainage and improvement of the reliability of make-up water to the pool ;
- accident management actions in case of major pool failure.

Further assurance that the probabilities and assumptions used so far are appropriate, still needs to be provided. Where significant pessimisms were first used in risk-significant sequences, justified new assumptions are being developed.

#### b. Incredibility Of Failure Case :

Another major issue is the defense against large breaks in the primary pipework.

Preliminary calculations raised some doubts about the effectiveness of the existing safety equipment to prevent core degradation after a large break in the primary pipework outside the containment-building.

New thermo-hydraulic analysis of large LOCA's and investigation of the siphon-break system associated with the defense against large LOCA's are being carried out.

Nevertheless the weight of the safety case will be based on the demonstration that such large breaks are extremely unlikely. This requires a extensive inspection and validation programme on the pipework in order to establish an incredibility of failure case (IOF).

The IOF shall be considered demonstrated if [5]:

- a thorough inspection does not show any significant weakening (i.e. cracks or overall wall thinning) of the pressure retaining boundary, or external damage on the piping or supports. Defect sizes and distribution should be within the limits specified by the appropriate code.
- a stress calculation report can confirm the adequacy of design. Existing documentation might supplement the report, if its review is found satisfactory.
- the "leak before break" can be demonstrated. This will be the case if it can be shown that longitudinal and circumferential cracks do not grow spontaneously once initiated. It should be demonstrated that the stresses at the ends of postulated cracks do not exceed the rupture stresses of the material.

#### c. Advanced Passive Reactor Features :

BR2 has many features of advanced reactor designs, in that the ultimate integrity of the core relies on physical and simple design features, i.e.

natural circulation removing the residual heat from the core and transferring it to a substantial heat-sink, the reactor pool.

In order to enhance the advanced passive reactor features (APR-features) and to increase safety, some minor changes in equipment and some modifications in the safety procedures are being studied. This particularly concerns some reengineering of the major block valves of the primary circuit : make them fail in safe position on loss of services, assure high integrity of the hydraulic systems local to the valves, upgrade their testability and review the philosophy of sequences of automatic actions.

Upgrading some key features to "passive safety" status will enable to downgrade in their safety importance some (more complex) electrical and hydraulic support systems.

d. Fire protection :

A study based on modern standards (prevention, detection, mitigation) has been carried out [6].

An ideal compartementalization and segregation plan has first been established. This plan has then been reviewed in function of the safety importance of the systems concerned. In this manner a realistic definition of compartments, detection and mitigation systems was obtained. At present the implementation plan is being established.

e. Seismic Risk Assessment :

In an earlier study, the sensible installations were identified and the consequences of the reference earthquake were evaluated [7]. The most important functions to be assured were found being the operability of the latch mechanisms of the control-rods and the preservation of an appropriated level of water in the reactor-pool. In order to confirm that all systems are able to support the reference earthquake, some additional verifications were suggested, mainly in relation with the possibility of total drainage of the reactor pool. An evaluation whether those verifications are required, taking into account the results produced by other studies, is underway.

## 5.2. Ageing issues

In phase 1 of the refurbishment programme, the potential ageing processes were identified and the equipments susceptible to ageing were identified and categorized.

In phase 2, detailed studies and inspections are carried out, in order to assess remaining life and define the refurbishment activities for phase 3 and 4.

The purpose is to ensure availability and reliability of the installation for the considered life extension period.

Only the most important issues are briefly discussed here below.

a. Be-matrix :

The issue is to establish the feasibility of using BR02 beryllium channels and their associated parts as a replacement for the current BR2-matrix, which

reaches its foreseen end-of-life around '96 (BR02 is the zero power nuclear mock-up of BR2).

The main conclusions, while inspection work is still ongoing, are the following [8]:

- the BR02 parts are fundamentally the same as the original BR2 matrix parts. Minor differences have been detected which require only limited modifications of the stainless steel extension pieces to ensure compatibility with BR2.
- there are some signs of corrosion. This corrosion is not deep and not expected to be a problem for future use of the matrix in BR2.

Some study and research work is still carried out and is focused on irradiation-induced swelling, cracking,  $^3\text{He}$  poisoning, radiological characterisation and corrosion [9,10,11].

At present the main findings can be summarized as follows :

- for low temperature irradiated Be, the swelling and the He content have been found linearly correlated with the fast ( $E > 1 \text{ MeV}$ ) neutron fluence ;
- annealing at higher temperatures is found to enhance strongly the swelling and to reduce the He content ;
- He release is found to be characterized by both "burst type" and "steady state type" release, depending on the temperature ;
- the qualitative similarity of He release characteristics with those of  $^3\text{H}$  release indicates a connection between the two ;
- evaluation of experimental results must take into account different influencing variables of the irradiation conditions (neutron spectrum, temperature, time) ;
- cracking of the BR2 beryllium channels is mainly due to mechanical interaction and only additionally caused by the irradiation-induced swelling ;
- the dominant gamma activity of the BR2-matrix is due to  $^{60}\text{Co}$  ;
- two types of corrosion have been identified on the BR02 channels : superficial white paste-like deposits resulting of a reaction between water and small carbide particles present within the parent material and some pitting corrosion, mainly near the top and bottom ends of the beryllium sections, close to the stainless steel parts ;
- passivation helps forming a protective oxide layer. Cleaning of the beryllium parts must be followed by a chemical passivation treatment.

b. Al-vessel :

The issue is to :

- evaluate the prospects for integrity insurance during the contemplated reactor-life extension period ;
- demonstrate acceptable failure risk during that period ;
- carry out a limited in-service inspection of accessible areas ;
- prepare a full in-service inspection for the refurbishment shutdown. A full inspection is only possible with the core matrix removed.



A materials characterisation action plan has been set-up [12], consisting of:

- a consultation agreement with off-site experts ;
- an improved dosimetrical characterisation of the neutron spectra at the vessel wall ;
- an investigation of remote control verification of the vessel beltline materials, particularly the vertical welds of the core forging ;
- thermal ageing of annealed specimens and future re-irradiation of these specimens ;
- a scoping evaluation of annealing potentials ;
- the establishment of guidelines and acceptance criteria for the full in-service inspection, possibly combined to an overpressure test.

As there is limited mechanical property data on irradiated type 5052-0 material, use of data for similar alloys is unavoidable, but is considered to be justifiable [13].

A first preliminary inspection of accessible part showed no signs of degradation and no deviation from the results of the detailed inspection, carried out 1980 in compliance with ASME XI. This improved the confidence in the acceptability of the vessel in advance of the full in-service inspection.

c. Instrumentation and control :

BR2 has two control-rooms : a "nuclear" control-room inside the containment-building and a "process" control-room outside.

The requirements for some nuclear control functions to be duplicated and located in an emergency control center outside the containment-building, are under consideration.

In the frame of the PSA, high-level failure mode effects analysis (FMEA) and dependant failure analysis of the electronic scram system and the shim-safety rods have been carried out. Diversity and segregation issues will be adressed following on from a fault tree assessment.

Several options (replacement, upgrading) are studied for the "process" instrumentation, as many pneumatic control systems are still under use. More specific issues concerning design and reliability of specific instruments are also adressed.

d. Electrical supplies :

General review and inspection identified the following work items :

- upgrading of the 110 V-DC net, i.e., split-up in several smaller nets and increase reliability ;
- segregation of some cabling. The results of the PSA and the fire protection study give valuable input to this issue ;

The installation of an additional separate emergency power generator is envisaged.

e. Pipework, pools and structures :

An extensive inspection programme has been set up and is being executed [14]. A general maintenance programme has been defined for the spent fuel storage pool. This involves some reshuffling of the fuel, made possible by the use of high-density storage racks [15].

## 6. FUTURE OPERATION

After the replacement of the beryllium matrix, it will be again possible to modify easily without any physical constraints - no He3 poisoning - the operation regime of the reactor.

A future operation regime should certainly be optimized and modified in function of the demands for irradiation programmes and commercial productions of radioisotopes and silicon neutron doping.

A choice has to be made between a continuous operation regime on a year basis with 8 to 10 cycles of 3 weeks operation and a discontinuous mode of operation where (very) long shutdowns are accommodated and the reactor is only brought into power on demand for specific (short) programmes.

Also in function of the expected short term scientific irradiation demands or commercial productions, the refurbishment programme could be realized in successive steps, starting with the necessary safety related upgradings and continuing later with replacements and modernizations during programmed extended shutdowns.

These various options are now still open and decisions will be taken early in 1994.

## 7. CONCLUSION

A final decision about the future of the BR2 reactor is expected early in 1994. A choice which has to be made on basis of technical, economical and programmatic considerations. It is the will of the CEN/SCK to keep open a performant test reactor for future scientific programmes within an international context. Various alternatives and scenarios are now being considered and evaluated to realize this option at the lowest cost.

## Références:

1. BR2 Refurbishment study, phase 1, BR2/JDP/DN01, AEA Engineering, January 1992.
2. Refurbishment BR2 - fase 2: organisatie, takenplan, masterplanning, NG.55/D2200/02/JD, 12.01.93.
3. Methodology plan for the BR2 PSA , BR2/FAW/12/MIS, issue 1, SRD/AEA, 04.11.92.
4. BR2 PSA Preliminary Report, BR2/FAW/61/REP, issue 1, SRD/AEA, 29.03.93.
5. Proposed path for the demonstration of IOF of the primary piping, NT.57/D2206/01/PB, 15.06.93.
6. Refurbishment BR2, Brandbeveiliging, TIERSI/4NT/144/01, Belgatom, 25.05.93.
7. CEN/SCK - Réévaluation de Sûreté, Etude des séismes, T.83346/627/NT.00020, Tractebel, 29.02.88.
8. Use of the existing BR02 parts in BR2, Final Report (preliminary issue), TN.D22/R0700/TG28, 28.04.93.
9. Réévaluation de la sûreté de BR2, § 5: matrice en beryllium, NT.72/R0576/EK, 01.06.91.
10. The effects of neutron irradiation on beryllium, JS&CDR, Paper presented at the 17th Symposium on Fusion Technology, Roma, Italy, Sept. 14-18, 1992.
11. Study on the corrosion of beryllium, Co.2535, Cebelcor, 01.07.93.
12. Long term integrity insurance of the BR2 aluminium vessel, D22/D2215/AF, 30.06.93.
13. Réévaluation de la sûreté de BR2, § 3.1: cuve du réacteur, NT.72/R0576/EK, 03.05.91.
14. Refurbishment BR2, Stand van zaken op 31.05.93, NT.55/D2200/01/JD, 14.06.93.
15. Extension de la capacité de stockage du canal, NT.D2860/PG, 03.05.93.

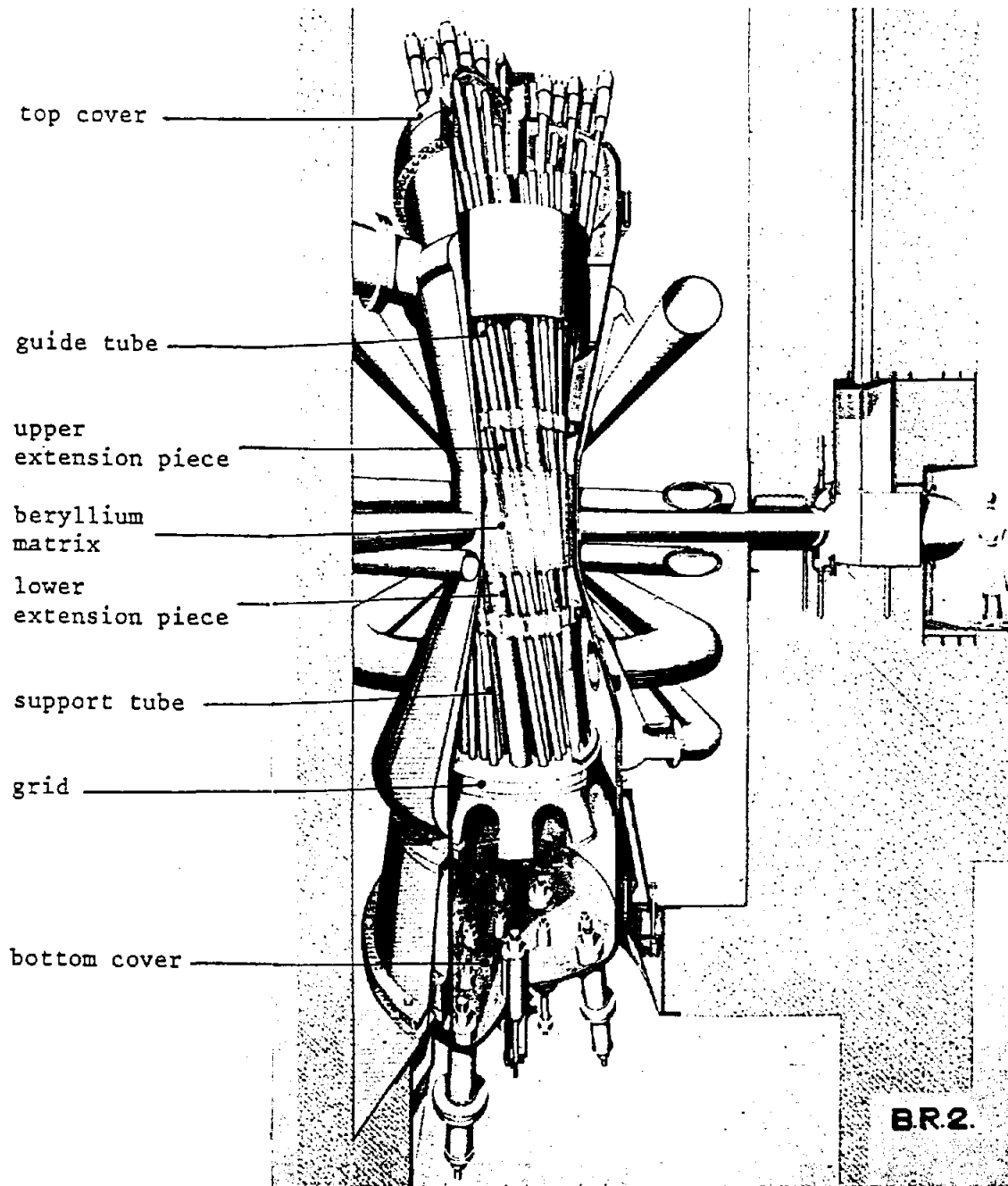


FIG.1 General view of the BR2 reactor

The Reactor and Cold Neutron Research Facility at NIST

H.J. Prask and J.M. Rowe

Reactor Radiation Division

National Institute of Standards and Technology

Gaithersburg, MD 20899

**ABSTRACT**

The NIST Reactor (NBSR) and Cold Neutron Research Facility (CNRF) are located at the Gaithersburg, MD site, and have been in operation since 1969 and 1991, respectively. A total of 26 thermal neutron facilities and 11 cold neutron stations are operating for studies in condensed matter physics and chemistry, materials science, chemical analysis, nondestructive evaluation, neutron standards, fundamental neutron physics, and irradiations. Thermal and cold neutron instruments which have become operational since the 2d IGORR Conference will be described. Major facility upgrades to be implemented in early 1994 will be outlined.

**INTRODUCTION**

Since the last IGORR meeting, progress on several fronts has continued at the NIST Reactor. This includes the installation of new instruments, near completion of other instruments, the expansion of use of the Cold Neutron Research Facility (CNRF) as a National Facility, and preparation for major facilities

improvements to be undertaken in 1994. These are described in this paper. Descriptions of instrumental capabilities have also been given elsewhere [1,2].

### FACILITIES DEVELOPMENT

In the fall of 1994, experimenters in the guide hall can expect an increase of at least a factor of five in the cold neutron flux to their instruments because of improvements to be made beginning in early 1994. Three major projects will be undertaken: installation of the remaining three guides of the CNRF; replacement of the cold neutron source; and replacement of the reactor heat exchangers. A shutdown of six to eight months is planned.

#### PRIMARY HEAT EXCHANGERS

A major upgrade of the reactor cooling systems has been scheduled, including replacement of the primary heat exchangers. Three new heat exchangers are being built as replacements (only two are needed for 20 MW), which will be installed during the shutdown. It will be necessary to move the instruments from the west side of the reactor in order to remove the heat exchangers from the building. The old helium refrigerator for the cold source will be removed at the same time. Completion of installation of the new heat exchangers will proceed in parallel with removal of the existing guides, the D<sub>2</sub>O cold source, and the Bi tip.

In addition to the heat exchangers, other major maintenance items are planned or contemplated, including the ion exchange system, shim arms, and D<sub>2</sub>O replacement for detritiation.

#### NEUTRON GUIDES

A number of improvements in the guides will result in a significant increase in the cold neutron flux received in the guide hall. The center plug (now containing only NG-3) and CTE, which have to be removed to replace the cold source, will be replaced with new in-pile pieces. NG-1 through NG-4 will be located in the new center plug, as shown in Figure 1. The sections comprising the next 4.5 m, currently helium filled<sup>1</sup>, will be encased in steel so that they may be evacuated. Because the casings are larger than the current guides, a single ex-core piece is needed for the first section of guides 5, 6, and 7. Guides 1, 2, and 4, along with the new in-pile pieces, will have supermirrors for their top and bottom surfaces, and <sup>58</sup>Ni sides.

Much of the shielding surrounding the guides will be replaced when the final three guides are installed. A 6 m guide, NG-0, will be installed at the end of CTW so that the cold neutron depth-profiling facility and neutron optical bench can occupy the space vacated by the old refrigerator. A 2 m section will be curved,

---

<sup>1</sup>Evacuated initially, these sections were filled with helium after a guide failure occurred. Details are given in the Proceedings of the 2d IGORR Conference.

with a 60 m radius; it is called a five-channel bender because it has 4 vertical surfaces within the guide. The curved guide will reduce the gamma-ray and fast-neutron background. All NG-0 surfaces will be supermirrors.

#### LIQUID HYDROGEN COLD NEUTRON SOURCE

A liquid hydrogen cold neutron source is being built to replace the D<sub>2</sub>O/H<sub>2</sub>O ice. A simple, passively-safe system has been designed, with multiple barriers preventing air from mixing with hydrogen. A thermosiphon will be used to maintain the LH<sub>2</sub> inventory in the moderator chamber, located in the cryogenic beam port. The thermosiphon relies on natural circulation; no pumps or moving parts are required to adequately cool the chamber. A hydrogen condenser, located on the face of the reactor above the guides, will be cooled by a new 3.5 kW helium gas refrigerator (1 KW required; 14 - 18K). A 2 m<sup>3</sup> ballast tank is connected to the condenser so the entire hydrogen inventory can expand freely into the tank, providing completely passive protection against refrigerator failures (see Figure 2).

The moderator chamber is a 2 cm thick spherical shell with an outside diameter of 32 cm and a volume of 5 liters; the interior is filled with vapor. A cold neutron flux trap is then created, as demonstrated by the annular cold source in the Orphée reactor at Saclay. A 20 cm diameter exit hole in the back side of the chamber shell fully illuminates the guides with cold neutrons from the flux



trap in the interior. Figure 1 shows the location of the cold source relative to the reactor core and the neutron guides. Monte Carlo calculations using MCNP [3] indicate the LH<sub>2</sub> source will increase the yield of long-wavelength neutrons (greater than 0.4 nm) by a large factor. The LH<sub>2</sub> source will be colder (21 K) than the D<sub>2</sub>O (40 K), and it will be 14 cm closer to the fuel (the Bi tip now shielding the D<sub>2</sub>O source can be removed).

MCNP calculations also indicate less than 1000 W will be deposited in the cold source from neutrons and gamma rays. Hydrogen will evaporate at 2 g/s and rise to the condenser, and condensed liquid will return by gravity to the moderator chamber. A concentric pair of tubes connect the chamber to the condenser, completing the thermosiphon. A full-scale model of the cryostat was built and tested by the Chemical Sciences and Technology Laboratory at NIST Boulder, which demonstrated that at least 2200 W can be removed from the chamber in this manner, with very stable two-phase return flow. The tests also indicated that the void fraction in the LH<sub>2</sub> at 900 W will be between 6% and 12%, depending on the pressure. The total hydrogen inventory is expected to be about 700 g (4 atm warm), with about 450 g of LH<sub>2</sub> while operating.

Each component of the hydrogen system is surrounded by a helium containment above atmospheric pressure. The containment provides another barrier preventing air from mixing with hydrogen, and makes it possible to immediately detect insulating vacuum leaks. If a

containment or insulating vacuum pressure varies outside its established limit, indicating that one of the barriers is compromised, the refrigerator will be shut down, allowing the hydrogen to expand into the ballast tank. The reactor will be shut down when the hydrogen pressure rises so as not to overheat the moderator chamber.

Once the tank is initially charged with hydrogen, the cold source can be operated and shut down any number of times without additional gas handling. Hydrogen will be removed only for major repairs, using a portable metal-hydride storage unit.

All components of the hydrogen system will be located within protective shields to eliminate the possibility of accidental ruptures. A safety analysis indicates that the cryostat components can withstand detonation of a stoichiometric mixture of hydrogen with the maximum amount of oxygen that may possibly be present in the component. In May, the U.S. Nuclear Regulatory Commission advised NIST that the  $\text{LH}_2$  source can be installed under the provisions of 10 CFR 50.59, subject to review and approval by the NBSR Safety Evaluation Committee.

The installation of the  $\text{LH}_2$  cold source will increase the yield of cold neutrons by at least a factor of three. Combined with other improvements, neutron intensities at the instruments of the CNRF are expected to be at least a factor of five greater than the

currently available intensities.

### INSTRUMENT DEVELOPMENT

Concurrent with the facilities modifications described above, a relocation of CNRF instruments is also planned for the shutdown period, as shown in Figure 3. Instruments which have come on line since IGORR-2 are described below.

#### THE NSF/NIST CENTER FOR HIGH RESOLUTION NEUTRON SCATTERING (CHRNS)

Much of what was envisioned when, in 1989, NIST and the National Science Foundation (NSF) agreed to establish the Center for High Resolution Neutron Scattering (CHRNS) at the CNRF has come to fruition in the past year. During that time the two CNRF instruments that the NSF has partially supported, a 30 m, high resolution, small angle neutron scattering (SANS) instrument and a cold neutron inelastic scattering spectrometer (known as SPINS for Spin Polarized Inelastic Neutron Scattering) have gone into operation. Guest researcher experiments approved by the CNRF'S Program Advisory Committee have been scheduled on the CHRNS SANS instrument since August, 1992, when the instrument was officially commissioned as part of the CNRF'S second Researchers' Group meeting. Since then roughly 75% of the available beam time on this instrument has been allocated to approved proposals, and, through June, 1993, 37 guest researcher experiments have been carried out. The SANS instrument (Figure 4) has a Q range extending from 0.015

to  $6 \text{ nm}^{-1}$ , and utilizes a 2-d detector of the ILL-type, capable of counting at rates in excess of 20,000/sec. Additional performance characteristics for the instrument are listed in Table 1.

The CHRNS SPINS spectrometer began phase I of its operation in the spring of 1993. The instrument is presently configured as a fixed incident energy, cold neutron triple-axis spectrometer, with focusing pyrolytic graphite monochromator and analyzer crystals, and is available part of the time for use by guest researchers for inelastic scattering measurements with unpolarized neutrons. In this mode the instrument also serves as a test bed for the development and testing of the wide-beam transmission polarizing devices and the Drabkin-type, energy-dependent spin flipper that will give this instrument its unique capabilities. When implemented over the next year, these devices will enable inelastic scattering measurements with full polarization analysis, and, in addition, will make it possible to partially decouple the momentum and energy resolution of the instrument to achieve high energy resolution ( $20 \text{ } \mu\text{eV}$ ) under conditions of moderately relaxed momentum resolution.

#### THE NIST/IBM/U. MINNESOTA NEUTRON REFLECTOMETER

The new reflectometer in the CNRF guide hall began operating in May 1993. This instrument is capable of reflectivity measurements from free liquid surfaces as well as solid surfaces. The new reflectometer permits the measurement of reflectivities as low as

$10^{-6}$ , which requires typical run times of ~8 h. A significant improvement in performance (~ 4-6 times increase in signal) is expected when the new liquid H<sub>2</sub> cold source is installed in 1994. As shown in Figure 5 a pyrolytic graphite monochromator array deflects neutrons onto a horizontal sample surface at a shallow angle of incidence. Reflected neutrons are measured by a detector after passing through an exit slit system. In a future version of the instrument, another detector will be added, capable of scanning a large angular range in order to perform surface diffraction measurements. Independent movement of both sample and detector will allow measurement of off-specular scattering. A position sensitive detector will also be installed in the near future. The performance characteristics are summarized in Table 1.

#### NEW POWDER DIFFRACTOMETER

The new high-resolution neutron powder diffractometer has been commissioned and is being scheduled for routine operation. The new instrument, shown schematically in Figure 6, has 32 detectors, arranged at 5° intervals around a circle in an assembly that can scan a 12° 2θ range, so that powder diffraction patterns can be collected over the entire range from 0° to 167°. There is a choice of three monochromator positions and takeoff angles, so that the peak-width minimum can be matched to the d-spacing range that is most important for each sample. Because of the excellent results from the old five-detector instrument for samples with large, but high symmetry, unit cells, one of the takeoff angles is 75°, with

a Cu 220 monochromator. A Si 531 monochromator at a takeoff angle of  $120^\circ$  gives high resolution for small, low symmetry unit cells, while a Cu 311 monochromator at a takeoff angle of  $90^\circ$  can be used for intermediate size cells. All choices have a neutron wavelength close to  $1.54 \text{ \AA}$ .

Selection of in-pile collimation of  $15'$  of arc permits rapid data collection for temperature-dependent studies, while  $7'$  of arc provides maximum resolution (as low as  $\sim 0.17^\circ$  FWHM,  $\Delta d/d = 9 \times 10^{-4}$ ). When compared with the five-detector instrument, the new diffractometer offers dramatic improvements in resolution (up to a factor of 3) and data collection time (up to a factor of 20). The three focusing monochromators all give Gaussian peak shapes, greatly facilitating Rietveld-refinement applications. In Figure 7 a comparison of data taken with the new and previous BT-1 instruments is made.

#### CNRF GUEST RESEARCHER PROGRAM

As a national facility dedicated to serving the needs of U.S. researchers in the area of cold neutron instrumentation, the CNRF issues calls for proposals twice yearly to inform the community about the opportunities it offers. The guest researcher program has now been functioning for almost two years. The fourth call for proposals was completed in July 1993, for beam time in the period

from Sept. 1993 to early 1994, until the start of the extended shutdown.

The response to the first three calls has shown steady growth, both in number and variety of proposals. The first call stimulated 39 proposals, requesting 165 instrument-days, while the third call elicited 65 proposals requesting 357 instrument-days. Proposals for SANS comprised almost all the first round proposals, but only about 60 percent of the total in the third round, with proposals for the new reflectometer, for the chemical analysis stations, and for the new inelastic scattering instruments making up the rest. The latest submissions spanned a very wide range of scientific areas ranging from biology to chemistry, physics, and materials science.

The Program Advisory Committee (PAC) is the body primarily responsible for determining the characteristics of the CNRF guest researcher program. First convened in 1989, it advises NIST administration on all aspects of CNRF operation. Twice yearly, the PAC meets to consider all proposals submitted in response to the most recent call, and determines whether each should receive beam time and how much time is to be allocated. Actual scheduling of beam time is carried out by NIST staff. An important element of the review process is peer review by mail, in which most proposals are sent out for external review before being considered by the PAC.

The CNRF Guest Researchers' Group is an independent body constituted to represent the interests of guest researchers at the facility. So far, it has had two meetings (in 1991 and 1992), with a third meeting planned for early 1994.

Finally, we note that the access procedures for guest researchers have been greatly simplified during the past year. For those with approved experiments at the CNRF or other facilities at the reactor, and who plan to spend less than 30 days in a calendar year at NIST (10 days for non-citizens), no prior paperwork is required beyond a letter of identification from the home institution.

#### ACKNOWLEDGEMENTS

The authors are indebted to a number of colleagues who contributed to sections of this manuscript.

#### REFERENCES

- [1] H.J. Prask, "The Reactor and Cold Neutron Facility at NIST," Neutron News 1, 9-13 (1990).
- [2] "NIST Cold Neutron Research Facility," J. Res. - NIST (Special Issue) 98, #1 (1993).
- [3] "MCNP - A General Monte Carlo Code for Neutron and Photon Transport (Version 3A)", LA-7396-M, Rev. 2, J.F. Briesmeister, Ed, Los Alamos National Lab (1986).



**Table 1. CHRNS 30-m SANS Characteristics and Performance**

Source:	neutron guide (NG-3), 6 × 6 cm <sup>2</sup>
Monochromator:	mechanical velocity selector with variable speed and pitch
Wavelength Range:	0.5 nm to 2.0 nm
Wavelength Resolution:	8% to 30% $\Delta\lambda/\lambda$ (FWHM)
Source-to-Sample Dist.:	3.5 m to 16 m in 1.5 m steps via insertion of neutron guide sections
Sample-to-Detector Dist.:	1.3 m to 13 m continuously variable
Collimation:	circular pinhole collimation
Sample Size:	0.5 cm to 2.5 cm diam
Q-Range:	0.01 to 6.0 nm <sup>-1</sup>
Size Regime:	0.5 nm to 500 nm
Detector:	65 × 65 cm <sup>2</sup> <sup>3</sup> He position sensitive proportional counter (1 × 1 cm <sup>2</sup> resolution), ILL type
Ancillary Equipment:	<ul style="list-style-type: none"> <li>- automatic multispecimen sample changer with temperature control from -10 to 200 C</li> <li>- electromagnet (0 to 15 Kgauss)</li> <li>- couette type shearing cell</li> <li>- cryostats and vacuum furnace (10 to 1800 K)</li> </ul>

Neutrons on Sample vs. $Q_{min}$	$Q_{min}$ (nm <sup>-1</sup> )	$I_s a$ (n/sec)
	0.015	$3.7 \times 10^3$
	0.030	$3.4 \times 10^4$
	0.050	$2.6 \times 10^5$
	0.10	$1.0 \times 10^6$
	0.20	$3.5 \times 10^6$

\*for 1.5 cm diam sample and  $\Delta\lambda/\lambda = .25$  at 15MW reactor power.

Table 2. Reflectometer Characteristics

Monochromator:	Pyrolytic graphite
Wavelength range:	0.235, 0.407, 0.47, and 0.55 nm
Wavelength resolution:	2.5% $\Delta\lambda/\lambda$
Beam size (continuously variable):	.05 x 50 mm to 4 x 50 mm
Q range:	0.03 to 4 nm <sup>-1</sup>
Q resolution:	Variable with slits from .04 to .15 $\Delta Q/Q$
Monochromator-to-sample distance:	2m
Sample-to-detector distance for reflectivity detector:	2m
Angular range for grazing incidence diffraction detector:	5° - 140°.

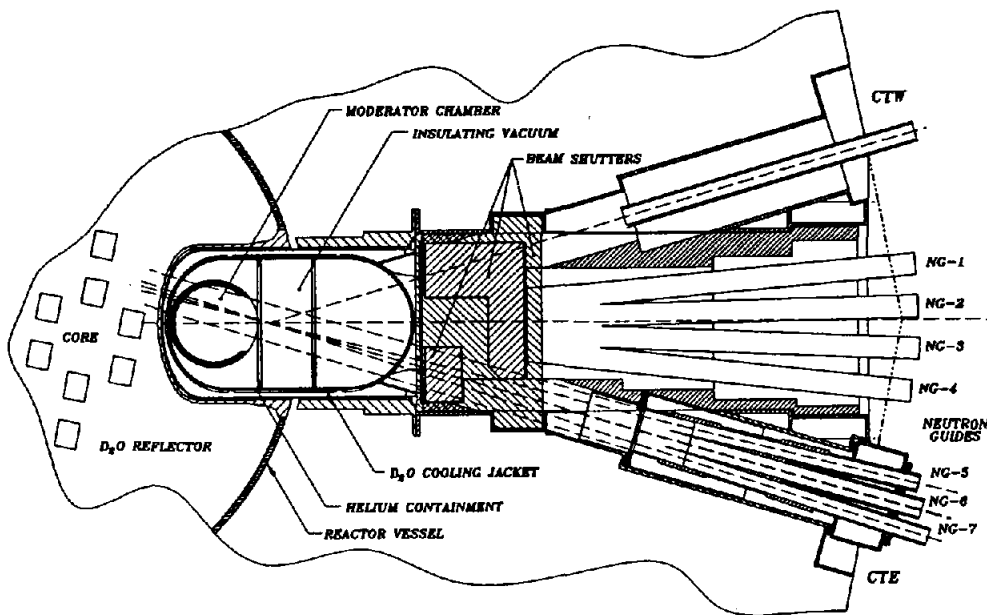


Figure 1. Plan view of the cold source region of the reactor.

**HYDROGEN COLD SOURCE THERMOSYPHON**

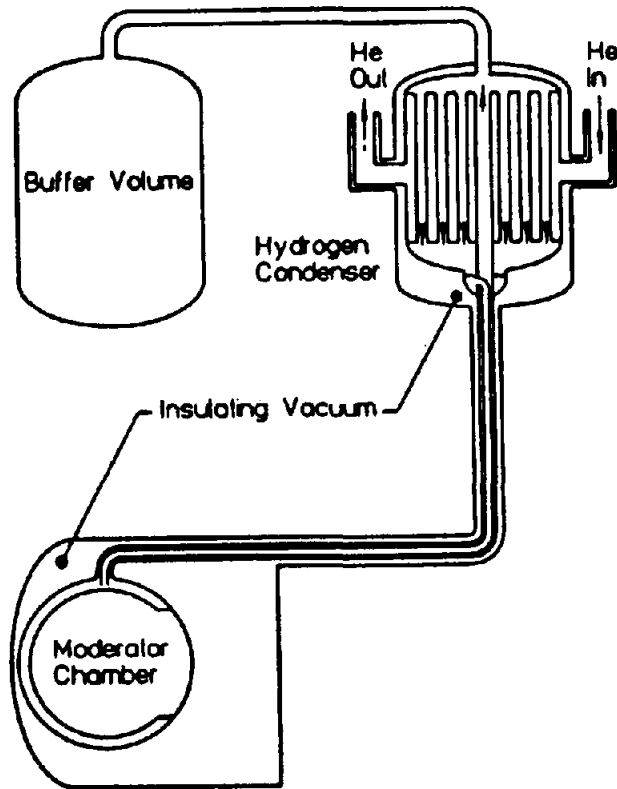


Figure 2. Schematic of the new L-H<sub>2</sub> cold source facility.

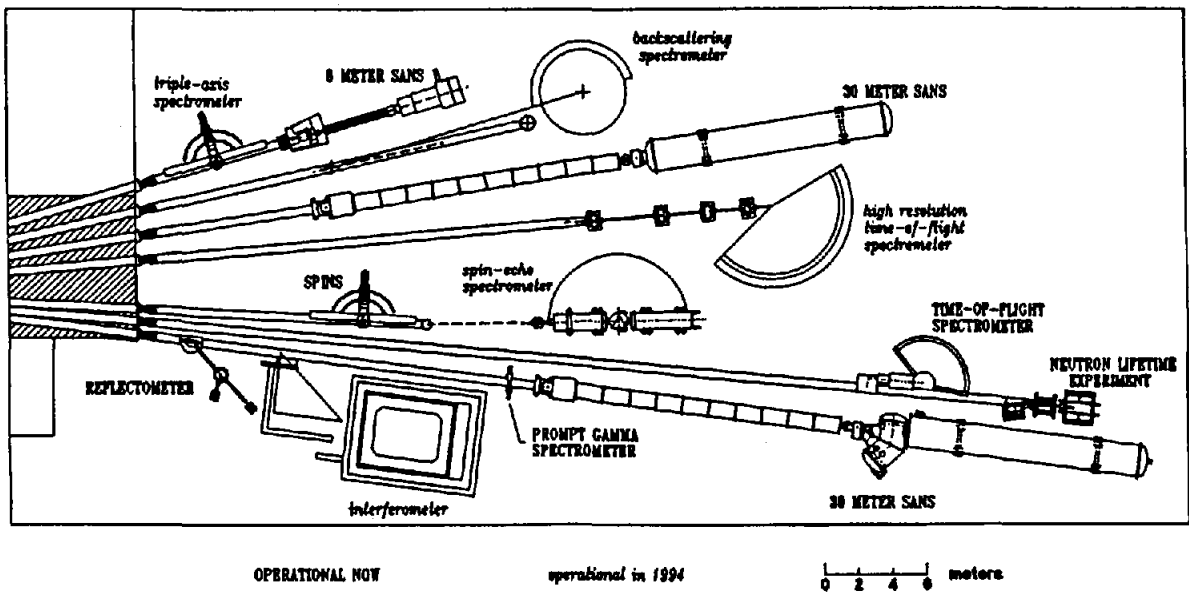


Figure 3. Floor plan of the CNRF after the 1994 shutdown.

CHRNS 30 METER SANS INSTRUMENT

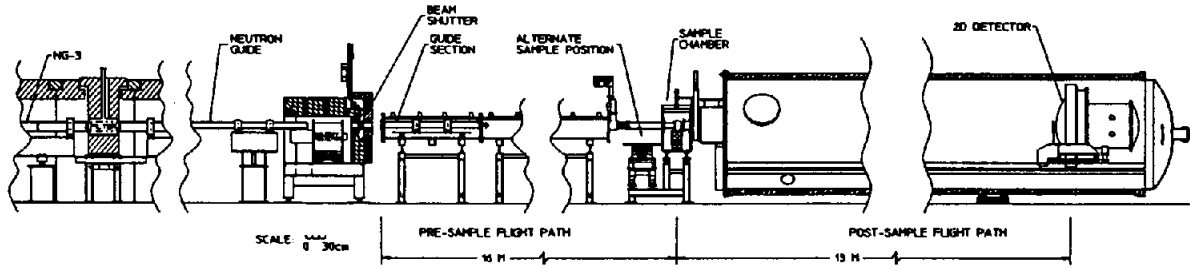


Figure 4. Schematic of the CHRNS 30-m SANS spectrometer.

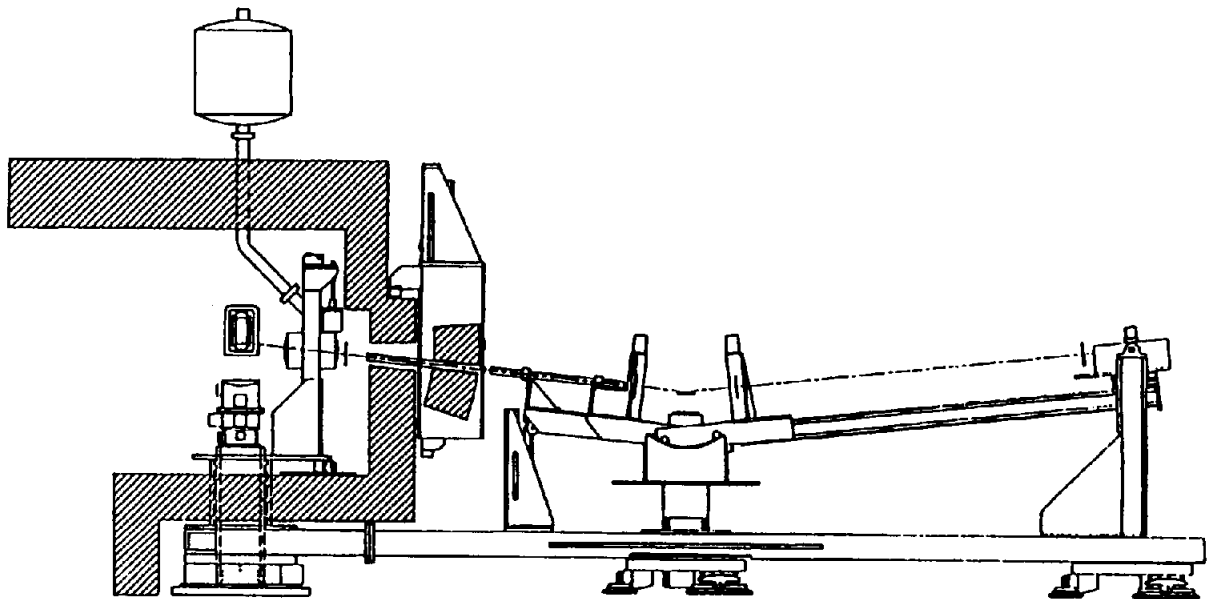
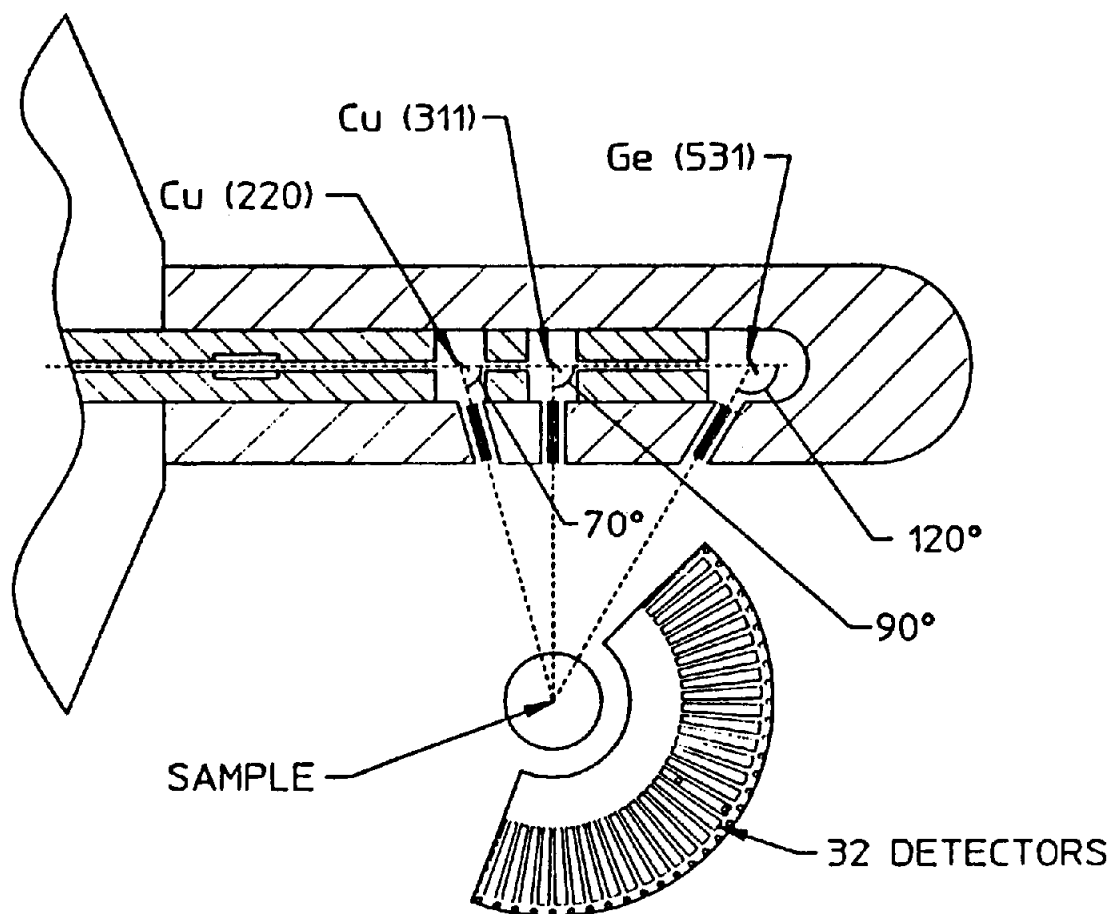
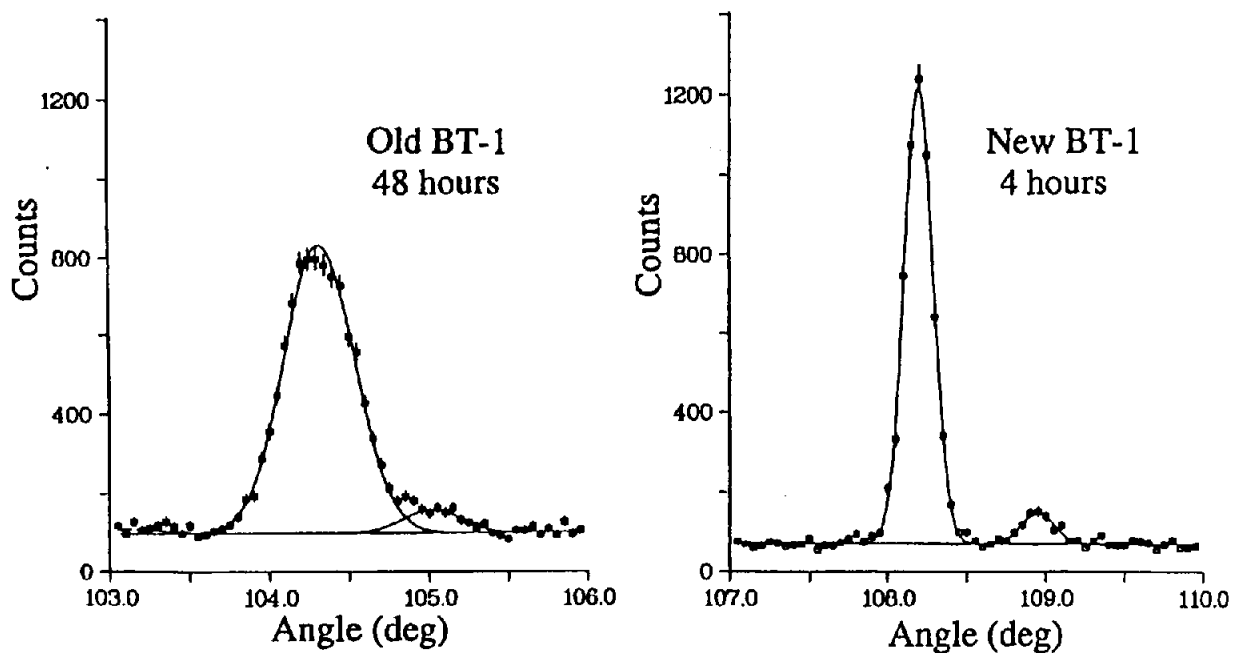


Figure 5. Schematic of the cold neutron reflectometer.



**Figure 6.** Schematic of the new high-resolution powder diffractometer, installed on BT-1.



**Figure 7.** A portion of the neutron diffraction pattern of  $Tb_2Ti_2O_7$ . Old BT-1: Cu 220 monochromator,  $\lambda = 1.54\text{\AA}$ , 10'-20'-10' collimation, FWHM =  $0.51^\circ$  New BT-1: Si 531 monochromator,  $\lambda = 1.57\text{\AA}$ , 15'-30'-7' collimation ("low" resolution option), FWHM =  $0.21^\circ$ .

## PRESENT STATUS OF JRR-3M

Eiji SHIRAI

Department of Research Reactor  
Japan Atomic Energy Research Institute  
Tokai-mura, Naka-gun, Ibaraki-ken 319-11, Japan

## INTRODUCTION

JRR-3 was a heavy water moderated and cooled tank type reactor with slightly enriched uranium fuels. JRR-3 was constructed by Japanese staff for studying the reactor technology in Japan. Its thermal output was 10MW and it was operated and utilized for about twenty years. But its thermal neutron flux was an order of  $10^{13}$  n/cm<sup>2</sup>-sec and slightly low for the recent demand of research and developments, therefore JRR-3 was modified and upgraded to JRR-3M. Modification works were started in 1986 and got the first criticality in March, 1990. After that, JRR-3M has been operated successfully.

## JRR-3M

JRR-3M is a light water moderated and cooled, heavy water reflected pool type reactor with 20MW. There are 26 standard fuel elements and 6 control rod elements with follower fuels in the core. Fuel elements are U-Alx dispersed MTR type fuels and their enrichment is about 20%. Its full power operation was established in November, 1990.1), 2), 3), 4)

JRR-3M is operated with seven or eight operation cycles in each year. Its operation cycle is basically consist of four weeks of full power operation and one week of shut down for refueling, irradiation capsule handling and maintenance works. Figure 1 shows the reactor operation data. The JRR-3M was operated twenty two cycles in total, and the integrated thermal power of 10,000 MWD was attained at the end of September, 1993 ( Table 1 ).

A core of the JRR-3M is divided into five parts for refueling, and the standard and follower fuels in each part are refueled during the shut down period. So, five or six standard fuels are exchanged to new ones in a cycle. Average burn up of standard fuels is about 21%U-235, and the maximum burn up of the fuels is about 40%U-235. Six follower fuels are refueled at intervals of five cycles. The averaged burn up of follower fuels just before the refueling is about 25%U-235, and the maximum burn up of the fuels is about 38%U-235. Figure 2 shows a change of excess reactivity from the beginning of the operation. Since it is difficult to divide the core equally and the reactivity of irradiation samples is changed every cycles, it shows unevenness of the reactivity at the beginning of cycle or the end of cycle.

Figure 1 shows nine unscheduled shutdowns experienced in JRR-3M. Most of the shutdowns are caused by natural phenomena directly or indirectly, that is an earthquake or a loss of electric power supply. Table 2 shows the unscheduled shutdowns including the results and the counter measures. The JRR-3M experienced three unscheduled shutdowns except that caused by an earthquake or a loss of electric power supply. First unscheduled shutdown was occurred in the 4th cycle and it caused by some confusion of an operation manual of experimental facilities. But the reactor itself had no damage and restarted its operation immediately. Control rods of the JRR-3M are held by electrical magnets. Trouble of this control rod holding circuit was occurred in the 13th operation cycle. It caused by an aging of fuses in the circuit. In the 20th cycle, a flow meter of secondary coolant of helium compressor in the Cold Neutron Source (CNS) facility made a signal of low flow rate and made the compressor stop. The reactor is designed to be shut down if the helium compressor in CNS facility stops. Actually, the secondary pump was running, and the trouble originated from noise by air in the flow meter. These troubles did not cause any significant impacts to reactor utilization and reactor itself.

### EXPERIMENTAL FACILITIES IN JRR-3M

JRR-3M has both of irradiation facilities and beam experimental facilities. The irradiation facilities using eighteen vertical irradiation holes are listed in Table 3. Nine irradiation holes are located in the core region for the capsule irradiation. They are used for material irradiation tests and radio isotope (RI) production. In the heavy water reflector region, nine vertical holes are arranged. One of the holes is used for the CNS facility and the others are used for the irradiation experiments such as an activation analysis, a semiconductor

production by silicon doping, RI production and so on. For the neutron beam experiment, JRR-3M has nine beam tubes. The thermal neutron flux measured at the end of the tubes are shown in Table 4. Two beam tubes are used for the neutron guide tubes. One of these is for thermal neutron beam and another is for cold neutron beam. The thermal neutron beam is separated into two beams, and the cold neutron beam is separated into three beams. All thermal / cold neutron beams are lead to the beam hall and served to beam experimental instruments.

The CNS facility in JRR-3M is a vertical thermosyphone type using liquid hydrogen at 20K as the moderator. A schematic diagram of the CNS facility is shown in Fig. 3, and design parameters and operational feature are shown in Table 5. This facility was operated all during the reactor operation. Table 6 shows the operation record of the CNS facility. The CNS facility experienced just one trouble throughout its operation, and this trouble was initiated by flow meter in the compressor cooling system, and there was no damage to the CNS facility.<sup>5)</sup>

A prompt gamma ray analyzing (PGA) system was constructed for a new experimental equipment at JRR-3M. This analysis is an elemental and isotopic analytical technique. The system can be set at cold and thermal neutron beam guides. A schematic diagram of the PGA system with the extended evacuated guide tube is shown in Fig.4. The system consists of a beam shutter, beam collimator, sample box, beam stopper, neutron and gamma ray shieldings, and a multi-mode gamma ray spectrometer. Using PGA system, it became to be able to analyze elements that cannot be determined by an instrumental neutron activation analysis.<sup>6)</sup>

Neutron radiography (NRG) facility is a non-destructive testing device which utilizes the penetrating nature of neutron. Figure 5 shows the JRR-3M NRG facility. It is used for many research works such as the inspection of spent fuels and irradiated capsules, the visualization of air-water two-phase flow, the observation of plant roots, the characterization of cancer and so on.

## CONCLUSION

JRR-3M started its operation in November, 1990, and the integrated thermal power of 10,000 MWD was attained in September, 1993. Throughout the operation, JRR-3M experienced nine unscheduled shutdowns due to minor troubles without any significant impacts to reactor utilization and reactor itself. JRR-3M serves thermal / cold neutrons to the beam hall through the neutron guide tubes, and nineteen beam experimental instruments are set up in the hall. PGA system is one of the instruments, and is useful for an elemental and isotopic

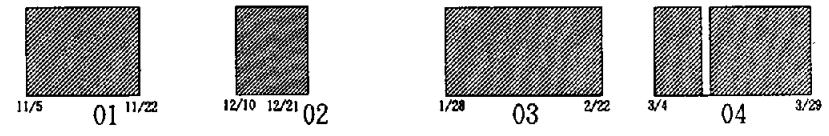


analysis. The NRG facility is also an useful instrument for analysis of thermohydraulic experiment and as an innovative technique.

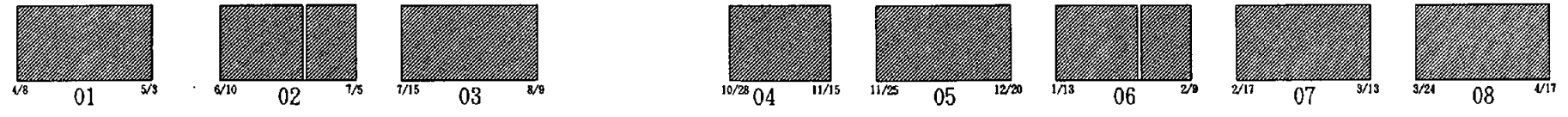
## REFERENCES

- 1) N. Onishi, H. Takahashi, M. Takayanagi and H. Ichikawa, "Reactor Design Concept and Commissioning Test Program of the Upgraded JRR-3", Proceedings of the American Nuclear Society International Topical Meeting on the Safety, Status and Future of Non-Commercial Reactors and Irradiation Facilities, Boise, USA, September 31 - Oct. 4, 1990.
- 2) H. Ichikawa, M. Takayanagi, M. Watanabe, N. Onishi and M. Kawasaki, "Commissioning Test of Low Enriched UAlx Fuel Core on Upgraded JRR-3", Proceedings of the Int. RERTR Meeting, Newport, USA, September 23-27, 1990.
- 3) K. Kakefuda, M. Tani and M. Issiki, "Completion of Reconstruction for Japan Research Reactor NO.3", Proceedings of the Third Asian Symposium on Research Reactor, Hitachi, Japan, November 11-14, 1991.
- 4) S. Matsuura and E. Shirai, "Current Status of Research and Test Reactors in JAERI", Proceedings of the IGORR- II , Saclay, France, May 18-19, 1992.
- 5) S. Matsuura, E. Shirai and M. Takayanagi, "The CNS Facility and Neutron Guide Tubes in JRR-3M", Proceedings of the IGORR- II , Saclay, France, May 18-19, 1992.
- 6) C. Yonezawa, A. K. H. Wood, M. Hoshi, Y. Ito and E. Tachikawa, "The Characteristics of the Prompt Gamma-Ray Analyzing System at the Neutron Beam Guides of JRR-3M", Nuclear Instruments and Methods in Physics Research A329, 1993.

FY 9 0

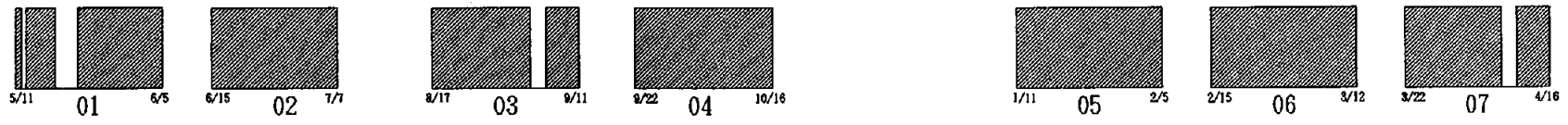


FY 9 1



— 08 —

FY 9 2



FY 9 3

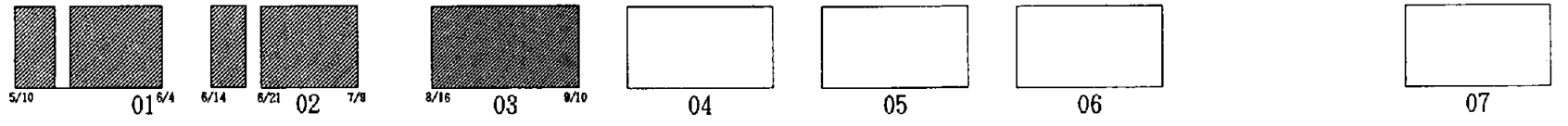


Fig. 1 Operation record of JRR-3M

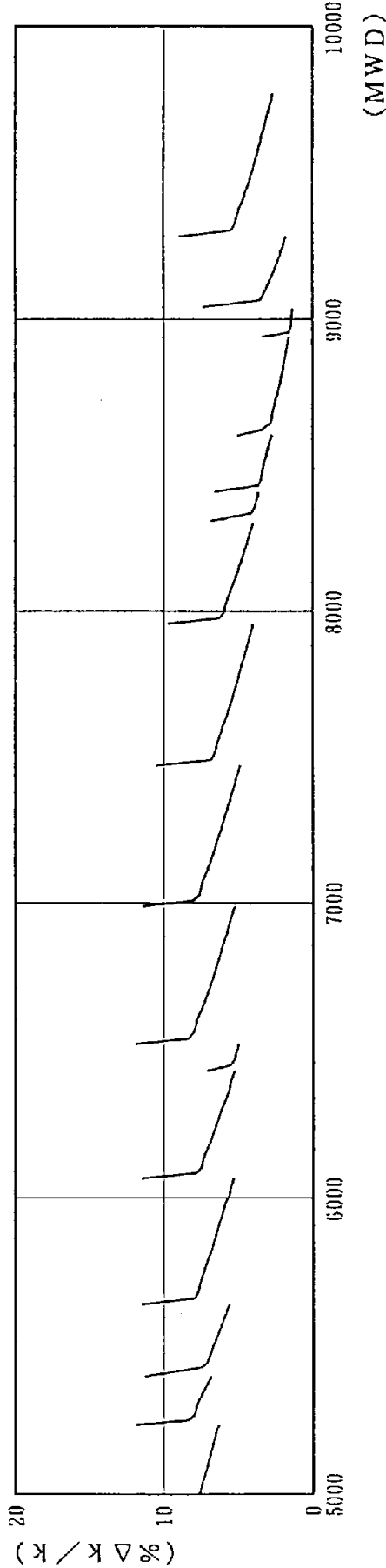
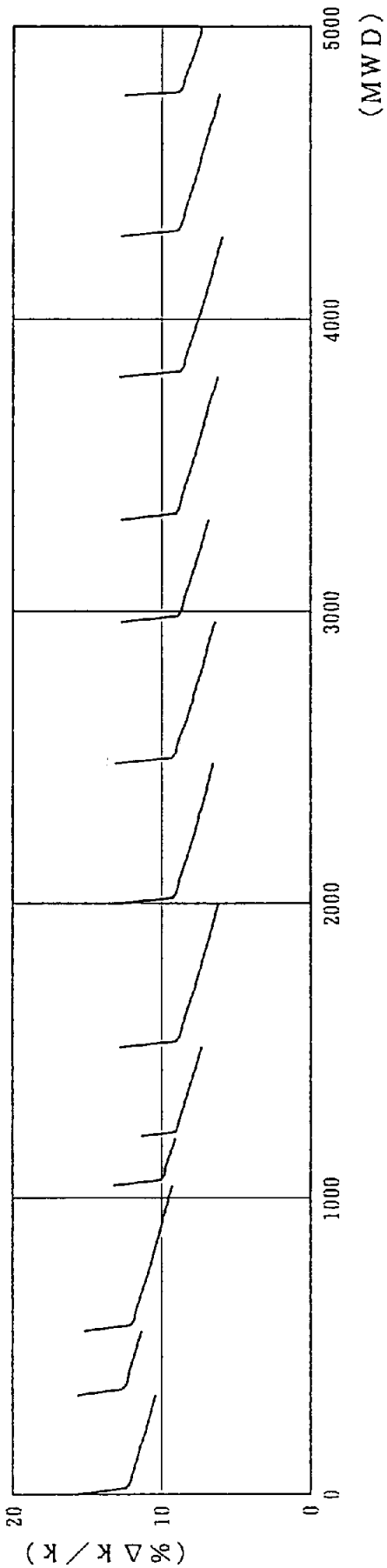


Fig. 2 Excess reactivity change with burn-up of JRR-3M

Table 1 Operation Record of JRR-3M

Fiscal Year	Cycle	Operation Time (Hr. Min)	Integrated Output (MWD)	Unscheduled Shutdown
1990	4	2638hr 53 min	1678.4	1
1991	8	4689hr 46 min	3725.4	2
1992	7	4001hr 38 min	3174.1	5
1993	3 (7)	1723hr 37 min	1370.7	1
TOTAL	22	13,053 hr 54 min	9948.6	9

( ) in Cycle shows the number of scheduled cycles

Table 2 Unscheduled Shutdown of JRR-3M

Date	Facilities	Equipment	Result	Counter Measure
Mar. 12, 91	Irradiation Facilities	Pneumatic tube	Operation error	Amendment of operation manual
Jun. 25, 91			Earthquake	
Feb. 1, 92			Loss of power	
May 11, 92			Earthquake	
May 18, 92	CRDM	Magnet Coil	Inspection	Change of coil
Jul. 7, 92	CRDM	CR holding circuit	Aging of fuse	Exchange of fuse Increase of capacity
Sep. 4, 92			Loss of power	
Apr. 9, 93			Loss of power	
May 17, 93	CNS	Flow meter of secondary coolant of helium compressor	Noise by bubbles	Increase of time constant

Table 3 Irradiation Facility in JRR-3M

Name	Size and Number	Neutron Flux (n/cm <sup>2</sup> ·sec)		Application
		Thermal	Fast	
Hydraulic rabbit (HR)	φ 37x2	1x10 <sup>14</sup>	1x10 <sup>12</sup>	·RI production
Pneumatic rabbit (PN)	φ 37x2	6x10 <sup>13</sup>	1x10 <sup>11</sup>	·RI production
Activation Analysis (PN3)	φ 20x1	2x10 <sup>13</sup>	4x10 <sup>9</sup>	·Activation analysis
Uniform irradiation (SI)	φ 170x1	3x10 <sup>13</sup>	3x10 <sup>11</sup>	·Material irradiation ·Silicon doping
Rotating irradiation (DR)	φ 140x1	8x10 <sup>13</sup>	2x10 <sup>11</sup>	·Large material irradiation
Capsule irradiation (RG,BR,VT-1,SH)	φ 60x5 φ 45x4 φ 100x1	3x10 <sup>14</sup> 2x10 <sup>14</sup> 8x10 <sup>13</sup>	2x10 <sup>14</sup> 5x10 <sup>13</sup> 2x10 <sup>11</sup>	·Exposure test ·RI production

Table 4 Measured Thermal Neutron Flux at the End of Beam Tubes at clean core

Beam Tube Name	Thermal Neutron Flux (n/cm <sup>2</sup> ·sec)
1 - G	1.2 × 10 <sup>9</sup>
2 - G	( not measured )
3 - G	3.3 × 10 <sup>9</sup>
4 - G	3.0 × 10 <sup>9</sup>
5 - G	( not measured )
6 - G	3.5 × 10 <sup>9</sup>
7 - R	1.2 × 10 <sup>9</sup>
8 - T	7.4 × 10 <sup>9</sup>
9 - C	1.5 × 10 <sup>9</sup>

Table 5 JRR-3M CNS Facility

DESIGN PARAMETERS

TYPE	Vertical Thermosyphone Type
MODERATOR	Liquid Hydrogen, 20K
COOLANT	Helium Gas
MODERATOR CELL	Flask Shape, 200mmH × 130mmW × 50mmT, 0.8ℓ Stainless Steel, 0.8mmt
VACUUM CHAMBER	φ154mm, 8mmt, Stainless Steel

OPERATIONAL FEATURE

PRESSURE OF HYDROGEN	1.2ata
VOLUME OF LIQUID HYDROGEN	1.5ℓ
NUCLEAR HEAT	400W
THERMAL RADIATION HEAT	150W
COLD NEUTRON GAIN	10 ( at the wave length of 0.5nm)

Table 6 Operation record of CNS facility

Fiscal Year	Operation Time ( Hour )	Trouble
1990	2,100	0
1991	4,870	0
1992	4,320	0
1993	1,860	1 ( Noise by Bubbles )
Total	13,150	1

At the end of 05-03 cycle

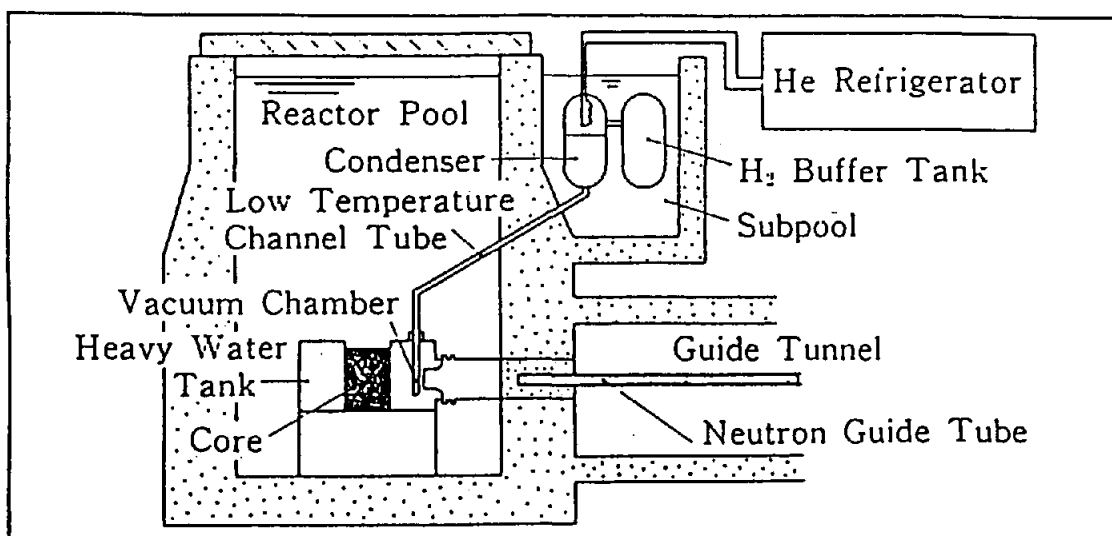


Fig. 3 Schematic diagram of JRR-3M CNS facility

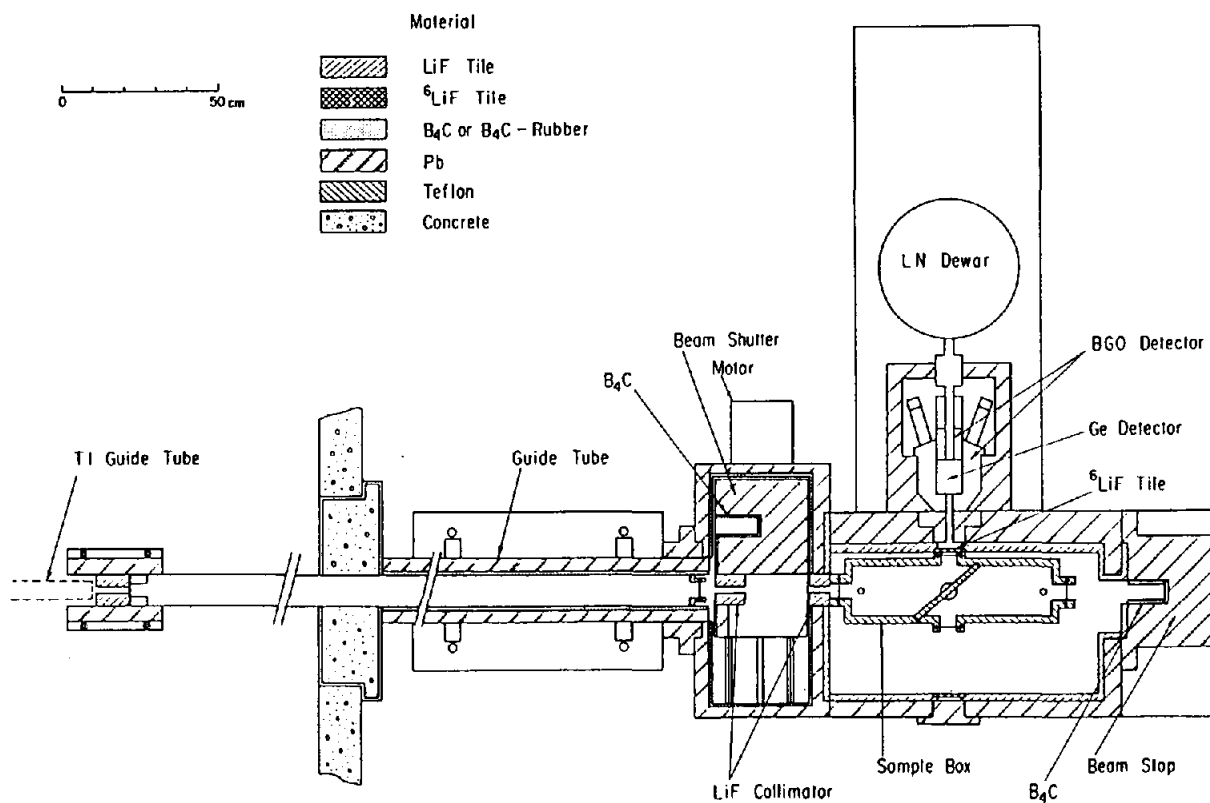


Fig. 4 Layout of the JRR-3M PGA system at the thermal neutron guide beam

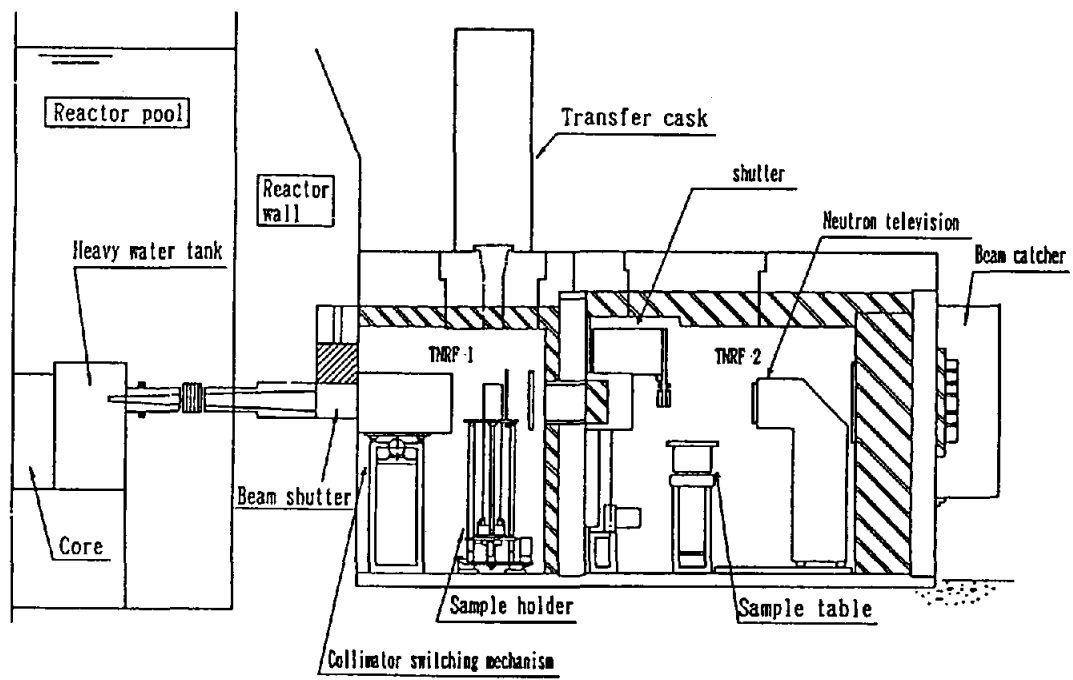


Fig. 5 Thermal neutron radiography facility in JRR-3M



**Status of FRJ-2 Refurbishment of  
Tank Pipes and  
Essential Results of Aging Analysis**

**G. Hansen**

**G. Thamm**

**M. Thomé**

**Forschungszentrum Jülich GmbH  
Zentralabteilung Forschungsreaktoren und  
Kerntechnische Betriebe**

**Summary**

An aging evaluation program for FRJ-2 (DIDO) of the Forschungszentrum Jülich GmbH has been developed and is currently executed in cooperation with the licensing and regulatory and TÜV experts in order to determine the overall life expectancy of the facility and to identify critical systems and components that need to be upgraded or refurbished for future safe reactor operation.

In Phase A (completed) a so called master list of the FRJ-2 mechanical, electrical and structural components was compiled on a system-by system basis and the operational documentation with respect to regular inspections, maintenance, repair and unusual occurrences was carefully examined. Critical components were selected and their ageing respectively life limiting mechanisms identified.

In Phase B (currently under way) special inspections, examinations and tests for critical systems/components are being elaborated, executed and evaluated.

Current work is being concentrated on non replaceable components (e.g. reactor aluminium tank (RAT) and the connecting pipes to the primary cooling circuit, the reactor steel tank and pipe work inside the concrete reactor block).

As a consequence of first results of the aging evaluation program and due to leaks in the weir and drain pipes of the RAT a repair/refurbishment program was set up for the Al-RAT pipes (risers, downcomers, weir and drain pipes) and the steel guide tubes. Details of the r/r program which is in far progress and first essential results of the aging evaluation will be presented.

The results achieved until today are encouraging with respect to safe reactor operation on short and medium term.

## 1. Introduction and Overview

First critical in November 1962 FRJ-2 reached its original design power of 10 MW in 1963. FRJ-2 is a heavy water moderated and cooled research reactor of DIDO-Type. Table 1 gives some important data of the facility.

Tab. 1: Some important Data of FRJ-2

Type:	Tank (MTR-tubular)
Construction:	1957-1962
1st Criticality:	November 1962
Power (MWM) Design/Upgrading:	10/15/23
Neutron Flux (1/s):	
- max. therm:	$2 \times 10^{14}$
- max. fast: ( $> 0.1$ MeV)	$1 \times 10^{14}$
Exp. Channels	
- vertical	
• core:	25
• reflector:	15 (D <sub>2</sub> O) + 10 (graphite)
- horizontal	
• reflector:	10 (D <sub>2</sub> O) + 21 (graphite)
No of Experiments (Simultaneous)	30-35
Utilization:	Beam Exp./Spec. Irradiations
Special features:	CNS/ELLA*) (1971) opt. CNS/ELLA (1986)
Status:	repair/refurbishment measures under way, operation scheduled begin 1994

\*) CNS: Cold Neutron Source; ELLA: External (Cold) Neutron Guide Hall

Figure 1 shows the reactor block and the primary cooling circuit. Although FRJ-2 originally had been designed for multipurpose experimental utilization there was a strong shift from a nearly balanced experimental operation (beamhole-/irradiation experiments) to beam experiment utilization (~ 90%) from the late seventies until today.

## **2. Aging Evaluation Program**

Although conceptual design studies for major modifications of FRJ-2 (DIDO) and even a new reactor to replace DIDO (/1/-/5/) have been elaborated in the past (starting in the late seventies and being continued with increased intensity and in cooperation with German and French companies from 1986 until today) it has been always inevitable to also evaluate the technical status of DIDO- now about 30 years old - with respect to further life expectancy. After many discussions with the atomic licensing and regulatory authority and TÜV experts the decision was taken end of 1990 to elaborate and execute an aging evaluation program for FRJ-2 (DIDO).

### **2.1 Features, Objectives, Phases**

The overall objective of the aging evaluation program (AEP) is to determine the life expectancy (residual working life) of FRJ-2 by executing suitable investigation (inspection) measures taking into account special design features of the facility, past operation period and operation experience. It also should be determined to what extent modification, refurbishment or replacement measures have to be taken today or in the near future to guaranty the safe operation of the facility according to the present state of the art of science and technology. The aging evaluation program is being focussed at the systems and components of the reactor only (not at experiments and experimental supply systems).

The AEP is being executed in a two phased approach (Phase A and B). The different working steps and the sequence of steps for the program can be seen in a schematic survey from Fig. 2.

In phase A an inventory of all systems and components is drawn up and relevant technical data including age are compiled. In parallel operation documents, results of regular inspections and unusual occurrences/events are evaluated in order to determine critical components with susceptibility to malfunction and aging effects. Comparable occurrences/events at other nuclear facilities are assessed to get additional indications on critical (groups of) components when compared with FRJ-2 experiences. Finally life limiting effects and aging/damaging mechanisms (e.g radiation, thermal embrittlement, corrosion, erosion, fatigue, wear) are identified and compiled for association with critical components. On completion of phase A all components that need further detailed inspection analysis will be selected for Phase B. As a first working step inspection programs and analysis methods for critical components have to be elaborated and executed. By a comprehensive safety evaluation of the

inspection/analysis results finally life expectancy (residual working life) shall be assessed. Furthermore requirements and technical/administrative measures necessary to continue reactor operation for the assessed residual working life have to be determined.

## **2.2 Some Results of Phase A /6/\* )**

First of all the inventory of all systems and components was taken and a so called master list was compiled. According to the master list consequently all relevant technical data including age of the component were collected and stored by using adequate computer software. The 3 remaining working steps of Phase A (see Fig. 2) were executed in parallel so that the analysis/evaluation of the operation experience, of the results from the regular inspections and of unusual occurrences/events directly was used to determine how and to what extent different life limiting factors and aging/damaging mechanisms were affected for critical components in the past. Some results will be given for selected factors/mechanisms:

### **- mechanical and thermal load.**

Since static pressures and temperatures below 100° are predominant at FRJ-2 particular damage/aging effects on components of metallic material can be excluded. Some investigations, however, on nonmetallic/nonferrous materials will be necessary.

Likewise structural investigations (calculations) for piping systems (mainly for the primary cooling circuit) taking thermal movements into account are being carried out. The results achieved to date are encouraging.

No unusual occurrences/events with the exception of a pressure leakage test in the lower part of one riser have been found where design data (limits) were exceeded in the past. The assessment of the mentioned (over)pressure during the leakage test did not reveal any damaging effects.

### **- corrosion**

Corrosion of components is dependent on environmental conditions and operating media. Corrosion might be induced and favored by leakages or operation with non specified media in gas or water systems.

Whereas no (significant) deviations from media specifications were found during operation in the past leakages of D<sub>2</sub>O into the annular gaps formed by the RAT-A1 pipes and the enclosing steel tubes (see. Fig. 3) were detected twice (1980 weir pipe, 1990 drain pipe).

---

\*) Work of the Phase A of the AEP mainly was done by TÜV experts being well familiar with DIDO

Therefore comprehensive investigations on the corrosion status of RAT and RAT pipes were carried out recently as an advanced part of Phase B of the AEP (see 2.3.2).

Since the leakages of the drain and weir pipes led to increased corrosion and deposition of corrosion products within the gaps - above all in the region of the stuffing box seals that have to provide for different thermal expansion of Al- and steel tubes (see Fig. 4) - reduction of the thermal movements and even solid seizure could not be excluded. Therefore a thermal stress/fatigue analysis of RAT (bottom region) also was carried out recently (see 2.3.1).

- **radiation**

Only structural parts of the RAT in the core or very near to the core are exposed to a fast neutron flux of about to  $10^{14}$  n/cm<sup>2</sup>s. The fast flux dose ( $E > 0.1$  MeV) accumulated from the startup Nov/1962 until now is about  $5 \cdot 10^{22}$  n/cm<sup>2</sup> in the core (median plane) and less than  $10^{22}$  n/cm<sup>2</sup> for the grid plate and 2TAN channel. The flux for all other parts of the RAT (including horizontal channels, RAT walls in the radial and bottom region) is much smaller (at least one or several orders of magnitude). Due to the relatively small fast dose ( $< 10^{22}$  n/cm<sup>2</sup>) damaging effects by radiation embrittlement on 2TAN and grid plate can be excluded today and also for the residual working life.

- **other factors/mechanisms**

particular (mechanical) wear must be taken into account for active components, e.g. "moving" piping systems, all types of bearings, slide ring sealings, cone belts etc. The extent of aging and wear depends on service life and cycles mainly. By the regular inspection program carried out by the operator to some extent in cooperation with TÜV experts affected components can be safely detected and replaced if necessary. This procedure (safe detection by inspection and subsequent replacement) is of particular importance for sliding/sealing parts of safety systems as the fast shut down system and the coarse control arms of FRJ-2. Therefore life limiting effects for these systems are of minor importance.

### **2.3 Status of Phase B, Essential Results**

During Phase A it became obvious that there were at least two issues which need urgent investigation so to speak as an advanced part of Phase B.

These issues are (see 2.2)

- corrosion of RAT and RAT pipes
- restricted thermal expansion of RAT pipes.

Therefore an investigation program on these issues was elaborated discussed in detail with representatives of regulatory bodies and TÜV and executed nearly completely to date.

Results will be given in 2.3.1 and 2.3.2. Furthermore for the refurbishment of the RAT pipes the primary cooling circuit had been dismantled to a great extent so that special aging investigations on dismantled and not dismantled components (e.g. x-ray inspection of welds, eddy current examination of heat exchanger tubes) were carried out. The results achieved to date are positive with no restrictions on further operation.

### 2.3.1 Stress/Fatigue Analysis of the RAT (Bottom)

The corrosion and deposition of corrosion products in the annular gaps between RAT-Al-tubes and the enclosing steel tubes caused great concern because restricted thermal movements of the RAT pipes against the steel tubes would give rise to thermal stress for the RAT at the positions where the tubes (risers, downcomers, drain and weir pipe) are welded to the RAT bottom. Efforts to measure the restricted thermal movements by heating up the RAT tubes in the lower part did not lead to satisfactory results. Therefore solid seizure for some of the RAT tubes could not be excluded. First calculations using a finite elements computer code revealed that under the pessimistic assumption of all RAT tubes being seized the elastic limits (yield strength) of the RAT bottom region would have been exceeded significantly.

During refurbishment work RAT-Al tubes and enclosing steel pipes were cut off together as one unit about 10 cm below the ceiling of the D<sub>2</sub>O plant room. 4 units (2 risers and downcomers each) were taken unchanged with respect to the corrosion state in the annular gap to determine the displacement of the Al tube against the steel tube as a function of the strength applied to the Al tube (fixed steel pipe) using a special device. The strength was determined up to and even exceeding the values that had been measured for the displacement after the power upgrade from 15 MW to 23 MW under normal operation (temperature) conditions in 1972.

By calculations using the measured displacement/strength function up to maximum D<sub>2</sub>O temperatures during operation it was found that around 1000 load cycles would be the permissible limit before formation of cracks will start /4/. Assumed that restrictions of the thermal movement of the RAT tubes were not significant before 1979 (first leakage observed by weir pipe 1980) about 200 load cycles must be taken into account from 1979 until 1990. This figure is well below the limit mentioned above so that damaging effects in the past can be

excluded. A fatigue analysis for the RAT bottom region with the replaced parts of Al/steel tubes (bellows in the enclosing steel pipes will provide for the different thermal expansion) considering the temperature differences during normal operation at RAT bottom has demonstrated that around 34000 load cycles will be upper limit /8/.

### 2.3.2 Investigations on the Corrosion Status of RAT and RAT-Pipes

Concerning the ageing evaluation program the reactor aluminium tank (RAT) and the 9 vertical RAT-pipes (Al 99.8) for D<sub>2</sub>O circulation were inspected (Fig. 3+4). Cut off parts of the RAT-pipes were also investigated. Inspections (Fig. 5) were done with optical methods (periscope, mirror, video microscope, videoscope) and other non-destructive methods of material testing (eddy current probe, ultrasonic probe). The cut off pipe parts were investigated using microscope, electron microscope and methods of analytical chemistry and metallography. To get data of the mechanical properties of the material, tensile and hardness measurements were made.

#### Results of inspections

##### RAT-pipe annular gaps

Gaps between RAT-pipes and the enclosing steel tubes (mild steel) partially filled with a reddish brown mixture of FeO<sub>x</sub> and AlO<sub>x</sub>

##### Inlet pipes (risers), wall thickness 7.1 mm

Outside (He-side):

(Fig. 6)

Pitting corrosion max. 2.8 mm deep - 12 mm  $\phi$ .

Above 2 m no indication of corrosion (ultrasonic)

Inside (D<sub>2</sub>O-side):

(Fig. 7)

Isolated pittings (Fig. 8) max. 2 mm deep - 2 mm  $\phi$ , orientated mainly in axial direction.

Above 1.25 m no indication of corrosion.

Important! Optical and ultrasonic inspection showed no indication of overlapping inside/outside pitting maximum.

##### Outlet pipes (downcomers), wall thickness 6.8 mm

Outside:

Pitting corrosion max. 2.8 mm deep - 11x6 mm  $\phi$ .

Above 0.65 m no indication of corrosion.

Inside:

Insignificant corrosion

#### Drain-/Weirpipe, wall thickness 3.5 mm

Outside:

(Fig. 9)

Both pipes with two penetrations each and pitting corrosion up to 1.05 m.

Decreasing denseness of pitting towards RAT.

Inside:

Insignificant corrosion

#### Enclosing steel tubes

Few isolated pittings with 30% wall thickness weakening inside.

#### RAT, wall thickness 12.7 and 17.4 mm

Inside and outside no significant corrosion.

#### Results of analytical chemistry investigations

##### Inside RAT-pipes (D<sub>2</sub>O-side)

Reddish brown layer of AlO<sub>x</sub> (15 $\mu$ m) and FeO<sub>x</sub> (2 $\mu$ m) on top.

Traces of chloride, no indication of heavy metals like copper (Fig. 11).

Corrosion mechanism:

Release of chloride by Chloroprene valve-membranes.

Traces of chloride in combination with residues of pipe manufacturing (Fig. 10) caused pitting corrosion.

##### Outside RAT-pipes (He-side)

Chloride (Fig. 12), highest concentration of 16% Cl<sup>-</sup> near Chloroprene gland, traces of copper.

Corrosion mechanism:

Release of chloride by Chloroprene gland.

Combination of chloride and humidity in Helium caused pitting corrosion. Certain influence of copper.



After completion of the major part of corrosion investigations the findings had been compiled in a status report (/9/) and discussed in detail with representatives of the licensing and regulatory authority and TÜV. Meanwhile an evaluation-report on the results was presented by TÜV (/10/)

### Evaluation

- Having the right conditions nearly complete stop of pitting corrosion will be possible.
- Due to the observed pitting corrosion D<sub>2</sub>O-leakage will start with a minor rate only.
- Due to the ductile pipe-material instantaneous failure (stress corrosion cracking) can be excluded.

### Recommendations

- Cleaning of RAT-pipes inside and outside.
- Exchange of Chloroprene (valves, seals) by EPDM-rubber.
- Strict control of D<sub>2</sub>O-purity.
- Limitation of humidity outside RAT-pipes in the He-graphite system.
- Reliable and fast detection of possible leaks (control of humidity and nuclides).
- RAT-pipe inspections within certain time intervalls.

## **3. Upgrading the RAT Pipes**

### **3.1 Problem Caused by the Original Design**

The four downcomers and three risers of the reactor aluminium tank (RAT) of FRJ-2 consist of aluminium pipes, size 7" and 9", positioned concentric in steel pipes (Fig. 4). The gaps formed by the aluminium and steel pipes are part graphite-helium-system. The gaps are sealed by stuffing boxes in the lower part to allow different thermal expansion between the steel tank and the RAT during start-up and shut-down of the Reactor.

The design of the drain- and the weir pipe is comparable to that of the downcomers and risers but the size is only 1,5".

In the past leaks in the drain and weir pipe let to the penetration of heavy water into the gaps. Consequent the gaps were filled up with corrosion products which gave the risk of solid seizure between the steel and the aluminium pipes

in the area of the stuffing box including the size of unacceptable stresses in the bottom of the RAT.

### **3.2 Design and Performance of the New Arrangement**

Due to the problems mentioned above the stuffing boxes areas of the RAT pipes had to be replaced by a new design using steel bellows and O-ring sealing. The lower parts of the steel and aluminium pipes of the downcomers and risers were cut in two steps using a compass saw and a milling cutter device. The radioactive corrosion products were removed from the gaps and new tube nozzels were welded to the steel and aluminium pipes using special shielding devices placed into the pipes. (Fig. 13). For the risers the shielding was given by a canister filled with water and for the downcomers a stainless steel cylinder was used fixed by an inflatable balloon device. The tritium release during welding was nearly totally avoided by preheating the used aluminium pipes. The preheating procedure has been optimized by tests with used aluminium pipe peaces cut before. For drain and the weir pipe a scaling device consisting of an internal pipe with steel bellow was developed. The scaling is realized by two O-rings in the upper region pressed to old aluminium pipe (Fig. 14).

### **3.3 Status of the Refurbishment Work**

The sealing devices for the drain and the weir pipe were installed in August 1992. Concerning the work for the downcomers and the risers the new tube nozzels were welded and the new steel bellows are available. The final installation will be finished in October 1993.

## **4. Final Remark**

The results of the Aging Evaluation Program achieved until today do not reveal significant aging/damaging effects on non replaceable parts of FRJ-2. Even the corrosion status of RAT and RAT tubes - issue of most concern - does not indicate severe effects on future safe reactor operation if the recommended and specified data for the primary coolant and the He-gas of the grahite system will be strictly kept during operation. Therefore modifications of the graphite He system are necessary and under construction.

The refurbishment of the RAT tubes is in far progress and will be completed within the next months. In addition several technical and administrative measures have to be realized before FRJ-2 can resume operation. Among the technical measures those to modify and upgrade several systems and components so

that they can meet the current seismic and fire protection standards are of particular importance because licensing procedures according to the German Atomic Energy Act are required for realization.

Among the administrative measures the operation manual is being adopted to the current regulations and an emergency handbook including accident management measures is being elaborated.

Due to the uncertainties with regard to the above mentioned licensing procedures a reliable date to resume reactor operation cannot be given. Under very optimistic assumptions FRJ-2 might start operation in the first quarter of next year.

## References

- /1/ G. Bauer, H. Friedewold, G. Thamm, J. Wolters,  
"Refurbishing Concepts for the FRJ-2 (DIDO) at KFA Jülich"  
Jahrestagung Kerntechnik, Aachen, 8-10 April 1986
- /2/ J. Wolters, G. Bauer, J. Nöcken, G. Thamm,  
"Modernisierung eines Jülicher Forschungsreaktors, Variante  
'Blockaustausch' beim FRJ-2 (DIDO)"  
Jahrestagung Kerntechnik, Travemünde, 17-19 Mai 1988
- /3/ G. Bauer, G. Thamm,  
"25 years of Research Reactor Operation at KFA Jülich, Changing  
Experimental Utilization in the Course of Time"  
Second Asian Seminar on Research Reactors  
(ASRR-II) Jakarta, Indonesia, 22-26 May 1989
- /4/ J. Wolters, A. Hainoun, J. Nöcken, Ch. Tiemann, H. Haas,  
"Studie zur Erneuerung des Forschungsreaktors FRJ-2 (DIDO) des  
Forschungszentrums Jülich"  
Jahrestagung Kerntechnik, Karlsruhe, 5-7 Mai 1992
- /5/ J. Wolters, P. Chapelot, P. Breant, H.J. Didie,  
"JUNO The Planned New Neutron Source for KFA Jülich"  
Jahrestagung Kerntechnik, Köln, 25-27 May 1993
- /6/ TÜV ARGE Kerntechnik West,  
"Zwischenbericht zur Lebensdaueruntersuchung des Forschungsreaktors FRJ-2  
in Jülich (Phase A)",  
Juni 1992
- /7/ TÜV ARGE Kerntechnik West  
"Stellungnahme zu  
- Berechnungen der Spannungen im RAT  
- Ausdrückversuchen Z5, Z6, R3, R4  
- Ermüdungsanalyse für den RAT Bodenbereich des DIDO"  
24.06.1993

- /8/ G. Breitbach,  
"Ermüdungsanalyse für den RAT-Bodenbereich des DIDO"  
Int. Bericht IRW, Feb. 1993
- /9/ H. Küpper, G. Thamm, M. Thomé,  
"Untersuchungen zum Zustand von RAT und RAT-Rohren"  
März 1993
- /10/ TÜV ARGE Kerntechnik West,  
"Stellungnahme zur Korrosion am RAT und an den RAT-Rohren"  
30.07.1993

## List of Figures

- Fig. 1: View on FRJ-2 reactor block and primary cooling circuit arrangement  
Aging Evaluation Programm for FRJ-2 (DIDO)
- Fig. 2: Schematic survey of working steps and sequence of steps
- Fig. 3: Vertical section of FRJ-2 reactor block
- Fig. 4: RAT-pipe and enclosing steel pipe stuffing box sealing (former design)
- Fig. 5: Schematic overview of inspections for RAT and RAT pipes
- Fig. 6: Riser (No 5), cut off part, view on outer surface
- Fig. 7: Riser (No 5), cut off part, view on inner surface
- Fig. 8: Riser (No 5), cut off part, metallographic sections inner surface (pitting corrosion)
- Fig. 9: Drain pipe, cut off part, view on outer surface (upper section cleaned)
- Fig. 10: Riser (No 5), cut off part, view on outer surface before and after cleaning
- Fig. 11: Riser (No5), chemical analysis inside pits by SEM-EDX method
- Fig. 12: Weir pipe, cut off part, radial distribution of elements in corrosion layer
- Fig. 13: Arrangement of Primary coolant inlet pipes, improved design
- Fig. 14: Arrangement of drain and weir pipe, improved design
- Fig. 15: Upgraded downcomers and risers of FRJ-2

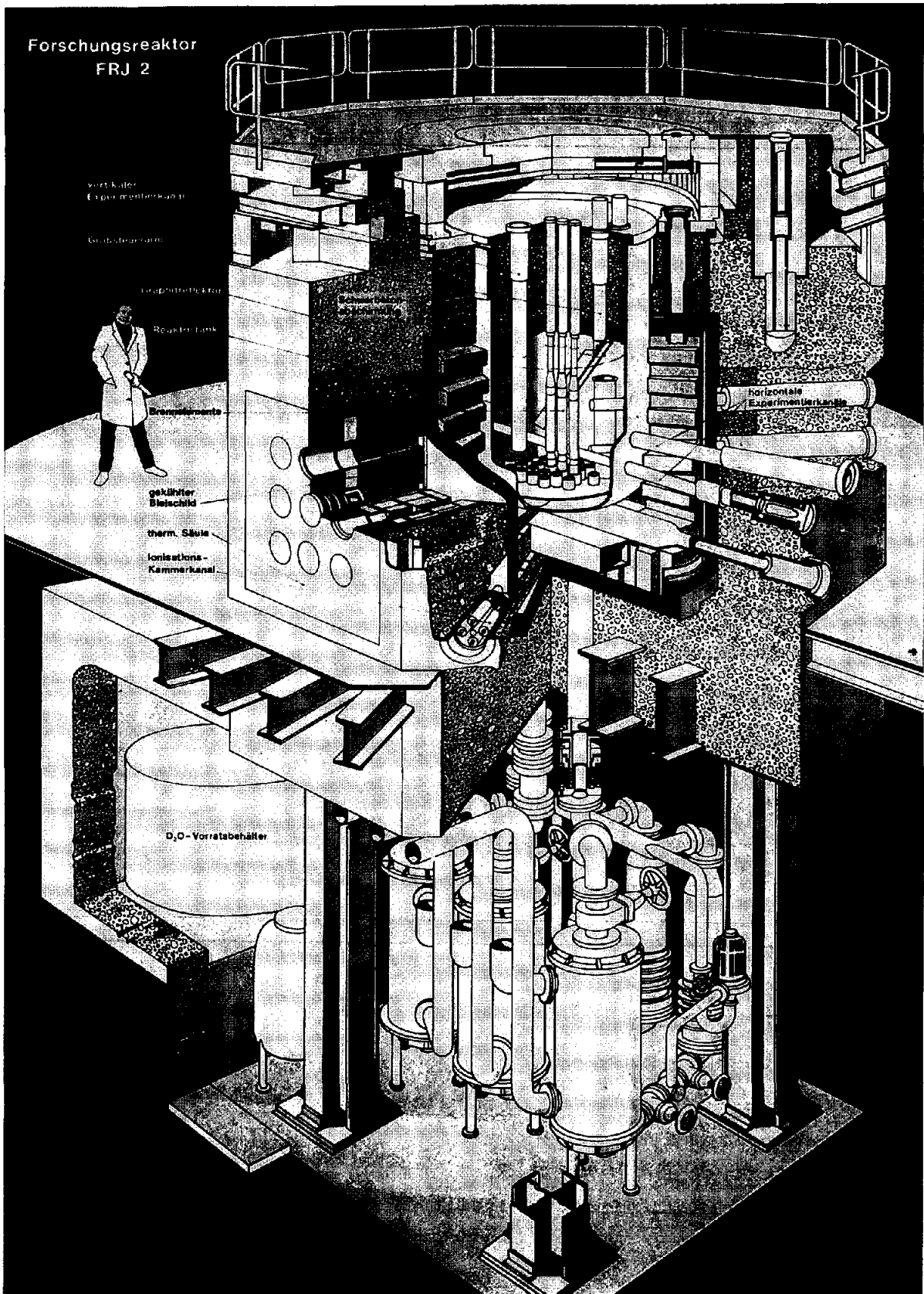


Fig. 1: View on FRJ-2 reactor block and primary cooling circuit arrangement

# Aging Evaluation Program for FRJ-2 (DIDO)

## PHASE A

## PHASE B

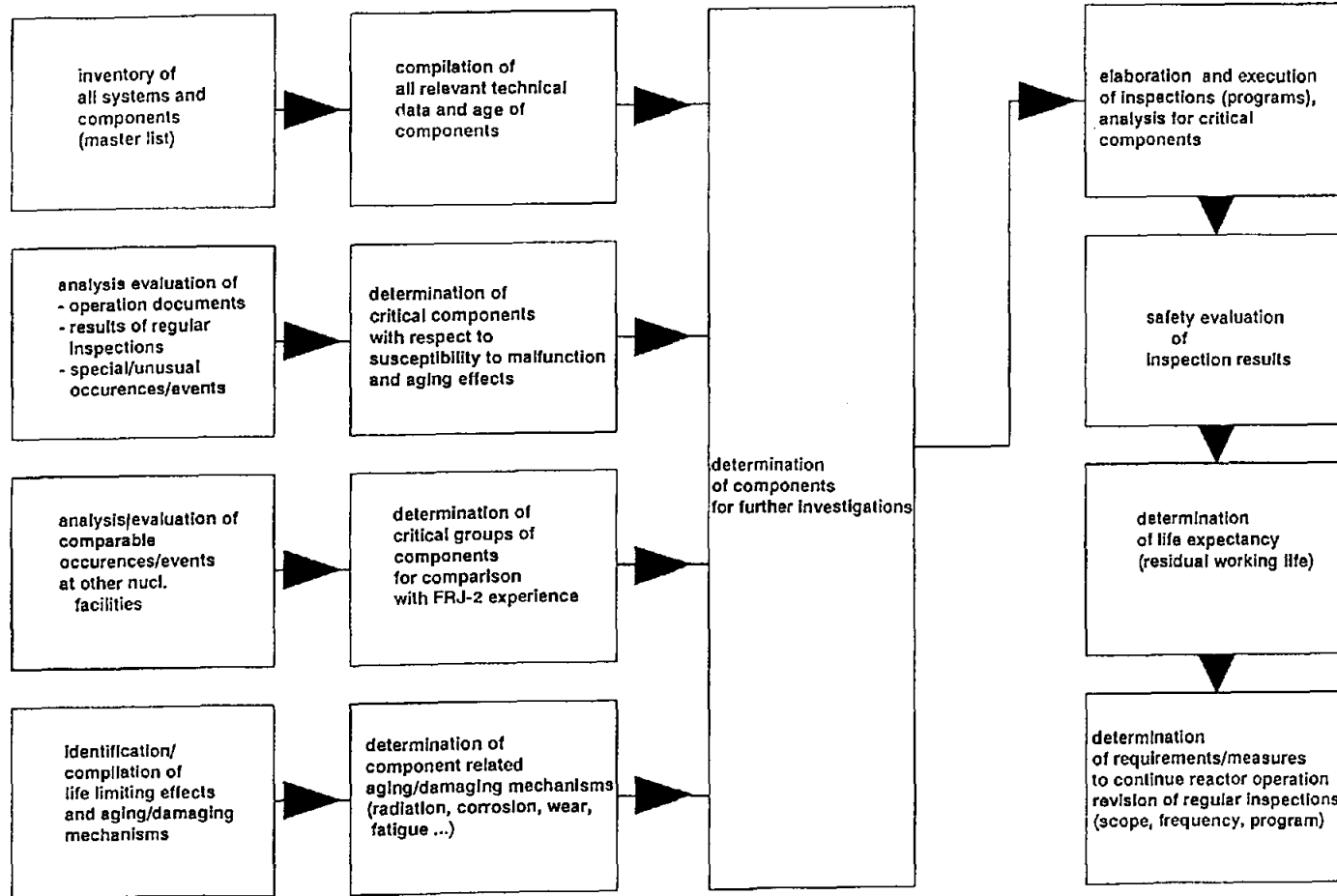


Fig. 2: Schematic survey of working steps and sequence of steps



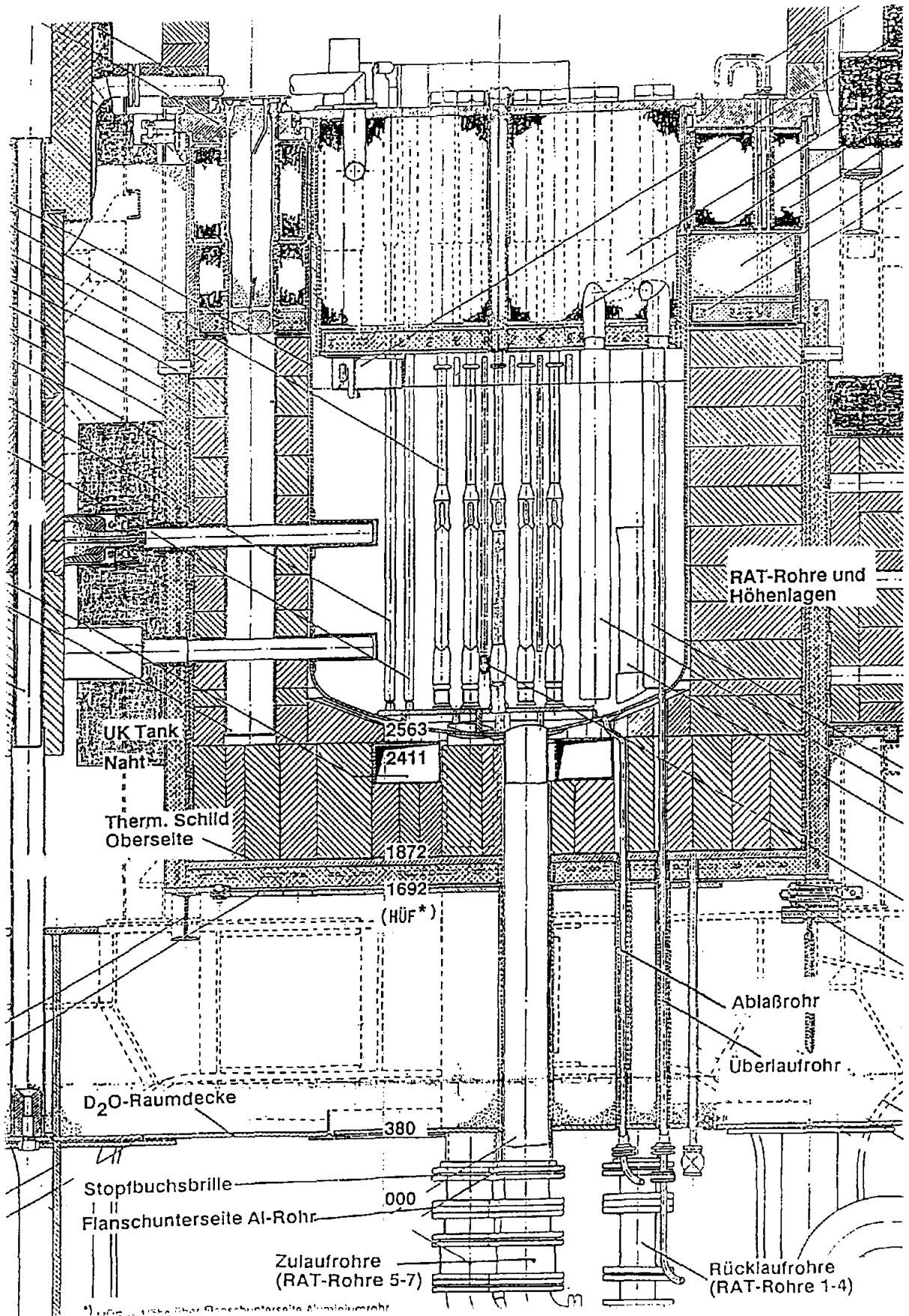


Fig. 3: Vertical section of FRJ-2 reactor block

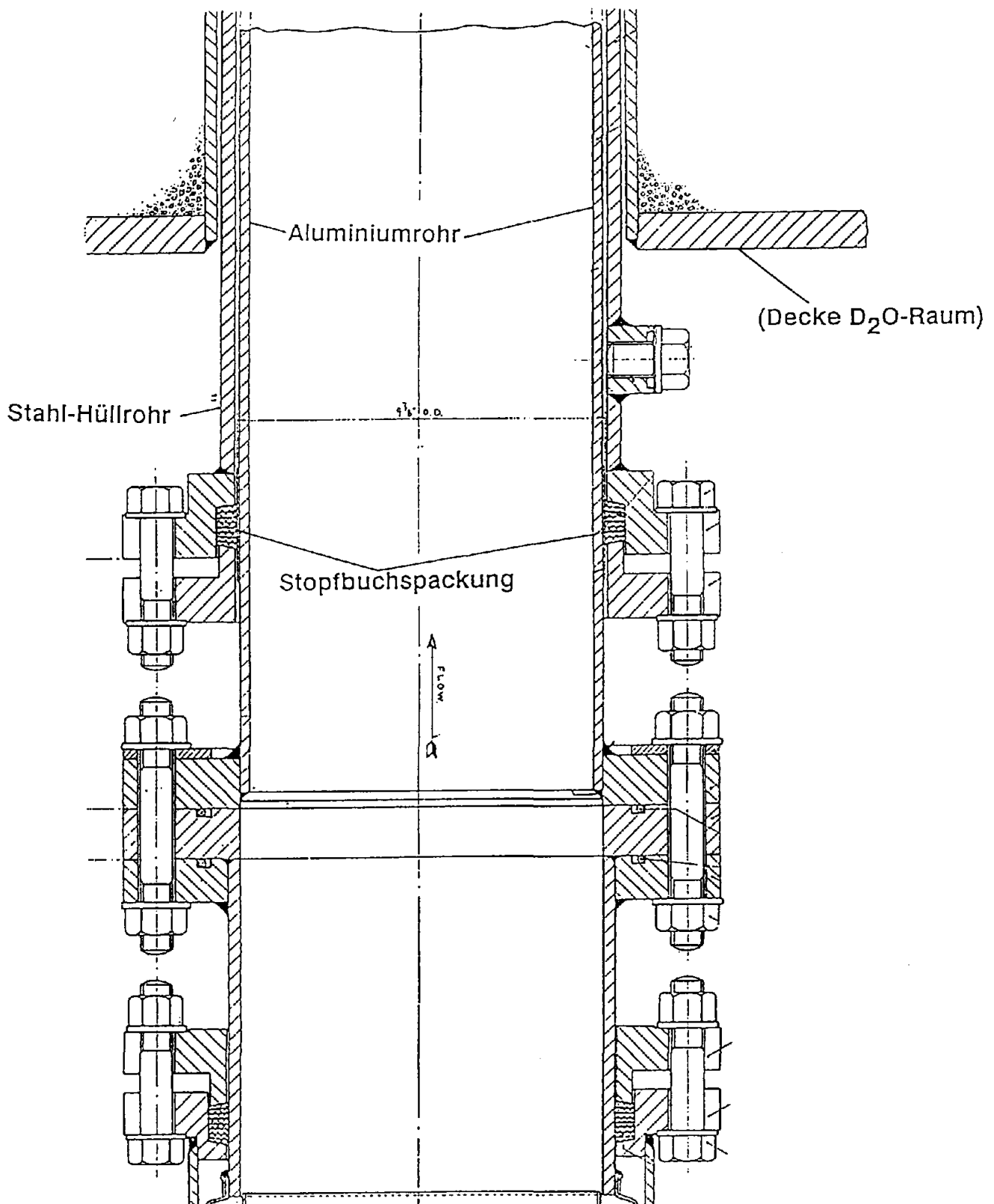


Fig. 4: RAT-pipe and enclosing steel pipe stuffing box sealing (former design)

**Visual inspections**

Periscope

Mirror

Videoscope

Videomicroscope

**RAT-Rohre**

Inlet pipes

Outlet pipes

**Eddy current measurement**

Cylindrical probe

Rotating probe

Drain-/Weir pipe

**Ultrasonic measurement**

Automatic drive

Manual drive

RAT

Side wall

Bottom

**Investigations**

Visual

Microscope

Analytical chemistry

SEM-EDX

Metallography

Tensile test

**Fig. 5: Schematic overview of inspections for RAT and RAT pipes**

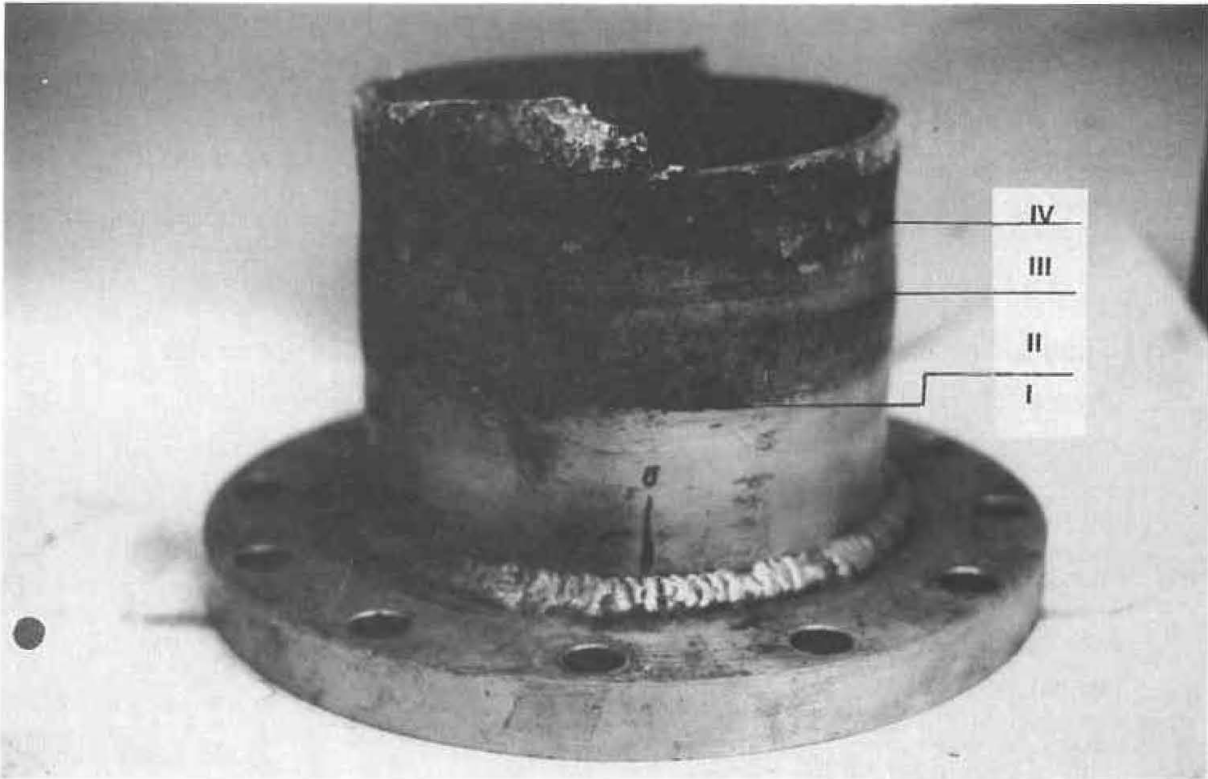


**Fig. 6: Riser (No 5), cut off part, view on outer surface**



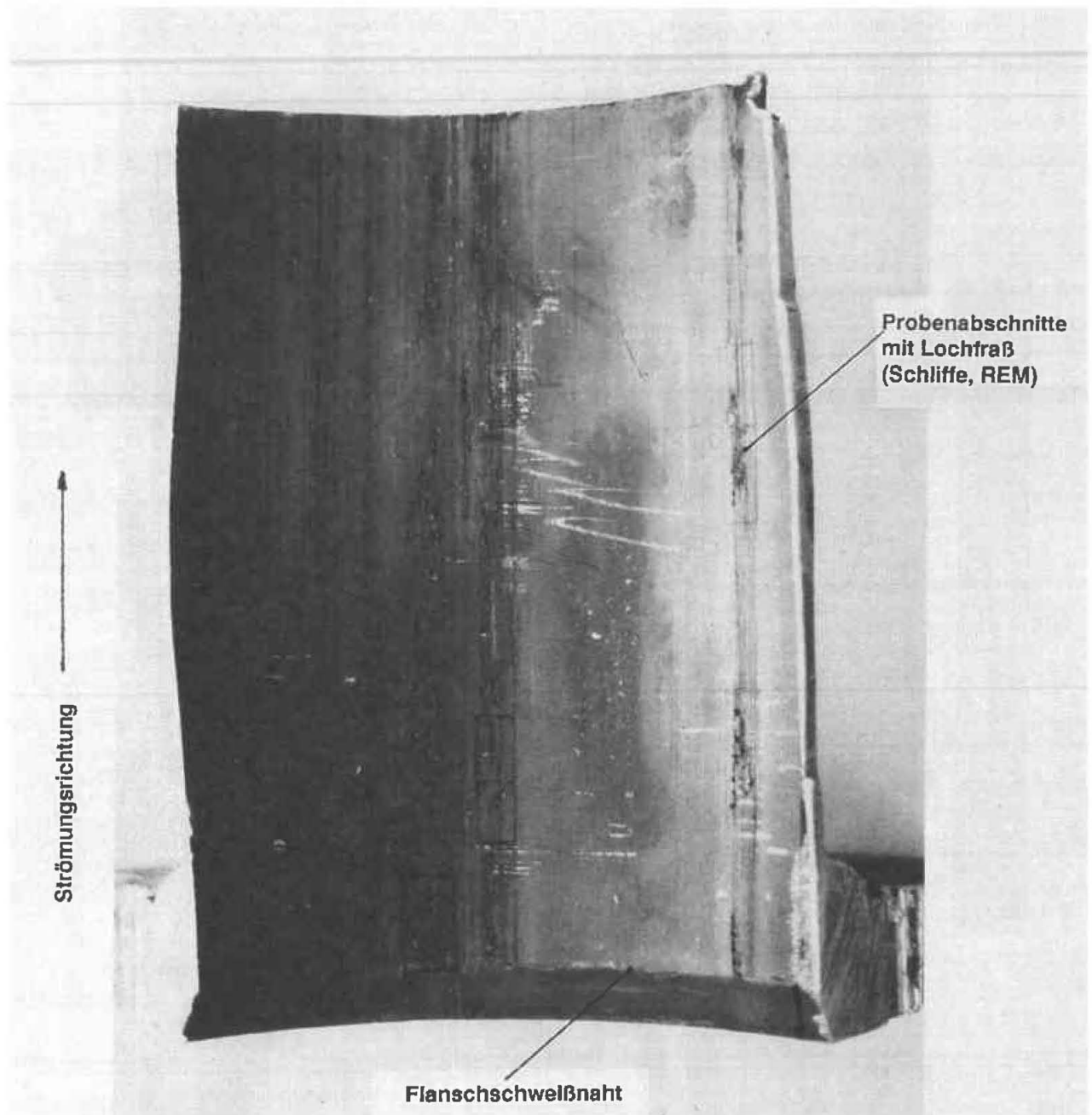
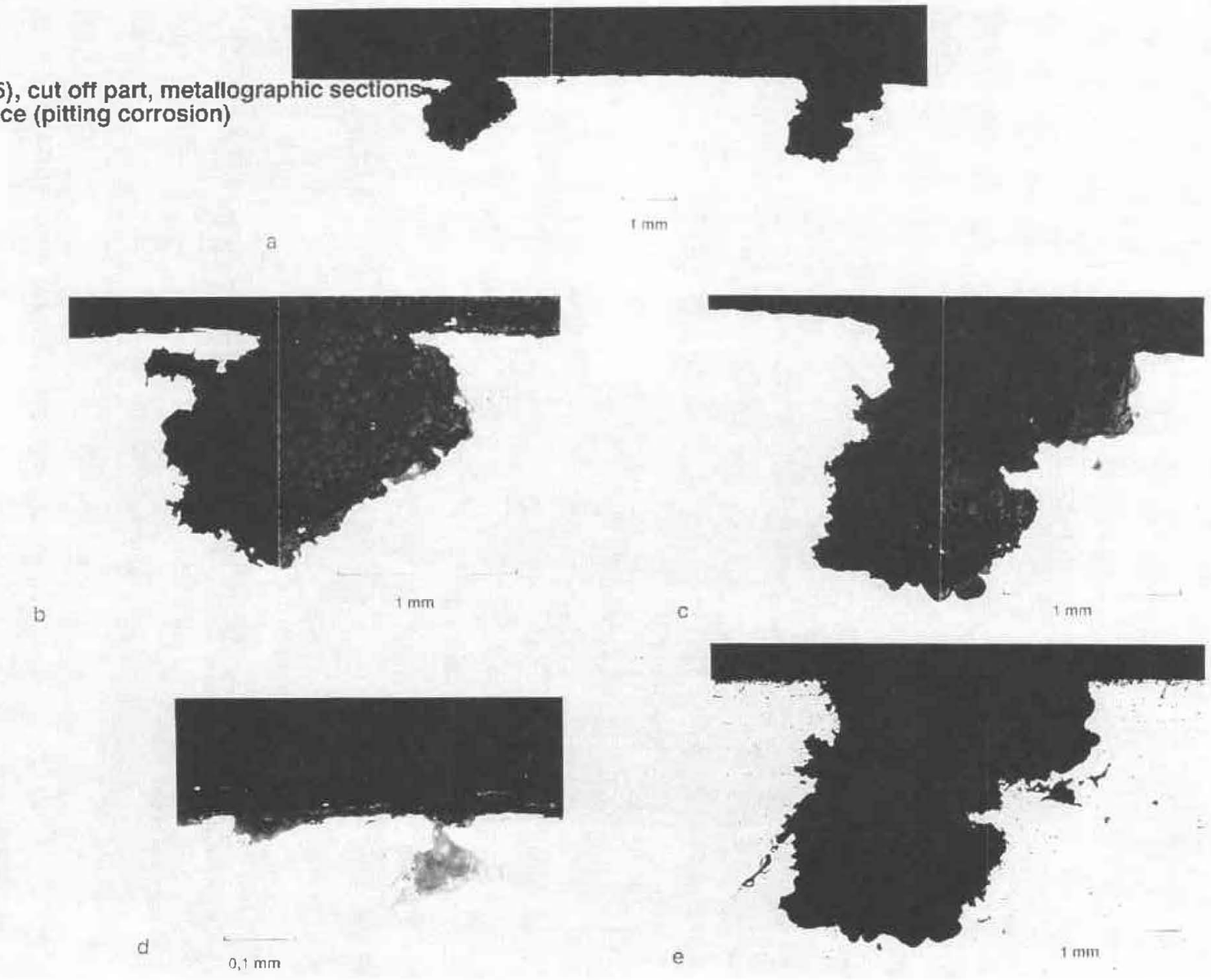


Fig. 7: Riser (No 5), cut off part, view on inner surface

Fig. 8: Riser (No 5), cut off part, metallographic sections  
inner surface (pitting corrosion)



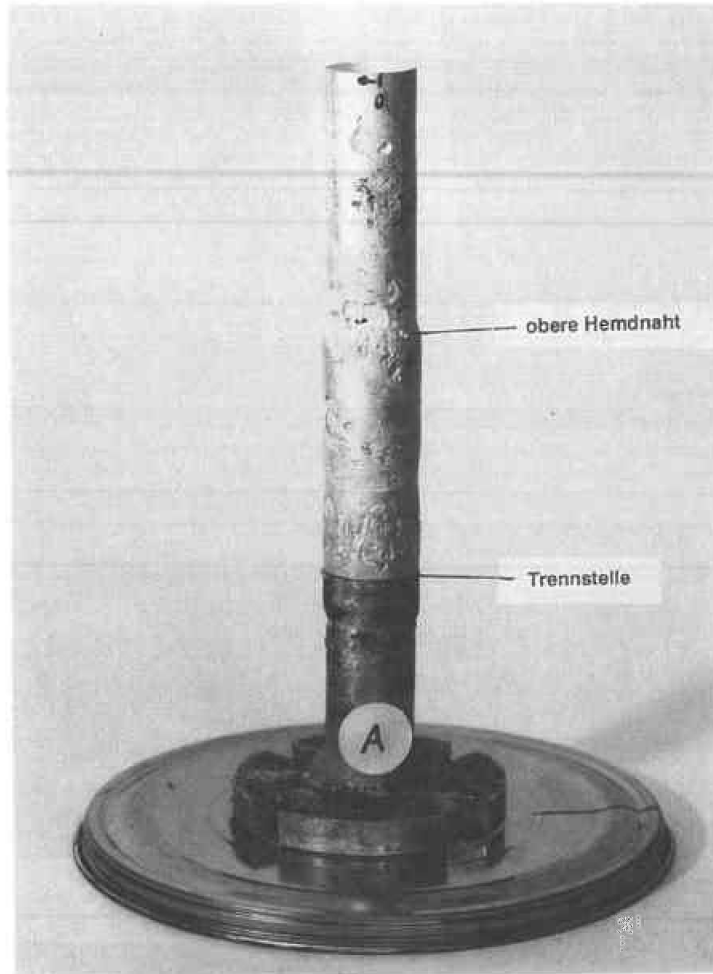


Fig. 9 Drain pipe, cut off part, view on outer surface (upper section cleaned)

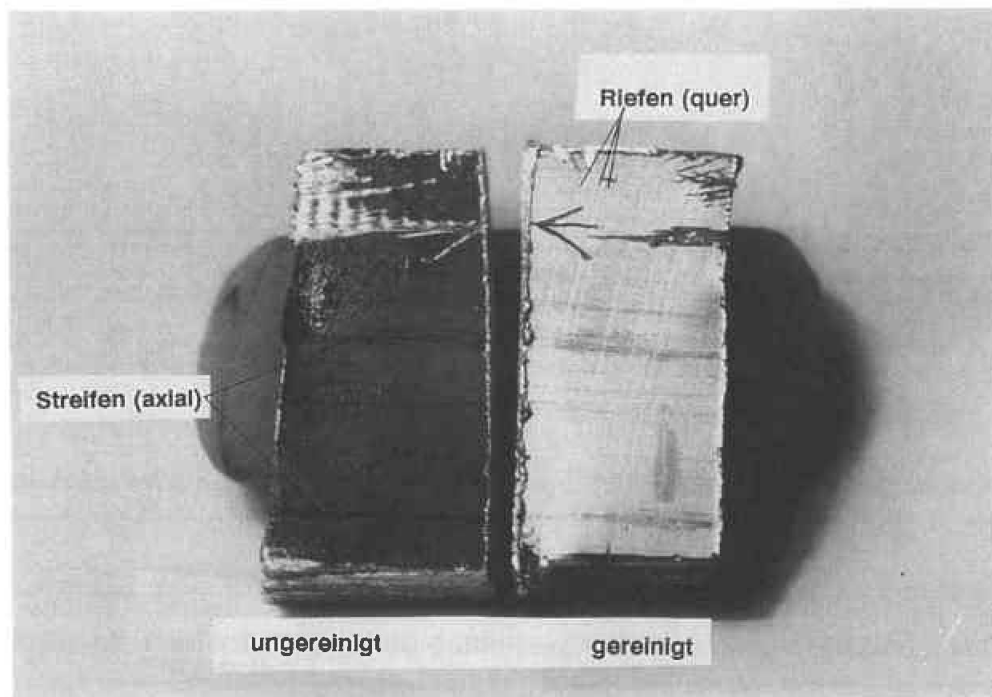
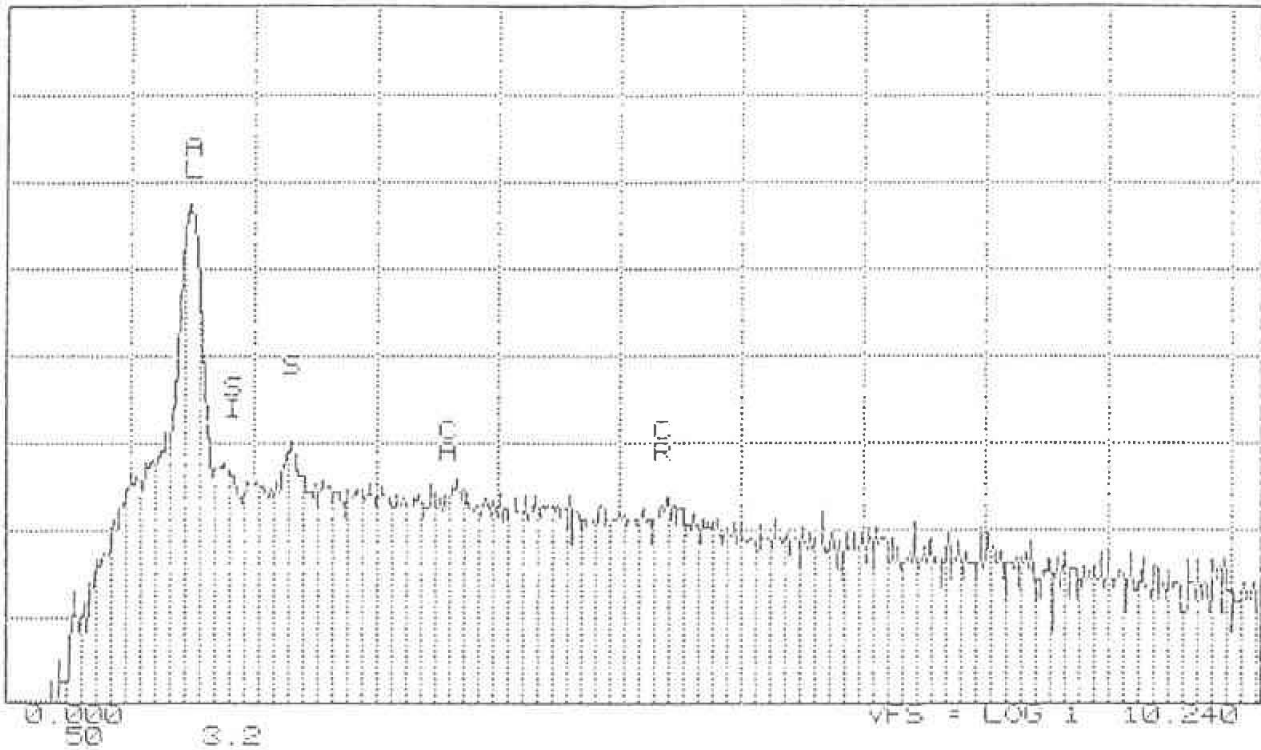


Fig. 10 Riser (No 5), cut off part, view on outer surface before and after cleaning



Tabellarische Auswertung des Spektrums der Abb. 15

Element	Netto-Zählrate	Gew-%
Al	33045 +/- 240	93.2
S	514 +/- 52	2.1
Na	188 +/- 57	1.4
Si	200 +/- 51	1.2
Cr	130 +/- 40	0.8
P	101 +/- 43	0.6
Cl	68 +/- 40	0.3

Fig. 11 Riser (No 5), chemical analysis inside plts by SEM-EDX method



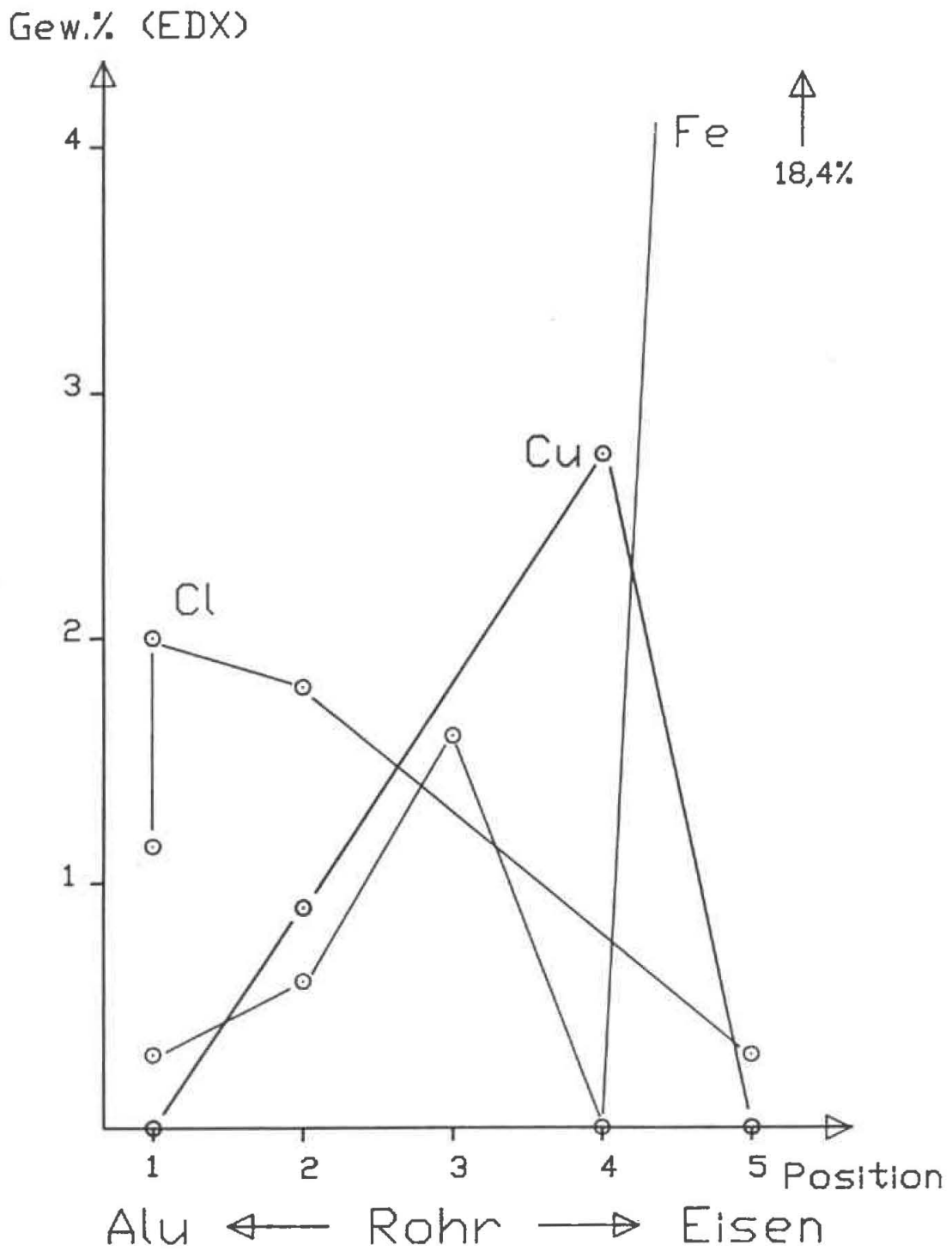
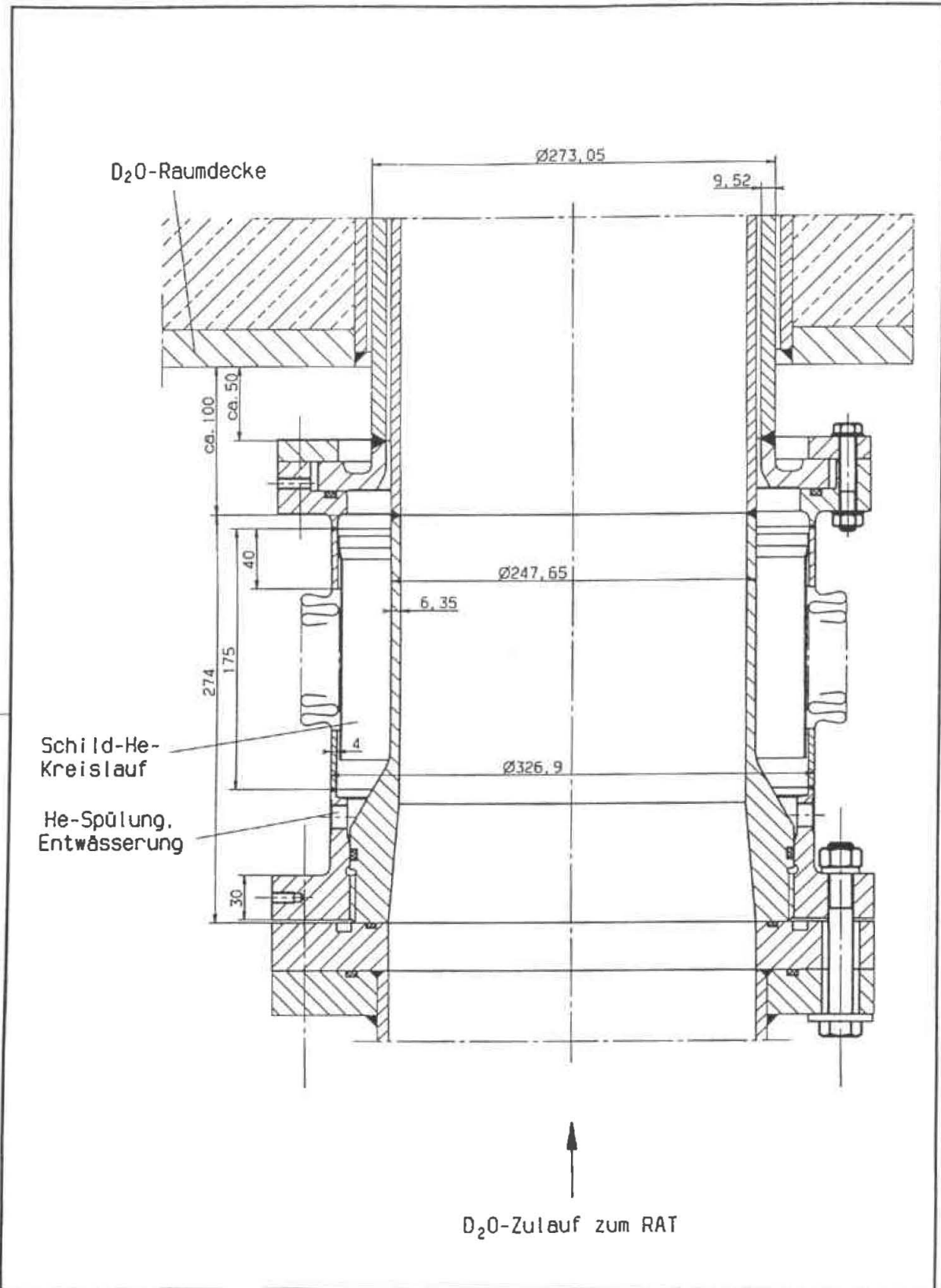


Fig. 12 Weir pipe, cut off part, radial distribution of elements in corrosion layer



KFA 57.20-06



Arrangement of Primary Coolant Inlet Pipes,  
Improved Design

Fig. 13



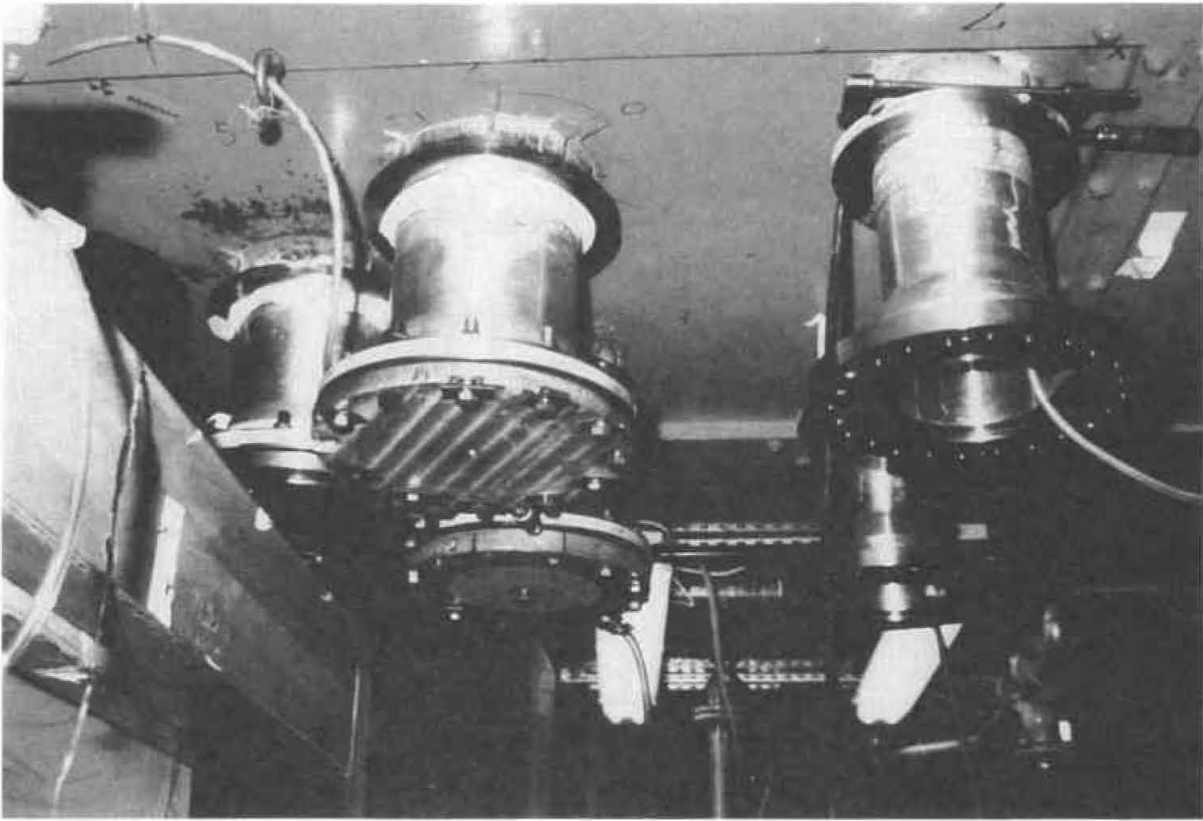


**Fig. 15: Upgraded downcomers and risers of FRJ-2**

## UPGRADE OF THE EXPERIMENTAL FACILITIES OF THE ORPHEE REACTOR

B.FARNOUX<sup>a</sup> and P.BREANT<sup>b</sup>

a) DSM, ORME des MERISIERS, CEN SACLAY F-91191 GIF SUR YVETTE

b) Service d'Exploitation ORPHEE, CEN SACLAY F-91191 GIF SUR YVETTE

## ABSTRACT

At the time of the design, the ORPHEE reactor has been equipped with a set of up-to-date experimental facilities such as nine tangential and horizontal beam holes, one hot source, two hydrogen cold sources and six neutron guides. After more than ten years of operations, all the neutron beams are now used by about twenty five spectrometers. A modernisation program is under progress with a two fold aim: upgrade of the existing facilities and creation of new beams. Some details of the six following points will be described: 1) replacement of the flat cold source cell by an hollow cylinder in order first to increase the cold neutron flux and secondly to facilitate the extraction of new cold neutron beams. 2) replacement of the old neutron guide elements coated with natural nickel by new elements with isotopic nickel or super mirror coating. 3) modification of the curvature of some existing neutron guides in order to increase the wavelength band transmission. 4) creation of new cold neutron beams by installation of benders on the existing neutron guides. 5) design of new cold neutron guides and a new guide hall. 6) design of a thermal neutron guide. The two last points will made extensive use of super mirrors allowed by new technical developments done at the Laboratoire LEON BRILLOUIN in connection with industry.

## 1. INTRODUCTION

The ORPHEE reactor is a medium flux neutron source for fundamental and applied research using neutron beams. It was designed by the end of the seventies, few years after the divergence of the High Flux Reactor of Grenoble (HFRG). In the design of the integrated experimental facilities, special features of a modern reactor like the HFRG were used: pool type reactor block of compact size, tangential beam tubes, hot and cold sources, neutron guides. With all these up-to-date items, the ORPHEE reactor is the best medium flux neutron source and the ideal complement of the HFRG. After twelve years of operation, all the neutron

beam positions are fully occupied with 30 experimental facilities including 25 scheduled spectrometers. These facilities are operated by the Laboratoire LEON BRILLOUIN (LLB), a common laboratory of the Commissariat à l'Énergie Atomique (CEA) and the Centre National de la Recherche Scientifique (CNRS).

The lifetime of the source being expected to be greater than 30 years, a modernisation programme of the integrated facilities, defined in close collaboration between the LLB and the operating reactor team, is under progress. In the context of the future development of an European neutron source, the aim of this programme is to enhance the quality of the neutron beams and to increase the number of beam positions. After a short recall of the ORPHEE characteristics, the modernisation programme will be presented in details.

## 2. THE ORPHEE REACTOR.

The ORPHEE reactor is the third reactor built after those of BROOKHAVEN (HFBR 1965) and GRENOBLE (HFRG 1971) specially dedicated to provide intense neutron beams for fundamental and applied research. The construction started on June 1976 and the reactor first went critical on December 19, 1980. Full power operation started on July 1981.

The reactor design [1] is similar to the HFRG: a compact core of fully enriched Uranium, is surrounded by a heavy water moderator to give a good thermal flux. The biological shielding is achieved by a light water pool and a heavy concrete wall. Great care was taken to minimise the distance between the source and the experiments and the overall diameter of the reactor block is only 7 meters. The neutron beams are issued from the reflector tank by nine horizontal beam ports in tangential position. The thermal power is 14 MW and the maximum thermal neutron flux is  $3 \times 10^{14}$  n/cm<sup>2</sup>/s. The reactor is operated for 250 days per year in two and half cycles of 100 days each.

The reactor is designed as a medium thermal neutron flux source. But many experiments require lower energy ( $E < 5$  meV) or high energy ( $E > 100$  meV). For this purpose the thermal moderator is locally replaced by either a low temperature (cold source) or high temperature (hot source) moderator.

The cold moderator is liquid Hydrogen. Helium refrigerator continuously liquefies Hydrogen gas inside a condenser. Liquid Hydrogen at 20 K circulates by thermosiphon between this condenser and a lenticular shaped cell ("flat" cell) located inside a vacuum chamber in front of the beam tube. In order to provide cold neutron beams to a large number of experimental facilities, two cold sources are located inside the heavy water tank at a distance of 400 mm from the core axis.

The hot source is a cylindrical Graphite block, 120 mm in diameter and 200 mm high, located in a vertical tube at a distance from the core of 270 mm, which allows to obtain a temperature of 1450 K by radiation heating only.

Nine horizontal beam tubes, made of aluminium alloy, penetrate the biological shielding and provide seventeen neutron beams (figure 1). Seven beam ports are located in the reactor experimental hall (figure 3), four located at the thermal source, two at the hot source and one at the cold source. The total number of neutron beams is eleven, six thermal, two cold and three hot. Two beam ports, located each on a cold source, provide six cold neutron beams to a large experimental hall by means of curved neutron guides, using natural Nickel as reflector.

The number of spectrometers is eleven in the reactor hall and eighteen in the neutron guide hall. In addition a laboratory for non destructive testing by neutron radiography is located at the end of a neutron guide (see figure 2).

### 3. THE MODERNISATION PROGRAMME.

Due to the modern design of the reactor and the fact that it is periodically and systematically maintained there are no plans for modernisation of the source itself. The modernisation programme described thereafter concerns only the neutron beams for a more efficient use. Six projects are under consideration and are at different level of achievement. The first one is linked to the production of cold neutron beams. The five others are aimed to the improvement of neutron beam transport by neutron guides afforded by new industrial developments of mirror coating. These developments are the result of a joint research program of the LLB and the CILAS, the company manufacturing the neutron guides [2].

### 3.1 New cold sources.

In the original design of the reactor, the choice of liquid Hydrogen for the moderator has led to two small cells in order to produce enough cold neutron beams. Due to the geometry of the beam tubes looking at the cold sources it was decided to design a "flat" cell in order to fully illuminate the corresponding beam tubes. The cell size, made of stainless steel, is 205 mm height, 125 mm large and 50 mm thick [3].

After twelve years, about 68 per cent of the experimental facilities are using cold neutron beams and the demand for such neutron beams is increasing. A preliminary study to give an answer to such a demand has been done and is the so-called ORPHEE PLUS project, presented in a following section. For this project it is necessary to modify the shape of the cold source cell in order to illuminate two beam tubes at orthogonal positions (beam tube number 1 and number 8, see figure 1). The best suitable shape is a cylinder of 130 mm in diameter. To reduce the neutron absorption this cylinder must be hollow. The thickness of the liquid Hydrogen layer was determined by calculations based on results of experimental studies done for the High Flux Reactor of Grenoble [3]. A value of 15 mm was determined for the best neutron gain below 7 Angstroms, the wavelength range used by the majority of the experimental set-up. The diameter is 130 mm and the maximum height 300 mm. The cell (figure 4) is formed by an external envelope in aluminium-magnesium alloy (3% Mg) with an external diameter of 130 mm and a thickness of 0.65 mm. The top and bottom are 0.7 mm thick. The liquid layer is obtained by a very thin magnesium insert 0.5 mm thick. The thickness layer is kept constant by two thin cylindrical spacers with many holes to insure free liquid and gas Hydrogen circulation. This insert is full of Hydrogen gas in normal operating conditions (reactor at full power). The total quantity of liquid is around 1.4 litres. The total structure weight not exceeds 250 g with 100 g for the liquid Hydrogen.

Full scale test experiment have been done during the summer 1991 in order to measure the gain of the cylindrical cell in comparison with the flat one. Time-of-flight measurement at the end of a neutron guide of the whole neutron flux with the flat and the new cells allows direct check of this gain. The result is presented on figure 5. As predicted, the gain with the new



geometry is always higher for the new cell than the flat cell ( 10 % in the range 4 to 8 Angstroms), but surprisingly the gain increases at both ends. For the long wavelength side the gain reflect the fact that the Hydrogen thickness is smaller, leading to a smaller absorption. In the short side the increase could be due to the better moderation by the two liquid Hydrogen layers.

The new cell shape is designed in the frame of the ORPHEE PLUS project. But looking at the increase in the neutron flux given by this geometry, the decision was taken to use the new cells as soon as possible. Two new cells are manufactured in 1993 and it is planned to replace the old cells by the end of 1994. This operation will be done with the total renewal of the old cryogenerator in operation since 1981. The new cryogenerator is based on a screw compressor, cryogenic turbine with gas shaft bearing and high quality electronic components. It has been designed for a power of 1850 watts. The main characteristics are: complete automatic operation system, automatic start-up after failure of electric power, no regeneration of helium circuit before restart and possible remote control and diagnostic.

### 3.2 Improvement of existing neutron guides.

In the design, the ORPHEE reactor was equipped with six cold neutron guides. The beam size was a compromise between mechanical constraints and maximum beam desirable. The size is the same for all guides defining a rectangular beam of 15 centimetres high and 2.5 centimetres large. The first step of the modernisation programme is to use the new results obtained in the processing of the mirrors for neutron guides. This allows to increase the transmission with the same geometry or allows to share the beam by using benders to extract new beams. When designed, more than twelve years ago, the neutron guide reflector was polished glass (with or without boron oxyde) coated with natural Nickel. Since that time a precise study of the surface structure [4], revealed by the new neutron reflectivity method used at the Laboratoire LEON BRILLOUIN [5], has shown that the near surface is perturbed by the mechanical processing used up to now. A new process has been designed to reduce the roughness of the glass surface and to minimise the perturbation of the near surface. Together with the use of isotopic Nickel

(Nickel 58) this led to an increase of the neutron guide transmission. Another new fact is the industrial production of efficient super mirrors with a characteristic critical angle twice that of natural Nickel [6]. These improvements were used or will be used to increase the cold neutron flux received in the guide hall.

### 3.2.1 New coating.

The reflectivity curve measured with the EROS reflectometer of Saclay for a natural Nickel coating and a new super mirror is depicted on figure 6. This is an example of the gain expected by the use of such a device. The reflectivity value in the range of the super mirror is at the present time around 90 per cent and is not enough for a very long guide but, compared to a "normal" guide, the increase in the transmitted intensity is significant. A first application of this new coating will be the replacement of the neutron guide elements of the existing highly curved guide G1 and G2 ( see table I). The characteristic wavelengths are respectively 6 Å and 4 Å. These values were defined at the time of the guide design to be fitted with the small angle spectrometers. By now, shorter wavelengths are commonly used. In the past the only way to change the characteristic wavelength was to increase the radius of curvature. With the use of super mirror coating, it is now possible to extend the transmission in the short wavelength range without modifications of the geometry. The figure 7 present the result of a calculation for the neutron guide G2. Two cases are compared to the present natural Nickel mirror, the isotopic Nickel and the super mirror. The gain given by the last case is evident. It is planned to replace the two guides G1 and G2 by super mirrors in the near future.

### 3.2.2 New geometry.

Another way to increase the transmitted flux is to replace the curved guide by a straight one. This operation has been done in 1991 for the guide G5 (characteristic wavelength 2 Å, see table I) together with a replacement of the natural Nickel coating by a Nickel 58 coating. This operation was done together with the installation of a bender (see below). The guide elements in the guide hall were all replaced by a smaller guide ( height 85 mm) in straight line. The only

curved part are the first 12.5 meters from the beam port up to the exit of the confinement building. After this modification an increase of 30 per cent of the total flux at the end of the guide (total length 56 meters) has been recorded.

### 3.2.3 New beams.

There is a tremendous demand of neutron guide ends. All the six ends are fully occupied (see table I), and the only way to get new neutron guide end is to graft benders on the existing guides. The beam is then shared in the vertical dimension between normal guide with a reduced size and a bender. Three benders have been installed on the guides G1, G3 and G5 (see table II). Due to the shorter radius of curvature, the transmitted beam is less intense in the short wavelength side. This is shown on figure 8 where the measured flux for the new guide G5 (see above) and the bender set at the beginning of this guide (see figure 2) are compared. This bender is based on the new super mirror coating: the vertical convex face is coated with a  $2\theta_c$  super mirror, the other faces are coated with Nickel 58. The flux transmitted by such a mirror compared with the classical multichannel bender G3 bis is presented on figure 9 [7]. The multichannel bender is set on guide G3 with the same characteristic wavelength as the guide G5 ( $2\text{ \AA}$ ) and it is composed of five channels of 4.6 mm each. the dividing walls are coated with Nickel 58 on both side.

Another way to get a new neutron guide end is to use a multilayer monochromator. Contrary to the bender, this device gives a fixed monochromatic beam adapted to a specific experiment. Such a monochromator with a wavelength of  $8\text{ \AA}$  and a resolution of 10 % has been included in the new guide G5 (figure 10) in 1992. The monochromatic beam will be used for a small angle machine, with a high monochromatic flux due to the fact that there is no mechanical selector.

### 3.3 New neutron guides.

Due to the complete use of all experimental positions, the only way to increase the number of experimental devices is to built a new neutron guide hall. The new development in the super mirror coating open now new possibilities for cold neutrons and even for thermal neutrons.

a) cold neutrons.

A preliminary study started in 1988 was based on the fact that a hole was provided in the confinement building in front of the third cold beam tube (beam tube 4F, see figure 3) giving the possibility to extract a neutron guide without modifications of this building. In this project, called ORPHEE PLUS, a important modification of all experiments located in the reactor hall will take place. Preliminary design of this project has been presented at the first IGORR meeting [8]. Since that time a precise study of the modifications was undertaken. In short, nearly all the beam tubes have to be modified, in particular the beam size will be increased from  $40 \times 80 \text{ mm}^2$  to  $50 \times 120 \text{ mm}^2$ . A part of implantation of the new neutron guide it is necessary to create a new cold neutron beam tube in order to maintain in operation the two cold neutron three axis spectrometers. This will be done by extending the tube of beam number 1 (see figure 1) up to the cold source number 1. This beam tube is nearly perpendicular to the beam tube number 8. In order to fully illuminate these two tubes, a new shape for the cold source cell has been designed as defined in section 3.1.

In this project, two straight neutron guides coated with a  $2 \theta_c$  super mirror, will be extracted from the cold beam tube. The in-pile collimator is under design. It will include a converging part in isotopic 58 Nickel in order to fully illuminate the super mirror neutron guide section. The beam size will be 160 mm height and 50 mm large from the reactor up to the containment wall. After this wall the two guides will be split in two guides each (see figure 11). The first one is split in the vertical dimension, leading to two neutron guides of same dimensions (50 mm width , 70 mm height), one with a radius of 148 metres and one straight. The second guide is divided in the horizontal dimension, giving one straight guide of 25 mm large and 160 mm high and a curved guide with the same dimension and a radius of 209 metres. A new neutron guide hall will be built. The number of experimental positions will be increased by 30 per cent. The project is now under design and the decision to built will be taken after the restart of the HFRG and is linked to possible participation of European laboratories.

b) thermal neutrons.

Another hole was provided in front of the thermal beam tube number six (see figure 3). In a preliminary design study, the possibility to extract thermal neutron up to the external adjacent

building has been evaluated. This will be possible with the use of highly efficient super mirror coating as depicted in figure 12 for the case of the thermal neutron guide H25 of the ILL.

#### 4. CONCLUSION.

Due to a possible future shortage of neutron beams in Europe and the predicted lifetime of the ORPHEE reactor (greater than 30 years), an increase of the experimental facilities is essential to provide neutrons beams in complement of the HFGR and the spallation source ISIS. The modernisation programme in progress concerns first the improvement of the production of cold neutrons. This will be achieved at the beginning of 1995 by the replacement of the present cold source cells and the cryogenerator. An immediate increase in the number of beam position has been done by setting three benders on the existing guides: G1 bis in 1986, G3 bis in 1988 and G5 bis in 1992. The change of the existing mirror guide elements by a super mirror coating will lead to a direct increase of the transmitted flux. This will be realized in the near future for the two most curved guides G1 and G2. The next important step will be the creation of a new cold neutron guides. This project (the ORPHEE PLUS project) under design, will increase the experimental facilities of the LLB by about 30 per cent with the installation of 7 to 8 new spectrometers. This increase will give to new scientific communities the opportunity for the access to neutron beams. Discussions with foreign laboratories for a possible participation to this project are in progress. Linked to this project, a major refurbishment of the collimator plugs in the reactor will increase the neutron flux on the spectrometers set around the reactor. This operation will take 3 years for the realisation of the components (collimator plugs, new biological shielding, new neutron guide, new guide hall...) and needs a rather long shut-down of the reactor (three months). It is not yet decided and could be done in 1997. A future possible extension could be the setting on the beam tube 6 of a thermal neutron guide, using very efficient super mirror guides under development.

## References.

- [1] D.CRIBIER, B.FARNOUX, P.BREANT. Design and operation of the ORPHEE reactor. CEA internal report AM 005 Np 001 , May 1983.
- [2] F.SAMUEL, B.FARNOUX, B.BALLOT, B.VIDAL. Development and industrialisation of super-mirrors multilayers used for neutron guides. SPIE proceedings July 19-25, 1992 San Diego (USA).
- [3] P.BREANT. New cold source for ORPHEE reactor. International workshop on cold neutron sources, March 5-8, 1990. Los Alamos, NM (USA)
- [4] M.MAAZA. Thesis PARIS VI October 31, 1991.
- [5] B.BALLOT, A.MENELLE, F.SAMUEL, K. ALUSTA, B.FARNOUX. Characterisation of neutron optics elements using multireflection experiment. Surface X-ray and neutron scattering. June 24-29, 1993 DUBNA (Russia).
- [6] F.SAMUEL, K.ALUSTA. Metallic multilayer coating. CILAS report 06/93 DT/KA 1993.
- [7] B.BALLOT, F.SAMUEL, B.FARNOUX. Super mirror neutron guide. SPIE proceedings, July 19-25, San Diego (USA).
- [8] P.BREANT. The ORPHEE reactor current status and proposed enhancement of experimental capabilities. IGORR I proceedings, February 28-March 2, 1990, Knoxville, Tennessee (USA)

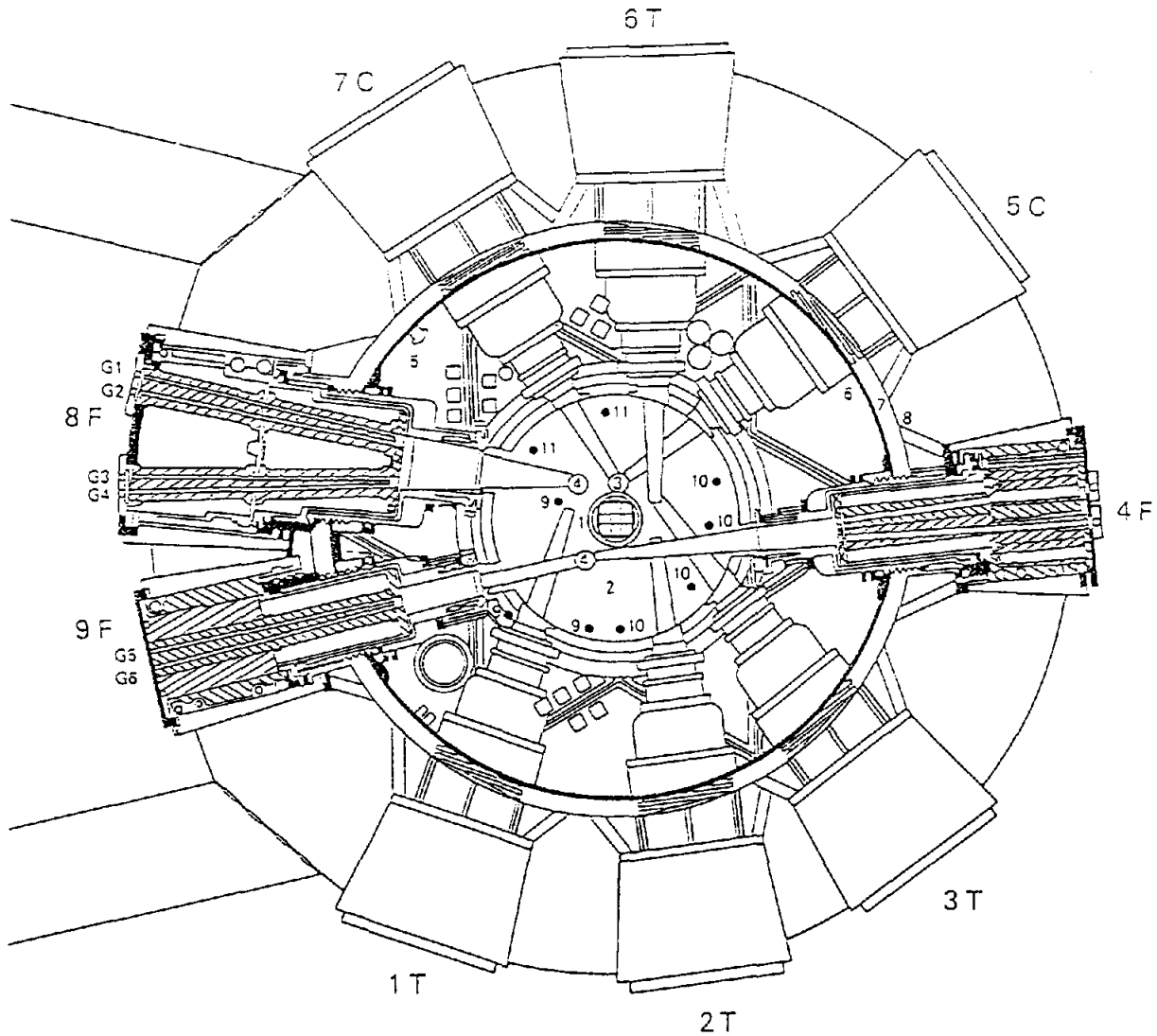
**TABLE I.** Characteristics of the ORPHEE neutron guides.

The total neutron flux measured at the end of the neutron guide by Gold foil activation is given in unit  $10^9$  n/cm<sup>2</sup>/s.

Cold source	Guide	Radius (m)	Characteristic wavelength (Å)	Curved length (m)	Straight length (m)	Experimental positions	End guide experiment	total flux at the end
1	G1	463	6	13.4	20	1	Small Angle	1.15
1	G2	1042	4	23.3	16.2	2	Small Angle	1.26
1	G3	4167	2	39.6	10	1	Spin Echo	1.61
1	G4	4167	2	42	21.2	5	Neutronography	0.91
2	G5	4167	2	12.5	43.3	5	Small Angle	1.88
2	G6	4167	2	27.2	12.5	2	Time-Of-Flight	2.07

**TABLE II.** Characteristics of the benders.

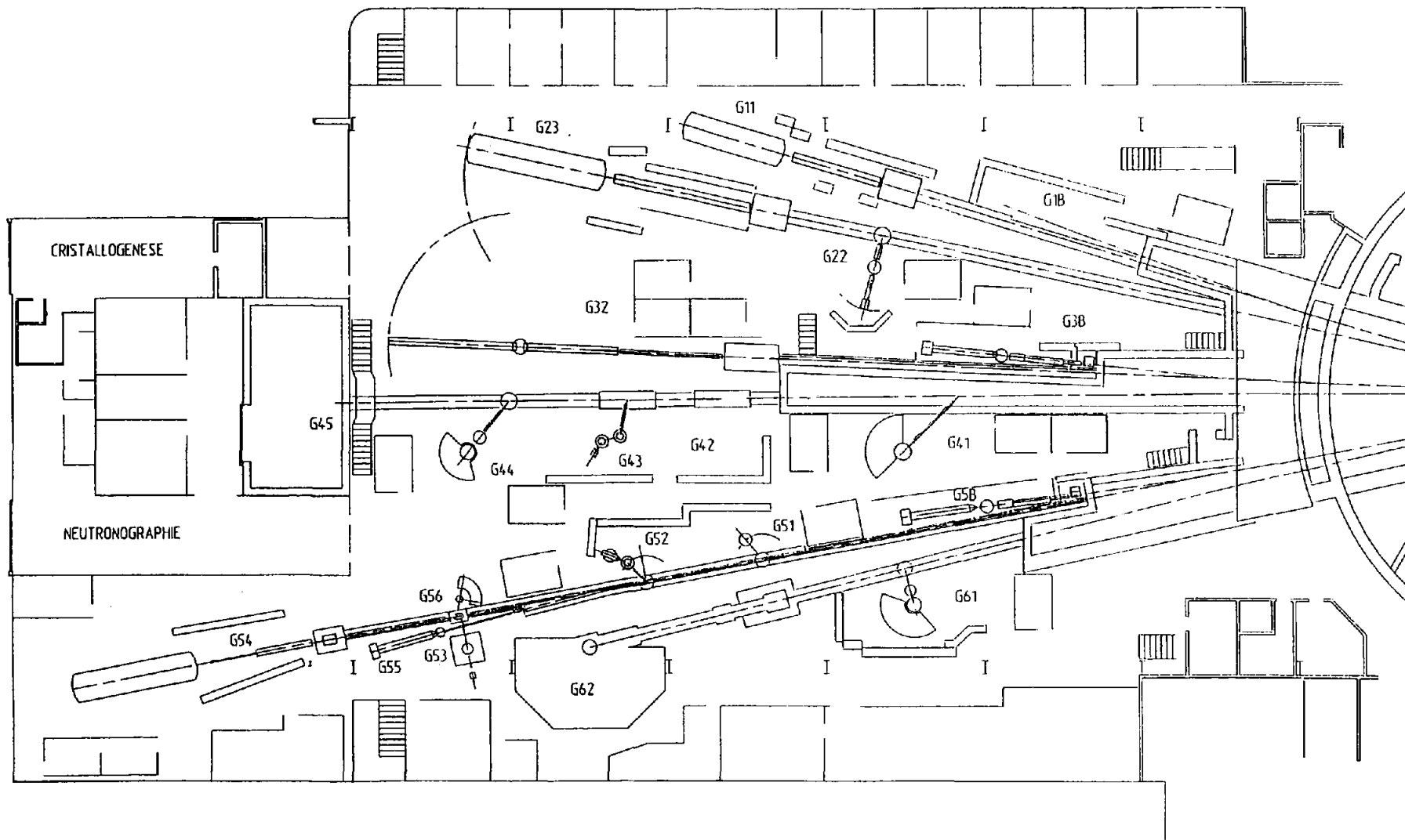
Bender	beam size (w x h) cm	type	radius (m)	length (m)	Total flux	date of operation
G1 bis	2.5 x 5	Multichannel	46.3	8	0.64	1986
G3 bis	2.5 x 5	Multichannel	46.3	9	0.73	1988
G5 bis	2.5 x 3.5	Supermirror	155	10	1.22	1992



1. core
2. heavy water reflector
3. high-temperature source
4. low-temperature source
5. pool
6. pool inner wall
7. annular space
8. pool outer wall
9. radio-isotope production channel
10. shuttle tube
11. vertical irradiation channel

Figure 1. Horizontal section of the ORPHEE reactor with the nine beam ports (T= thermal, F= cold and C= hot).





ORPHEE-HALL DES GUIDES LLB / 25-03-93

Figure 2. Neutron guide hall with the six cold neutron guides G1 to G6.

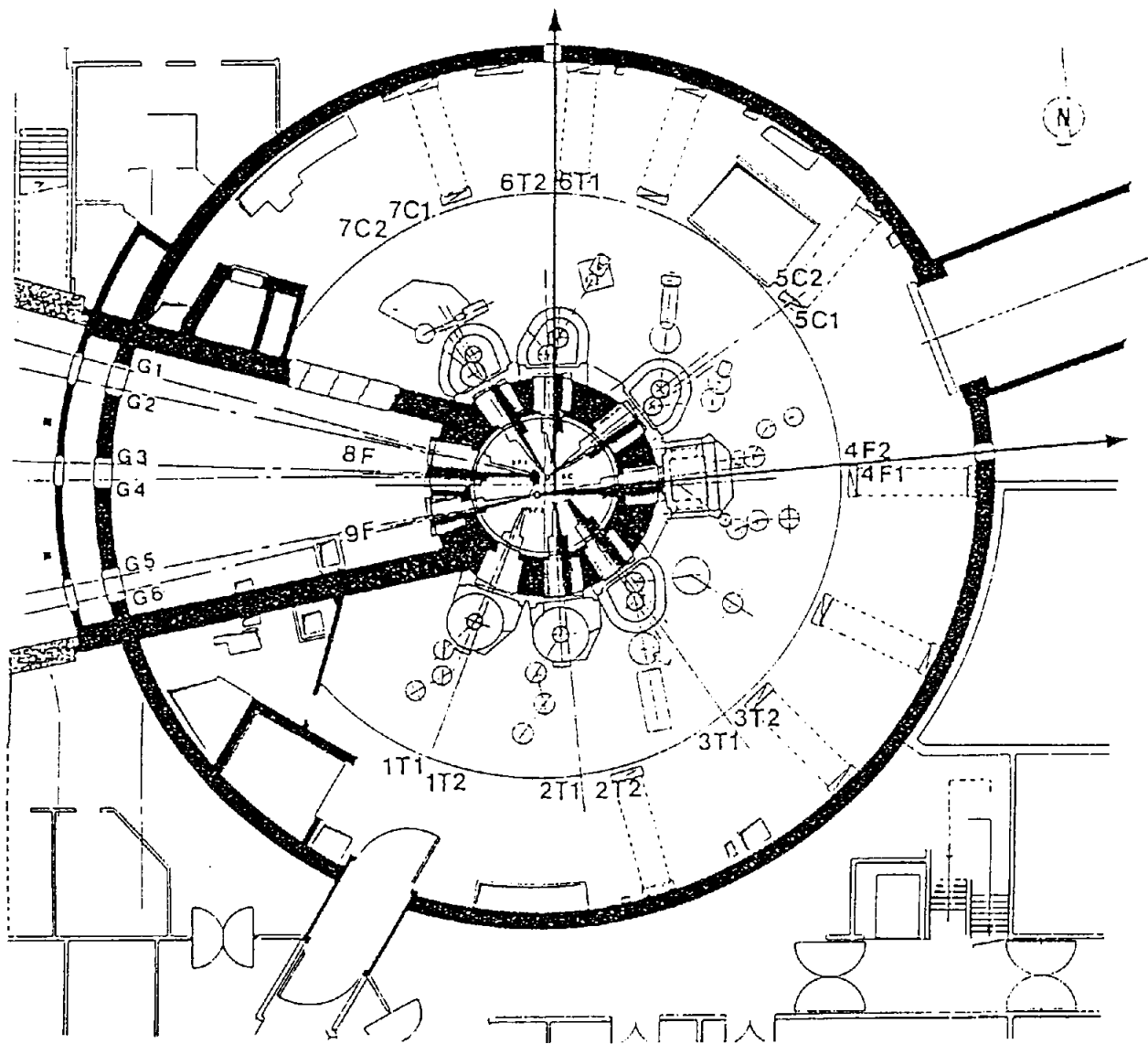


Figure 3. Reactor hall with seven beam ports distributed on the thermal source (T), the hot source (C) and the cold source (F). Two holes are provided in the confinement building for future neutron guides.

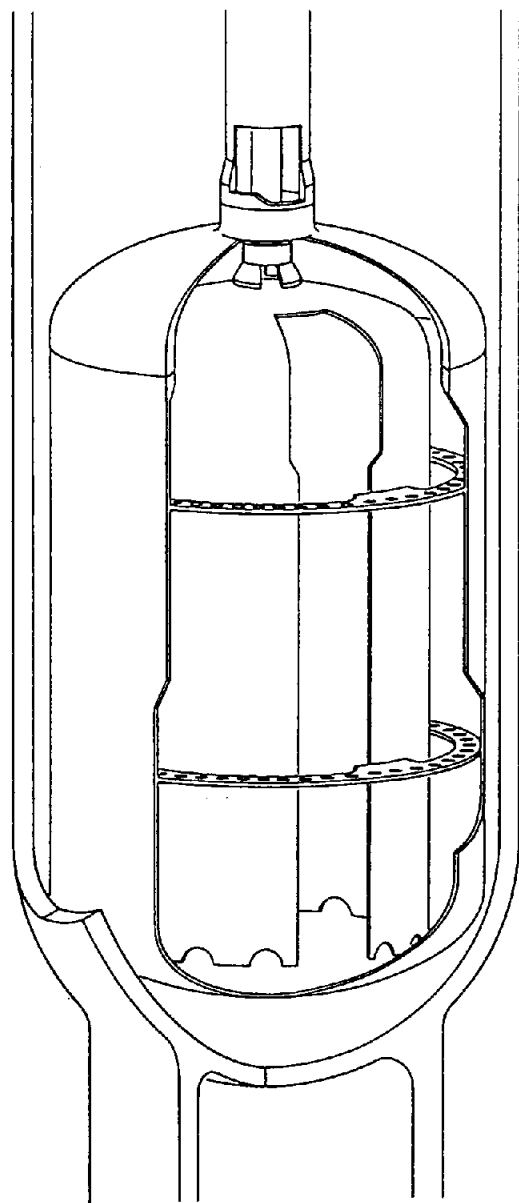


Figure 4. Schematic view of the annular cold source cell.

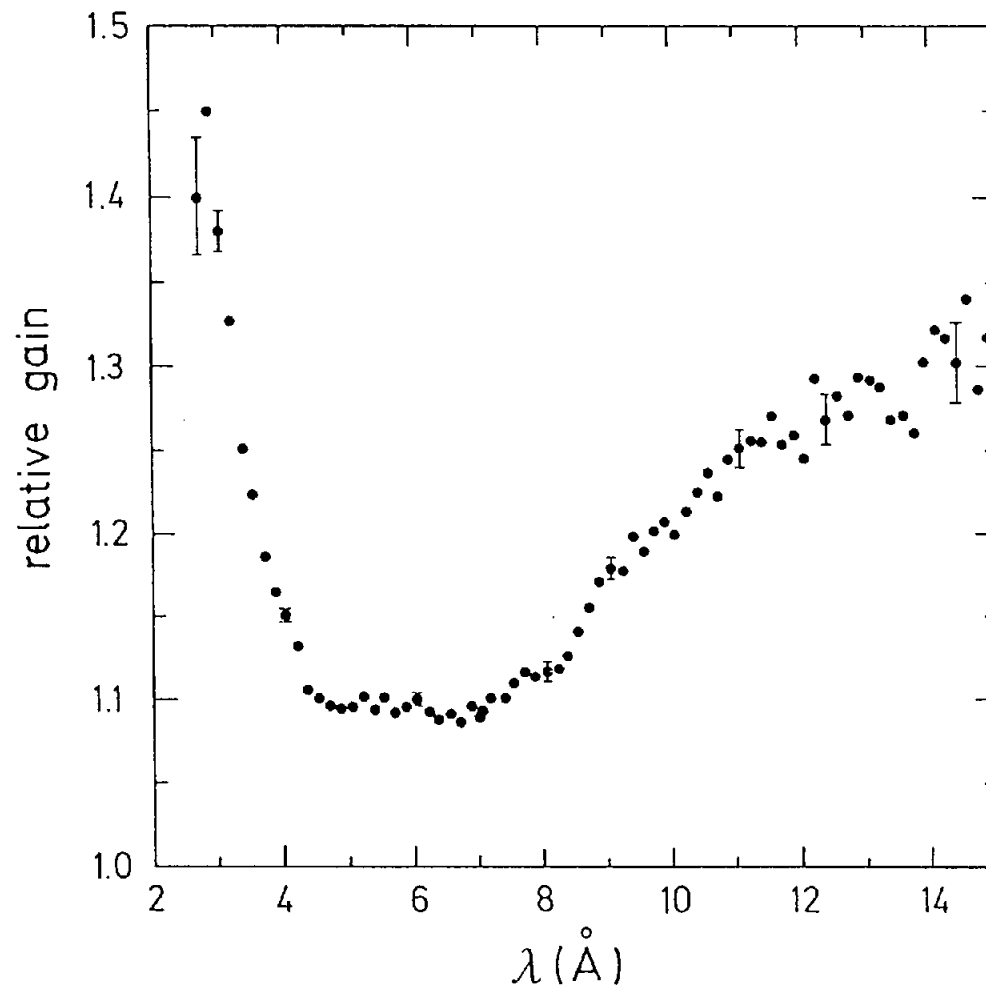


Figure 5. Relative gain of the annular cell compared to the flat cell.

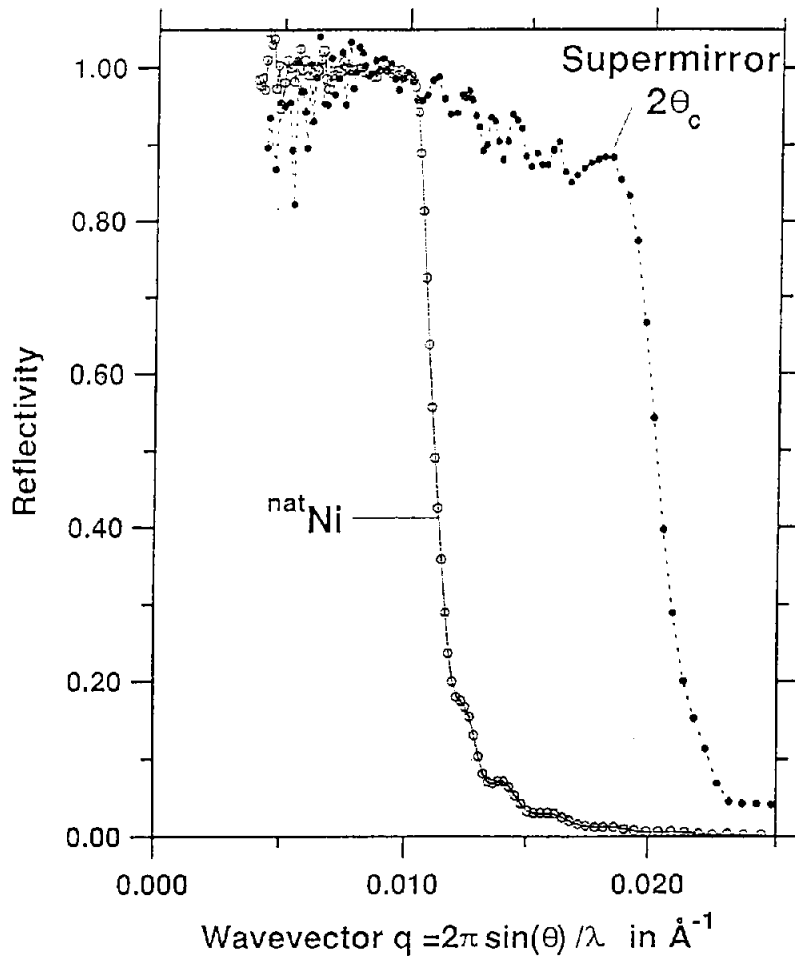


Figure 6. Measured reflectivity of neutron guide mirrors with natural Nickel and super-mirror coatings.

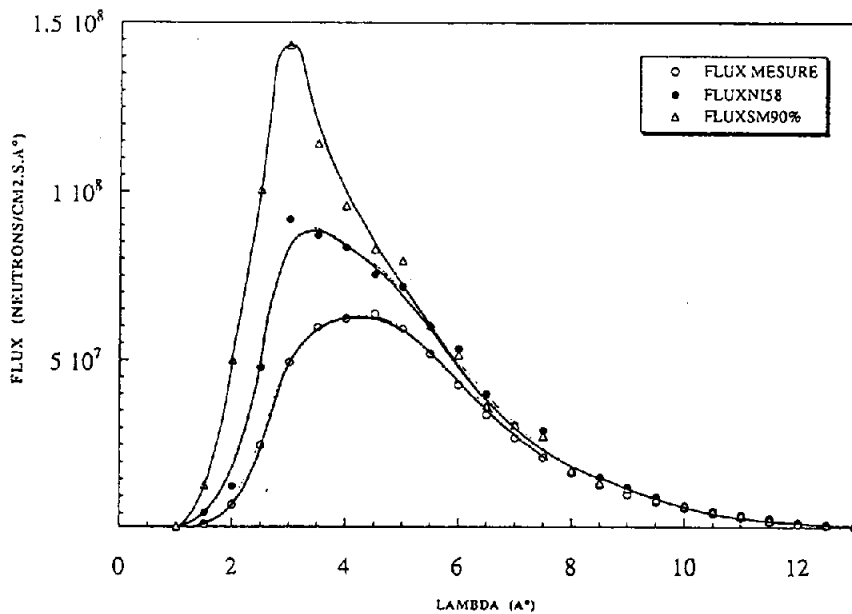


Figure 7. Neutron flux for the guide G2 for three coatings: Natural nickel (open circles, measured), isotopic Nickel (closed circles, calculated), super-mirror (triangles, calculated).

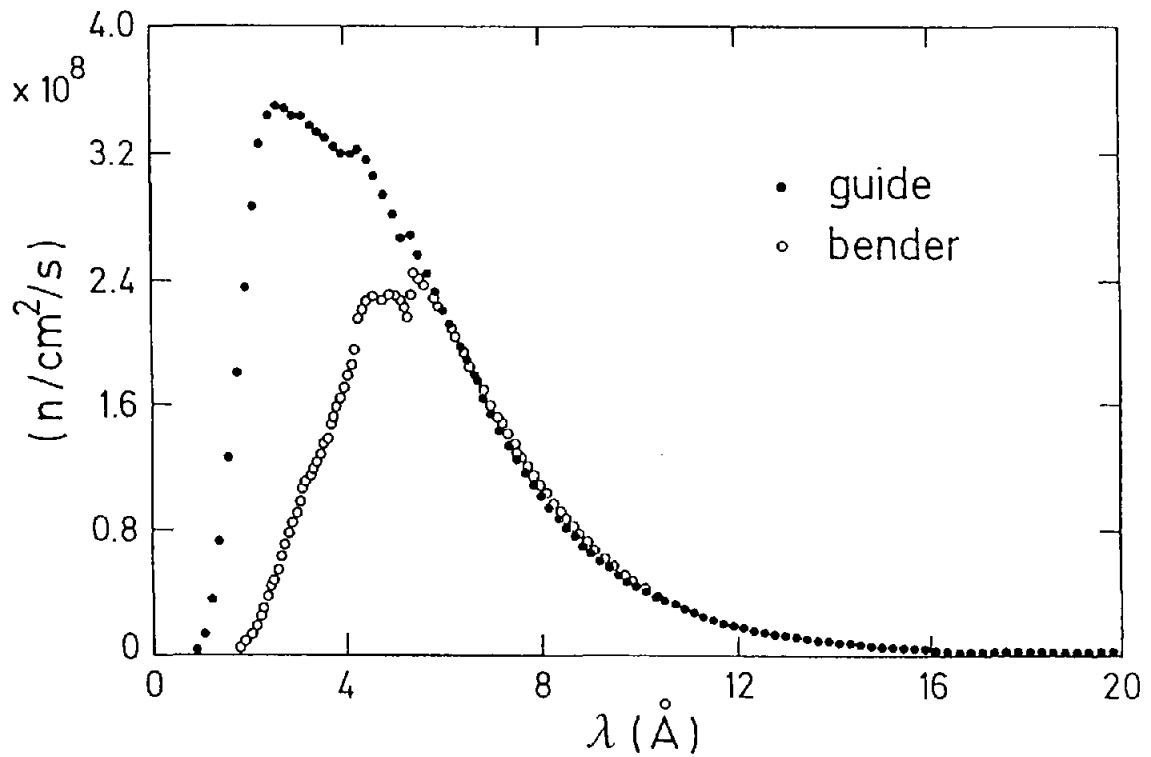


Figure 8. Measured flux at the end of the guide G5 and the bender G5 bis.

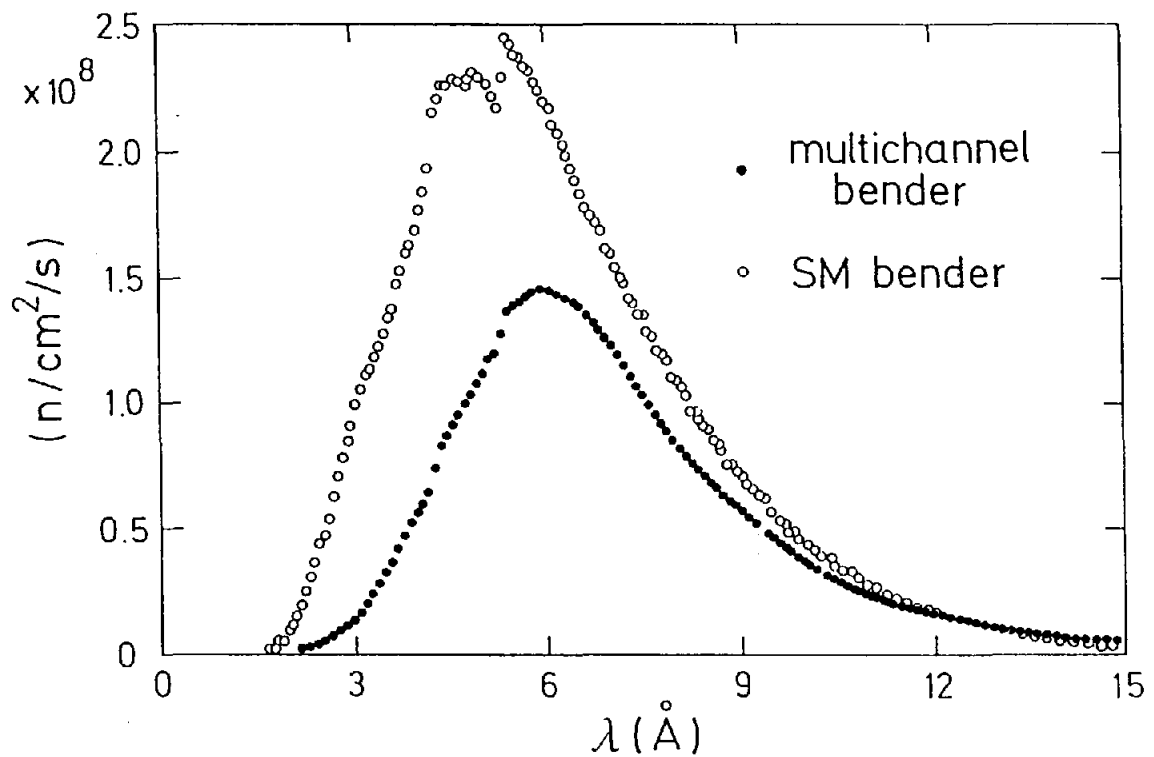
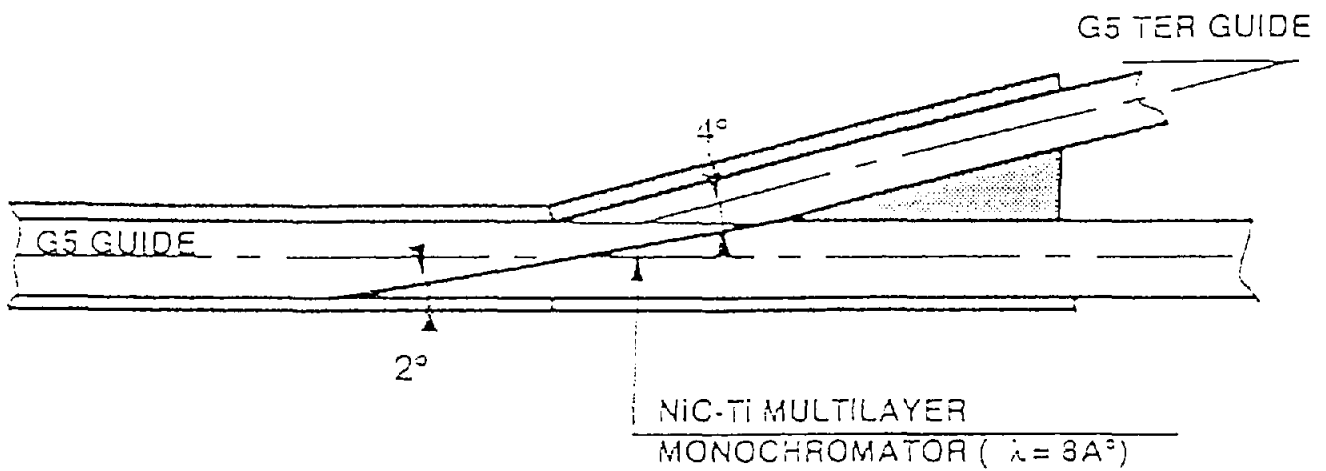


Figure 9. Measured flux at the end of a multichannel bender (G3 bis) and a supermirror bender (G5 bis).



- Coating: Nickel-Carbon/ Titanium
- Substrate: Silicon
- Dimension: 300 mm x 35 mm

Number of layers	Period	incl	$R_{\max}$	$\lambda_{\max}$	$\Delta\lambda/\lambda$	$I(\lambda/2)/I(\lambda)$
60	119 Å	2°	90 %	3 Å	10 %	$10^{-2}$

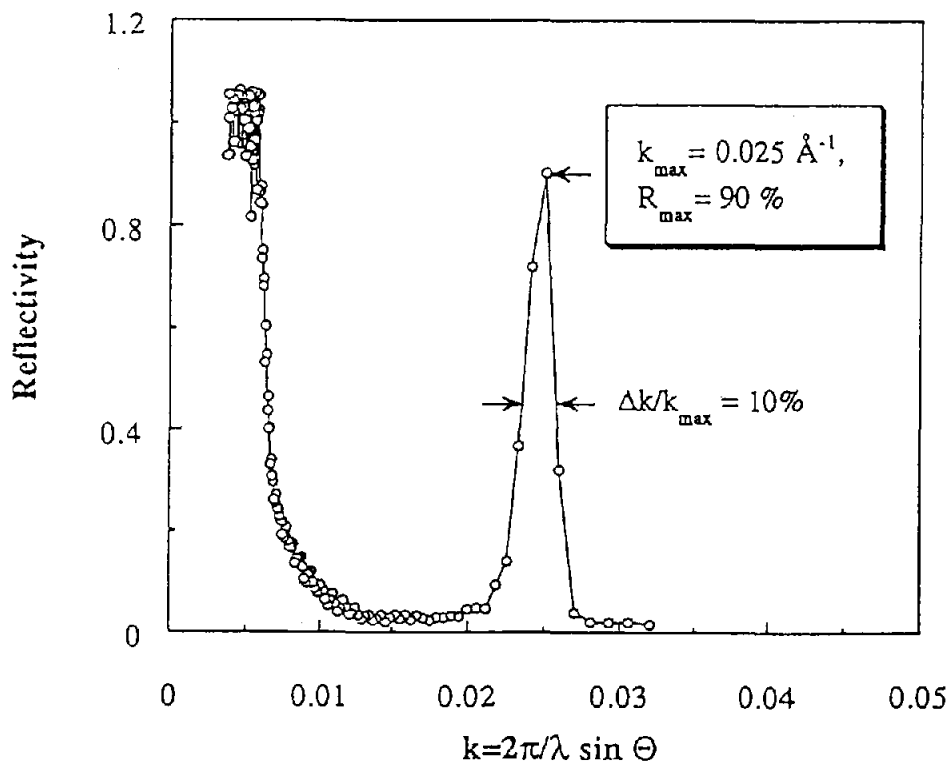


Figure 10 Characteristics of the multilayer monochromator (G5 ter).

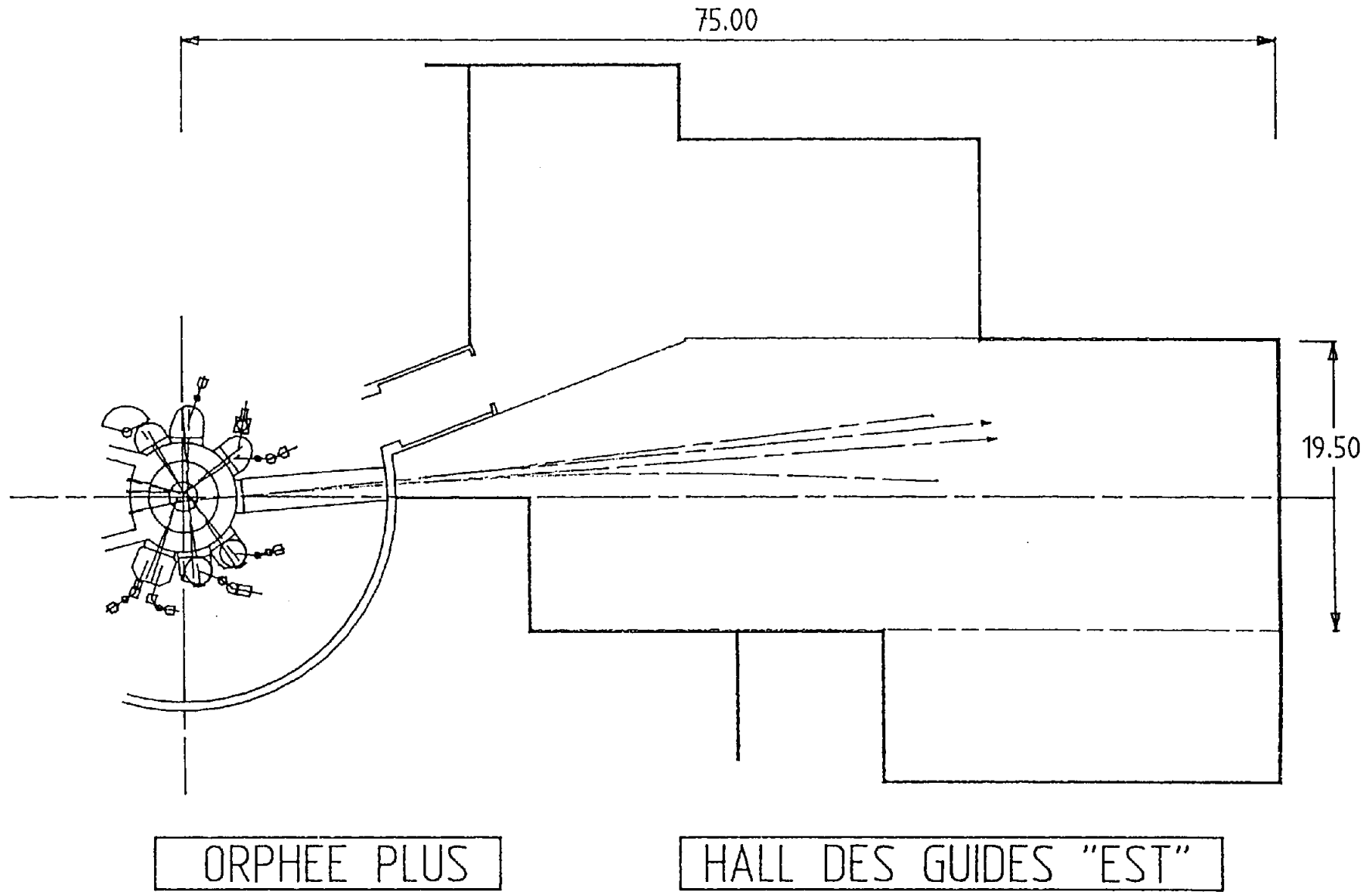


Figure 11. Implantation of new cold guides on the beam port 4F.

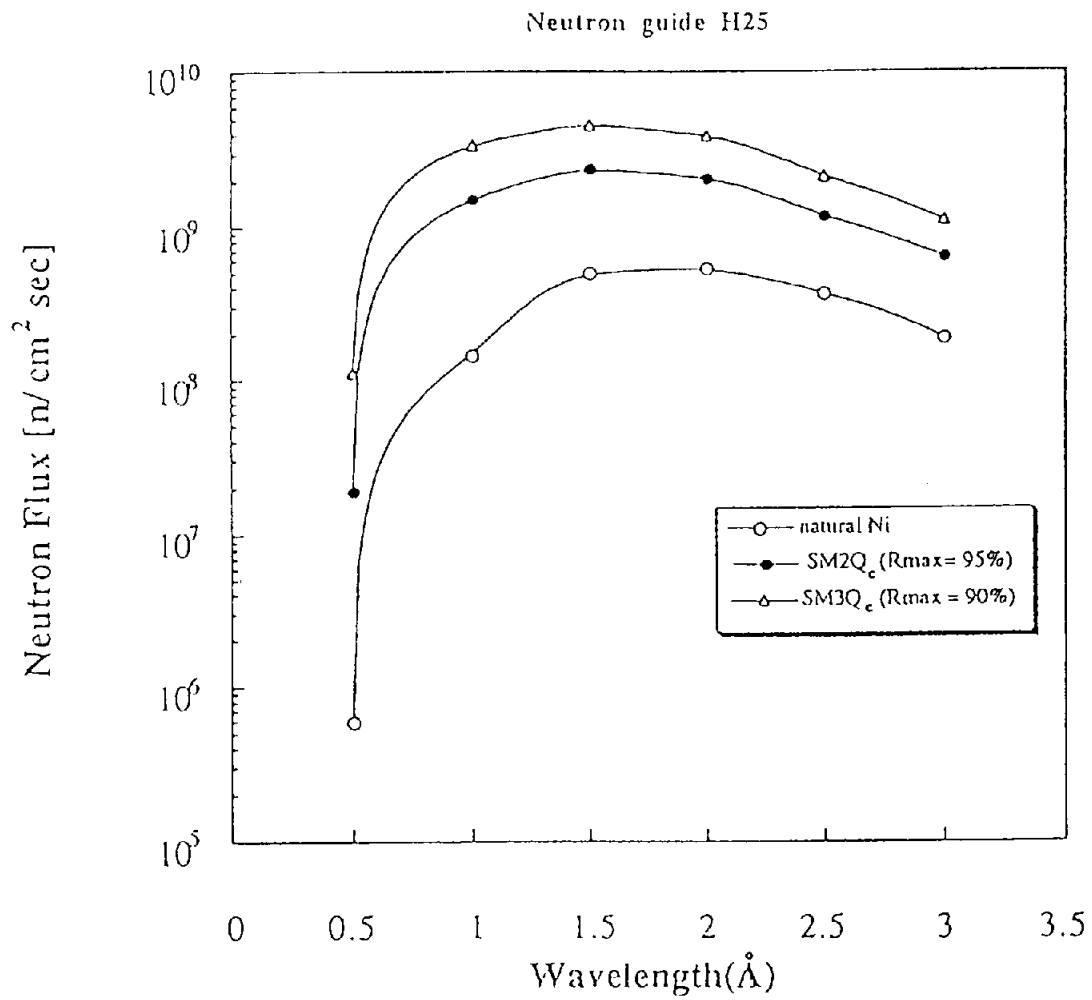
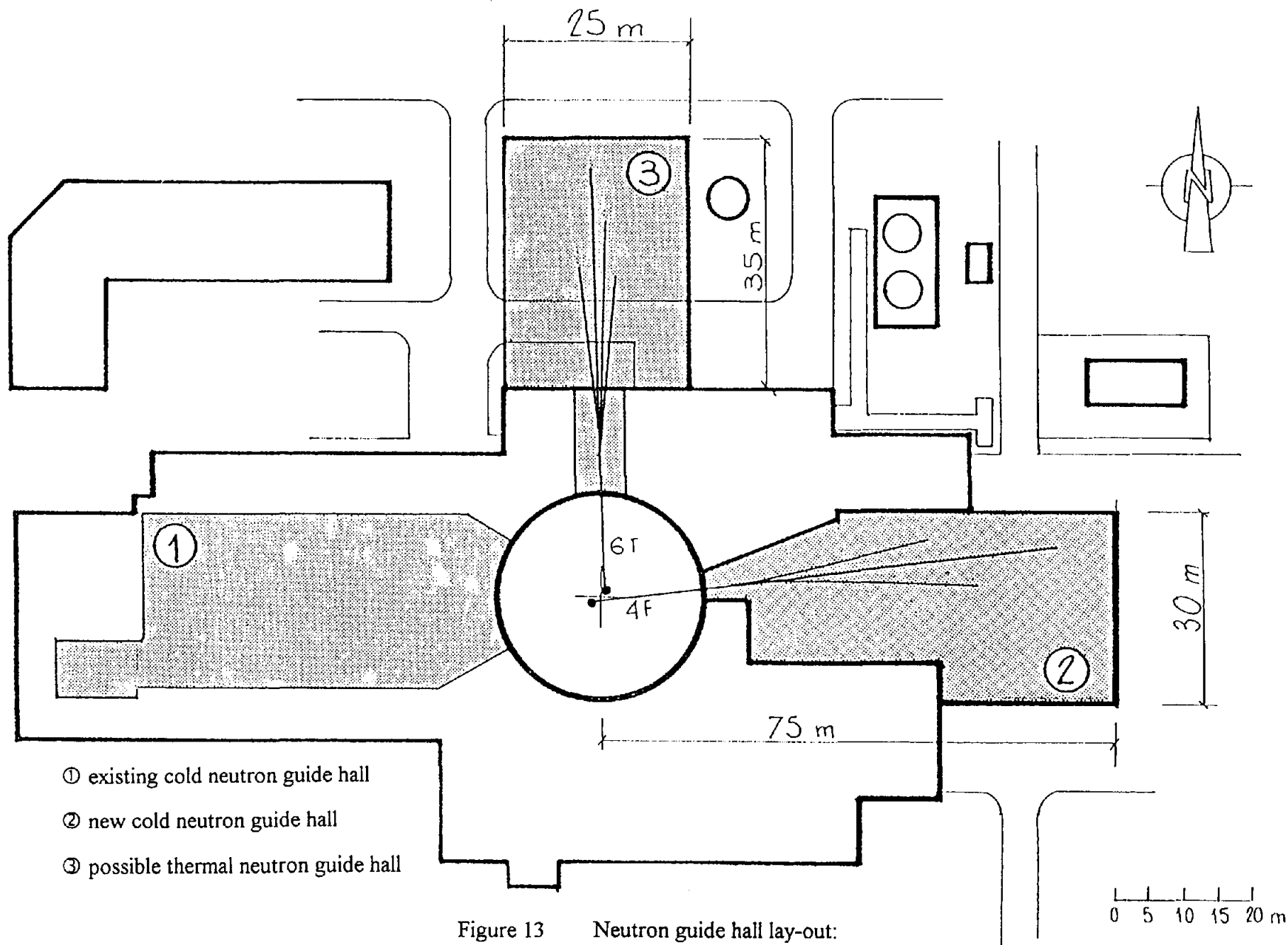


Figure 12. Measured (natural Nickel) and calculated transmission (super-mirrors 2 and 3 times the critical angle of natural Nickel) for the ILL thermal neutron guide H25





## **SESSION II**

# **Research Reactors in Design and Construction**

**STATUS OF THE FRM-II PROJECT**

K. Böning  
Fakultät für Physik E21, Technische Universität München,  
D-85747 Garching, Germany

**ABSTRACT**

The new research reactor FRM-II at Garching near Munich is planned to become a high performance source of slow neutrons in Germany. Its design concept provides for a very compact reactor core cooled by light water and placed within a heavy water moderator tank, where a high thermal neutron flux will be obtained at only 20 MW power. - This paper begins with an overview over some of the essential design features and some more recent design modifications. It then reports on the status of the project, the most important event being a positive decision which the Bavarian State Government has made in January 1993 and which represented a green light for the project to enter the next project phase. Consequently, two official requests have been made by the Technical University of Munich, one for the nuclear licensing of the facility and the other for the so called "Raumordnungsverfahren". In this context the final version of the FRM-II safety report has been submitted to the nuclear licensing authority.

**THE FRM-II PROJECT**

The FRM-II facility is planned to be a high performance national neutron source which shall be built by the Technical University of Munich on its research campus at Garching to replace its existing 4 MW swimming pool research reactor FRM (FRM stands for "Research Reactor Munich"). The FRM-II will have a power of 20 MW; its design has been optimized primarily with respect to beam tube applications, but it will also be very attractive for the utilization of slow neutrons in other fields of research and applications. So the FRM-II will actually represent a multipurpose high flux research reactor.

## FEATURES OF THE FRM-II DESIGN

Reports on the design concept of the FRM-II facility have already been given on the two previous IGORR Meetings /1,2/. To recall some of the essential design features, the reactor core of the FRM-II consists of a single fuel element which is cooled by light water and surrounded by a large heavy water moderator tank. This single fuel element is particularly compact as is shown in Fig. 1. Because of these small dimensions it has to use highly enriched uranium in combination with the new high density silicide fuel. Since this compact core is very undermoderated, about 50 % of the fast fission neutrons immediately leak out into the moderator tank where they are slowed down to yield a high flux level and a pure spectrum of thermal neutrons in a large usable volume. The ratio of flux to power is particularly high for this "compact core" reactor, the unperturbed thermal flux maximum in the D<sub>2</sub>O tank being  $8 \cdot 10^{14} \text{ cm}^{-2}\text{s}^{-1}$  at 20 MW power. The cycle length will be about 50 full power days.

Fig. 2 shows a horizontal cross section of the reactor pool at about core level. The compact core is placed in a vertical core channel tube in the center of the D<sub>2</sub>O moderator tank. The moderator tank has a diameter of 2.5 meters and will be penetrated by 10 horizontal beam tubes, by two slant tubes and by various vertical channels to be used for the irradiation of samples. The spectrum of the slow neutrons can be modified locally by cold and hot sources, and fast fission neutrons can be extracted from one of the beam tubes if a converter plate with uranium has been shifted to its nose.

A horizontal cross section of the reactor block - at a vertical position for above the core - is shown in Fig. 3. The reactor pool, on the right hand side of the figure, is placed in the center of the reactor building (experimental hall). Further to the left follows the storage pool which is used for the decay of spent fuel elements and other radioactive equipment. A transport vehicle allows to bring radioactive material under water to the lower end of a vertical channel through which it can be pulled up into a hot cell. On the far left of Fig. 3 one sees the "limited volume" primary cell which contains the four pumps and two heat exchangers of the primary core cooling circuit.

During the last year the conceptual design of the FRM-II has been worked over and some potential for its further optimization has been identified. As an example, the storage pool of the FRM-II could be enlarged considerably, as becomes evident if Fig. 3 of this paper were compared with Figs. 2 and 3 of Ref. /2/. This has become possible by improving the design concept of the primary cells and reducing their number from 2 to 1; so the axes of the primary pumps are vertical now instead of horizontal. As a further example, the boundary of the D<sub>2</sub>O region in the beam tubes has been shifted as close as possible to the moderator tank; this is not only more economic but also reduces the possible contamination of D<sub>2</sub>O by H<sub>2</sub>O during some processes of maintenance as e.g. the replacement of the core channel tube (Fig. 2). Finally, the statics of the reactor building will be further enforced so that the building will provide protection not only with respect to smaller air-

crafts, but also to larger civil or military jets; this measure has become necessary to improve the public acceptance of the FRM-II project.

## STATUS OF THE FRM-II PROJECT

The conceptual design and the safety concept of the FRM-II facility have been established and a first draft of the safety report has been completed already in the year 1991. (Note: According to German regulations, the safety report is mainly provided for the benefit of the public so that individuals can consider whether or not they might be affected by the project. The licensing authority requires much additional and more detailed information).

During the years 1991 and 1992 the design concept was reviewed and some design simplifications with the potential of cost reductions were identified /2/ as well as some further optimizations of the design, some examples of which were given in the last section. All these efforts could only be made at a strongly reduced speed, however, since a new political decision on whether or not the project could go ahead had to be waited for.

On January 19, 1993, the Bavarian State Government decided to authorize the Technical University of Munich to enter the next phase of the FRM-II project. Since the ministries involved of the German Federal Government had already signalled their agreement earlier, this Bavarian decision represented the long expected green light to go ahead.

The aim of this next project phase is to go through the public procedures as required by law. As a consequence, two official requests have been made in February 1993 by the president of the Technical University of Munich. The first of these requests involves an examination of whether or not the FRM-II complies with the official structural and development plans of the area ("Raumordnungsverfahren"), which also involves an environmental impact investigation. The resulting comment of the responsible Bavarian State authority is expected to become available in about fall of 1993.

The second request is for the nuclear licensing of the FRM-II facility. For this end, an updated draft of the safety report as mentioned above has been submitted to the nuclear licensing authority, the Bavarian State Ministry of Environment. This authority has appointed a Bavarian technical surveillance company, the "TÜV Bayern-Sachsen", as an independent assessor of the facility design. The preceding formal and overall examination of the safety report has already been completed, whence the final version of the FRM-II safety report (together with an environmental impact report) has been submitted to the authority in August 1993. It is anticipated that the safety report could be presented to the public during late summer 1993 so that the public hearing act could be performed in early 1994. In parallel to and after this procedure the detailed design of the FRM-II facility will

be further established for all those components which are essential for nuclear safety. It is hoped that the corresponding detailed examination of the TÜV company and of the nuclear licensing authority will lead - by about the end of 1994 - to the award of the first partial construction permit including a positive safety assessment of the design concept of the facility as well as the permission to construct the FRM-II reactor building.

The final decision on the construction of the FRM-II will be made - by the Bavarian State as well as the German Federal Governments - after the first partial construction permit has been granted. If everything goes well, this final political decision could be expected for the first half of 1995 and the FRM-II could achieve first criticality in about the year of 2000.

### ACKNOWLEDGEMENTS

This paper represents a summarizing report on a project which many colleagues and co-workers from various institutions have contributed to. These include numerous members of the Faculty of Physics E21 of the Technical University of Munich as well as of the Siemens AG (previously Interatom GmbH) company.

### REFERENCES

- /1/ K. Böning: "The Project of the New Research Reactor FRM-II at Munich". Proceedings of the 1st Meeting of the International Group on Research Reactors (IGORR-1), Knoxville, Tenn. (USA), Feb. 28 - March 2, 1990; Report of the Oak Ridge National Laboratory, CONF - 9002100, page 1 - 11 (1990).
- /2/ K. Böning: "Status Report on the FRM-II Project". Proceedings of the 2nd Meeting of the International Group on Research Reactors (IGORR-2), Saclay, France, May 18 - 19, 1992; Bericht des französischen Commissariat a l'Energie Atomique CEA und der Firma Technicatome, Seite 1 - 9 (1992).

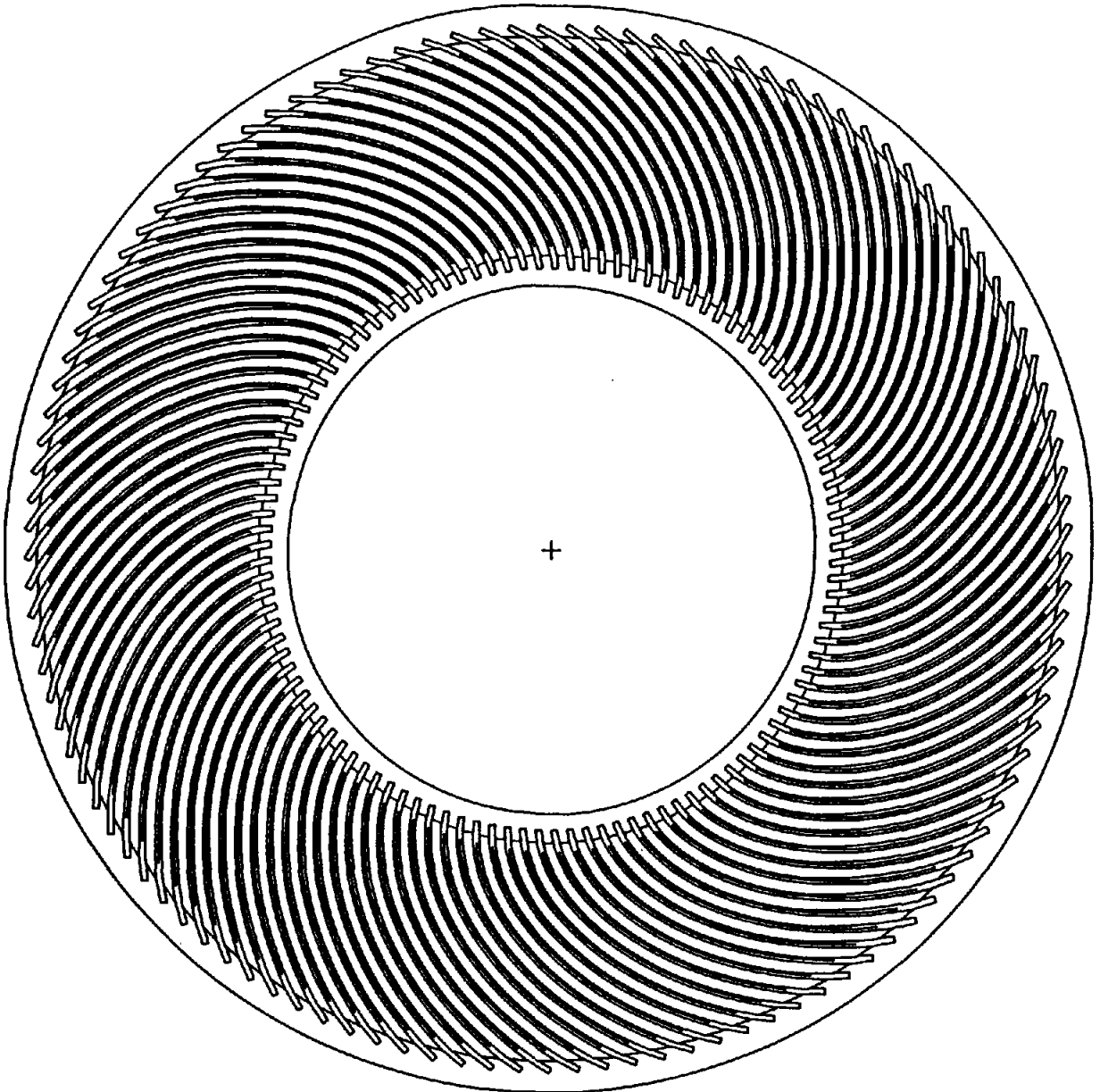


**Fig. 1:** The single fuel element of the FRM-II. The outer and inner diameters of the two core tubes are 243 and 118 mm, respectively. The 113 fuel plates have involute curvature, the axial dimension of the fuel zone being 700 mm and its volume 17.6 liters.

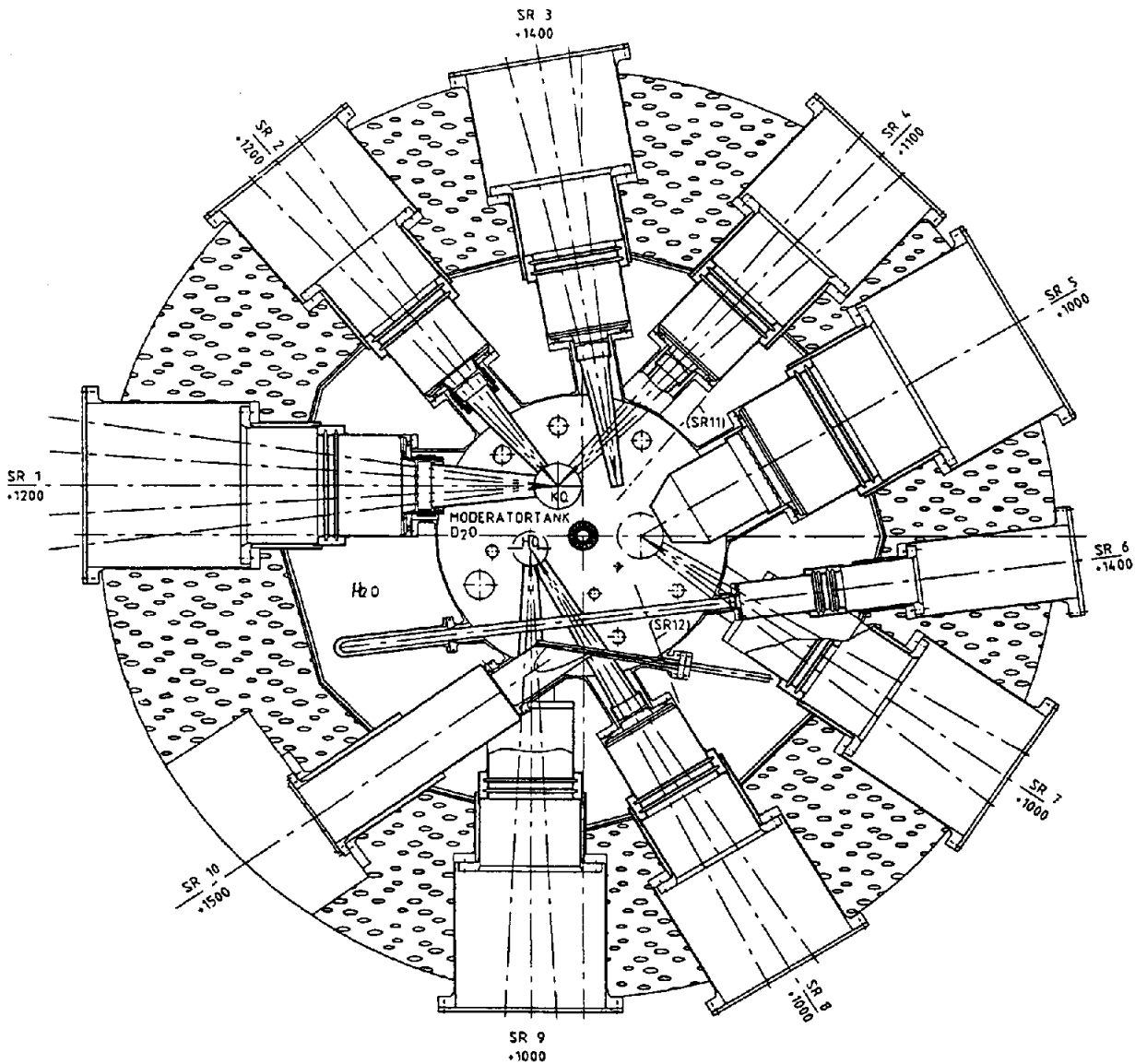


**Fig. 2:** Horizontal cross section of the reactor pool at about core midplane level. The pool is filled with light water  $H_2O$ , the biological shield having an outer diameter of 8.0 meters and consisting of heavy concrete. The moderator tank is full of heavy water  $D_2O$ , where the high neutron flux levels can be used by 10 horizontal beam tubes (SR1-SR10, with positions above ground floor given in mm), two slant tubes (SR11-SR12) and various vertical irradiation channels. There further are cold (KQ) and hot (HQ) sources and an uranium converter (SR10).



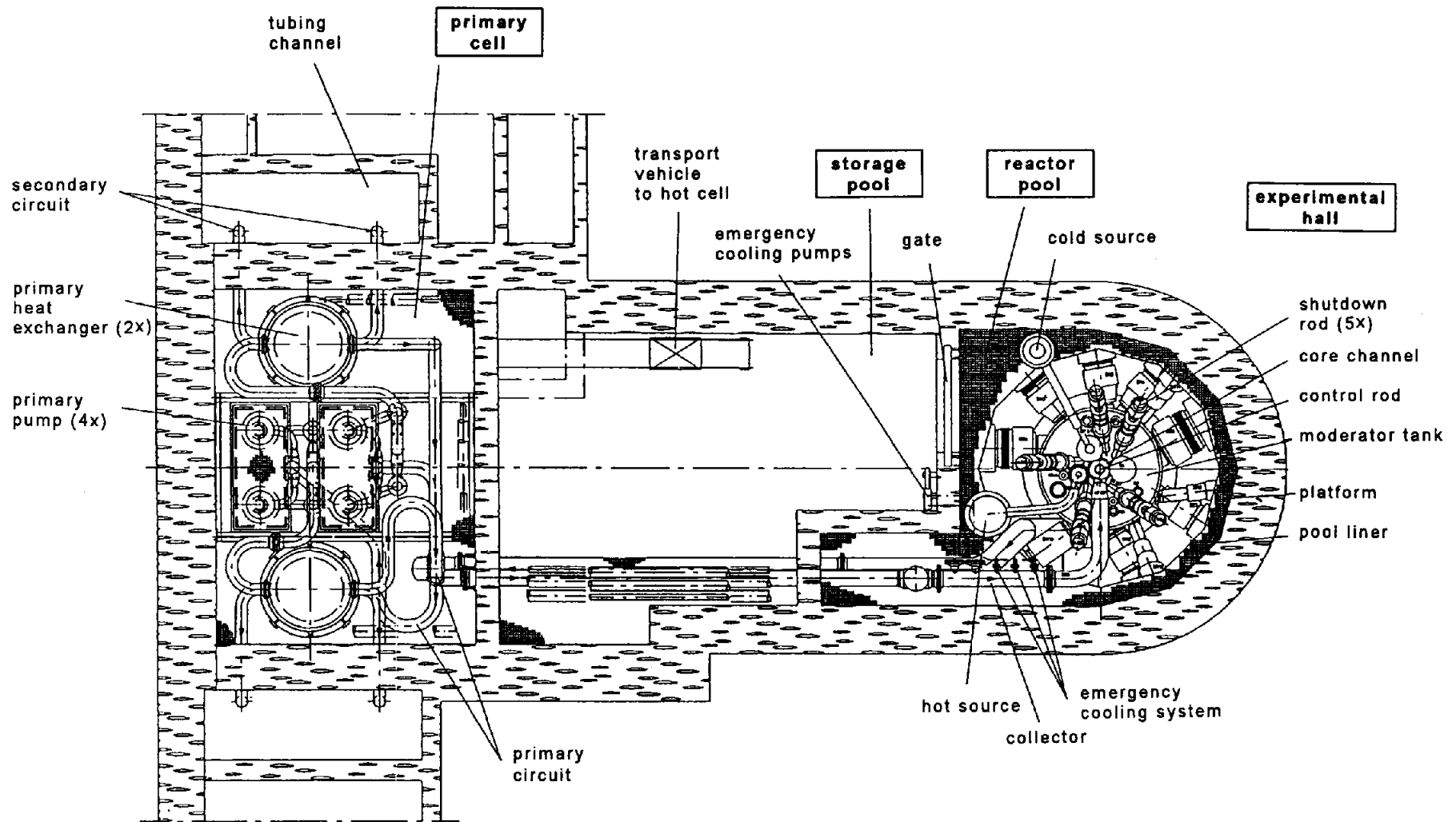


Fig. 3: Horizontal cross section of the reactor block showing the reactor pool, the storage pool and the primary cell. The position of the cutting plane is about 9 m above the ground floor level of the experimental hall.

## PROGRESS TOWARDS A NEW CANADIAN IRRADIATION-RESEARCH FACILITY

by

A.G. Lee and R.F. Lidstone

AECL RESEARCH

### 1. INTRODUCTION

As reported at the second meeting of the International Group on Research Reactors, Atomic Energy of Canada Limited (AECL) is evaluating its options for future irradiation facilities [1]. During the past year significant progress has been made towards achieving consensus on the irradiation requirements for AECL's major research programs and interpreting those requirements in terms of desirable characteristics for experimental facilities in a research reactor. The next stage of the study involves identifying near-term and long-term options for irradiation-research facilities to meet the requirements. The near-term options include assessing the availability of the NRU reactor and the capabilities of existing research reactors. The long-term options include developing a new irradiation-research facility by adapting the technology base for the MAPLE-X10 reactor design [2]. Because materials testing in support of CANDU<sup>1</sup> power reactors dominates AECL's irradiation requirements, the new reactor concept is called the MAPLE Materials Testing Reactor (MAPLE-MTR).

Parametric physics and engineering studies are in progress on alternative MAPLE-MTR configurations to assess the capabilities for the following types of test facilities:

- fast-neutron sites, that accommodate materials-irradiation assemblies,
- small-diameter vertical fuel test loops that accommodate multi-element assemblies,
- large-diameter vertical fuel test loops, each able to hold one or more CANDU fuel bundles,
- horizontal test loops, each able to hold full-size CANDU fuel bundles or small-diameter multi-element assemblies, and
- horizontal beam tubes.

### 2. RESEARCH REACTOR IRRADIATION REQUIREMENTS

To achieve a consensus on the requirements for a new irradiation-research facility, AECL has established a committee that represents all user groups. As CANDU reactor support is the most important program for justifying a new AECL irradiation-research, particular attention has been devoted to examining its major components, namely, fuel technology, reactor materials technology and reactor safety research, and to identifying the aspects of the research that require a source of neutrons.

---

1. CANDU (CANada Deuterium Uranium) is a registered trademark of AECL.

## 2.1 FUEL TECHNOLOGY

The fuel-technology program is a very crucial part of the AECL program because the CANDU fuel bundle is different from the fuel assemblies used in light-water power reactors. It consists of relatively short (0.5 m) lengths of fuel elements, clad in thin-walled collapsible sheaths and assembled with welded end plates. The fuel-technology program investigates the irradiation behaviour:

- of new (e.g., the 43-element CANFLEX bundle) and existing power reactor fuel designs, to improve and further qualify fuel for existing CANDU reactors under normal operating conditions and at extreme limits, and
- of new fuel designs for the next generation of CANDU reactors, including enriched and higher burnup fuels, low void and other passive safety designs, and improved fuel cycles.

## 2.2 REACTOR MATERIALS TECHNOLOGY

The reactor materials technology program is a AECL program because CANDU pressure tubes and calandria tubes are exposed to high neutron fluxes. The reactor materials technology program involves long-term research into:

- parametric studies to further develop and test predictive models for deformation, corrosion and fracture potential,
- end-of-life materials studies that allow the behavioural models to cover the full operational lifetime of the components,
- basic research to improve the fundamental understanding of in-reactor materials and
- development of improved materials and components.

## 2.3 REACTOR-SAFETY RESEARCH

The reactor-safety research program develops information to protect the investment in current CANDU plants and to ensure that future CANDU reactors can be licensed and operated safely. The program is directed at:

- improving the understanding of fuel and fuel-channel behaviour under the high-temperature conditions that characterize various loss-of-coolant accident and severe-fuel-damage scenarios,
- providing data to validate the computer codes and models for safety assessments and licensing of CANDU reactors in an anticipated environment of stricter regulatory requirements and an increased emphasis on passive safety design, and
- characterizing fission-product release, transport and deposition to fully quantify the source-term.

## 2.4 SPECIFIC EXPERIMENTAL REQUIREMENTS FOR CANDU SUPPORT

To achieve the foregoing objectives the irradiation-research facility must provide irradiation conditions that both match and exceed those found in a CANDU reactor. During this past year, a consensus has been reached on the specific experimental requirements described below.

### 2.4.1 Specific Fuel Technology Requirements

The peak linear heat ratings for current and future CANDU fuel range from 50 to 70 kW/m. Hence, there is a requirement to irradiate experimental fuel elements at these ratings. However, the enrichment is expected to vary from 0.71 wt% ( $^{235}\text{U}$  in total U) for the present once-through natural uranium fuel cycle to 1.9 wt% or more for low-void-reactivity (LVR) fuel that achieves an exit burnup of 21 GWd/MgU). Even without the extra enrichment required to support burnable poisons, the need for enriched CANDU fuels is inherent in the target of higher exit burnups (e.g., 1.2 wt% enrichment fuel for 21 GWd/MgU). CANDU fuel-irradiation requirements are summarized in Table 1.

As shown in Table 1, the corresponding fissile content of standard 13-mm elements varies proportionately from 7.5 g/m to ~20 g/m. Accordingly, CANDU fuel-irradiation facilities must cater to a range of fuel ratings per unit initial fissile content, from 2.5 to 9.3 kW/g  $^{235}\text{U}$  (27-99 kW/m/wt%  $^{235}\text{U}$ ). For high-burnup advanced CANDU fuels, the principal range of interest is 2.5-5.5 kW/g fissile (27-58 kW/m/wt%  $^{235}\text{U}$ ).

**TABLE 1**  
**CANDU FUEL-IRRADIATION REQUIREMENTS**  
**(standard 13-mm elements for 37-element bundles)**

Reactor or Fuel Type	Enrichment (wt%)	Fissile Content (g/m)	Fuel Rating (kW/m)	Fuel Rating Per Unit Fissile	
				(kW/m/wt%)	(kW/g fiss)
C-6 or OH OH (Br/Da) C-6	0.71	7.5	70	99	9.3
	0.71	7.5	63	89	8.4
	0.71	7.5	51	72	6.8
SEU*	1.2	12.7	70	58	5.5
	1.2	12.7	50	42	3.9
LVR	1.88	19.9	70	37	3.5
	1.88	19.9	50	27	2.5

\* slightly enriched uranium

Through consulting with the users and analyzing their requirements, the following experimental specifications for irradiation-research facilities have been established:

1. Large-diameter loop facilities for development and prototype-demonstration of full-diameter CANDU fuel bundles:
  - capacity for at least four fuel bundles,
  - minimum flux length of 1.0 m for each test section,
  - representative CANDU conditions (flux, coolant temperature and coolant pressure), and
  - linear fuel-element ratings of 50 to 70 kW/m.
2. Small-diameter loop facilities for fuel-element testing:
  - single elements or partial-bundle multi-element assemblies,
  - representative CANDU conditions (flux, coolant temperature and coolant pressure),
  - capacity for four test sections,
  - linear fuel-element ratings of 50 to 70 kW/m, and
  - capability to vary coolant conditions.
3. Diagnostic capability using:
  - in-pool beam tube for neutron radiography of irradiation fuel (thermal-neutron flux of  $\sim 0.7 \times 10^{18} \text{ n}\cdot\text{m}^{-2}\cdot\text{s}^{-1}$ ), and
  - external beam tube for neutron radiography (thermal-neutron flux of  $\sim 2 \times 10^{18} \text{ n}\cdot\text{m}^{-2}\cdot\text{s}^{-1}$ ).

#### 2.4.2 Specific Reactor Materials Technology Requirements

Linear heat ratings of 50 to 70 kW/m in the CANDU fuel corresponds to fast-neutron ( $E \geq 1 \text{ MeV}$ ) fluxes at the pressure tube of  $0.3 \text{ to } 0.7 \times 10^{18} \text{ n}\cdot\text{m}^{-2}\cdot\text{s}^{-1}$ . The specific requirements of the reactor materials technology program are related to the conditions required to represent the CANDU reactor and the conditions that allow accelerated ageing of CANDU fuel-channel components.

In consultation with the users, the following experimental specifications have been established:

1. Facilities to test full-diameter CANDU fuel-channel sections:
  - capacity for four fuel-channel sections and
  - representative CANDU conditions (flux, coolant temperature and coolant pressure).
2. Deformation and fracture facilities for irradiating small specimens in three fast-neutron ( $E_n \geq 1 \text{ MeV}$ ) flux environments:
  - medium  $0.7 \times 10^{18} \text{ n}\cdot\text{m}^{-2}\cdot\text{s}^{-1}$  (4-5 capsules),
  - high  $1.8 \times 10^{18} \text{ n}\cdot\text{m}^{-2}\cdot\text{s}^{-1}$  (2 capsules), and
  - ultra high  $3.0 \times 10^{18} \text{ n}\cdot\text{m}^{-2}\cdot\text{s}^{-1}$  (2-3 capsules).

3. Corrosion-testing loops for irradiating small specimens:
  - fast-neutron fluxes of  $\sim 0.7 \times 10^{18} \text{ n}\cdot\text{m}^{-2}\cdot\text{s}^{-1}$ ,
  - stainless-steel loops with standard or variable coolant chemistry, and
  - recirculating gas loop.
4. Diagnostic capability using:
  - external beam tube for neutron radiography (thermal-neutron flux of  $\sim 2 \times 10^{18} \text{ n}\cdot\text{m}^{-2}\cdot\text{s}^{-1}$ ), and
  - beam tube access for three instruments: one for residual strain determination, one for texture determination and one for chemical phase and annealing studies (thermal-neutron flux of  $\sim 3 \times 10^{18} \text{ n}\cdot\text{m}^{-2}\cdot\text{s}^{-1}$ ).

#### 2.4.3 Specific Reactor-Safety Research Requirements

In consultation with the users, the following experimental specifications have been established:

1. Test section to handle fuel elements under accident conditions:
  - horizontal orientation to match CANDU fuel-channel orientation,
  - representative flux, coolant temperature and coolant pressure conditions,
  - linear fuel-element ratings of 50 to 70 kW/m,
  - single elements or partial-bundle multi-element assemblies with instrumentation, and
  - high-integrity loop system to study accident conditions.
2. Diagnostic capability using:
  - in-pool beam tube for neutron radiography of irradiation fuel (thermal-neutron flux of  $\sim 0.7 \times 10^{18} \text{ n}\cdot\text{m}^{-2}\cdot\text{s}^{-1}$ ), and
  - external beam tube for neutron radiography (thermal-neutron flux of  $\sim 2 \times 10^{18} \text{ n}\cdot\text{m}^{-2}\cdot\text{s}^{-1}$ ).

#### 2.5 NEUTRON BEAM REQUIREMENTS

The AECL condensed matter science program provides a materials analysis capability in support of CANDU development and participates in AECL's national laboratory role. At present, the study team has concentrated on the requirements to support CANDU development. Accordingly, efforts will be made to match the beam-tube capabilities (i.e., thermal-neutron fluxes of  $\sim 2.0 \times 10^{18} \text{ n}\cdot\text{m}^{-2}\cdot\text{s}^{-1}$ ) of the NRU reactor in any new reactor and possibly to allow a cold neutron source to be added in the future.

#### 3. MAPLE MATERIALS TEST REACTOR DESCRIPTIONS

Several configurations (P0 - P6) of the MAPLE-MTR concept have been studied to explore the range of capabilities that can be provided. The features included in each of the seven configurations (Figure 1) are summarized in Table 1. All MAPLE-MTR configurations were based on the following basic features:

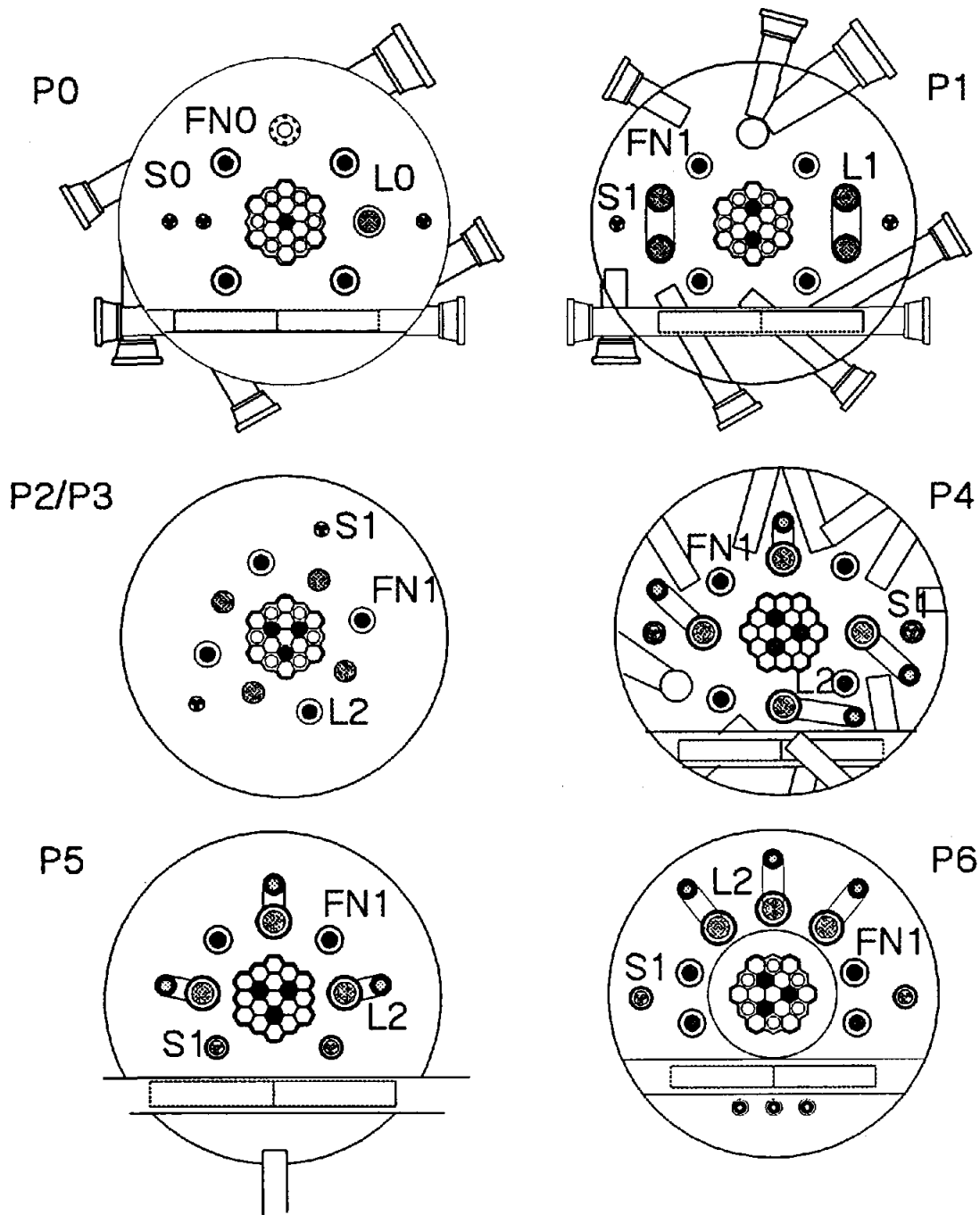


Figure 1: MAPLE-MTR Configurations

TABLE 2

SUMMARY OF FEATURES IN MAPLE-MTR CONFIGURATIONS

FEATURE	CONFIGURATION						
	P0	P1	P2	P3	P4	P5	P6
<b>CORE</b>							
# HEX. FUEL	12	11	10	10	16	16	10
# CYL. FUEL	6	6	6	6	0	6	6
# IRRAD. SITES	1	2	3	3	3	3	3
POWER (MW)	15	15	15	20-25	20-25	21	15
<b>FN-RODS</b>							
TYPE	FNO	FN1	FN1	FN1	FN1	FN1	FN1
NUMBER	4	4	4	4	4	2	4
<b>LOOPS</b>							
# LARGE DIA./TYPE	1/L0	4/L1	4/L2	4/L2	4/L2	3/L2	3/L2
# SMALL DIA./TYPE	3/S0	2/S1	2/S1	2/S1	2/S1	2/S1	2/S1
# HORIZ.	1	1	0	0	1	1	1
BEAM TUBES	5	7	0	0	10	1	0
COLD SOURCE	1	1	0	0	1	0	0

- hexagonal 36-element driver fuel assemblies,
- cylindrical 18-element fuel assemblies for the control and shutdown sites,
- hafnium absorbers for reactivity control, and
- a D<sub>2</sub>O reflector with a dump system to provide a diverse shutdown mechanism.

The P0 to P2 configurations examined the capabilities to provide the desired fast-neutron fluxes and fuel-irradiation conditions for several CANDU fuel elements. The P3 configuration focussed on increasing the fast-neutron flux and the power output from the fuel test loops by using an alternative driver fuel to achieve higher power from the core. The P4 to P6 configurations focussed on the performance of experimental facilities for full-diameter CANDU fuel bundles and for safety-related tests. The P3 to P5 configurations require some departures from the basic core design and imply further development work. The P6 configuration features the basic core design described above.

Two versions of the fast-neutron (FN) rods were examined as part of the study:

- FNO consisted of 42 MAPLE-type fuel elements with two rings, and a central irradiation space of 60 mm inner diameter, and
- FN1 consisted of 58 MAPLE-type fuel elements with two rings, and a central irradiation space of 75 mm inner diameter for compatibility with the materials irradiation rigs for the core.



Two versions of the small-diameter fuel test loops were examined as part of the study:

- a re-entrant test section (S0) to hold from one to four elements and
- a re-entrant test section (S1) to hold from one to seven elements.

Three versions of the large-diameter fuel test loops were examined as part of the study:

- a re-entrant test section (L0) to hold one CANDU fuel bundle,
- a U-shaped test section (L1) with one or two CANDU bundles in each leg of the 'U', and
- a once through test section (L2) with one or two CANDU bundles.

For the re-entrant test section, the coolant flows down an outer annulus and up through the CANDU fuel bundle. For the U-shaped test section, the coolant flows down through one CANDU bundle and up through the second. For the once-through test section, the coolant flows down through a small diameter pipe and up through the CANDU fuel bundle(s). The CANDU bundles for the vertical test loops differ from the actual CANDU bundles in that the centre fuel element is replaced with a solid support rod. Hence the test bundles have 36 CANDU fuel elements arranged in three rings.

#### 4. RESULTS OF PHYSICS CALCULATIONS

The physics calculations for the early (P0 to P2) MAPLE-MTR configurations predict that perturbed fast-neutron fluxes of at least  $1.4 \times 10^{16} \text{ n}\cdot\text{m}^{-2}\cdot\text{s}^{-1}$  are achieved at a core power output of 15 MW. The calculations also showed that the minimum requirements for fast-neutron fluxes for accelerated-ageing investigations can be met in the MAPLE-MTR core.

For the early MAPLE-MTR configurations, perturbed fast-neutron fluxes of  $0.4\text{-}0.6 \times 10^{16} \text{ n}\cdot\text{m}^{-2}\cdot\text{s}^{-1}$  can be achieved in the FN-sites with a core power output of 15 MW. These fast-neutron fluxes match normal operating conditions in CANDU reactors.

For the P0 MAPLE-MTR configuration, the S0 small-diameter fuel test loop provides:

- peak linear ratings of 67 kW/m in each of four natural  $\text{UO}_2$  fuel elements at a distance of 100 mm from the core, and
- peak linear ratings of 47 kW/m in each of four natural  $\text{UO}_2$  fuel elements at a distance of 270 mm from the core.

A parametric assessment of the small-diameter fuel test loop has produced the results shown in Figure 2 for the S1 small-diameter fuel test loop. These calculations were performed with the P6 MAPLE-MTR configuration with a core power output of 15 MW. The linear element ratings in a typical CANDU bundle are also shown in Figure 2 for comparison. These results show that this type of small-diameter fuel test loop can be used to simulate the element ratings for

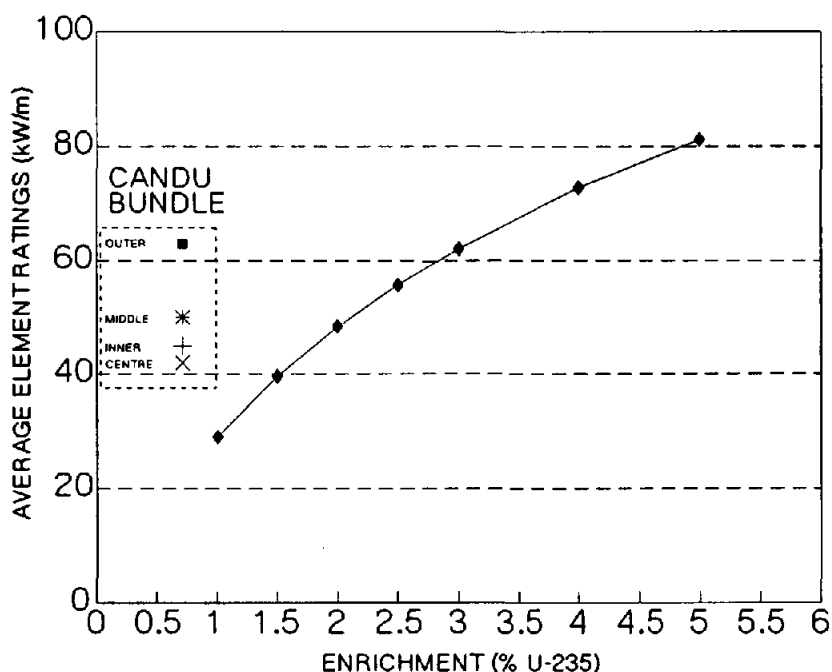


Figure 2: Average CANDU Element Ratings as a Function of  $^{235}\text{U}$  Enrichment in a Small-Diameter Test Loop with Six CANDU Elements

the different rings of elements in a CANDU bundle by adjusting the enrichment in the test assembly.

A parametric assessment of the large-diameter fuel test loop has produced the results shown in Figure 3 for the L2 large-diameter fuel test loop. These calculations were performed with the P6 MAPLE-MTR configuration with a core power output of 15 MW. The linear element ratings in a typical CANDU bundle are also shown in Figure 3 for comparison. It is expected that this type of large-diameter fuel test loop can be used to simulate a wide range of conditions for the CANDU bundle by suitable adjustment of the enrichment.

The fast-neutron fluxes within the CANDU fuel bundle are shown in Figure 4. For comparison, the fast-neutron flux in the centre of the hottest channel, the outside of the hottest channel and the outside of an average channel in a BRUCE-A CANDU unit are also shown in Figure 4. The results in Figure 4 indicates that the test bundle can be adjusted either to match the range of fast-neutron flux conditions in the CANDU reactor by suitable adjustment of the enrichment or to exceed the fast-neutron flux conditions and accelerate damage effects for the cladding.

These parametric assessments help define the capabilities that can be included in a new irradiation facility based on the MAPLE-MTR concept. Further assessments are in progress to understand the trade-offs among different types of experimental facilities as well as to understand the mix of irradiation capabilities required.

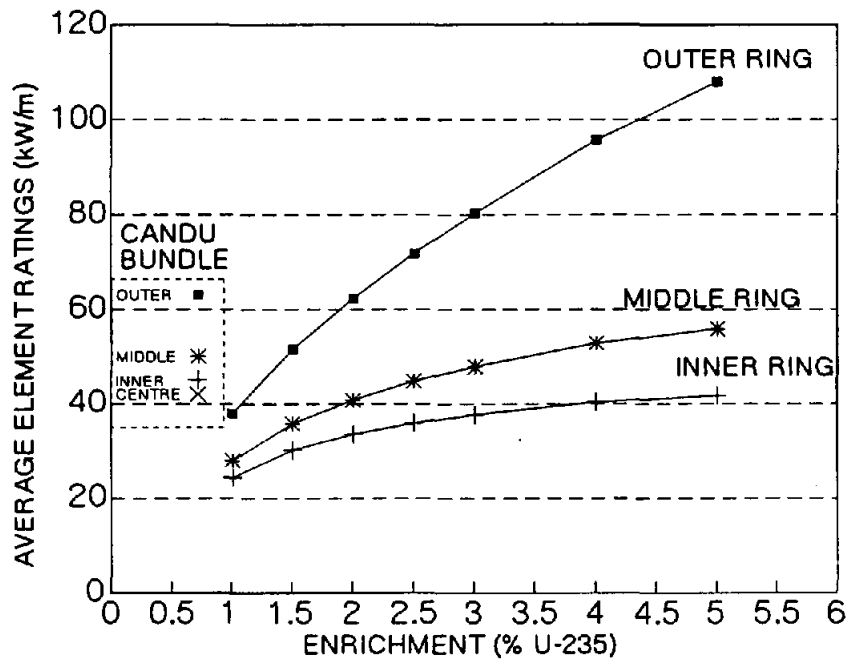


Figure 3: Average CANDU Element Ratings as a Function of  $^{235}\text{U}$  Enrichment in a Large-Diameter Test Loop with a 36-Element CANDU Bundle

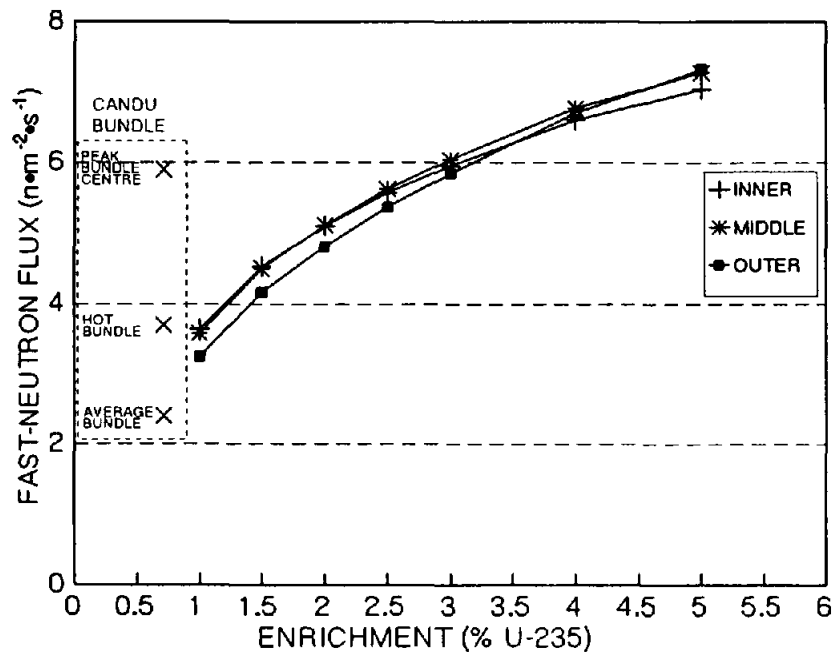


Figure 4: Fast-Neutron Fluxes in a CANDU Bundle as a Function of  $^{235}\text{U}$  Enrichment

## 5. SUMMARY

AECL is at an early stage in its evaluation of options for future irradiation facilities. During the past year the irradiation requirements for the CANDU support research programs have been reviewed and a consensus on these requirements has been achieved. Work is currently in progress to interpret these irradiation requirements to provide detailed technical performance specifications for experimental facilities.

Computer simulations of experimental facilities needed to satisfy various irradiation requirements are in progress. The initial calculations have identified how individual experimental facilities could perform in a MAPLE-MTR. Further analyses of fuel test loops and materials test rigs are under way to characterize interactions among the experimental facilities. As part of the options assessment, work has also been initiated to identify what irradiation capabilities can be provided in existing research reactors to cover near-term requirements.

## ACKNOWLEDGEMENT

The authors wish to acknowledge the contributions of J.R. Lebenhaft, J.V. Donnelly and G.R. Dyck in performing the reactor simulations to characterize power distributions and neutron fluxes.

## REFERENCES

1. Lee, A.G., Lidstone, R.F. and Donnelly, J.V., "Planning a New Research Reactor For AECL: The MAPLE-MTR Concept," Proceedings of the 2<sup>nd</sup> meeting of the International Group on Research Reactors, Saclay, France, 1992 May 18 and 19.
2. Lee, A.G., Bishop, W.E. and Heeds, W., "Safety Features Of The MAPLE-X10 Design," Proceedings of The Safety, Status And Future Of Non-Commercial Reactors And Irradiation Facilities, Boise, Idaho, 1990 September 30 to October 4.

## II-3

# A STATUS REPORT ON THE ADVANCED NEUTRON SOURCE PROJECT

C. D. West  
Oak Ridge National Laboratory

### Introduction

The Advanced Neutron Source (ANS) will be a new laboratory for neutron research, centered around a 330 MW(f) research reactor cooled and reflected by heavy water and including extensive experiment systems and support facilities.

The major components of the baseline design, occupying about 16 heetares, are a guide hall/research support area, containing most of the neutron beam experiment systems, shops and supporting laboratories; a 60 m diameter containment building housing the reactor and its primary coolant system, and selected scientific research facilities; an operations support building with the majority of the remaining plant systems; an office/interface complex providing a carefully designed, user friendly entry point for access control; and several other major facilities including user housing, an electrical substation, a diesel generator building, a cryorefrigerator building, and heavy water cleanup and upgrade systems.

### Conceptual Design

Conceptual design of the ANS began in fiscal year 1988, and the Conceptual Design Report (CDR) was issued in June 1992. The DOE requirements for a CDR are quite stringent, and especially so for a project involving a nuclear reactor. Table 1 lists the documents that, together, make up the CDR. Of special note are the cost and schedule estimates, and the Safety Analysis Report (SAR): this is the first time that such a detailed safety analysis has been prepared at the conceptual design stage.

A massive DOE review (involving more than 75 reviewers) in November and December 1992 identified no insuperable technical difficulties, and accepted the conceptual design as a basis for future work. An independent cost estimate (ICE) performed for DOE by Foster Wheeler Corporation was within 2% of the estimate contained in the project's CDR.

Immediately upon completion of the conceptual design, the ANS Project Office initiated value engineering studies using in-house staff and expert help from the U.S. Corps of Army Engineers. Our studies revealed a number of potential cost savings on the baseline design (for example, placing the buildings so that safety related structures and non-safety related structures are not

contiguous can increase the site preparation costs, but it reduces building costs by even more because of the less stringent seismic criteria). Those changes leading to evident cost savings were processed through the project's configuration control system and documented. The overall savings are illustrated in Table 2. The building layout associated with the April 1993 revision of the design concept is shown in Figure 1.

Table 3 lists some of the potential cost saving changes that are still under consideration. A detailed study is underway of the effects on reactor availability of using different primary cooling system configurations (4 x 33% loops, 3 x 33% loops, and 4 x 25% loops).

### Kohn Committee

The U.S. Department of Energy requested another study of reactor and spallation neutron sources. The task was assigned to the department's Basic Energy Sciences Advisory Committee, who formed a special Panel on Neutron Sources under the chairmanship of Professor Walter Kohn. The Panel visited each of the four DOE laboratories with neutron facilities and organized a broad review of neutron sources and applications from September 10-12, 1992: that review involved 70 national and international experts on neutron research, sources, and instrumentation.

The major thrust of the panel's findings is captured in this paragraph from the Executive Summary of their report.

"After reviewing different alternatives for capability and cost-effectiveness, the Panel concluded that the nation has a critical need for a complementary pair of sources: a new reactor, the Advanced Neutron Source (ANS), which will be the world's leading neutron source; and a 1-MW pulsed spallation source (PSS), more powerful than any existing PSS and providing crucial additional capabilities, particularly at higher neutron energies. The ANS is the Panel's highest priority for rapid construction. In the Panel's view, any plan that does not include a new, full-performance, high-flux reactor is unsatisfactory because of a number of essential functions that can be best or only performed by such a reactor."

### Experiment Systems

The ANS cold source concept has been advanced significantly. The baseline design is now a single phase, forced circulation liquid deuterium system. For safety reasons, no part of the system is below the freezing point of

deuterium, and a double or triple containment philosophy is applied throughout. Cryogenic tests of the commercially supplied circulators are planned to begin in December of this year. The basic scheme is shown in Figure 2.

Work has begun on the design of a hot source. In support of this effort, the scattering kernels of carbon have been improved, and arrangements have been made to measure the thermal conductivity of CBCF (carbon bonded carbon fiber) insulation at very high temperatures both in vacuum and in various gases.

A design concept for a positron source has begun to evolve. It comprises a system for irradiating microspheres of copper, or of copper coated on a substrate, in a rabbit facility. The spheres are then transferred to a vacuum system, where they are spread out into a monolayer which provides a large area source of positrons from  $^{64}\text{Cu}$  decay. The positrons are moderated to low energy and focussed into a relatively intense beam. The concept is illustrated in Figure 3. The positron beam current is expected to be 10-100 nanoamps, 2-3 orders of magnitude higher than the best existing slow positron sources.

#### Summary

Design work on the Advanced Neutron Source facilities has progressed significantly, with cost saving changes to the buildings and other systems. The cold source design has advanced considerably, and in addition design work has been initiated on the hot neutron source and on a positron source.

#### References

F. J. Peretz, *Conceptual Design Summary*, ORNL/TM-12184, Martin Marietta Energy Systems, Inc., Oak Ridge Natl. Lab., September 1992

Table 1. Conceptual design documents

- Conceptual Design Report Summary
- Technical Information Document
- Plant Design Requirements
- Cost and Schedule Document (8 volumes)
- Conceptual Safety Analysis Report (4 volumes)
- Phase I Environmental Report for the ANS at ORNL
- Plans required by DOE or MMES/ORNL Orders, policies, procedures, and guidelines (19 plans in 4 volumes)
- Work Breakdown Structure (3 volumes)
- Integrating Systems Design Descriptions (5)
- Hardware Systems Design Descriptions (35 in 12 volumes)
- Engineering Drawings (376 printed in "D" size)

Table 2. Comparison of CDR and post-value-engineering cost estimates

Funding category	(Constant 1992 dollars) in millions)		Actual year dollars in millions)	
	June 1992 CDR	April 1993 revision	June 1992 CDR	April 1993 revision
Construction line item	1700	1642	2217	2024
Operating expenses	365	395	505	498
Capital equipment	10	18	11	21
Additional instruments <sup>a</sup>	35	33	45	41
Prior year costs	45 <sup>b</sup>	86 <sup>c</sup>	45 <sup>b</sup>	86 <sup>b</sup>

<sup>a</sup> Beyond the initial complement recommended by the ANS National Steering Committee. Many or all of these additional instruments are expected to be funded by industrial or other participating research teams.

<sup>b</sup> Cost of preparing the conceptual design (actual year dollars).

<sup>c</sup> All prior year costs, per DOE instructions (actual year dollars).



Table 3. Items still under consideration but not yet incorporated into the ANS design

Change	Potential saving
Reduce reactor primary and secondary cooling loop capacity	14,418,000
Eliminate emergency heat exchangers	12,040,000
Reduce the size of the main heat exchangers by using the emergency heat exchangers during normal operation	165,000
Use plastic materials in lieu of stainless where feasible	247,000
Delete detritiation/upgrade plant in lieu of lease arrangement	99,540,000
Reduce instrument channels from eight to four	470,000
Compress schedule where possible	15,000,000
Negotiate a reduction in the Tennessee Sales Tax on out of state purchases	0 - 50,000,000
Eliminate Integrating Contractor	17,354,000
Eliminate operating basis earthquake as a design loading	1,190,000
Use site specific wind criteria for Category 1L structures	780,000
Relocate detritiation facility	140,000
Other design suggestions (not well enough developed to assign cost savings)	
Use ANS waste heat	
Utilize passive solar heating	
Use bends in safety class piping in lieu of fittings	
Eliminate 1E diesels	
Substitute metal panel exterior wall in lieu of precast concrete panel system	

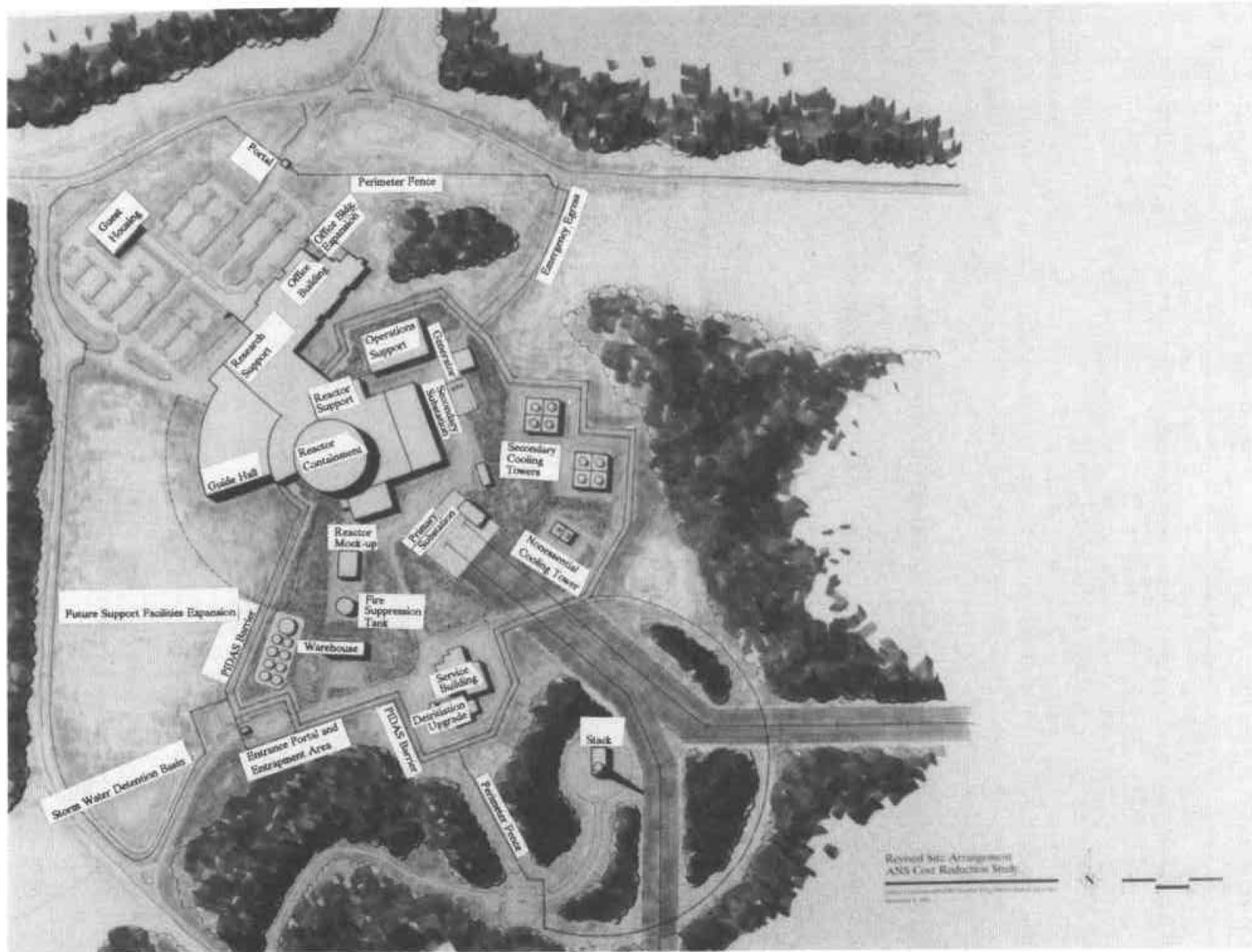


Figure 1

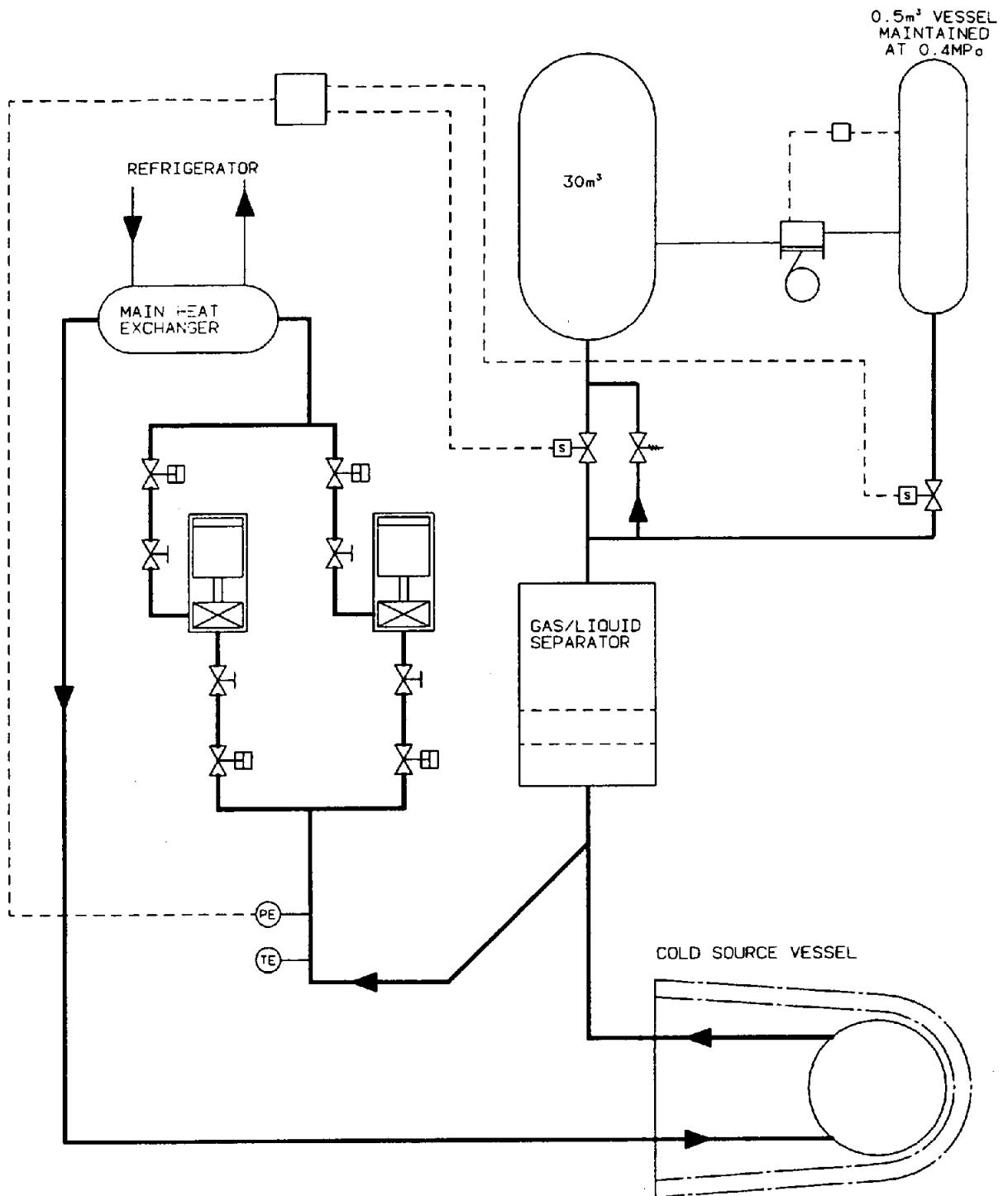


Figure 2



# THE DESIGN CHARACTERISTICS AND CURRENT STATUS OF KMRR

J. T. Lee, J. B. Lee and B. K. Kim  
Korea Atomic Energy Research Institute  
Dukjin-Dong 150, Yoonsung-Ku, Taejon, 305-353, Korea  
Tel:82-42-868-2284, Fax:82-42-861-0209

## ABSTRACT

The construction of the Korea Multi-purpose Research Reactor (KMRR) is scheduled to be completed by the end of 1994.

The KMRR is equipped with several vertical holes for fuel test loop or capsule for the irradiation of reactor's structural materials, radioisotope production, neutron transmutation doping and neutron activation analysis. It also has several beam tubes for the neutron beam experiments.

In this paper, the characteristics of neutron fluxes from physics analysis are summarized for the irradiation sites and experimental sites in the KMRR. And, the experimental facilities of the KMRR including hot cells for radioisotope production and irradiated material experiments are briefly described. Finally, mention is made of the construction status of the KMRR.

## 1. Introduction

The KMRR is a 30 MW open-tank in pool type research reactor. The compact core, which consequently results in high power density and high neutron flux, is cooled by upward forced convection of light water and reflected by heavy water. Even though the core is compact, it gives enough space to install capsules and/or loops within it for material irradiation tests which require high neutron flux. The heavy water reflector tank provides large space of high thermal neutron flux field for various irradiation and experiments.

The specific utilization programs of KMRR comprise;

- fuel and material testing to support the manufacturing and developing projects of fuel and reactor components for PWRs and CANDUs,
- the production of key radioisotopes including Tc-99m, I-131, Ir-192, Co-60, etc.,
- the production of neutron transmutation-doped silicon,
- neutron beam experiments including neutron radiography and,

- neutron activation analysis.

To satisfy these functions of variety, many vertical holes and horizontal beam tubes are required. The neutron flux requirements for the experimental sites are summarized with their geometrical characteristics, in Table 1.

In addition to the experimental holes and beam tubes, two kinds of experimental facilities with several hot cells in the KMRR site are required. One is radioisotope production facility(RIPF) to process radioisotopes irradiated from the reactor, and the other is irradiated material examination facility(IMEF) for fuel performance and material tests. Design of the KMRR was accomplished on the basis of the above requirements.

## 2. The Design Characteristics of KMRR

The KMRR core configuration is shown in Fig. 1. The hybrid-type core is composed of inner and outer core. The inner core is compact, modular, and cooled and moderated by light water. The outer core in the peripheral zone of the inner core is cooled by light water and moderated by heavy water.

The inner core, forming corrugated rectangular shape, consists of 23 hexagonal flow tubes and 8 cylindrical flow tubes. The outer core is composed of 8 cylindrical flow tubes embedded in the D<sub>2</sub>O reflector tank. For the sake of neutron economy, all the core structure is made of zircaloy-4. The flat-to-flat distance between hexagonal flow tubes is uniformly 8.01 cm. Adjacent flow tubes are separated by a 2.5 mm gap that is normally filled with light water.

In normal operation of KMRR, thirty six element fuel assemblies are loaded in 20 hexagonal flow tubes while 18 element fuel assemblies are charged in 12 cylindrical flow tubes. The reactor is controlled by 4 shutoff and 4 control absorbers. The absorber has the shape of hollow cylinder which surrounds an 18 element fuel assembly so as to keep a compact core and to have larger control rod worth. It is composed of 4.5 mm thick hafnium shroud. The reactor is located at the bottom of light water pool with 4 meters in diameter and 13 meters in height.

The fuel element is rod type with finned aluminum cladding and aluminum end plugs. It has a nominal composition of 61.4 w/o U<sub>3</sub>Si and 38.6 w/o Al and contains low enriched uranium of 20 w/o U-235. There are two types of fuel elements in KMRR: One is the standard fuel meat element of which the meat diameter is 6.35 mm; and the other is the reduced fuel meat element of which the meat diameter is 5.49 mm. The active length of the both fuel elements is 700 mm.

The 36 element fuel assembly uses two kinds of fuel elements. Inner ring and middle ring consist of standard fuel meat elements while outer ring is comprised of reduced fuel meat elements. The 18 element fuel assembly makes use of standard fuel meat elements. The KMRR fuel assembly is depicted in Fig. 2.

The characteristics of reactor physics and thermal-hydraulics of KMRR are given in Table 2. The maximum thermal flux of the reactor core is estimated at  $4.4 \times 10^{14}$  n/cm<sup>2</sup>.sec at the central flux trap with dummy fuel loading. As shown in Fig. 1, the KMRR core has various experimental holes and beam tubes. Overall neutron characteristics of each vertical hole and nose of beam tube are presented in Tables 3 and 4.

Three neutron flux traps in the inner core (CT, IR1, and IR2) and irradiation holes in the outer core (OR3,4,5, and 6) where high fast and epithermal neutron fluxes are available, are very useful for the loop and capsule irradiation tests of power reactor fuel and material, and radioisotope production of Tc-99m, Ir-192 and Co-60.

In the D<sub>2</sub>O reflector tank region, there are 5 large holes from 10 cm to 22 cm in diameters for the each specific purpose described in Table 1, twenty holes of 6 cm in diameter for various radioisotope production and neutron activation analysis, and 7 beam tubes. The LH hole is useful to install a fuel test loop for the power reactor. The neutron flux level and spectrum are suitable for the PWR and CANDU fuel performance evaluation. The CNS hole will accept a cold neutron source which provides high monoenergetic neutron beam to the neutron guide tube. The HTS hole is used to install a hydraulic transfer system for radioisotope production. Two neutron transmutation doping holes (NTD1 and 2) are wide enough to dope commercial size silicon ingots. Three NAA holes (NAA1, 2 and 3) give variety of flux level for neutron activation analyses. NAA1 is used to install a pneumatic transfer system by manual mode while others to install pneumatic transfer system by automatic mode. Seventeen IP holes (IP1 -IP17) give variety of neutron flux level and spectrum for various radioisotope productions.

Six tangential neutron beam tubes are carefully designed to maximize thermal neutron flux and to provide enough space for spectrometer layout with minimized fast neutron and gamma fluxes. For typical neutron spectrometer applications, four standard beam tubes (ST1-ST4) are designed to have rectangular shape. In conjunction with the CNS thimble, CN beam tube will be dedicated to cold neutron beam experiments. The neutron radiography facility will be attached to NR beam tube. Utilization of IR beam tube is foreseeing mainly the irradiation-induced material damage research.

### **3. RIPF and IMEF Buildings**

In the KMRR site, Radioisotope Production Facility (RIPF) and Irradiated Material Examination Facility (IMEF) are being constructed in conjunction with the KMRR.

The RIPF has 4 heavy concrete hot cells with 1.2 m shielding thickness, 17 lead hot cells with 15 cm or 10 cm shielding thickness and several experimental laboratories. Hot cells are prepared to process radioisotopes irradiated from the KMRR core. The RIPF provides also activation analysis room, radioisotope laboratory, labelled compound isotope laboratory, silicon processing room and beam tube laboratory.

The IMEF has 7 heavy concrete hot cells with 1.2 m shielding thickness, 2 lead hot cells with 19 cm shielding thickness, and a water pool to transfer a fuel assembly into the hot cell. Hot cells are prepared to accomplish material tests and fuel performance tests.

#### 4. Current Status of KMRR

Excavation work for the KMRR facilities started in February 1989. Concrete structure work including embedments was completed by May 1992, while the installation of pool liners consisting of reactor pool, service pool and spent fuel storage pool was completed by the end of 1992. The installation of mechanical equipment such as piping, primary pumps, heat exchangers, etc., was completed by May 1993. The installation of reactor and reactivity control unit is on-going to be completed by March 1994.

Recently non-nuclear commissioning tests for construction acceptance test (CAT) and system performance test (SPT) are being performed. Test procedures for CAT and SPT have already been prepared to accomplish successful commissioning works. Non-nuclear tests will be finished by June 1994. Nuclear test procedures are under development aiming at the completion by the end of 1993. At this stage, first criticality will be scheduled in December 1994.

#### References

1. S. K. Oh, H. J. Kim and Y. K. Kim, "Reactor Experimental Facility Layouts", KM-00100-021-900.08, June 1986.
2. S. T. Baek, J. B. Lee, et al., "KMRR Utilization Plan", Proceedings of the Korea Nuclear Society Autumn Meeting, Vol.2, Oct. 1992.
3. H. R. Kim, W. S. Park, et al., "Reactor Physics Design Manual of KMRR", to be published.



Table 1. Experimental Facility required to KMRR

Location	Hole	Shape	No	Size (cm)	Neutron Flux(n/cm <sup>2</sup> .sec)		Purpose	
					Fast	Thermal		
Core	Inner core	CT	HEX	1	7.44	$1.3 \times 10^{14}$	$5.0 \times 10^{14}$	capsule or loop
		IR	HEX	2	7.44	$1.0 \times 10^{14}$	$1.3 \times 10^{14}$	capsule or loop
	Outer core	OR	Cyl	4	6.0		$3.0 \times 10^{14}$	capsule
Reflector	Hole	CNS	Cyl	1	16.0		$2.0 \times 10^{14}$	cold neutron source
		NTD	Cyl	2	22.0		$2.0 \times 10^{14}$	silicon doping
						18.0		$1.5 \times 10^{14}$
		LH	Cyl	1	15.0		$1.0 \times 10^{14}$	fuel test loop
		HTS	Cyl	1	10.0		$1.0 \times 10^{14}$	hydraulic transfer system
		NAA	Cyl	3	6.0		$1.0 \times 10^{14}$	pneumatic transfer system
		IP	Cyl	17	6.0		$0.5 \sim 2.5 \times 10^{14}$	RI production
	Beam Tube	ST	Rectangular	4	7×14		$3.0 \times 10^{14}$	spectrometer
		CN	"	1	7×15		$2.0 \times 10^{14}$	cold neutron beam
		NR	Cyl	1	10.0		$0.7 \times 10^{14}$	neutron radiography
IR		Cyl	1	10.0		$2.5 \times 10^{14}$	irradiation test	

Table 2 Main Characteristics of KMRR

	Description
Reactor Power (MWth)	30
Reactor Type	Open-tank-in-Pool
Coolant	H <sub>2</sub> O
Reflector	D <sub>2</sub> O
Nuclear Properties	
Excess Reactivity (mk)	114
Control Rod Worth (mk)	143
Shut off Rod Worth (mk)	175
Temperature Coefficient (mk/°C)	
fuel	-0.0122
coolant	-0.0143
Prompt Neutron Lifetime (sec)	$0.822 \times 10^{-4}$
Delayed Neutron Fraction	$0.763 \times 10^{-2}$
Max. Neutron Flux (n/cm <sup>2</sup> sec)	
core	
thermal flux	$4.5 \times 10^{14}$
fast flux	$2.1 \times 10^{14}$
Reflector	
thermal flux	$2.0 \times 10^{14}$
fast flux	$2.3 \times 10^{12}$
Thermal-Hydraulic Properties	
Coolant Temperature (°C)	35/45
Flow Rate (kg/sec)	635
Pressure (MPa)	0.4
Max. Fuel Temperature (°C)	307
MCHFR	3.42

Table 3 Characteristics of Neutron Flux in  
Experimental Holes in KMRR

(unit : n/cm<sup>2</sup>.sec)

Site	Hole Name	Fast Flux (>0.8 Mev)	Thermal Flux (<0.625 ev)
Inner core	CT	$2.10 \times 10^{14}$	$4.40 \times 10^{14}$
	IR1	$1.88 \times 10^{14}$	$3.82 \times 10^{14}$
	IR2	$1.95 \times 10^{14}$	$3.93 \times 10^{14}$
outer core	OR3	$2.13 \times 10^{13}$	$3.06 \times 10^{14}$
	OR4	$1.98 \times 10^{13}$	$2.72 \times 10^{14}$
	OR5	$2.07 \times 10^{13}$	$2.94 \times 10^{14}$
	OR6	$2.25 \times 10^{13}$	$3.36 \times 10^{14}$
Reflector (D <sub>2</sub> O Tank)	CNS	$1.32 \times 10^{12}$	$1.73 \times 10^{14}$
	LH	$6.62 \times 10^{11}$	$9.77 \times 10^{13}$
	NTD1	$6.98 \times 10^{11}$	$3.93 \times 10^{13}$
	NTD2	$1.10 \times 10^{10}$	$6.20 \times 10^{13}$
	HTS	$9.84 \times 10^{11}$	$8.17 \times 10^{13}$
	NAA1	$6.33 \times 10^{10}$	$3.63 \times 10^{13}$
	NAA2	$1.70 \times 10^{11}$	$9.37 \times 10^{13}$
	NAA3	$1.34 \times 10^{12}$	$1.62 \times 10^{14}$
	IP 1	$1.96 \times 10^{10}$	$4.80 \times 10^{13}$
	IP 2	$8.25 \times 10^{10}$	$2.87 \times 10^{13}$
	IP 3	$1.37 \times 10^{12}$	$1.62 \times 10^{14}$
	IP 4	$1.21 \times 10^{10}$	$3.44 \times 10^{13}$
	IP 5	$9.91 \times 10^{11}$	$7.30 \times 10^{13}$
	IP 6	$1.62 \times 10^{10}$	$4.67 \times 10^{13}$
	IP 7	$1.51 \times 10^9$	$2.44 \times 10^{13}$
	IP 8	$4.08 \times 10^{10}$	$5.78 \times 10^{13}$
	IP 9	$3.43 \times 10^{11}$	$1.51 \times 10^{14}$
IP10	$9.41 \times 10^{10}$	$7.68 \times 10^{13}$	
IP11	$7.71 \times 10^{11}$	$1.02 \times 10^{14}$	
IP12	$5.00 \times 10^{10}$	$4.25 \times 10^{13}$	
IP13	$1.12 \times 10^{11}$	$9.64 \times 10^{13}$	
IP14	$4.06 \times 10^9$	$3.96 \times 10^{13}$	
IP15	$2.26 \times 10^{12}$	$1.99 \times 10^{14}$	
IP16	$1.99 \times 10^{10}$	$5.47 \times 10^{13}$	
IP17	$8.61 \times 10^{11}$	$7.70 \times 10^{13}$	

Table 4 Characteristics of Neutron Flux  
in Experimental Holes in KMRR

(unit :  $n/cm^2 \cdot sec$ )

Beam Tube	Fast Flux	Thermal flux	$\Phi_{ep}/\Phi_{th}$	Rcd
IR	$3.45 \times 10^{14}$	$2.83 \times 10^{14}$	0.17	6.7
CN	$1.00 \times 10^{14}$	$1.41 \times 10^{14}$	0.03	34.0
ST1	$2.26 \times 10^{14}$	$1.82 \times 10^{14}$	0.14	8.2
ST2	$2.51 \times 10^{14}$	$2.35 \times 10^{14}$	0.10	11.3
ST3	$2.52 \times 10^{14}$	$2.75 \times 10^{14}$	0.09	11.8
ST4	$1.69 \times 10^{14}$	$2.25 \times 10^{14}$	0.08	14.0
NR	$4.40 \times 10^{13}$	$4.49 \times 10^{13}$	0.02	60.4

\*  $\Phi_{ep}$  : Epithermal flux (9.0 Kev~0.625 ev)

\*\* Rcd : Cadmium Ratio =  $1 + \Phi_{th}/\Phi_{ep}$

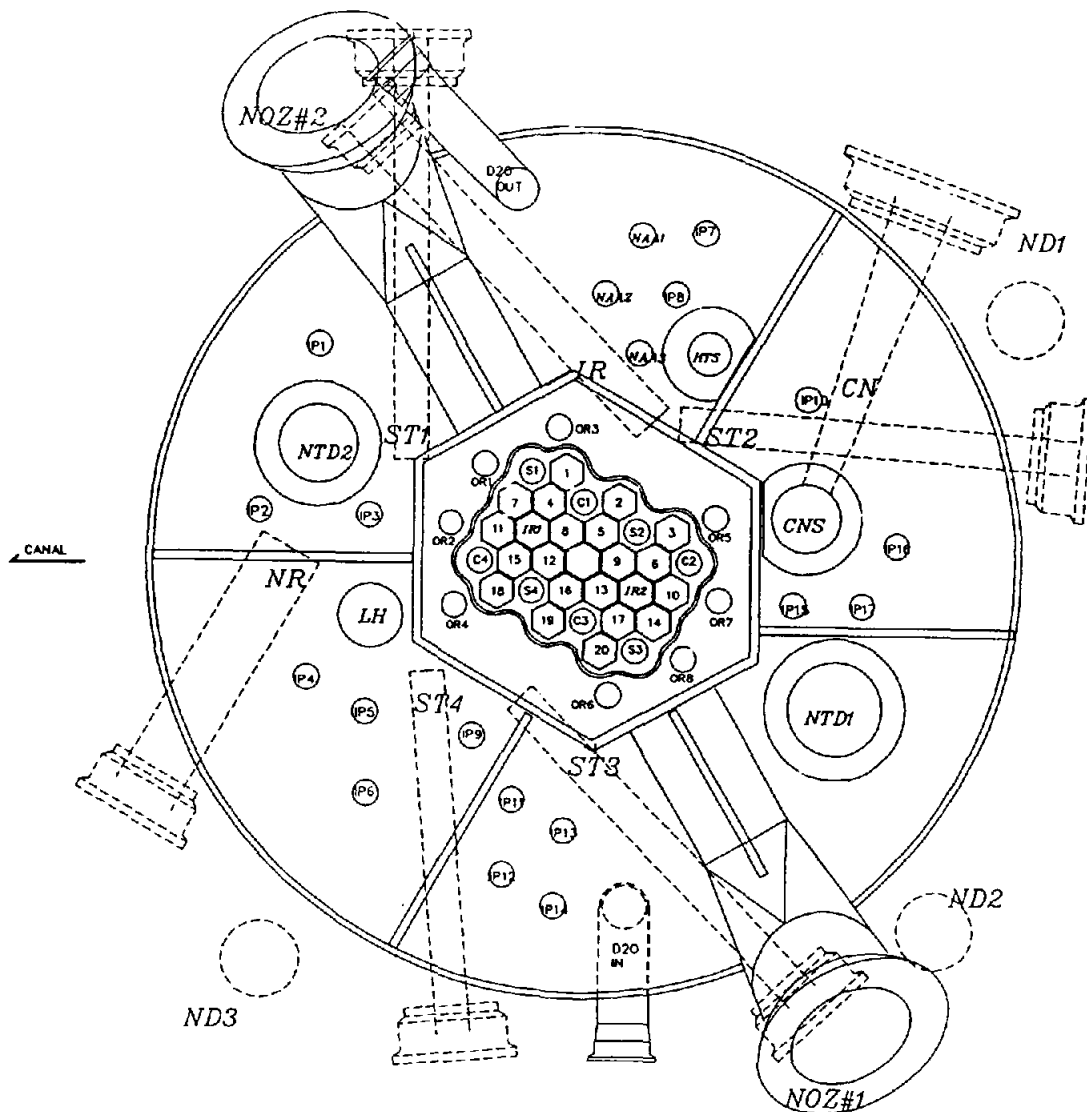
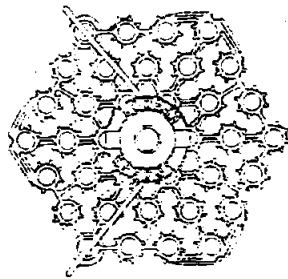
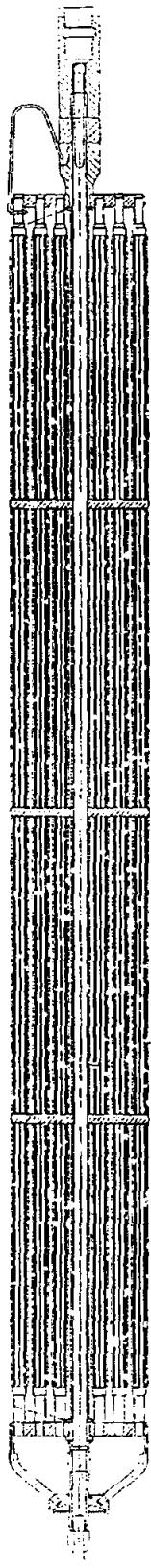
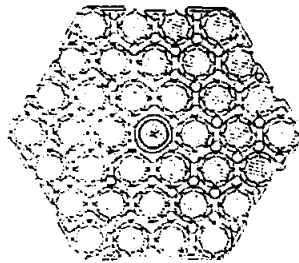


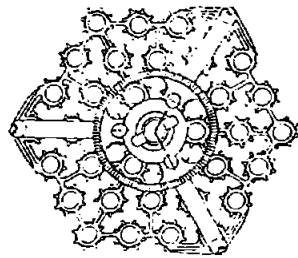
Fig.1 KMRR Core Configuration



TOP VIEW

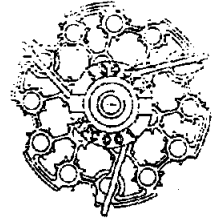
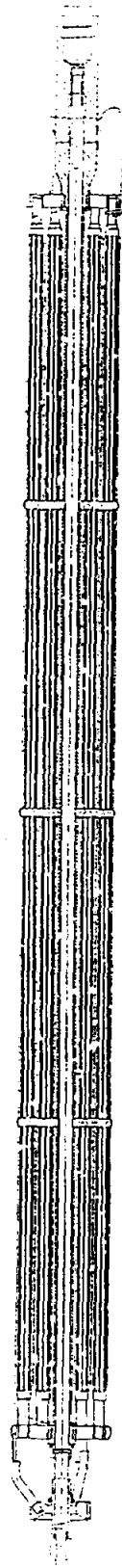


SECTION AT SPACER  
PLATE LOCATION

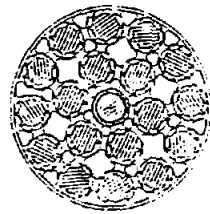


BOTTOM VIEW

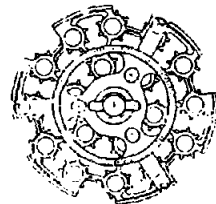
36 Element Assembly



TOP VIEW



SECTION AT SPACER  
PLATE LOCATION



BOTTOM VIEW

18 Element Assembly

FIG. 2 KMRR FUEL ASSEMBLIES

# THE RESIDUAL HEAT REMOVAL SYSTEM OF KMRR AND FLAP VALVE DESIGN

I. C. Lim, Y. S. Yang, H. T. Chae, and C. Park  
Korea Atomic Energy Research Institute  
Dukjin-Dong 150, Yoosung-Ku, Taejon, 305-353, Korea  
Tel:82-42-868-2000, Fax:82-42-861-0209

C. H. Han  
Samshin Limited  
Dujong-Dong 63-6, Chonan, Chungnam, 330-210, Korea  
Tel:82-417-62-3401, Fax:82-417-62-1950

## Abstract

A 30 MW<sub>th</sub> research reactor, the so-called KMRR (Korea Multi-purpose Research Reactor), has been developed by the Korea Atomic Energy Research Institute. The KMRR is an upward-flowing, light-water-cooled and heavy-water-reflected research reactor with an open-tank-in-pool arrangement. At normal operation, the core heat is removed by forced convective flow maintained by two pumps in parallel and then discharged to the secondary cooling system (SCS) through two plate type heat exchangers. When the core power is less than 50% of the full power (FP) or one of the primary cooling system pumps should fail, KMRR can be operated with only one pump and one heat exchanger at a reduced power level. During reactor shutdown, the core decay heat is removed by the natural circulation through primary cooling system (PCS Natural Circulation) when the secondary flow is available. Otherwise, the core decay heat is dumped into the pool by gravity-driven circulating flow via the flap valves inside the pool (Pool Natural Circulation). This paper describes the residual heat removal capability by the natural circulation and the flap valve design in detail.

## 1. Introduction

KMRR is a 30 MW<sub>th</sub> research reactor with the arrangement of open-tank-in-pool, as shown in Fig. 1 and Fig. 2 [1]. As in Fig. 1, the core is composed of inner core and outer core. The inner core, 50 cm in effective diameter and 1.2 m in height, has 23 hexagonal and 8 circular flow channels. Each hexagonal flow channel formed by the hexagonal flow tube is loaded with the 36-element driver fuel assembly. The circular flow channel formed by the circular flow tube is loaded with the 18-element fuel assembly. Outside the circular flow tube, a hafnium control or shut-off shroud tube can be moved up and down for the control and reactor shutdown. 3 out of 23 hexagonal flow channels are used to accommodate the fuel and material test facilities. The outer core consists of eight circular flow channels embedded in the reflector vessel whose effective diameter is 2 m and the height is 1.2 m. 4 of 8 outer flow channels are to be

used as the irradiation sites while the remainders are used as the 18-element fuel sites.

Fig. 3 shows the schematic diagram of PCS. The 90% of total coolant flow of 780 kg/s passing through the pumps and heat exchangers directs to the reactor core. About 10% of total PCS flow, 77 kg/s, is fed to the bottom of the pool through bypass line, and slowly rises through the reactor pool, and then drawn into the chimney. This prevents the core flow having  $N^{16}$  from escaping onto the pool surface. The core flow of 703 kg/s passing into the reactor inlet plenum flows through the flow channels and the gap. The coolant flow rate per channel is 19.6 kg/s for the hexagonal flow channel and 12.7 kg/s for the circular flow channel. The gap flow of 50 kg/s traveling through the gap between the innershell and the flow tubes cools the inner shell surrounding the inner core. Both the bypass flow and the core flow are sucked into the two outlets in the chimney and circulate through the PCS.

During the reactor shutdown, the core decay heat is removed by the PCS Natural Circulation (Outlet-Pump-Heat exchanger-Inlet line-Inlet plenum-Core) when SCS is available. Otherwise, the core decay heat is removed by the pool natural circulation via the flap valves attached on the core inlet line (Chimney top-Pool-Flap valves-Inlet line-Inlet plenum-Core).

This paper describes the residual heat removal capability by the natural circulation and the flap valve design in detail.

## 2. Residual Heat Removal System

### 2.1 Design Objective

There are two design objectives for the residual heat removal system:

#### a. Safe Cooling Objective

To prevent fuel overheating, the safety limits imposed on the fuel shall be met by the residual heat removal system design.

#### b. Environment Objective

To protect experimental facilities placed in the reactor hall, residual heat removal should be adequate to maintain the pool water temperature below 50°C during normal shutdown and the anticipated operational occurrences of the reactor.

### 2.2 Methods of Residual Heat Removal

#### 2.2.1 PCS Natural Circulation

When SCS is available, the core decay heat is removed by the natural circulation through PCS. The elevation difference between the core and the heat exchanger is 7.7 m. Especially, for the case of the Loss-of-Offsite Electric Power (LOEP), the cooling

water in the cooling tower basin is driven to the secondary side of the heat exchanger by gravity. It acts as a heat sink for one hour and, eventually, the decay heat is removed by the pool natural circulation. The analysis results showed that the core could be cooled by the PCS natural circulation up to 6% FP without impairing the fuel safety.

### 2.2.2 Pool Natural Circulation

When SCS is not available due to the loss of SCS circulation, loss of cooling tower circulation, and the pipe break in SCS or when SCS pump is stopped for the prolonged reactor shutdown, the decay heat is removed by the pool natural circulation via the flap valves. The flap valve is the most important component for the establishment of the natural circulation pass, and its design feature is described in Chap. 3. It was estimated that the core could be cooled by the pool natural circulation up to 6% FP without impairing the fuel safety.

### 2.2.3 EWSS and Sump Recirculation

In case of the pool water inventory loss due to the beam tube failure or the break of PCS pipe, even though their occurrences would be very seldom, the emergency water supply system (EWSS) is provided to make up the pool water. The schematic diagram of the EWSS is shown in Fig. 4. The major components of EWSS are the EWSS tank and the sump pumps. When the EWSS is activated, the water in the EWSS tank is injected into the core through the inlet line and the injection rate is 11.4 kg/s for 2.4 hrs after the start of injection. The operation of the sump pumps follows the emergency water injection at the recirculation rate of 13.1 kg/s.

## 3. Flap Valve

### 3.1 Requirements

The flap valve is the most important component for the establishment of the pool natural circulation path. It opens when the pool side pressure is greater than the pressure at the core coolant inlet line at the same location. This pressure difference is achieved by the decrease in the PCS natural circulation flow rate and the increase in the coolant inlet temperature due to the loss of the secondary cooling. The greater the pressure difference is, the easier the design of the valve is. But the required opening pressure is limited in a very narrow range considering the safe cooling of the fuel. Also, the flow resistance of the valve should be as low as possible to achieve the enough pool natural circulation flow rate. Considering those factors, the design requirements were set as:

- a. The valve should start to open when the pressure difference is less than 100 Pa.
- b. The flow rate through one valve should be greater than 8.5 kg/s when the pressure difference is 300 Pa.



### 3.2 Design Characteristics [2]

To satisfy the requirements, the mechanical and hydraulic resistance of the valve should be minimized. Many types of the valves were considered and, finally, the counter weight flap valve was selected. The cross-sectional view of the valve is shown in Fig. 5. The arrangement of the valve disc and counter weight is depicted in Fig. 6. The design characteristics are as follow: When the PCS natural circulation is maintained, the valve is closed as the moment of the disc set is greater than that of the counter weight set. As the coolant inlet temperature increases due to the loss of SCS, the pool side pressure becomes higher than the coolant pressure at the inlet line. By the time when the summation of moment by the pressure difference between the inlet and outlet of the flap valve and the counter weight is greater than the summation of the moment by the disc set and the friction force on the shaft bearing, the valve starts to open. When the pressure difference becomes much greater, the valve becomes fully open.

### 3.3 Functional Test

To confirm the design of the flap valve, the functional test was performed using the test facility in Fig. 7. The test was performed using the pressure difference between the inlet and outlet of the valve created by the difference of the pool water depths between pool B and pool C in Fig.7. The test results showed that the current flap valve design is acceptable. Another series of test is in progress to confirm the operation of the valve by the pressure difference created by the density difference using the test section simulating the core and the reactor pool. Also, more functional tests will be repeated to get the reliability data.

## 4. Demonstration of Residual Heat Removal Capability

### 4.1 Loss of Offsite Electric Power

LOEP is estimated to occur about twice a year, and it is a kind of anticipated operational occurrence for which the core decay heat is removed by the pool natural circulation. When LOEP occurs, the PCS flow and the SCS flow coast down. The reactor is shutdown by SOR (Shut Off Rod) due to the coast down of the SOR pressurizing pump, which is energized by the offsite power at normal operation. Also, the valve connecting the cooling tower basin to the secondary side of PCS heat exchangers automatically opens and thus, the basin water acts as the heat sink for a while. Following the loss of secondary heat sink, the pool natural circulation is established and the core decay heat is removed by this mechanism. The variation of the core flow at LOEP is illustrated in Fig. 8. The variation of the core coolant temperature is shown in Fig. 9. In this analysis, the secondary cooling water from the basin of the cooling tower was neglected. The analysis results shows that the core can be cooled safely by the pool natural circulation.

## 4.2 Long-term Cooling for Prolonged Shutdown

For the prolonged shutdown, one PCS pump will run for two hours after the reactor shutdown. After stopping of the PCS pump, the secondary cooling pumps will also be stopped subsequently. Then, the core decay heat will be removed by the pool natural circulation. Thus, the pool water is the heat sink for the prolonged shutdown. The total inventory of the pool water in the reactor pool, the transfer canal and the service pool is 340 tons. The analysis shows that the pool water temperature will reach 50°C at 29 hours after the PCS pump stop. At that time, operator will start one PCS pump and one SCS pump to cool the pool water. This operation is needed to satisfy the environmental objective for the residual heat removal.

## 5. Summary

During the shutdown of KMRR, the core decay heat is removed by the natural circulation through primary cooling system (PCS Natural Circulation) when the secondary flow is available. Otherwise, the core decay heat is dumped into the pool by a gravity-driven circulating flow via the flap valves inside the pool (Pool Natural Circulation). The flap valve is the most important component to achieve the pool natural circulation. The counter weight flap valve was designed through the functional test. The analysis show that the core can be cooled by the PCS/Pool natural circulation up to 6% of FP without impairing the fuel safety. For the prolonged shutdown, the decay heat is dumped into the pool by the pool natural circulation, and the operator will start one PCS pump and one SCS pump when the pool water temperature reaches 50°C to keep abreast with the environmental objective.

## References

- [1]. KMRR Safety Analysis Report, KAERI/TR-322/92, KAERI, 1992.12.
- [2] Functional Test Procedure for 6" Flap Valve, T-008-002, Samshin Limited, 1993. 8.

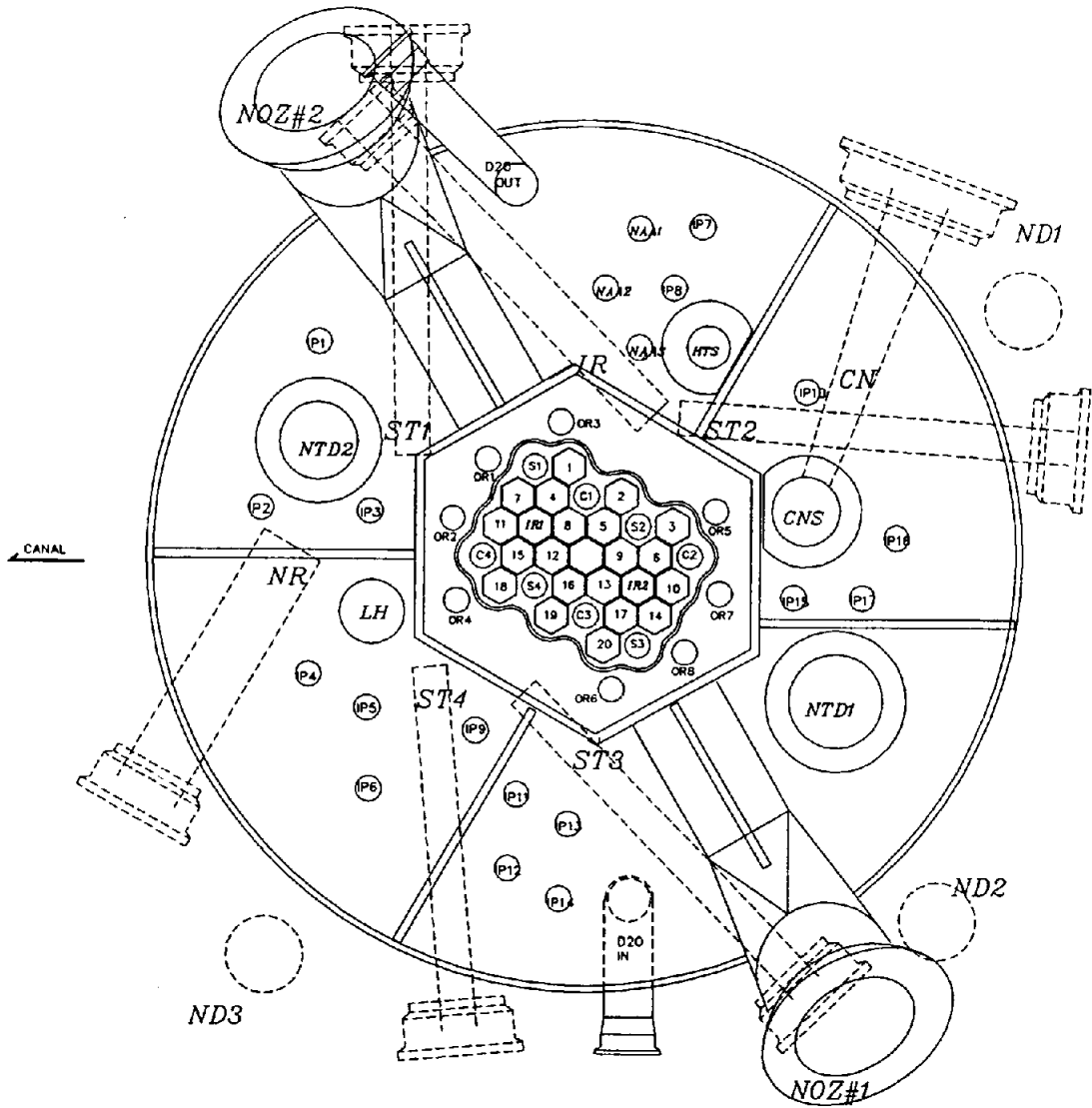


Fig. 1 Top View of Reactor

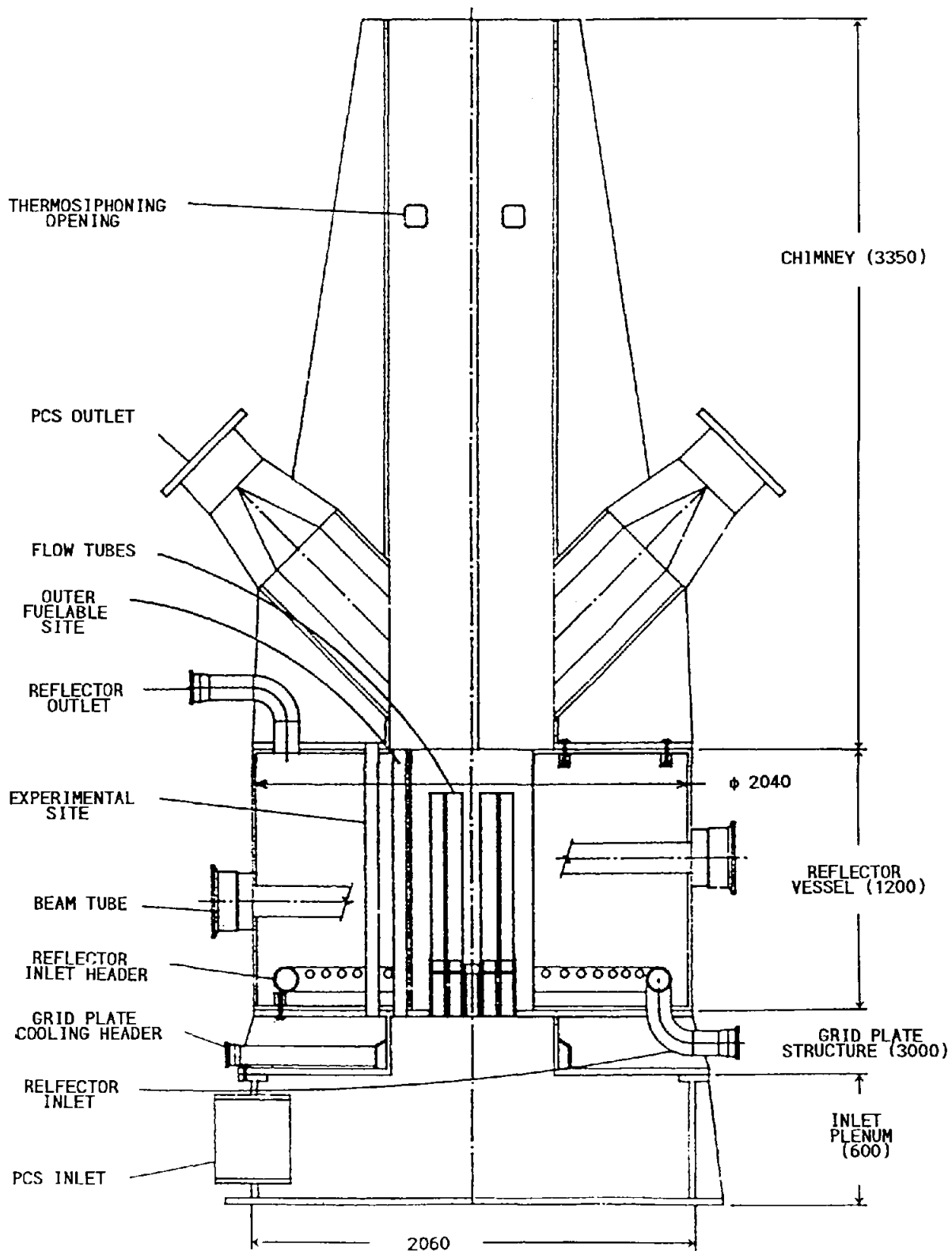


Fig. 2 Vertical View of Reactor

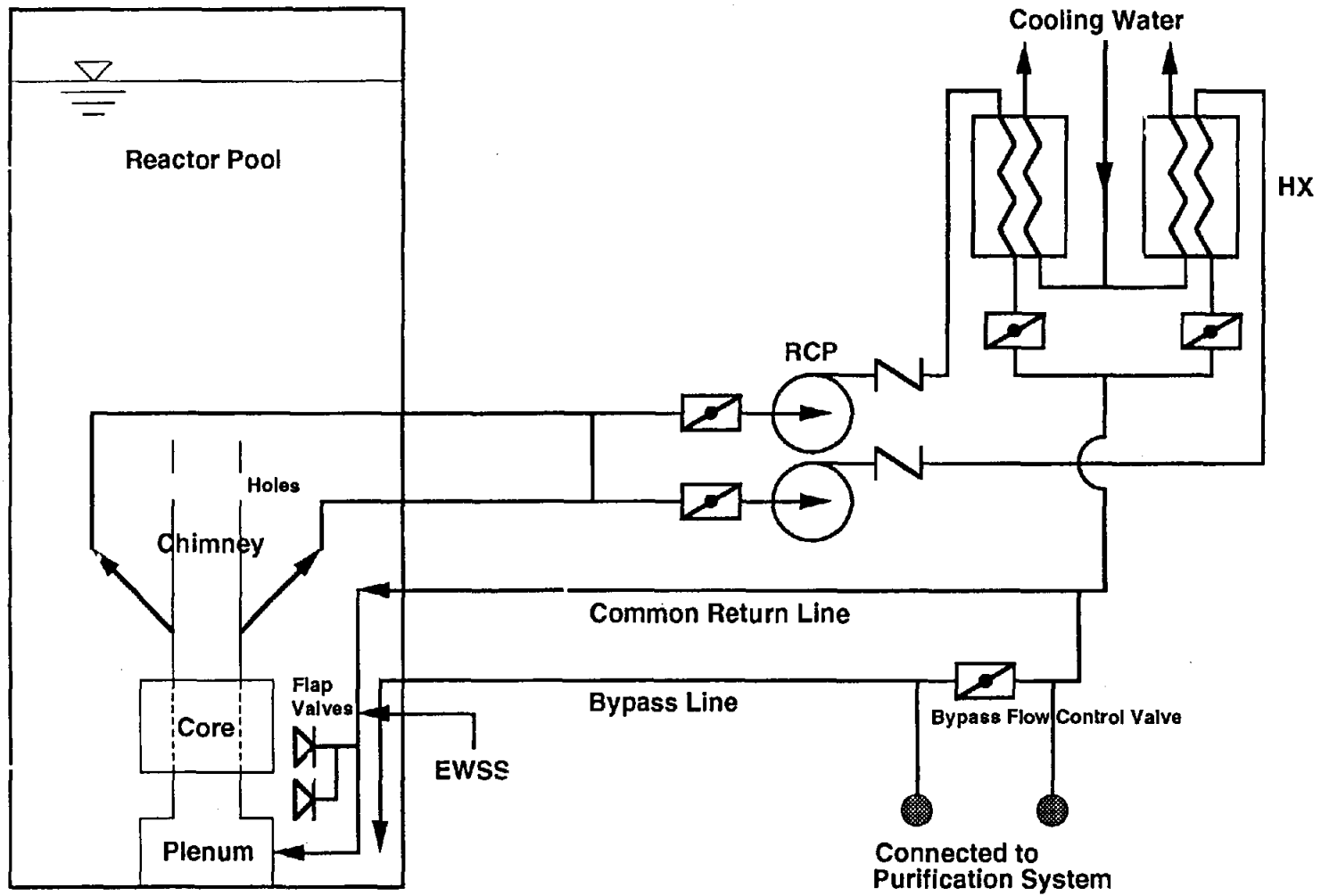


Fig. 3 Schematic Diagram of Primary Cooling System

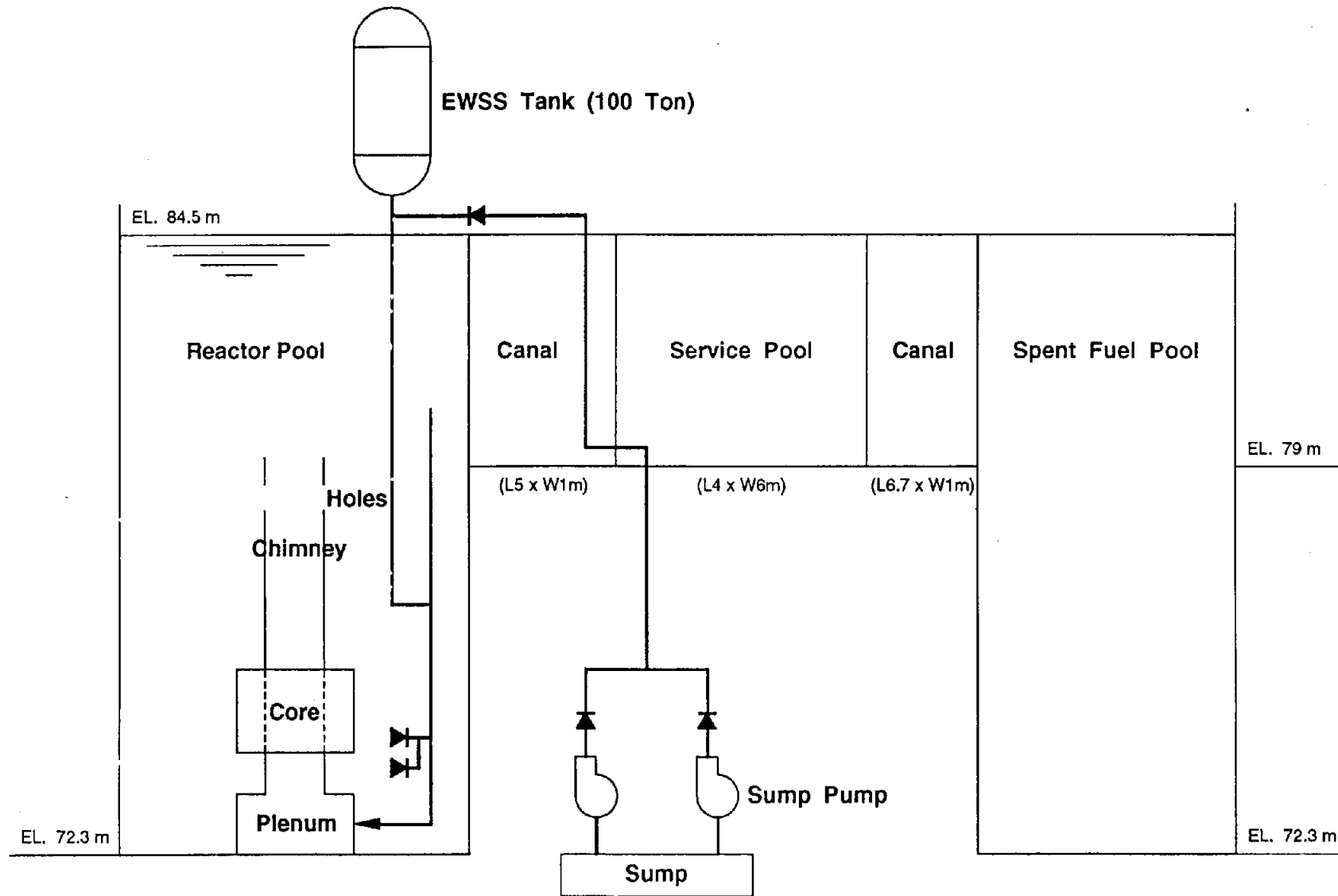


Fig. 4 Schematic Diagram of EWSS and Sump Recirculation

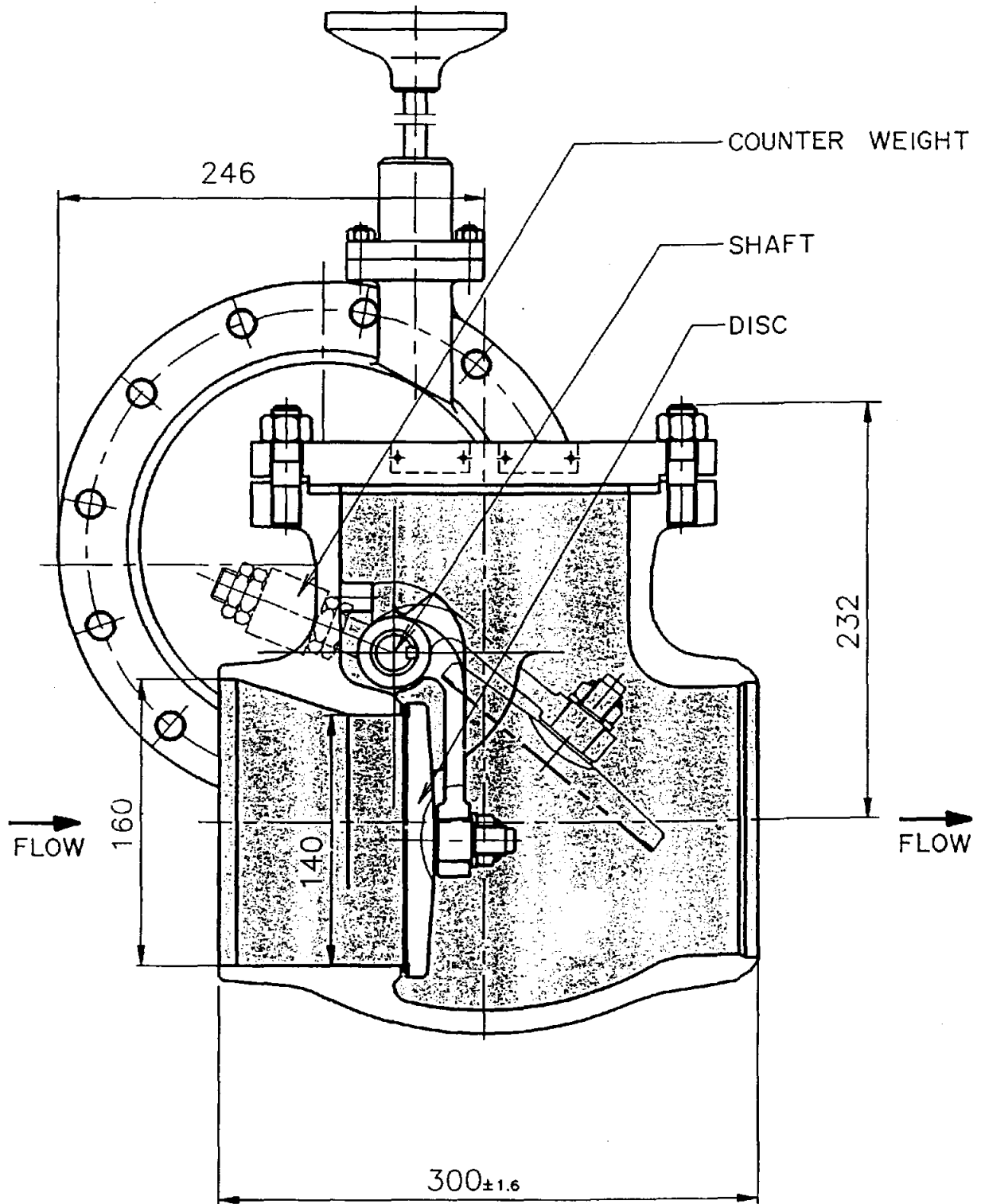


Fig. 5 Sectional View of Flap Valve

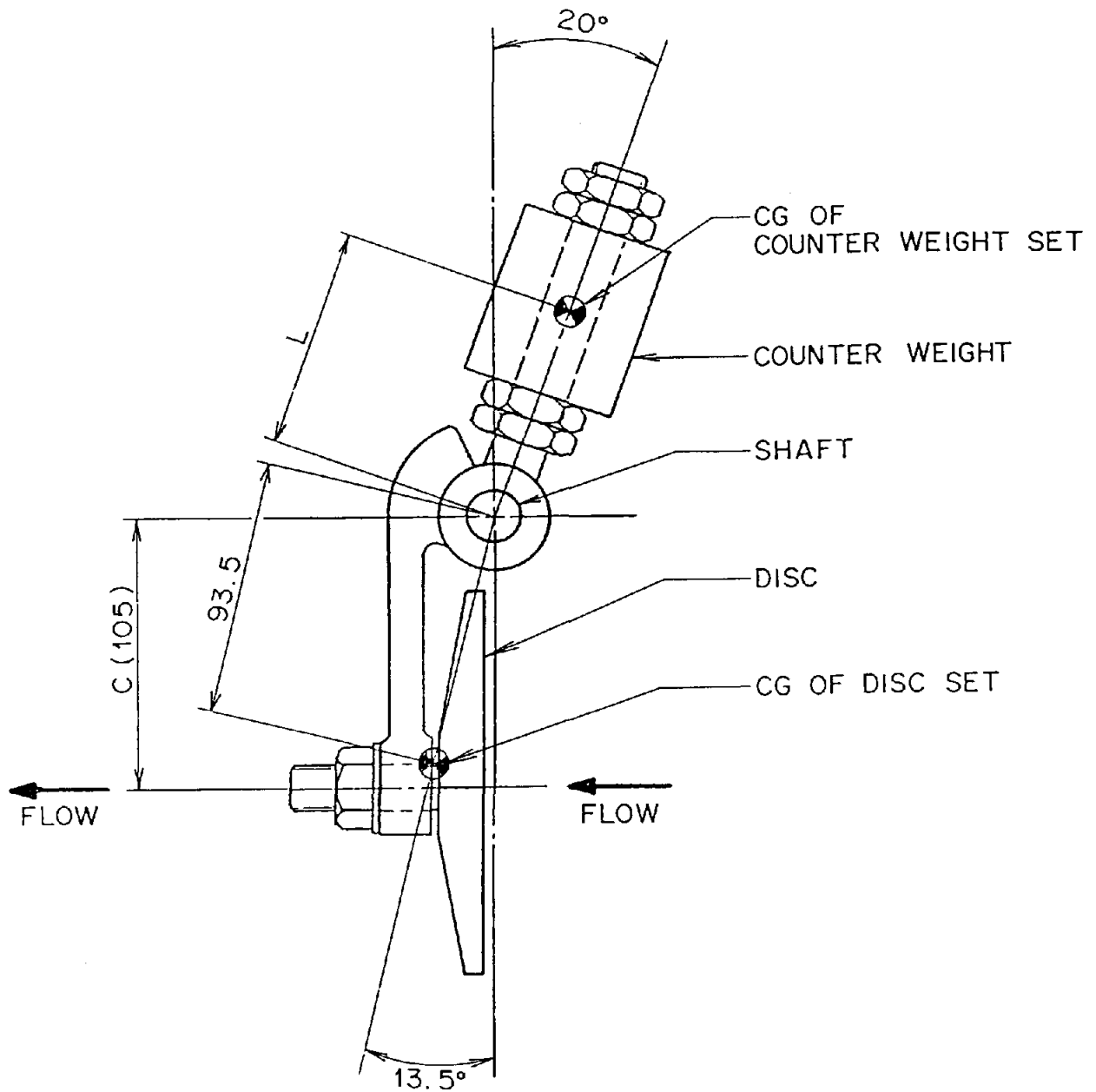


Fig. 6 Arrangement of Valve Disc and Counter Weight



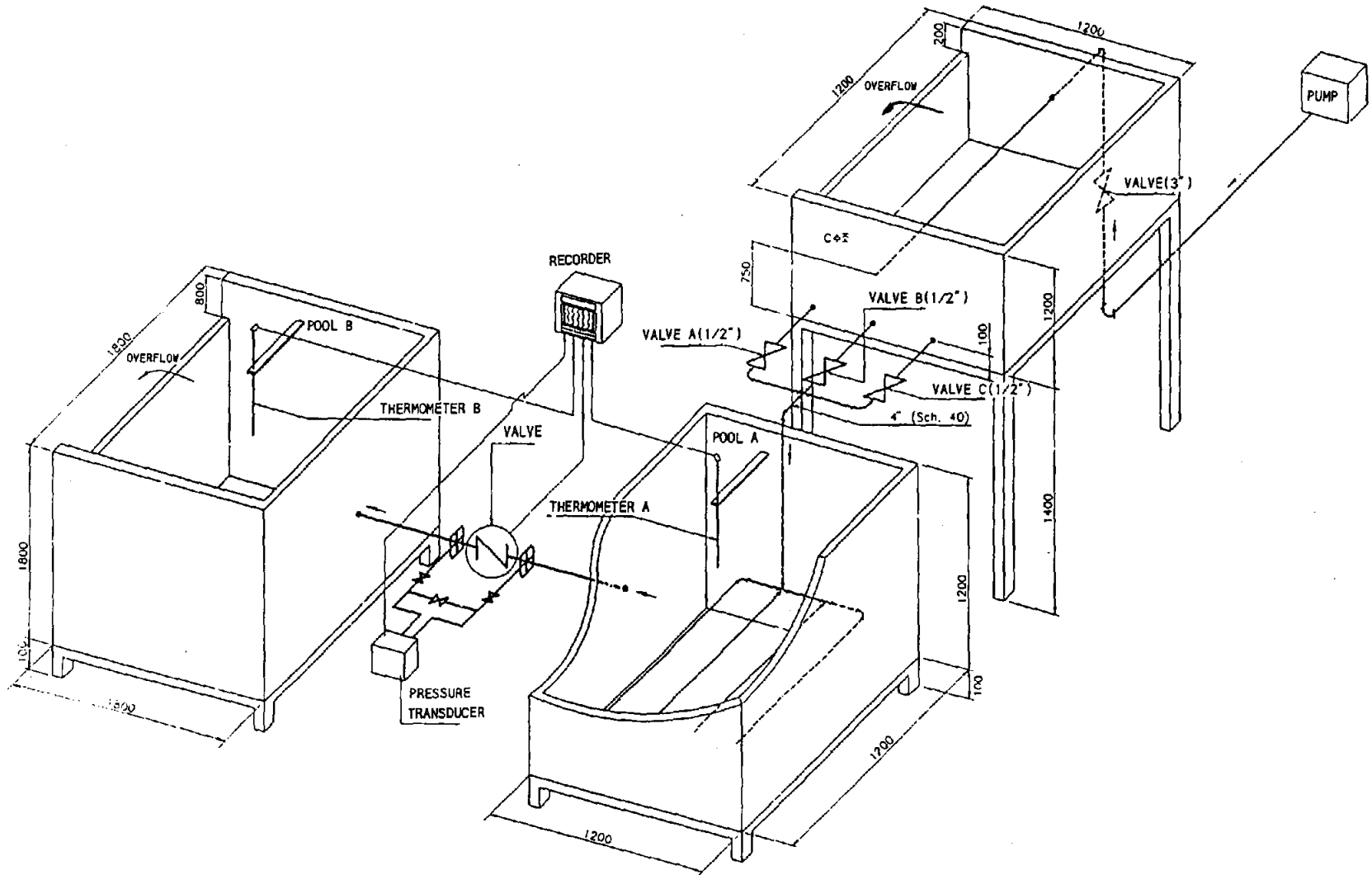


Fig. 7 Test Facility for Functional Test of Flap Valve

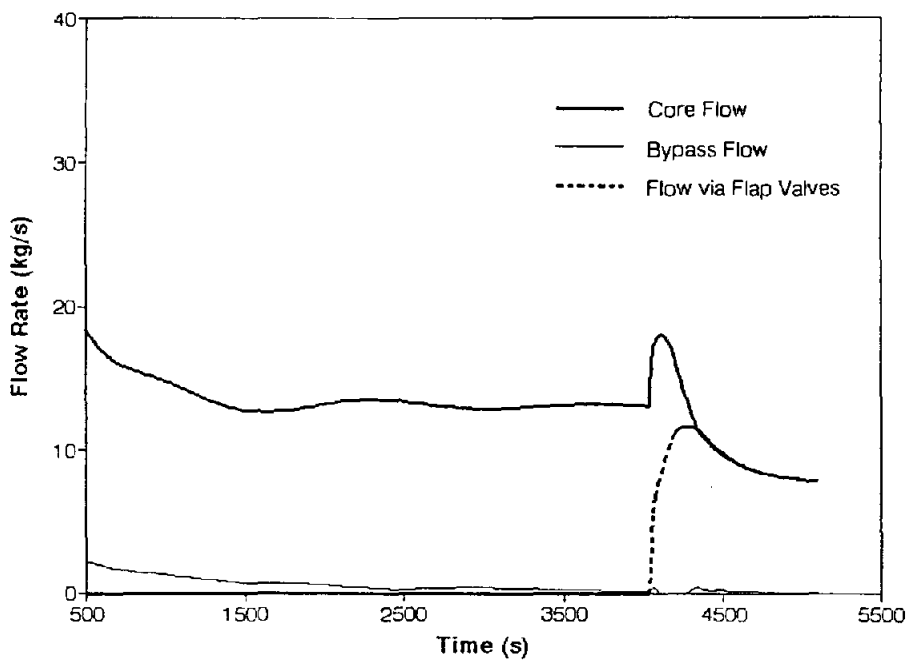
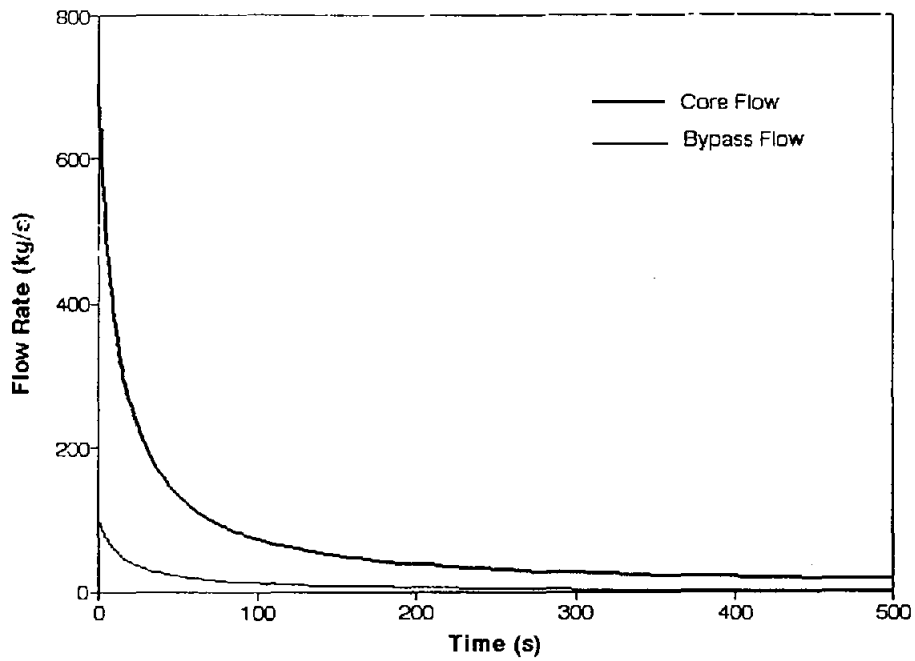


Fig. 8 Variation of Core Flow at LOEP

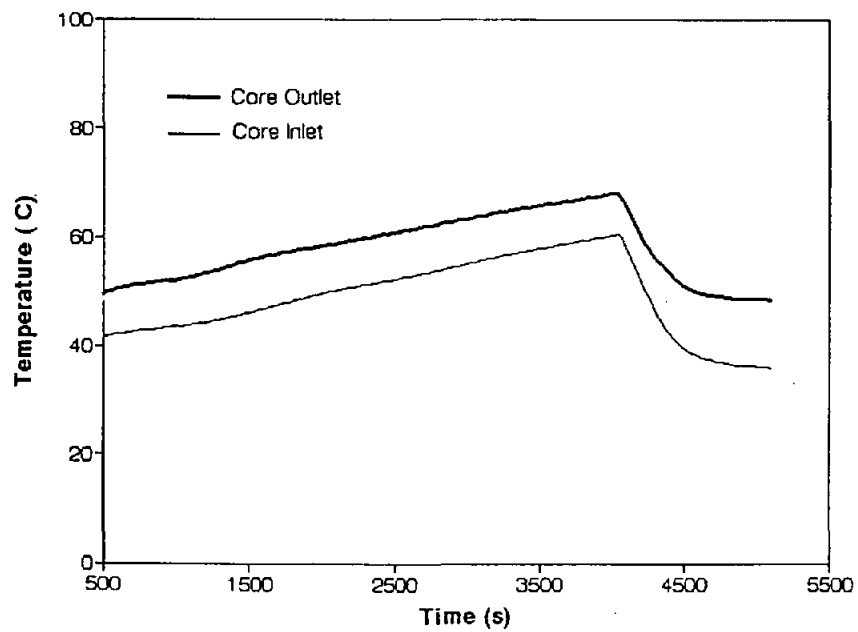
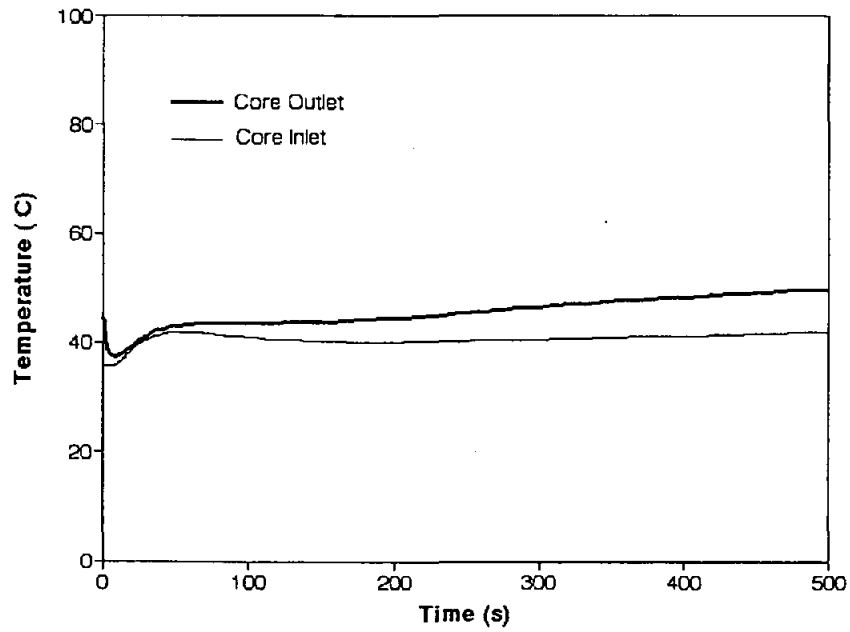


Fig. 9 Variation of Coolant Temperature at LOEP

## Preliminary conceptual studies of REX 2000

---

F. MERCHIE, C. BAAS, A. BALLAGNY, M. CHAGROT

G. FARNY, M. BARNIER, A. PATTOU

CEA, France

### ABSTRACT

Nuclear R and D programs are, to some extent, completely dependent on research reactors availability. In France and others european countries, the major materials testings reactors were built in the sixties and are consequently ageing and reaching the end of their life, some of them having already been shut down. A situation with not a single large research reactor available in first half of next century cannot be imagined, given all the benefits drawn from the use of research reactors. The CEA has therefore started to evaluate the needs for neutron sources in the next four or five decades so as to design the most suitable new facilities to take over from the existing ones. REX 2000 is a new dedicated reactor project intended to meet the needs for fuels and materials testings after the year 2000. The preliminary conceptual studies which have been carried out along the last 18 months are presented and commented.

# **PRELIMINARY CONCEPTUAL STUDIES OF REX 2000**

- 1. INTRODUCTION**
- 2. PRESENT SITUATION OF R.R.**
- 3. WHAT TYPE OF R.R. FOR WHAT TYPE OF NEEDS  
AFTER YEAR 2.000 ?**
- 4. FUELS AND MATERIALS TESTING IN R.R.**
- 5. REX 2000 PREMIMINARY OPTIONS**
- 6. CONCLUSIONS**

## **2. PRESENT SITUATION OF RESEARCH REACTORS**

- AGEING**
- SAFETY**
- UTILIZATION FACTOR AND EXPERIMENTAL NEEDS**
- OTHERS ISSUES**

**FUNDING**

**STAFF PROFICIENCY AND TRAINING**

**PUBLIC ACCEPTANCE**

## RESEARCH REACTORS IN OPERATION IN WESTERN EUROPE

$P \geq 10$  MW

---

AUSTRIA	ASTRA	10 MW	1960
BELGIUM	BR-2	80	1961
DENMARK	DR-3	12	1960
FRANCE	ORPHEE	14	1980
	OSIRIS	70	1966
	RHF	57	1971
	SILOE	35	1963
GERMANY	BER	10	1973
	FRJ-2	23	1962
NETHERLANDS	HFR	45	1961
NORWAY	HBWR	25	1959
SWITZERLAND	SAPHIR	10	1957
SWEDEN	R-2	50	1960

**3. WHAT TYPE OF R.R. FOR WHAT TYPE  
OF NEEDS AFTER YEAR 2.000 ?**

- **MULTIPURPOSE REACTORS**
- **DEDICATED REACTORS**
- **REX 2000 PROJECT MAIN PURPOSES**

**4. FUELS AND MATERIALS TESTING IN R.R.**

- **ACKNOWLEDGED ADVANTAGES OF IRRADIATION  
EXPERIMENTS IN R.R.**

**INSTRUMENTATION**

**FLEXIBILITY**

**LOW COST**

**MULTIPLICITY**

- **DEBATED QUESTIONS**

**NPP REPRESENTATIVITY**

**NEUTRON FLUX AND SPECTRUM**

**GAMMA HEATING**

**THERMOHYDRAULICS**

**TEST GEOMETRY**

**STATISTICAL RESULTS**

## **5. REX 2000 PREMIMINARY OPTIONS**

- **SMALL PWR OR MTR TYPE**
  
- **IRRADIATION VOLUME AND LOCATIONS**
  - AT THE CORE PERIPHERY**
  - IN THE CORE**
  - CENTRAL CROSSING LOOP**
  
- **OPEN CORE OR CLOSED VESSEL**
  
- **DOWNWARD OR UPWARD COOLING**
  
- **DRIVING CORE (LEU)**
  - FUEL PLATES**
  - FUEL RODS**



## Present Status of High-Temperature engineering Test Reactor(HTTR) Program

Toshiyuki TANAKA, Osamu BABA, Shusaku SHIOZAWA,  
Minoru OKUBO, Toshiaki TOBIOKA

Department of HTTR Project  
Japan Atomic Energy Research Institute  
Oarai-machi, Higashiibaraki-gun, Ibaraki-ken, Japan

### Abstract

The 30Mwt HTTR is a high-temperature gas-cooled reactor(HTGR), with a maximum helium coolant temperature of 950°C at the reactor outlet.

The construction of the HTTR started in March 1991, with first criticality to be followed in 1998 after commissioning testing. At present the HTTR reactor building(underground part) and its containment vessel have been almost completed and its main components, such as a reactor pressure vessel(RPV), an intermediate heat exchanger, hot gas pipings and graphite core structures, are now manufacturing at their factories at the target of their installation starting in 1994.

The project is intended to establish and upgrade the technology basis necessary for HTGR developments. Japan Atomic Energy Research Institute(JAERI) also plans to conduct material and fuel irradiation tests as an innovative basic research after attaining rated power and coolant temperature. Innovative basic researches are now in great request.

The paper describes major features of HTTR, present status of its construction and research and test plan using HTTR.

### 1. Introduction

It is essentially important in Japan, which has limited amount of natural resources, to make efforts to obtain more reliable and stable energy supply by extended use of nuclear powers including high temperature heat from nuclear reactors. Hence, efforts are to be continuously devoted to establish and upgrade HTGR technologies and to make much of human resources accumulated so far. It is also expected that making basic researches at high temperature using HTGR will contribute to innovative basic research in future. Then, the construction of HTTR was decided by the Japanese Atomic Energy Commission(JAEC) and is now under way by the JAERI.

The HTTR aims at establishing and upgrading the technology basis necessary for HTGR developments, serving at the same time as a potential tool for innovative basic researches.

The paper summarizes the HTTR project and research and test program using

HTTR.

## 2. HTTR Project

In Japan, the R&D on HTGRs has been carried out for more than 20 years, firstly as the multi-purpose Very High Temperature Gas-Cooled Reactor program for direct utilization of nuclear process heat and then as the HTTR Project, reflecting the change of social and energy situation.

Since 1969, the JAERI has carried out R&D works on HTGRs in the areas of fuel, graphite and high temperature alloy, high temperature in-core instrumentations, high temperature components, reactor physics, heat transfer and fluid dynamics, fission products plate-out etc.. At present, the JAERI is constructing the HTTR which can supply high temperature coolant up to 950°C at the outlet of the RPV, which has been realized with the results of these R&D works. The block type fuel is adopted in the HTTR considering the ease of irradiation experiments as well as the advantages of fuel zoning, control of coolant flow rate in each column, easy insertion of control rods in the core, and so on. Major features of the HTTR and the construction schedule are given below.

### 2.1 Major Features of HTTR

The HTTR has been so designed as to be an engineering test reactor which aims to establish and upgrade the technological basis necessary for HTGR developments and to conduct various irradiation tests for innovative basic researches.

The HTTR plant is under construction in the Oarai Research Establishment of the JAERI. The reactor building is centered in the HTTR plant. The main reactor facilities of the HTTR such as the RPV, primary cooling system, reactor containment vessel and refueling machine are housed in the reactor building, as illustrated in Fig.1. The RPV made of 2 1/4 Cr-1Mo steel is 13.2m high and 5.5m in diameter, and contains the core consisting of fuel and control rod guide block columns, permanent and replaceable reflector blocks, metallic and graphite core support structures as illustrated in Fig.2. The main cooling system(MCS) is composed of a primary cooling system, a secondary helium cooling system and a pressurized water cooling system. The primary cooling system has two heat exchangers, an intermediate heat exchanger and a primary pressurized water cooler, in parallel.

The major specification of the HTTR is shown in Table 1.

The reactor core is graphite moderated, helium gas cooled and hexagonal fuel elements are used. The active core consists of 30 fuel block columns and 7 control rod guide block columns, where each column is composed of 5 blocks (2.9m) stuck. The active core of 2.3m in diameter is surrounded by 15 replaceable reflector columns and 9 reflector-zone control rod guide block columns. Some of replaceable reflector columns are used as irradiation test columns. The permanent reflector surrounds the replaceable reflector and is made up of large polygonal graphite blocks fixed by core restraint mechanism. Each hexagonal graphite block, which is made of the domestic IG-110, has three dowel-pins on its top and three associated sockets at its bottom, and the blocks are fixed by setting dowel-pins into sockets.

A standard fuel element, 36cm across flats and 58cm high is made up of fuel rods and a hexagonal graphite block, as shown in Fig.3. The fuel consists of TRISO coated particles of low enriched uranium oxide whose average enrichment is about 6% and the kernel diameter is 600μm. The particles are dispersed in the graphite matrix and sintered so as to form a fuel compact. These compacts are contained in

a graphite sleeve to form a fuel rod. The fuel rods of 3.4cm in diameter are contained inside vertical holes of 4.1cm in diameter within a graphite block. Helium gas flows through an annular channel between a vertical hole and a fuel rod inserted in it to remove heat produced by fission and gamma heating.

Reactivity is controlled by 16 pairs of control rods, which are individually supported by the rod drive mechanisms located in standpipes connected to the hemispherical top head of the RPV and inserted into the channels in the active core and replaceable reflector regions. The reactor shutdown under the high temperature condition is made by inserting 9 pairs of control rods into the reflector region at first, then the other 7 pairs of control rods in the core region are inserted after the active core region temperature decreases. Back-up shutdown capability is provided by dropping boron carbide/graphite pellets into the holes in the control rod guide blocks.

Major nuclear and thermal-hydraulic characteristics of the HTTR is shown in Table 2.

The reactor cooling system is composed of an MCS, an auxiliary cooling system (ACS) and two reactor vessel cooling systems (VCSs). The reactor cooling system is schematically shown in Fig.4. The ACS is in the stand-by condition during the normal reactor operation and is operated to remove the residual heat from the core when the reactor is scrammed. Both VCSs are operated at each 100% flow rate during the normal operation in order to cool biological shielding concretes around the RPV, and they serve to cool the RPV and the core under such accident conditions as a pipe break of the primary cooling system, when the core is no longer cooled effectively by neither the MCS nor the ACS.

## **2.2 Construction Status and Schedule of HTTR project**

The JAERI applied for the permission of installation of the HTTR to the Science and Technology Agency (STA) for the safety review by the Government in February 1989 and the safety review by Nuclear Safety Commission (NSC) followed and finished in November 1990.

In parallel, the graphite structural design code and high temperature structural design code had been developed by the JAERI. The inspection criteria for the fuel and the graphite components had also been established by the JAERI. These codes and criteria were endorsed by the STA in December 1990.

The construction schedule of the HTTR is shown in Table 3. The construction of the HTTR was initiated in March 1991 and the excavation of ground were completed in August 1991. The construction of concrete base-matt was also completed in May 1992 and the construction of reactor building is under way. Its underground part has been almost completed. The assembling and installation of containment vessel was completed with a success of its pressure-proof and leakage tests in November 1992. Photo 1 shows the construction status on the site. Several large tanks such as for helium gas storage and supply have been already installed in the reactor building. Other main components are now being manufactured at their factories and the RPV and the intermediate heat exchanger will be installed in 1994. It will take another five years for the construction and fuel fabrication, and the first criticality will be attained in June 1998.

## **3. Research and Test Program Using HTTR**

### **3.1 Reactor Performance Tests for Establishing HTGR Technologies**

Reactor performance data will be accumulated through the HTTR criticality, zero

power and power increase tests and also full power operation. These data are quite valuable for design, safety evaluation and licensing of advanced HTGRs. They are most effectively utilized for establishing the technology basis necessary for HTGR developments.

### **3.2 Irradiation and Demonstration Tests for Upgrading HTGR Technologies**

To upgrade the technology basis for HTGRs, many kinds of tests are planned as follows.

#### **(1) Irradiation Tests**

To develop advanced HTGRs (reactor outlet coolant temperature about 1100°C, power density 3–6 w/cm<sup>3</sup> and fuel burnup about 100GWd/t are targeted respectively), many kinds of irradiation tests such as fuel irradiation tests, material irradiation tests are planned.

#### **(2) Safety Demonstration Tests**

The following safety demonstration tests are planned in the HTTR to verify inherent safety features of HTGRs:

- 1) Abnormal control rod withdrawal tests and
- 2) Coolant flow reduction tests.

#### **(3) Nuclear Heat Application Tests**

A heat utilization system is planned to be connected to the HTTR and demonstrated at the later stage of the first core. A steam-reforming or thermo-chemical hydrogen production system is under discussion for a possible candidate of the system, which will be promoted by the IAEA as one of international coordinated research programs. A closed cycle gas-turbine system will be also investigated if the demonstration test by the HTTR is found to be effective.

### **3.3 High Temperature Irradiation Tests for Innovative Basic Researches**

Many irradiation regions are reserved in the HTTR to be served as a potential tool for an irradiation test reactor in order to promote innovative basic researches such as materials, fusion reactor technology, radiation chemistry and so on, besides fuel and material irradiation tests as shown in 3.2. Specific irradiation capabilities in the HTTR are to be able to irradiate a large-sized sample up to 25cmφ×50cmL or block size with installed instruments at elevated temperature although maximum thermal and fast neutron fluxes are in the order of 10<sup>13</sup>neutrons/(cm<sup>2</sup>·s).

Innovative research subjects are now in great request. Some examples of testing at high-temperature and under irradiation are shown below.

- (1) New semi-conductors, super-conductors, composite materials development,
- (2) Material properties changes and irradiation damages research on metals, ceramics and composite materials and functionally gradient materials,
- (3) Tritium production and continuous recovery testing of fusion reactor blanket materials, and
- (4) Radiation chemistry such as decomposition of high molecular compounds and synthesis of fulleren including actinide elements.

The operation and the test plan in the HTTR is shown in Table 4.

## **4. Concluding Remarks**

The HTTR is a high temperature gas cooled test reactor which has various aims and operational modes. The construction of the HTTR has progressed smoothly so far

and its first criticality is foreseen in June 1998.

The various tests by the HTTR will make a great contribution to confirm salient characteristics of HTGRs including high inherent safety and reliable supply of heat as high as 950°C and the application of high temperature heat from HTGRs to various fields will also contribute to resolve global environmental problems.

Furthermore, the HTTR has a unique and superior capability for carrying out high temperature irradiation tests for innovative basic researches. The HTTR is highly expected to contribute so much to promoting the international cooperation in these fields.

Table 1 Major specification of the HTTR

<b>Thermal power</b>	<b>30 MW</b>
<b>Outlet coolant temperature</b>	<b>850°C/950°C</b>
<b>Inlet coolant temperature</b>	<b>395°C</b>
<b>Fuel</b>	<b>Low enriched UO<sub>2</sub></b>
<b>Fuel element type</b>	<b>Prismatic block</b>
<b>Direction of coolant flow</b>	<b>Downward-flow</b>
<b>Pressure vessel</b>	<b>Steel</b>
<b>Number of main cooling loop</b>	<b>1</b>
<b>Heat removal</b>	<b>IHX and PWC (parallel loaded)</b>
<b>Primary coolant pressure</b>	<b>4 MPa</b>
<b>Containment type</b>	<b>Steel containment</b>
<b>Plant lifetime</b>	<b>20 years</b>

Table 2 Major nuclear and thermal-hydraulic characteristics of the HTTR

Thermal power	30 MW
Core diameter	2.3 m
Core height	2.9 m
Average power density	2.5 W/cm <sup>3</sup>
Fuel loading	off-load, 1 batch
Excess reactivity	15 % $\Delta k$
Uranium enrichment	3~10 wt%
average	about 6wt%
Fuel burn up (average)	22 GWd/t
Reactivity coefficient	
Fuel temperature coefficient	$-(1.5 \text{ to } 4.6) \times 10^{-5} \Delta k/k/^{\circ}\text{C}$
Moderator temperature coefficient	$(-17.1 \text{ to } 0.99) \times 10^{-5} \Delta k/k/^{\circ}\text{C}$
Power coefficient	$-(2.4 \text{ to } 4.0) \times 10^{-3} \Delta k/k/\text{MW}$
Prompt neutron lifetime	0.67~0.70 ms
Effective delayed neutron fraction	0.0047~0.0065
Total coolant flow	10.2kg/s (950°C Operation)
Inlet coolant temperature	395 °C
Outlet coolant temperature	950 °C (max.)
Power peaking factor	
Radial	1.1
Axial	1.7
Effective core coolant flow rate	88 %
Max. fuel temperature	1492 °C

Table 3 Construction schedule of HTTR

ITEM \ FY <sup>*1</sup>	1990	1991	1992	1993	1994	1995	1996	1997	1998
MILESTONE	Construction start ▽					Electricity receive ▽			Fuelling ▽ Criticality ▽
Safety review	▬								
Approval of design and construction method	▬	▬	▬	▬	▬				
Site renovation	▬								
Excavation of reactor building		▬							
Reactor building			▬	▬	▬				
Containment vessel			▬						
Cooling system					▬	▬	▬		
Reactor pressure vessel and core internals					▬	▬	▬		
Fuel fabrication				▬	▬	▬	▬	▬	

\*1 Fiscal year of Japan starts in April and ends in March



Table 4 Operation and test plan in HTTR

Items	Fiscal Year	1998	1999	2000	2001	2002	2003~
1. Establishment of HTGR Technologies		Initial Core					Advanced Core
	▼ Criticality						
2. Upgrading of HTGR Technologies		Reactor Performance Tests				30MW 850~950°C	30MW 950°C
			Irradiation Tests in Capsules or Full-sized Samples				Irradiation Tests
			Safety Demonstration Tests	Demonstration Tests of Nuclear Heat Application System			
3. Innovative Basic Researches			<ul style="list-style-type: none"> <li>• Development of Very High Temperature Heat-Resisting Materials</li> <li>• Tritium Production and Recovery Tests, etc.</li> </ul>				

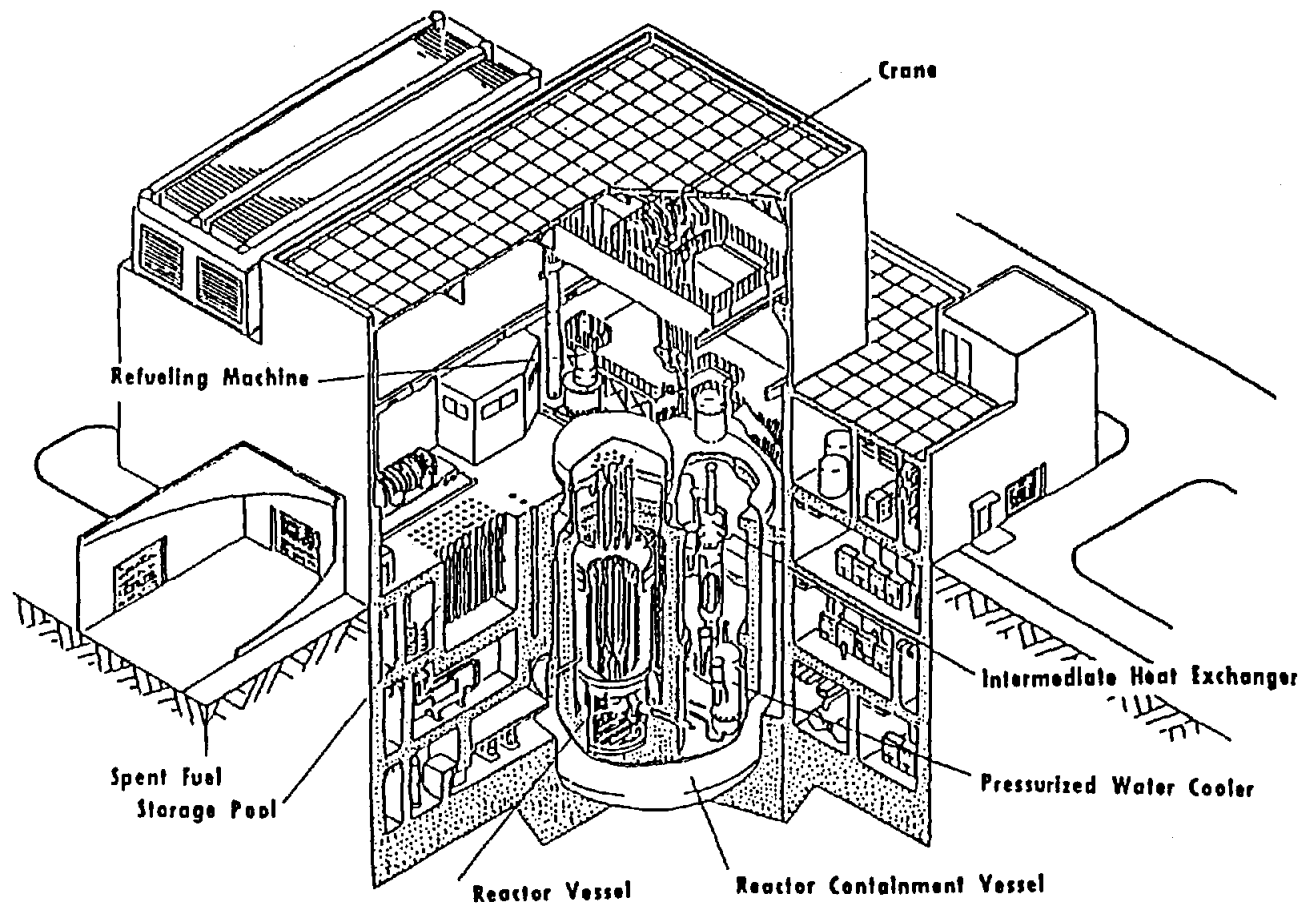


Fig.1 HTTR reactor building

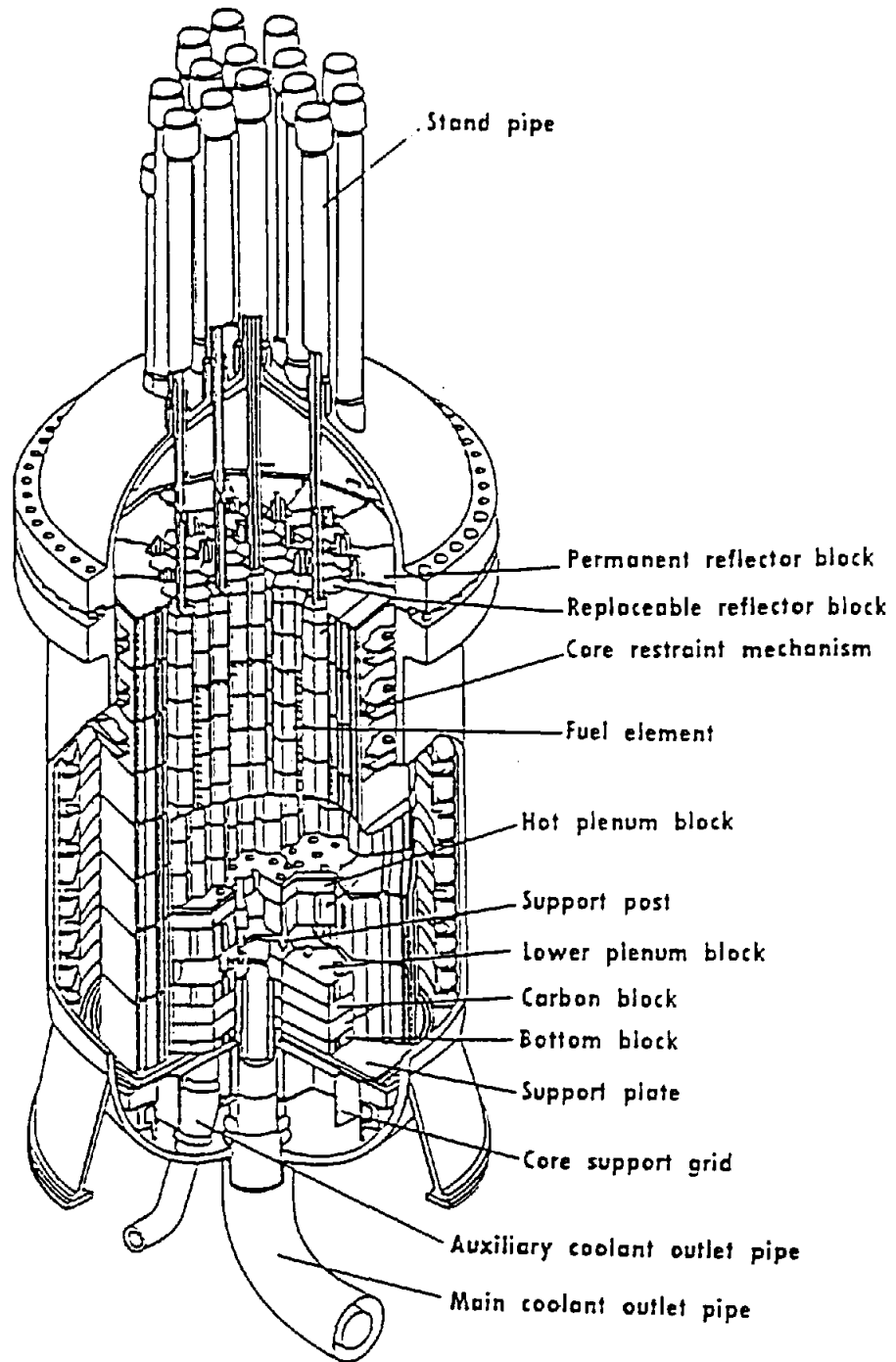


Fig.2 Bird's eye view of the reactor pressure vessel and core

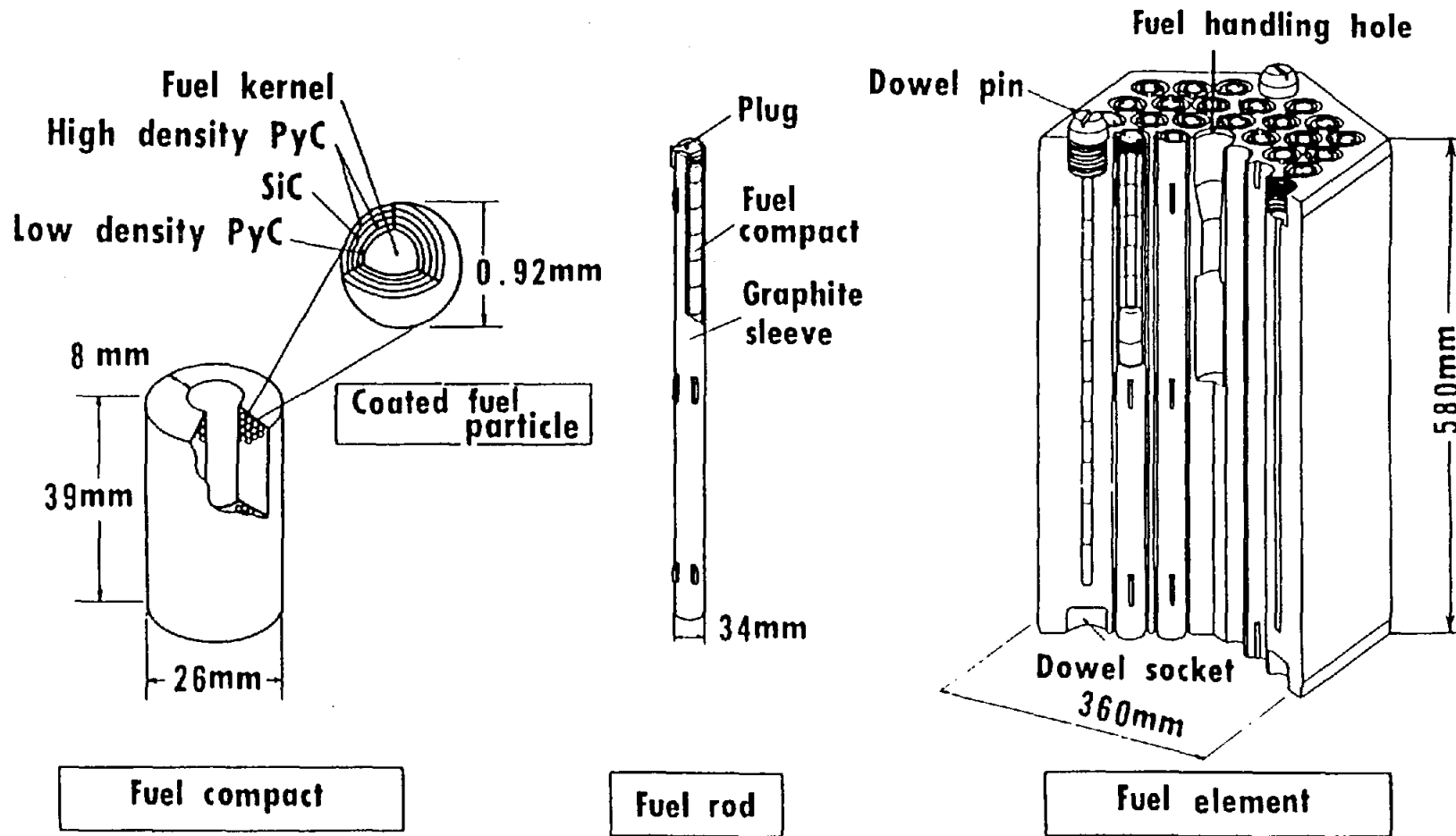


Fig.3 Structure of the HTTR fuel element

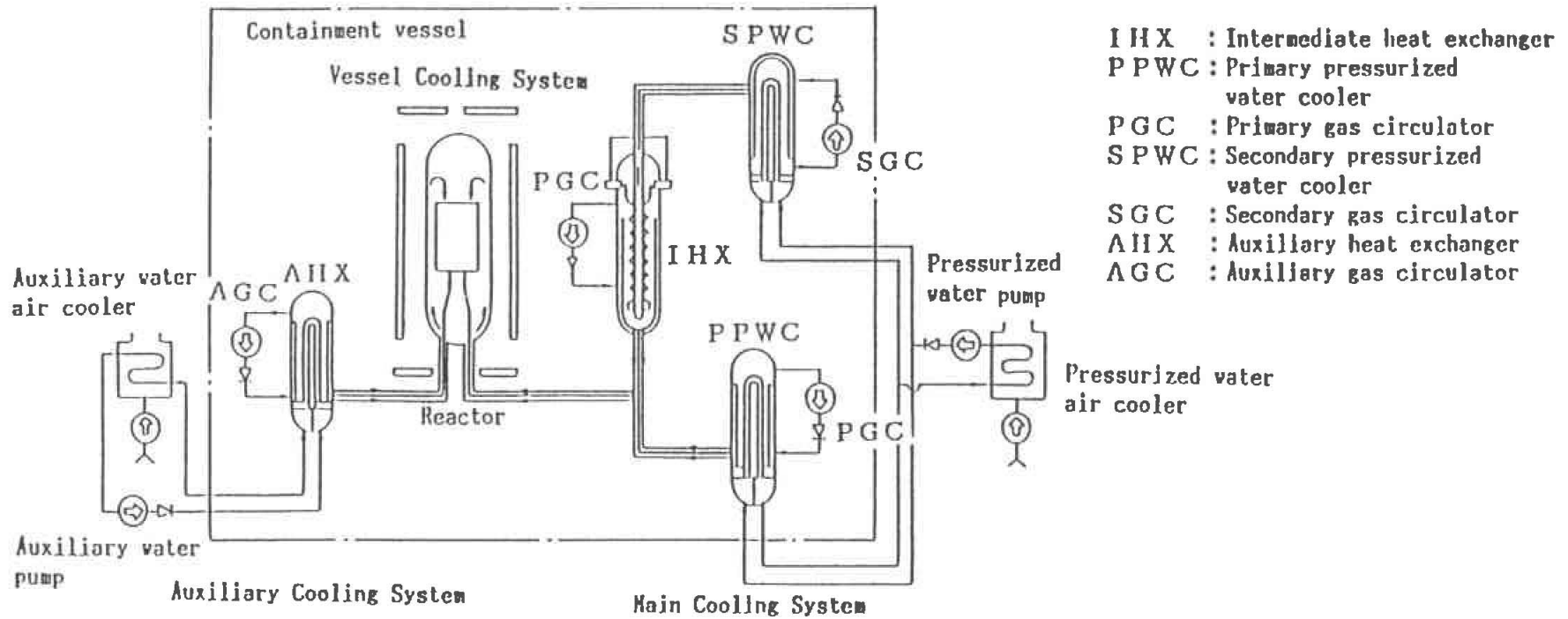


Fig.4 Cooling system

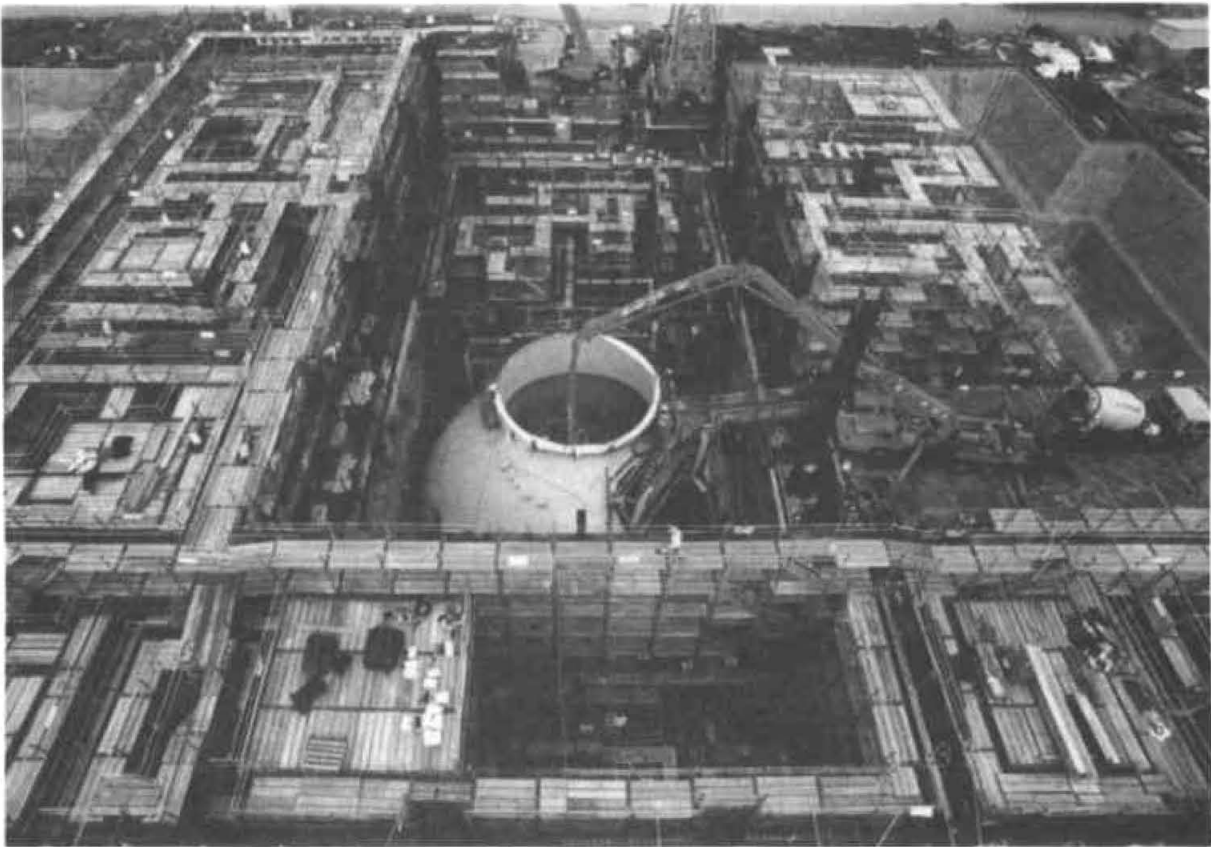


Photo 1 HTTR's construction status on the site

TRIGA RESEARCH REACTORS WITH  
HIGHER POWER DENSITY

by

W. L. Whitemore  
General Atomics  
San Diego, California

## ABSTRACT

The recent trend in new or upgraded research reactors is to higher power densities (hence higher neutron flux levels) but not necessarily to higher power levels. The TRIGA LEU fuel with burnable poison is available in small diameter fuel rods capable of high power per rod ( $\approx 48$  kW/rod) with acceptable peak fuel temperatures. The performance of a 10-MW research reactor with a compact core of hexagonal TRIGA fuel clusters has been calculated in detail. With its light water coolant, beryllium and  $D_2O$  reflector regions, this reactor can provide in-core experiments with thermal fluxes in excess of  $3 \times 10^{14}$  n/cm<sup>2</sup>·s and fast fluxes ( $>0.1$  MeV) of  $2 \times 10^{14}$  n/cm<sup>2</sup>·s. The core centerline thermal neutron flux in the  $D_2O$  reflector is about  $2 \times 10^{14}$  n/cm<sup>2</sup>·s. and the average core power density is about 230 kW/liter. Using other TRIGA fuel developed for 25-MW test reactors but arranged in hexagonal arrays, power densities in excess of 300 kW/liter are readily available. A core with TRIGA fuel operating at 15-MW and generating such a power density is capable of producing thermal neutron fluxes in a  $D_2O$  reflector of  $3 \times 10^{14}$  n/cm<sup>2</sup>·s. A beryllium-filled central region of the core can further enhance the core leakage and hence the neutron flux in the reflector.

## 1. Introduction

The recent trend in medium powered research reactors (5 to 15 MW) is toward higher power density, hence higher neutron fluxes. Part of the means to improve the power density for reactors with fuel rods is to use a compact hexagonal cluster typically with 19 or 37 rods per cluster. Such an improved hexagonal fuel cluster design was reported at the Second Meeting of the International Group of Research Reactors<sup>1</sup>. A measure of the improvement in the reactor performance is the average power density. The standard 10-MW TRIGA research reactor<sup>2</sup> and the 14-MW Romania TRIGA test reactor<sup>3</sup> have average power densities of about 87 kW/liter and 118 kW/liter, respectively. Please refer to Table 1. These two reactors use the standard square cluster of 4 x 4 or 5 x 5 fuel rods. As will be shown below, use of the compact hexagonal fuel cluster can increase the average power density by a factor of two or more.

## 2. TRIGA Reactor with Compact Hexagonal Core

The compact hexagonal fuel cluster with TRIGA LEU fuel has been considered for a very compact core as shown in Fig. 1. The core is cooled with light water. The core with its partial beryllium reflector is surrounded by a tank of D<sub>2</sub>O that extends 14 inches (356 mm) in the radial direction outward to a graphite outer reflector 24 inches (610 mm) thick radially.

The core contains 16 hexagonal clusters each of which contains 19 TRIGA fuel rods with

---

<sup>1</sup> W. L. Whittemore, et. al., "*TRIGA HEXAGONAL FUEL ELEMENT DEVELOPMENT*," Session II, IGORR Proceedings, Saclay, France, 18-19 May 1992.

<sup>2</sup> "*10 MW TRIGA-LEU FUEL AND REACTOR DESIGN DESCRIPTION*", GA document UZR-14 (Rev), Oct. 1979.

<sup>3</sup> "*10 YEARS OF OPERATING EXPERIENCE AT THE STEADY STATE REACTOR IN ROMANIA*," by M. Ciocanescu, et.al., Eleventh European TRIGA Users' Conference, Heidelberg, Germany, Sept. 1990.



13.7 mm diameter. The vertical height of the fuel is 22 inches (559 mm). Three in-core experimental regions are available for the thermal or fast neutron irradiations. As shown in Fig.1, these experimental locations were evaluated for fast neutron irradiations assuming that each region was filled with an experiment equivalent to a metal whose density was 0.5 that of stainless steel.

For 10 MW operation, the average power density is about 230 kW/liter, a significant improvement over the values for TRIGA reactors using the standard square fuel cluster. The thermal neutron flux in in-core experimental regions was calculated to be about  $3 \times 10^{14}$  n/cm<sup>2</sup>·s. With in-core irradiation locations filled with half-density stainless steel, the fast neutron flux (>0.1 MeV) was calculated to be  $2.1 \times 10^{14}$  n/cm<sup>2</sup>·s. The unperturbed peak thermal flux in the D<sub>2</sub>O reflector at about core centerline was calculated to be  $1.95 \times 10^{14}$  n/cm<sup>2</sup>·s. These values together with other pertinent parameters are tabulated in Table 1.

### 3. Higher Power Density TRIGA Reactor

For TRIGA reactors with larger power levels ( $\geq 20$  MW), a smaller diameter fuel rod has been designed to assure that the peak fuel temperatures remain at acceptable low values. A fuel rod with diameter of 9.50 mm has been evaluated in detail for use in a square (6 x 6) fuel cluster. Use of this same fuel rod in the higher performance hexagonal cluster will significantly improve the performance of a 10 to 15 MW TRIGA reactor. The hexagonal cluster with this fuel would have 37 fuel rods. The average power density for a 15 MW TRIGA reactor could easily be as high as 330 kW/liter. With a large D<sub>2</sub>O reflector the thermal flux in a central flux trap region can be about  $4 \times 10^{14}$  n/cm<sup>2</sup>·s. The thermal flux near the core centerline in the D<sub>2</sub>O reflector should be about  $3 \times 10^{14}$  n/cm<sup>2</sup>·s based on the performance of the 10 MW compact core with its average power density of 230 kW/liter and thermal flux in the D<sub>2</sub>O reflector of about  $2 \times 10^{14}$  n/cm<sup>2</sup>·s.

#### 4. Discussion: Safety and Performance

The TRIGA LEU fuel is very robust. Its clad (Alloy 800H) is rugged enough to provide a large margin of safety including such abnormal events as loss of forced cooling. The UZrH fuel matrix together with the Alloy 800H clad assure that no fuel damage will occur during any credible reactivity accident. A high performance TRIGA reactor using the hexagonal fuel cluster for operation at 10 to 15 MW is a particularly user-friendly reactor.

It is interesting to compare the geometry of the 10 to 15 MW compact TRIGA core with that for Orphée<sup>4</sup>. For the TRIGA LEU core, the approximately circular core has a diameter of 14.5 - 19.5 in. (368 - 495 mm) with a fueled height of 22 in. (559 mm). The ratio of height to diameter ranges from 1.13 to 1.52. By comparison the Orphée reactor has a square parallelepiped core 250 x 250 mm<sup>2</sup> with a fueled height of 900 mm. The ratio of its core height to core width is about 3.6, a value which is quite far from an optimum value of about 1.0.

The performance of the 10 MW research reactor MURR<sup>5</sup> is particularly efficient for in-core experiments. Its core occupies a small volume giving it a large average power density of 303 kW/liter. This is higher than the corresponding average power density for Orphée (i.e., 282 kW/liter) even though its power level is noticeably smaller. Its central flux trap doubles the unperturbed thermal flux ( $6 \times 10^{14}$  n/cm<sup>2</sup>·s) compared to the quoted value for Orphée. However, the leakage flux in the reflector available for beamports is about half that reported for Orphée due to the use of a beryllium and graphite reflector compared to Orphée's D<sub>2</sub>O reflector. A TRIGA reactor operating at 15 MW with the small diameter fuel (9.5 mm) can produce an average power density (~ 332 kW/liter) larger than those for either the Orphée or MURR. The neutron fluxes for such a TRIGA reactor can exceed those reported for the above two reactors.

---

<sup>4</sup> Orphée, CEN Saclay; *DIRECTORY OF NUCLEAR RESEARCH REACTORS*, IAEA, Vienna 1989, p 136 ff.

<sup>5</sup> University of Missouri Research Reactor: *RESEARCH, TRAINING, TEST AND PRODUCTION REACTOR DIRECTORY*, Publ. by American Nuclear Society, 3rd edition, 1988, p 423 ff.

Table 1. Performance Characteristics of Several Higher Power TRIGA Reactors and Other Intermediate Power Reactors

Parameters	Standard 10-MW TRIGA	Romania TRIGA	TRIGA Compact Hex Clusters	ORPHÉE	MURR
Power (MW)	10	14	10	14	10
No. of fuel clusters	30	27	16	8	--
Fuel rods/clusters	4 x 4	5 x 5	19-Hex	- plate fuel -	
No. of fuel rods	480	675	304	--	--
Length of fuel (mm)	559	559	559	900	610
Diam. of fuel rod (mm)	13.7	13.7	13.7	--	--
Avg. power density (kW/liter)	87	118	230	282	303
Reflector type	H <sub>2</sub> O	Be/H <sub>2</sub> O	Be/D <sub>2</sub> O	D <sub>2</sub> O	Be/Gr
$\phi$ (th), central core region (n/cm <sup>2</sup> .s)	2.9 (14)	2.8 (14)	3 (14)	3 (14)	6 (14)
$\phi$ (fast), central core region (n/cm <sup>2</sup> .s)	2 (14)	2.4 (14)	2.1 (14)	--	1.4 (14)
$\phi$ (th) reflector peak (n/cm <sup>2</sup> .s)	1 (14)	1.1 (14)	1.95 (14)	2 (14)	~1 (14)

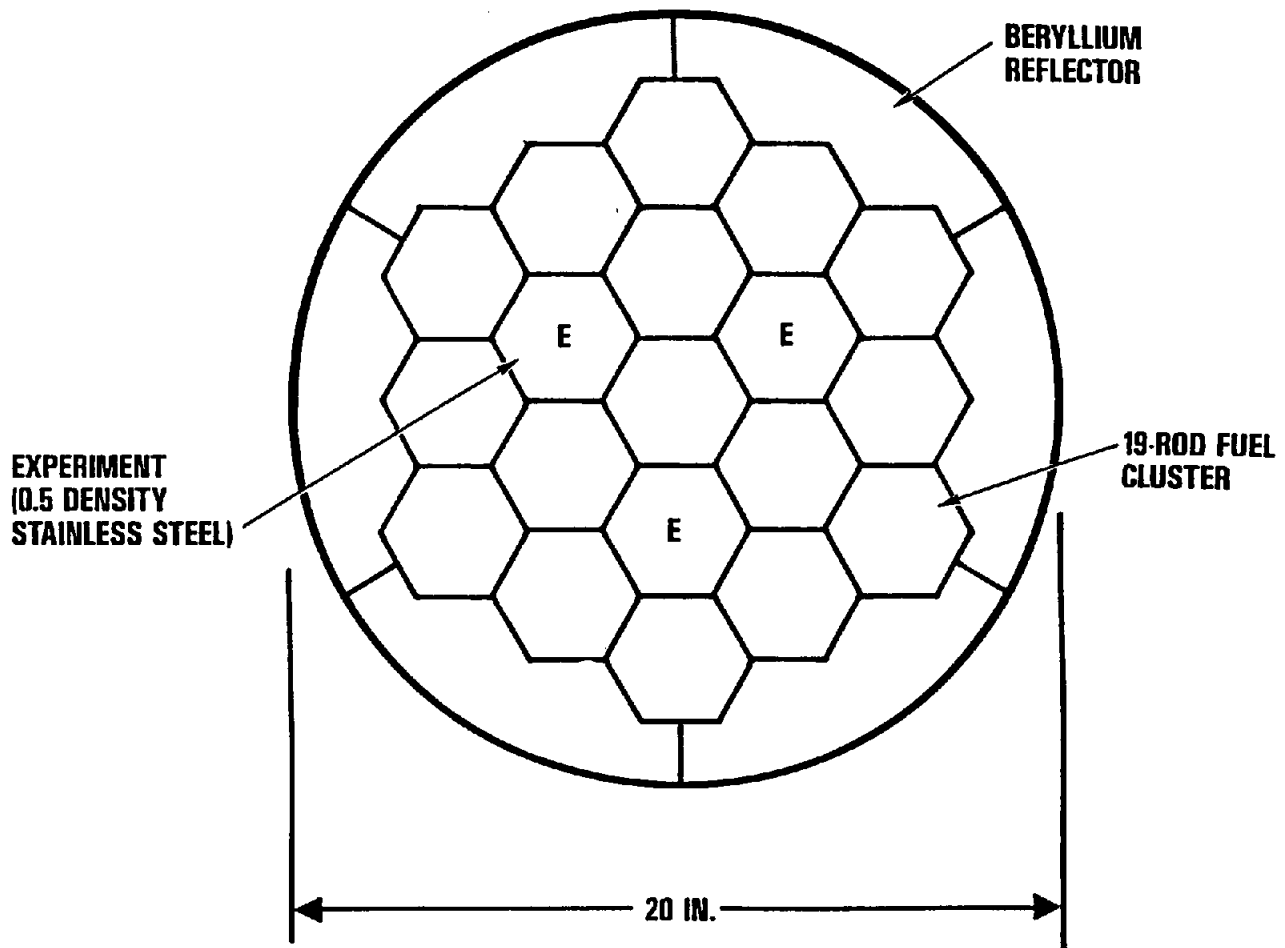


**FIGURE 1. CORE CONFIGURATION WITH TRIGA  
19-ROD HEXAGONAL FUEL CLUSTERS**

## **SESSION III**

### **Research, Development and Analysis Results**

INSTRUMENTATION OF FUEL ELEMENTS  
AND FUEL PLATES

J.P. Durand - Y. Fanjas

C E R C A  
Zone Industrielle "Les Bérauds"  
B.P. 1114  
26104 ROMANS SUR ISERE - FRANCE

ABSTRACT

When controlling the behaviour of a reactor or developing a new fuel concept, it is of utmost interest to have the possibility to confirm the thermohydraulic calculations by actual measurements in the fuel elements or in the fuel plates.

For years, CERCA has developed the technology and supplied its customers with fuel elements equipped with pressure or temperature measuring devices according to the requirements.

Recent customer projects have lead to the development of a new method to introduce thermocouples directly into the fuel plate meat instead of the cladding.

The purpose of this paper is to review the various instrumentation possibilities available at CERCA.

1. INTRODUCTION

Thermohydraulic conditions are of critical importance for the safety of research reactors. Reliable computer codes have been designed throughout the world to determine them by calculation.

However it is often deemed necessary to check the calculation results and the validity of physical model used by experimental measurements.

This is particularly true when major changes occur in an existing reactor such as :

- nominal power reactor increase
- modification of core configuration according to the experimentator's needs
- replacement of HEU by LEU fuel in the frame of the non proliferation policy

Or when new reactor is built or is under design.

In any case, for the new as well as for the existing reactors it is of great interest to have the possibility to confirm the thermohydraulic calculations by actual measurements of pressure or temperature in the fuel elements or in the fuel plates.

For years CERCA has developed the technology and supplied its customers with the fuel elements equipped with pressure or temperature measuring devices according to the need.

The purpose of this paper is to review the various instrumentation possibilities available at CERCA.

## **2. THE MEASUREMENT OF PRESSURE WITHIN A FUEL ELEMENT**

Our customers often need to measure :

- The dynamic pressure between the fuel plates in the coolant direction
- The static pressure on the surface of a fuel plate

The pressure can be measured by means of Pitot tubes installed in the fuel element. This technology has been applied to the JRR3 fuel elements.

Slide 1 shows Pitot tubes crossing plates to measure the static pressure on the plate surface and the dynamic pressure in the water channel.

Slide 2 shows a draft with general views of the fuel element and the path followed by the Pitot tubes between the plates to get out through the end fitting.

From this technique, it can be noticed that it is possible to measure the pressure anywhere in the fuel element (in the side plates, in the end fitting) but the number of tubes is limited by the hydraulic losses generated by the devices within the fuel element.

If the pressure is to be measured in the central part of the water channel, the instrumented plates must be inert ones since holes must be drilled to allow the Pitot tubes to cross the instrumented plates. However the other plates of the element can be normal fuel plates if necessary.

## **3. THE MEASUREMENT OF A FUEL PLATE TEMPERATURE**

It is interesting to know the temperature of the fuel plate cladding to check the heat exchange and the thermohydraulic conditions in the coolant water.

It may also be requested to measure the temperature within the meat of the plate to evaluate the thermal behaviour of the meat itself.

We will successively speak of both techniques.

### 3.1 TEMPERATURE OF THE PLATE CLADDING

CERCA has developed special techniques with special tools and adequate procedures to introduce thermocouples within a plate cladding.

Slide 3 shows a draft with a general view of an instrumented plate. The path followed by the thermocouples to reach the cladding above the meat can be seen. Section "B" shows the plate with the thermocouple completely embedded in the cladding. It should be noted that the thermocouple does not touch the meat.

The number of thermocouples is limited by their diameter and the available space between the meat and the longitudinal edge of the plate. Typically, a maximum of ten thermocouples can be installed in a fuel plate, in any location.

It can be noticed that this technique allows to insert thermocouples in a curved as well as in a flat plate.

### 3.2 TEMPERATURE OF THE PLATE MEAT

Last year, the ANS project team expressed its wish to check the feasibility of the temperature measurement within the meat of a mini plate. In addition, in order to avoid the possible influence of individual fuel grains on the measured temperature, it was also requested to prevent direct contact between the fuel particules and the thermocouple. This was requiring the development of a new technique.

Therefore, the aim of the development was to demonstrate the feasibility to introduce an aluminium clad thermocouple within a thin meat containing hard particles. Furthermore, the clad thermocouple had to stand exactly in the middle of the meat thickness to keep symetrical uranium distribution around it in order to get a representative measurement.

Slide 4 shows a micrograph of a mini plate with its clad thermocouple. For the manufacturing tests, the thermocouple was replaced by a stainless steel wire representative of the actual dimensions of a real one.

The thermocouple is homogeneously covered with an aluminium sheet avoiding a direct contact with uranium. The termocouple with its aluminium sheet is symmetrically embedded in the thickness of the meat.



The manufacturing tests required the design and production of special and accurate tools to demonstrate the feasibility of the ANS team wish.

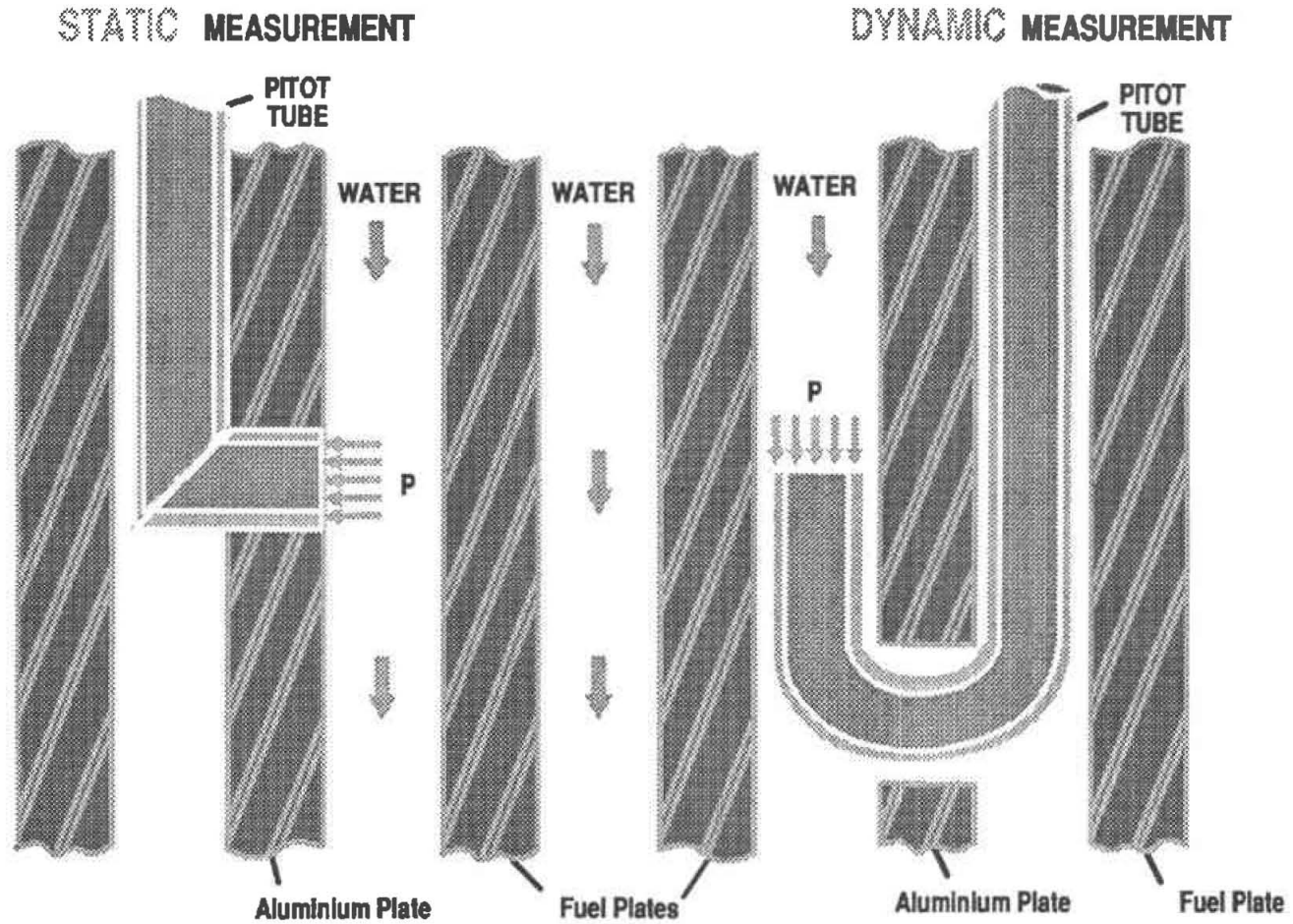
Now, as the manufacturing technique has been developed, the next step will be to produce plates with real thermocouples.

#### 4. CONCLUSION

For years CERCA has gained a wide expertise and developed special tools and techniques for the instrumentation of fuel elements for the measurement of pressure and temperature.

Since each fuel element has a different design and each case is a particular one, CERCA has got a large flexibility to be able to study and manufacture a wide range of instrumentation devices adapted to the needs of its customers.

# THE MEASUREMENT OF PRESSURE WITHIN A FUEL ELEMENT



# INSTRUMENTED FUEL ELEMENT WITH PITOT TUBES

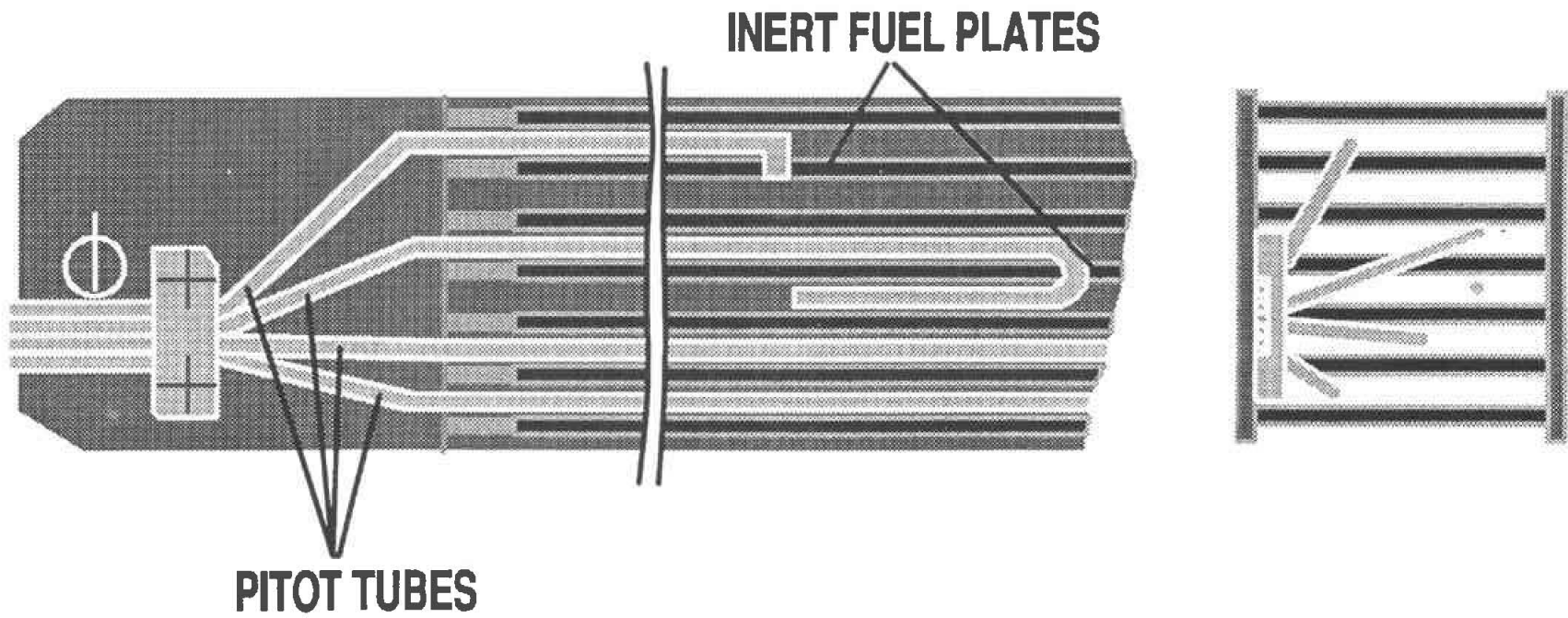
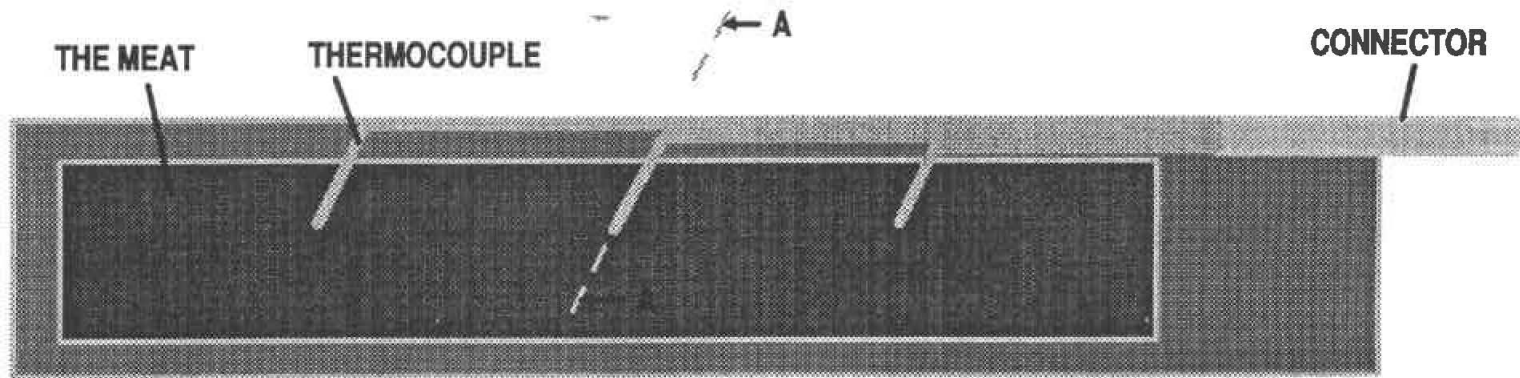
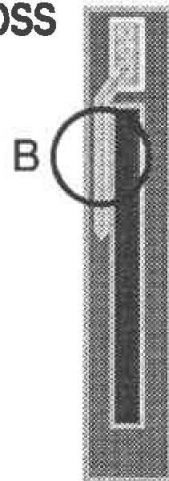


# PLATE CLADDING : MEASUREMENT OF THE TEMPERATURE



A : DETAIL OF THE CROSS SECTION



B : MICROGRAPH OF THE CROSS SECTION

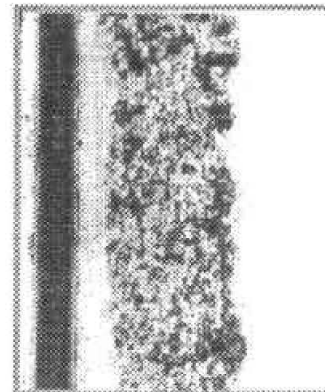
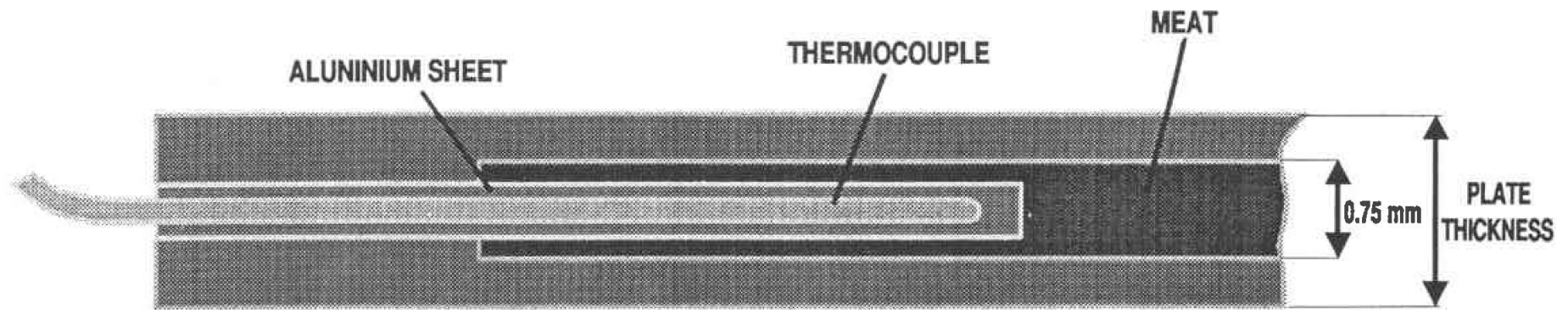
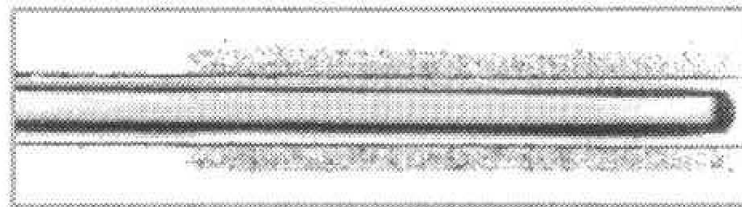


# PLATE MEAT : MEASUREMENT OF THE TEMPERATURE



MICROGRAPHIC RESULT : x 25



MECHANISM OF  $^{232}\text{U}$  PRODUCTION IN MTR FUEL  
EVOLUTION OF ACTIVITY IN REPROCESSED URANIUM

G. Harbonnier, B. Lelièvre -  
Y. Fanjas, - SJP. Naccache

C E R C A  
Zone Industrielle "Les Bérauds"  
B.P. 1114  
26104 ROMANS - FRANCE

ABSTRACT

The use of reprocessed uranium for research reactor fuel fabrication implies to keep operators safe from the hard gamma rays emitted by  $^{232}\text{U}$  daughter products.

CERCA has carried out, with the help of French CEA and COGEMA, a detailed study to determine the evolution of the radiation dose rate associated with the use of this material.

FOREWORD

One of the major problems of reactors operators is to get rid of spent fuel, whose accumulation on reactor site leads to technical and administrative problems and could, in some cases, lead to reactor shutdown due to a lack of storage space on the site.

Highly enriched fuel elements can be reprocessed, and the recovered uranium can be converted by dilution into low enriched uranium.

CERCA has carried out with the help of specialized teams of the French CEA and COGEMA Pierrelatte a study to evaluate the consequences of the introduction of such material in the production lines. In this study, CERCA has also taken profit of the experience of FBFC (the French PWR fuel Manufacturing Company) located on the same site, which is currently handling reprocessed fuel in its workshop.

The purpose of this paper is to focus on the mechanism of formation of  $^{232}\text{U}$  and its daughter products, and their importance in radiation problems.

## 232U PRODUCTION MECHANISMS AND AMOUNT IN REPROCESSED URANIUM

There are mainly three ways for 232U production : from 234U, 235U and 236U isotopes (slide 1).

The first two ways concern 234U and 235U :

Before irradiation, these products are decaying with alpha reaction to Pa and Th which build up in the metal. During irradiation, by neutron capture and beta decay, these products lead to 232U.

The third way concerns 236U :

236U is formed by neutron capture of 235U which, by another neutron capture, gives 237U whose decay leads to Np and 236Pu. 236Pu, by alpha decay with a half life of 2.8 years, leads to 232U.

As a consequence, there are three important periods in the life of uranium since its conversion into metal :

### - Fresh metal life time

During the first period, between the last purification of fresh uranium (which is usually corresponding to the conversion into metal) and the irradiation in reactor, Pa and Th are accumulating by decay of 234U and 235U.

### - Irradiation

During the second period, irradiation in reactor occurs. Pa and Th are transformed into 232U, and 236U into 236Pu.

### - Decay time

During the third period, between irradiation and reprocessing, 236Pu decays into 232U.

Immediately after irradiation, the 234U way accounts for about 80 % of the 232U content.

But, after irradiation, 236U way (via 236Pu) is increasing with time and accounts for about a quarter of 232U after a cooling period of ten years (slide 5).

After irradiation, the spent fuel has a final enrichment of 70 to 80 % assuming a burn up of 50 %.

As the uranium will finally be used as 19,75 % material, reprocessed U has to be blended with depleted uranium to an approximate dilution factor of 4.

A study of French MTR fuel history performed by CEA with the KAFKA code shows that, after reprocessing, the 232U content in HEU stands between 2 and 18 ppb, depending on the reactor. Therefore, after blending, the 232U content stands between 0.5 and 4.5 ppb.

As a conclusion to this chapter, it has to be remembered that the initial  $^{232}\text{U}$  content is depending upon the uranium history : composition and storage time before irradiation, irradiation conditions, storage time between irradiation and reprocessing.

## CONTAMINATION AND RADIATION

Handling of U always induces a certain amount of contamination and radiation, which is examined below for various kinds of uranium.

### Fresh Uranium

With fresh uranium, the major problem is atmospheric contamination induced by  $^{234}\text{U}$  and its decay products which are presented in slides 2 and 3.

As far as radiation is concerned, the corresponding activity level is very low and comes from the  $^{235}\text{U}$  and  $^{238}\text{U}$  families and their Pa and Th decay products.

However, usual fresh uranium, called "Virgin" uranium is not as virgin as it is supposed to be, as it may have an  $^{236}\text{U}$  content as high as 0.5%, and  $^{232}\text{U}$  content up to 0,2 ppb.

### Uranium from Critical Experiments

For several years CERCA has been manufacturing fuel elements with uranium coming from critical experiments.

This uranium, generally with a nominal enrichment of 19,75 %, has not produced much energy, but is nevertheless slightly irradiated. Therefore, the quantity of fission products and transuranic products is not neglectible as all these products are not removed by any treatment since uranium is used as it is.

The amount of  $^{232}\text{U}$  in this uranium is generally almost undetectable and in the order of magnitude of less than 0.01 ppb.

Provided additional radiation measurements are carried out at the various working stations and production wastes are treated according to a special procedure, this material can be used without difficulty from atmospheric contamination and radiation dose rate points of view.



## Reprocessed Uranium

Contamination associated with reprocessed uranium is, as in fresh uranium, mainly due to  $^{234}\text{U}$  to the condition that  $^{241}\text{Pu}$ , which is a powerful beta emitter, is kept below 1Bq/gU. Since the  $^{234}\text{U}$  content remains approximately constant during irradiation, reprocessed uranium creates no particular difficulties from the atmospheric contamination point of view.

Fission products and transuranic elements are a rather simple matter, as they are chemically removed during reprocessing, and, if a high degree of purification is reached, they should not appear in LEU with a much higher level than the previous case. Therefore, contribution to the radiation level should be of the same order of magnitude as with uranium coming from critical experiments. For the calculation of these dose rates, the following fission products and transuranics contents have been taken into account :

$^{240}\text{Pu}$ :	6 Bq/g U, i.e. $7.12 \cdot 10^{-10}$ g/g U
$^{239}\text{Pu}$ :	6 Bq/g U, i.e. $2.66 \cdot 10^{-9}$ g/g U
$^{238}\text{Pu}$ :	6 Bq/g U, i.e. $9.55 \cdot 10^{-12}$ g/g U
$^{237}\text{Np}$ :	23 Bq/g U, i.e. $8.93 \cdot 10^{-12}$ g/g U
$^{241}\text{Am}$ :	22 Bq/g U, i.e. $1.73 \cdot 10^{-10}$ g/g U
$^{144}\text{Ce}$ :	3150 Bq/g U
$^{137}\text{Cs}$ :	160 Bq/g U
$^{134}\text{Cs}$ :	75 Bq/g U
$^{106}\text{Ru}/^{106}\text{Rh}$ :	840 Bq/g U
$^{103}\text{Ru}$ :	210 Bq/g U
$^{95}\text{Zr}/^{95}\text{Nb}$ :	140 Bq/g U
$^{60}\text{Co}$ :	42 Bq/g U

The major factor for radiation dose rate is the initial amount of  $^{232}\text{U}$  after reprocessing because the activity level increases with this amount which is directly depending upon the fuel history from metal production to reprocessing (slide 5).

During reprocessing,  $^{232}\text{U}$  decay products are chemically removed. But  $^{232}\text{U}$  remains untouched, and immediately after, the build up of its decay products starts again.

As can be seen on slide 4, these alpha decay products lead to  $^{212}\text{Bi}$  and  $^{208}\text{Tl}$  which are very active gamma emitters with an energy of 0.79 Mev and 2.63 Mev respectively.

These two are the most important products in radiation induced by  $^{232}\text{U}$ . Knowing the half lives of  $^{232}\text{U}$  and its decay products, computation using the CHAINURA code developed by CEA in CADARACHE shows that the build up of activity is maximum ten years after reprocessing, but has reached half of its maximum level after only three years (slide 6).

## CONCLUSION

This paper has shown how  $^{232}\text{U}$  is formed and why it has a major consequence on utilization or reprocessed uranium.

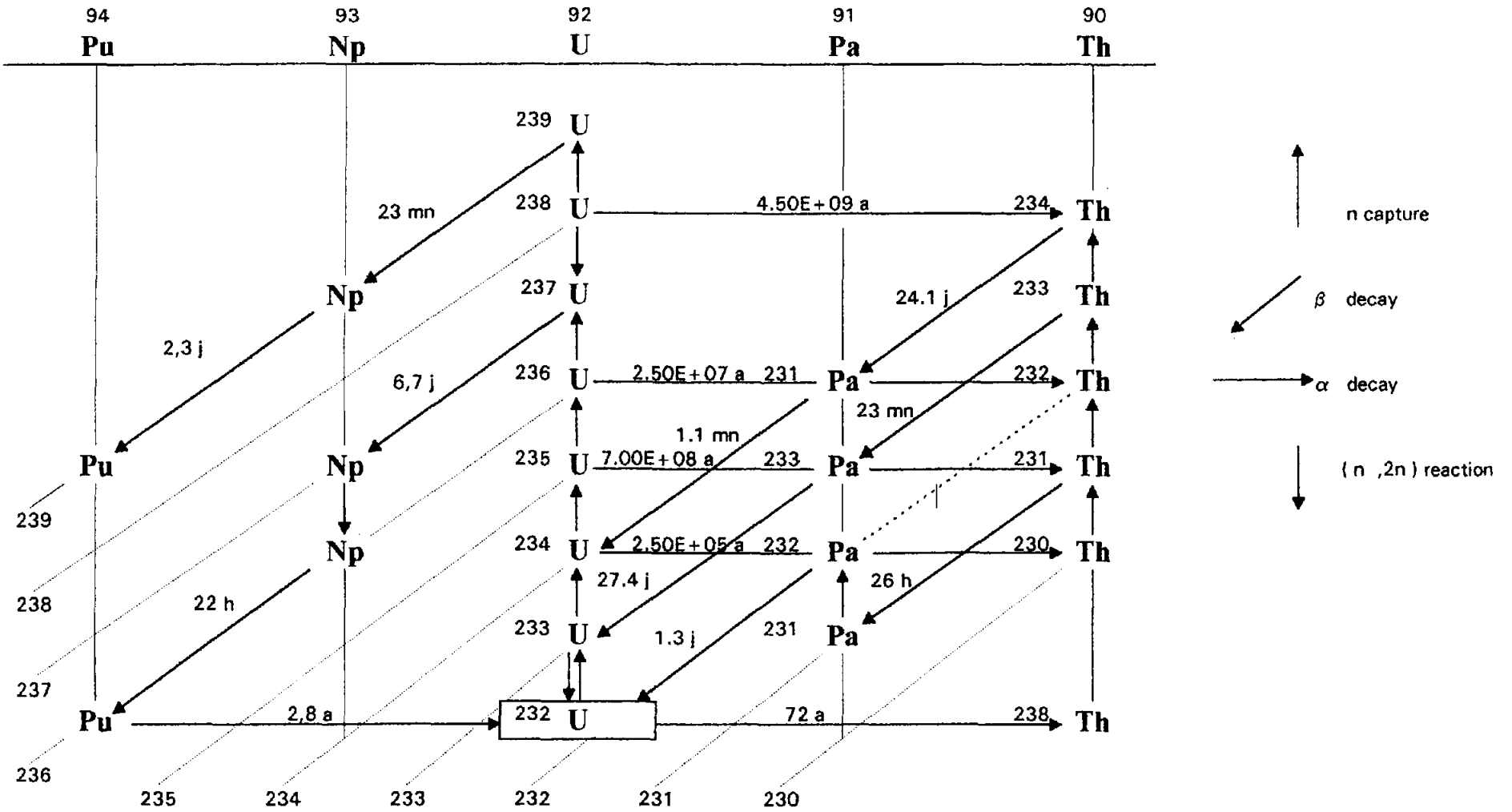
Further studies concerning the practical implications in the workshop have been carried out, and their results will be presented at the RERTR meeting in OARAI.

## References

- 1- Retraitement du combustible MTR  
D. BERETZ - F. TOURNEBIZE (CEA GRENOBLE)
  
- 2- Etude de l'évolution des débits de dose aux postes de travail de CERCA en présence d'URT.  
Gérard COUTY - Nicole GALLIANO - Claude LEUTHROT (CEA CADARACHE)
  
- 2- Recycling of reprocessed Uranium from Research Reactors.  
S. BOUCHARDY - J.F. PAUTY (COGEMA)  
Presented during the RERTR meeting at Roskilde

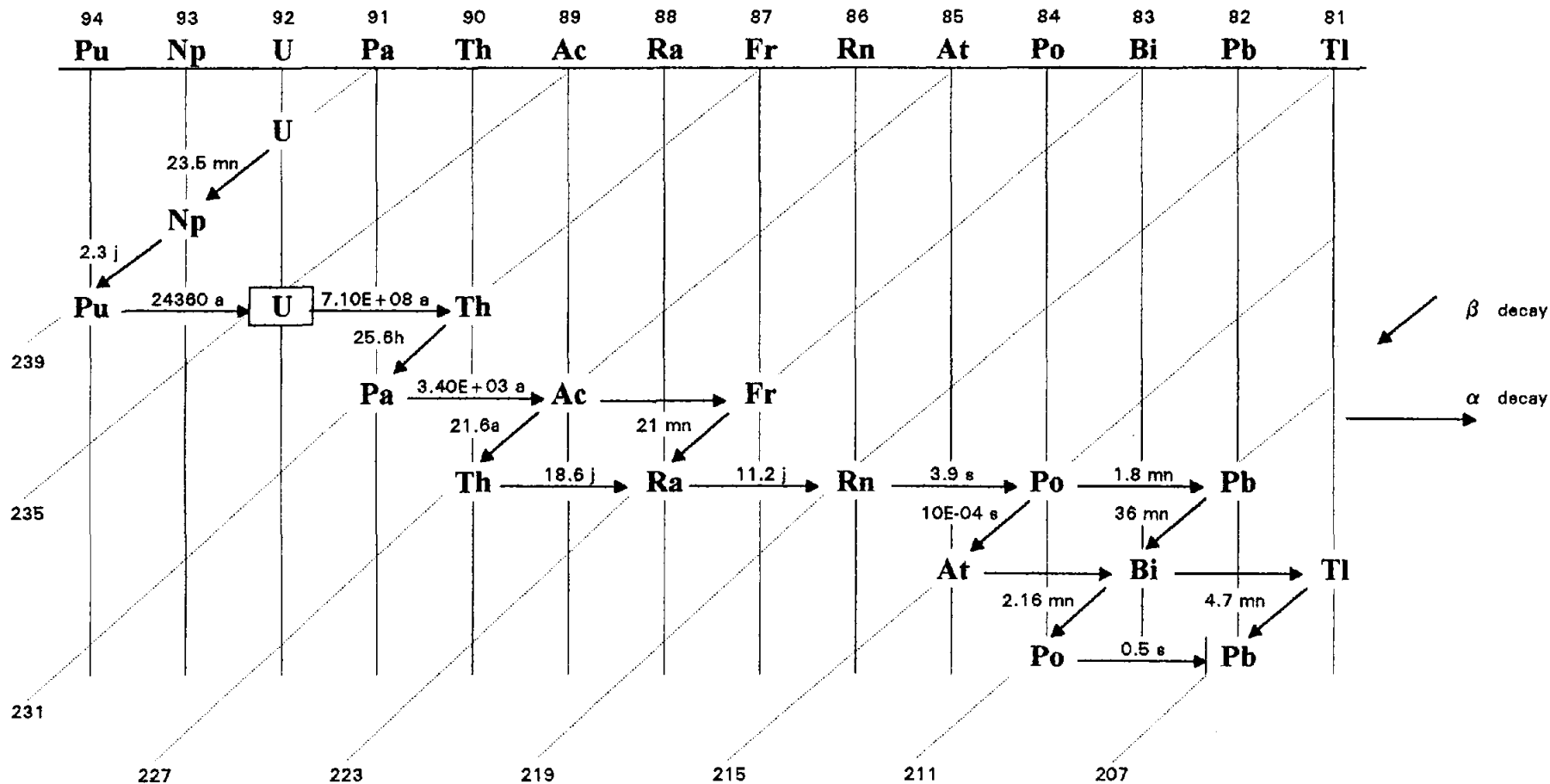
RADIOACTIVE BEHAVIOUR OF URANIUM ISOTOPES

224



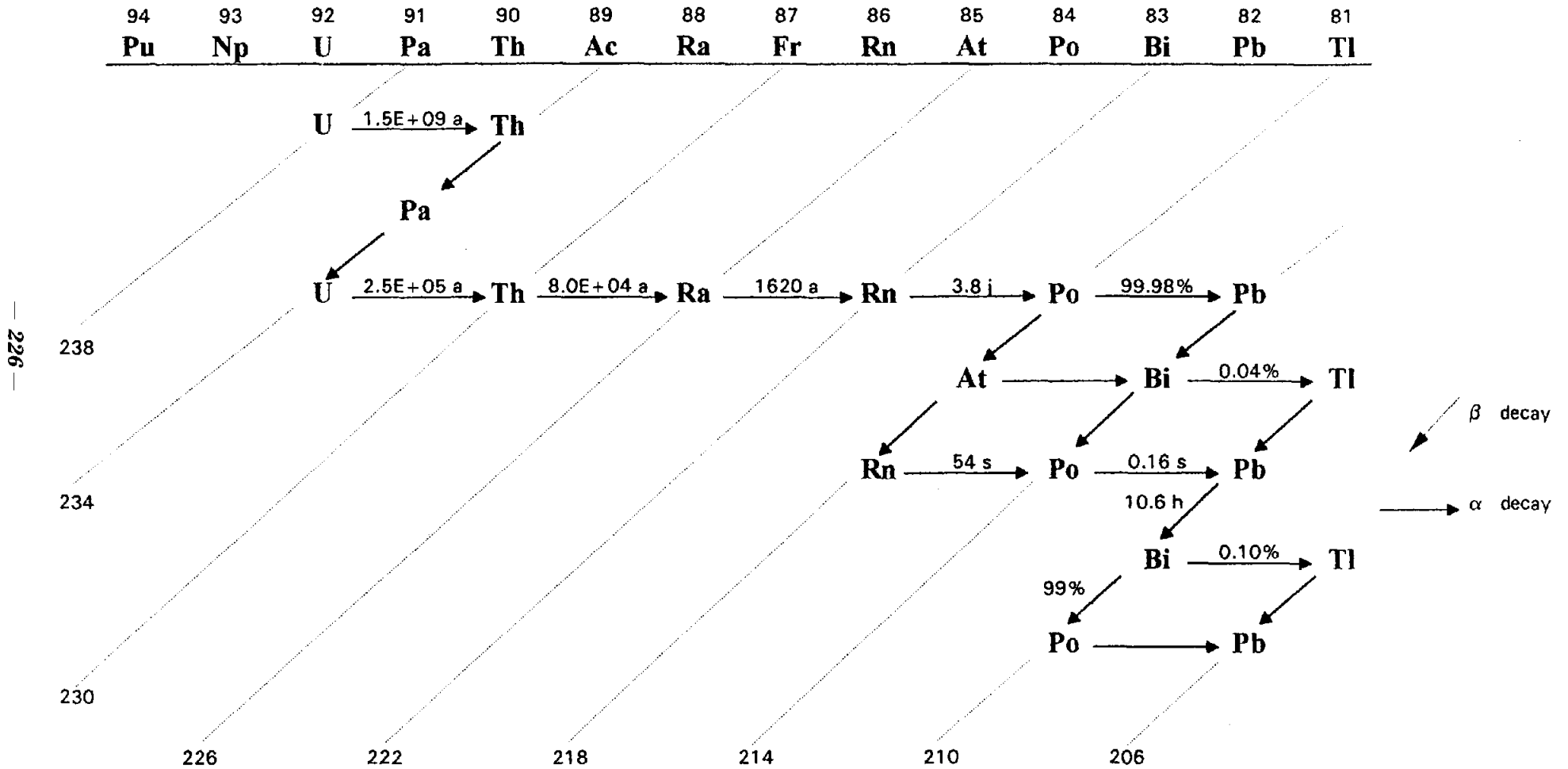
CERCA

URANIUM 235 RADIOACTIVE FAMILY

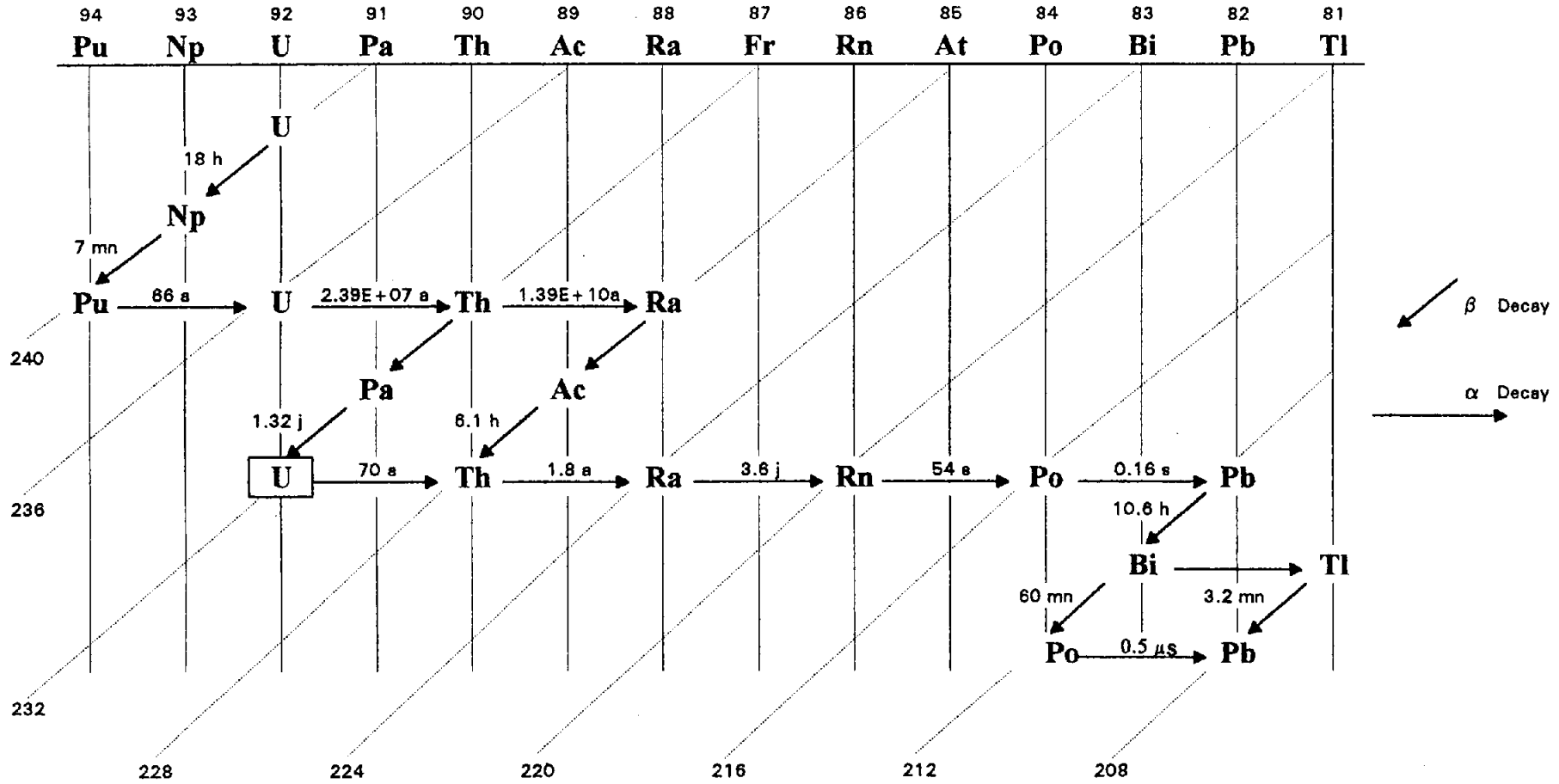


— 225 —

URANIUM 238 RADIOACTIVE FAMILY



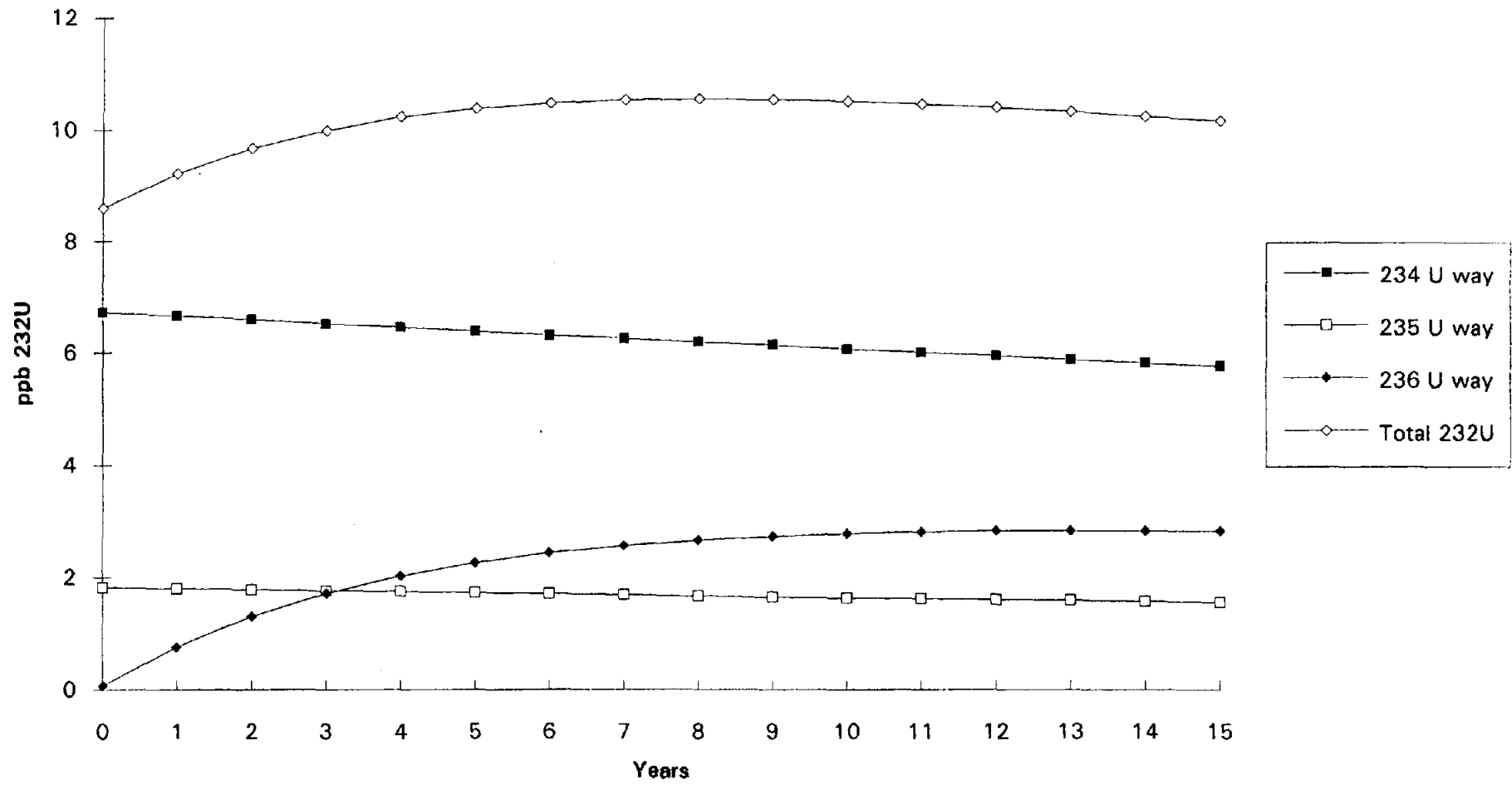
URANIUM 232 RADIOACTIVE FAMILY



227

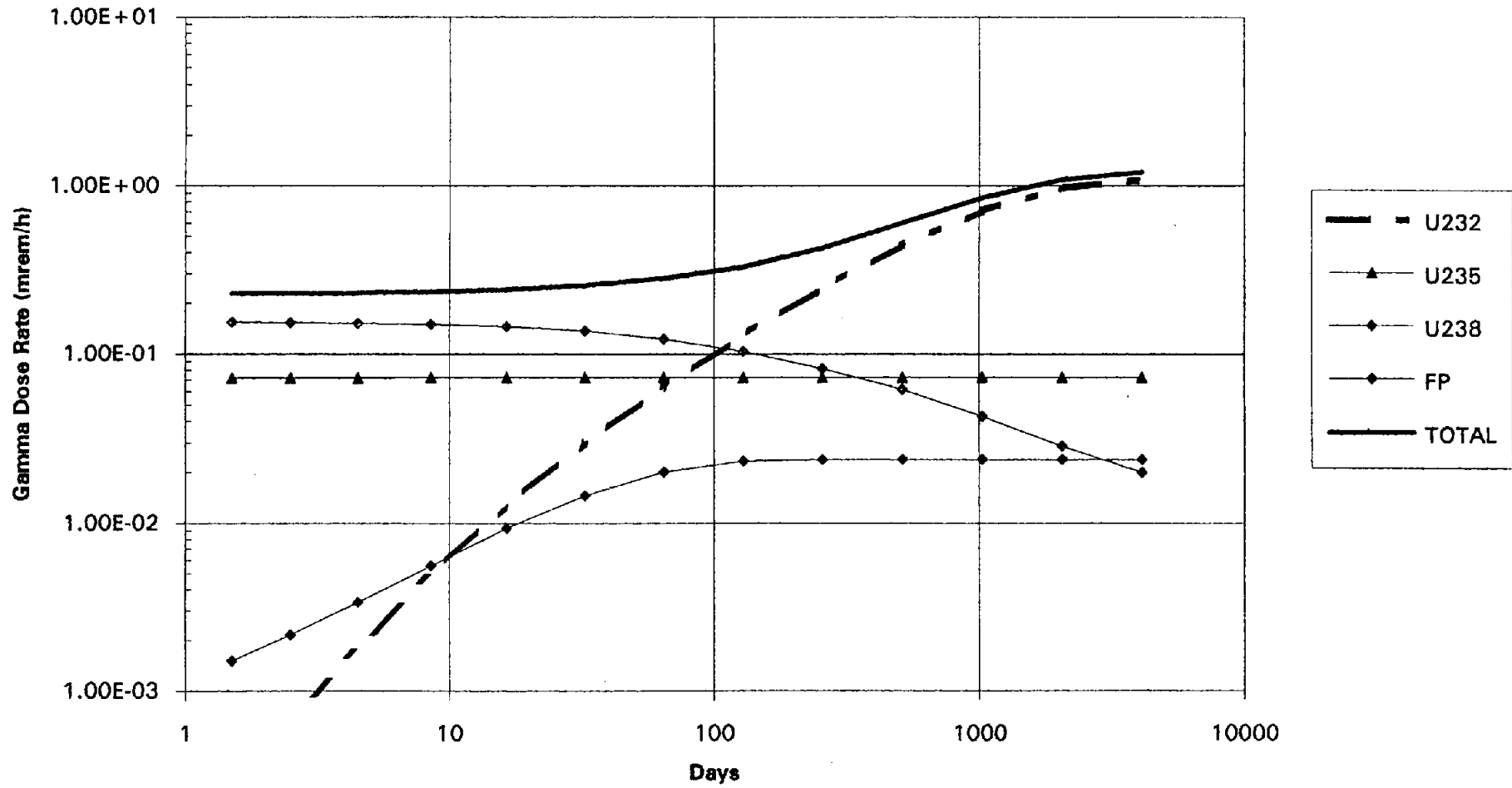
**232U EVOLUTION AFTER END OF IRRADIATION**

— 228 —



22 PLATES ELEMENT 5ppb U232

50 cm distance





### III-3

#### TWO DESIGN ASPECTS CONNECTED WITH THE SAFETY OF THE PIK REACTOR PRESENTLY UNDER CONSTRUCTION.

V.V.Gostev, A.S.Zakharov, K.A.Konoplev,  
N.V.Levandovskii, L.M.Ploshchanskii, and S.L.Smolsky

Neutron Research Department

Petersburg Nuclear Physics Institute

Russian Academy of Sciences

#### 1. PIK REACTOR

The PIK reactor [1] is designed for physical research with neutron beams and sample irradiation. In the central trap the thermal neutrons flux is  $4 \times 10^{15}$  n/cm<sup>2</sup> s. The reactor power is 100 MW, the thermal neutron flux in the reflector at the maximum of distribution is  $1 \times 10^{15}$  n/cm<sup>2</sup> s. The core with a high uranium concentration of 600 g/l is light water-cooled, heavy water being used in the reflector (fig.1,2,table).

The Chernobyl disaster happened at the time of equipment assembly at the PIK. The code revision, a change of the authors ideas about the safety, and a shift of public attitude toward nuclear installations resulted in a stopping down of construction and project revision. While it was certainly hard to make a decision of disassembling the equipment already installed and, particularly, of introducing changes into constructions, the new project or, as it was called, the reconstruction project has led to a change of all safety systems and involved in various degrees all essential reactor systems. The construction is presently resumed; however the economic difficulties plaguing Russia preclude specifying the term of its completion (fig.3). In January 1993, the reactor was inspected by experts from a number of European countries, USA, and European Commission delegated by

their governments to prepare a report on whether supporting the construction to its completion would be reasonable [2]. In the course of the examination, the experts expressed doubts concerning two systems, namely, the containment and scram. It is these points that will be discussed in the present communication.

## 2. CONTAINMENT: ACCIDENT LOCALIZATION SYSTEM

The PIK design is based on unit configuration, namely, the technological circuits are separated from the experimental zone and housed in separate buildings (fig.4). This precludes construction of a common containment that would enclose all the PIK buildings. To confine leakage of radioactive products under normal operating conditions or in an accident, the rooms with radioactive sources are provided with seals for maintaining in these rooms the air pressure lower than that in the adjacent premises, as well as with a special system for collecting the leaked-out liquids. These rooms are housed in four separate containments differing in the equipment confined, in the presence or absence of personnel, and in the character and probability of possible emergencies (fig.5). We shall consider below only three of these containments, since the fourth, similar in design to the first, houses the heavy water reflector equipment and contains considerably less radioactive material than the circuits associated with the core cooling in containment 1.

### Containment 1

This containment houses the primary circuit equipment and pipelines. During reactor operation there are no people inside the containment, all operations being performed by remote control. The containment is made up of seven interconnected rooms sealed off airtight from the remainder of the building. Inside the building, the rooms of this containment are arranged in such a way that between the containment and the outer brick wall there are at least two inner brick or reinforced-concrete walls. The containment proper is made of single-piece "heavy" reinforced-concrete of density  $3,6 \text{ t/m}^3$  and not less than 1 m thick. The rooms are provided by air-tight doors, the pipeline and cable laying penetrations being likewise air-tight. The floor is covered with a water-tight stainless steel tray, and the walls and ceiling, with epoxy-resin covering. Any leakage in these rooms is drained through stainless-steel pipelines into an emergency tank. A rarefaction of 15-20 mm water is maintained inside the containment, which is about 10 mm lower than the pressure in the adjoining rooms. The air removed from the containment is purified by passing it through aerosol filters and charcoal sorbents. The air is discharged through a 100 m-high stack. The total volume of containment is  $6000 \text{ m}^3$ , the total ventilation-air flow rate under normal conditions being about  $12000 \text{ m}^3/\text{hr}$ . Each of the seven rooms housed in the containment is provided with a separate gate valve on the ventilation pipeline, thus permitting one to cut each room

off from the others in the case of emergency and, hence, to increase the delay of the radioactive gas discharge. The available instrumentation, including dosimetric equipment, provides continuous monitoring of the state of the equipment inside the containment. The containment ensures safety of the personnel and environment both under the conditions of planned primary - circuit water leakage occurring during repairs or tests, and in emergencies associated with a sudden water leakage during reactor power operation. The design of the containment provides adequate protection against external interference. The reactor reconstruction project did not practically introduce any changes into the design of container 1, except for using more reliable packing for the electric cables passing through the containment walls.

#### Containment 2 (Fig.6).

The change introduced into the design of this containment are so profound that its reconstruction dominates presently the reactor construction. This containment houses only one room, namely, the technological hall. The surface of the water from the reactor vault, spent fuel element pool, and fuel assembly transfer channel looks into this hall. The containment is located in the top part of the building and is about 15 m high, 100 m long, and approximately 8 m wide. In contrast to containment 1, containment 2 is not surrounded by any rooms and forms the outer wall of the reactor building in its upper part. Note that the reactor vault lies between containment 1 and 2 ; rather, by its water leakage collection system it belongs to

containment 1, and by the ventilation system, to containment 2. The reactor vault is about 12 m deep and is filled with water which contacts with the primary water circuit in the case of refueling. The spent fuel element pool and reactor vault cooling loops are not connected in any way with the reactor cooling loop. Under normal operation, as well as in basic project accidents occurring inside the reactor building, containment 2 could not be destroyed already before the reconstruction. An analysis showed that external impacts (for example, explosions) could, however, damage it. The reactor reconstruction project envisages building a second high-strength reinforced-concrete shell. As a result, the containment will consist of two shells, namely, an inner one of sectional and, partially, of single-piece reinforced concrete, 600 mm thick, and an outer one made up of a steel inner wall and a single-piece reinforced-concrete wall 40 cm thick separated by an air gap. The hall floor is covered by a water-tight stainless steel tray. The walls and ceiling are coated by a layer of epoxy resin. The pipe and electric cable penetrations are air-tight. Air-tight doors are installed. Accidental leaks in the hall are collected through traps and pipelines into emergency tanks the air being discharged through a 100 m-high stack. Under emergency conditions the air flow rate is reduced to the lowest level that still ensures absence of leakage apart anywhere except through the stack. One of the goals of the present work has been to analyze the efficiency of the additional measures taken to reduce the

release from containment 2 in an accident. The results of this analysis will be presented below. It should be borne in mind that during reactor operation personnel may be present inside containment 2; so that the people should be removed, and some necessary electrical commutations should be made, for which three minutes are allotted, before transition to the emergency ventilation regime can be effected.

#### Containment 3 (Fig.5).

The containment encloses two experimental halls, namely, the horizontal channel hall and inclined channel hall. It is of cylindrical shape of radius 13.6 m and extends from 0.00m to the 16.00m-level. The containment is situated inside the building and is surrounded by two (horizontal channel hall) or three (inclined channel hall) rows of rooms with brick walls. The hall walls are made of single-piece reinforced concrete 600 mm thick. The containment is coated by epoxy resin and is provided with drains to collect spilled liquids into the emergency tank. The doors and technological penetrations are air - tight. Under normal conditions ventilation is effected by a separate system through the stack without purification. No radioactive water pipelines or open radioactive water surface are present in the halls. Under normal operation, surface or air contamination can appear during disassembly of experimental equipment or channels. The heavy water contains a tritium of up to 2 Cu/l.

In the case of an accident involving rupture of an experimen-

tal channel some heavy water may get access into the experimental hall, although its major part should drain into containment 1. During reactor operation, both reactor personnel and experimenters may be present in containment 3. In the case of accident, the people are evacuated, after which the ventilation is switched over to the emergency regime involving reduced flow rate and air filtration.

### 3. ANALYSIS OF CONTAINMENT EFFICIENCY.

While the rules adopted in the Russian Federation for the accident localization systems require dose limitation for the population, they do not require the construction of an overall containment. The PIK reactor containments meet the regulatory standards. Nevertheless it is of interest to analyze possibilities of a further reduction of radioactive gas and aerosol release for the PIK containments. The release of radioactive products into the rooms is the largest in the primary circuit equipment containment, which is associated primarily with repairs and regular testing of the equipment. The analysis yields also for this containment the highest probability of accident involving release of radioactive contamination.

Actually, a containment is equivalent to a delay line for the nuclides before their release into the atmosphere. To evaluate the containment efficiency, we assume that an amount  $N_0$  of a radioactive isotope has released in the containment and became uniformly distributed over the volume. The amount released out of

the containment will be

$$M = \int_0^{\infty} \frac{N(t)}{V} Q dt = N_0 \frac{Q/V}{\lambda + Q/V} \quad (1)$$

where V is the containment volume,

Q is the air discharge from the containment,

$\lambda$  is the decay constant.

If the containment is a double-shell design or is provided with an additional volume preceding air discharge into the atmosphere, then

$$M = N_0 \frac{Q_1/V_1}{\lambda + Q_1/V_1} \times \frac{Q_2/V_2}{\lambda + Q_2/V_2} \quad (2)$$

where the indices 1 and 2 refer to the containment and additional volume, respectively. Since the air circulation ratios  $Q_2/V_2$  adopted at research reactors are much larger than  $Q_1/V_1$ , the effect of the latter factor is usually small.

The PIK design value of the parameter  $Q/V$  does not exceed  $10^{-6} \text{ s}^{-1}$ , thus permitting considerable suppression of the release of all radioactive noble gas isotopes with the exception of Xenon-133 ( $\lambda = 1.5 \cdot 10^{-6} \text{ s}^{-1}$ ). The best design values of research reactor containments permit substantial delay of Xenon-133 release [3]. Straight forward calculation of the population dose burden associated with an accident on the PIK reactor have yielded values below the code-allowed levels. Maximum design-basis accident - 0.08sZv while allowed dose - 0.5sZv.



To reduce the release still further, we are considering the possibility of installing air recirculation and filtration inside the containments.

The recirculation efficiency can be analyzed using an equation similar to (1) for the total radioactivity release

$$M/M' = 1 + \frac{\sum q/V}{\lambda + Q/V} \quad (3)$$

where  $M'$  is the release with recalculation at the flow rate  $q$  and efficiency  $\xi$ .

Obviously, recirculation can be useful only provided  $q \gg Q$ . It is technically feasible to reduce by recirculation by tens and hundreds of times the released activity of long-lived nuclides with a halflife in excess of 10 days for which the efficiency of a containment as a delay line is low. This relates to Cesium-137, Strontium-90, Zirconium-144, and some other nuclides. Direct calculation of the dose load for the case of recirculation carried out for containment 2 has yielded a dose reduction down to several times. This conclusion of the usefulness of developing a recirculation system and of the possibility of improving the filtration systems for containment 2 of the PIK reactor is the main result of the above consideration.

#### 4. SHUTTER SEPARATION.

The PIK reactor is controlled by means of eight rods in the heavy-water reflector and an absorbing cylinder at the boundary between the core and the central light-water neutron trap

(fig.7).The rods are used for emergency protection and reactor start-up. The central control cylinder called here the shutter serves several functions, namely, as scram, automatic control, and burnup compensation. The delay time before the onset of negative reactivity is 1.05 sec for rods, and 0,25 sec for the shutter.

The shutter is made up of two cylinders moved symmetrically in opposite directions by the same electric drive, thus ensuring symmetric energy release in the core. The weight of the control elements was measured in the critical assembly representing an exact replica of the PIK core and reflector. The weight of the rod in the reflector at the beginning of the campaign is  $0.66 \beta_{\text{eff}}$ , which yields  $2.64 \beta_{\text{eff}}$  for four rods, and, taking into account interference,  $4.5 \beta_{\text{eff}}$  for the eight. The shutter weighs  $9.5 \beta_{\text{eff}}$ : Since the mobility of the shutter is checked by the step servo motor of the automatic control, the probability of its seizing is extremely small. Nevertheless, independent drives to operate each half of the shutter are presently under development (fig.8). Symmetrical motion of the two halves with respect to the core medial plane will be ensured by their position indicators. Should the shutter seize when the emergency protection is actuated, the negative reactivity margin will be determined by the time of reactor shutdown. The margin will be the lowest soon after the reactor power - up, i.e. when a sizable amount of Iodine-135 has already accumulated but the shutter is not yet driven wide apart to compensate for burnup.

If at this moment the reactor is shut down, and simultaneously one of the two shutter halves seizes, then at the time the reactor escapes from iodine well the subcriticality will be  $1.2-1.7\beta_{\text{eff}}$  depending on the actual operating mode (Fig.9). This value lies at the limit of reliable shutdown, and therefore additional slow emergency protection is employed in this case. The absorber solution should be introduced into the gap between the reactor shroud and vessel during the first day after the reactor shutdown. When gadolinium nitrate is used, the protection system provides additionally  $1\beta_{\text{eff}}$ . Before the separation of the shutter into two halves, the additional negative reactivity was produced by draining off the reflector or by discharging the core.

The above values of reactivity were obtained under the assumption that when only one (upper or lower) half of the shutter is introduced the corresponding change in the reactivity will be one half of the result when both are driven in. While on the critical assembly this assumption was partially confirmed, three-dimensional calculations with inclusion of burnup are certainly required.

## References

-----

1. A.N.Erykalov, O.A.Kolesnichenko, K.A.Konoplev,  
V.A.Nazarenko, Yu.V.Petrov, S.L.Smolsky  
PIK REACTOR  
Academy of sciences of Russia  
Petersburg nuclear physics institute, preprint No 1784  
St.-Petersburg, 1992.
2. C.West  
PIK Reactor, Gatchina  
International Group on Research Reactors.  
IGOGG News.March 1993.
3. Summary Report of the ANS.  
Containment workshop.  
September 1990. CONF-9008150, Draft.

Table 1. PIK reactor parameters.

Power	100 MW
Flux of thermal neutrons in the trap	$4.10^{15} \text{ n/cm}^2 \text{ s}$
Flux of thermal neutrons in the reflector	$1,3.10^{15} \text{ n/cm}^2 \text{ s}$
Moderator and coolant	H <sub>2</sub> O
Reflector	D <sub>2</sub> O
Diameter	2,4 m
Height	2,5 + 2,0 m
Core	
Inner diameter of the vessel	0,39 m
Height	0,5 m
Volume occupied by fuel assembly	51 liters
Fraction of water in the fuel assembly	0,59
Load <sup>235</sup> U (90% enrichment)	27,5 kg
Type of the fuel elements	cross-shape section pins
Specific heat-transfer surface of the fuel elements	6,5 cm /cm <sup>2</sup>
Pitch of triangle grating of the fuel elements	5,23 mm
Primary circuit	
Core input pressure	5 MPa
Core pressure drop	1 MPa
Water flow	to 3000 m <sup>3</sup> /t
Shielding	
D <sub>2</sub> O	1 m
Heterogeneous iron-water shielding	0,55 m
Heavy concrete (p=3,6 g/cm <sup>2</sup> )	0,9 m
Movable shielding	1 m

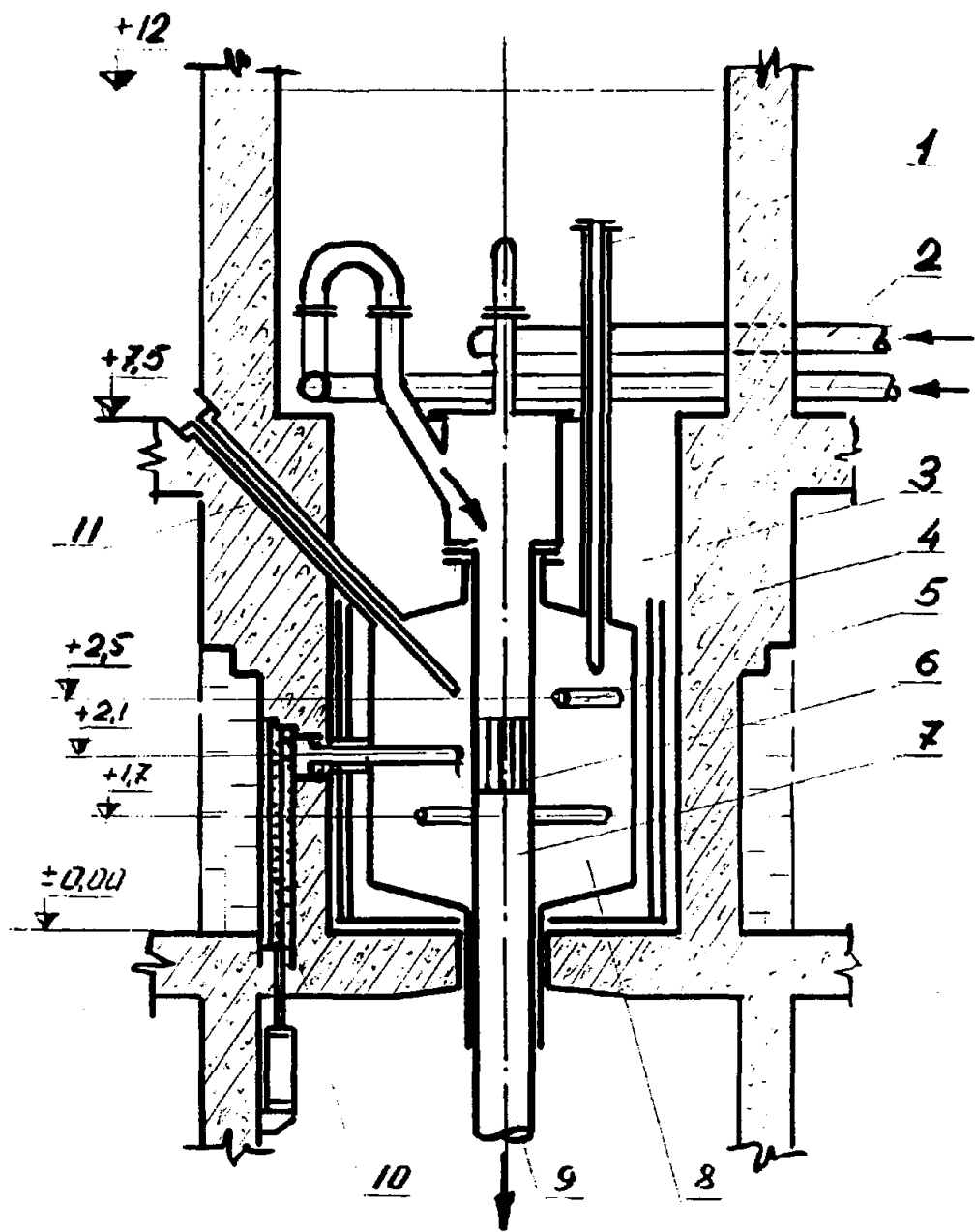


Fig. 1. Schematic vertical section of the PIK reactor.

1 - vertical channel; 2 - coolant inlet; 3 - water pool; 4 - biological shielding; 5 - horizontal experimental beam channel; 6 - core; 7 - replaceable vessel; 8 - heavy water reflector; 9 - coolant outlet; 10 - plug; 11 - inclined experimental beam channel.

Shown on the left are the distances from the floor of the experimental hall in meters.



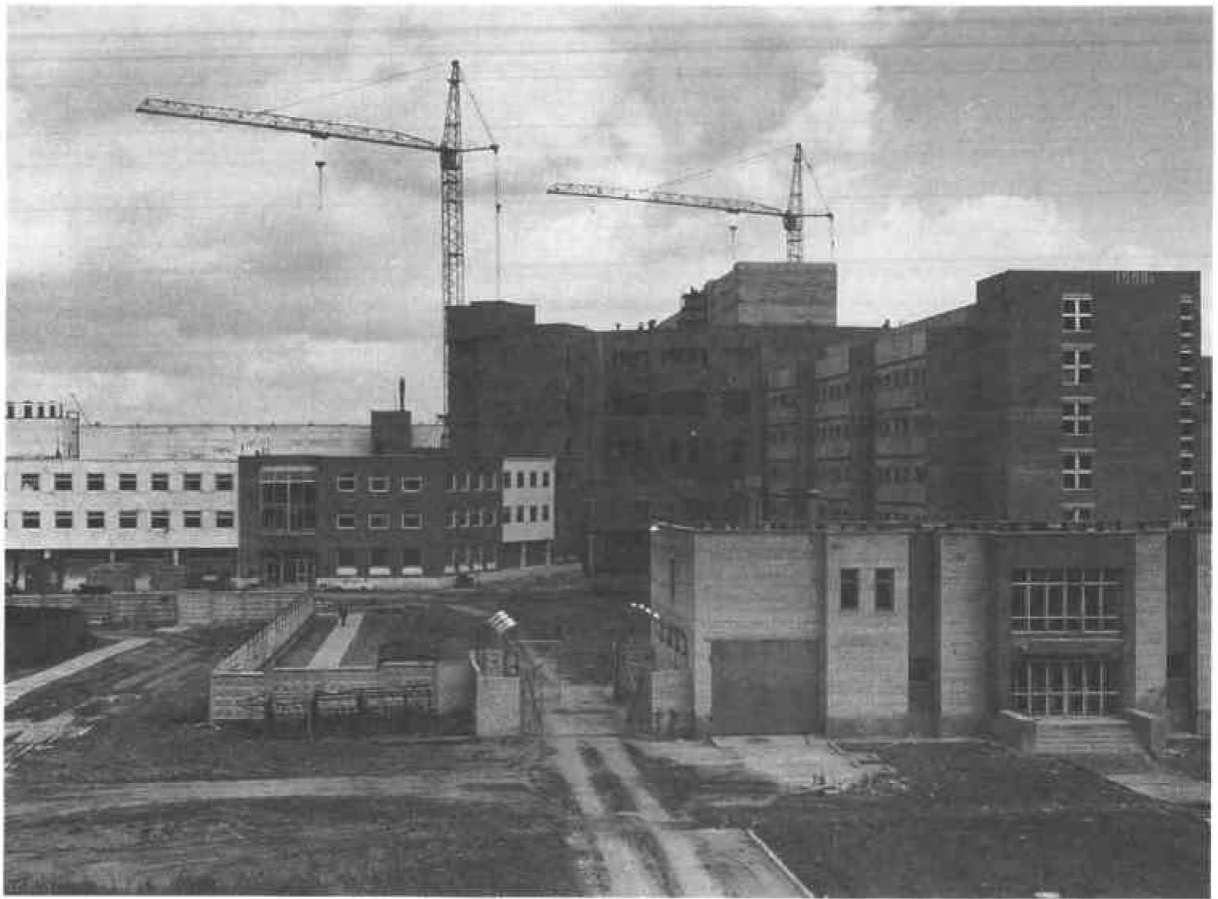


Fig.3. View to PIK reactor complex (1993).



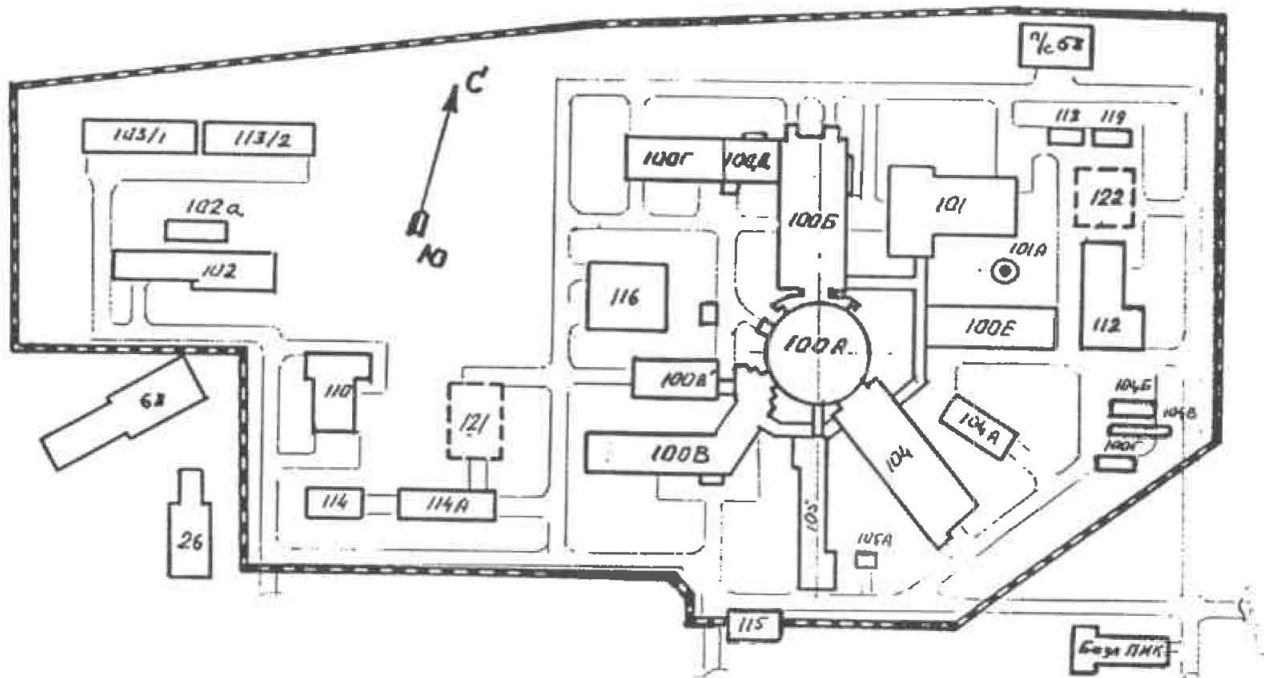
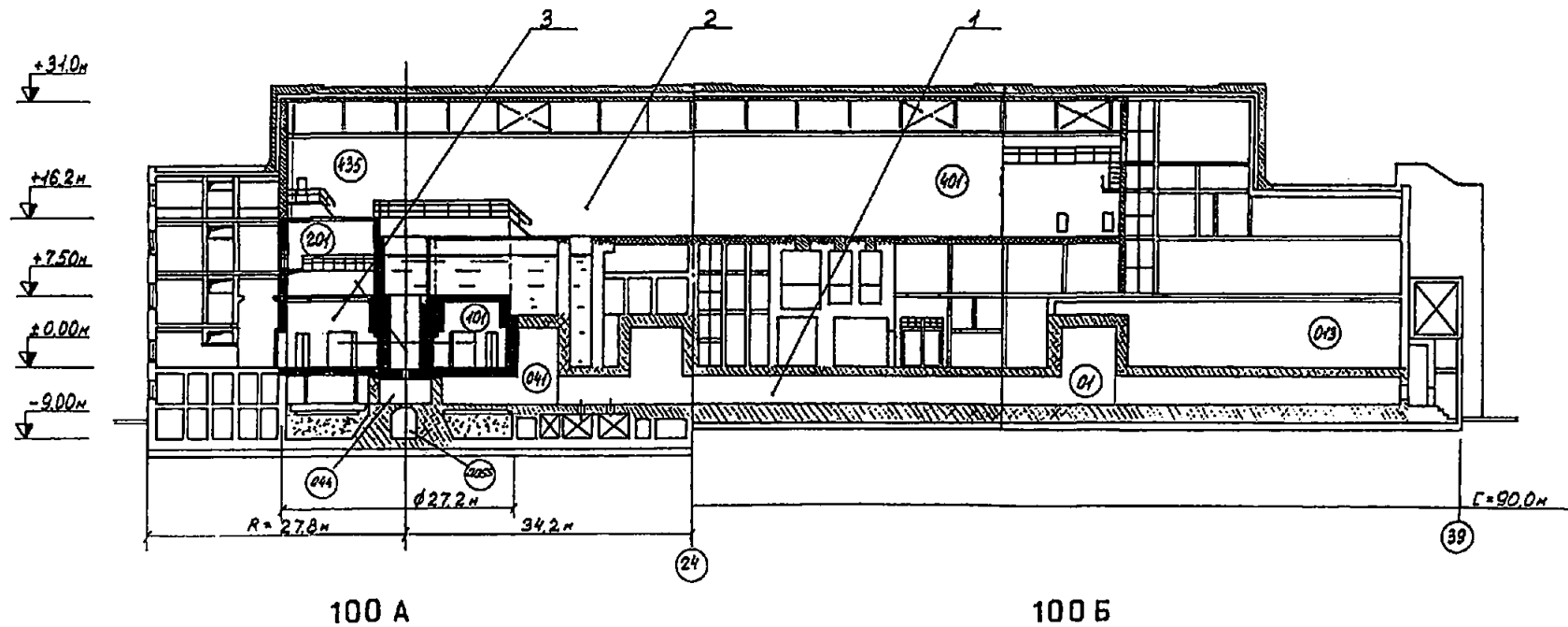


Fig.4. PIK reactor buildings plan.

100A - reactor and laboratories; 100B - disinfection post and ventilation; 100C - pumping block of the intermediate circuit; 100D - energy block; 100E - cryogenic station; 101 - ventilation center; 101A - ventilation stack; 102 - water circulation pumping block; 102A - cold water chamber; 103 (1,2) - water - cooling tower; 104 - neutron guide hall and laboratories; 104 A - technological block; 104B - water circulation pumping block; 104 C - cold water chamber; 105 - physics laboratories; 105 A store-house; 106 - carbon acid block; 110 - compressor block; 112 - isotope purification block; 114 - storehouse; 114 A - storehouse; 115 - guard hall; 116 - emergency diesel power station; 118 - nitrogen station; 121 - operators training simulator; 122 - drain tank for irradiated liquids; 26 - chemical water cleaning; 58 - electric substation; 68 - emergency tank.

*Building 100A and 100B side section  
containments 1, 2 and 3*



*Fig 5*

*Contaiment N°2 cross-section*

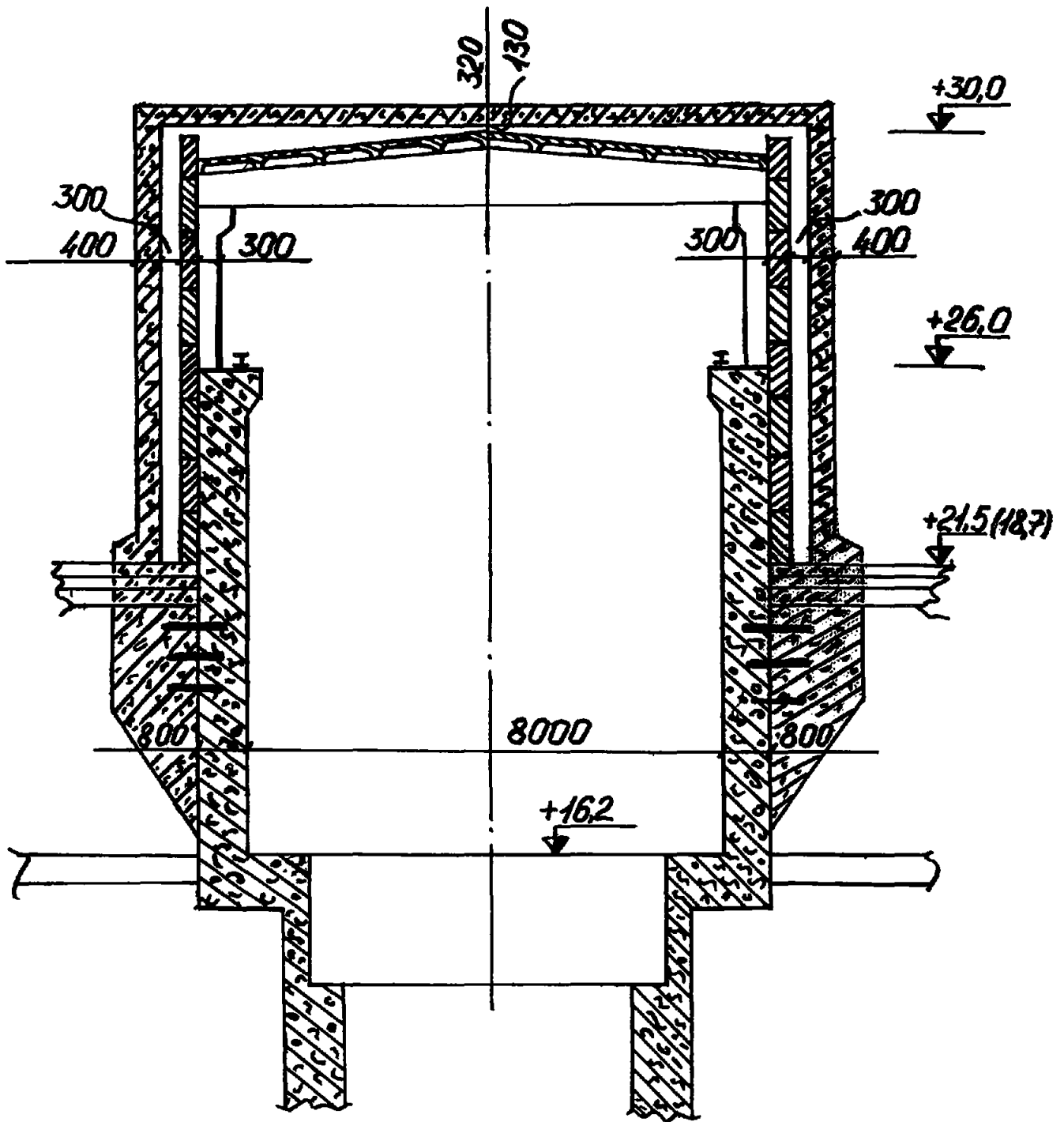
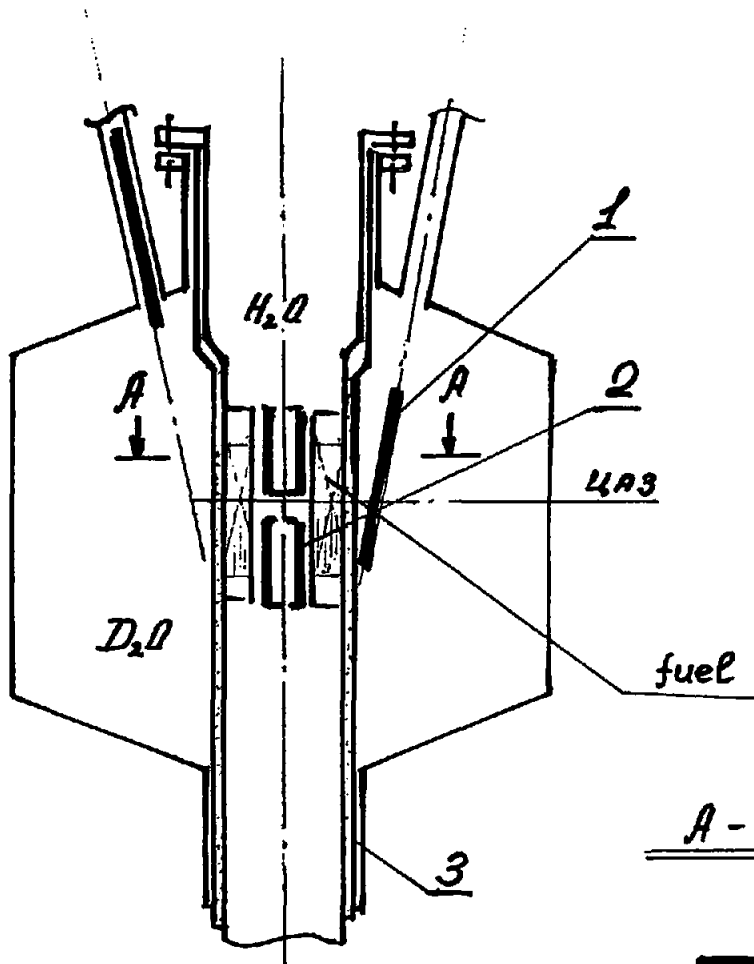


*Fig 6*

# PIK Reactor Control elements.



- 1 Outer blade ( $\text{Eu}_2\text{O}_3$ )  
( $0,66 \pm 0,05$ )  $\beta_{\text{eff}}$ .
- 2 Inner cylinder  
( $9,5 \pm 0,5$ )  $\beta_{\text{eff}}$ .
- 3 Additional slow emergency shut-down.  
Absorbing solution injection in vessel cooling water.

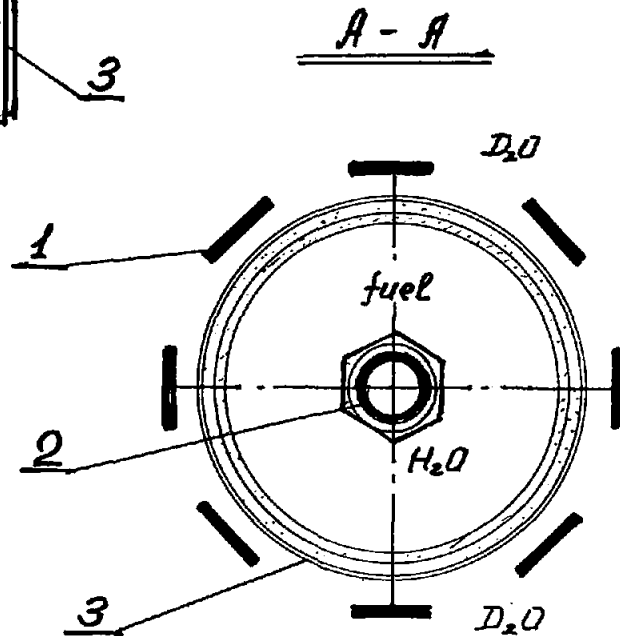
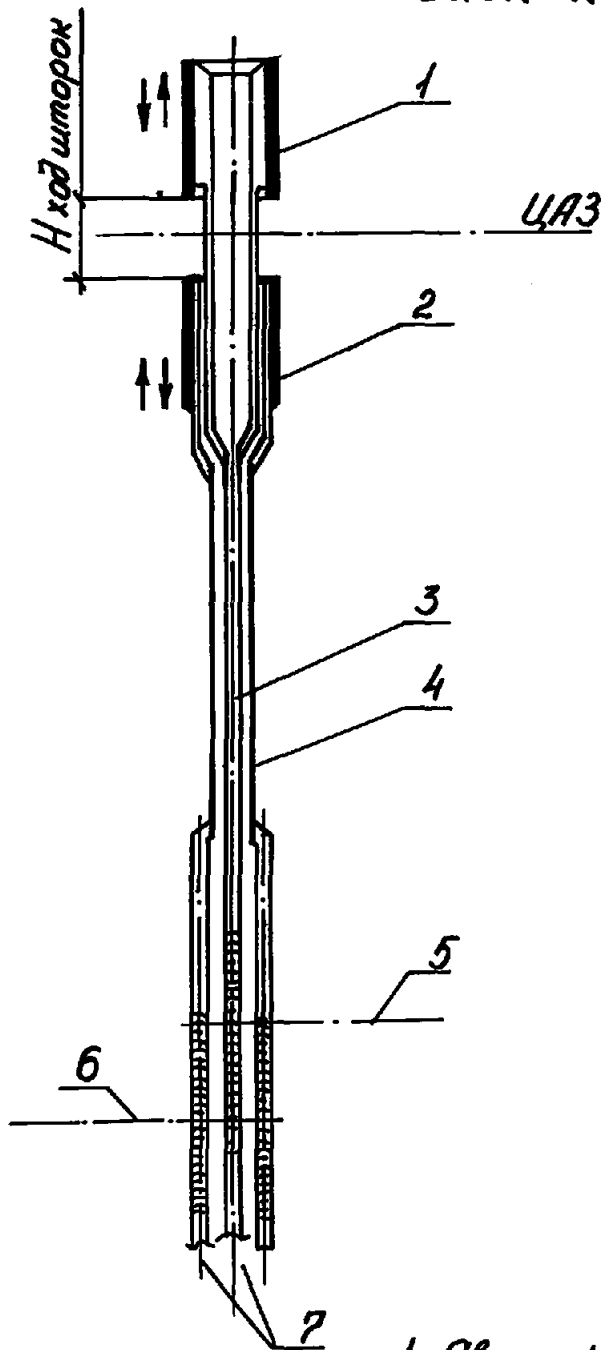


fig. 7

*Individual drive for  
each half of absorption  
cylinder*



- 1-Absorption cylinder upside
- 2- — " — — — downside
- 3,4-Traction tubes
- 5,6-Servo-motors axles
- 7-Rack with brakes

*Fig 8*

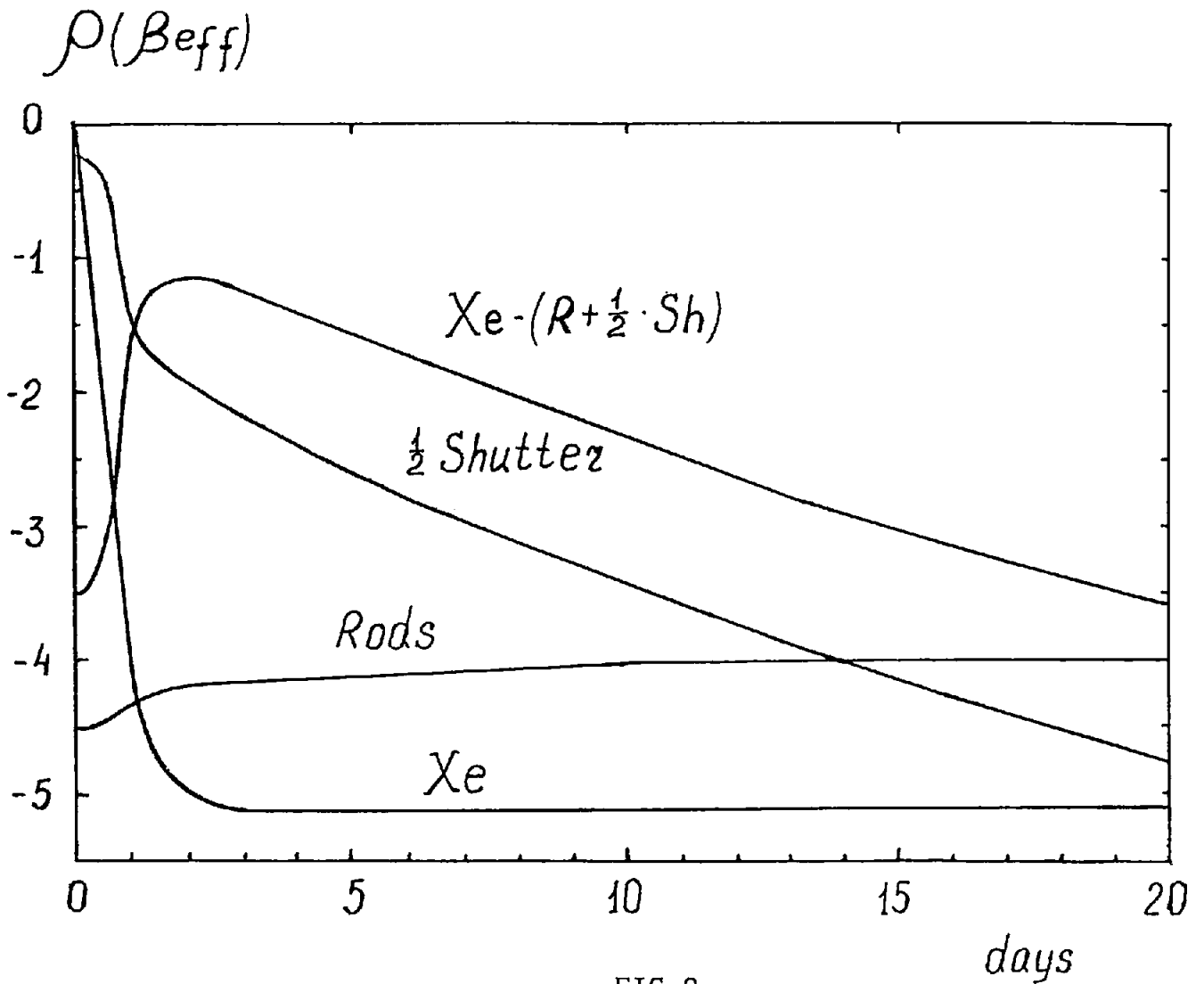


FIG. 9

REACTOR PIK SUBCRITICALITY AFTER IODINE WELL AND  
WHILE 1/2 SHUTTER IS SEIZED IN UPPER POSITION.

# PRESENT STATUS OF PIK GADOLINIUM CONTROL

Petrov Yu.V., Garusov E.A., Shustov V.A.  
 Petersburg Nuclear Physics Institute  
 Gatchina, 188350 St.Petersburg, Russia

**Introduction.** A liquid control element (LCE) containing a water solution of gadolinium nitrate  $Gd(NO_3)_3$  was originally planned for use at the PIK reactor for partial compensation of poisoning and fuel burnup [1-3] (Fig.1). However, a further analysis has shown that quick forcing-out, boiling up or flowing-out of the absorbing solution (though of low probability) can lead to the dangerous prompt overcriticality of the reactor. In the following sections the results of the analysis are presented as well as the upper limit of the reactivity, quick insertion of which still is safe for the reactor.

1. The LCE is shown in Fig.2 [4]. Its normal parameters as well as permissible range of the deviations are given in Table 1. The total amount of the solution in the LCE loop is equal to 1.7 m<sup>3</sup> which includes: 2l is in the sectional gap at the core [5]; 0.28 m<sup>3</sup> is in the 35 m long pipe line after the gap; 0.5 m<sup>3</sup> is in a pressure compensation vessel (PC), 0.45 m<sup>3</sup> is in a heat exchanger (HE) and the rest being in the high pressure branch of the loop.

Though the PIK core has a negative power coefficient of reactivity, the replacement or heating of the LCE lead to positive reactivity, hence such situations must be investigated carefully according to the IAEA safety laws for research reactors [6].

2. The forcing-out of the LCE by the primary coolant can be caused by cracks in the reactor vessel (e.g. in the welding joints). The probability of the break for one of the three welding joints amounts to  $10^{-5}$  within three years, the crack probability is  $10^{-4}$ . As a result of such an accident, the core water (5 MPa pressure) will quickly replace the absorbing solution (pressure  $P_0 = 1.3 - 1.6$  MPa) in the gap. The replacement rate depends on the hydraulic resistance of the crack  $\xi_p$  and its surface  $S_p$ . For a large break cross section (small  $\xi_p/S_p^2$  value), the core pressure will close a check (non-return) valve from the pressure pumps of LCE (RV in Fig.2) and stop the LCE feeding in the gap. The rest of the absorber will be moved to the core in  $\tau_c < 1s$ , and the absorber will go away in  $\tau_r \sim 0.1 - 0.15 s$  (Fig.3). For small cracks, the pressure drop is considerable, the check valves remain open and the absorber will be forced out from the gap by mixture with the primary coolant. The asymptotic value of the inserted positive reactivity is determined

by the difference between the initial and final concentrations of the absorbing solution. The parameters of the new hydraulic and temperature regime of LCE are still in the acceptable region (see Table 1), and the emergency signal will be caused by the power excess only. As seen from Fig.3, the reactivity insertion will be very quick in this case. In a delay time ( $\tau_i \lesssim 1$  s) the asymptotic flow regime will be set up.

In case of the rupture of the reactor vessel at a core level, there is a little time for the asymptotic flow regime to be set up. The moment and the rate of the reactivity insertion are determined by the process of compression of the solution outside the gap, i.e. by the propagation of the acoustic waves. It depends on the initial pressure jump  $\Delta P$ , solution properties (density  $\gamma$ , compressibility  $\beta \equiv (\gamma c^2)^{-1}$ , sound velocity  $c^2 \equiv (\partial P / \partial \gamma)_s$ ) as well as on the hydraulic parameters and the geometry of the loop units. The change of the volume fraction of the absorbing solution  $\psi$  in several damaged sections is described by a balance equation

$$\gamma \frac{V}{S} \frac{\partial \psi}{\partial t} = -\gamma u(o, t) \equiv -G(o, t), \quad (1)$$

where  $V$  is the total volume of the damaged sections, and  $S$  is the cross section area.

The rate of the solution removal  $u(x, t)$  is obtained via the flow  $G$  (see (1)) from the eq. of continuity and Euler's equation (momentum conservation) [7]

$$\frac{\partial \gamma}{\partial t} + \frac{\partial G}{\partial x} = 0; \quad \frac{\partial G}{\partial t} + \frac{\partial G^2}{\gamma x} + \frac{\partial P}{\partial x}, \quad (2)$$

which are solved in a linear approximation (since  $u = G/\gamma \ll c$ ) at the prompt pressure jump in the contour inlet  $\Delta P(o, t) = \Delta P \delta(t)$ . The contour model consisted of two pipes with the same cross section everywhere, connected to a point-like heat exchanger volume. The whole hydraulic resistance was reduced to a flow regulator before the PC. The pressure in the PC (pressure compensator) was considered to be constant and equal to 0.8 MPa. Fig.4 shows the time dependence of the relative velocity  $\omega(o, t) \equiv u(o, t) / \Delta P / \gamma c$  at the pressure jump  $\Delta P$  [8]. Integrating this dependence in eq.(1) over time, one obtains for pressure jumps greater than the pump pressure ( $\Delta P \sim 2 \div 5$  MPa) the result that the gadolinium solution is removed from the damaged sections in a very short time  $\tau_r \sim 0.05 - 0.15$  s.

**3. Boiling-up of the absorbing solution with following forcing-out to the LCE loop by the own vapor is possible (though with low probability) by flow blockage in five or less sections (out of 8 [5]).** Deviations of the controlled parameters will not exceed the acceptable values in this case (see Table 1). The blocked solution will be heated up to the saturation temperature  $T_s$  in a few seconds by the  $\gamma$ -rays and fast neutrons ( $\sim 40 - 50$  W/g  $D_2O$  [9]) as well as by the heat of the environment ( $30 \div 40$  W/g  $D_2O$ ). Insertion of a small positive reactivity caused by heating the solution will be compensated by the automatic control system.



Since the heat transfer to the stopped solution is weak, the vessel temperature will increase considerably (see Fig.5). This will lead to a doubling of the total accumulated energy, increase of the vaporization and to a pressure jump in the gap. This, in turn, will lead to the propagation of acoustic waves in the LCE loop similar to the case of the vessel break. The pressure will relax by removing of the solution. In order to obtain the time dependence of the volume vapor fraction in the blocked sections,  $\varphi(z, t)$ , the system of equations (2) (where  $\gamma \equiv \gamma_e(1 - \varphi) + \gamma_g\varphi$ ,  $\psi + \varphi \equiv 1$ ,  $i = e$  corresponds to the solution,  $i = g$  is to vapour) was solved together with the vapour balance equation, the equations of state in the gap

$$\frac{\partial}{\partial t}(\gamma_g\varphi) + \frac{\partial G_g}{\partial z} = \frac{Q_r(z, t)}{r} \cdot F(\varphi, P, T, \dots); \quad \gamma_i \equiv f_i(P, T) \quad (3)$$

and equations (1) and (2) for the whole loop. The initial conditions are  $\varphi(z, 0) = 0$ ;  $u(z, 0) = 0$ ;  $P(z, 0) = P_0 = 1.25$  MPa. The vapour and solution velocities inside the sections are considered to be the same and equal at the point of blockage to zero. The value of  $Q_r(z, t)$  in eq.(3) is the specific energy yield which is spent to vaporization of the solution

$$Q_r(z, t) = Q_v(z, t) - C_p\gamma_e \left( \frac{\partial T_e}{\partial P} \right) \cdot \frac{\partial P}{\partial t}. \quad (4)$$

Here,  $C_p$  is the specific heat capacity,  $r$  is the specific vaporization heat,  $F(\varphi, P, T)$  is a function which determines the vapour generation and condensation according to the thermodynamic conditions, and  $Q_v(z, t)$  is the total specific energy yield taking into account the heat transfer from the vessel. Since the vessel temperature does not change during the time  $\tau_r$ ,  $Q_v$  may be considered to be constant. With the same accuracy, it is considered to be constant along the height of the core. In this case,  $\varphi(z, t)$  is also independent of  $z$  and equal to the average value in the gap  $\bar{\varphi}(t)$ , while  $F = 1 - \bar{\varphi}$ . If the process in the LCE loop is described via the Green function, its convolution with the variable pressure value in the gap  $P(t)$  transforms eq.(1) to the integrodifferential one with respect to the values  $\bar{\varphi}(t)$  and  $P(t)$ . The second relation for them comes from the solution of the system (2)–(3), which gives the dependence  $P(\bar{\varphi})$  with account to the state equation. The dependencies  $\bar{\varphi}(t)$  in the five blocked sections of the LCE at various assumptions are given in Fig.6.

**4. Reactivity at the total forcing - out of the solution by vapour amounts to about  $3\beta_{eff}$  ( $\beta_{eff} = 0.8$ ).** When 5 sections of 8 are emptied, it is about  $2\beta_{eff}$ . If the absorbing solution is forced out by a primary coolant, the positive reactivity reaches the value  $4\beta_{eff}$ .

The emergency rods begin to influence the situation only after 1.4s. For this reason it is important to determine the limit of the positive reactivity what can be managed by help of the inherent passive reactor safety.

**5. The limits of the inherent safety of the PIK reactor** with respect to the quick insertion of positive reactivity was studied in a series of a thermohydraulic calculations, taking into account the reactor kinetics. In order to obtain the reactor response, the

equations were solved in a point kinetics approximation, which describes compact cores of the research reactors sufficiently well.

The feedback reactivity was calculated taking into account local statistical weights of voids [10,11] is

$$\rho_b = -\bar{\omega} \sum_i^n \bar{\varphi}_i \kappa_i \eta_i, \quad (5)$$

where  $\bar{\omega} = 0.28$  means the void reactivity coefficient,  $\bar{\varphi}_i$  is a node void volume, due to the decrease of water density, thermal expansion of the fuel elements and vaporization of water,  $\kappa_i$  is the statistical weight (the importance) of the given node volume, and  $\eta_i$  is the relative fraction of the node volume. The summation in eq.(5) is performed over all  $n$  nodes of the core (in Fig.7  $n = 15$ ).

The equations of the two phase hydrodynamics for a hot channel include conservation of mass and momentum (eq.(2)); for energy conservation, we write

$$\frac{\partial(\gamma i)}{\partial t} = Q_v - \frac{\partial(Gi)}{\partial z}; \quad \text{with } Q_v = \frac{\alpha F}{V} [T_f - T_e], \quad (6)$$

where  $i$  is enthalpy,  $\alpha$  is heat transfer coefficient from the walls to the water,  $F$  is the surface  $T_f(z)$  is local temperature of the fuel, and  $T_e(z)$  is the local temperature of liquid.

In eq.(2) for the momentum one should keep the nonlinearity and add to the right-hand side a term, taking into account friction:  $-\xi G |G| / 2D\gamma$  ( $D$  is hydraulic diameter,  $\xi$  is dimensionless friction coefficient). One should include also the vapor generation, eq.(3), state equation and the local equations which determine the fuel temperature.

The result of one of the typical calculations taking into account vaporization at the insertion of the reactivity  $\rho_0 = 1\beta_{eff}$  during to 0.4 s is presented in Fig.8. For a running reactor with stationary power 100 MW, the peak of power in 0.3 s exceeds 200 MW (Fig.8a). The vaporization process in the PIK reactor is almost explosive because of the high specific energy yield (up to 10 MW/l at the power peak). As seen from Fig.8c, the vapour content in a hot channel changes by 30% in 15 ms. The vapour arising pushes the solution to both sides, decreasing the flow rate at the channel entrance (and increasing it at the channel outlet). At some instant, the inlet flow rate becomes negative (flow inversion) and the channel drying goes on very fast (Fig. 8d), leading to fuel melting, i.e. to a serious accident. Therefore the absence of flow inversion of the coolant should be the criterion of the reactor safety.

Taking into account a great variety of different processes of low probability leading to a positive reactivity excess, it is reasonable divert from a concrete situation and to form a general safety curve for a variety of values  $[\rho_0, t_0]$  (Fig.9, curve 1). Such a criterion is considerably more strict than that of the absence of the fuel element melting at a fixed flow rate (curve 2). One should note that the calculations were performed for a hat hydraulicity isolated channel. Water admixture from neighbour channels can improve the situation a little.

Conclusions about the use of the LCE can be formed by comparing the reactivity excess arising as a result of the LCE accident (up to  $2 - 4\beta_{eff}$  for a time interval less than 1s) with  $1\beta_{eff}$ , which is tolerable according to the safety curve (curve 1, Fig.9). On the base of this analysis it was decided not to use the LCE for the PIK reactor control. It can be used probably for the partial compensation of the reactivity excess after the  $^{135}\text{Xe}$  decay at the stopped reactor.

#### Acknowledgement

One of the authors (Yu.P.) is greatly indebted to Dr. Sh.Matsura (JAERI) and Prof. K.Nagamine (RIKEN) for the generous invitation to Naka-machi. The revision of the english manuscript by F.M.Wagner (Reactorstation Garching) is gratefully acknowledged.

Table 1.

$D_n$	Parameter to be controlled	Magnitude	
		Nominal	Accident value
$D_1$	Outlet temperature, °C	60	90
$D_2$	Pressure in PC (MPa)	0.8	> 1.0 < 0.5
$D_3$	Solution level in the PC (mm)	700	500
$D_4$	Flow rate in the LCE loop (l/s)	15.3	12.2
$D_5$	Pressure at the gap entrance (MPa)	1.6	> 1.9 < 1.3
$D_6$	Pressure difference between the primary cooling system and LCE (MPa)	3.7	> 4.0 < 3.4

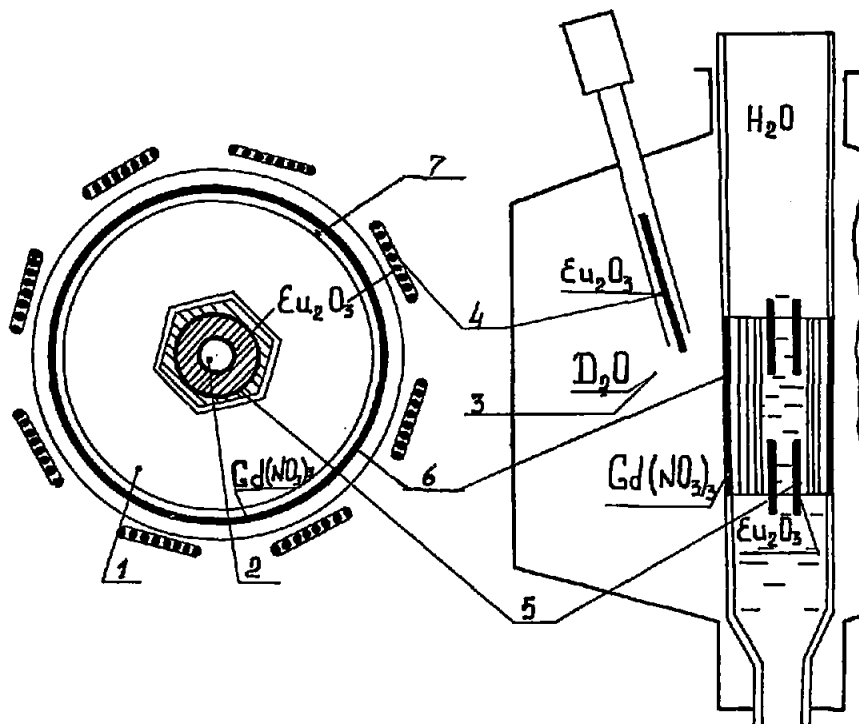


Fig.1. Scheme of the control of the PIK reactor [2].  
 1 core; 2 central experimental channel; 3 heavy water reflector; 4 emergency rod;  
 5 automatic control blind; 6 liquid control element (LCE); 7 reactor vessel.

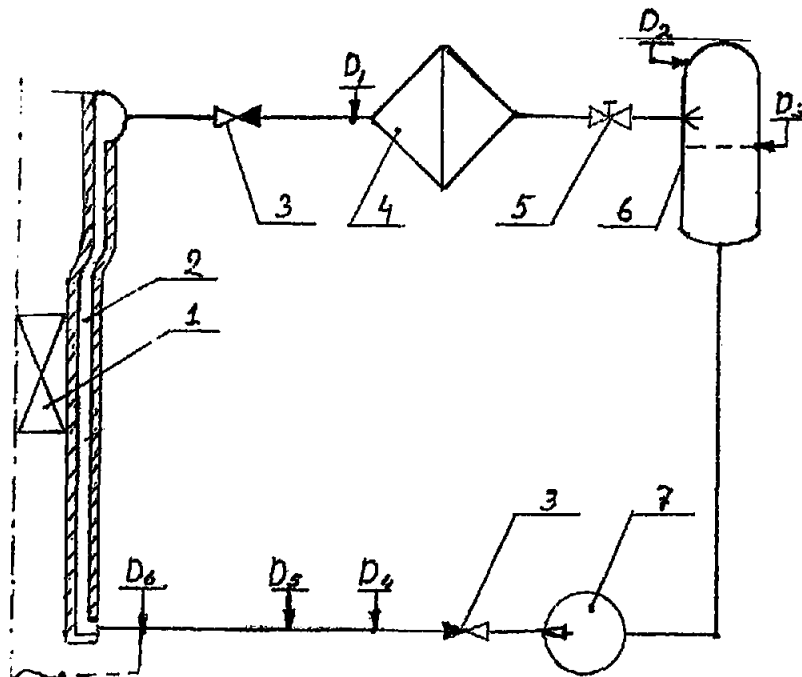


Fig.2. LCE loop [4]  
 1 core; 2 gap with absorber; 3 a check valve (CV); 4 heat exchanger (HE); 5  
 flow rate regulator; 6 pressure compensator (PC); 7 centrifugal pump (CP);  $D_k$  are  
 the control points of the LCE loop parameters, giving a signal to the emergency control  
 rods (see Table 1).

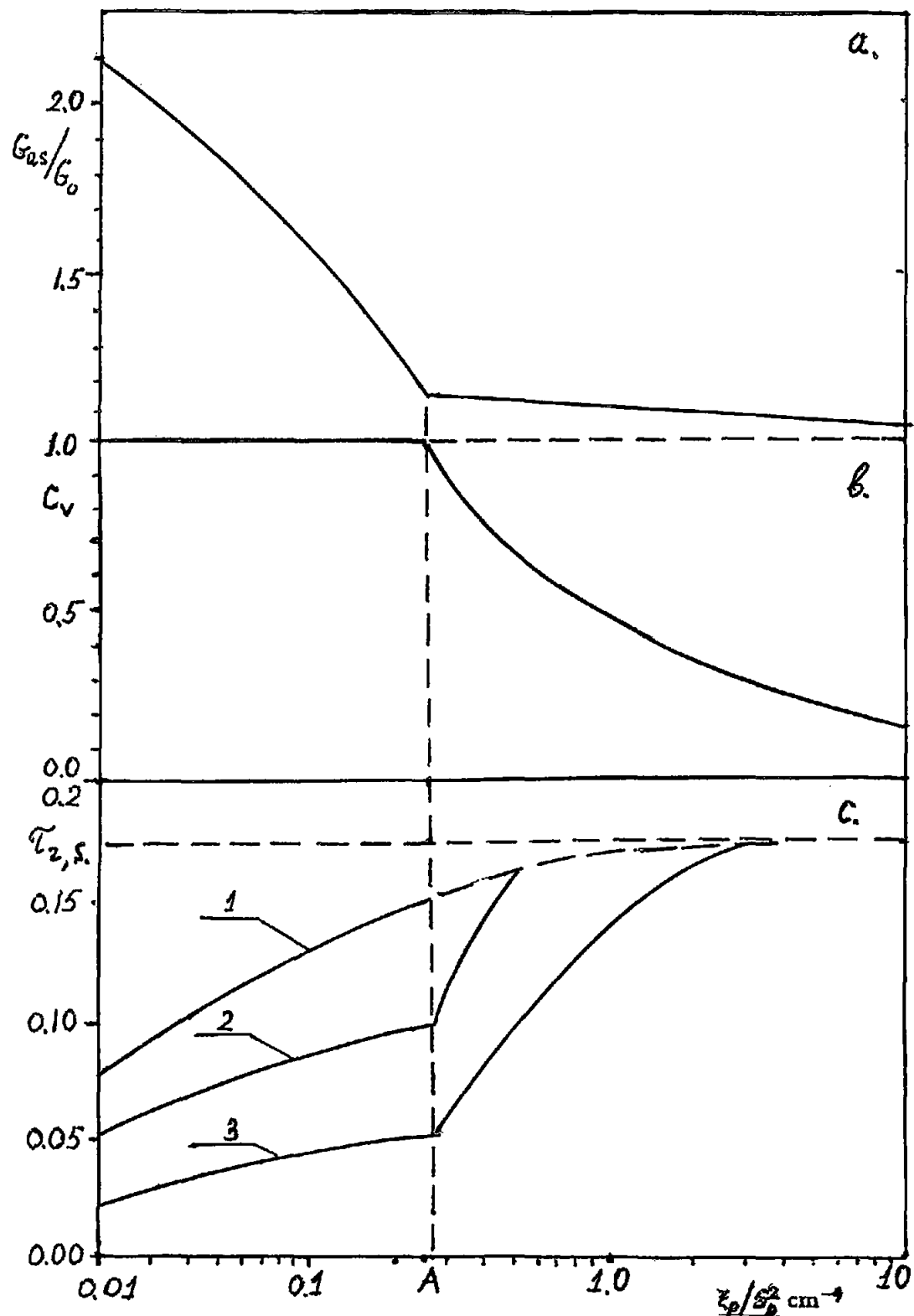


Fig.3. Forcing out of the LCE solution due to the breakdown of the vessel welding joints under the core. Dependencies on the effective hydraulic resistance of the crack  $\xi_p/S_p^2$  cm<sup>-1</sup>: a) asymptotic flow rate; b) volume fraction of the primary coolant in the LCE ( $C_V = G_p/G_{as}$ ); c) removal duration  $\tau_r$  of the volume fraction of the LCE: 1  $C_V = 1$ ; 2  $C_V = 0.67$ ; 3  $C_V = 0.3$ . The bending point A at the curves corresponds to the instant opening of the CV.

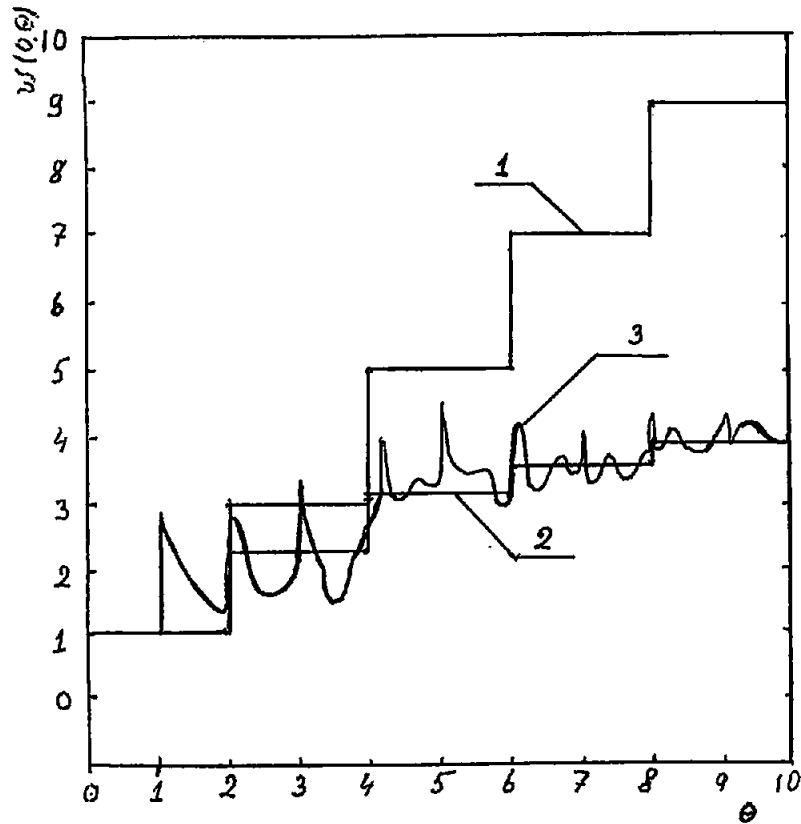


Fig.4. Relative velocity of the solution at the entrance of the LCE:  $w(0, \theta) \equiv u(0, \theta)/\Delta P/\gamma c$  versus relative time  $\theta \equiv ct/L$  for various loop models ( $L/c = 23$  ms)  
 1 a pipe without friction; 2 pipe with friction; 3 pipe with friction and heat exchanger.

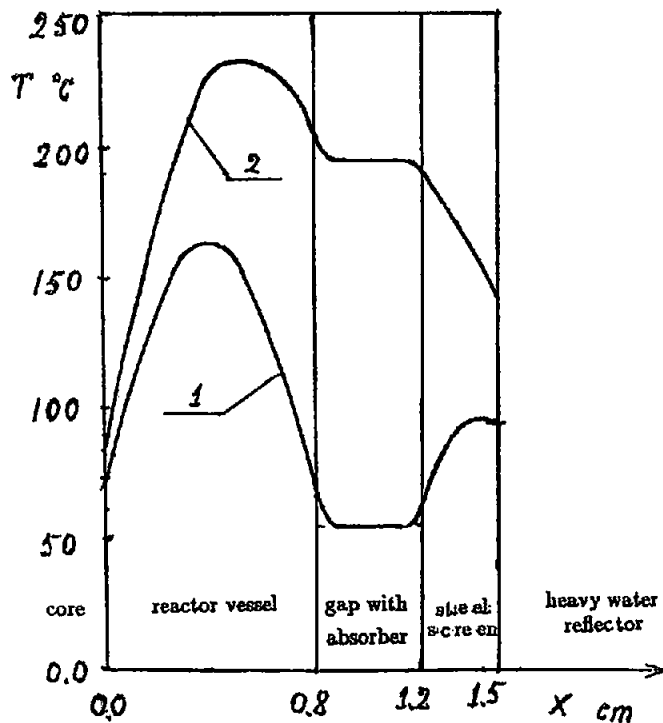


Fig.5. Spatial temperature distribution in a gap of the LCE loop and environment at a central plane of a core.  
 1 stationary state of the reactor at 100 MW; 2 start of the volume vaporization in the LCE loop.

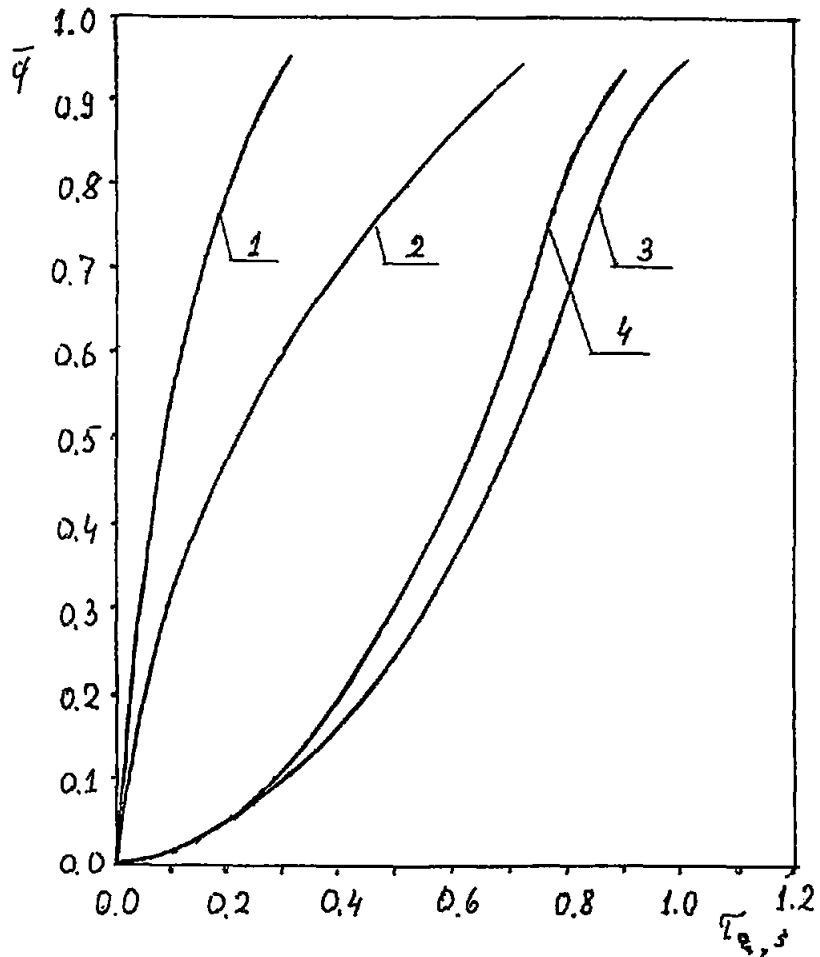


Fig.6. Volume fraction of the absorber vapour in the LCE  $\bar{\varphi}$  versus duration time of solution removing  $\tau_s$ ; initial pressure is 1.25 MPa:

1 without vapour outlet from the gap to the loop,  $T_s = const$ ; 2 with vapour outlet,  $T_s = const$ ; 3 with vapour outlet,  $T_s(P)$ ; 4 increase of the reactor power is taken into account.

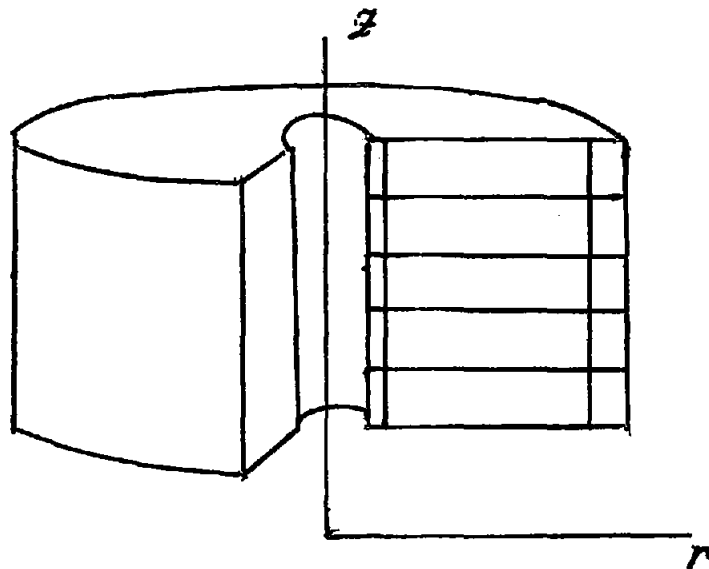


Fig.7. Core dividing to nodes.

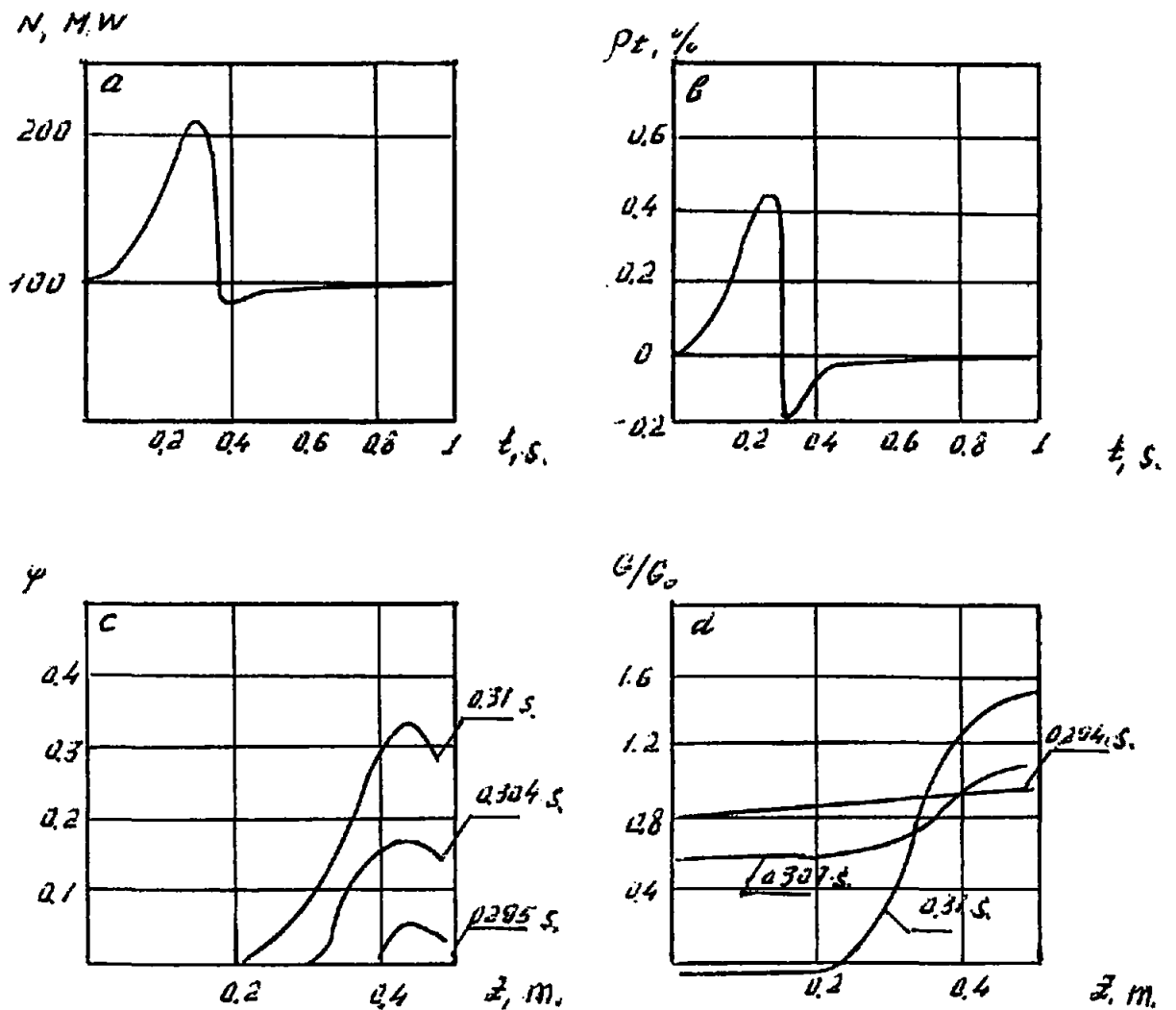


Fig.8. PIK reactor response to the reactivity insertion  $\rho_0 = 0.8\%$  during  $t_0 = 0.4s$  ( $K_V = 2.8$ ;  $G_0 = 10^4 \text{ kg/m}^2\text{s}$ ).  
a a reactor power  $N$ ; b total reactivity  $\rho_t$  including the reactivity of feedback;  
c volume vapour content  $\varphi$ ; d relative flow rate  $G/G_0$ .



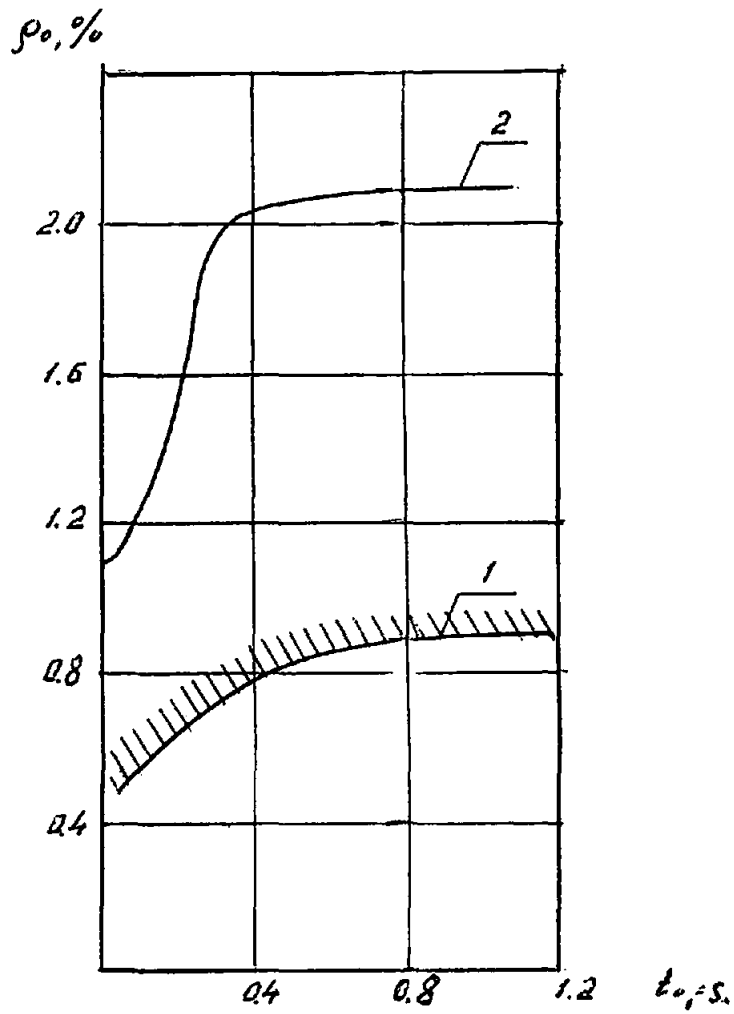


Fig.9. Safety curves for the PIK reactor.  $\rho$  amplitude of the reactivity inserted;  $t_0$ ; insertion duration.  
 1 with flow rate  $G$  determined by the hydrodynamic equations ( $K_V = 2.8$ ); 2 with constant flow rate  $G = 10^4$  kg/m<sup>2</sup>s ( $K_V = 3$ )

## References

- [1] Erykaiov A.N., Kondurov I.A., Konoplev K.A., Krasotsky Z.K., Petrov Yu.V., Sumbaev O.I., Trunov V.A. Research feasibility of the PIK reactor. Preprint LNPI - 852, Leningrad, 1985, 25 p.
- [2] Erykaiov A.N., Kirsanov G.A., Kolesnichenko O.A., Konoplev K.A., Petrov Yu.V., Shustov V.A. Some aspects of the safety of the high flux research PIK reactor. AECL - 9926, (1990), v.2, p.689 - 708.
- [3] Petrov Yu.V. Reactor PIK. IGOR-2 - Meeting Saclay, France, May 18 - 19, 1992.
- [4] Gausha V.D., Konoplev K.A., Mashchetov V.P., Orlov S.P. LNPI Applied Research Report, Leningrad, 1988, p. 160 - 161.
- [5] Abramkov E.L., Avaev V.N., Bolshakov V.V., Vasil'ev G.Ya. et al. Radiation characteristics of the PIK reactor. Preprint LNPI - 1471, Leningrad, 1988, 28 p. (in Russian).
- [6] Research reactor safety, N 35-S1, Stj/Pub/927, IAEA, Vienna, 1992, 54 p.
- [7] Landau L.D., Lifshitz E.M. Hydrodynamic, M., "Science", 1988, 733 p.
- [8] Garusov E.A., Grachev S.D., Petrov Yu.V. Nuclear danger of strongly poisoned fluids in reactor core. Preprint PNPI - 1871, TH-2-1993, (Uatchina, 54 p. (in Russian).
- [9] Garusov E.A., Petrov Yu.V. Radiation energy release in the PIK reactor vessel. Reactors Physics and Technology. Proceedings of LNPI Winter School, Leningrad, 1986, p.116 - 140 (in Russian).
- [10] Dyck G.R., Shustov V.A. Reactor Kinetic Models: one and a few points approach. Preprint LNPI - 1612, Leningrad, 1990, 29 p. (in Russian).
- [11] Petrov Yu.V., Sakhnovsky E.G. Reactor kinetics equations with nonlinear temperature dependent feedback. Atomic Energy (Russian) 71(4), 1991, p.298 - 303.

## Core Thermal Hydraulic Tests for ANS

M. Kaminaga

Japan Atomic Energy Research Institute  
Tokai-mura, Naka-gun, Ibaraki-ken, 319-11, Japan

M. Siman-Tov

D.K. Felde

G.L. Yoder

C.D. West

Oak Ridge National Laboratory  
P.O.Box 2009  
Oak Ridge, TN 37831-8045, U.S.A.

## ABSTRACT

The Advanced Neutron Source Reactor (ANSR) is currently being developed by the Oak Ridge National Laboratory (ORNL) to become the world's highest-flux, steady-state, thermal neutron source for measurements and experiments in fields such as materials science and engineering, biology, chemistry and nuclear science. The ANSR is both cooled and moderated by heavy water and uses highly enriched uranium silicide fuel. The core has average and peak heat fluxes of 5.9 and 12 MW/m<sup>2</sup>, respectively. Highly subcooled, heavy-water coolant flows vertically upward at a velocity of 25 m/s through parallel aluminum fuel-plates. In this configuration, both flow excursion (FE) and critical heat flux (CHF) represent potential thermal limitations. The availability of existing experimental data for both FE and CHF at the conditions applicable to the ANSR is very limited. A Thermal Hydraulic Test Loop facility was designed and built to simulate a full-length coolant subchannel of the core, allowing experimental determination of both thermal limits under the expected ANSR thermal-hydraulic conditions.

A series of FE tests with light water flowing vertically upward was completed over a nominal heat flux range of 6-14 MW/m<sup>2</sup> and a corresponding velocity range of 8-21 m/s. Both the exit pressure (1.7 MPa) and inlet temperature (45 °C) were maintained constant during these tests, while the loop was operated in a "stiff" (constant flow) mode.

To the authors' knowledge, no other FE data have been reported in the literature that cover the range and combination of conditions reported in this paper. Experimental work is currently proceeding to higher heat fluxes and coolant velocities. Final correlation of the FE data is postponed until the remainder of the experiments are performed.

## INTRODUCTION

The Advanced Neutron Source (ANS) is a state-of-the-art research reactor facility to be built at the Oak Ridge National Laboratory (ORNL) and is designed to become the world's most advanced thermal neutron flux source for scientific experiments. The core of the ANS reactor (ANSR) must therefore be designed to accommodate very high power densities using a very high coolant mass flux and subcooling level. The ANSR is both cooled and moderated by heavy water, and uses highly enriched uranium silicide fuel. The core is composed of two concentric annular core halves, each shifted axially and radially with respect to the other. Fig.1 shows the core configuration and the fuel plate arrangement. There are 684 parallel aluminum clad fuel plates (252 comprise the inner-lower core and 432 comprise the outer-upper core), each 1.27 mm thick, arranged in an involute geometry which effectively creates an array of thin rectangular channels. The coolant channels have a 1.27 mm gap width, spans of 87 mm (lower core) and 70 mm (upper core), and a 507 mm heated length. Each fuel plate has 10 mm unheated leading and trailing edges with all the channels having common inlet and outlet plenums with common nominal pressure of 3.2 and 1.7 MPa, respectively. The coolant flows vertically upward at an inlet velocity of 25 m/s. The inlet and average outlet temperatures are 45 °C and 85 °C, respectively. The average heat flux is 5.9 MW/m<sup>2</sup> with a radial and axial maximum of 12 MW/m<sup>2</sup>. The ANSR thermal-hydraulic (T/H) operating conditions can be classified as having high subcooling, high flow, very high heat flux, a narrow channel gap, a very high length to diameter ratio, and moderate pressure. The ANSR core configuration with multiparallel-channels is subject to a potential excursive instability, called flow excursion (FE), and is distinguished from a true critical heat flux (CHF) which would occur at a fixed channel flow rate. The correlations currently used in the ANSR T/H analysis are discussed by Siman-Tov et al.[1].

A Thermal Hydraulic Test Loop (THTL) was designed and built to provide known T/H conditions to a simulated full-length coolant subchannel of the ANS reactor core, allowing experimental determination of both FE and CHF thermal limit under the expected ANSR T/H conditions. Determination of these two thermal limits and the relationship between them is the main objective of the THTL facility. However, the facility is also designed to examine other T/H phenomena, including onset of incipient boiling, single-phase heat transfer coefficients and friction factors, and two-phase heat transfer and pressure drop characteristics.

Although the facility's primary aim is to develop the T/H correlations at the ANSR nominal conditions for normal operation and safety margin analysis, tests will also be

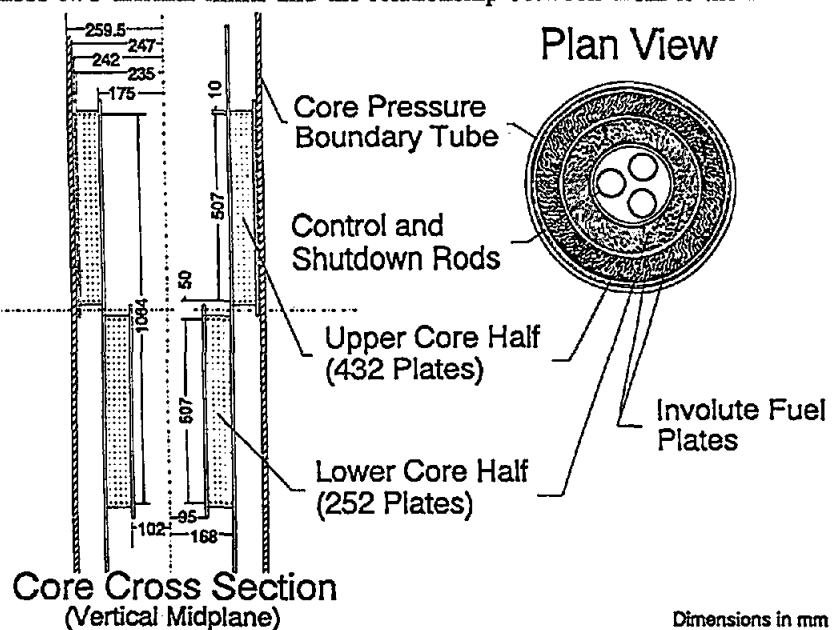


Fig. 1 ANS core assembly and fuel plates arrangements

conducted that are representative of decay heat levels at both high pressure (e.g., loss of off-site power) and low pressure [e.g., a loss of coolant accident (LOCA)] as well as other quasi-equilibrium conditions encountered during transient scenarios. This paper will present the initial experiments focused on the FE phenomena at ANS nominal conditions as well as a few true CHF experiments for comparison.

## DESCRIPTION OF THE THTL FACILITY AND THE TEST SECTION USED IN THE THTL

An isometric view of the THTL facility is shown in Fig.2 and a schematic diagram of the loop and its major components and instrumentation is presented in Fig.3 [2]. In the design process, special consideration was given to include the proper pump, test section bypass configuration, and system valving and piping, allowing operation of the system in either a "stiff" mode for true CHF experiments (actual primary burnout) and FE experiments with no actual burnout, or in a "soft" mode for true FE experiments (with actual secondary burnout). The Moyno primary circulation pump is driven by a variable speed motor through a gear drive. Using the variable speed of the motor drive provides capability for operating over most of the flow-pressure diagram up to  $2.5 \times 10^{-3}$  m<sup>3</sup>/s flow and 4.1 MPa differential pressure across the pump at 750 rpm. In combination with the test section bypass line, a very wide range of mass flow conditions at the test section is possible. In the "stiff" mode, with a closed bypass, a near-constant test section mass flux in the range of 7 to 42 Mg/m<sup>2</sup>s can be used (the maximum mass flux being limited by the test loop overall pressure rating). In the "soft" mode, with a bypass flow ratio of 10 to 1, a maximum mass flux of 12 Mg/m<sup>2</sup>s at a near-constant bypass pressure drop can be used. At a 5 to 1 bypass flow ratio, this maximum increases to 23 Mg/m<sup>2</sup>s.

Fig.4 shows the cross-section of the test section used in the THTL experiments. The cross-

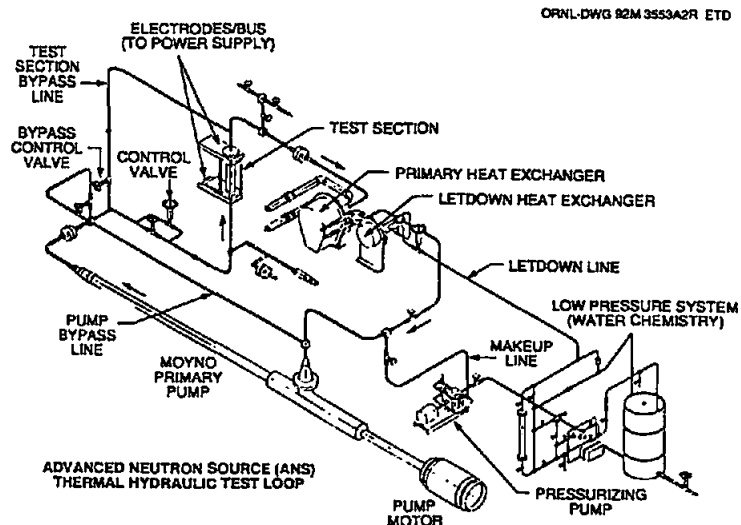


Fig. 2 ANS Thermal Hydraulic Test Loop

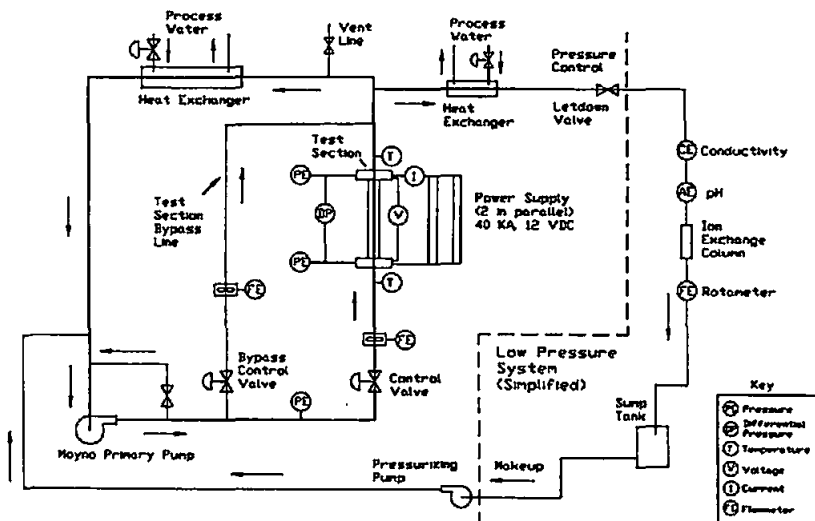


Fig.3 Schematic diagram of the THTL primary components and instrumentation

section design was similar to that used by Gambill and Bundy [3] but is modified in accordance with the ANS characteristics as shown in Fig.4. The test section simulates a single subchannel in the ANS reactor core with a cross section that has a full length (507 mm), the same flow gap (1.27 mm), the same material (aluminum). The channel span was scaled down to 12.7 mm (87 mm and 70 mm for the upper and lower core halves in the ANSR) in order to limit total power requirements to the test section. The involute shape of the plates was not simulated. The test section wall thickness at the flat portion of the test channel (Rectangular channel) is 2.54 mm. The reduced wall thickness at the curved ends is designed to reduce the heat flux and prevent the coolant bulk temperature from peaking on the curved ends of the channel (Semicircular channel) which could lead to premature burnout. The ratio of heat flux on the curved ends to that on the flats for the design shown in Fig.4 is about 36 %. The flow channel gap is measured at locations along the axial length using a capacitance-type probe inserted into the channel. This data is

- 1.27 x 12.7 mm coolant channel
- Full length = 507 mm
- Directly heated using dc current

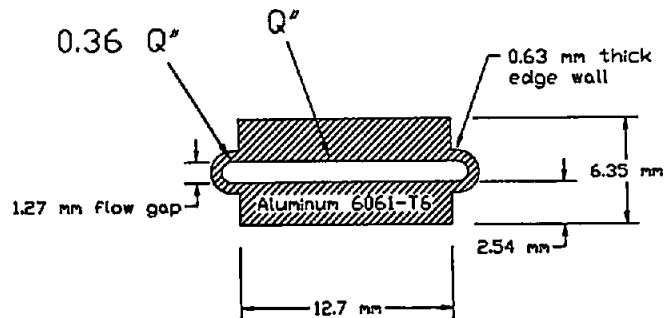


Fig. 4 Cross-section of the test channel in the THTL

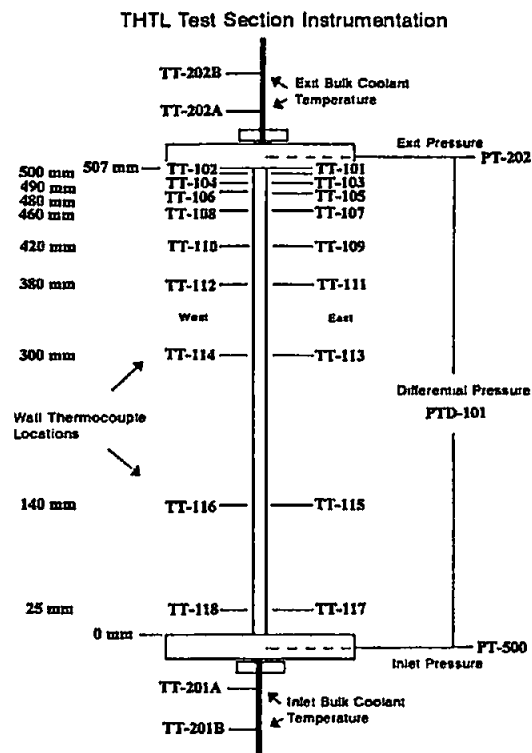


Fig.5 THTL test section instrumentation

used to provide improved conversion of volumetric flow measurements to local velocities in the channel. The test channel is instrumented on the back of the channel wall with type N thermocouples. The location of these thermocouples on the test section are shown in Fig.5. Measurements are made on both sides of the channel for the axial locations shown in Fig.5 for redundancy. Pressure and temperature of the water are measured at the test section inlet and outlet with the pressure taps installed in the test section flanges as shown in Fig.5. The taps are located axially 12.7 mm from the "heated" channel at each end allowing a closer determination of the pressure-drop across the heated region. The test channel is enclosed inside a stainless pressure backing and is isolated thermally and electrically from this backing by Micalex insulation. The test channel is either welded or brazed on both ends into aluminum flanges, each 2.54 cm thick. The test section flanges are sandwiched between two 2.54 cm thick aluminum electrical bus plates.

## RESULTS AND DISCUSSION

The THTL experimentation for the ANSR T/H correlations is still in its initial stages. The current THTL (Figs. 2 & 3) and test section design (Figs. 4 & 5) are the result of a number of initial shakedown and benchmark tests, which led to successive modifications both in the loop and the test section design. The initial emphasis was placed on the FE phenomena at nominal conditions. The first goal was to proceed from low levels of heat flux and velocity and then extend the tests to the extremely high heat flux levels required by the ANSR operating conditions. The experiments completed so far include the following T/H conditions [4]:

- coolant: water,
- inlet coolant temperature: 45 °C,
- exit coolant pressure: 1.7 MPa,
- nominal average heat flux range: 6-14 MW/m<sup>2</sup> (goal is 17 MW/m<sup>2</sup>),
- corresponding velocity range: 8-21 m/s (goal is 27 m/s), and
- channel configuration (Figs. 4 and 5): 1.27 x 12.7 x 507 mm (rectangular).

A nonpowered data set of pressure-drop measurements across the test section as a function of velocity was made before powered operation and repeated after every few runs in the test sequence. The nonpowered data set serves as a reference for the modeled single-phase pressure drop under isothermal conditions. Intermittent repetition of the nonpowered operation also effectively monitors any possible accumulated channel geometry changes from previous powered operation(s). The heat fluxes covered so far include the nominal values of 6, 9, 11, 12, 13, and 14 MW/m<sup>2</sup>, with the resulting respective average velocities of 8.3, 12.9, 17.1, 17.8, 19.3, and 21.0 m/s, are determined at the point of minimum pressure drop. Acquiring FE data at this level of heat fluxes and velocities is of significance for two reasons. First, to the authors' knowledge, no data is available for velocities higher than 10 m/s [5-7], except those reported by Waters [8] at 16 m/s in experiments supporting the Advanced Test Reactor (ATR). Second, the heat flux achieved is beyond the ANS nominal peak heat flux of 12 MW/m<sup>2</sup>. The corresponding limiting velocity of 17.8 m/s is well below the ANS nominal velocity of 25 m/s; even at the highest local heat flux tested (14 MW/m<sup>2</sup> nominal and 16.1 MW/m<sup>2</sup> at the exit), the corresponding velocity of 21.0 m/s is well below the ANSR nominal operating velocities. This implies, on a

Table 1 Results summary of flow excursion test in the THTL<sup>a)</sup>

Test Case	Date	Q <sup>b)</sup> (MW/m <sup>2</sup> )		V <sub>o</sub> <sup>c)</sup> (m/s)	ΔP <sub>min</sub> <sup>d)</sup> (MPa)	P <sub>exit</sub> <sup>e)</sup> (MPa)	T <sub>bulk</sub> <sup>f)</sup> (°C)	Q <sub>loss</sub> <sup>g)</sup> (%)
		Q <sub>av</sub> <sup>h)</sup>	Q <sub>exit</sub> <sup>i)</sup>					
FEB17A	08/17/92	No power		N/A <sup>j)</sup>	N/A	N/A	N/A	N/A
FE903A	09/03/92	No power		N/A	N/A	N/A	N/A	N/A
FEN17A	11/17/92	No power		N/A	N/A	N/A	N/A	N/A
FEN17D	11/17/92	No power		N/A	N/A	N/A	N/A	N/A
FEN19A	11/19/92	No power		N/A	N/A	N/A	N/A	N/A
FEN20C	11/20/92	No power		N/A	N/A	N/A	N/A	N/A
FEN30B	11/30/92	No power		N/A	N/A	N/A	N/A	N/A
FED15A	12/15/92	No power		N/A	N/A	N/A	N/A	N/A
FED17B	12/17/92	No power		N/A	N/A	N/A	N/A	N/A
FED28A	12/28/92	No power		N/A	N/A	N/A	N/A	N/A
FEB17C	08/17/92	6.2-5.7	6.7-6.0	8.3	0.110	1.653	182.5	6.8
FE904A	09/04/92	6.4-5.8	6.9-6.4	8.4	0.147	1.670	190.1	4.3
FE904B	09/04/92	9.6-8.8	10.4-9.7	12.9	0.307	1.617	188.0	4.2
FEN17B	11/17/92	9.3-7.6	9.9-7.9	12.9	0.297	1.728	182.5	7.6
FE904C	09/04/92	11.8-11.1	13.0-12.2	17.1	0.456	1.571	178.3	3.5
FE904D	09/04/92	12.9-12.4	14.5-14.1	18.1	0.545	1.530	182.3	3.3
FEN17C	11/17/92	12.5-10.6	13.5-11.3	18.0	0.310	1.705	178.1	6.4
FED15B	12/15/92	12.7-11.6	13.7-13.0	17.6	0.547	1.718	181.9	5.5
FEN20A	11/20/92	13.7-12.0	15.1-13.6	19.6	0.607	1.739	178.6	6.3
FED15C	12/15/92	13.8-13.0	14.9-14.7	19.2	0.634	1.733	181.3	5.1
FEN20B	11/20/92	14.9-13.7	16.7-16.0	21.1	0.744	1.728	180.0	4.8
FEN30A	11/30/92	14.9-13.6	16.6-15.8	21.1	0.757	1.725	180.7	4.6
FED17A	12/17/92	14.6-14.4	16.3-16.1	21.2	0.750	1.701	176.8	6.1
FED28B	12/28/92	14.8-14.6	15.5-15.5	20.6	0.768	1.738	181.1	5.5

a) In all cases P<sub>exit</sub> = 1.7 MPa and T<sub>in</sub> = 45 °C.

b) Q<sup>b)</sup> - heat flux.

c) Q<sub>av</sub><sup>h)</sup> - average nominal heat flux (range reflects uncertainty).

d) Q<sub>exit</sub><sup>i)</sup> - local heat flux at the exit (range reflects uncertainty, see Fig. 7).

e) V<sub>o</sub><sup>c)</sup> - value at the minimum pressure drop point.

f) ΔP<sub>min</sub><sup>d)</sup> - pressure drop at the minimum pressure drop point.

g) P<sub>exit</sub><sup>e)</sup> - exit pressure at the minimum pressure drop point.

h) T<sub>bulk</sub><sup>f)</sup> - bulk coolant temperature at the exit.

i) Q<sub>loss</sub><sup>g)</sup> - heat losses from the test section.

j) N/A - not applicable.

preliminary basis, that a good margin exists in the ANSR operating velocity.

The actual data from the sequences performed for each case on decreasing velocity are summarized in Table 1 and in Fig. 6, including a nonpowered case. It is worth emphasizing that the heat fluxes indicated for each curve are nominal average values. The actual local heat fluxes close to the exit (where the FE phenomena is supposed to start), taking into account in a preliminary way internal axial and lateral heat redistribution, are indicated in Table 1 as the  $Q_{ex}^*$  values, which

are at the exit higher than the average in all cases as a result of the aluminum resistivity change with temperature. For example, the local heat flux at the exit corresponding to the 14 MW/m<sup>2</sup> nominal is 15.8 MW/m<sup>2</sup> (after losses), which is the value used for comparison with correlations. As illustrated in Fig. 6, the minimum points could be clearly detected, and the true CHF (or the subsequent expected burnout) was not encountered before that minimum (the point where FE would occur) in any of the experiments. A single case of true CHF was also performed at 12 MW/m<sup>2</sup> using the stiff system mode (closed bypass). The corresponding CHF velocity was 12.2 m/s as compared to the corresponding FE velocity of 17.8 m/s. This shows an additional margin in velocity of ~30% compared to the FE velocity and of ~50% margin compared to the ANSR nominal velocity.

Although the final correlation of the FE data will be postponed until the remainder of the experiments are performed (by extending the heat flux and corresponding velocity ranges up to 17 MW/m<sup>2</sup> and ~27 m/s, respectively), the collected data were plotted in Fig. 7, and comparisons were made with correlations by Costa [9], Whittle & Forgan [10], and Saha & Zuber [11]. The Costa correlation is the one currently being used for the preliminary ANSR T/H design and analysis. Whittle and Forgan (W&F) and Saha and Zuber (S&Z) correlations are widely used in the United States with the S&Z correlation being well established in many computer codes for nuclear safety analysis. For a given coolant (water), physical properties, and geometry ( $L/D=199.6$ ), all three correlations can be rearranged and simplified to the same general formulation as follows:

$$Q_{fe}^* / (T_s - T_b) = CV^n, \quad (1)$$

where  $C = 1/0.0128$  and  $n = 0.5$  (Costa);  $C = 1/0.0382$  and  $n = 1.0$  (S&Z); and  $C = 1/0.0427$  and  $n = 1.0$  (W&F).

In the Costa correlation, the FE heat flux is proportional to the square-root of velocity, whereas both W&F and S&Z (as well as most other FE correlations) show a linear dependence. Based on this formulation, the Costa correlation will yield the same result as the W&F correlation at a

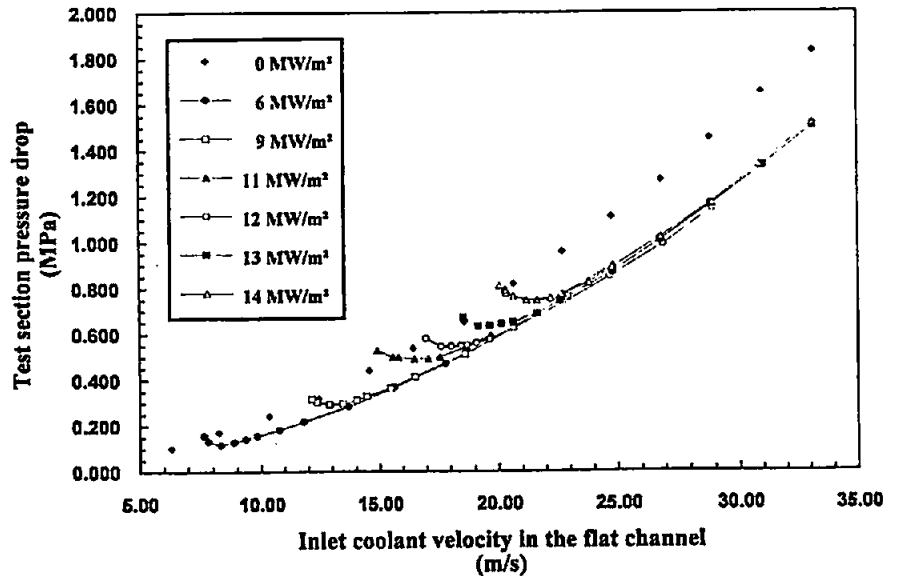


Fig. 6 Flow excursion data from THTL experiments  
(The inlet bulk coolant temperature is 45 °C, and the exit pressure is 1.7 MPa)



velocity of 11.1 m/s and, in comparison, will be too optimistic (higher heat flux) at lower velocities and too conservative at higher velocities (33% more conservative than W&F at the ANSR nominal velocity of 25 m/s). The Costa correlation will show the same trend when compared with the S&Z correlation, except that the equality will occur at 8.9 m/s. At 25 m/s, the Costa correlation will be ~40% more conservative than S&Z.

Since the above correlations are based on data for relatively low coolant velocities (maximums of 9.14, 7, and 7.66 m/s for W&F, Costa, and S&Z, respectively), it is quite interesting to see the trend of our data in terms of dependence on velocity. A comparison of the data with the three correlations is shown in Fig. 7. All three correlations seem to be conservative when compared to the data, with S&Z being the most accurate. Excluding three of the four data points taken with test section TSD-3/B (a steam leak in the gasket occurred), the agreement with S&Z is quite good, with the correlation skirting the lower bound of the data. The FE heat flux dependence on velocity seems to be between 0.5 power (Costa) and 1.0 (S&Z and W&F), more nearly in the 0.8-0.9 range. This result is in agreement with the conclusion recently arrived at by Lee & Bankoff [12], and Rogers & Li [7] who relate the heat flux to the turbulent heat-transfer coefficient (which is approximately proportional to the 0.6-0.8 power of velocity). As indicated before, the actual correlation of the ANSR FE data is postponed to a later stage.

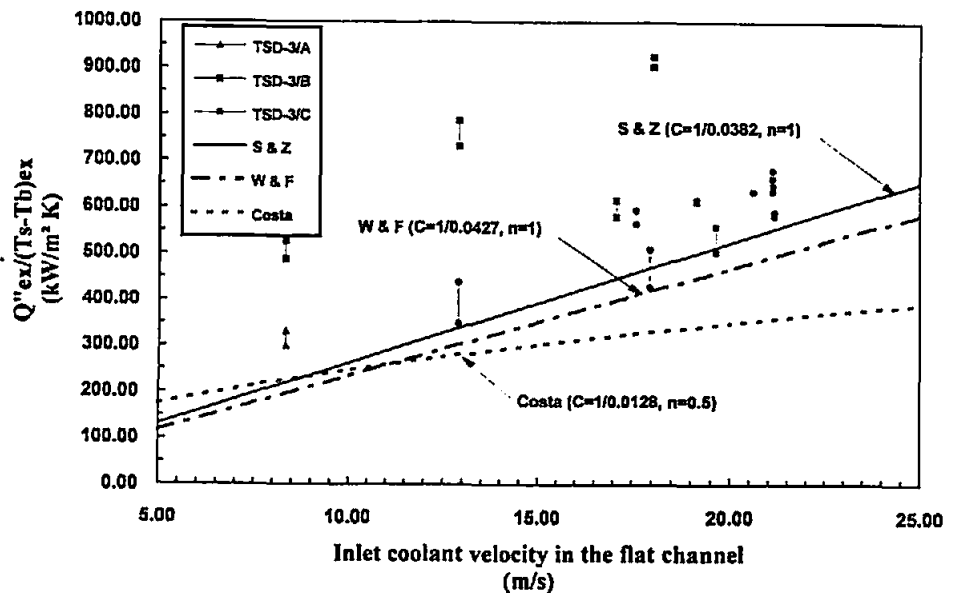


Fig.7 Comparison of flow excursion data from THTL experiments (Bars represent uncertainty related to axial and lateral internal heat redistribution by conduction)

## SUMMARY AND CONCLUSIONS

1. Although the experiments performed so far are in their initial stages, preliminary conclusions were derived by comparing the data to three well-known FE correlations of Costa [9], Whittle and Forgan [10], and Saha and Zuber [11]. All three correlations seem to be conservative when compared to the data, with the best agreement occurring with the Saha and Zuber correlation. The FE heat flux dependence on velocity seems to be somewhere between the 0.5 power (Costa) and 1.0 (S&Z and W&F), more nearly in the 0.8-0.9 range.
2. Acquiring FE data at this level of heat flux and velocity is of great significance for numerous reasons. Most of the available FE data is in the low velocity range (<10 m/s). The data reported in this paper are beyond any previously available, except those reported by Waters [8] in support of the Advanced Test Reactor. The heat flux achieved (14 MW/m<sup>2</sup> nominal and 15.8 MW/m<sup>2</sup> at the exit) is well beyond the ANSR peak heat flux of 12 MW/m<sup>2</sup>, and, yet, the corresponding limiting velocity is 17.3 m/s - well below the ANSR nominal velocity of 25 m/s.

The true CHF (or the subsequent expected burnout) was not encountered before the minimum pressure drop (FE) point in any of the experiments performed thus far. Furthermore, a true CHF test at 12 MW/m<sup>2</sup> showed a corresponding velocity of 12.2 m/s as compared to the 17.8 m/s for the FE velocity (30% margin) and 50% margin compared to the ANSR nominal velocity. On a preliminary basis, this result implies the existence of a good safety margin in the ANSR operating velocity for both thermal limits.

3. In the near term, the current series of experiments will be continued to achieve or exceed the ANSR nominal set point conditions, which include the nominal velocity of 25 m/s and the corresponding heat flux of 16 MW/m<sup>2</sup>. The final correlation of the data for FE and CHF as a function of the major T/H parameters at the ANSR conditions range will be postponed until the remainder of the experiments is performed.

### ACKNOWLEDGMENT

The authors would like to acknowledge the support of the ANS Project Office that made this work possible and the support received from Marshall McFee, Bill Nelson, Art Ruggles, Ronald Boyd, and other contributors.

### NOMENCLATURE

$C$	= a constant [Equation (1)]	$T$	= temperature (K)
$P$	= pressure (Pa)	$V$	= coolant velocity (m/s)
$Q$	= heat rate (kW)	$n$	= exponential constant [Equation (1)]
$Q''$	= heat flux (kW/m <sup>2</sup> )	$\Delta P$	= pressure drop (Pa)

### Subscripts

$av$	= average across and along the test section	$loc$	= local
$b$	= bulk coolant	$loss$	= losses from test section
$c$	= value at the minimum $\Delta P$ point	$s$	= saturated
$fe$	= at the flow excursion point	$ts$	= test section
$ex$	= exit		

### REFERENCES

1. Siman-Tov, M. et al, "Thermal-Hydraulic Correlations for the Advanced Neutron Source Reactor Fuel Element Design and Analysis," ASME HTD-Vol. 190, Winter Annual Meeting, Atlanta, GA, (December 1991).
2. Felde, D.K., Yoder, G.L., and Skrzycke, D., "The Advanced Neutron Source Thermal Hydraulic Test Loop," presented at 8th Power Plant Dynamics, Control & Testing Symposium, Knoxville, TN, (May 1992).
3. Gambill W.R., and Bundy, R.D., "Heat Transfer Studies of Water Flow in Thin Rectangular Channels, Part I: Heat Transfer, Burnout, and Friction for Water in Turbulent Forced Convection," Nucl. Science and Eng., 18, 69-79, (1964).
4. Siman-Tov M., Felde, D.K., Kaminaga, M., and Yoder, G.L., "Experimental Investigation of Thermal Limits in Parallel-Plate Configuration for The Advanced Neutron Source Reactor," presented at National Heat Transfer Conference, Atlanta, GA, (August 1993).

5. Duffey, R.B. and Hughes, E.D., "Static Flow Instability Onset in Tubes, Channels, Annuli, and Rod Bundles," ASME HTD-Vol. 150, Winter Annual Meeting, Dallas, TX, (November 1990).
6. Lee, S.C., Dorra, H., and Bankoff, S.G., "A Critical Review of Predictive Models for the Onset of Significant Void in Forced-Convection Subcooled Boiling," ASME HTD-Vol. 217, Winter Annual Meeting, Anaheim, CA, (1992).
7. Rogers, J.T. and Li, J., "Prediction of the Onset of Significant Void in Flow Boiling of Water," ASME HTD-Vol. 217, Winter Annual Meeting, Anaheim, CA, (November 1992).
8. Waters, E.D., "Heat Transfer Experiments for Advanced Test Reactor," BNWL-216, UC-80 (TID-4500), (May 1966).
9. Costa, J., "Measurement of the Momentum Pressure Drop and Study of the Appearance of Vapor and Change in the Void Fraction in Subcooled Boiling at Low Pressure," ORNL/TR-90/21, Martin Marietta Energy Systems, Inc., Oak Ridge National Laboratory, (1967).
10. Whittle, R.H. and Forgan, R., "A Correlation for the Minima in the Pressure Drop vs. Flow-Rate Curves for Sub-Cooled Water Flowing in Narrow Heated Channels," Nuclear Eng. & Design, 6, 89-99, (1967).
11. Saha, P. and Zuber, N., "Point of Net Vapor Generation and Vapor Void Fraction in Subcooled Boiling," Proc. of 5th Int. Heat Transfer Conf., Tokyo, IV, 175-179, (1974).
12. Lee, S.C. and Bankoff, S.G., "Prediction of the Onset of Significant Void in Down Flow Subcooled Nucleate Boiling," ASME HTD-Vol. 197, Proc. of 28th National Heat Transfer Conference and Exhibition, San Diego, CA. (August 1992).

## SOME RESULTS FROM THE ANS RESEARCH WORK

Presented by

C. D. West

October 1, 1993

<u>Subject</u>	<u>Contact</u>	<u>Fax No.</u>
Fuel Grading Profile	B. A. Worley	615-574-9619
Comparison of MCNP with FOEHN critical experiments	J. Ryskamp	208-525-5562
Status of ASME Code Case	G.T. Yahr	615-574-0740
Fuel testing	G. Copeland	615-576-3894
NSRR experiments	R. Taleyarkhan	615-574-8216
	T. Fuketa	81292826160
Graphite kernels	B.A. Worley	615-574-9619

# DURING THE PAST YEAR, THE FUEL GRADING PROFILE HAS BEEN GREATLY IMPROVED

Limiting power,\* MW<sub>t</sub> (95%  
certainty), with two different  
fuel gradings

---

Limiting phenomenon	CDR**	6693 grading
Critical heat flux	440	531
Incipient boiling	332	403
Fuel-centerline temperature	308	402
Fuel-oxide $\Delta T$	295	388

\*

Includes control and measurement uncertainties.

\*\*

With the L7 grading used in the Conceptual  
Safety Analysis Report.

## FOEHN CRITICALS

- FOEHN -- a critical experiment for the Franco-German High Flux Reactor at Institut Laue Langevin
- Purpose of experiment -- verification of design calculations and methods
- Experiment constructed in EOLE at CEN Cadarache

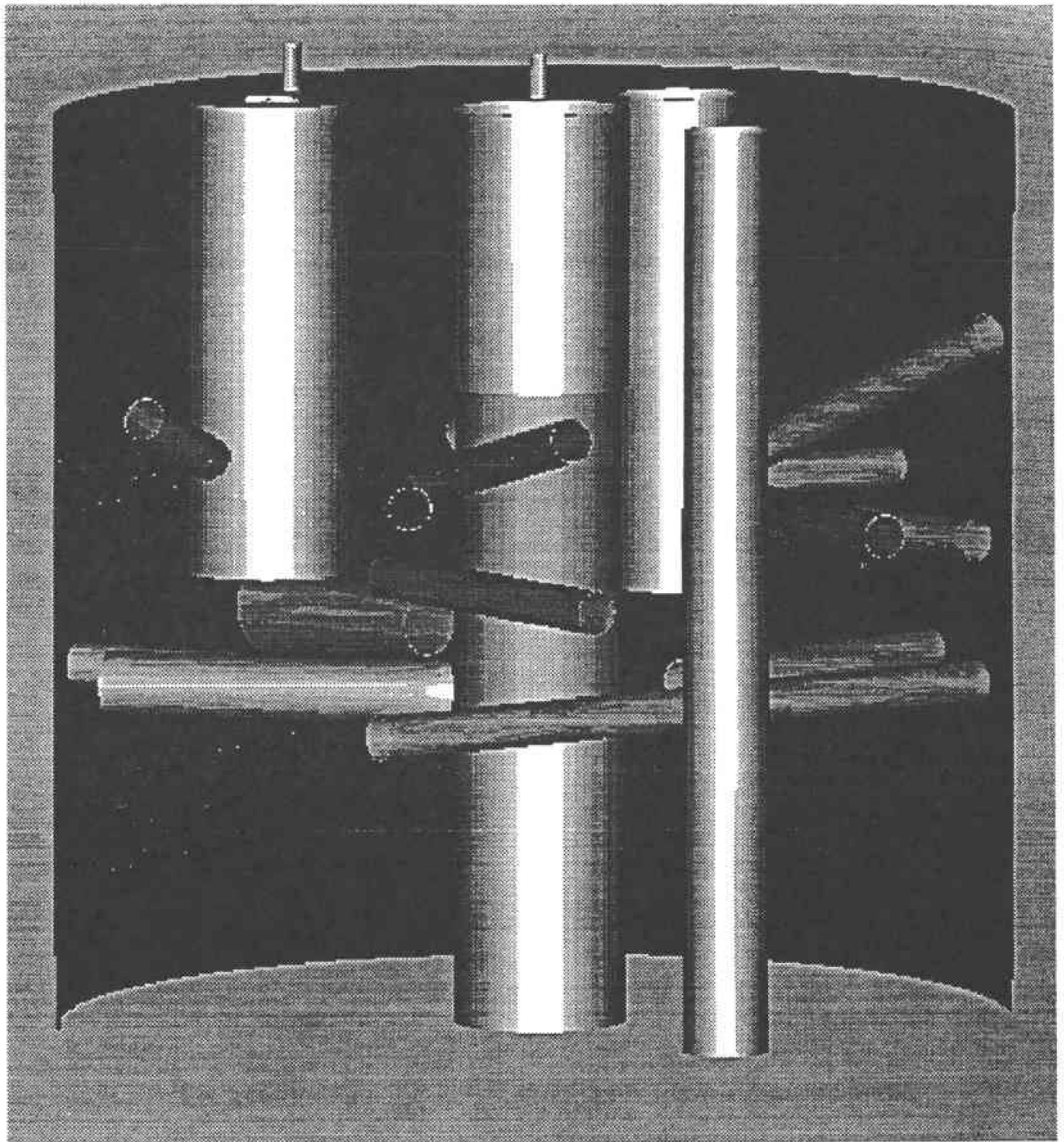
## FOEHN CONFIGURATIONS

- No B endplates, no reflector internals
- B endplates, no reflector internals
- Complete assembly with B endplates

# MCNP MODEL OF FOEHN

- Explicit geometric model of FOEHN
  - homogenized core
  - neglected Al seal plate at top and bottom of core (no dimensions)
  - no other geometric approximations
- Reactor materials as described for each component
  - exception - Al used for AG3-NE
  - due to initial lack of composition
  - later analysis showed effect of alloy was small ( $\sim 0.7\% \Delta k$ )
- ENDF/B-V continuous energy cross sections
- All reflector internals explicitly represented
- All three configurations modelled

SABRINA Diagram of the FOEHN MCNP Model

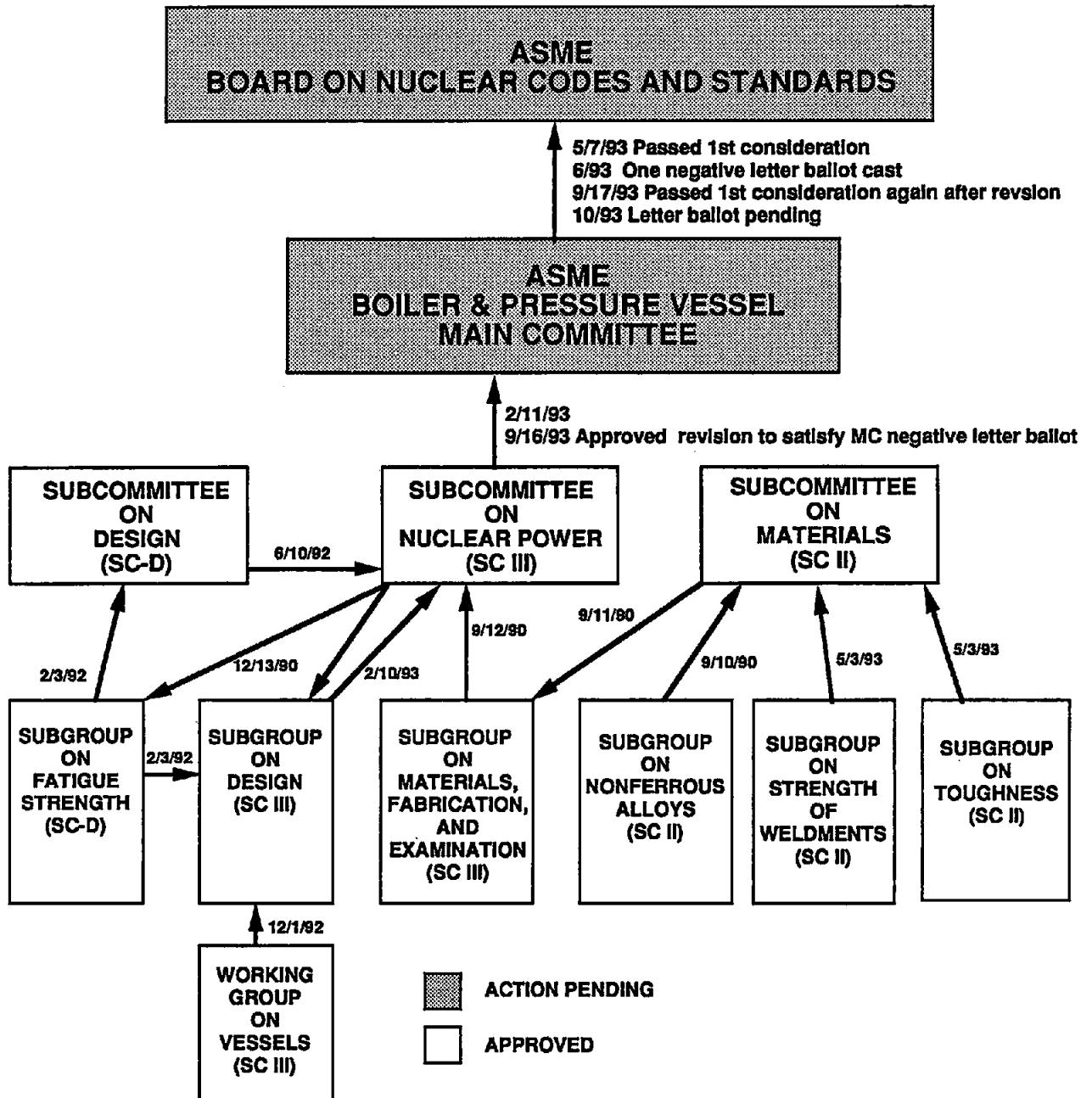




EXAMPLES OF MCNP CALCULATED CORE  
MULTIPLICATION FACTORS FOR FOEHN  
CRITICAL REACTOR STATES

Configuration No.	Control rod position (m)	boron conc.(g/L)	keff
1	1.438	0.2477	1.0028±0.0028
1	0.714	0.5386	0.9974±0.0032
2	1.2578	0.2100	1.0059±0.0035
2	0.946	0.371	1.0090±0.0034
3	1.361	0.078	1.0055±0.0034
3	0.899	0.311	1.0091±0.0027

**CODE CASE N-519: Use of 6061-T6 and 6061-T651 Aluminum for Class 1 Nuclear Components, Section III, Division I is going to the ASME Board on Nuclear Codes and Standards for final approval after second ASME Boiler & Pressure Vessel Main Committee letter ballot**



## IRRADIATION BEHAVIOR OF $U_3Si_2$ -Al DISPERSION FUEL UNDER ANS-LIKE CONDITIONS

- The following concentric microstructural pattern exists after high burnup at high temperature
  1. An outer rim of  $U(AlSi)_3$  formed by Al diffusion prior to grain refinement. This rim has  $UAl_3$ -like irradiation behavior.
  2. A  $U(AlSi)_3$  shell comprising most of the fuel volume that has undergone grain refinement prior to Al diffusion. This shell has  $U_3Si_2$ - $USi$  like irradiation behavior.
  3. An inner core of low U-silicide where Al diffusion has been inadequate for transformation to  $U(AlSi)_3$ .

This core exhibits gas bubble coarsening similar to amorphized  $U_3Si$ .

- The combined swelling behavior of the various zones result in a doubling of the fuel particle diameter.
- Our fuel behavior model in DART has been updated to reflect the above outlined fuel behavior under ANS conditions.

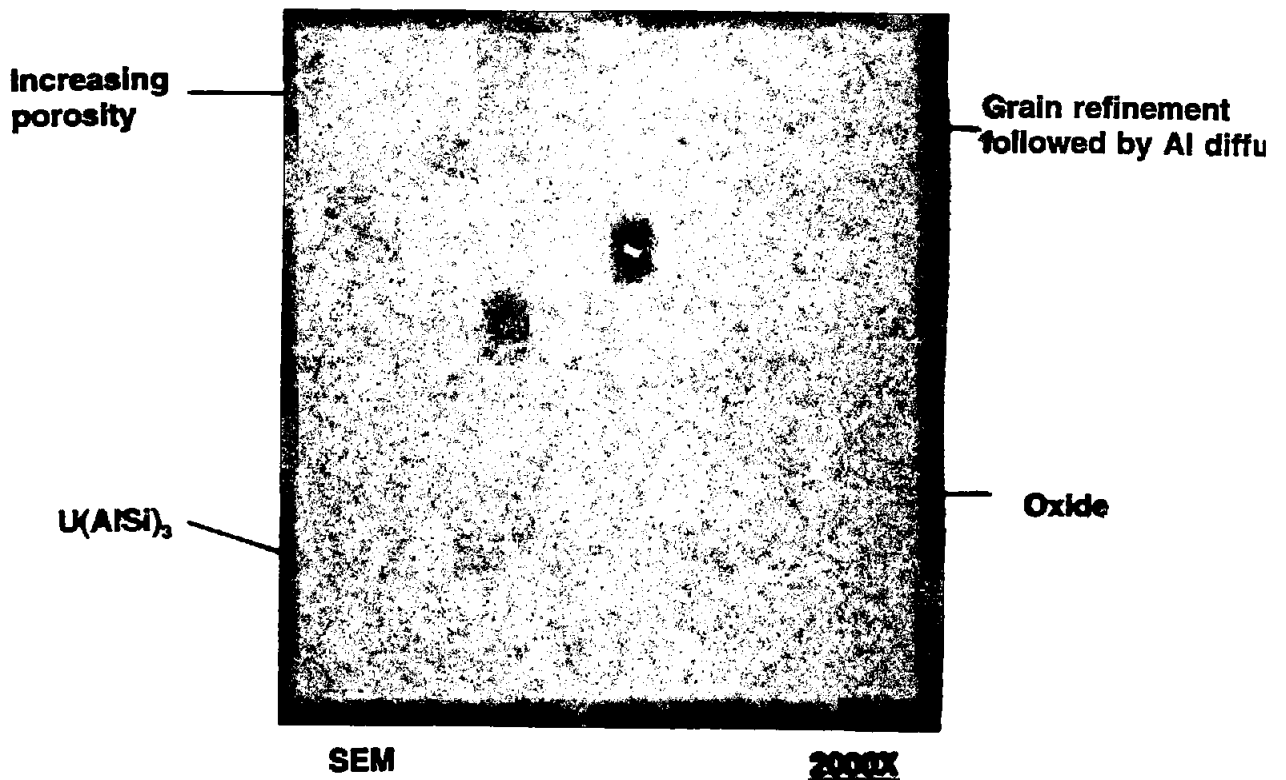
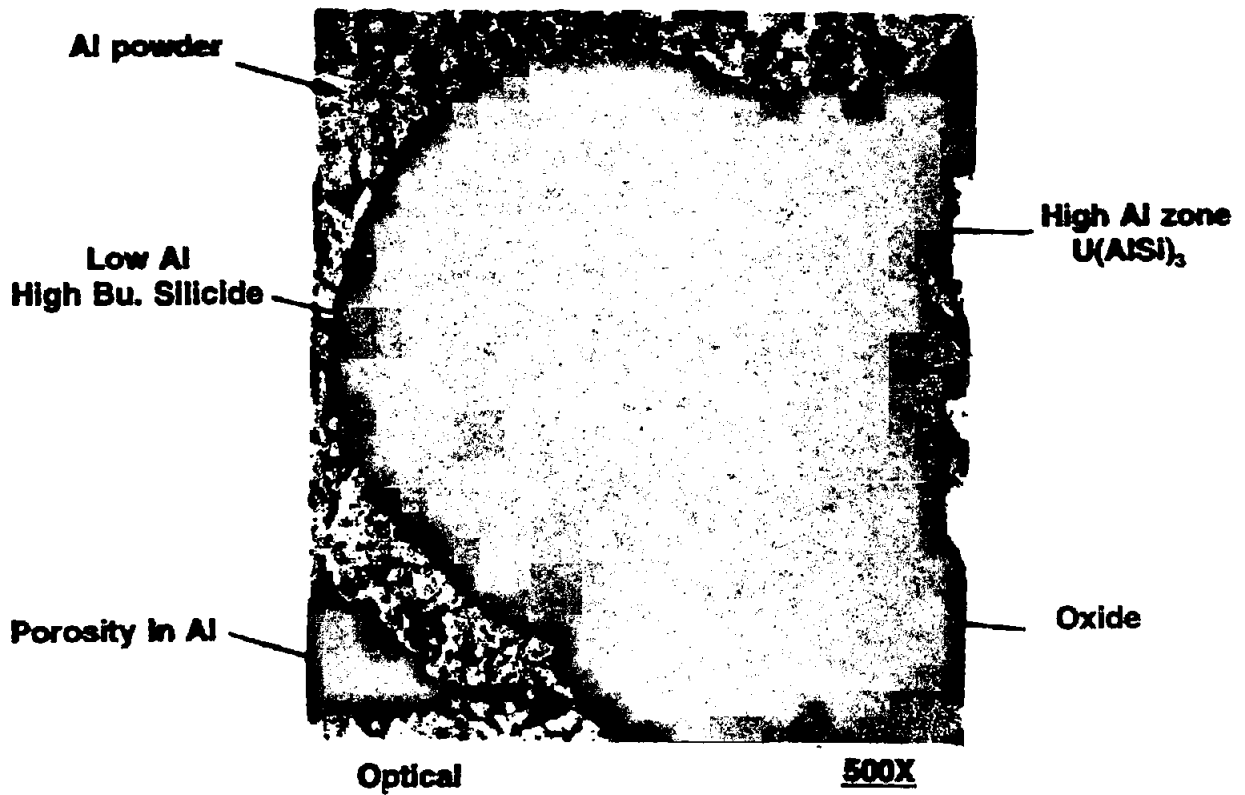


Fig. 1. Microstructure of  $U_2Si_2$ -Al Dispersion Fuel Irradiated to 90% Burnup in HFIR at ANS Conditions.

# JAERI-ORNL TESTS IN NSRR

## o ANS FUEL PLATES ARE QUITE DIFFERENT FROM JMTR PLATES

- Clad and meat thicknesses are significantly different (e.g., for ANS meat thickness = 0.76 mm, JAERI meat thickness = 0.5 mm)
- For ANS, the fuel meat thickness is variable (from 0.71 mm to 0.1 mm)
- ANS fuel density loadings in plates are significantly lower

## o TESTING IN JAERI'S NSRR PROVIDE VALUABLE DATA

- Design limits (plate cracking, bowing, material dispersion thresholds)
- Explosive FCI modeling (thermal-to-mechanical energy conversion)
- Fuel meat geometrical positioning (i.e., centered vs skewed)

## o TWO EXPERIMENTS HAVE ALREADY BEEN CONDUCTED (Under Analysis)

- Five more planned for 1993-94

## o FUTURE TESTS MAY INCLUDE PREIRRADIATED PLATE SPECIMENS

***RESULTING DATABASE WILL BE OF CONSIDERABLE SCIENTIFIC VALUE TO SILICIDE-FUELED RESEARCH REACTORS WORLDWIDE***

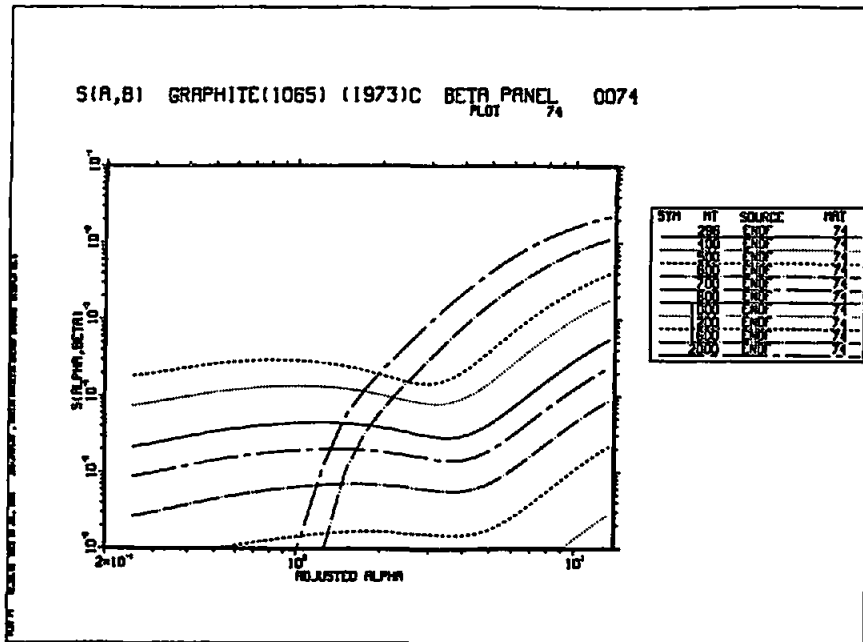
## RECENT WORK ON ANS FUEL DEVELOPMENT

- Irradiation of the HANS-2 capsule was completed in the target region of the HFIR during February 1993
  - capsule contained powder samples of  $U_3Si_2$ ,  $U_3O_8$ , and  $UAl_x$
  - capsule was disassembled in July-August
  - fuel samples have been shipped to ANL for microstructural evaluation
  
- Fabrication development has continued at B&W during the year
  - 18 HFIR outer plates were fabricated with 3 different lots of  $U_3Si_2$ 
    - homogeneity of all lots were equivalent to the oxide HFIR plates
  - 2 lots of miniature plates were fabricated for pulse testing in the NSRR
  - fabrication of a series of plates to demonstrate feasibility of dual fuel gradients is in progress

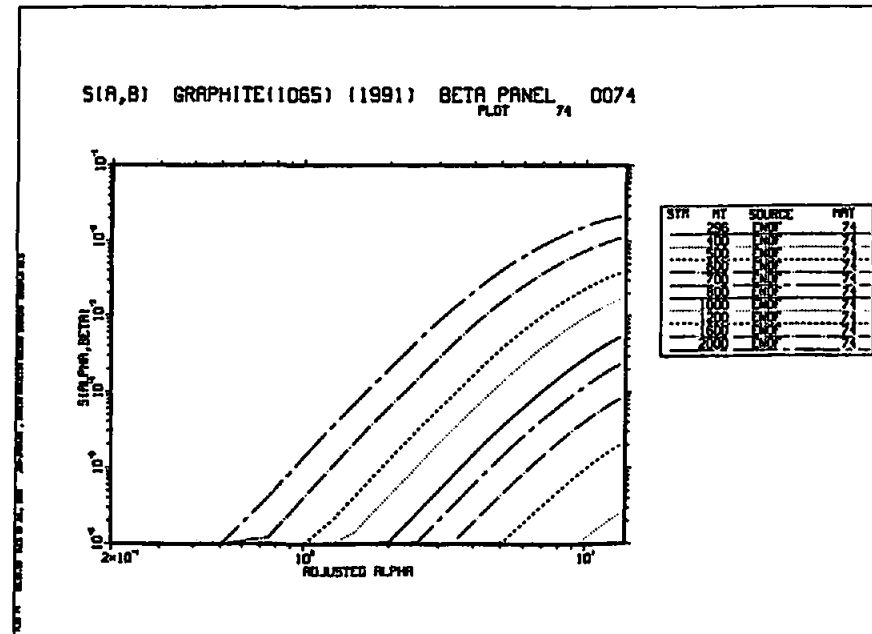
# GRAPHITE SCATTERING DATA IN ENDF FILES IS INCORRECT

CORRECTED DATA HAS BEEN GENERATED BY ORNL

OLD



NEW



# III-7

COMMISSARIAT A L'ENERGIE ATOMIQUE  
CENTRE D'ETUDES DE SACLAY  
FRANCE

PAPER TO BE PRESENTED AT THE THIRD MEETING OF THE  
INTERNATIONAL GROUP ON RESEARCH REACTORS (IGORR - III)  
SEPTEMBER 30 - OCTOBER 1, 1993 IN NAKA-MACHI, IBARAKI-KEN, JAPAN

## OSIRIS : THE FIRST M.T.R. WITH A NEW INSTRUMENTATION AND CONTROL SYSTEM BASED ON DIGITAL LOGIC OF VOTE

C. JOLY, C. THIERCELIN, J. CORRE, J.F. DUBOIS, G. DE CONTENSON

### 1 - INTRODUCTION

OSIRIS, one of the french C.E.A. research reactors located at SACLAY, near PARIS, is since 27 years mainly devoted to production and irradiation technologies. To satisfy these objectives, OSIRIS is equipped by different test sections allowing mainly :

- . the long time irradiation of different materials including fuel rods, reactor vessel materials, fusion reactor components...,
- . the power ramps of fuel rods,
- . the Silicon doping,
- . the radioelements production,
- . the neutronography of materials and test sections.

In most of the loops, the nuclear reactor conditions are fully simulated to approach as far as possible the exact behaviour of the materials.

Through the new irradiation facilities under development, let's cite the OPERA test section foreseen for the simultaneous irradiation of 32 fuel rods with a maximum length of 2 m.

To guarantee the safety and the high performances of the reactor, a continuous maintenance and improvement programme took place during the whole life of the reactor.

The paper gives an overview of the part of this programme devoted to the replacement of the instrumentation and control system of the reactor. After 5 years study and development, the on site work took place in the second part of 1992 allowing a reactor start up beginning of 1993.



## 2 - OBJECTIVES

The new instrumentation and control system of the reactor OSIRIS is organized to insure a large availability of the reactor and a high precision of its control and monitoring.

To reach both objectives with respect to quality insurance and safety rules, the equipment is formed by three parts :

- . a protection - or safety - system using the most modern technology, i.e. microprocessors,
- . a control system adapted to the process requirements and associated to a fully computerized monitoring system,
- . a central process system of all informations, called "T.C.I." , including a computer and a fast acquisition station, called "C.A.R." .

Figure 1 schematizes the designed system based on the 3 hereabove mentioned parts.

The control involves to collect a large number of data related to the reactor and to the experiments : "T.C.I." and "C.A.R." facilitate this task.

The safety requirements lead to different automatic actions : limitation of the running ranges, impossibility of incompatible configurations and automatical control of the reactor.

Furthermore, the safety is also guaranteed by the system which takes into account a 2/3 digital voting logic.

The computerization of process data on P.C.'s in the new ergonomic reactor control room enables the operating shift to be kept informed and to take all decisions with respect to the orders and to the reactor programme.

## 3 - SAFETY PROTECTION SYSTEM

### 3.1. Reactor Power Measurement and Control

To maintain the neutron flux in the experiments the reactor power is stabilized at its nominal level of 70 MW : the reactor is conducted at constant power, the control rods being successively raised following a predetermined order .

The power is carefully measured by three different ways :

- . the thermodynamical power using mass flow rates and temperature differences in equilibrium state,
- . the power based on the N16 specific activity of the primary cooling water and allowing a rapid power estimation,
- . the nuclear power measured by
  - .. three low power level starting chambers taking into account their position relatively to the reactor core,

- .. three high power level safety linear chambers,
- .. a control chamber.

The nuclear power can't directly served as power value but has to be compared to the two other power measurements.

From subcritical regime till 1 MW, the reactor power is given by the starting chambers.  
From 1 MW till the nominal power of 70 MW, the compensated safety chambers are used for the follow-up of the power level.

For the reactor control, the non compensated ionisation control chamber gives the exact reference value of the power.

One of two running regimes may be selected, one excluding the other one,

- . a low power level regime, till 1,7 MW, characterized by natural convection cooling conditions and allowing loading and unloading of the reactor core,

- . a high power level regime, characterized by forced convection cooling conditions, functioning of all safety circuits but inhibition of the low power level starting chambers.

### 3.2. Basic conception of the safety protection system

As the renovation to be performed deals with an existing plant, the following international and C.E.A. rules have been approached as far as possible :

- . international standards : CEI 231A, CEI 880
- . C.E.A./I.P.S.N./D.A.S. rules : SAM 13 for safety software, SAM 17 for safety programmable automatons, SAM 33 for electrical supply and for control and safety system.

Mainly the following criteria have been respected :

- . single failure criteria : the system plays its role if a single failure occurs,
- . independence criteria : the system insures physical separation and galvanic insulation of all components and equipments,
- . functioning tests : the system allows self control tests when running as well as periodical tests when shutdown,
- . quality insurance : the system was concerned and realized with respect to a complete quality insurance programme.

As organized, the whole system, whose architecture has been pre-defined by a safety study, fulfils the most stringent safety standards hereabove mentioned.

Special preliminary tests ensure the qualification of the equipment according to imposed nuclear equipment specifications.

### 3.3. Safety circuits [figure 2 ]

As far as the safety is concerned :

. the safety channels are physically separated and are composed of three redundant SIREX elements - called ASX1, ASX2, ASX3, - for the neutronic parameters and of three safety automatons - called ASU1, ASU2, ASU3 - for the thermodynamical parameters and the fuel clad failure detection,

. the safety actions induced by the three hereabove mentioned channels are taken into account by a 2/3 digital voting logic, the two voting logics being also physically separated but using the same software.

All the components of the new system uses the latest electronic technology - use of 16 bits MOTOROLA microprocessors, digital technology using multilayer printed circuit, static relays... - leading to extremely fast response times, i.e.,

- . triggering of an emergency shutdown control from a nuclear parameter in less than 60 ms ,
- . execution of a polling function and control in 5 ms.

Fully exhaustive digital information is transmitted to the new ergonomic control room, thus making it possible to perform consistency checks and to produce measurement validity diagnostics to simplify repair and reduce maintenance time.

The parameters specific to the process are controlled and modified by the operator, giving a system which can be adapted to variations in the time imposed by the process.

### 4 - CONTROL SYSTEM [Figures 3, 4, 5, 6, 7, 8, 9 ]

The control system uses five APRIL 5000 type programmable automatons

. three programmable automatons treat all TOR and analogic informations necessary to the reactor operator,

- . two programmable automatons treat all mechanical and electrical parameters.

These five programmable automatons are integrated in five unit racks called UT1, UT2, UT3, UT4, UT5.

Rack UT1 includes

- . the first programmable automaton receiving all informations from safety racks ASXi, ASUj and ASUj,  $i = 1, 2, 3$  and  $j = A, B$ ,
- . the two chains for neutronic measurements,
- . the control equipment,
- . the N16 specific activity control system,
- . the follow up of the alimentation of the control rods motors.

Rack UT2 includes

- . the second programmable automaton receiving, as UT1, all informations from safety racks ASXi, ASUi and ASUj,
- . the fuel clad failure detection information,
- . the temperature measured values.

Rack UT3 includes

- . the analogical informations related to the control rods positions,
- . the temperature measured values,
- . the values from the vibration monitoring systems.

Racks UT4 and UT5 treat all TOR and analogical values from the electrical net and from the mechanical components.

All control equipment is interconnected via a redundant local area communication network, FACTOR type, which centralized data in the control room where these are visualized by means of four supervisors :

- . two supervisors for the reactor monitoring,
- . two supervisors for the follow up of electrical and mechanical informations.

Examples of visualization synoptics are given by figures 4 up to 9.

The redundancy allow the reactor monitoring even in a degraded mode in which case the operator has the minimum of important data.

Two printers, associated to these programmable automatons, work continuously or on request of the operator.

Furthermore, all information managed by the programmable automatons are transmitted to the calculator (T.C.I.) by specific J BUS type connection.

## **5 - CENTRAL PROCESS SYSTEM [figure 10]**

The central process system, called T.C.I. , includes a computer with its peripheral equipments and a fast acquisition system, called C.A.R., and is used

- . to memorize and to treat all informations with a view to rereading or editing of tables, curves...,
- . to precisely date the T.O.R. and analogical data making it possible the history of any event,
- . to support the reactor control and monitoring.

The main component of the T.C.I. is a HEWLETT PACKARD computer, type HP9000 433 S, with two discs allowing a memory of 600 and 330 Mo. A magnetic support, streamer type, of 133 Mo allows to safe all data of a reactor cycle.

A console located on the desk in the control room gives all the information to guarantee the availability and the fiability of the reactor. Two other consoles are devoted to informatical system and to parametric applications. Two printers and one tracer are used for editing. Selected informations are transmitted to 14 P.C.'s through a internal net. The fast acquisition system is connected to the computer through the same net. At present, the computer manages 1800 TOR and 600 ANA.

. The system allows daily overview by storage of all TOR and ANA informations measured each 2 s and related to the last twelve hours.

. The system stores all data, averaged on 10 mn, of the last 45 days.

. The computer controls important safety parameters, editing messages when the limits are overpassed together with 450 values before the event occurence and 180 values after.

The C.A.R. receives 220 TOR informations and 9 ANA informations . The software of the C.A.R. allows to surround any event occurence which can then be analyzed and explained.

## 6 - CONCLUSION

. The components of the OSIRIS reactor control room and associated equipments have been completely redesigned.

. Since the beginning of 1993, the new control system of OSIRIS is operating with a high satisfactory manner proving its large reliability and safety level.

. All the hereabove mentioned replacement and improvement work on the OSIRIS reactor was realized mainly with the collaboration of the following firms :

. MERLIN GERIN, GRENOBLE, FRANCE, for the safety protection and control systems

. COMELOG ESIA, PARIS, FRANCE, for the central process system.

. The new console was developed taking into account the up to date ergonomics principles .

The computerization of process data on two PCs enables

. the operator to be kept informed,

. data to be classified by themes and repair work to be simplified

The traditional interfaces have been redesigned using new technology.

The use of industrial hardware and software allow the user to update or modify the application.

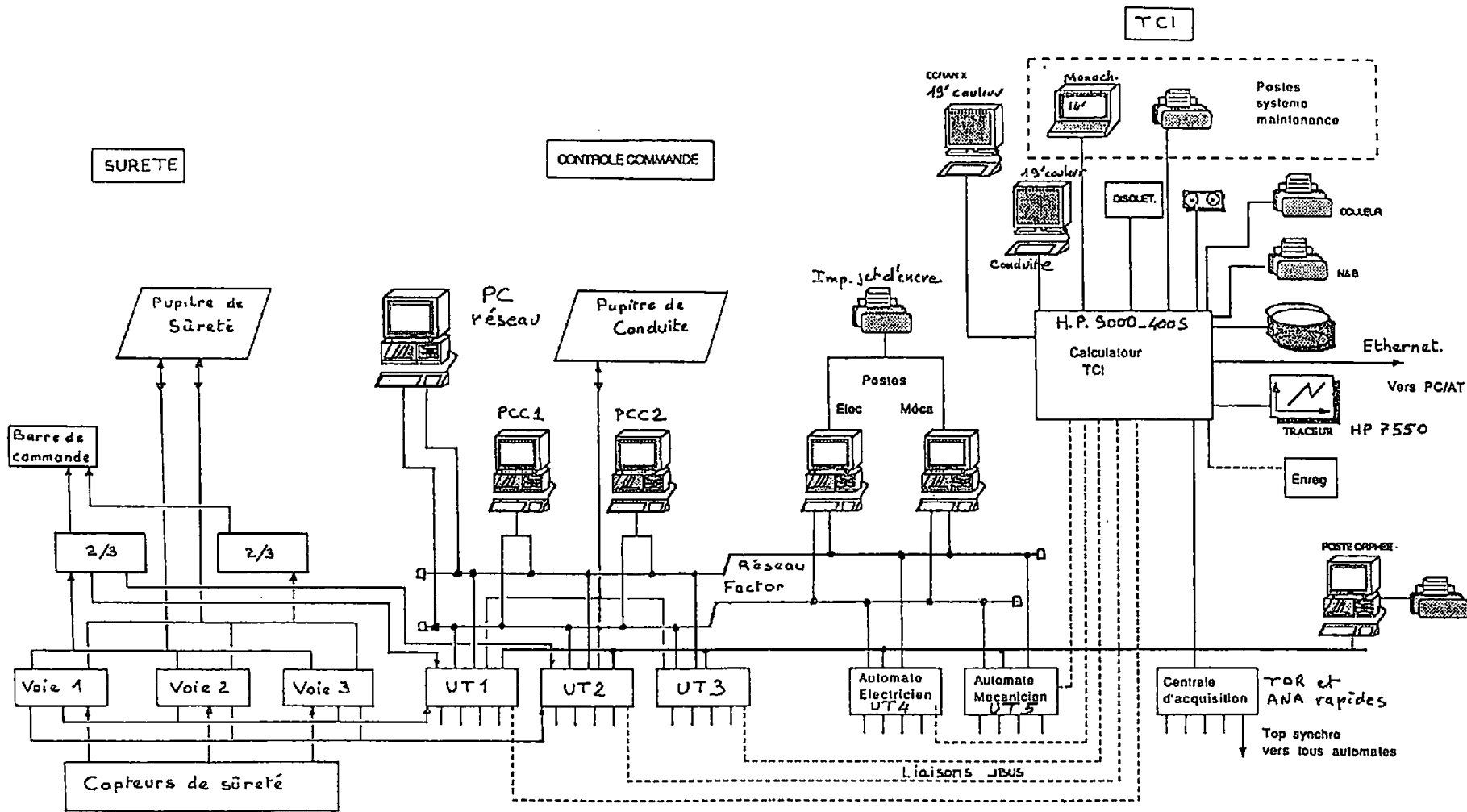


Figure 1 : Schematic representation of the new instrumentation and control system of OSIRIS

SYNOPTIQUE GENERAL

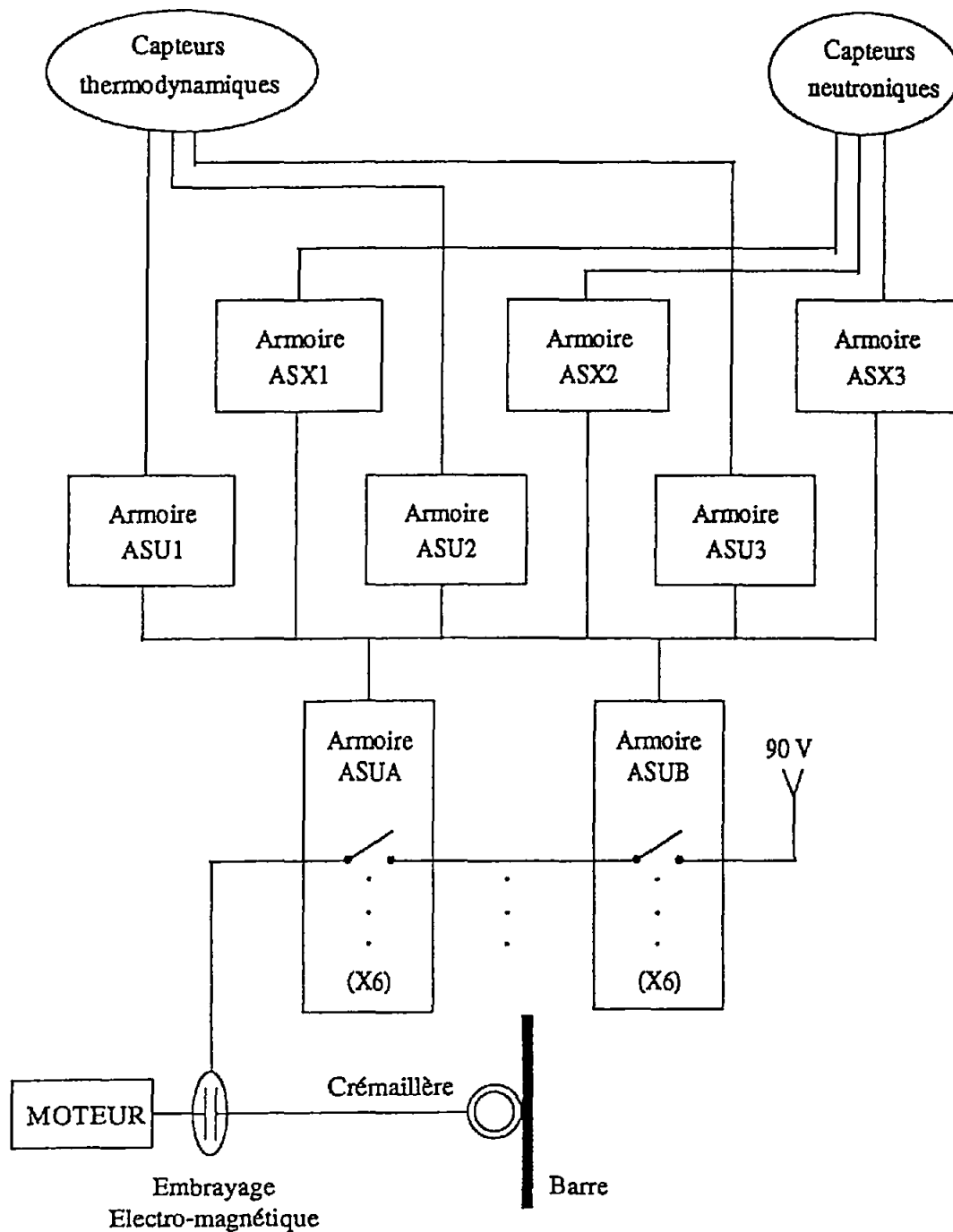


Figure 2 : OSIRIS - General representation of the safety circuits

RENOVATION DU Cle-Cde OSIRIS.

Circuits de conduite.

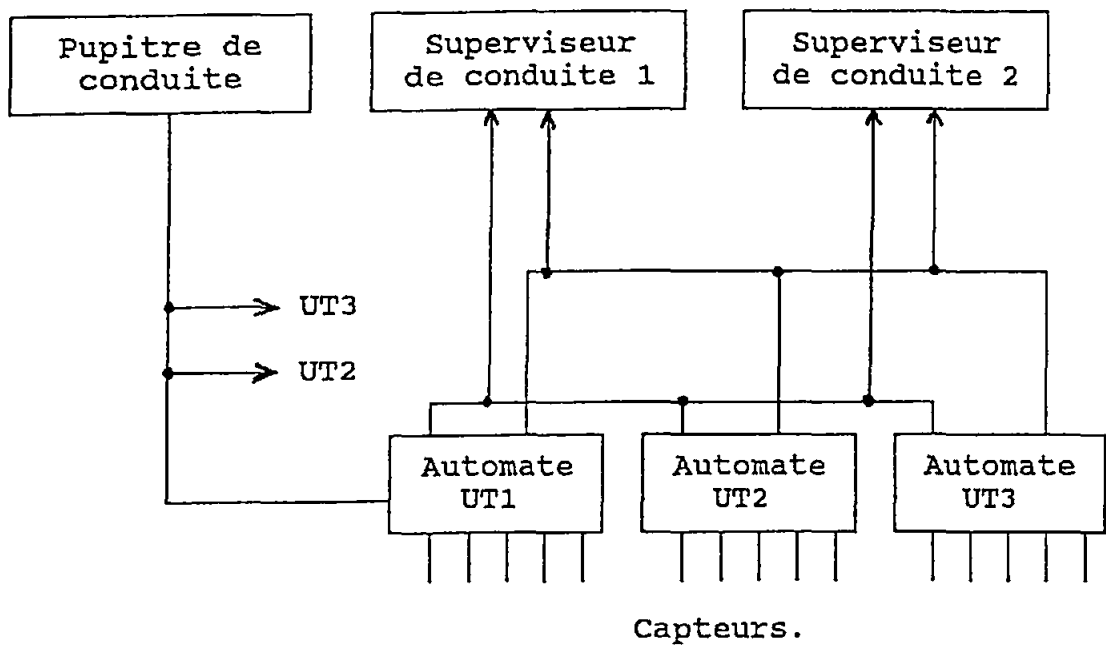


Figure 3 : OSIRIS \_ General representation of the control system



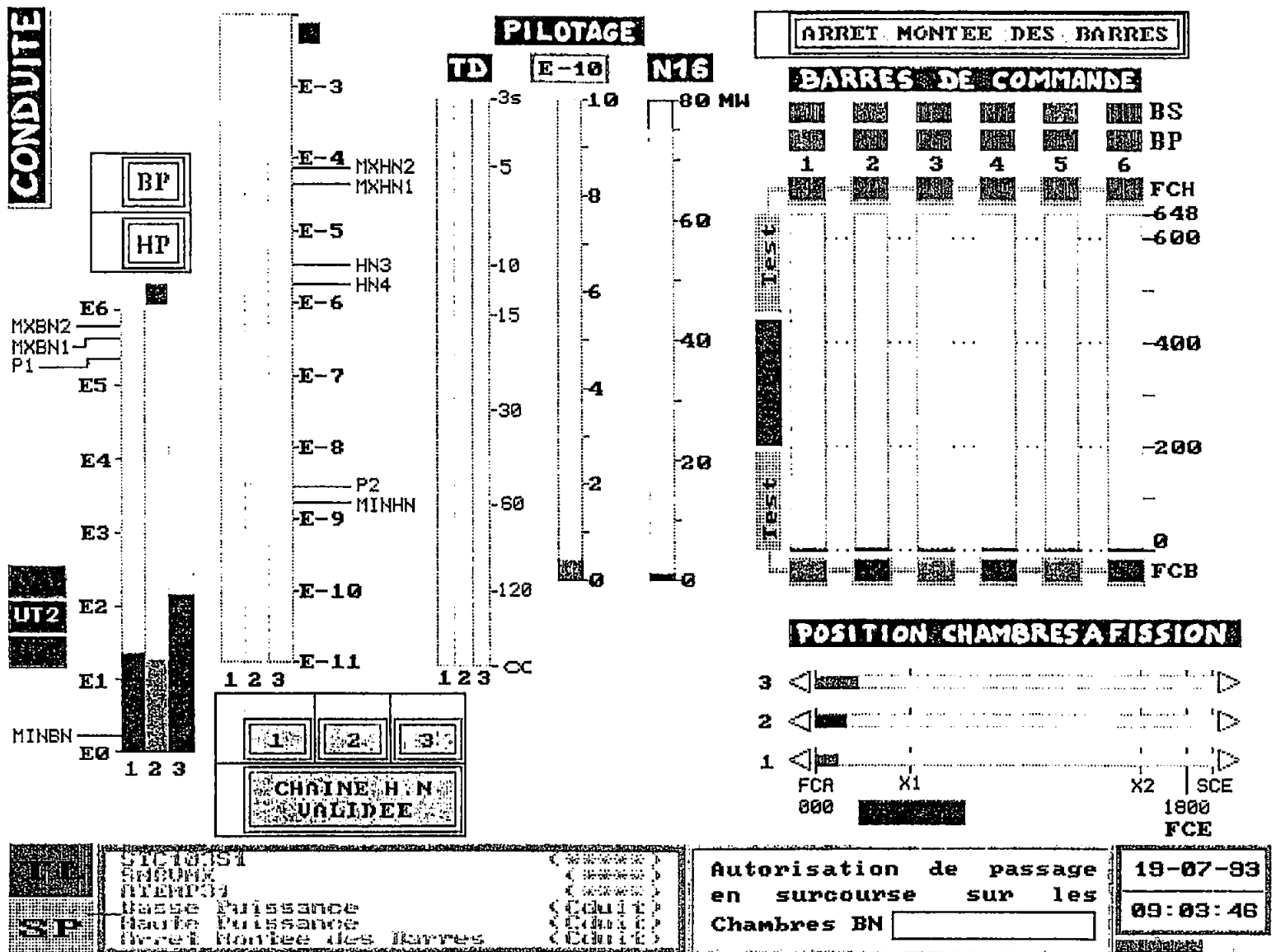


Figure 4 : OSIRIS - Typical synoptics of the control system

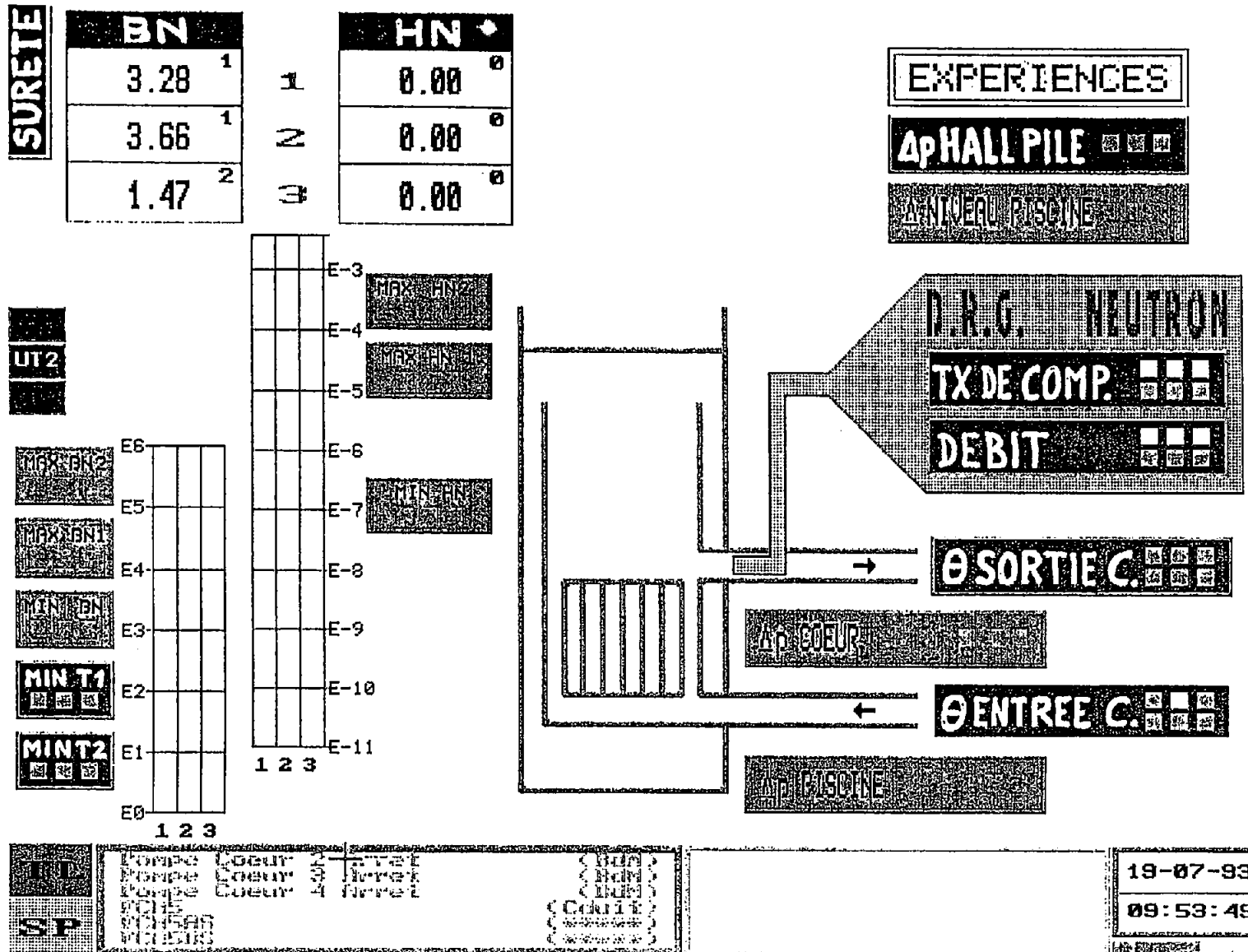


Figure 5 : OSIRIS - Typical synoptics of the control system

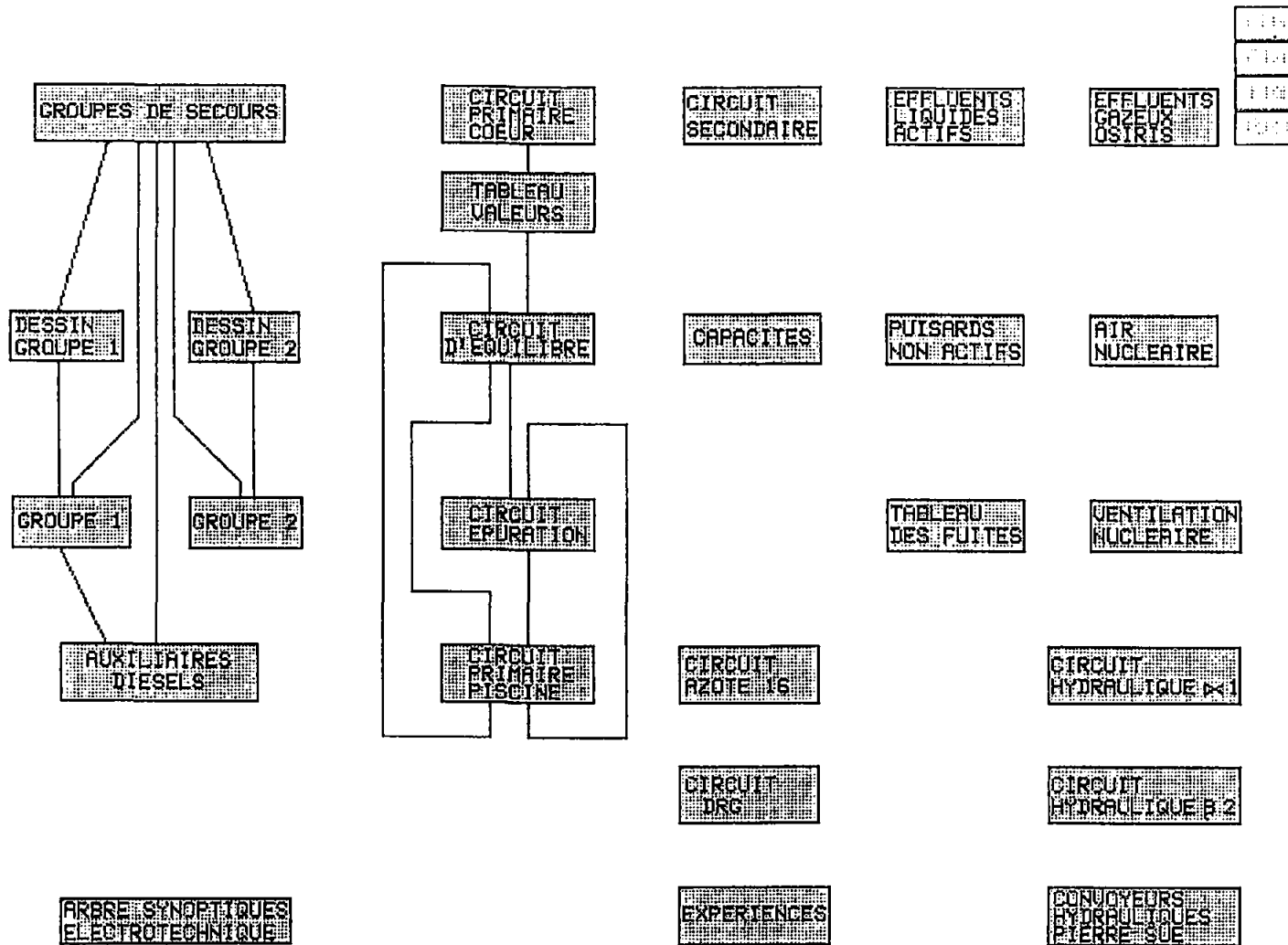


Figure 6 : OSIRIS - General mechanical synoptics

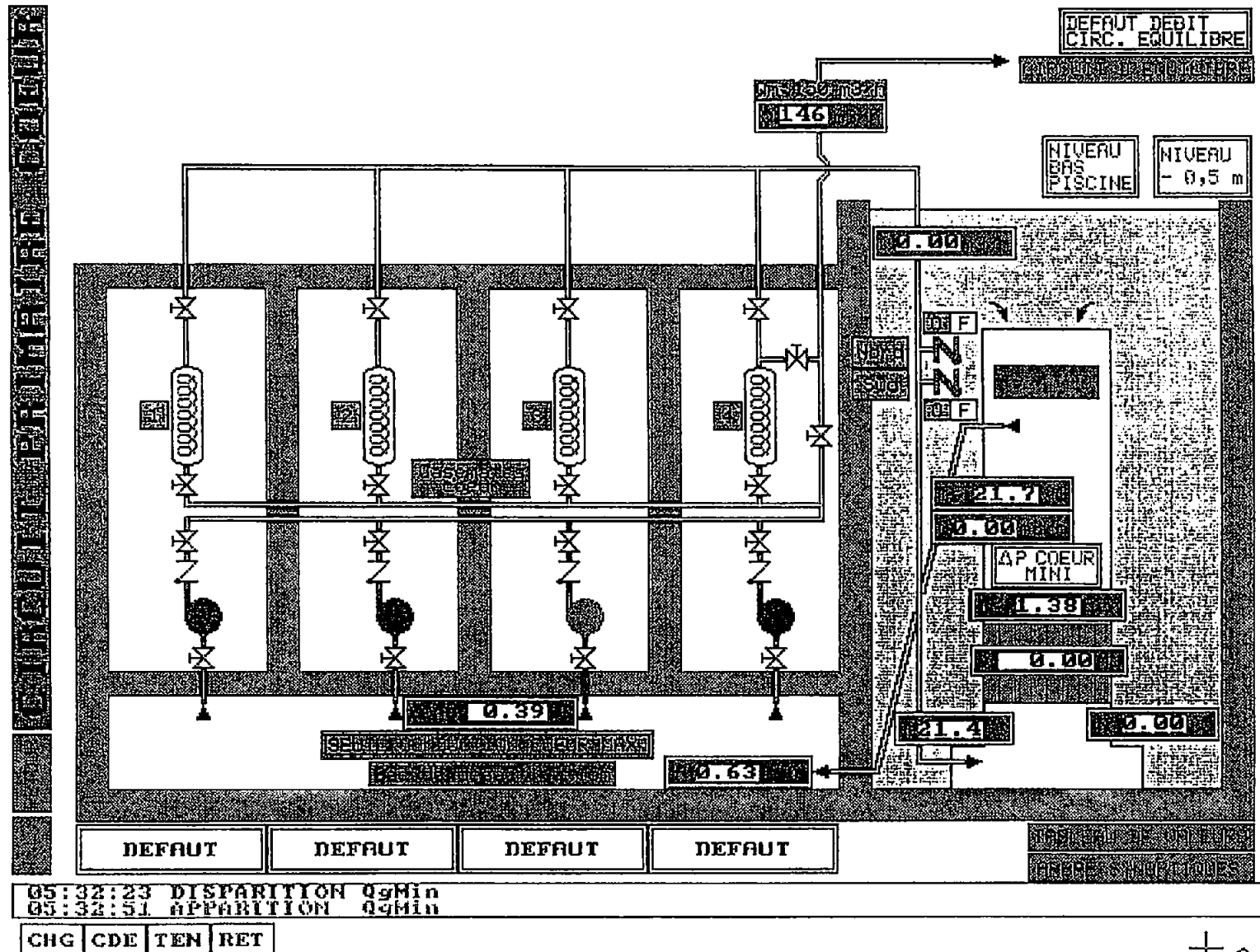


Figure 7 : OSIRIS : Typical mechanical synoptics

# ARBRE SYNOPTIQUES ELECTROTECHNIQUE

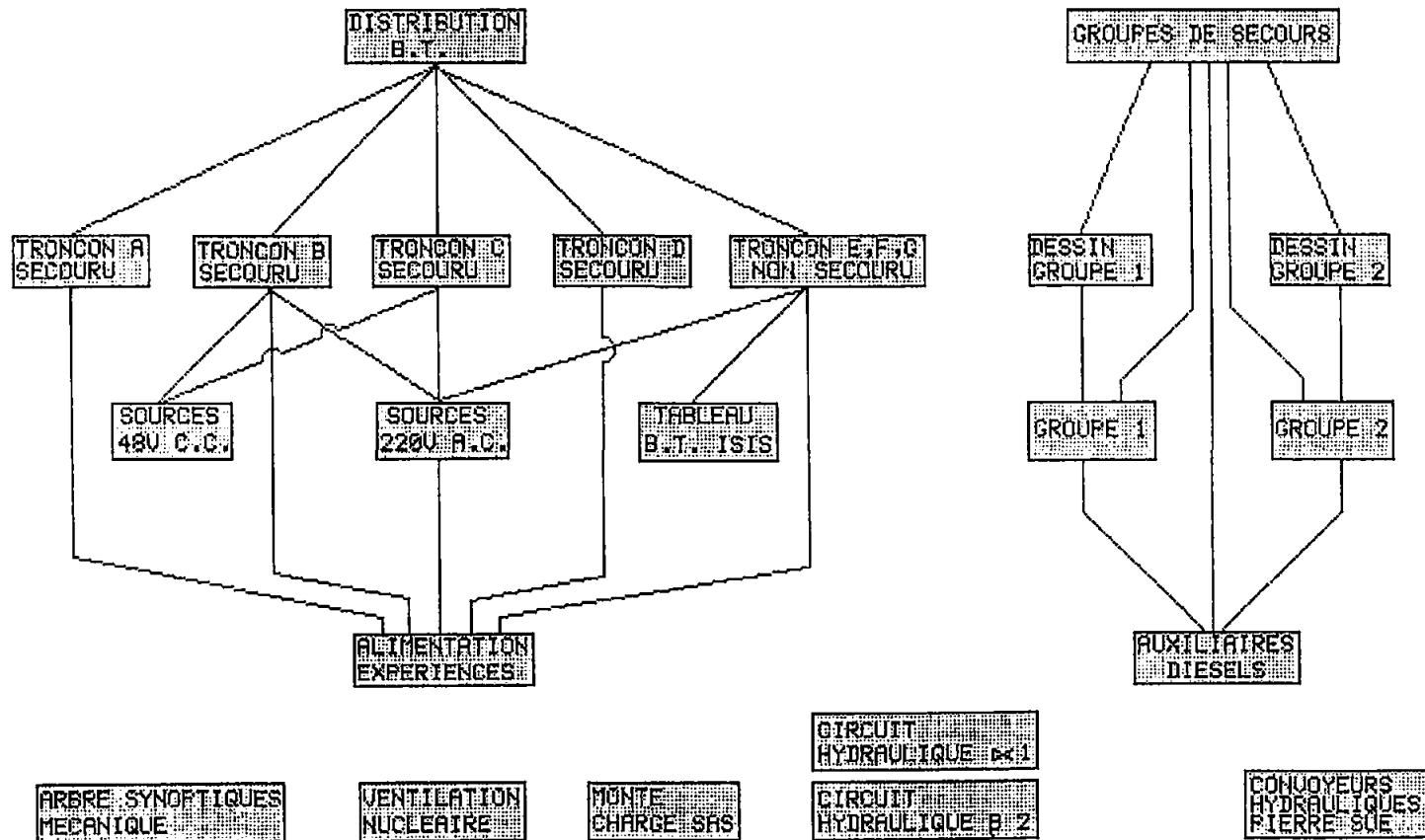


Figure 8 : OSIRIS - General electrical synoptics



RENOVATION DU Cle-Cde OSIRIS.

Circuits du Traitement Centralisé des Informations.

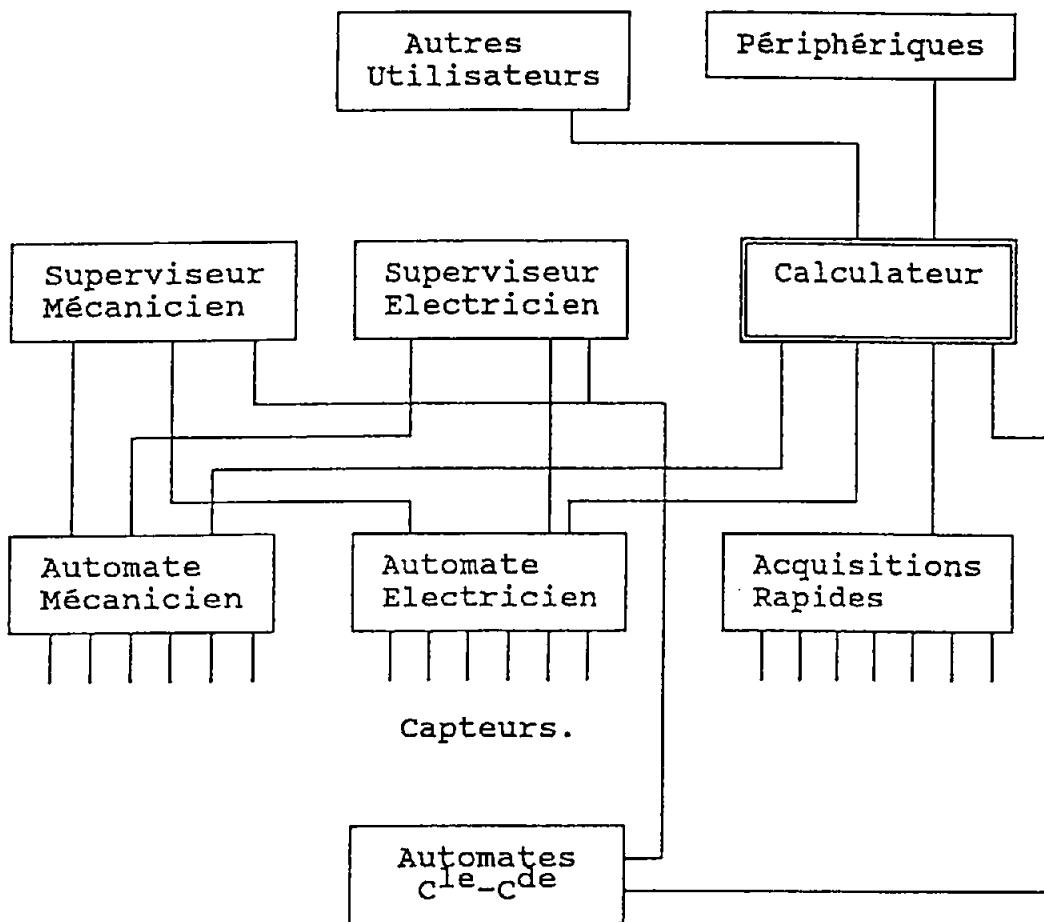


Figure 10 : OSIRIS - General representation of T.C.I. - C.A.R.

**PROBABILISTIC SAFETY ANALYSIS FOR FRJ-2  
MOTIVATION, METHODOLOGY AND RESULTS**

by

J. Wolters

Institute for Safety Research and Reactor Technology, Research Center Juelich, FRG

**ABSTRACT**

A PSA of the Research Reactor FRJ-2 was performed to check the twenty-year-old safety system for weak points and to develop accident management as a 'fourth line of defence' against severe accidents according to a German initiative. The total core damage frequency proved to be  $1.5 \cdot 10^{-4}/a$ , which is consistent with figures found for other research reactors. Minor plant modifications will reduce the value by roughly a factor of 4, resulting in a frequency of  $3 \cdot 10^{-7}/a$  for a major release of fission products into the environment caused by an independent failure of the containment. The integrity of the gas-tight steel containment proved not to be endangered by any core damage accident. From the results and insights gained by the PSA, many accident management measures could be identified and defined for the emergency handbook. The most important measure is primary feed and bleed, for which the feed line already exists.

**1. INTRODUCTION**

The FRJ-2 at the Research Center Jülich (KFA) is the most powerful research reactor in Germany. It was commissioned in 1962. In the late sixties and at the beginning of the seventies, the power was increased in two steps from the originally designed power of 10 MW to 15 MW and then 23 MW. At the beginning of the nineties, a level-3 probabilistic safety analysis (PSA) was initiated by the Board of Directors of KFA for two reasons: firstly to check the twenty year old safety concept for weak points, and secondly to provide the basis for an accident management handbook, which is being prepared at present and which was required by a safety review ordered by the supervising authority in the aftermath of the Chernobyl disaster.

The Institute for Safety Research and Reactor Technology (ISR) of KFA was charged with supervising the analyses and it introduced other institutions from KFA and the German companies INTERATOM and Battelle. The level-1 PSA was performed by a team of analysts from ISR and from the Safety and Reliability Directorate (SRD, part of the UK Atomic Energy Authority). Co-operation with SRD facilitated the utilization of previous PSA findings from similar studies for the UK reactors DIDO & PLUTO (Harwell) to be applied to the FRJ-2.



## 2. PLANT DESCRIPTION

The FRJ-2 is a DIDO-class tank-type research reactor cooled and moderated by heavy water passing through the core in the upward direction. The core consists of 25 so-called tubular MTR fuel elements accommodated within an aluminum tank (Fig.1). The tank is surrounded by a graphite reflector enclosed within a double-walled steel tank. This steel tank, together with its liner tubes for the various penetrations, constitutes the second containment for the reactor tank. All penetrations are sealed at the outside of the biological shield so that a leak in the reactor tank and its pipes would only fill the aluminum/steel tank interspace, which is designed such that the water circulation would not be interrupted.

The reactor is equipped with two independent and diverse shutdown systems, the so-called Coarse Control Arms (CCAs) and the Rapid Shutdown Rods (RSRs). In the case of a demand, the six CCAs are released from their electromagnets and drop in by gravity, whereas the three RSRs are shot in by their pneumatic actuators. Both systems are demanded in the case of reactivity accidents, but in the case of cooling accidents only the CCAs are demanded. The CCAs are lowered and raised by the reactor control system in order to control power levels in normal operation, whereas the RSRs are permanently in their upper position.

The primary circuit is housed in a closed but not air-tight plant room beneath the reactor block. The main circuit consists of the three main pumps, the two shutdown pumps, the three heat exchangers and all associated valves and pipework. The operation of all three main pumps is required for full power operation, and the reactor is tripped if one pump fails although core cooling is not directly compromised. In the case of a stoppage of all main pumps, one shutdown pump is switched on automatically for after-heat removal from the core to the heat exchangers. Forced convection is not absolutely necessary for after-heat removal from the core to the bulk  $D_2O$  in the tank as has been demonstrated by reactor experiments /1,2/. But the tank water would be heated up to boiling temperature within 30 min.

The primary circuit transfers the power via the three heat exchangers to the closed secondary circuit, which is cooled by dry cooling towers. Two of the four main pumps of the secondary circuit are equipped with a pony motor for after-heat removal in the case of a switch-off of the main motors. The fans of the cooling towers are not needed for after-heat removal.

Because the maintenance of a minimum coolant inventory in the reactor tank is of crucial importance to the reactor, there are several systems which provide this function. Two of them operate in the event of accidental loss of  $D_2O$  inventory. They are the Emergency Core Cooling System (ECCS) and the Emergency Light Water Injection System (LWIS). The ECCS consists of two automatically controlled pumps, which can circulate water from the plant room sump back to the reactor tank, and the associated pipework (Fig. 2). The LWIS, which is manually operated from outside the reactor hall, provides a means for water from the fire system or the mains to be injected into the reactor tank as a last resort. In the case of a leak, depending on its size, there are two different cooling modes for the fuel elements, either forced or natural convection or cooling by a falling water film.

The reactor hall is a steel shell designed for an overpressure of 300 mbar and a leak rate at this pressure of 1 vol.%/d. In the case of an accident with the release of radioactive substances into the hall, the containment isolation is initiated automatically. Isolation means that the redundant flaps in the extract and air conditioning pipes and a motor-operated valve in the waste water pipe are closed. The latter pipe is also sealed passively by a water column.

### 3. ADOPTED METHODOLOGY AND SCOPE OF THE ANALYSES

The methodology adopted within the level-1 analysis was designed to provide a pragmatic utilization of manpower and resources within the overall standard analysis required for a comprehensive PSA. The first phase was the qualitative development of the 'Risk Model', which consists of the following components:

- Definition of safety functions of the reactor, and the systems which provide those functions
- Identification of initiating events
- Determination of success criteria and
- Event tree development.

Once an initial risk model was established an initial screening quantification exercise was commenced. Within the screening quantification, initiating event frequencies and the failure probabilities of the safety systems were assigned taking into consideration such factors as level of redundancy/diversity within systems, feasibility of human actions, feasibility of recovery actions etc. From this screening quantification exercise, a list of risk dominant core damage scenarios were derived, which were then re-examined, using specific assessments for the particular accident scenario. At this stage, the results of the fault tree and human factor analysis etc. were available and were incorporated into the re-assessment.

In order to structure the analysis within the PSA the initiating events were grouped as follows:

- A: Loss of primary coolant
- B: Increase in reactivity
- C: Failure of support systems (including grid supply)
- D: Other initiating events (e.g. reduction in primary flow)
- E: External events like fire, flood.

The data utilized in the fault trees came from a number of sources and where possible plant specific data was used. Where this was not possible generic information from the DIDO reactor family was utilized to estimate an appropriate probability. The common mode failure (CMF) probability of redundant systems was evaluated by the so-called  $\beta$ -factor method with a fraction of 10 % of the independent failure rate, in general; only for the CCAs was a specific

investigation of the CMF probability carried out on the basis of historical failures due to sticking CCA blade bearings.

Two types of human actions were considered explicitly, both concerned with hypothetical situations where the automatic safety systems are assumed to have failed. These are: specific emergency procedures, well defined, and recovery procedures, less well defined. The so-called THERP model was used for assessing human reliability, taking into account the complexity and time available for the specific procedure. In general, a lower limit of  $1 \cdot 10^{-3}$  was placed on the failure probability of any single operator action.

The containment analysis (level-2 PSA) was separated from the level-1 PSA. It encompassed the assessment of the failure probability of the isolation function and the deterministic analysis of the containment behavior and its retention capability for fission products in the most probable core melt-down scenarios. The fault tree analysis for the isolation function took into account interdependence with other safety functions, for instance due to common support systems or due to a common signal of the plant protection system.

According to the objective of the analyses, emphasis was placed on the evaluation of direct radiation from the reactor hall in the case of a core melt-down accident, since the accessibility of the periphery of the unshielded hall is a crucial aspect for the feasibility of mitigating accident measures. The results of the source term estimation for the most probable core melt-down scenarios were used to assess the radiation exposure in the environment on the basis of the calculation procedure required for design basis accidents. This pessimistic procedure is consistent with the objective of the analyses, but contradicts the procedure of a risk analysis.

The full-scope PSA included a number of deterministic analyses in order to clarify the response of the plant to the various accident conditions and determine the success criteria of the safety systems /3/. A lot of difficulties were encountered due to the lack of computational tools and knowledge, particularly in the range of those beyond design basis accidents associated with damage to the core. Thus, some results were based on engineering judgment and assessments.

#### 4. MAIN RESULTS

Table 1 gives a summary of the main results of the level-1 PSA. The total core damage frequency amounts to  $1.5 \cdot 10^{-4}/a$ . This value is consistent with the results of PSA for other research reactors like DIDO & PLUTO at Harwell and the HFBR at Brookhaven /4/.

The dominant contribution (about 62 %) stems from the so-called interfacing system LOCAs by-passing the ECCS because the leaking water does not return to the  $D_2O$  plant room. The underlying leak is of such a size that it is difficult to isolate manually in time. Additionally, there is not enough time for the LWIS to be brought into operation with a high degree of reliability. More than two thirds of this contribution is caused by the rupture of a measuring pipe which leads from the primary circuit to instrumentation outside the plant room. The re-

maintaining one third of the dominant contribution refers to a certain leak category within the D<sub>2</sub>O purification plant outside the D<sub>2</sub>O plant room. This sequence includes failure of the redundant isolation valves automatically closed in a LOCA. It should be mentioned that the comparatively high frequency of this sequence is caused by rather pessimistic estimates of LOCA frequencies for the purification plant, the installation of which outside the D<sub>2</sub>O plant room at FRJ-2 is unique for the family of DIDO reactors.

LOCAs combined with the early failure of the ECCS also contribute significantly to the overall core damage frequency but they proved less dominant than the NON-LOCAs Without Scram. This group, as well as the group of LOCAs Without Scram, includes sequences in which there is a sudden loss of flow because the main pumps are tripped either spuriously or legitimately. These events normally result only in the demand of the CCA shutdown system, leaving the RSR system without any signal to operate. Common mode failure of the CCA system will then create an accident without scram, resulting in some core damage /3/. It should be noted that the integrity of the primary circuit is not affected by the core damage and remains closed unless the initiating event itself has violated the integrity.

All dominant groups except the LOCAs with early ECCS failure can be reduced in frequency by minor plant modifications. These modifications are:

- Interfacing System LOCAs:

The installation of throttling discs into the measuring pipe and the feedback of primary coolant leakages from the purification plant into the D<sub>2</sub>O plant room.

- Non-LOCA and LOCA Without Scram:

The additional demand of the RSR system to shut the reactor down in accidents involving an initial loss of flow.

These three modifications would reduce the core damage frequency to about  $4 \cdot 10^{-5}$ /a. Most of the sequences result in a core melt-down due to the loss of coolant inventory either by boil-off or by leakage. In both cases, the integrity of the primary circuit is violated so that fission products are released into the reactor hall where they are retained with a high degree of reliability. The failure probability of the containment isolation proved to be  $7 \cdot 10^{-3}$  per demand so that the overall frequency of a major release of fission products from the plant is about  $3 \cdot 10^{-7}$ /a after the minor modifications of the plant have been realized.

One of the major findings of the deterministic analyses was the fact that core damage accidents do not cause an overload of the reactor hall. Even if the residual power after a core melt-down is consumed completely for continuous steam production, the pressure inside the hall would not exceed one third of the design overpressure. Three effects are responsible for this behavior, namely the thermal power decreasing with time, the heat dissipation to the environment increasing with temperature and the leak rate of the shell increasing with pressure. The quantity of deuterium produced in the event of a severe power excursion is limited by the

quantity of aluminum available to such a value that flammability limits can only be exceeded locally but would, by far, not be reached globally.

The quantity of volatile fission products released into the reactor hall in the event of a core melt-down accident proved to depend significantly on whether or not the release path leads via the D<sub>2</sub>O plant room because the room has a good retention capability. This is especially true of cases where the secondary circuit is still running since the heat exchangers provide a large cold surface area for steam condensation and thus for the washout of volatile fission products. The LOCAs with early ECCS failure, representing more than 50 % of the total core melt-down frequency after the above mentioned modification, are included in this group. For iodine, a retention between 87 % and 95 % depending on the operation of the secondary circuit have been assessed.

The total escape factor (quantity of fission products escaping into the environment to the quantity escaping from the core) for 7 days has been assessed to be 4.2 % for noble gases and 0.11 % for aerosols. The dose calculation based on these figures revealed that the effective dose and the bone surface dose of young children and adults remain in the range of the dose limits set by the German Radiation Protection Ordinance /5/ for design basis accidents. The same is true of the thyroid dose at a distance greater than 500 m (adults) and 1100 m (young children), provided the ingestion of foodstuff grown in the vicinity is forbidden after 24 h.

## 5. ACCIDENT MANAGEMENT MEASURES

One important accident management measure proved to be the pressure relief of the reactor tank by opening a manually operated valve in the case of a total failure of after-heat removal by a loss of forced convection either of the primary or of the secondary circuit. The opening of the valve is not necessary to avoid a core melt-down accident, but would avoid a plastic deformation of the aluminum tank, which could occur if the pressure in the tank rises to the set point of the bursting disc in the cover gas circuit. The opening of the valve also facilitates primary feed by the LWIS and bleed for long-term after-heat removal.

Another preventive accident management measure proved to be secondary feed of the heat exchangers from the secondary circuit by discharging the water after it had been heated in the heat exchangers into the sump of the hall. The inventory of the circuit above the heat exchanger level is adequate in combination with heat dissipation from the primary circuit surface for long-term after-heat removal. Secondary bleed also seems to be an appropriate and simple measure to remove the residual heat from the primary circuit in the case of a loss of flow in the secondary circuit. It requires only the manual opening of a vent valve on top of a manifold in order to let the steam produced in the heat exchangers escape. The primary circuit pressure would increase to the acceptable value of 600 mbar.

The LWIS is also very important as a backup system for the ECCS in the case of small LOCAs or any LOCAs associated with late ECCS failure. Depending on the cooling mode of the fuel elements, however, it might be necessary to suck off the water from the reactor hall

into a tank lorry and to re-feed it into the LWIS in order to avoid excess flooding of the hall. This is only possible as long as the core remains intact. In the case of core damage the radiation level around the reactor hall might be too high within the first few days (Fig. 3) /6/. In such a case, an unlimited stay is only possible in the adequately shielded emergency control room and perhaps a short-term stay in its entrance area from where the LWIS is initiated. The shift will be instructed in the emergency handbook to initiate the LWIS even if a core melt-down has already occurred since it is expected that the consequences will be mitigated by such a measure. But the quantity of injected water must then be limited to some tens of tons.

## 6. CONCLUSIONS

As had been expected when the PSA was commissioned, there are possibilities for accident management which strengthen the defence in depth of the plant safety systems without any need for major modifications. The accident management procedures and indicators for minor modifications arise naturally from those PSA insights resulting from investigations beyond the original design basis of the plant.

The PSA has revealed the importance of primary feed and bleed for the overall safety of the plant. If this accident management measure were not possible the core damage frequency would be significantly higher than the value given above. However, the achievement of some numerical reduction in accident probabilities was not the main intention of the PSA-based accident management but rather the logical investigation of possibilities with the outcome of increasing the qualitative depth of defence.

## 7. REFERENCES

- /1/ J. D. C. Henderson and S. A. G. Bottril  
High Power Test Run in D.M.T.R. from 15 to 25 MW  
TRG Memorandum 3593, August 1966.
- /2/ J. Wolters  
Wärmetechnische Anfahrexperimente während und nach der Leistungserhöhung des Reaktors FRJ-2 auf 15 MW (Thermohydraulic Start-Up Experiments during and after the Power Increase of the Reactor FRJ-2 to 15 MW).  
Internal Report ZFR/R2 1/70, April 1970.
- /3/ R. Nabbi, J. Wolters  
Loss of Main Pumps at the Research Reactor FRJ-2 with Delayed or without Scram.  
HTD-Vol. 192, Thermal Hydraulics of Severe Accidents  
Editors: R. M. Singer, and M. S. El-Genk, Book No. H00750-1992.
- /4/ T. L. Chu et al.  
Quantification of the Probabilistic Risk Assessment (PRA) of the High Flux Beam Reactor (HFBR) at Brookhaven National Laboratory (BNL).  
Proceedings of the Safety, Status and Future of Non-Commercial Reactors and Irradiation Facilities, Sept. 31 - Oct. 4, 1990, Boise, Idaho, pp. 607 - 609.
- /5/ German Radiation Protection Ordinance (Verordnung über den Schutz vor Schäden durch ionisierende Strahlen- Strahlenschutzverordnung- in der Fassung der Bekanntmachung vom 30. Juni 1989)  
Bundesgesetzblatt I, pp. 1321/-1962.
- /6/ O. Schaffer  
Strahlenbelastung durch Gammastrahlung aus der Reaktorhalle des FRJ-2 als Folge eines Kernschmelzunfalls mit Spaltproduktfreisetzung (Radiation Exposure by Gamma-Radiation from the Reactor Hall of the FRJ-2 as a Consequence of a Core Melt-Down with Release of Fission Products).  
Document No. KFA-ASS/NST 911, Sept. 1991

Table 1

Accident Group	Core Damage Frequency Contribution	
	exist. Plant	modif. Plant
Non-LOCA Without Scram (U2)	23,8	4
Non-LOCA Without Scram (U1)	0,2	0,2
LOCA Without Scram (U2)	4,0	1
LOCA/Interfacing Systems (U3)	94,8	1
LOCA/Early ECCS Failure (U3)	16,9	16,9
LOCA/Late ECCS Failure (U3)	0,5	0,5
Non-LOCA/Early Primary Flow Failure (U3)	0,5	0,5
Non-LOCA/Late Primary Flow Failure (U3)	3,3	3,3
LOCA/Primary Flow Failure (U3)	1,1	1,1
Non-LOCA/Early Heat Removal Failure (U3)	3,8	3,8
Non-LOCA/Late Heat Removal Failure (U3)	0,3	0,3
Miscellaneous (U3)	4,4	4,4
<b>Total</b>	<b>153,6</b>	<b>37</b>

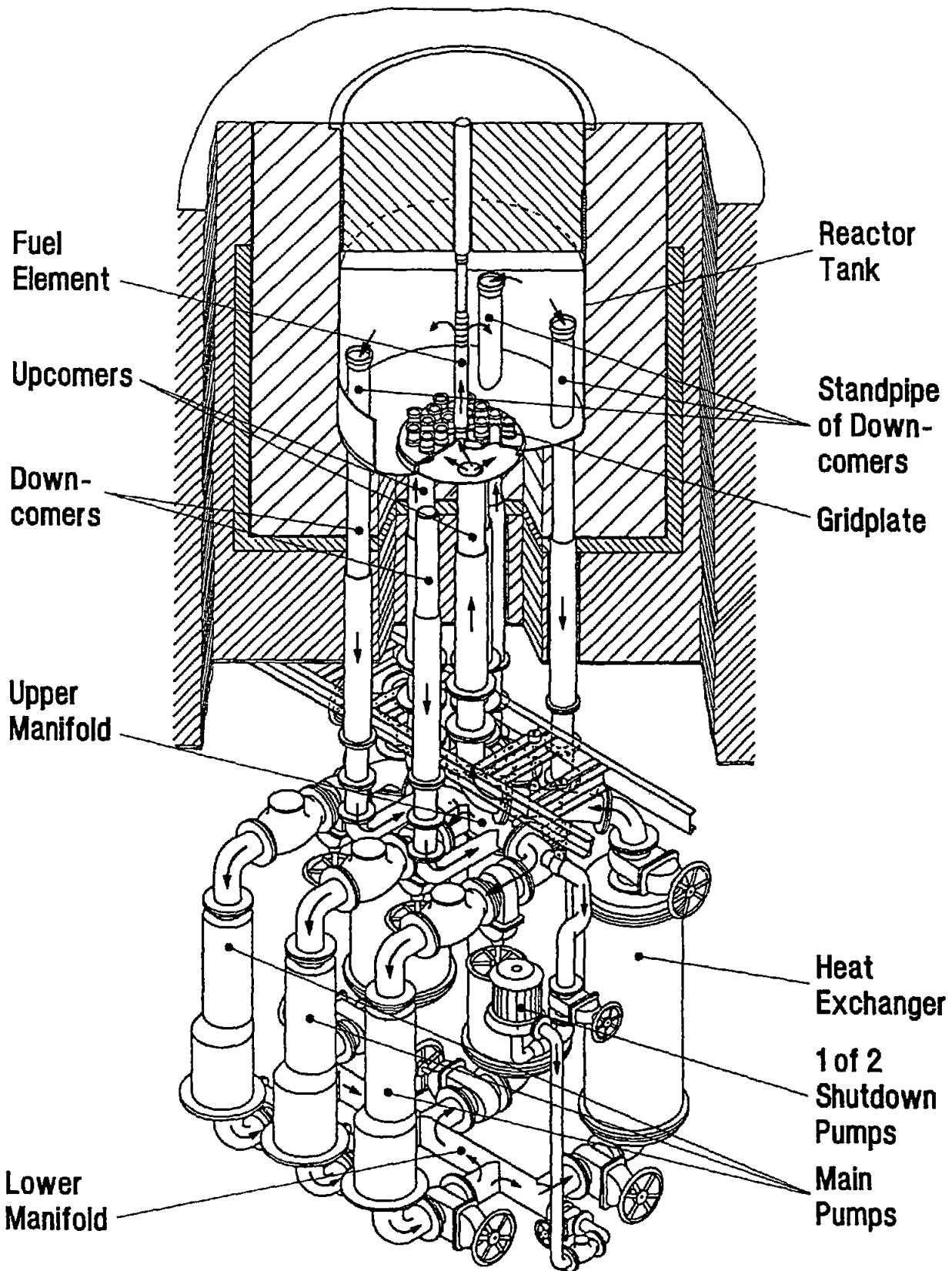
Core Damage Frequency by Accident Groups in Units of  $1 \cdot 10^{-6}/a$

U1 Fast Core Melt-Down

U2 Damage of a Few Fuel Elements

U3 Slow Instantaneous or Delayed Core Melt-Down

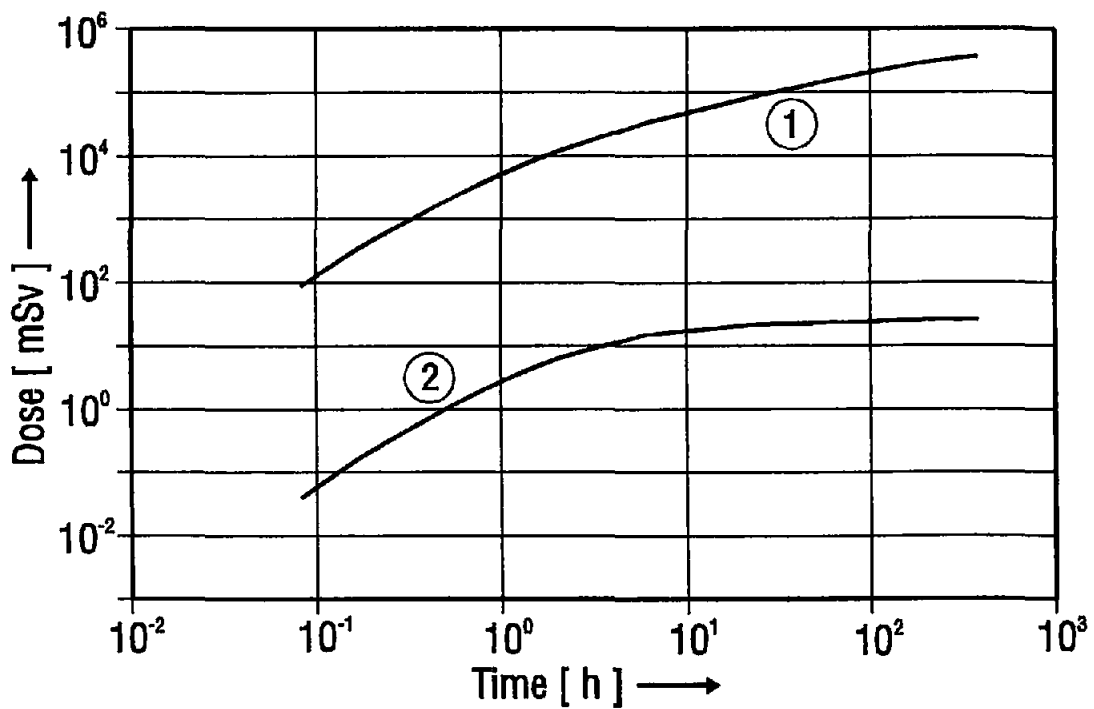
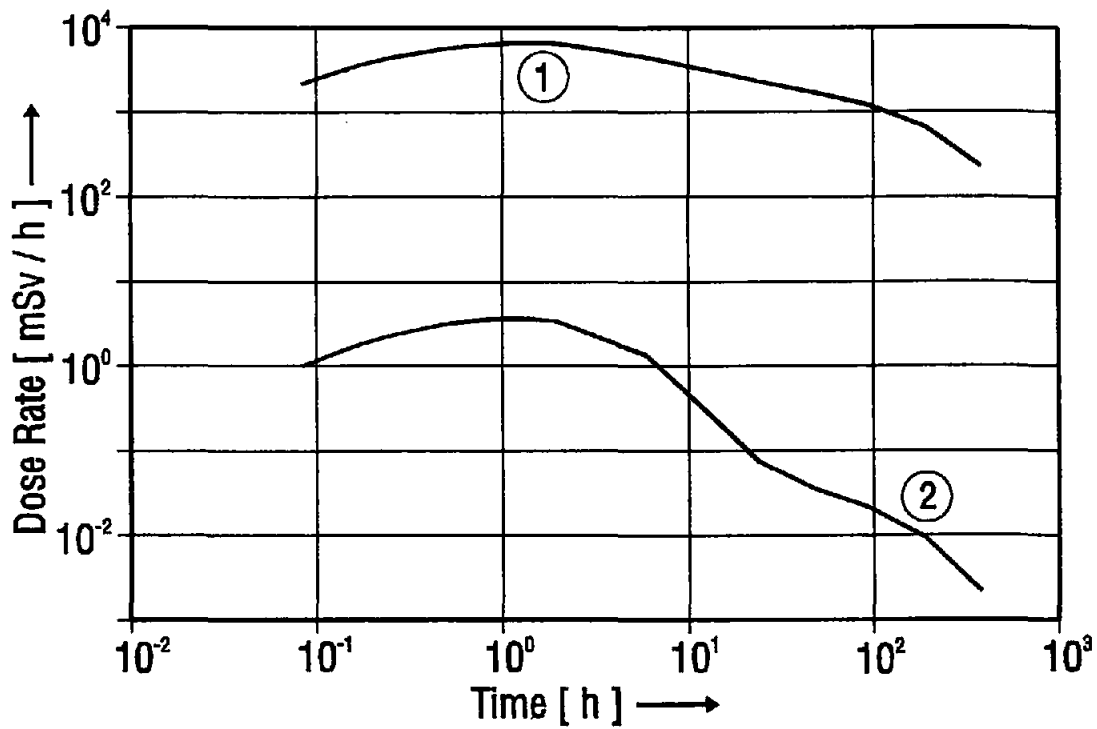




**Perspective View of the Arrangement of the Reactor and the Primary Circuit of FRJ-2**

**Fig. 1**





Radiation Exposure versus Time in a Distance of 50 m from the Center of the Reactor Hall

- ① Unshielded Area
- ② Emergency Control Room ( 0.9 m Concrete )

Fig. 3

## III-9

### NEUTRON SOURCES FOR THE RESEARCH OF CONDENSED MATTER

W. KNOP

1. INTRODUCTION  
(EXAMPLES)
2. NEUTRON SCATTERING  
AND INSTRUMENTATION
3. NEUTRON FLUX -- INSTRUMENTATION
4. SMALL REACTORS (GKSS)
5. CONCLUSION

#### Examples for application

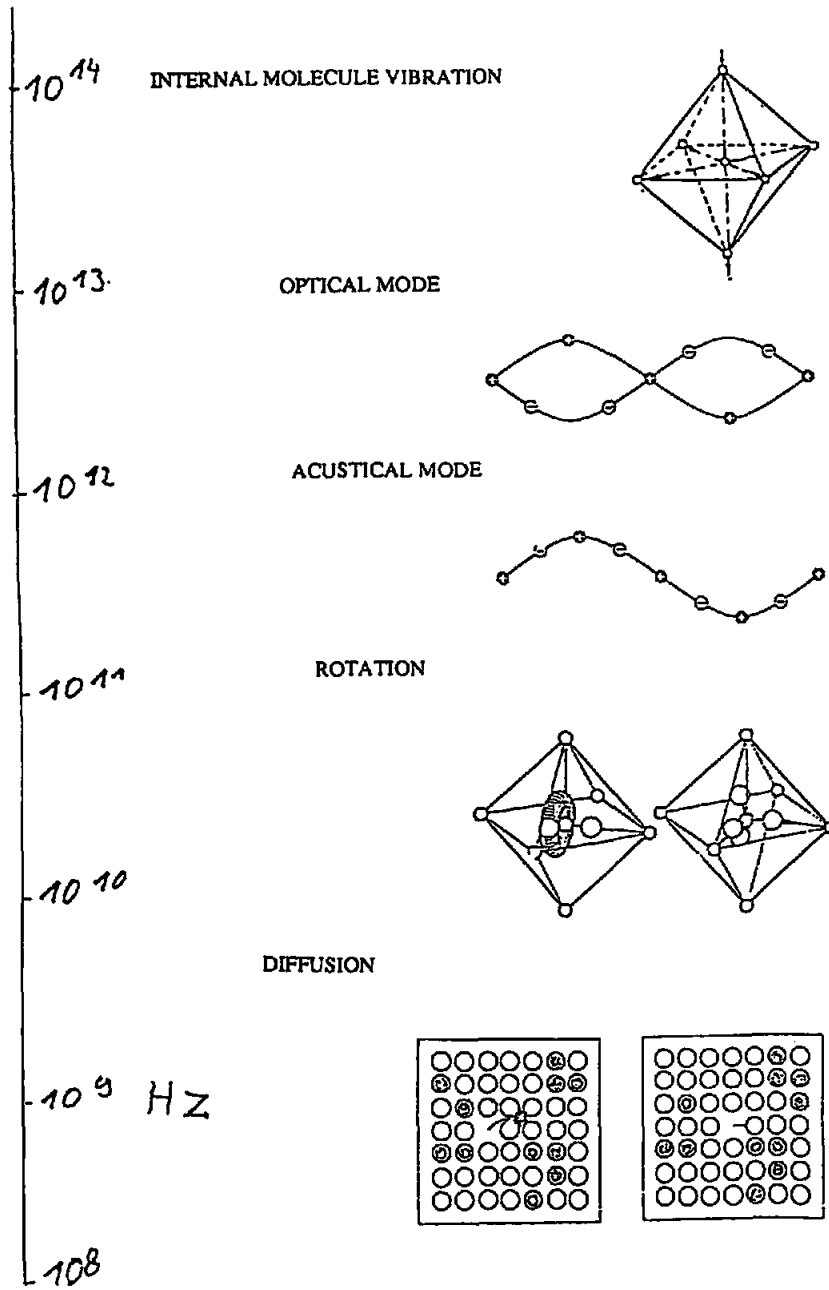
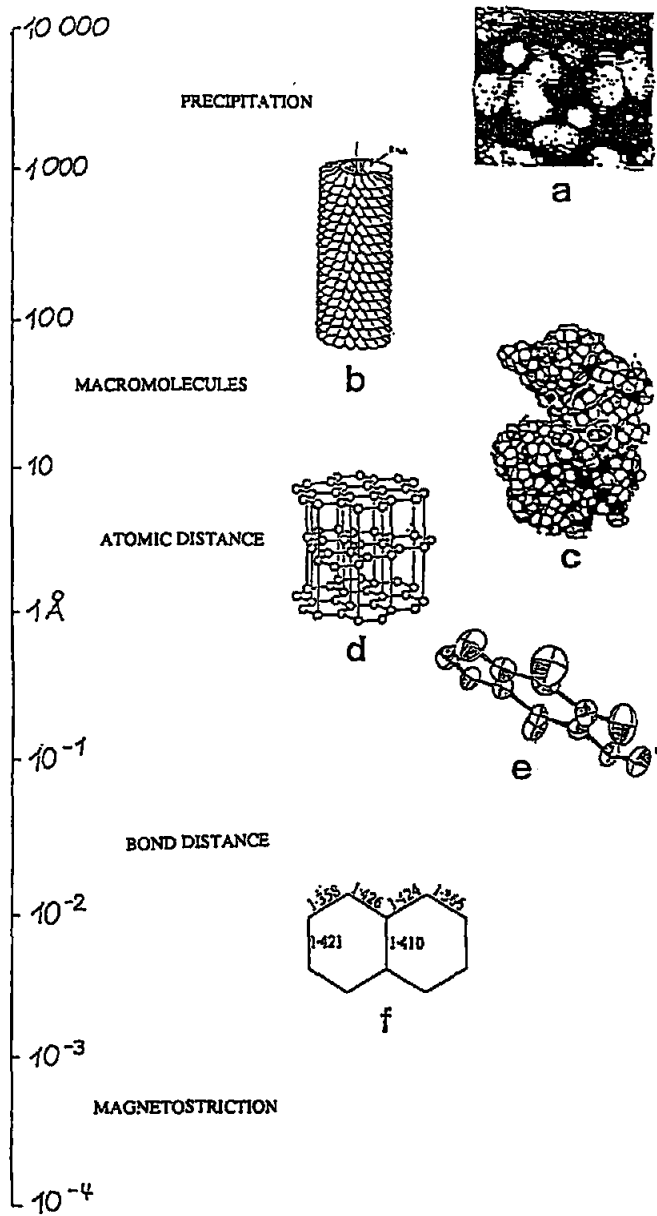
Knowledge of the structure and dynamics on a microscopic (atomic) level is necessary for understanding the macroscopic behavior of matter.

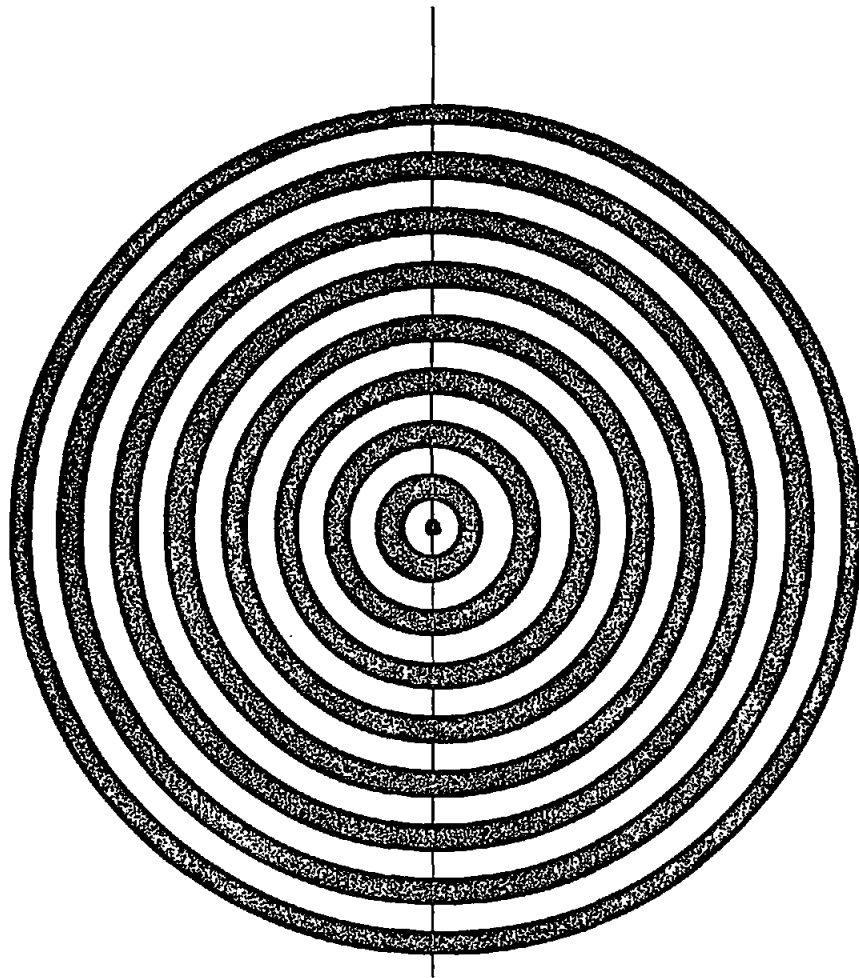
Examples :

Structure	Dynamic
crystall structure	lattice dynamic
magnetism	magnetic excitation
phase transition (order / disorder)	dynamics of liquids
biological structure	molecular dynamic
material	diffusion
texture	
configuration of polymer	
imperfection	
conduction electrons density	
radiation damage	
chemical bond distance	

Therefore

Neutron scattering experiments are a powerful technique to study the microscopic behavior of matter for physics, chemistry, material research, biology and geology.





WEAK INTERACTION

THICK SAMPLE

NUCLEUS SCATTERING

HYDROGEN (PROTONS)  
ISOTOPS  
*different scattering  
length for isotops*

MAGNETIC MOMENT

*interaction with  
the magnetic moment  
of electrons and nucleus*

WAVELENGTH  
COMPARABLE TO  
ATOMIC DISTANCE

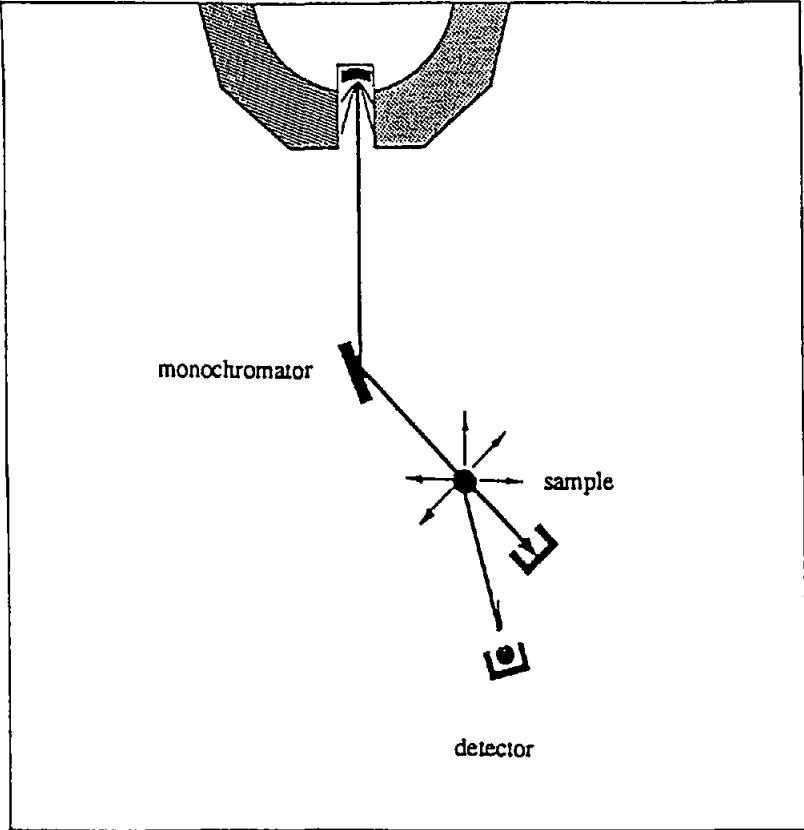
*determination of  
lattice parameter and  
atom position*

*Energy comparable  
to momentum  
of atoms*

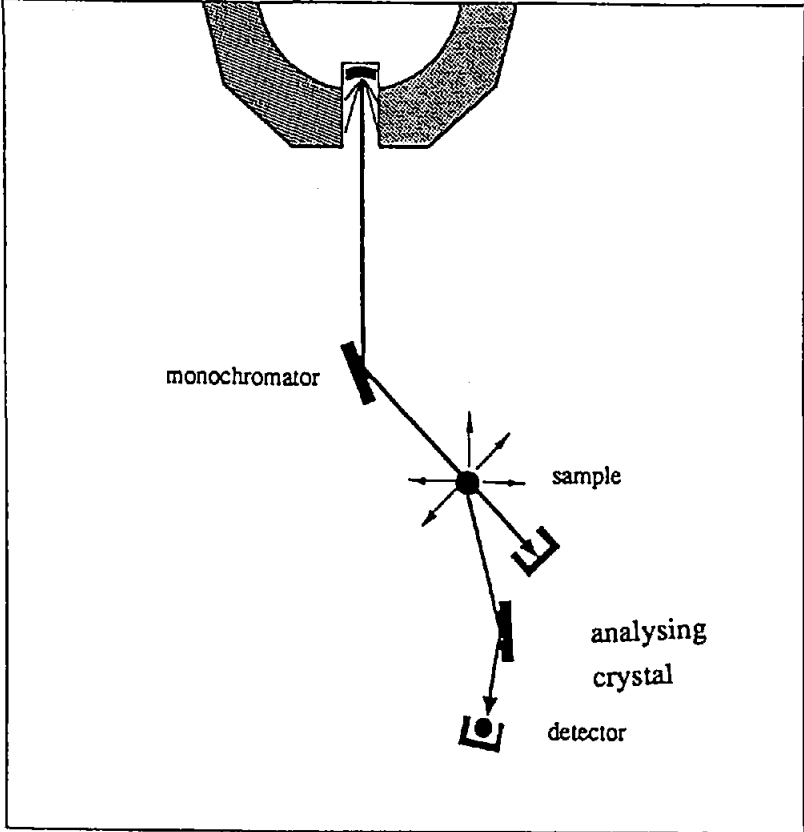
*direct determination  
of the forces between  
the atoms.*

# Neutrons scattering instrumentations

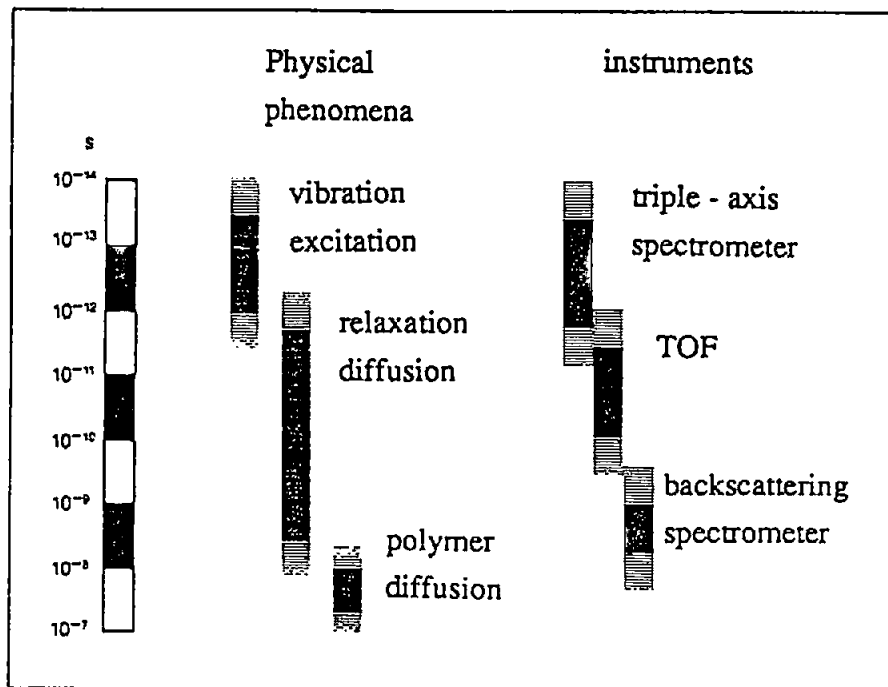
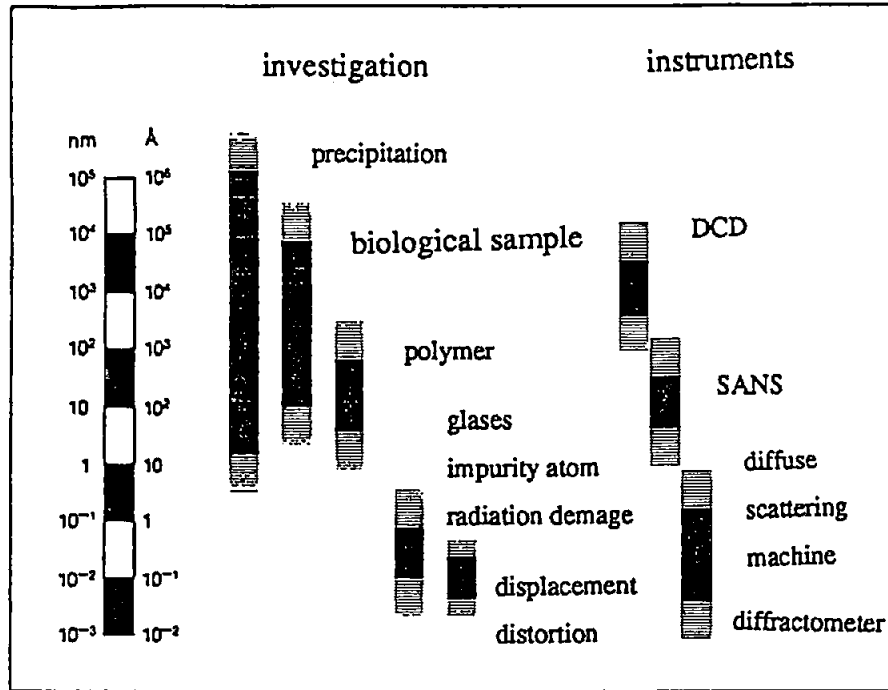
elastic scattering



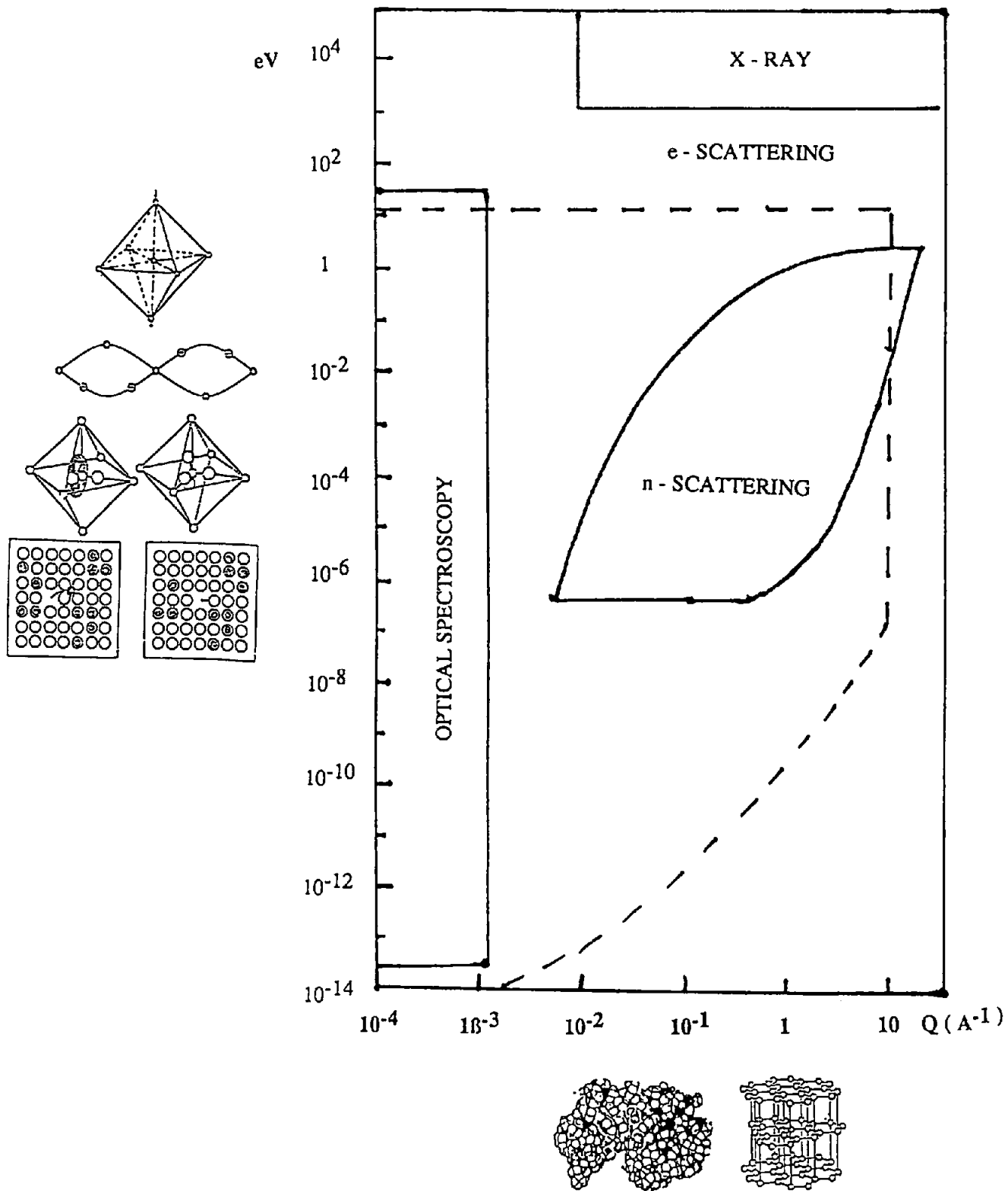
triple - axis spectrometer  
inelastic scattering



## Opposition of the different instruments and investigations







$$\sigma_{TOT} = \sigma_{coh,nucl} + \sigma_{coh,magn} + \sigma_{quasiel} + \sigma_{inel} + \sigma_{inc} + \sigma_{pol}$$

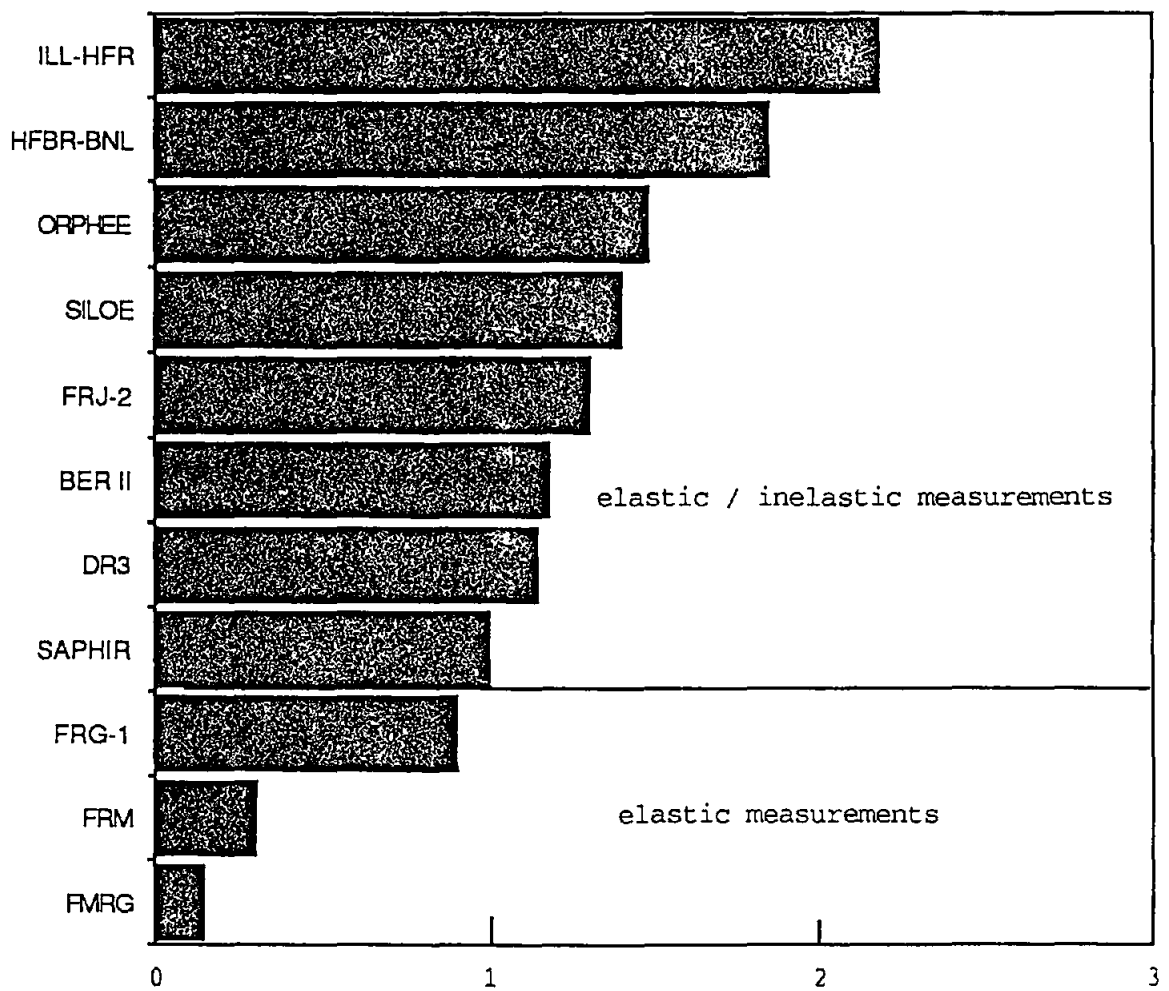
long range order

SRO

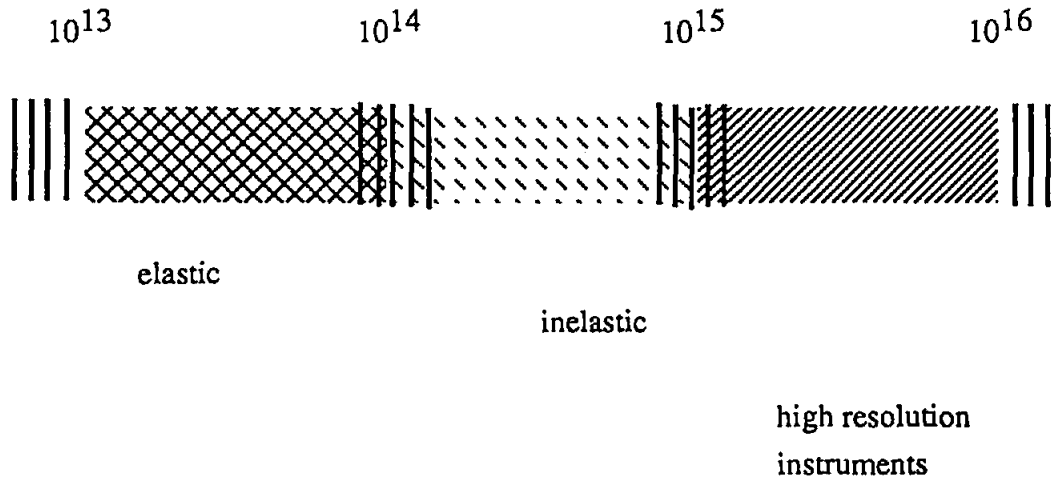
excitations

elastic scattering

inelastic scattering



## General opposition of neutron flux and experimental technics



HFR : -- make it possible to use advanced diffractometer as for high energy - and momentum - transfer resolution about magnetudes.  
Novel and unforeseen results are expected with these instruments.

-- short measurement times

-- more proposales as measurement time  
( strong limitation of measurement - times )

**Therefore we need a new high flux neutron source ( ANS ) .**

## " SMALL " REACTORS P < 10 MW

**Advantage :** No strong limitation of time of measurement as for HFR.

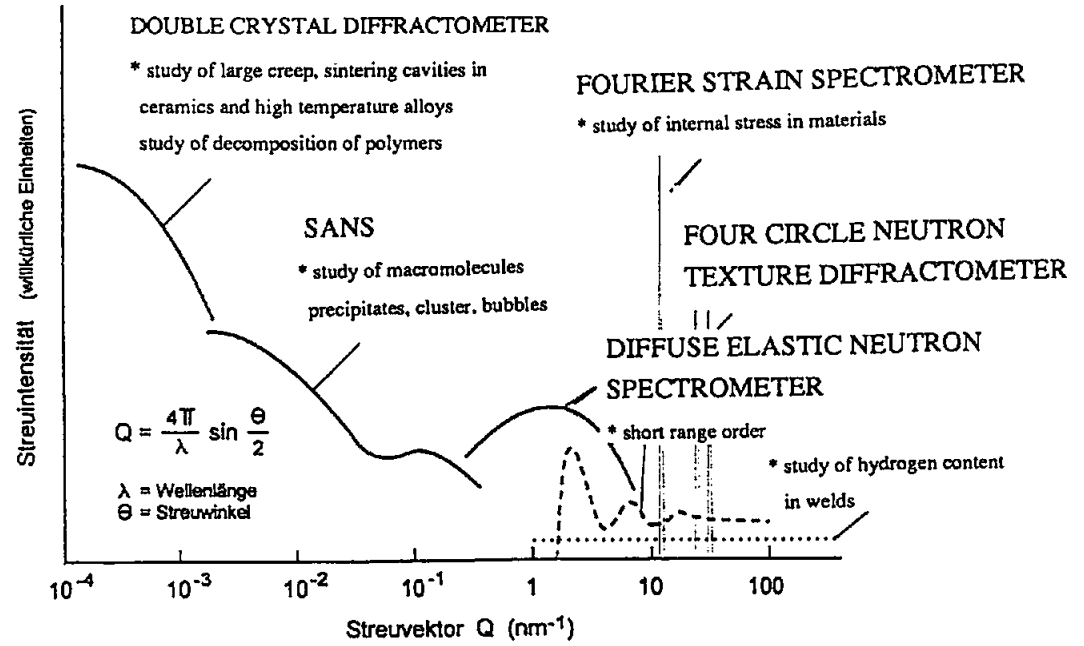
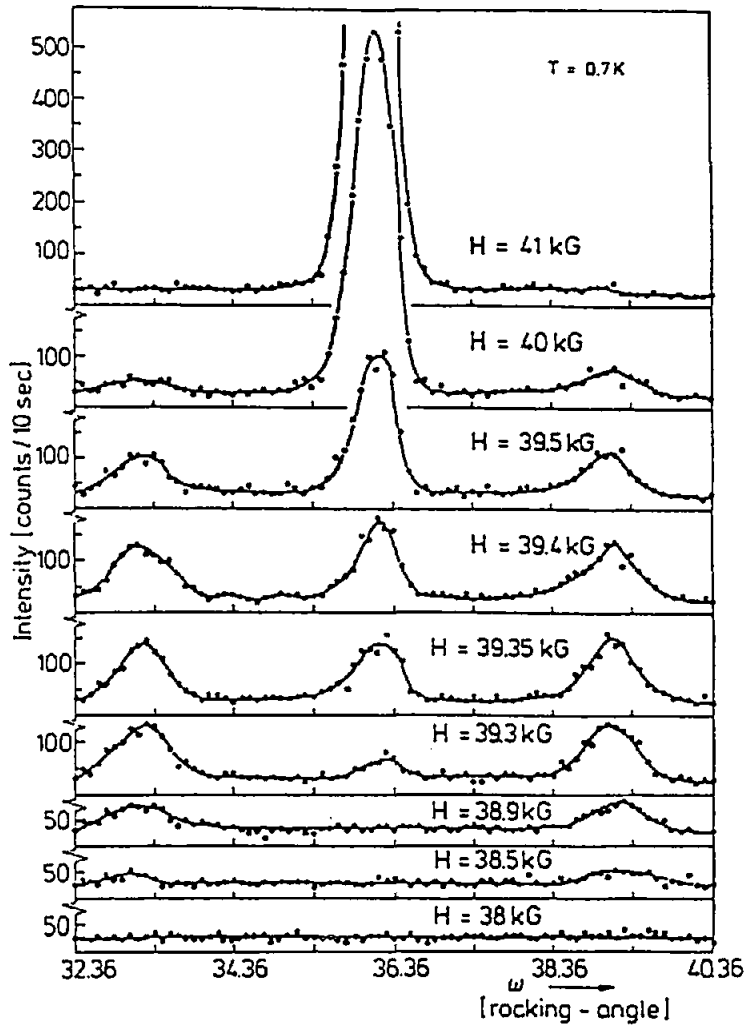
Therefore it is possible to study in detail structure and phase diagram etc.

### Improvement of experimental facilities ( example GKSS )

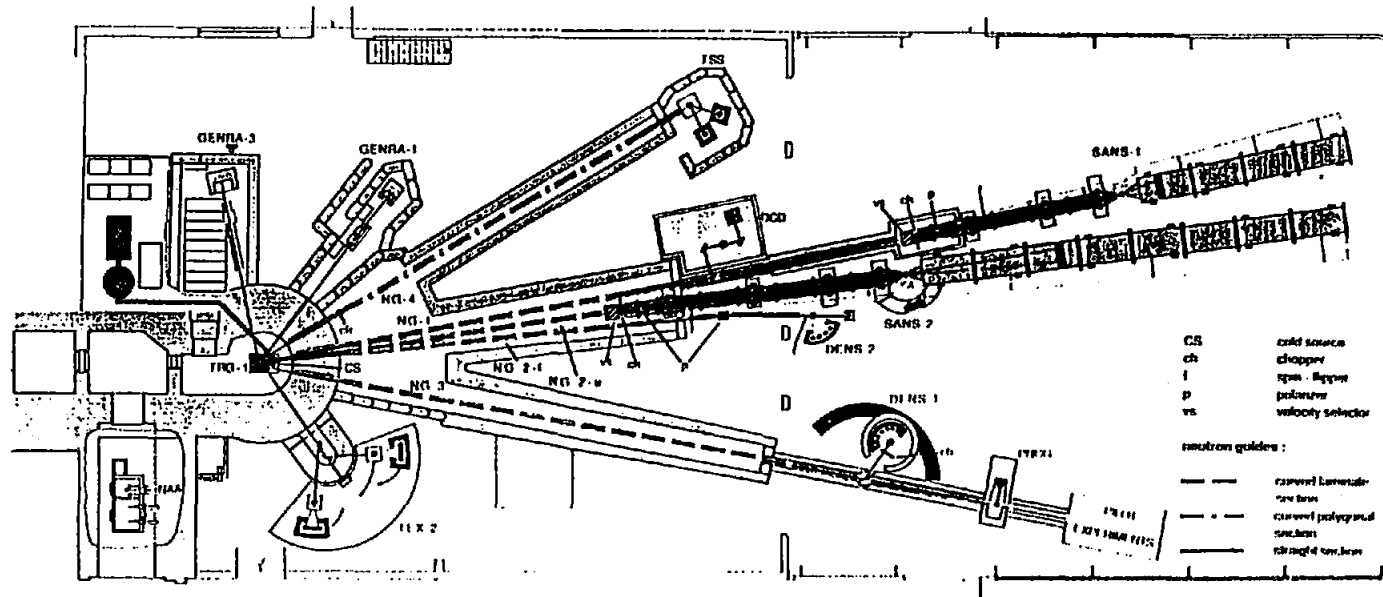
Improvement	Gain
<u>reactor</u>	
HEU --> Leu compact core	2
<u>experiment</u>	
better selector	1.25
detector / electronic	1.2
	-----
	3

in addition : using multi - or area detectors for simultaneous neutron measurements.

Figur 1



Neue Experimente und neue Neutronenleiter am FRG-1 Forschungsreaktor  
 New Instrumentation and Novel Neutron Guides at the FRG - 1 Research Reactor



323

**NEUTRON SCATTERING FACILITIES FOR MATERIALS RESEARCH**

- SANS:** **SMALL ANGLE NEUTRON SCATTERING FACILITY**
- SANS 1: study of organic macromolecules using the interaction of polarized neutrons with polarized targets
  - SANS 2: study of precipitates, clusters, voids and bubbles in crystalline and amorphous solids with unpolarized or polarized neutrons
- DCD:** **DOUBLE CRYSTAL DIFFRACTOMETER**  
 study of large empty, tubular and swirling cavities in ceramics and high temperature alloys  
 study of decomposition of polymers
- DENS:** **DIFFUSE-ELASTIC NEUTRON SPECTROMETER**
- DENS 1: study of short range order and clustering
  - DENS 2: study of hydrogen content in welds and heat affected zones
- FSS:** **FOURIER STRAIN SPECTROMETER**  
 study of internal stresses in materials
- TEX-2:** **FOUR-CIRCLE NEUTRON TEXTURE DIFFRACTOMETER**  
 study of textures in metals, alloys and geological samples

**USE OF NEUTRONS FOR ENVIRONMENTAL RESEARCH PURPOSES**

- NAA:** **NEUTRON ACTIVATION ANALYSIS**  
 detection of trace elements in samples for environmental research  
 chemical analysis of alloys
- PNCG:** **PROMPT NEUTRON CAPTURE GAMMA-RAY SPECTROMETER**  
 detection of trace elements in samples for environmental research
- GENRA-1; GENRA-3:** **GEESTRACHT NEUTRON RADIOGRAPHY FACILITIES**  
 non-destructive analysis of materials

**NEUTRON GUIDES**

Neutron Guide	l	g/mm	A <sub>0</sub> /mm	A <sub>1</sub> /mm	R/mm	L <sub>1</sub> /m	L <sub>2</sub> /mm	coating
NG 1	3	9.0	30	90	1040	13	0.20	<sup>238</sup> U
NG 2 <sub>W</sub>	2	14.1	30	40	900	13	0.28	<sup>238</sup> U
NG 2.1	3	9.0	30	40	270	14	0.45	<sup>238</sup> U
NG 3	4	9.1	42	100	4400	24	0.10	<sup>238</sup> U and SM
NG 4			15	106	3000	19	0.16	1a (nat)

(l) number of channels in laminate section, A<sub>0</sub>: total beam width; A<sub>1</sub>: beam height; R: curvature radius, L<sub>1</sub>: length of curved section, L<sub>2</sub>: characteristic wavelength, SM: supermirror coating on top and bottom

Abb. 10/fig. 10:

CS: Kälte Neutronenquelle; GENRA: Neutronen-Radiographie; FSS: Fourier Spannungs-Spektrometer; DCD: Doppel Kristalldiffraktometer; SANS: Neutronen-Kleinwinkel-Streueinrichtung; DENS: Diffus-elastisches Neutronen-Spektrometer; PNCG: Prompte Neutronen-Einfang-Spektroskopie; TEX-2: Vierkreis Neutronen-Textur-Diffraktometer; NAA: Neutronen Aktivierungsanalyse.

## CONCLUSION

- \* Neutron scattering experiments are a powerful probe for the study of the microscopic behavior. Therefor an increasing need of new neutron sources exist world wide.
- \* For the future, high flux sources are necessary to measure novel and unforeseen results with high resolution instruments.
- \* Small reactors can be used for extensive and detailed neutron measurements. The neutrons which are at disposel, should be effectly used by improvement of the facility.

## Development of Supermirror and Neutron Bender

Kazuhiko SOYAMA Masatoshi SUZUKI Yuji KAWABATA\*

Department of Research Reactor  
Tokai Research Establishment, JAERI  
Tokai-mura, Naka-gun, Ibaraki-ken, 319-11

\*Research Reactor Institute  
Kyoto University  
Kumatori-cho, Sennan-gun, Osaka 590-04

### ABSTRACT

The morphology and multilayer structure of Ni/Ti supermirrors which were deposited by evaporation system, have been investigated using neutron spectroscopy, Heterodyne profiler, TEM, and ESCA profiler. High reflectivity supermirror ( $>0.90$ ) has been made by restraining surface roughness of the substrate, and the possibility to make a titanium oxide for diffusion barrier has been offered. The design of its application such as a neutron bender and a supermirror guide system applied to irradiation facility for cancer treatment, will be described.

### 1. Introduction

The concept of supermirror<sup>1</sup> which was first proposed by F.Mezei in 1976, is based on Bragg diffraction by multilayer<sup>2,3,4</sup>, whose bilayer thickness is gradually changed to enlarge the critical angle of total reflection and to obtain reflectivity over a wide band of wavelength. The critical angle of total reflection for natural nickel is  $1.7\text{mrad}/\text{\AA}$ , and that of  $^{58}\text{Ni}$  is  $2.0\text{mrad}/\text{\AA}$ . The supermirror can extend the critical angle of total reflection 2~3 times larger than that of natural nickel. It has the advantage that if the critical angle can be increased by a factor  $m$  then the flux gain at the end of a neutron guide would be increased up to  $m^2$ . So we may get higher neutron flux by one order of magnitude by replacing the existing nickel guide to the supermirror guide.

It was confirmed at the early stage of supermirror development that measured reflectivity is smaller than theoretical estimation, and it is caused by imperfections which are dependent on flatness and roughness of the substrate, crystallization in the layer, and inter-diffusion between layers. In these two decades, many works were made to improve the performance of supermirror, especially to minimize the imperfections in the layers and obtain high reflectivity.<sup>5,13,14</sup>

There are now increasing demands for the multilayer and supermirror in order to transport, monochromate, focus, and polarize neutron beam for various beam experiment such as neutron scattering, prompt- $\gamma$  activation analysis, neutron radiography and so on. Recently JAERI has upgraded JRR-3,<sup>6,7,8,9</sup> and installed the cold neutron source and the neutron guide tubes to meet the increasing demands. The development of neutron optical device and its application has been progressed.<sup>15,16,17,18</sup>

This paper describes the development of Ni/Ti supermirror at JAERI. The morphology and multilayer structure in the supermirror were investigated in order to improve the performance by various methods of neutron spectroscopy, heterodyne profiling, transmission electron microscopy, ESCA depth profiling from the point of roughness of the substrate, crystallization in the layer, and inter-diffusion between layers. We present the design of



application devices using supermirror such as a neutron bender and a supermirror guide tube also.

## 2. Reflectivity of supermirror

The neutron reflectivity of supermirror was estimated by using neutron optical method which was introduced by Yamada et al.,<sup>11</sup> Schelton and Mika.<sup>12</sup> In this method, each layer of a supermirror is described by one-dimensional square potential for the component of the incident plane wave perpendicular to the surface. The heights of the potential is given in a homogenous layers by the average value of the Fermi pseudopotential as follows:

$$V = \frac{2\pi h^2 \rho b}{m}$$

where  $\rho$  is the number of atoms per unit volume,  $b$  is the average coherent scattering length,  $h$  is Planck' constant, and  $m$  is the neutron mass. They are related to the refractive indices of the layers:

$$n = (1 - \lambda^2 2mV/h^2)^{1/2} = (1 - \lambda^2 \rho b/\pi)^{1/2}$$

where  $\lambda$  is the wavelength of the incident neutron.

Since the conditions of continuity for wavefunction and its derivative are imposed, a matrix characterizing each layer was obtained. In the supermirror composed of  $N$  layers, the reflectivity  $R$  and transmittivity  $T$  of the multilayer are expressed by the following equations:

$$R = |r|^2, \quad T = |t|^2 n_g/n_0$$

$$\begin{pmatrix} t \\ i n_g \end{pmatrix} = M \begin{pmatrix} 1 + r \\ i n_0 (1 - r) \end{pmatrix}$$

$$M = \sum_{j=1}^N M_j \quad M_j = \begin{pmatrix} \cos n_j k_0 d_j & n^{-1} \sin n_j k_0 d_j \\ n^{-1} \sin n_j k_0 d_j & \cos n_j k_0 d_j \end{pmatrix}$$

where  $n_0$  and  $n_g$  are the refractive indices of the media before and behind the multilayer respectively.  $n_j = (\lambda^2 \rho_j b_j / \pi - 1)^{1/2}$  and  $k_0$  is the wave vector of the incident neutron perpendicular to the surface.  $d_j$  is the thickness of the  $j$ th layer.

An empirical relation for the thickness of supermirror was used to calculate reflectivities of supermirrors which was proposed by Yamada et al..<sup>11</sup> The decrements of thickness of layers are given by,

$$d_{j-1} - d_j = \Delta (d_{\max}/d_{j-1})^a, \quad j=2, \dots, N;$$

$$d_1 = d_{\max}$$

with  $d_N \leq d_{\min} < d_{N-1}$

where  $d_j$  is the thickness of the  $j$ th layer, and  $d_{\max}$  and  $d_{\min}$  are the maximum and the minimum thickness respectively.  $\Delta$  is the initial decrement and  $a$  is the parameter which determines the distribution of thicknesses.

### 3. Supermirror deposition

Ni/Ti supermirror and multilayer were deposited by a vacuum evaporation system with electron beam gun. Pressure in the chamber before the deposition process is less than  $1 \times 10^{-6}$  Torr. The deposition process was carried out at  $7 \times 10^{-6}$  Torr. The deposition rate was  $0.5 \text{ \AA sec}^{-1}$  and are monitored with quartz crystal oscillator. Substrates were polished float-glass  $300 \times 100 \text{ mm}^2$  and silicon substrate. The vacuum chamber has a large volume of 80 cm diameter and 100cm height.

### 4. Characterization

#### 4.1 Experimental method

##### Neutron reflectometry

Reflectivity measurements were performed on a time of flight spectrometer installed at the JRR-3M at JAERI. Experiments were done at a grazing angle  $\theta \approx 1 \times 10^{-2}$  rad, with an angular resolution  $\Delta\theta/\theta$  of the order of  $1 \times 10^{-3}$  rad and with neutrons of wavelength over a spectral range of  $\lambda$  from 1 to  $8 \text{ \AA}$ . A schematic diagram of the TOF spectrometer at the JRR-3M is shown in Fig.1.

##### Heterodyne profiler

The surface roughnesses of the float glass substrates, were measured by Heterodyne profiler, Zygo5500 which is the interferometer optomechanical system using laser. Repeatability and height sensitivity of less than  $1 \text{ \AA rms}$ .

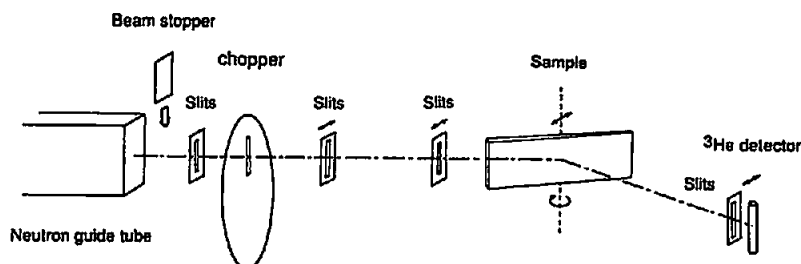


Fig.1 A schematic diagram of the TOF spectrometer at the JRR-3M

##### Transmission electron microscopy (TEM)

The morphology and multilayer structure in the layers were studied using JEM-4000EX, high resolution electron microscope operated at 400kV. The lattice resolution is  $1.4 \text{ \AA}$ , and the grain resolution is  $1.8 \text{ \AA}$ . Samples were cut and bonded face-to-face. They were mechanically polished to around  $100 \mu\text{m}$ , and finally perforated by ion milling caused by Ar-sputtering .

##### Electron spectroscopy for chemical analysis (ESCA)

Depth profiles of atomic density were studied by using ESCA-850, electron spectroscopy for chemical analysis. Deposited samples were cut by diamondcutter. Cross-sectional samples  $5 \times 5 \text{ mm}^2$  were prepared, and were studied by Ion milling caused by Ar-sputtering operated at  $1.5 \text{ kV}, 25 \text{ mA}$ . The depth resolution is around  $40 \text{ \AA}$

#### 4.2 Experimental results

##### Surface roughness of the substrate

The reflectivity measurements of the supermirror deposited on float-glass substrates with different surface roughness, were performed on a TOF spectrometer installed at the JRR-3M. The surface roughness of the polished substrate is  $5.1 \text{ \AA rms}$  and  $30.9 \text{ \AA peak-to-valley}$ , that of non polished substrate is  $7.6 \text{ \AA rms}$  and  $45.4 \text{ \AA peak-to-valley}$ , and the rough polished

substrate is 10.0 Å rms and 59.8 Å peak-to-valley, measured by Heterodyne profiler. Table 1 shows the surface roughness of each float-glass substrate. Fig.3 shows the estimated and measured reflectivities of the Ni/Ti supermirrors with 125 layers whose minimum width of layer is 75 Å.

The estimation of reflectivity of the supermirror was based on the neutron optical method. In this model, flat surface was assumed at the interface between substrate and supermirror, and also at interface between layers. The line shows the estimated reflectivity of the supermirror with the critical wavelength 300 Å, which is as half as that of natural Ni. It is almost unity for wavelength longer than the critical wavelength. The measured reflectivities increase rapidly also at the critical wavelength. It becomes higher with increasing neutron wavelength up to unity for wavelength longer than the critical wavelength of natural Ni. The reflectivity of supermirror in the bragg peak region, strongly depends on the surface roughness of the substratum. The reflectivity of supermirror deposited on the polished substrate is greater than 90%.

### Crystallization

The morphology and multilayer structure of the supermirror were observed using Transmission Electron Microscopy (TEM). Fig.4 shows the TEM image for the Ni/Ti multilayer consisting of 20 bilayers with  $d=150$  Å near the silicon substrate. The dark layers correspond to Ni layers and the bright layers correspond to Ti layers. It is seen the Ni/Ti multilayer had smooth and uniform interface. Fig.5 shows the TEM image for the same sample which was observed in the upper bilayers. The layer is beginning to undulate with increasing the number of layers. The  $d$ -spacing is maintained, but interface has big undulation in layer thickness. The crystallization of the Ni layers is observed, and Ti layers shows amorphous structure with some crystallized regions.



Fig.4 Cross-sectional TEM image for the Ni/Ti multilayer near the silicon substrate

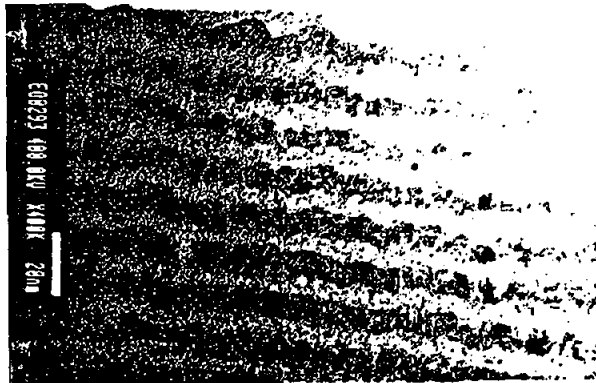


Fig.5 Cross-sectional TEM image for the Ni/Ti multilayer in the upper layers

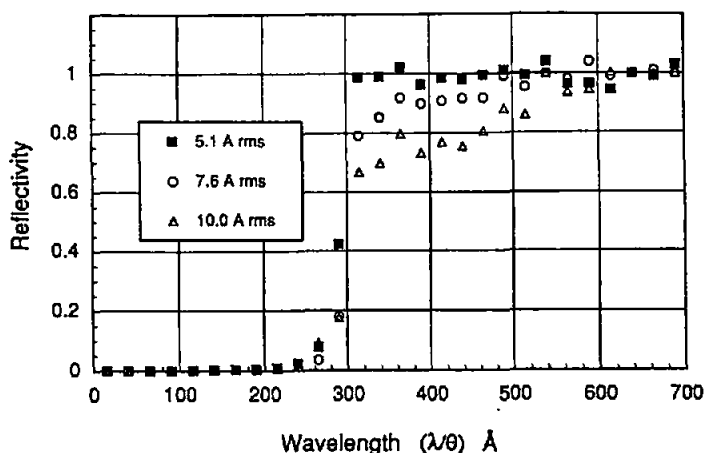


Fig.3 Neutron reflectivity profiles of the supermirrors consisting of 125 layers with  $2q_{Ni}$  as a function of neutron wavelength. The surface roughness of each float-glass substrate is 5.1 Å rms, 7.6 Å rms, and 10.0 Å rms.

Table 1 Surface roughness of the float-glass substrates

	rms (Å)	P - V (Å)
Polished sample	5.1	30.9
Normal sample	7.6	45.4
Rough polished sample	10.0	59.8

## Inter-diffusion and Oxidation

The depth profile of atomic density for the multilayer consisting of 40 layers with each thickness of  $100\text{\AA}$ , were performed using ESCA profiler. The multilayers were deposited on silicon substrates under different conditions of oxygen pressure. For the first sample, pressure in the chamber was  $1 \times 10^{-6}$  Torr before the deposition process. For the second sample, it was  $1 \times 10^{-3}$  Torr because oxygen gas was let in the chamber. Fig.6 shows the depth profile for the first sample near the silicon substrate. It was seen that the signals for Ni and Ti are clearly contrasted and in phase opposition, and mixing layer of Ni and Ti is observed in the interfacial region. It is observed that Ni diffused to the deepest region of Ti layer, and the Ni content at the deepest region of Ti layer is 20% of that of Ni layer. The signal for oxygen rises at the beginning of Ti layers. Obviously, Ti oxidized. Fig.7 shows the depth profile for the second sample. It is significant that Ti absorbed oxygen more than that for the first sample case, and Ni content at the deepest region of Ti layer is less than 2% of that of Ni layer.

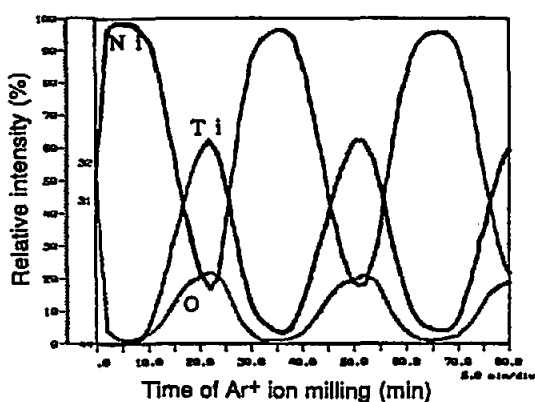


Fig.6 ESCA profile for the Ni/Ti multilayer ( $d = 200 \text{ \AA}$ ,  $P = 1 \times 10^{-6}$  Torr)

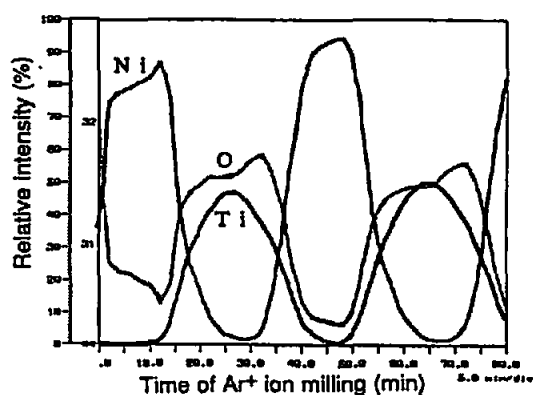


Fig.7 ESCA profile for the Ni/Ti multilayer ( $d = 200 \text{ \AA}$ ,  $P_0 = 1 \times 10^{-3}$  Torr)

The multilayer consisting of 40 layers with each thickness of  $50\text{\AA}$ , were studied by using ESCA profiler. For the third sample, pressure in the chamber was  $1 \times 10^{-6}$  Torr before the deposition process. For the fourth sample, it was  $1 \times 10^{-3}$  Torr because oxygen gas was let in the chamber before deposition process. Fig.8 shows the depth profile for the third sample. It is observed that the signal for Ni at the deepest region of Ti layers is half of that of Ni layer. We can not observe well defined multilayer. Fig.9 shows the depth profile for the fourth sample. It is significant that signal for the Ni at the deepest region of Ti layer is only 30% of that of the Ni layers. We can observe that the signal for Ni and Ti are clearly well contrasted and in phase opposition.

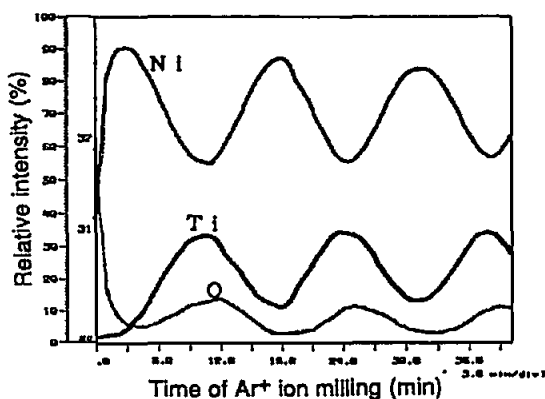


Fig.8 ESCA profile for the Ni/Ti multilayer ( $d = 100 \text{ \AA}$ ,  $P = 1 \times 10^{-6}$  Torr)

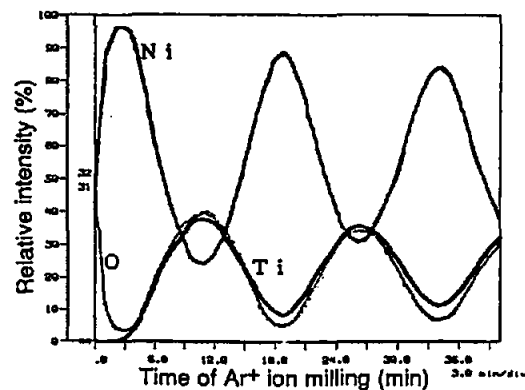


Fig.9 ESCA profile for the Ni/Ti multilayer ( $d = 100 \text{ \AA}$ ,  $P_0 = 1 \times 10^{-3}$  Torr)

## 5. Neutron bender and Supermirror guide tube

### 5.1 Neutron bender

A neutron bender using Ni/Ti supermirror has been designed.<sup>16,17</sup> The scheme of a supermirror bender is shown Fig.10. The neutron bender can branch off a white beam from the main beam main beam line, and creat a new beam port for various beam experiments. The bender using supermirror can makes radius of curvature to be smaller, and makes it much easier to separate a neutron beam. This bender has eleven channels which are divided by float glass plates. Both side of the glass plate are coated by Ni/Ti supermirror with  $3\theta_{Ni}$ . The thickness of glass plate is 0.5mm, and the width of each channel is 2.0mm. The beam size of this bender is 150mm height by 27mm width. Total length is 2m, and the exit of this bender is 28cm distant from the main beam tube. The characteristic wavelength at the exit of the bender is  $8\text{\AA}$ .

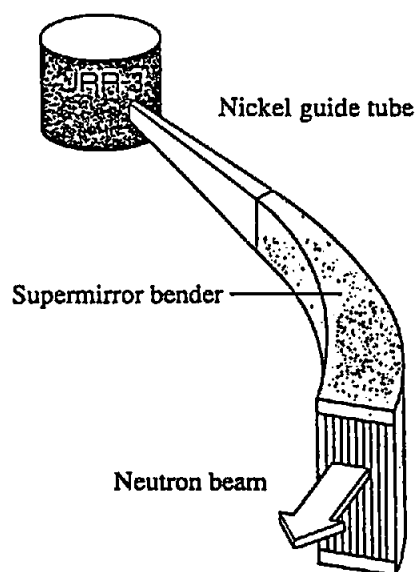


Fig.10 General scheme of a supermirror bender

### 5.2 Supermirror guide tube applied for cancer treatment

An irradiation facility for cancer treatment based on the Boron Neutron Capture Therapy (BNCT),<sup>19</sup> has been designed by using Ni/Ti supermirror guide tube at the JRR-3M.<sup>17</sup> Some irradiation conditions such as thermal neutron flux of  $10^9$  n/cm<sup>2</sup>/s, large beam size, and low background, are required by medical researcher for successful BNCT treatment. Neutron guide tube can transport low energy neutron from the reactor to the neutron facilities at distant place, and can reduce the background of fast neutron and gamma rays. So "pure" thermal neutrons are obtained at the end of neutron guide tube, it would be a most suitable neutron field for BNCT treatment.

The outline of the proposed irradiation facility is as follows. A schimatic view of a irradiation facility for cancer treatment is shown in Fig.8. The existing thermal nickel guide tube of 20m in the biological shielding, guide tunnel, and shielding room, is replaced by the Ni/Ti supermirror guide tube. The radius of curvature is as same as that of the existing one. Moter-operated nickel guide tube are set between the supermirror guide tube and the nickel one. The irradiation space for cancer treatment is set after moving this guide tube.

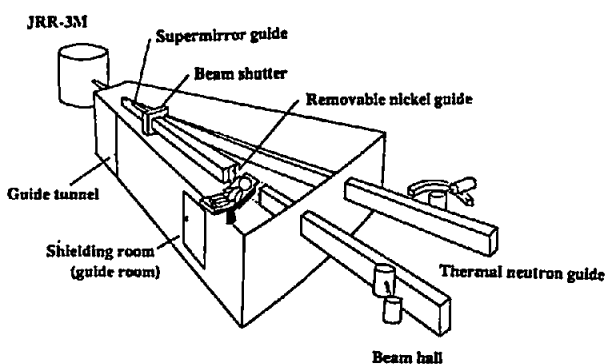


Fig.11 General scheme of irradiation facility for cancer treatment

The movable element can transport neutron beam to the neutron facilities at the beam hall, if the treatment isn't done. The unit of supermirror guide is divided into three channels of 2mm width by glass substrata of 5mm width. The total beam cross-section is 70mm x 200mm. Background dose is quite low at the shielding room, gamma dose rate measured just by the side of existing nickel guide was 350 $\mu$ Sv/h at a reactor power of 20MW. Thermal neutron flux at this irradiation field is expected to be  $1.4 \times 10^9$  n/cm<sup>2</sup>sec<sup>-1</sup> evaluated by the NEUGT code. This facility meet the requirements for succesful BNCT treatment. It would be a most suitable medical irradiation field for BNCT treatment.

## 6. Conclusions

The morphology and multilayer structure of Ni/Ti supermirrors have been investigated using neutron spectroscopy, Heterodyne profiler, TEM, and ESCA profiler. High reflectivity (>0.90) supermirror can be made using vacuum evaporation system by restraining surface roughness of the substrate, and the possibility to make a titanium oxide for diffusion barrier has been offered to improve the performance.

The development of application devices using supermirror such as a neutron bender and guide tube applied to irradiation facility for cancer treatment, has been progress to meet the increasing demands and to open up new research areas.

## 7. References

1. F. Mezei, *Comm. Phys.* 1, 81 (1976)
2. B. P. Schoenborn, D. L. D. Casper and O. F. Kammerer, *J. Appl. Cryst.* 7, 508 (1974)
3. A. M. Saxena and B. P. Schoenborn, *Acta Cryst.* A33, 805-813 (1977)
4. C. F. Majkrzak and L. Passell, *Acta Cryst.* A41, 41-48 (1985)
5. A. M. Saxena, *J. Appl. Cryst.* 19, 123-130 (1986)
6. N. Onishi, H. Takahashi, M. Takayanagi, H. Ichikawa, M. Kawasaki, *J. At. Energy Soc. Japan* 32, 10, 962-969 (1990)
7. Y. Kawabata, M. Suzuki, H. Takahashi, N. Onishi, A. Shimanuki, Y. Sugawa, N. Niino, T. Kasai, K. Funasyo, S. Hayakawa, K. Okuhata, *J. Nucl. Sci. Technol.* 27, 12, 58-66 (1990)
8. Y. Kawabata, *J. Nucl. Sci. Tech.* 27, 12, 1138-1146
9. Y. Kawabata, M. Suzuki, K. Tsuruno, N. Onishi, *Physica B* 180&181, 987 (1992)
10. T. Ebisawa, N. Achiwa, S. Yamada, T. Akiyoshi and S. Okamoto, *J. Nucl. Sci. Technol.* 16, 647-659 (1979)
11. S. Yamada, T. Ebisawa, N. Achiwa, T. Akiyoshi and S. Okamoto, *Annu. Rep. Res. Reactor Inst. Kyoto Univ.* Vol. 11, 8-27 (1978)
12. J. Schelten and K. Mika, *Nucl. Instrum. Meth.* 160, 287-294 (1979)
13. J. E. Keem, J. Wood, N. Grupido and K. Hart, S. Nutt, D. G. Reichel and W. B. Yelon, *SPIE* 983, 38-52 (1988)
14. F. Samuel, B. Farnoux, B. Ballot, B. Vidal, *SPIE* 1738, 54-66 (1993)
15. S. Tasaki, *J. Appl. Phys.* 71, (5), 1 (1992)
16. K. Soyama, Y. Kawabata and M. Suzuki, *Proc. 3rd Asian Symp. on Research Reactor*, JAERI-M92-028 (1991)
17. K. Soyama, M. Suzuki, K. Kawabata, H. Ichikawa and T. Kodaira, *Proc. The fifth International Symposium on Advanced Nuclear Energy Research* (1993)
18. K. Soyama, M. Suzuki, K. Kawabata and H. Ichikawa, *Proc. The fifth International Symposium on Advanced Nuclear Energy Research* (1993)
19. G. L. Locher, *Am. J. Roentgenol. Radium Therapy*, 36, 1-13 (1936)

## **SESSION IV**

### **Workshop on R&D Needs**

## REPORT ON THE WORKSHOP ON R&D NEEDS

Colin D. West and Klaus Böning

As in previous meetings, the R&D needs of IGORR members were discussed to identify common areas in which research work or results might be shared.

Of the R&D needs identified at IGORR-I and IGORR-II, several topics have been investigated and reported on by some members. These results, listed in the table below, have been shared through IGORR and through the normal publication routes.

Topics	Investigators
Thermal-hydraulic tests and correlations	JAERI, ANS
Corrosion tests and analytical models	ANS
Fuel plate fabrication	FRM-II/CERCA, ANS/B&W
Fuel plate stability	ANS
Fuel irradiations	ANS, JAERI, MURR
Structural materials irradiation tests	Several groups
Instrumentation upgrading and digital control systems	MIT, OSIRIS
Man-machine interface	MIT

To the extent that IGORR has been instrumental in helping to identify and publicize this work, it has performed a valuable service to the community.

Some of the research issues previously identified still need to be addressed (results have not been explicitly reported to IGORR meetings). They are shown in the next table.

Topic	Organizations needing results
Multidimensional kinetic analysis for small cores	ANS, FRM-II, MAPLE
Burnable poison irradiation tests	FRM-II, ANS
Neutron guide irradiation tests	JAERI, ANS, FRM-II
Cold source materials irradiation tests	ANS
Cold source LN <sub>2</sub> tests	ANS
Cold source LH <sub>2</sub> -H <sub>2</sub> O reaction	BNL, JAERI, FRM-II, ANS



There was considerable discussion of the need, pointed out by Dr. Roegler, for more information on the accident and safety analysis methods and codes used by the various organizations in different countries. It was agreed that members will be asked to provide information on the methods they use, on benchmarking results, and on other methods of code verification and validation. Colin West will solicit the input, and Albert Lee volunteered to compile the results. This is clearly a key issue for IGORR to address in the coming year.

Some other R&D needs identified during this workshop are also listed in the table below.

Topic	Notes
Accident and safety analysis codes and benchmarks	IGORR members will be asked to supply and share information on the methods they use
Thermophysical properties of D <sub>2</sub> O liquid and vapor	Risø has prepared a report on this, with 150 references, and will publish a heavy water handbook* in about six months IGORR members will be informed.
Chemical and other energy release from core melt events	Need better estimates of steam production for containment and design (Lee/AECL)
Fission product release from a molten MTR core	
Thermal conductivity of irradiated fuel meet	Analytical, or better still experimental, data are needed (West/ANS)
Tests of cryogenic circulators for single-phase forced-convection cold source	
Flow blockage tests	ANS will measure flow and heat transfer effects in the wake of a partial blockage and will use the results to benchmark a computational fluid dynamics model. Results will be reported.

We will continue to encourage members to report the availability of research results through the IGORR meetings and the newsletters.

\*) See attachment 1

## Attachment 1

# HEAVY WATER HANDBOOK

Evaluation of Available Thermophysical Properties of Heavy Water (D<sub>2</sub>O) Liquid and Vapour

Prof. Ing. Jan, J, Bukovsky, M.Sc., DCAe.  
University of West Bohemia, Plzen, Czech Republic

Karsten Haack, M.Sc.  
Riso National Laboratory

Povl Wiig, Scient.ass.  
Riso National Laboratory

Riso National Laboratory, DK-4000 Roskilde, Denmark, August, 1993

**Abstract** Numerous publications on the thermophysical data of heavy water (D<sub>2</sub>O) have been published since D<sub>2</sub>O became commercially available in the 1930'es. Some of these data are in mutual disagreement. This has led to confusion among the scientific and technical staffs who needed the information on the D<sub>2</sub>O thermophysical data.

Correct thermophysical data must be consistent, i.e. their mutual relations must be in accordance to the fundamental thermophysical laws. The work behind this publication has been focussed at collecting all available D<sub>2</sub>O data and checking the data mutually by means of these fundamental thermophysical criteria.

Depending on the various production methods, the oxygen content of the D<sub>2</sub>O is enriched more or less in the heavier oxygen isotopes <sup>17</sup>O and <sup>18</sup>O. This, together with the amount of impurities and dissolved gases in the D<sub>2</sub>O samples of the various references, might - to some extent - explain the discrepancies between the data sources. Only a few references contain informations on these subjects.

The D<sub>2</sub>O data sets which were found to be the most reliable are presented in chapter 9, in tables as well as in diagrams, together with the corresponding H<sub>2</sub>O data for comparison. The diagrams are commented for reliability where it was found necessary.

Furthermore, the publication contains short descriptions on the heavy water sources, availability, production processes, economy, material and energy demands for production.

A comprehensive list of references is enclosed.

## Attachment 2

Following presentation was made by Dr. Yuan Luzheng (CIAE, China) at the beginning of the workshop on R&D needs.

### A New Research Reactor Scheduled in CIAE

Yuan Luzheng, Huang Daoli and Kang Yalun

China Institute of Atomic Energy  
Beijing, P. R. of China

Since 1958 when the heavy water research reactor (HWRR) first went critical, two modifications have been performed on it. The first modification was finished in 1980 and changed the reactor core into a more compact neutron-trap-type. The enrichment of  $^{235}\text{U}$  was increased from 2% to 3% but the fuel assembly configuration and uranium metal as the fuel meat was kept the same. The second modification was done in 1983. It kept the same core configuration but changed the fuel assembly into cluster type and used  $\text{UO}_2$  with 3% enrichment of  $^{235}\text{U}$  as the fuel.

Obviously, these two upgrades only dealt with the reactor core and were subjected to many limitations for improving the reactor further. Following the requirements for a more advanced research reactor possessing higher flux and additional capabilities from various users in China, and HWRR approaching retirement, China has decided to design and construct a new research reactor. Now, having made several discussions and negotiations with users in various fields, we have planned to make a new research reactor with higher neutron flux, for example,  $5 \times 10^{14}$  n/s.cm<sup>2</sup> or more.

The new research reactor to be designed will meet mainly two rather different requirements, radioisotope production and neutron scattering experiments. So, the final design will be a compromise between these two requirements.

Now we are in the conceptual design stage and two reactors seem to be attractive for us as our references. One is JRR-3M and the other is FRM-II.

China has got experience in fabricating plate-type fuel but not involute-shaped plates. So, if the involute-shaped plate is chosen as our future reactor's fuel, international collaboration between China and other countries is required. If standard plate-type fuel is adopted, the core configuration of "inverse neutron trap" type is to be considered in the following way. For making the core more compact, there will be no position in the core for control rods and irradiation channels, meanwhile four lattice cells in the center will be provided for a central control rod with a square shape instead of a cylindrical one like FRM-II. Fig. 1 shows the conceptual diagram. In this case, we should use fuel with higher enrichment, for example, more than 45%. Also  $\text{U}_3\text{Si}_2\text{-Al}$  dispersion fuel with as high as possible uranium density is to be used.

For both cases, more information and experience on designing a new research reactor are welcome.

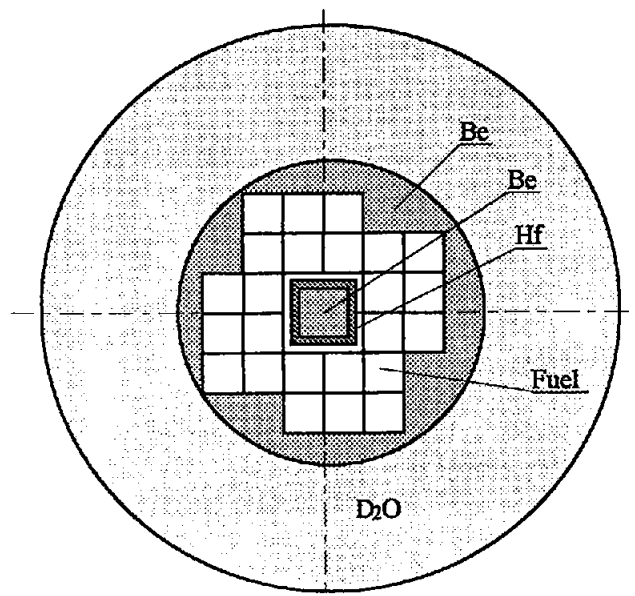


Fig. 1 Conceptual Design of China's  
New Research Reactor  
(Plate type fuel)

## **SESSION V**

### **Business Session**

## IGORR BUSINESS MEETING

Colin D. West

The entire group expressed thanks to our Japanese hosts for the outstanding organization of this meeting and for the support provided by the Secretariat. Earlier, a message of thanks for her work on the technical program had been signed by most attendees and sent to Kathy Rosenbalm at Oak Ridge, whose organization regrettably had not authorized her attendance at the meeting.

After some discussion, the group agreed that the next meeting, IGORR-IV, should be held in the United States following the sequence already established of the United States, Europe, and Asia. In his presentation on the proposed new Chinese research reactor, Dr. Yuan Luzheng had already offered to host a future meeting.

An offer to organize IGORR-IV in the East Tennessee area was accepted. It was agreed that the spring of 1995, about 18 months after this meeting, would be an appropriate time. Past meetings have evolved into a greater proportion of R&D reports as compared with facility status reports; it is expected, and hoped, that this trend will continue.

Colin West was unanimously reelected as chairman until the next meeting (author's note: thank you).

The meeting adjourned, and attendees were taken for a tour of the JRR-3M.

## **IGORR-III PARTICIPANTS LIST**

## List of Participants of IGORR-III

Edgar KOONEN  
BR2 Department  
Belgian Nuclear Research Center  
CEN/SCK  
Boeretang 200, B-2400 MOL  
Belgium

Albert G. LEE  
AECL Research  
Whiteshell Laboratories  
Pinawa, Manitoba, ROEILD  
Canada

Karsten HAACK  
Riso National Laboratory  
P. O. Box 49  
DK-4000 Roskilde  
Denmark

Anore CHAPELOT  
TECHNICATOME  
B. P. 17  
91192 Gif Sur Yvette Cedex  
France

Christian DESANDRE  
TECHNICATOME  
B. P. 17  
91192 Gif Sur Yvette Cedex  
France

Jean-Pierre DURAND  
CERCA  
P. O. Box 1114  
26104 Romans Cedex  
France

Bernard FARNOUX  
CEA/DSM  
ORME Des Merisiers  
C.E.N. Saclay  
91191 Gif Sur Yvette Cedex  
France

Gerard HARBONNIER  
CERCA  
P. O. Box 1114  
26104 Romans Cedex  
France

Charles JOLY  
C.E.A. DRN/DRE  
C.E.A. Saclay  
91191 Gif Sur Yvette Cedex  
France

Francis MERCHIE  
C.E.A. DRN/DRE  
C.E.N.G. - 85 X  
38041 Grenoble Cedex  
France

Pascal ROUSSELLE  
TECHNICATOME  
B. P. 17  
91192 Gif Sur Yvette Cedex  
France

Anton AXMANN  
Dept. Research Reactor BER II  
Hahn-Meitner-Institute Berlin GmbH  
Glienicke Strasse 100  
Postfach 390128  
D-14109 Berlin 39  
Germany

Klaus BÖNING  
Fakultät für Physik E21  
Technischen Universität München  
Reaktorstation  
D-85747 Garching  
Germany

Horst Walter HASSEL  
JECTA Consulting GmbH  
Japanese/European Consulting and Trade Agency  
63755 Alzenau-Horstein  
Postfach 3526  
Germany

Wolfgang KNOP  
GKSS Forschungszentrum  
Max-Planck-Strasse  
D-2054 Geesthacht  
Germany

Hans-Joachim ROEGLER  
Siemens AG  
Friedrich-Ebert-Str.  
D-51429 Bergisch-Gladbach 1  
Germany

Johannes WOLTERS  
Institute für Sicherheitsforschung und  
Reaktortechnik (ISR)  
Forschungszentrum Jülich GmbH  
D-52425 Jülich 1 - Postfach 1913  
Germany

Bakri ARBIE  
PRSG, BATAN  
PUSPIPTEK, Serpong,  
Tangerang, Jawa Barat  
Indonesia

Otohiko AIZAWA  
Musashi Institute of Technology  
971 Ozenji, Ashou-ku  
Kawasaki-shi, Kanagawa-ken  
Japan

Yoshiaki FUJITA  
Research Reactor Institute,  
Kyoto University  
Noda, Kumatori-machi,  
Sennan-gun, Osaka  
Japan

Mitsuho HIRATA  
Invited Researcher, JAERI  
2-4 Shirakata-Shirane,  
Tokai-mura, Naka-gun, Ibaraki-ken  
Japan

Michio ICHIKAWA  
Deputy Director General, JAERI  
2-4 Shirakata-Shirane,  
Tokai-mura, Naka-gun, Ibaraki-ken  
Japan

Masanori KAMINAGA  
Department of Research Reactor, JAERI  
2-4 Shirakata-Shirane,  
Tokai-mura, Naka-gun, Ibaraki-ken  
Japan

Mitsunobu KANEKO  
Nuclear Fuel Industries, Ltd.  
3135-41 Muramatsu, Tokai-mura,  
Naka-gun, Ibaraki-ken  
Japan

Masaru KOBAYASHI  
Pechiney Japon  
Mitsui-Building  
2-1-1 Nishishinbashi, Shinjuku-ku  
Tokyo, Japan

Shojiro MATSUURA  
Director General, JAERI  
2-4 Shirakata-Shirane,  
Tokai-mura, Naka-gun, Ibaraki-ken  
Japan

Masaru NAKAI  
Toshiba Corporation  
4-1 Ukishima-cho, Kawasaki-ku,  
Kawasaki-shi, Kanagawa-ken  
Japan

Noboru NAKAO  
Hitachi, Ltd.  
4-6 Kanda-Surugadai, Chiyoda-ku  
Tokyo, Japan

Hirokatsu NAKATA  
Ibaraki Prefectural Office  
1-5 Sannomaru, Mito-shi, Ibaraki-ken  
Japan

Hideaki NISHIHARA  
Research Reactor Institute,  
Kyoto University  
Noda, Kumatori-machi,  
Sennan-gun, Osaka  
Japan

Yoshiaki OKA  
University of Tokyo  
2-22 Shirakata-Shirane,  
Tokai-mura, Naka-gun, Ibaraki-ken  
Japan

Arahiko OOKI  
Musashi Institute of Technology  
971 Ozenji, Ashou-ku  
Kawasaki-shi, Kanagawa-ken  
Japan

Isao SAITO  
University of Tokyo  
2-22 Shirakata-Shirane,  
Tokai-mura, Naka-gun, Ibaraki-ken  
Japan



Atsushi SASAZAWA  
Hitachi, Ltd.  
4-6 Kanda-Surugadai, Chiyoda-ku  
Tokyo, Japan

Toshikazu SHIBATA  
Kinki University  
3-4-1 Kowakae, Higashi-Osaka-shi  
Osaka, Japan

Yoshio SHIMIZU  
Nissho Iwai Corporation  
2-4-5 Akasaka, Minato-ku  
Tokyo, Japan

Eiji SHIRAI  
Department of Research Reactor, JAERI  
2-4 Shirakata-Shirane,  
Tokai-mura, Naka-gun, Ibaraki-ken  
Japan

Kazuhiko SOYAMA  
Department of Research Reactor, JAERI  
2-4 Shirakata-Shirane,  
Tokai-mura, Naka-gun, Ibaraki-ken  
Japan

Kenji SUMITA  
Osaka University  
1-1 Yamadaoka, Suita-shi  
Osaka, Japan

Toshiyuki TANAKA  
Department of HTTR Project, JAERI  
Oarai-machi, Higashi-ibaraki-gun,  
Ibaraki-ken  
Japan

Junsaku TSUNODA  
Radiation Irradiation Application Association  
2-4 Shirakata-Shirane,  
Tokai-mura, Naka-gun, Ibaraki-ken  
Japan

Takao TSURUTA  
Kinki University  
3-4-1 Kowakae, Higashi-Osaka-shi  
Osaka, Japan

Tadashi WATANABE  
NKK Corporation  
2-1 Suehiro-cho, Tsurumi-ku,  
Yokohama, Kanagawa-ken  
Japan

Jong Tai LEE  
Korea Atomic Energy Research Institute  
Dukjin-Dong 150, Yoosung-Ku,  
Taejon, 305-353  
Korea

In Cheol LIM  
Korea Atomic Energy Research Institute  
Dukjin-Dong 150, Yoosung-Ku,  
Taejon, 305-353  
Korea

Huang DAOLI  
China Institute of Atomic Energy  
P. O. Box 275  
Beijing  
P.R. of China

Yuan LUZHENG  
China Institute of Atomic Energy  
P. O. Box 275  
Beijing  
P.R. of China

Kang YALUN  
China Institute of Atomic Energy  
P. O. Box 275  
Beijing  
P.R. of China

Kir A. KONOPLEV  
Petersburg Nuclear Physics Institute  
Russian Academy of Science  
188350 Gatchina, St. Petersburg  
Russia

Yuri V. PETROV  
Petersburg Nuclear Physics Institute  
Russian Academy of Science  
188350 Gatchina, St. Petersburg  
Russia

Mikael GROUNES  
Studsvick Nuclear AB  
S-61182 Nykoping  
Sweden

Erik B. JONSSON  
Sweden  
Studsvick Nuclear AB  
S-61182 Nykoping  
Sweden

Ka-Yu HUANG  
Institute of Nuclear Energy Research  
P. O. Box 3  
Lung-Tan  
Taiwan, R.O.C.

Lee-Chung MEN  
Institute of Nuclear Energy Research  
P. O. Box 3  
Lung-Tan  
Taiwan, R.O.C.

Der-Jhy SHIEH  
Institute of Nuclear Energy Research  
P. O. Box 3  
Lung-Tan  
Taiwan, R.O.C.

Kuan-Chywan TU  
Institute of Nuclear Energy Research  
P. O. Box 3  
Lung-Tan  
Taiwan, R.O.C.

Jim E. MAYS  
Babcock & Wilcox  
P. O. Box 785  
Lynchburg, VA 24505  
USA

Gerry L. McCORMICK  
Babcock & Wilcox  
P. O. Box 785  
Lynchburg, VA 24505  
USA

Henry J. PRASK  
Reactor Radiation Division  
National Institute of Standards and Technology  
Gaithersburg, MD 20899  
USA

Colin D. WEST  
Oak Ridge National Laboratory  
P.O. Box 2009, FEDC Building  
Oak Ridge, TN 37831-8218  
USA

## Participants from JAERI

T. ISE  
S. FUNAHASHI  
N. MINAGAWA  
Y. MORI  
T. TSUKADA  
K. WATANABE  
M. ISSHIKI  
I. TANAKA  
M. KIYOTA  
M. KUROSAWA  
T. ISHII  
M. MIYAZAWA  
C. NAKAZAKI  
T. NIHO  
R. OYAMADA  
H. TSURUTA  
T. HOSHI  
Y. NAKAGAWA  
T. KUGO  
T. SASA  
T. TONE  
K. TSUCHIHASHI  
S. BUCKMAN (ANSTO)  
T. GENKA  
K. KUSHIDA  
M. TANASE  
N. YAMABAYASHI  
T. KIKUCHI  
Y. TOGASHI  
N. FUJIMOTO  
S. NAKAGAWA  
N. SAKABA  
T. SHIBATA  
Y. HORIGUCHI  
K. KAKEFUDA  
T. KISHI  
T. KUMAI  
T. NAKAJIMA  
M. NAKANO  
D. NEMOTO  
M. OHTAKE  
A. OHTOMO  
M. TAKAYANAGI  
M. TANI  
A. TSURUNO  
T. YAMADA  
S. YAMAGUCHI  
K. HOTTA  
T. ISHII  
K. KITAHARA  
H. MATSUSHIMA  
S. TOYOKAWA

Y. IKEDA  
S. AHBA  
I. TAKESHITA  
K. YANAGISAWA

2-4 Shirakata-Shirane,  
Tokai-mura, Naka-gun, Ibaraki-ken  
Japan

N. NABABAN  
PRSG, BATAN  
PUSPITEK, Serpong,  
Tangerang, Jawa Barat  
Indonesia

Marco A. LUCATERO  
Department of Nuclear Systems  
National Institute of Nuclear Research of Mexico  
Sierra Mojada No. 447  
Lomas de Barrilaco  
11010, Mexico, D. F.

**IGORR-III Secretariat Staff**  
**Department of Research Reactor,**  
**JAERI**

N. ARAI  
K. ARIGANE  
Y. FUNAYAMA  
A. HIROSE  
Y. HOSHI  
H. ICHIKAWA  
T. INOUE  
K. IZUMO  
M. KAMINAGA  
H. KIKUCHI  
M. KINASE  
T. KODAIRA  
T. KURIBAYASHI  
T. KUROSAWA  
T. MARUO  
Y. MITADERA  
A. MORIAI  
Y. MURAYAMA  
Y. NAKANO  
T. NEMOTO  
K. NISHINO  
T. OBATA  
M. OGAWA  
N. OHNISHI  
K. OKUMURA  
M. SATOH  
S. SATOH  
E. SHIRAI

H. SHITOMI  
K. SOYAMA  
T. TABATA  
H. TAKAHASHI  
Y. TORII  
T. YAMADA  
K. YAMAMOTO  
A. YANAGISAWA  
K. YOKOO

Department of Research Reactor, JAERI  
2-4 Shirakata-Shirane,  
Tokai-mura, Naka-gun, Ibaraki-ken  
Japan

**IGORR-III Technical Program**  
**Chairman**

Kathy F. Rosebalm  
Oak Ridge National Laboratory  
P.O. Box 2009, FEDC Building  
Oak Ridge, TN 37831-8218  
USA